



**HAL**  
open science

# Importance of mitochondrial hydrogen sulfide oxidation in liver pathophysiology

Inês Mateus

► **To cite this version:**

Inês Mateus. Importance of mitochondrial hydrogen sulfide oxidation in liver pathophysiology. Tissues and Organs [q-bio.TO]. Université Paris Cité, 2021. English. NNT : 2021UNIP5049 . tel-03617849

**HAL Id: tel-03617849**

**<https://theses.hal.science/tel-03617849>**

Submitted on 23 Mar 2022

**HAL** is a multi-disciplinary open access archive for the deposit and dissemination of scientific research documents, whether they are published or not. The documents may come from teaching and research institutions in France or abroad, or from public or private research centers.

L'archive ouverte pluridisciplinaire **HAL**, est destinée au dépôt et à la diffusion de documents scientifiques de niveau recherche, publiés ou non, émanant des établissements d'enseignement et de recherche français ou étrangers, des laboratoires publics ou privés.

Université de Paris

École doctorale Bio Sorbonne Paris Cité 562

Laboratoire U1016 Institut Cochin

# Importance of mitochondrial hydrogen sulfide oxidation in liver pathophysiology

**Inês MATEUS**

**Thèse de doctorat de Physiologie et Physiopathologie**

Dirigée par **Carina PRIP-BUUS**

Présentée et soutenue publiquement à l'Institut Cochin le 3 mai 2021

Devant le jury composé de:

Béatrice MORIO (DR) – Université de Lyon	Rapporteuse
François BLACHIER (DR) - Université Paris-Saclay	Rapporteur
Cecília RODRIGUES (PU) – Université de Lisbonne	Examinatrice
Carles CANTÓ (MCU-HDR) - École polytechnique fédérale de Lausanne	Examinateur
Christophe MAGNAN (PU) – Université de Paris	Examinateur
Carina PRIP-BUUS (DR) – Université de Paris	Directrice de thèse

Université de Paris

École doctorale Bio Sorbonne Paris Cité 562

Laboratoire U1016 Institut Cochin

# Importance of mitochondrial hydrogen sulfide oxidation in liver pathophysiology

**Inês MATEUS**

**Thèse de doctorat de Physiologie et Physiopathologie**

Dirigée par **Carina PRIP-BUUS**

Présentée et soutenue publiquement à l'Institut Cochin le 3 mai 2021

Devant le jury composé de:

Béatrice MORIO (DR) – Université de Lyon

Rapporteuse

François BLACHIER (DR) - Université Paris-Saclay

Rapporteur

Cecília RODRIGUES (PU) – Université de Lisbonne

Examinatrice

Carles CANTÓ (MCU-HDR) - École polytechnique fédérale de Lausanne

Examineur

Christophe MAGNAN (PU) – Université de Paris

Examineur

Carina PRIP-BUUS (DR) – Université de Paris

Directrice de thèse

*This doctoral thesis is part of a project that has received funding from the European Union's Horizon 2020 research and innovation programme under the Marie Skłodowska-Curie grant agreement No 722619.*

## Acknowledgments

To all the members of the jury: Dr. François Blachier, Dr. Béatrice Morio, Professor Cecília Rodrigues, Dr. Carles Cantó and Dr. Christophe Magnan. Thank you for the time you took to read and evaluate my thesis. It was my deepest honour to discuss my work with such accomplished researchers. I was truly humbled.

A tous les membres de mon Comité de Suivi : Dr. François Blachier, Dr. Catherine Postic et Dr. Ludivine Doridot. Merci de m'avoir fait l'honneur de juger mon travail de thèse.

A Carina. Merci d'avoir accepté de diriger cette thèse. Ta grande rigueur scientifique et ton sens du détail m'ont permis de grandir en tant que chercheuse. J'ai toujours ressenti que tu étais «my back», professionnellement et personnellement. D'entre tous mes collègues du Foie Gras je peux dire que j'étais l'une des rares chanceuses. Je te suis profondément reconnaissante pour tout ce que tu as fait pour moi. Tu étais un mentor, une instructrice, et, surtout, une amie. Une chose est sûre : je ne t'oublierai jamais.

A Véronique, merci pour ton aide. Il y a longtemps, j'ai dit que tu étais mes yeux dans le labo. Ce sera toujours vrai. Je n'aurais rien pu faire sans toi !

A Frédéric, merci pour votre sympathie, nos discussions scientifiques ainsi que vos nombreux conseils.

A ma petite Angèle. Tu es vraiment un rayon de lumière dans cette équipe. N'arrête jamais de briller. Ne perds jamais ton sourire.

Je tiens également à remercier les autres membres de l'équipe : Anne, Céline, Clotilde, Emmanuel, Maïly, Khawla, Noureddine et Renaud.

Merci à mes voisins de couloir pour leur sympathie et leur soutien pendant ces 4 années : Anne-Françoise, Bolaji, Boris, Catherine, Dalale, Fadila, Florian, Lucia, Mélanie, Michèle, Sandra, Thais et Wafa.

A Paula. Muchas gracias por quererme y soportarme durante estos cuatro años. Aunque el tiempo nos aleje, siempre guardaré y recordaré con cariño a mi caracola. Muchas gracias por todo mi amiga.

Às senhoras do bar da Faculdade. Pode parecer pouco, mas o café e os dois dedos de conversa que partilhámos faziam o meu dia. Um grande beijinho.

To all members of the Foie Gras advisory board and PI team. Thank you for all the professional advice and scientific debates. More than a researcher, this program has made me grow as an individual.

To Professor Cecília Rodrigues and Professor Hans Zischka for welcoming me into their labs and for treating me as part of the team.

To my Foiegrinos. Looking back, I cannot think of a more spectacular group of people with whom I could have shared this experience. Even if time and distance take us apart, be sure that I will always hold you dear in my heart. *Obrigada. Gracias. Gràcies. Grazie. Hvala. Dhanyavaad. Tomake Donnobadh. Ameseginalehu.*

À minha mãe e ao meu pai, as pessoas mais importantes da minha vida. Se fizesse uma lista de todas as coisas pelas quais tenho de agradecer-vos, esta tese não teria espaço suficiente para ela. Assim sendo, agradeço só ao destino por, de entre milhões de pessoas, me ter feito vossa filha. Esta é mais uma conquista de nós os três.

À minha Tia Lena, por toda a preocupação e todo o carinho. É uma alegria poder contar com a sua presença na minha vida. Um beijinho enorme.

Ao meu Luís. Quando olho para ti vejo tudo o que poderias ter sido e te roubaram de ser. Tu inspiras-me a ser melhor e, tudo quanto vivo, tento vivê-lo pelos dois. Adoro-te.

Ao meu Tio Zé, por todos os telefonemas, todas as mensagens e todo o interesse. Existem várias formas de dizer “Gosto de ti” e, “Atão comé?” é uma delas. Agradeço-te do fundo do coração.

À minha avó Piedade. Todos os abraços e beijinhos que você me mandou por telefone chegaram cá. Obrigada Vó! Adoro-a.

À Irmandade dos Magníficos. Quando a amizade é verdadeira nem o vento a leva, nem a distância a separa. Agradeço à vida todos os dias por ter feito cruzar os nossos caminhos. Adoro-vos, corações.

À Sara Castro. Mesmo longe estiveste sempre a meu lado e sempre me fizeste companhia. És o melhor presente que Coimbra me deu. Adoro-te, miga.

Bozorgtarin moohebate zendegi, doosti ast va man aan ra az Minoos daryaft karde’am.  
Merci.

To all people who somehow supported me during these past 4 years, THANK YOU!

# Table of contents

List of illustrations.....	vii
Abstract.....	xi
Résumé.....	xiii
Abbreviations.....	xvii
Publications.....	xxiii
Posters and oral communications.....	xxiii
Secondments.....	xxiv
Complementary training.....	xxiv
<b>I. Introduction.....</b>	<b>1</b>
<b>1. Hydrogen sulfide: a double-edged sword.....</b>	<b>3</b>
1.1. In the beginning.....	3
1.2. Environmental pollutant.....	5
1.3. Gasotransmitter.....	7
1.3.1. Definition.....	7
1.3.2. Discovery.....	7
1.3.3. Crosstalk.....	8
1.4. Characteristics of the H <sub>2</sub> S molecule.....	9
1.4.1. Physical and chemical properties.....	9
1.4.2. Intracellular H <sub>2</sub> S pools.....	11
1.5. Sources of H <sub>2</sub> S in the body.....	13
1.5.1. Exogenous.....	13
a) Inhalation.....	13
b) Dietary intake.....	15
1.5.2. Endogenous.....	15
a) Gut microbiota.....	15
b) Tissue.....	17
Non-enzymatic production.....	17
Enzymatic production.....	19
Cystathionine β-synthase.....	21
Cystathionine γ-lyase.....	23
3-mercaptopyruvate sulfurtransferase.....	26
1.6. Catabolism of H <sub>2</sub> S.....	29
1.6.1. Expiration.....	29
1.6.2. Methylation.....	30
1.6.3. Mitochondrial oxidation.....	31
a) Enzymes involved in H <sub>2</sub> S mitochondrial oxidation.....	31
Sulfide Quinone Oxireductase (SQR).....	31
Ethylmalonic encephalopathy protein 1 (ETHE1).....	32
Thiosulfate sulfurtransferase (TST).....	33
Sulfite oxidase (SUOX).....	33
b) Steps of mitochondrial H <sub>2</sub> S oxidation.....	34
Step 1.....	34
Step 2.....	37
Step 3.....	37

c) A double-faced molecule.....	37
1.7. Biological effects of H <sub>2</sub> S.....	38
1.7.1. Vasorelaxation/Vasoconstriction.....	38
1.7.2. Inflammation.....	41
a) Anti-inflammatory.....	41
b) Pro-inflammatory.....	42
1.7.3. Apoptosis and cell proliferation.....	43
1.7.4. Oxidative stress.....	44
1.7.5. Protein modification.....	44
a) The reaction.....	47
b) Importance of protein persulfidation.....	48
1.8. Inhibitors of H <sub>2</sub> S biosynthesis.....	48
1.9. Donors of exogenous sulfide.....	48
1.9.1. Fast-release donors.....	48
a) Sulfide salts.....	48
b) Thiosulfate (SSO <sub>3</sub> <sup>2-</sup> ).....	49
1.9.2. Slow-release donors.....	50
a) GYY4137.....	50
b) Other donors.....	51
1.10. Methods of H <sub>2</sub> S quantification.....	51
1.10.1. Lead-acetate strips.....	51
1.10.2. Methylene blue method.....	53
1.10.3. Monobromobimane derivatization.....	53
1.10.4. Gas chromatography.....	54
1.10.5. Ion sensitive electrodes.....	54
1.10.6. Polarographic sensors.....	55
1.10.7. Fluorometric probes.....	55
<b>2. Non-Alcoholic Fatty Liver: a disease of the modern world.....</b>	<b>57</b>
2.1. Description.....	57
2.2. Epidemiology.....	57
2.3. Diagnosis.....	61
2.3.1. Non- or minimally invasive methods.....	61
a) Biomarkers.....	61
Hepatic transaminases.....	61
MicroRNAs (miRNAs).....	62
b) Imaging techniques.....	63
Magnetic Resonance Imaging (MRI).....	63
Transient elastography (TE).....	63
Ultrasonography .....	65
Computed tomography (CT).....	65
2.3.2. Invasive methods.....	65
a) NAFLD Activity Score (NAS).....	67
b) Algorithm of Bedossa.....	67
2.4. Etiology of NAFLD.....	69
2.4.1. “Two-hits” hypothesis.....	69
a) “First hit”: hepatic steatosis and insulin resistance.....	69
Increase in dietary fatty acids.....	69



Increase in adipose tissue lipolysis.....	71
Increase in hepatic lipogenesis.....	73
Decrease in VLDL synthesis and export.....	77
Changes in mitochondrial homeostasis.....	78
Increased FAO in non-mitochondrial pathways.....	84
Accumulation of toxic metabolites.....	86
a) “Second hit”: further insults.....	90
Inflammation.....	90
Endoplasmic reticulum-associated stress.....	91
Oxidative stress.....	93
2.4.2. “Multiple-hits” hypothesis.....	95
a) Gut microbiota.....	95
b) Gut-liver axis and intestinal dysbiosis in the development of NAFLD.....	97
c) Genetic polymorphisms.....	100
2.4.3. Controlling the disease.....	101
a) Diet and physical activity.....	101
b) Pharmacological treatment.....	102
Metformin.....	102
Thiazolidinediones.....	103
Vitamin E.....	104
Coenzyme Q10.....	105
Betaine.....	106
Statins.....	106
Bariatric surgery.....	107
<b>3. H<sub>2</sub>S and liver pathophysiology: what lies beyond the stink.....</b>	<b>108</b>
3.1. Context.....	108
3.2. H <sub>2</sub> S in liver functions.....	109
3.2.1. H <sub>2</sub> S and hepatic glucose metabolism.....	109
3.2.2. H <sub>2</sub> S and hepatic lipid metabolism.....	113
3.2.3. H <sub>2</sub> S and hepatic mitochondrial function.....	115
3.2.4. H <sub>2</sub> S and hepatic oxidative stress.....	117
3.2.5. H <sub>2</sub> S in hepatic differentiation and liver cancer.....	120
a) Hepatic differentiation.....	120
b) Hepatocarcinoma.....	120
3.3. H <sub>2</sub> S in NAFLD and fibrosis.....	122
3.3.1. NAFLD.....	123
a) Alterations in H <sub>2</sub> S metabolism in the development of NAFLD.....	123
b) H <sub>2</sub> S donors as a therapeutic agent in NAFLD.....	125
3.3.2. Fibrosis.....	127
3.4. Mitochondrial H <sub>2</sub> S oxidation in liver metabolism.....	129
<b>II. Methodology.....</b>	<b>133</b>
1. Animals.....	137
2. Fasting/Refeeding experiments.....	137
3. NAFL and NASH animal models.....	137
4. In vivo supplementation of sodium thiosulfate.....	138
5. In vivo injection of adenovirus.....	139
6. Physiological parameters.....	139

7. Isolation of mitochondria.....	139
8. Measurement of mitochondrial respiration and sulfide oxidation.....	141
9. Lipidomics analysis.....	144
10. Fecal microbiota analysis.....	144
11. Primary cultures of mouse hepatocytes.....	145
12. Analysis of mRNA expression by Real-Time Quantitative PCR.....	145
13. Western blots.....	147
14. Electron microscopy.....	147
15. Statistical analysis.....	147
<b>III. Results.....</b>	<b>149</b>
<b>Chapter 1: Mitochondrial H<sub>2</sub>S oxidation in liver physiology.....</b>	<b>151</b>
Problematic.....	153
Results.....	153
Conclusions.....	154
Original paper.....	155
Supplementary results.....	201
<b>Chapter 2: Mitochondrial H<sub>2</sub>S oxidation in liver pathology.....</b>	<b>205</b>
Problematic.....	207
Results.....	207
1. Animal model of NAFL.....	207
1.1. HF/HS-diet challenge for 10 weeks.....	209
a) Body weight, glucose tolerance and insulin sensitivity.....	209
b) Liver mitochondrial H <sub>2</sub> S oxidation and respiration.....	209
c) Liver protein expression levels of key enzymes involved in H <sub>2</sub> S oxidation and biosynthesis.....	213
1.2. HF/HS-diet challenge for 20 weeks.....	213
a) Body weight, glucose tolerance and insulin sensitivity.....	213
b) Liver mitochondrial H <sub>2</sub> S oxidation and respiration.....	217
c) Liver protein expression levels of key enzymes involved in H <sub>2</sub> S oxidation and biosynthesis .....	219
d) Plasma and liver lipids.....	219
1.3. Impact of HF/HS diet and STS supplementation on gut microbiota.....	224
2. Animal model of NASH.....	224
2.1. Impact of MCD diet and STS supplementation on mouse phenotype.....	228
2.2. MCD diet increases liver mitochondrial H <sub>2</sub> S oxidation capacity.....	228
2.3. MCD diet and STS supplementation increase liver SQR expression.....	229
2.4. Impact of MCD diet and STS supplementation on plasma and liver lipids.....	235
2.5. MCD diet and STS supplementation have an impact on gut microbiota.....	235
3. Human obese patients.....	236
3.1. Characteristics of the patients.....	236
3.2. NAFL patients present lower SQR protein expression.....	236
Discussion.....	239
Conclusions.....	244
<b>IV. General discussion.....</b>	<b>247</b>
<b>V. Annexes.....</b>	<b>257</b>
<b>VI. Bibliography.....</b>	<b>273</b>

## List of illustrations

- Figure 1:** Biological pools of labile sulfide and factors involved in its release
- Figure 2:** Sources of H<sub>2</sub>S in the human body
- Figure 3:** Non-enzymatic production of H<sub>2</sub>S
- Figure 4:** Transsulfuration pathways
- Figure 5:** Protein structure and reactions catalysed by CBS
- Figure 6:** Reactions catalysed by CSE
- Figure 7:** Mitochondrial biosynthesis of H<sub>2</sub>S by the enzymes CAT/MPST or DAO/MPST
- Figure 8:** Mitochondrial oxidation of H<sub>2</sub>S in a mammalian cell
- Figure 9:** Stimulation of cellular respiration by H<sub>2</sub>S in various cell types
- Figure 10:** Biological effects of H<sub>2</sub>S
- Figure 11:** Protein thiol modifications mediated by either the incorporation of H<sub>2</sub>S (persulfidation), NO (nitrosylation) or GSH (glutathionylation)
- Figure 12:** H<sub>2</sub>S quantification in different tissues and using different methods
- Figure 13:** Different stages of Non-Alcoholic Fatty Liver Disease (NAFLD)
- Figure 14:** Worldwide prevalence of NAFLD in the general population (A) and among patients with T2DM (B)
- Figure 15:** Steatosis detection using ultrasounds, computed tomography and magnetic resonance imaging
- Figure 16:** Algorithm of Bedossa proposed for the diagnosis of NAFLD
- Figure 17:** Mechanisms behind Non-Alcoholic Fatty Liver Disease (NAFLD)
- Figure 18:** Synthesis and secretion of VLDL
- Figure 19:** Glycolysis (A), mitochondrial FA β-oxidation (B) and the Tricarboxylic Acid Cycle (C)
- Figure 20:** Structure and designation of fatty acids
- Figure 21:** Fatty acid metabolism
- Figure 22:** Microsomal and peroxisomal fatty acid oxidation
- Figure 23:** Intracellular accumulation of toxic metabolites
- Figure 24:** Participation of inflammation in the development of Non-Alcoholic Fatty Liver Disease (NAFLD)
- Figure 25:** Endoplasmic reticulum (ER)-associated stress and unfolding protein response (UPR)
- Figure 26:** “Multiple-hits” hypothesis
- Figure 27:** Intestinal dysbiosis in the development of Non-Alcoholic Fatty Liver Disease (NAFLD)

**Figure 28:** Hepatic regulation of glucose and lipid metabolism in a post-prandial (A) and fasting (B) state

**Figure 29:** H<sub>2</sub>S regulation of liver glucose metabolism

**Figure 30:** H<sub>2</sub>S regulation of liver lipid metabolism

**Figure 31:** Impacts of H<sub>2</sub>S on mitochondria

**Figure 32:** H<sub>2</sub>S as an antioxidant molecule

**Figure 33:** Studies demonstrating the protective role of H<sub>2</sub>S in Non-Alcoholic Fatty Liver Disease (NAFLD)

**Figure 34:** H<sub>2</sub>S and Non-Alcoholic Fatty Liver Disease (NAFLD)

**Figure 35:** Diagram of the different animal models and techniques used

**Figure 36:** O<sub>2</sub> consumption of isolated mitochondria was measured using an O2k oxygraph (Oroboros)

**Figure 37:** Protocol to assess mitochondrial H<sub>2</sub>S oxidation

**Figure 38:** Protocol to assess H<sub>2</sub>S oxidation capacity in isolated mitochondria

**Figure 39:** Impact of 10 weeks of HF/HS feeding on mouse body weight (A), liver weight (B), adipose tissue weight (C), glucose tolerance (D) and insulin sensitivity (E)

**Figure 40:** Impact of 10 weeks of HF/HS-feeding on liver mitochondrial H<sub>2</sub>S oxidation and respiration

**Figure 41:** Protein expression level of enzymes involved in H<sub>2</sub>S oxidation and biosynthesis

**Figure 42:** Impact of 20 weeks of HF/HS feeding plus or minus STS supplementation on mouse body weight (A), liver weight (B), adipose tissue weight (C), muscle weight (D), glucose tolerance (E) and insulin sensitivity (F)

**Figure 43:** Impact of 20 weeks of HF/HS feeding plus or minus STS supplementation on liver histology (A) and on different plasma parameters (B)

**Figure 44:** Impact of 20 weeks of HF/HS-feeding plus or minus STS supplementation on liver mitochondrial H<sub>2</sub>S oxidation and respiration

**Figure 45:** Protein expression level of enzymes involved in H<sub>2</sub>S oxidation and biosynthesis

**Figure 46:** Effect of HF/HS diet and STS supplementation on circulating lipids

**Figure 47:** Effect of HF/HS diet and STS supplementation on liver lipids

**Figure 48:** Effect of HF/HS diet and STS supplementation on gut microbiota diversity

**Figure 49:** Effect of HF/HS diet and STS supplementation on gut microbiota composition

**Figure 50:** Impact of MCD feeding and STS supplementation on liver histology (A), body weight (B), liver weight (C), adipose tissue weight (D), muscle weight (E) and on different plasma parameters (F)

**Figure 51:** Impact of MCD feeding and STS supplementation on liver mitochondrial H<sub>2</sub>S oxidation and respiration

**Figure 52:** Protein expression level of enzymes involved in H<sub>2</sub>S oxidation and biosynthesis

**Figure 53:** Effect of MCD diet and STS supplementation on circulating lipids

**Figure 54:** Effect of MCD diet and STS supplementation on liver lipids

**Figure 55:** Effect of MCD diet and STS supplementation on gut microbiota diversity

**Figure 56:** Effect of MCD diet and STS supplementation on gut microbiota composition

**Figure 57:** Protein expression level of enzymes involved in H<sub>2</sub>S oxidation and biosynthesis

**Table 1:** Human physiological responses to different concentrations of H<sub>2</sub>S

**Table 2:** Properties of the different gasotransmitters

**Table 3:** Classification of patients according to the NAFLD Activity Score (NAS) (A) and the different criteria that compose the classification system (B)

**Table 4:** Primers used for Real-time Quantitative PCR

**Table 5:** Primary antibodies used for Western blot

**Table 6:** Determination of V<sub>max</sub> and K<sub>m</sub> values for mitochondrial H<sub>2</sub>S oxidation in SD-, HF/HS-fed mice and HF/HS+STS mice

**Table 7:** Determination of V<sub>max</sub> and K<sub>m</sub> values for mitochondria H<sub>2</sub>S oxidation in SD-, MCD-fed mice and MCD+STS mice

**Table 8:** Characteristics of the human obese patients

**Table 9:** Summary of the main findings



## Abstract

Hydrogen sulfide (H<sub>2</sub>S) is the third gasotransmitter described in mammals. Colourless and water-soluble, H<sub>2</sub>S is a highly effective inhibitor of mitochondrial cytochrome c oxidase when present at high concentrations. However, when present at low concentrations, H<sub>2</sub>S can act as an inorganic energetic substrate for mammalian mitochondria. To oxidize H<sub>2</sub>S, mitochondria need the sulfide oxidizing unit (SOU), a set of three specific enzymes: sulfide quinone reductase (SQR), dioxygenase (ETHE1) and thiosulfate sulfurtransferase (TST). Liver metabolism, finely regulated by hormones and nutrients, is central to energy homeostasis, and liver metabolic inflexibility is known to be associated with several metabolic diseases, such as Non-Alcoholic Fatty Liver Disease (NAFLD). The unique position of this organ makes it likely to be exposed to high levels of H<sub>2</sub>S coming from both exogenous (gastrointestinal tract) and endogenous (metabolism of sulfur-containing amino acids) sources. Recently, impaired liver H<sub>2</sub>S biosynthesis has been reported in animal models of NAFLD, and in vivo supplementation of H<sub>2</sub>S donors prevented the further escalation of the illness into steatohepatitis (NASH). Almost all studies exploring the hepatic pathological relevance of H<sub>2</sub>S are usually focused on H<sub>2</sub>S biosynthesis pathway and/or using exogenous donors. As intrahepatic H<sub>2</sub>S levels can also be controlled by its mitochondrial oxidation, the objectives of my PhD were to investigate the pathophysiological importance of this pathway in liver metabolism and in the development of NAFLD.

First, we showed that, physiologically, the liver nutritional status regulates hepatic mitochondrial H<sub>2</sub>S oxidation capacity and SQR protein expression, both being downregulated by fasting while overnight refeeding abolished the fasting inhibitory effect. Adenovirus-mediated overexpression of human SQR in mouse liver clearly demonstrated that SQR is the key regulatory enzyme of mitochondrial H<sub>2</sub>S oxidation. Enhancing this pathway i) increased in vivo glucose tolerance and liver insulin signalling, ii) stimulated glucose metabolism in primary cultures of mouse hepatocytes (<sup>13</sup>C-glucose fluxomics), and iii) decreased liver fatty acid oxidation capacity. Second, when exploring the context of NAFLD, we observed that liver mitochondrial H<sub>2</sub>S oxidation capacity was downregulated in mice fed high fat/high sucrose (HF/HS) diet (NAFL model) and surprisingly was upregulated in mice fed methionine-choline deficient (MCD) diet (NASH model). In vivo supplementation with sodium thiosulfate (STS), an H<sub>2</sub>S donor, abrogated the inhibitory effect of HF/HS diet while it had no impact in the NASH model. Additionally, STS supplementation had no effect on body weight, glucose tolerance and insulin sensitivity in the NAFL model, and on liver steatosis in both NAFL and NASH models. However, STS supplementation did have an impact in the composition of gut microbiota. Similarly to the NAFLD mouse models, in morbid obese patients with simple steatosis (NAFL), liver SQR protein expression was found decreased, while in individuals with NASH SQR expression was found increased. Altogether, these studies, which confirmed that SQR is the key rate-limiting enzyme for liver mitochondrial H<sub>2</sub>S oxidation, clearly demonstrated for the first time that this pathway is finely regulated by the nutritional status of the liver and is altered in animal models of NAFLD and obese NAFLD patients. The novel observation that increasing hepatic mitochondrial H<sub>2</sub>S oxidation capacity increases hepatic glucose metabolism opens a new door in the field of liver pathophysiology, with this pathway being a potential protective target against the development of liver insulin resistance.

**Keywords:** Hydrogen sulfide, Mitochondria, Liver metabolism, Homeostasis, Non-Alcoholic Fatty Liver Disease





## Résumé

Le sulfure d'hydrogène ( $H_2S$ ) est le troisième gasotransmetteur décrit chez les mammifères, les deux autres étant NO et CO. Le  $H_2S$  est un inhibiteur de la cytochrome c oxydase mitochondriale lorsqu'il est présent à des concentrations élevées. Cependant, lorsqu'il est présent à de faibles concentrations, le  $H_2S$  peut agir comme un substrat énergétique inorganique pour les mitochondries de mammifères. Pour oxyder le  $H_2S$ , les mitochondries ont besoin de l'unité d'oxydation de sulfure (SOU), comprenant trois enzymes spécifiques: la sulfure quinone réductase (SQR), la dioxygénase (ETHE1) et la thiosulfate sulfurtransférase (TST). Le métabolisme hépatique, finement régulé par les hormones et les nutriments, est au cœur de l'homéostasie énergétique, et l'inflexibilité métabolique du foie est connue pour être associée à plusieurs maladies métaboliques, telles que la stéatose hépatique non alcoolique (NAFLD). La NAFLD englobe toutes les lésions hépatiques de la stéatose isolée à la stéatohépatite (NASH), qui peuvent évoluer vers la fibrose, la cirrhose et le carcinome hépatocellulaire. La NAFLD est fréquemment observée chez les sujets obèses. Elle est considérée comme la manifestation hépatique du syndrome métabolique, touchant 100% des sujets obèses atteints de diabète de type 2. Il est actuellement admis que le développement de la NASH résulte d'une sensibilité accrue du foie au stress oxydant et à l'inflammation. Cependant, les mécanismes responsables du développement de la NAFLD, et notamment de la NASH, chez les sujets obèses ne sont pas encore élucidés. La position unique du foie le rend susceptible d'être exposé à des niveaux élevés de  $H_2S$  provenant à la fois de sources exogène (tractus gastro-intestinal) et endogène (métabolisme des acides aminés soufrés). Récemment, une altération de la biosynthèse hépatique de  $H_2S$  a été rapportée dans des modèles animaux de NAFLD, et la supplémentation in vivo de donneurs de  $H_2S$  prévient l'évolution de la maladie vers la NASH. Presque toutes les études explorant la pertinence pathologique du  $H_2S$  dans le foie sont axées sur la voie de biosynthèse du  $H_2S$  et/ou utilisent des donneurs exogènes de  $H_2S$ . Comme le contenu intrahépatique en  $H_2S$  peut aussi être contrôlé par son oxydation mitochondriale, les objectifs de ma thèse étaient d'étudier : i) si l'oxydation mitochondriale du  $H_2S$  dans le foie de souris est régulée dans différentes situations nutritionnelles, ii) si l'oxydation mitochondriale hépatique du  $H_2S$  est régulée dans des modèles murins de NAFLD et chez des patients obèses, et iii) les effets physiopathologiques de la modulation du métabolisme du  $H_2S$  par une supplémentation in vivo de  $H_2S$  et une surexpression hépatique de la SQR.

Au fil des ans, plusieurs études ont démontré que le  $H_2S$  joue un rôle régulateur dans le métabolisme hépatique du glucose, le  $H_2S$  favorisant la gluconéogenèse et inhibant l'utilisation du glucose. Premièrement, nous avons montré que, physiologiquement, l'état nutritionnel du foie régule sa capacité mitochondriale à oxyder le  $H_2S$  et l'expression de la protéine SQR, tous deux étant diminués par le jeûne (caractérisé par une gluconéogenèse accrue) tandis que la réalimentation (caractérisée par une utilisation accrue du glucose) abolit l'effet inhibiteur du jeûne. La surexpression, par approche adénovirale, de la SQR humaine dans le foie de souris démontre clairement que la SQR est l'enzyme régulatrice clé de l'oxydation mitochondriale du  $H_2S$ , cette surexpression augmentant de 500% l'oxydation hépatique du  $H_2S$ . La surexpression de SQR i) augmente in vivo la tolérance au glucose et la signalisation hépatique de l'insuline, ii) stimule le métabolisme du glucose dans des cultures primaires d'hépatocytes de souris (13C-glucose, fluoxomique), et iii) diminue l'oxydation hépatique des acides gras. Fait intéressant, les souris surexprimant dans le foie la SQR présentent une oxydation hépatique du  $H_2S$  qui n'est plus diminuée par le jeûne, et ont à jeun une signalisation hépatique de l'insuline et une glycémie augmentées. Ces résultats originaux indiquent que non seulement la biosynthèse du  $H_2S$  mais aussi l'oxydation mitochondriale du  $H_2S$  joue un rôle important dans la physiologie du foie. Ceci

représente un nouveau mécanisme de régulation du métabolisme hépatique jusqu'alors ignoré. Ainsi, ces études révèlent que la SQR peut moduler la tolérance au glucose et la signalisation hépatique de l'insuline avec le potentiel d'être une cible contre le développement de la résistance hépatique à l'insuline. Des expériences complémentaires seront nécessaires pour étudier la capacité gluconéogénique des hépatocytes de souris surexprimant SQR. Deuxièmement, les résultats obtenus lors de ma thèse montrent pour la première fois que l'oxydation hépatique mitochondriale du H<sub>2</sub>S est régulée différemment selon le stade de développement de la NAFLD. Dans un contexte d'obésité associée à une stéatose hépatique (modèle NAFL), la capacité mitochondriale du foie à oxyder le H<sub>2</sub>S était diminuée chez les souris nourries avec un régime riche en lipides et en sucrose (HF/HS) et était en revanche augmentée chez les souris nourries avec régime déficient en méthionine-choline (MCD) (modèle NASH). La supplémentation in vivo avec du thiosulfate de sodium (STS), un donneur de H<sub>2</sub>S, abolit l'effet négatif du régime HF/HS sur l'oxydation hépatique du H<sub>2</sub>S alors qu'elle n'a aucun impact dans le modèle NASH. Notre étude montre également que l'administration de STS à des souris HF/HS ne permet pas de contrecarrer la stéatose hépatique, l'intolérance au glucose et l'hypercholestérolémie induites par le régime HF/HS. De même, l'administration de STS à des souris MCD ne diminue pas la stéatose, la fibrose et l'inflammation hépatiques induites par le régime MCD. Cependant, la supplémentation en STS abolit l'augmentation des lipides circulants induite par le régime HF/HS. Cet effet semble être associé à une plus grande accumulation de lipides dans le tissu adipeux des souris HF/HS+STS en comparaison des souris HF/HS. Néanmoins, dans leur ensemble, nos résultats ne reproduisent pas les effets bénéfiques de donneurs de H<sub>2</sub>S précédemment rapportés dans la littérature dans des modèles animaux de NAFLD. Une hypothèse serait que ces études utilisent l'hydrosulfure de sodium (NaHS) ou le sulfure de sodium (Na<sub>2</sub>S) comme donneur de sulfure alors que l'utilisation du STS en tant que donneur de H<sub>2</sub>S dans le cadre de la physiopathologie hépatique et de la signalisation cellulaire est toute récente. A souligner cependant que la supplémentation en STS modifie la composition du microbiote intestinal des souris HF/HS et MCD. L'augmentation de *Bifidobacterium* chez les souris HF/HS+STS est tout particulièrement intéressante car plusieurs études ont proposé *Bifidobacterium* comme probiotique et agent anti-inflammatoire dans le traitement de la NAFLD. En effet, nos résultats ont montré que ces souris HF/HS+STS présentaient une tendance à avoir des niveaux hépatiques d'ARNm plus faibles de Toll-like receptor 4 (TLR4) et d'interleukine-1 $\beta$  (IL-1 $\beta$ ), marqueurs classiques d'inflammation. Dans tous les cas, nos souris HF/HS ne présentaient pas deux caractéristiques phénotypiques classiques attendus : une stéatose hépatique importante et une résistance à l'insuline. L'explication la plus logique pour nous était l'existence d'un régime alimentaire douteux. En effet, dans une première série d'alimentation diététique HF/HS (dans la même animalerie), les souris nourries HF/HS présentaient à la fois une intolérance au glucose et une résistance à l'insuline. Cependant, étant donné que les souris nourries par HF/HS de cette première série ont également montré une diminution de l'oxydation mitochondriale H<sub>2</sub>S et une plus faible expression de la protéine SQR, nous avons conclu que les petits changements induits par HF/HS observés dans la deuxième série étaient suffisants pour déclencher un changement dans la voie. Néanmoins, les résultats concernant le modèle animal NAFL doivent être interprétés avec prudence. Nous avons également associé l'augmentation de la population de *Bifidobacterium* chez les souris alimentées par HF/HS et supplémentées avec STS à la diminution des taux de lipides circulatoires.

Même si nos souris HF/HS ne présentaient pas deux caractéristiques phénotypiques classiques attendus (stéatose hépatique importante et résistance à l'insuline), les altérations observées de la capacité hépatique à oxyder le H<sub>2</sub>S dans ces modèles apparaissent en accord avec nos résultats obtenus dans des biopsies de foie de patients obèses. En effet, les patients obèses ayant une stéatose hépatique simple présentaient une diminution de l'expression hépatique de la

protéine SQR par rapport aux patients obèses sans NAFLD, suggérant une capacité mitochondriale hépatique plus faible à oxyder le H<sub>2</sub>S. Inversement, les patients obèses ayant une NASH avaient une expression hépatique de la protéine SQR plus élevée que les patients obèses NAFL, l'expression protéique étant similaire à celle mesurée chez les patients obèses sans NAFLD.

Alors qu'un nombre croissant de rôles de signalisation et d'effets physiologiques sont attribués au H<sub>2</sub>S, notre compréhension de la voie d'oxydation mitochondriale du H<sub>2</sub>S et de ses conséquences sur le métabolisme hépatique et l'homéostasie énergétique n'en est qu'à ses débuts. L'ensemble de mes résultats, qui confirme que la SQR est l'enzyme clé limitante de l'oxydation hépatique mitochondriale du H<sub>2</sub>S, démontre clairement pour la première fois que cette voie est finement régulée par l'état nutritionnel et est altérée dans des modèles animaux de NAFLD et chez des patients obèses NAFLD. Cependant, dans le contexte de la NAFLD, les implications de nos résultats restent ouvertes à l'interprétation, car il est, à ce stade, difficile de déchiffrer si les changements dans l'expression hépatique de la protéine SQR sont un mécanisme causal ou une réponse adaptative aux effets des régimes HF/HS et MCD. La démonstration qu'une augmentation de la capacité mitochondriale du foie à oxyder le H<sub>2</sub>S augmente le métabolisme hépatique du glucose ouvre de nouvelles perspectives en physiopathologie hépatique, cette voie étant une cible potentielle pour lutter contre le développement de la résistance hépatique à l'insuline. Ce travail souligne également que toutes les études précédentes liant les perturbations cellulaires aux dérèglements de la biosynthèse du H<sub>2</sub>S ont ignoré un acteur majeur de la régulation cellulaire centrée sur le H<sub>2</sub>S, à savoir l'oxydation du H<sub>2</sub>S médiée par la SQR. Bien que la production et l'oxydation de H<sub>2</sub>S soient toutes deux importantes pour maintenir les niveaux de H<sub>2</sub>S à l'état d'équilibre, la façon dont ces voies contrôlent les actions de H<sub>2</sub>S dans une cellule peut varier. La production de H<sub>2</sub>S aurait un impact sur sa capacité à modifier les résidus de cystéine et à réguler l'expression et l'activité des protéines, tandis que l'oxydation de H<sub>2</sub>S participerait à la respiration mitochondriale, contrôlant les niveaux d'O<sub>2</sub> ainsi que la production de espèces réactives de l'oxygène (ROS) et espèces soufrées réactives (RSS). Ainsi, il devient impératif d'explorer l'oxydation mitochondriale du H<sub>2</sub>S dans les études évaluant les effets d'une dérégulation du métabolisme du H<sub>2</sub>S dans des scénarios pathologiques, d'autant plus que nos résultats suggèrent que l'oxydation et la biosynthèse de H<sub>2</sub>S sont étroitement interconnectées. De plus, l'observation que des modifications de l'oxydation mitochondriale hépatique du H<sub>2</sub>S seraient associées à des changements du microbiote intestinal soulève la question de savoir si cette voie pourrait également être affectée par des changements intestinaux induits par l'alimentation. Une telle observation pourrait avoir des implications directes sur notre vie quotidienne, puisque les habitudes alimentaires occidentalisées sont remplies d'additifs alimentaires et de conservateurs, dont certains sont à base de soufre. En conclusion, étant donné la prévalence élevée des maladies métaboliques, l'oxydation mitochondriale du H<sub>2</sub>S pourrait être considérée comme une cible thérapeutique potentielle à l'avenir.

**Mots-clés:** Sulfure d'hydrogène , Mitochondrie , Métabolisme hépatique , Homéostasie , Stéatose hépatique non alcoolique



# Abbreviations

**3-MP:** 3-mercaptopyruvate  
**4-HNE:** 4-hydroxynonenal  
**ACC:** acetyl CoA carboxylase  
**ACS:** acyl-CoA synthetase  
**AE1:** anion exchange protein  
**AFL:** alcoholic fatty liver  
**Akt:** protein kinase B  
**ALT:** alanine aminotransferase  
**AMPK:** 5' adenosine monophosphate-activated protein kinase  
**ApoB:** apolipoprotein B  
**ARF-1:** ADP-ribosylation factor 1  
**AST:** aspartate aminotransferase  
**ATF4:** activating transcription factor 4  
**ATP:** adenosine triphosphate  
**ATPase:** ATP synthase  
**Bcl-2:** B-cell lymphoma 2  
**BMI:** body mass index  
**C/EBP $\alpha$ :** CCAAT/enhancer binding protein alpha  
**CACT:** carnitine acylcarnitine translocase  
**cAMP:** cyclic adenosine monophosphate  
**CAT:** cysteine aminotransferase  
**CBS:** cystathionine  $\beta$ -synthase  
**CD/AA:** choline deficient amino acid specific diet  
**ChREBP:** carbohydrate-responsive element-binding protein  
**CO:** carbon monoxide  
**CPT:** carnitine palmitoyltransferase  
**CSE:** cystathionine  $\gamma$ -lyase  
**CVD:** cardiovascular diseases  
**CYP2E1:** cytochrome P450 Family 2 Subfamily E Member 1  
**DAG:** diacylglycerols  
**DAO:** D-aminoacid oxidase

**DHLA:** dihydrolipoic acid  
**DNL:** *de novo* lipogenesis  
**DTT:** dithiothreitol  
**ECM:** extracellular matrix  
**EE:** ethylmalonic encephalopathy  
**ER:** endoplasmic reticulum  
**ERK1/2:** extracellular signal-regulated protein kinase  
**ETC:** electron transport chain  
**ETHE1 :** ethylmalonic encephalopathy protein 1  
**FAD:** flavin adenine dinucleotide  
**FAS:** fatty acid synthase  
**FBPase:** fructose-1,6-bisphosphatase  
**FCSD:** flavocytochrome c sulfide dehydrogenase  
**FDA:** Food and Drug Administration  
**FFA:** free fatty acid  
**FXR:** farnesoid-X activated receptor  
**G6Pase:** glucose-6-phosphatase  
**GABA:** gamma-amino butyric acid  
**GAPDH:** glyceraldehyde 3-phosphate dehydrogenase  
**GC:** gas chromatography  
**GGT:** gamma-glutamyltransferase  
**GLP-1:** glucagon like peptide-1  
**GPx:** glutathione peroxidase  
**GSH:** glutathione  
**GSSG:** glutathione persulfide  
**GST:** glutathione-s-transferase  
**GGY4137:** morpholin-4-ium 4 methoxyphenyl(morpholino) phosphinodithioate  
**H<sub>2</sub>O<sub>2</sub>:** hydrogen peroxide  
**H<sub>2</sub>S:** hydrogen sulfide  
**HbCO:** carboxyhemoglobin  
**HCC:** hepatocellular carcinoma  
**HDL:** high-density lipoprotein  
**HF/HS:** high fat/high sugar diet

**HFD:** high fat diet  
**HO-1:** heme oxygenase-1  
**HPLC:** high performance liquid chromatography  
**HSCs:** hepatic stellate cells  
**IBD:** inflammatory bowel diseases  
**ICAM-1:** intracellular adhesion molecule-1  
**IL-1 $\beta$ :** interleukin 1- $\beta$   
**IL-6 :** interleukin 6  
**IMM :** inner mitochondrial membrane  
**IP :** intraperitoneal  
**IR :** insulin resistance  
**ITT:** insulin tolerance test  
**IV:** intravenous  
**JNK:** c-Jun terminal kinase  
**K<sub>ATP</sub>:** ATP-sensitive potassium channel  
**KD:** knock-down  
**KO:** knock-out  
**LCFA:** long chain fatty acid  
**LC-MS/MS:** liquid chromatography with tandem mass spectrometry  
**LDH:** lactate dehydrogenase  
**LXR:** liver X receptor  
**MAPK:** p38 mitogen-activated protein kinase  
**MB:** methylene blue method  
**MBB:** monobromobimane derivatization  
**MCD:** methionine-choline deficient diet  
**MCFA:** medium chain Fatty acid  
**MDA:** malondialdehyde  
**mFAO:** microsomal Fatty acid oxidation  
**miRNA:** micro RNA  
**MPST:** mercaptopyruvate sulfurtransferase  
**MPTP:** mitochondrial permeability transition pore  
**MS:** metabolic syndrome  
**mtDNA:** mitochondrial DNA

**mtFAO:** mitochondrial fatty acid oxidation

**Na<sub>2</sub>S:** sodium sulfide

**NADH:** nicotinamide adenine dinucleotide

**NADPH:** nicotinamide adenine dinucleotide phosphate

**NAFL:** non-alcoholic fatty liver

**NAFLD:** non-alcoholic fatty liver disease

**NaHS:** sodium hydrosulfide

**NAS:** NAFLD activity score

**NASH:** non-alcoholic steatohepatitis

**NF-κB:** nuclear factor-kappa B

**NH<sub>3</sub>:** ammonia

**NMDA:** N-methyl D-aspartate

**NO:** nitric oxide

**NOS:** nitric oxide synthase

**Nrf2:** nuclear receptor factor 2

**O<sub>2</sub><sup>-</sup>:** superoxide

**OGTT:** oral glucose tolerance test

**OMM:** outer mitochondrial membrane

**ONOO<sup>-</sup>:** peroxynitrite

**p21:** cyclin-dependent kinase inhibitor 1

**PAG:** propargylglycine

**PC:** pyruvate carboxylase

**PEPCK:** phosphoenolpyruvate carboxykinase

**pFAO:** peroxisomal fatty acid oxidation

**PGC-1α:** peroxisome proliferator-activated receptor gamma coactivator 1-alpha

**PKA:** protein kinase A

**PLP:** pyridoxal-phosphate

**PNPLA3:** patatin-like phospholipase domain-containing protein 3

**PPARα:** peroxisome proliferator-activated receptor alpha

**Ppm:** parts per million

**PPRC1:** peroxisome proliferator-activated receptor-γ coactivator-related protein 1

**ROS:** reactive oxygen species

**RSS:** reactive sulfur species



**SAM:** S-adenosylmethionine  
**SAT:** subcutaneous adipose tissue  
**SCD1:** stearyl-CoA desaturase-1  
**SCFA:** short-chain fatty acid  
**SdB:** sulfide dibimane  
**-SH:** thiol  
**siRNA:** small interfering RNA  
**SIRT1:** sirtuin 1  
**SMA:** smooth muscle actin  
**SNP:** sodium nitroprusside  
**SOD:** superoxide dismutase  
**SQR:** sulfide quinone oxireductase  
**SRB:** sulfur reducing bacteria  
**SREBP-1c:** sterol regulatory element-binding protein 1  
**-SSH:** persulfide  
**STS:** sodium thiosulfate  
**SUOX:** sulfite oxidase  
**T2DM:** type 2 diabetes mellitus  
**TCA:** tricarboxylic acid cycle  
**TG:** triglyceride  
**TLR4:** toll-like receptor 4  
**TM6SF2:** transmembrane 6 superfamily member 2  
**TMT:** thiol s-methyltransferase  
**TNF $\alpha$ :** tumor necrosis factor alpha  
**tRNA:** transfer RNA  
**TST:** thiosulfate sulfurtransferase  
**UC:** ulcerative colitis  
**UPR:** unfolding protein response  
**VAT:** visceral adipose tissue  
**VLCFA:** very-long chain fatty acid  
**VLDL:** very-low density lipoprotein



## Publications

- **“Hydrogen sulfide oxidation via mitochondrial SQR impacts liver glucose metabolism”**  
**Inês Mateus**, Sara Guerra\*, Véronique Lenoir\*, Fabrizia Carli, Renaud Dentin, Frédéric Bouillaud, Amalia Gastaldelli, Carina Prip-Buus#  
Article. To be submitted to *Antioxidants and Redox Signalling* (in preparation)
- **“H<sub>2</sub>S, liver metabolism and NAFLD: what lies beyond the stink?”**  
**Inês Mateus** and Carina Prip-Buus  
Review. Part of the special issue **“Foie Gras: Bioenergetic Remodelling in the Pathophysiology and Treatment of Non-Alcoholic Fatty Liver Disease (NAFLD)”**. *European Journal of Clinical Investigation* (in preparation; not included in the PhD manuscript)
- **“Dietary supplementation of Sodium Thiosulfate alters gut microbiota and increases mitochondrial hydrogen sulfide oxidation in mice fed high fat/high sucrose diet”**  
**Inês Mateus**, Sara Guerra, Véronique Lenoir, Fabrizia Carli, Frédéric Bouillaud, Amalia Gastaldelli, Benoit Chassaing, Carina Prip-Buus\*  
Article. (in preparation; not included in the PhD manuscript)

## Posters and oral communications

### Posters:

- **Colloque MeetOchondrie (May 27<sup>th</sup> to May 30<sup>th</sup> 2018, Pornichet, France)**  
“Impact of starvation on mitochondrial hydrogen sulfide oxidation in mouse liver”
- **MitoPorto (July 13<sup>th</sup> 2018, Porto, Portugal)**  
“Impact of starvation on mitochondrial hydrogen sulfide oxidation in mouse liver”
- **Spetses Summer School (August 25<sup>th</sup> to August 31<sup>st</sup> 2018, Spetses, Greece)**  
“Impact of starvation on mitochondrial hydrogen sulfide oxidation in mouse liver”
- **The International Liver Congress - EASL (April 10<sup>th</sup> to April 14<sup>th</sup> 2019, Vienna, Austria)**  
“Liver mitochondrial hydrogen sulfide oxidation: from nutritional physiology to Non-Alcoholic Fatty Liver pathology”

### Oral communications:

- **53<sup>rd</sup> Annual Scientific Meeting of the European Society for Clinical Investigation (May 22<sup>nd</sup> to May 25<sup>th</sup> 2019, Coimbra, Portugal)**  
“The scope of liver mitochondrial hydrogen sulfide oxidation: from nutritional physiology to Non-Alcoholic Fatty Liver pathology”
- **PhD annual days (February 24<sup>th</sup> and 25<sup>th</sup> 2020, Paris, France)**  
“Mitochondrial H<sub>2</sub>S oxidation in liver pathophysiology”  
*Won an award for 2<sup>nd</sup> best presentation*

## Secondments

- Secondment 1:  
Laboratory: **Helmholtz Zentrum München (Munich, Germany)**  
Mentor: **Prof. Dr. Hans Zischka**  
Duration: **May 14<sup>th</sup> 2017 - May 18<sup>th</sup> 2017 (1 week); October 28<sup>th</sup> 2017 - January 31<sup>st</sup> 2018 (3 months and 1 week)**
- Secondment 2:  
Laboratory: **Faculty of Pharmacy of the University of Lisbon (Lisbon, Portugal)**  
Mentor: **Prof. Dr. Cecília Rodrigues**  
Duration: **September 30<sup>th</sup> 2019 - January 24<sup>th</sup> 2020 (~4 months)**

## Complementary training

### Formations within the Doctoral School and Institute:

- Animal experimentation: **“Regulatory Course for project designers (rodents & lagomorphs) – designer level” (50h);**
- Lessons of French: intermediary level (30h);
- Chairman during the PhDs days of 2020 (3h).

#### **Formations within the Foie Gras consortium:**

- 1<sup>st</sup> FOIE GRAS Networking School: **“Tools and Rationale for measuring mitochondrial function in intact cells and isolated mitochondria”** – 18<sup>th</sup>-23<sup>th</sup> September 2017, Coimbra, Portugal (3h);
- 2<sup>nd</sup> FOIE GRAS Networking School: **“Tools for the study of Gut-Liver crosstalk and energy fluxes in NAFLD”** – 3<sup>rd</sup>-5<sup>th</sup> July 2018, Pisa, Italy (3h);
- 3<sup>rd</sup> FOIE GRAS Networking School: **“Biomarkers for NAFLD staging, prognosis and treatment”** – 10<sup>th</sup>-12<sup>th</sup> July 2019, Lisbon, Portugal (3h);
- 4<sup>th</sup> FOIE GRAS Networking School: **“NAFLD: modulation by lifestyles and therapies”** – May 26<sup>th</sup>, online (3h);
- Short course on public communication given by Dr. Marisa Azul from the Center for Neuroscience and Cell Biology (Coimbra, Portugal) – 12<sup>th</sup>-13<sup>th</sup> July 2018, Coimbra, Portugal (18h).



# ***I. Introduction***

---





## I. Introduction

### 1. Hydrogen sulfide: a double-edged sword

#### 1.1. In the beginning...

The role of hydrogen sulfide ( $H_2S$ ) in the development of life as we know it dates back millions of years to a time when the outlook of earth was very grim. In the late Permian Period (250 million years ago), the single most devastating extinction event of all time was under way [1]. Something that nearly brought life on Earth to an end. Among several theories hypothesized as causes to this massive destruction, scientists have long believed that large-scale volcanic eruptions in the Siberian Traps could be behind it [1]. Surely Siberian volcanoes did not wipe out thousands of biological creatures by swamping the world with lava. Instead, as volcanic gases like carbon dioxide and methane poured into the skies, a global warming effect would have taken place rapidly [1]. As the oceans became warmer, their capacity to absorb oxygen grew dimmer. Although this would be incredibly suffocating for oxygen-breathing species, anaerobic organisms would have thrived under such conditions. According to biomarkers found in oceanic sediments from the latest part of the Permian, an ocean-wide upsurge of  $H_2S$ -consuming bacteria took place around that time, which would have caused a widespread anoxia (severe deficiency of oxygen) [2]. Geoscientists Lee R. Kump and Michael A. Arthur have shown that oxygen levels decreased so much in the oceans that the anoxic condition favoured the proliferation of deep-sea anaerobic bacteria in upper layers of the oceans [3]. In fact, these microbes were found in extremely shallow marine strata, which is itself a marker indicating that even the surface of the oceans at the end of the Permian was oxygen-free but  $H_2S$ -rich [2]. This would have caused a large-scale euxinia (production of  $H_2S$ ) throughout the world, which would have resulted in horrific bubbles of toxic  $H_2S$  gas diffusing from the oceans into the air, obliterating Flora and Fauna on land. By the end of the Permian extinction, 90% of marine species and 70% of terrestrial ones had vanished [1].

If we take these events into account, the organisms that sustained that catastrophe and survived were the ones able to tolerate and, in some cases, even consume  $H_2S$ . In fact, until this day several organisms are known to dwell in  $H_2S$ -rich environments due to the ecological opportunities they offer. After all,  $H_2S$  is the “sun-light of the deep ocean”. This is the case of several types of seashells and sea worms, which take advantage of the harsh conditions to increase their resource availability and reduce not only competition but also potential enemies [4]. Perhaps mankind’s affinity for this gas may well be a remnant from those primordial times.

Concentration (ppm)	Concentration (mg/m <sup>3</sup> )	Expected effects/Symptoms
0.00011-0.00033	0.000165-0.000495	Typical background concentrations
0.003 – 0.02	0.0045-0.03	Odor threshold
20-30	30-45	Strong offensive odor (“rotten eggs”)
30	45	Sickening sweet odor
50	75	Conjunctivital irritation
50-100	75-150	Irritation of respiratory tract
100-200	150-300	Loss of smell (olfactory fatigue)
150-200	225-300	Olfactory paralysis
250-500	375-750	Pulmonary edema
500	750	Anxiety, headache, ataxia, dizziness, amnesia, unconsciousness
500-1000	750-1500	Respiratory paralysis, immediate collapse, neural paralysis, cardiac arrhythmias, death

*Adapted from Rubright et al. 2017 [6]*




**Table 1: Human physiological responses to different concentrations of H<sub>2</sub>S**

**ppm:** parts per million

## 1.2. Environmental pollutant

Modern evidence of H<sub>2</sub>S as an environmental toxin dates back to the 18<sup>th</sup> century. Carl Wilhelm Scheele in 1775 managed to isolate H<sub>2</sub>S by treating pyrite (ferrous sulfide) with a mineral acid. C.W. Scheele immediately noticed the release of a stinking gas, which he called “Schwefelluft” (sulfur air) [5]. Over the following two hundred years, the toxicological properties of this gas, now referred to as H<sub>2</sub>S, would be thoroughly investigated [5]. Easily recognizable by its characteristic scent of rotten eggs, H<sub>2</sub>S is considered an environmental pollutant and its toxic effects on humans have been thoroughly characterized. H<sub>2</sub>S constitutes the number-one occupational hazard at oil and gas field wellheads, pipelines, processing plants and refineries [5]. Human beings can smell H<sub>2</sub>S in the air from concentrations above 0.0047 part per million (ppm). At 500 ppm consciousness is lost and a 5-minute exposure to concentrations above this threshold result in death (**Table 1**) [6]. This increasing toxicity has depicted H<sub>2</sub>S as a potential chemical weapon, which was actually put to use by the British Armed Forces during World War I [7]. Several disasters throughout the years have constantly reminded mankind of how incredibly poisonous H<sub>2</sub>S can be. Sudden release of huge amounts of this gas from oil wells or refineries leads to infamous “knock-down” phenomenon of oilers and other petrochemical workers, an instant loss of consciousness often associated with respiratory failure. Quite recently, in February 2020, 14 workers and hundreds of nearby residents of a main port in the city of Karachi (Pakistan) died or fell sick from apparent poisoning [8]. The Environmental Protection Agency of the area blamed the massive H<sub>2</sub>S gas emissions from the oil installation at the port [8].

However, despite numerous evidence showing physiological impairment in cases of H<sub>2</sub>S-prolonged exposure, one particular discovery has generated a lot of attention towards the potential duality of this gas. In 2005, Roth *et al.* reported that “H<sub>2</sub>S induces a suspended animation-like state in mice” [9]. In their study, mice placed in atmospheres of 20-80 ppm (30-120 mg/m<sup>3</sup>) of H<sub>2</sub>S exhibited dose-dependent reductions in core body temperature and metabolic rate. Over the course of several hours, the metabolic rate of the animals went down to 10% and when the chamber where the animals were kept was cooled down, their body temperature reached 15°C. These effects were found completely reversible upon resuscitation at room air and warming of the chamber [9]. H<sub>2</sub>S toxicity to mammals is quite evident, and yet several species present pathways of H<sub>2</sub>S biosynthesis, humans among these. Over the last century, nearly 20 000 papers related to “Hydrogen sulfide” were published but few of those examined the physiological importance or even beneficial role of this gas. It was only from the 21st century that a true biological role was granted to H<sub>2</sub>S: the role of gasotransmitter.

	 H <sub>2</sub> S	 CO	 NO
<b>Main substrate</b>	Cysteine	Heme	Arginine
<b>Generating enzymes</b>	CBS, CSE	Heme oxygenases	NO synthases
<b>Scavengers</b>	Hemoglobin	Hemoglobin	Hemoglobin
<b>Inducers</b>	NO	Free radicals	Acetylcholine, endotoxin
<b>Course of action</b>	K <sub>ATP</sub> channel, cAMP	K <sub>Ca</sub> channel, cGMP	K <sub>Ca</sub> channel, cGMP
<b>Half-life in solution</b>	Minutes	Minutes	Seconds

*Adapted from Wang 2002 [11]*

**Table 2: Properties of the different gasotransmitters**

**CBS:** cystathionine  $\beta$ -synthase; **CSE:** cystathionine  $\gamma$ -lyase; **K<sub>ATP</sub> channel:** ATP-sensitive potassium channel; **K<sub>Ca</sub> channel:** calcium-sensitive potassium channel; **cGMP:** cyclic guanosine monophosphate

## 1.3. Gasotransmitter

### 1.3.1. Definition

Advances in cellular studies have split the classification of signalling molecules into two major categories according to their completely unique profiles: neurotransmitters and gasotransmitters [10]. The first category includes all molecules synthesized by neurons whose release requires exocytotic vesicles and whose actions are dependent of membrane receptors. Classified as neurotransmitters are a handful of low molecular weight endogenous substances, such as acetylcholine, catecholamines, serotonin, histamine, glutamate, glycine, gamma-Amino Butyric Acid (GABA) and adenosine triphosphate (ATP) or its metabolites [10]. Concerning the second category, in 2002, Dr. Rui Wang defined a series of specific criteria which molecules should absolutely meet in order to be classified as gasotransmitters [11]. This class of signalling molecules is far less extent than that of neurotransmitters, and, to this day, only three molecules are known to compose it: nitric oxide (NO), carbon monoxide (CO) and H<sub>2</sub>S. The criteria that allow a molecule to be defined as a gasotransmitter are the following:

- a. To be a gas, capable of moving freely across membranes without the use of transporters.
- b. To be endogenously and enzymatically generated, and to have its synthesis regulated.
- c. To have well-defined specific functions at physiologically relevant concentrations.
- d. To act upon specific cellular and molecular targets with or without the aid of second messengers.

### 1.3.2. Discovery

Despite the common traits that recognize all three as members of the same family, NO, CO and H<sub>2</sub>S differ in their production, course of action and durability (**Table 2**) [11].

**NO** was the first molecule to enter the class of gasotransmitters [12]. Originally dubbed as “endothelium-derived relaxing factor” or “EDRF” by Dr. Robert Furchgott, NO is known to be used by the endothelium of blood vessels to signal the surrounding smooth muscle to relax, thus prompting vasodilation and increasing blood flow [12, 13]. Unlike CO and H<sub>2</sub>S, the effects of NO as mediator of biological functions were known even before its endogenous synthesis was described.

The second molecule to be proposed as gasotransmitter was **CO** back in 1993 by the team of Dr. Snyder [14]. CO has its strongest function in the neuronal system where it regulates the

release of neurotransmitters and neuropeptides and intervenes in the acquisition and retention of learning skills and memories [15]. Aside its role in the central nervous system, CO has also been described as an important vasorelaxant and cardiac protector in cases of ischemia-reperfusion injury [16].

The first time **H<sub>2</sub>S** was proposed as the third gasotransmitter dates back to 1996, when the group of Dr. Kimura described in first-hand the endogenous production of the gas in the central nervous system [17]. However, it was not until 2001 that the participation of H<sub>2</sub>S in an actual physiological situation – cardio vasorelaxation - was described [18]. The *in vitro* incubation of rat aortic tissues with H<sub>2</sub>S was able to induce tissue-relaxation through the modulation of ATP-sensitive potassium channels (K<sub>ATP</sub> channels) without the need of a second messenger.

### 1.3.3. Crosstalk

All three gasotransmitters share the same beginning, in that they were initially regarded by the scientific community as toxic and poisonous molecules. Eventually, evidence showed that all life forms, from bacteria to large mammals, are equipped with specific pathways to synthesize or detoxify CO, NO and H<sub>2</sub>S in order to keep their concentration at a level that allows these molecules to accomplish specific cellular functions [11, 19]. Although the precise mechanisms through which CO, NO and H<sub>2</sub>S divide their responsibilities are not fully understood, it has been established that all gasotransmitters work together, sharing a substantial number of pathophysiological functions and signalling transduction pathways [11, 18, 20].

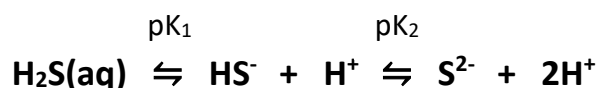
Given that all gasotransmitters show affinity (however to different extensions) for the hemoglobin sink, one single gasotransmitter can potentiate or mask the biological effect of another gasotransmitter. Evidence has shown that the use of sodium nitroprusside (SNP), a NO donor, can enhance the endogenous production of H<sub>2</sub>S in rat aortic tissues by increasing the expression level of cystathionine  $\gamma$ -lyase (CSE) [18]. On the other way around, preincubation of rat aortic tissues with sodium hydrosulfide (NaHS) significantly enhanced the vasorelaxant effect of SNP [20]. This type of interaction appears to also exist between CO and H<sub>2</sub>S. In rat aortic smooth muscle cells, the downregulation of the CO/HO pathway with zinc protoporphyrin increases CSE expression and H<sub>2</sub>S levels [21]. Furthermore, the use of NaHS decreased the expression of heme oxygenase-1 (HO-1) and the content of carboxyhemoglobin (HbCO) [21].

## 1.4. Characteristics of the H<sub>2</sub>S molecule

### 1.4.1. Physical and chemical properties

H<sub>2</sub>S is a colourless and flammable gas with an unmistakable scent of rotten eggs. It is the sulfur analogue of the water molecule (H<sub>2</sub>O) and it displays a higher vapor density (d) than air (1.19 against 1.0, respectively) [22]. The average half-life of H<sub>2</sub>S in the air is 25h but this time is influenced by temperature and so, in winter, the half-life of this gas can be prolonged up to 37h [23]. Despite the same covalent hydride structure, the sulfur (S) atom present in this molecule makes it less polar and more acidic than H<sub>2</sub>O. In fact, one of the reasons that led H<sub>2</sub>S to be considered a gasotransmitter was its hydrophobic nature, which allows it to easily penetrate the lipid bilayer of cell membranes, even those containing cholesterol and sphingomyelin [24]. Interesting fact regarding this matter, considering that intracellular pH is lower than extracellular pH, H<sub>2</sub>S privileges the extracellular flow, being quantitatively more exported than imported by a cell.

H<sub>2</sub>S is a weak acid and its dissociation comprises two sequential reactions in which two different dissociation constants (pK<sub>1</sub> and pK<sub>2</sub>) are involved, as shown in the acid-base equilibrium reaction:



The first reaction has a pK<sub>1</sub> of 6.98 or 6.76 at 25°C or 37°C, respectively, which in a solution of pH 7.4 allows H<sub>2</sub>S to exist in its diprotic form or as the hydrosulfide anion (HS<sup>-</sup>). The second reaction of dissociation in which HS<sup>-</sup> renders disulfide (S<sup>2-</sup>) has a pK<sub>2</sub> above 14. The exact constant value is not known due to contamination from polysulfides formed during the measurements. However, the most accepted value for pK<sub>2</sub> ranges between 18.5 and 19.2 [25, 26]. Given that pK<sub>2</sub> is much higher than 14, the concentration of S<sup>2-</sup> in biological tissues is virtually negligible. However, in solution, it is still sufficient to cause precipitation of metal sulfides [27].

In mammalian cells, HS<sup>-</sup> crosses membranes through an anion channel. This anion exchange protein (AE1) transports HS<sup>-</sup> in exchange for chloride (Cl<sup>-</sup>). Theoretical calculations by Mathai *et al.* indicate that the transport of HS<sup>-</sup> by AE1 is unlikely to occur under physiological conditions [24]. However, AE1 was found to transport HS<sup>-</sup> in exchange for Cl<sup>-</sup> in erythrocytes, which may act as a sink for H<sub>2</sub>S [28].

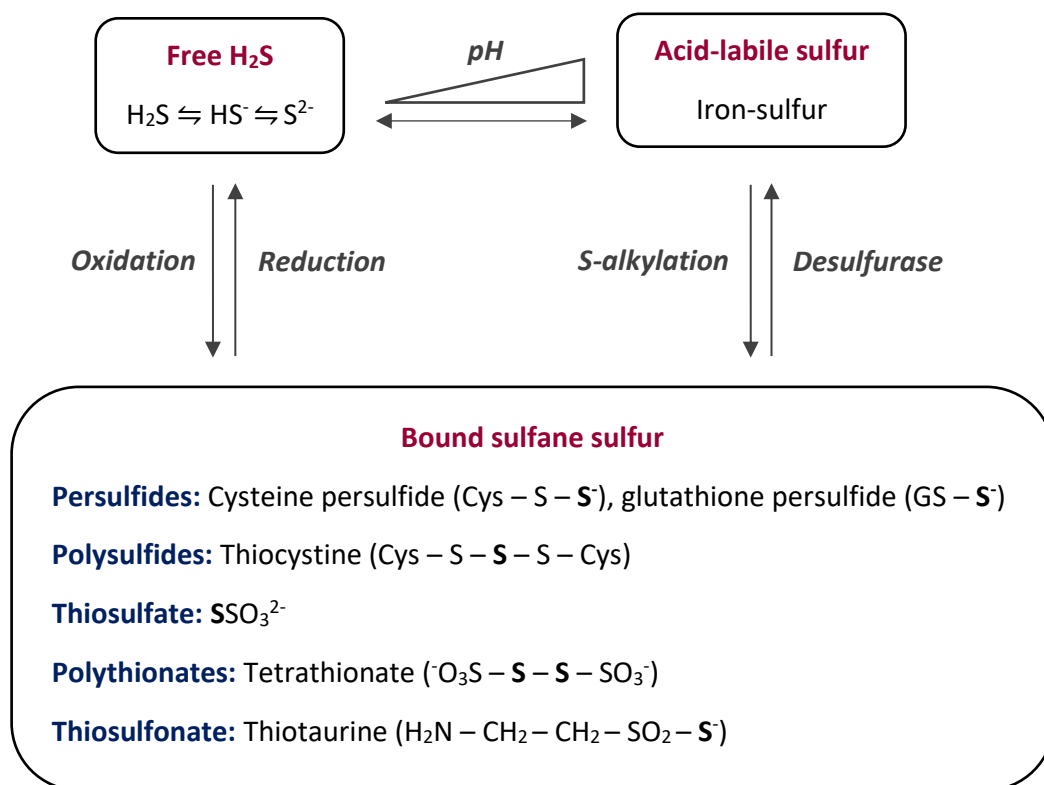


**Figure 1: Biological pools of labile sulfide and factors involved in its release**



At physiological pH and 37°C, H<sub>2</sub>S and HS<sup>-</sup> are in fast equilibrium, existing in approximately 20% and 80%, respectively. However, at 25°C, about 40% of all sulfide will be present as H<sub>2</sub>S [28]. It should be emphasised that H<sub>2</sub>S and HS<sup>-</sup> may both contribute directly to the biological action of hydrogen sulfide, and that HS<sup>-</sup> is a nucleophile, which readily binds to metal centres in biological molecules. The concentration of H<sub>2</sub>S in a given solution can be determined from its absorption at 230nm [29]. However, air oxidation and formation of polysulfides can interfere with this determination.

The proximity of pK<sub>1</sub> to the physiological pH becomes an advantage considering that we can replace the H<sub>2</sub>S gaseous form by a physical salt (sulfide donor), which is easier to manipulate. However, when using H<sub>2</sub>S donors, such as NaHS or sodium sulfide (Na<sub>2</sub>S), in chemical or biological studies it is necessary to consider that these species create strong alkaline solutions when dissolved in water, which makes the adjustment of the pH of the medium imperative [22]. It is also important to bear in mind that sulfide solutions are quite unstable at physiological pH, given that H<sub>2</sub>S tends to equilibrate between the liquid phase (ex: tissues) and the external atmosphere in which sulfide concentrations are extremely low. This particular aspect of gas evasion complicates experiments where solutions of H<sub>2</sub>S are manipulated. In fact, *in vivo*, this phenomenon of exhalation represents one way of biologically eliminate endogenous H<sub>2</sub>S.

Throughout this manuscript the words “H<sub>2</sub>S” or “sulfide” are used to collectively designate H<sub>2</sub>S and its ionized forms of HS<sup>-</sup> and S<sup>2-</sup>, acknowledging the equilibrium in which they exist in biological fluids. Indeed, all forms remain in a perfect acid-base balance so that if one form suddenly drains out, the other two will dissociate or protonate according to the pH of the medium and restore the lost balance.

#### 1.4.2. Intracellular H<sub>2</sub>S pools

H<sub>2</sub>S can either directly interact with signalling molecules and cause immediate biological effects or have its sulfur atom stored first and released later in response to a physiological trigger. In mammalian cells, aside free H<sub>2</sub>S, there are two main forms to store sulfur: acid-labile sulfur and bound sulfane sulfur [30] (**Figure 1**).

The acid-labile sulfur pool releases sulfur from the iron-sulfur clusters of mitochondrial proteins when the surrounding conditions become acidic or when the proteins are subjected to detergents or protein denaturants [31, 32]. Acid-labile sulfur has been quantified in the brain, heart, liver, kidney and spleen of rats [31]. Results showed that, among all tissues, the largest pool of acid-labile sulfur was found in the heart. As to the subcellular distribution, among whole tissue

extracts, nuclei, mitochondria, microsomes and cytoplasm, acid-labile sulfur was found greatest in the mitochondrial fraction [31]. The maximal pH for H<sub>2</sub>S release from acid-labile forms is 5.4 [33]. However, given that mitochondria are not in an acidic condition (pH of the mitochondrial matrix 7.8 and pH of the intramembrane space 7.0-7.4), acid-labile sulfur may not be a physiological source of H<sub>2</sub>S [33, 34]. Additional evidence has revealed that at a pH of 1.5, H<sub>2</sub>S gas release is maximal, with values of 400nmol/g protein in the heart and 170nmol/g protein in the liver and brain [33].

Reduction-labile sulfur or bound sulfane sulfur consists of chains of sulfur atoms that are covalently bound only to sulfur atoms (**Figure 1**) [31]. They are incorporated into proteins as persulfides or polysulfides, acting as intracellular storage units of sulfur and releasing H<sub>2</sub>S under reducing conditions, such as excess thiols [31, 33]. For this purpose, glutathione (GSH) and cysteine are the major cellular reducing compounds. According to Ogasawara *et al.*, bound sulfur is most abundant in cytosolic fractions of liver and kidney [31].

Sulfane sulfurs are not electronically charged (represented as S<sup>0</sup>). Instead, the attachment to the carrier protein occurs via a covalent bond between the S<sup>0</sup> atom, with its six valence electrons, and other sulfur atoms [35]. This molecule always exists in a sulfur-attached form and never in a stand-alone form, and can be present as elemental sulfur (S<sub>8</sub>), persulfides (RSSH), polysulfides (RSSSH or RSSSR), thiosulfonates (RSSO<sub>2</sub>R), polythionates (S<sub>n</sub>O<sub>6</sub><sup>2-</sup>) and thiosulfate (S<sub>2</sub>O<sub>3</sub><sup>2-</sup>) (**Figure 1**) [35].

One unique property of a sulfane sulfur is that it can reversibly transfer to other sulfur atoms (process of trans-sulfidation), such as thiols, to form the corresponding persulfide/polysulfide species and consequently increase the length of the polysulfur. Interestingly, sulfane sulfur can also react with the cyanide ion to form thiocyanate, which is easily quantifiable and much less toxic than cyanide. In fact, sulfane sulfur is most often quantified by cold cyanolysis and colorimetric measurement of ferric thiocyanate [36]. The direct measurement of H<sub>2</sub>S levels using either gas chromatography analysis of headspace gas or methylene blue spectrometry would not differentiate acid-labile sulfur from bound sulfane sulfur.

Sulfur is a multifaced atom with multiple oxidation states such as -2 in H<sub>2</sub>S, 0 in S<sub>8</sub>, +2 in sulfur oxide (SO), +4 in sulfite (SO<sub>3</sub><sup>2-</sup>) and +6 in sulfate (SO<sub>4</sub><sup>2-</sup>). Given that -2 in H<sub>2</sub>S is the lowest oxidation state of sulfur, H<sub>2</sub>S is a reductant and can only be oxidized.

Several proteins have been openly described as carriers of sulfane sulfur, such as albumin in the plasma and thiosulfate sulfurtransferase (TST), cystathionine γ-lyase (CSE), 3-mercaptopyruvate sulfurtransferase (MPST) and cysteine aminotransferase (CAT) in the cell [37].

In fact, cells that express MPST and CAT show a nearly two-fold increase in bound sulfane sulfur than cells that do not express MPST and CAT [38]. This sulfane sulfur can be released as H<sub>2</sub>S/HS<sup>-</sup>. In the brain, after neuronal excitation, the increase of extracellular K<sup>+</sup> leads to an increase in the intracellular pH of astrocytes, which in turn promotes the release of H<sub>2</sub>S from the bound sulfur groups [32].

H<sub>2</sub>S must be oxidized to bind to proteins as a persulfide or a polysulfide. This oxidation typically occurs by the means of the mitochondrial enzyme sulfide quinone oxidoreductase (SQR) [39]. Since exogenously applied H<sub>2</sub>S is absorbed and stored in proteins, it is highly likely that endogenous H<sub>2</sub>S produced by enzymes may also be incorporated into proteins for later release according to the cell needs [33, 35]. According to literature, sulfane sulfur has regulatory effects in several biological systems such as post-translational modifications of transfer RNA (tRNA) and synthesis of sulfur-containing cofactors (ex: iron-sulfur clusters) and vitamins (biotin, lipoic acid and thiamine) [40, 41]. Sulfane sulfur has been also associated to the covalent modification of -SH groups of receptors and enzymes, which can directly influence their biological activity [37]. Oxidoreductases containing iron or molybdenum atoms appear to be part of the enzyme set whose activity is modulated by sulfane sulfur [42].

## 1.5. Sources of H<sub>2</sub>S in the body

### 1.5.1. Exogenous

#### a) Inhalation

The inhalation of H<sub>2</sub>S is an important environmental, occupational, and public health concern (**Figure 2A**). H<sub>2</sub>S is released from pulp and paper mills, natural gas production, animal containment and manure handling, volcanoes and geothermal power plants [6]. The yearly emissions of H<sub>2</sub>S from all sources on land can reach 27–150 million metric tons [43]. Although the odor of H<sub>2</sub>S is easily identifiable, olfactory fatigue occurs in cases of high concentrations or under continuous exposure to low concentrations [44]. Combining this feature with the fact that the gas is rapidly absorbed and distributed through the blood, H<sub>2</sub>S can quickly escalate from a signalling agent to a death sentence. Nonetheless, some researchers claim that the inhalation of H<sub>2</sub>S may be exploitable for organ protection. Blackstone *et al.* described that pre-inhalation of H<sub>2</sub>S improved the survival rate of mice exposed to acute hypoxia [45]. Other studies have additionally reported that inhalation of H<sub>2</sub>S protects against cotton smoke inhalation- and ventilator-induced lung injury [46, 47].

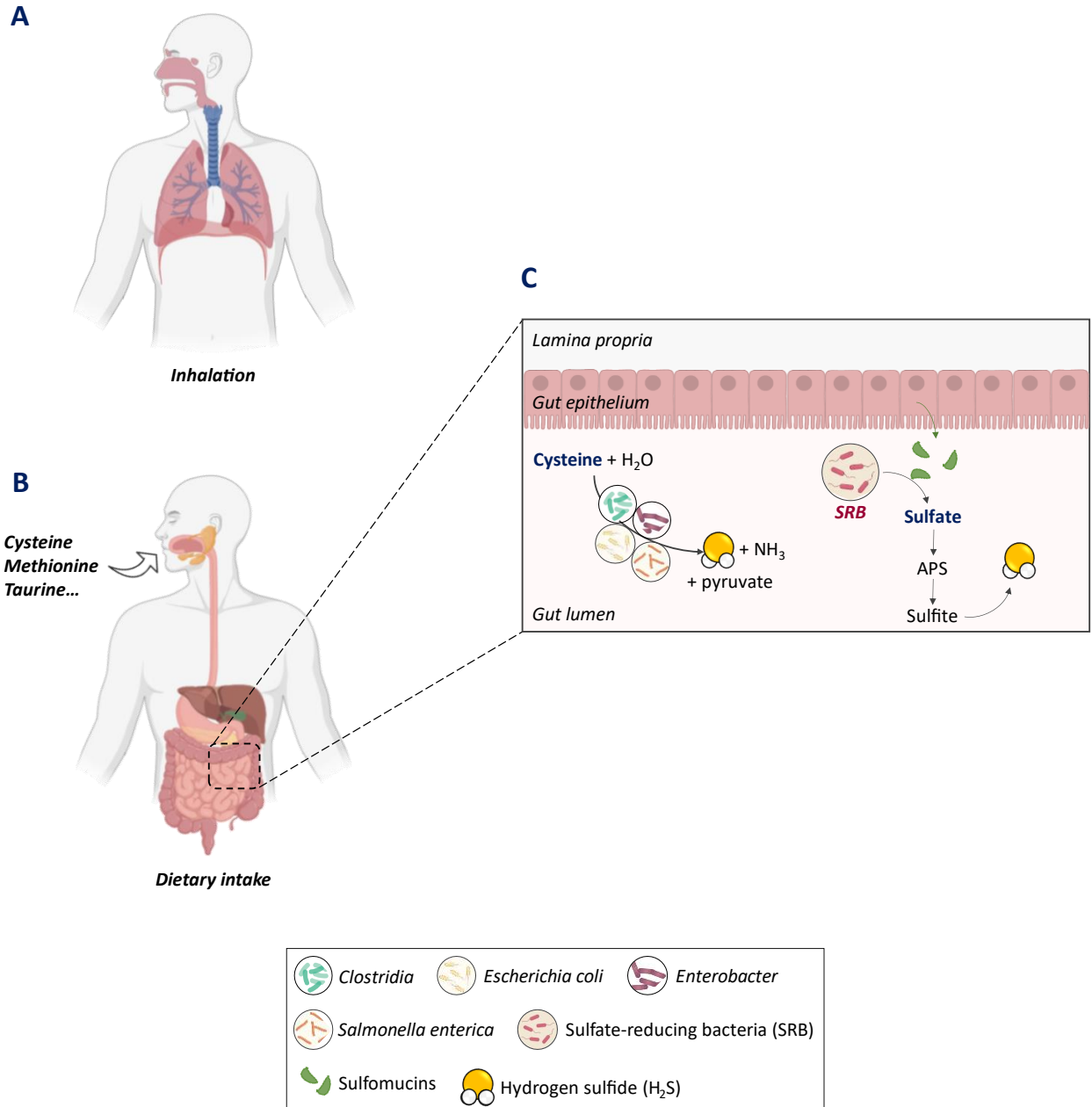


**Figure 2: Sources of H<sub>2</sub>S in the human body**

Humans may be exposed to H<sub>2</sub>S from both exogenous and endogenous sources. On one hand, exogenous H<sub>2</sub>S can enter the body via inhalation (A) or diet intake (B). On the other hand, endogenous gut production of H<sub>2</sub>S has proven itself to be a substantial source of this gas (C). In the colonic lumen, certain bacteria, such as *Escherichia coli* and *Clostridia*, are capable to produce H<sub>2</sub>S from the desulfhydration of cysteine. Other, namely the sulfate-reducing bacteria (SRB), are able to reduce the sulfate present in epithelium-released sulfomucins to produce H<sub>2</sub>S.

**RB:** sulfate-reducing bacteria; **NH<sub>3</sub>:** ammonia; **APS:** adenosine 5' phosphosulfate

## **b) Dietary intake**

The amount of sulfur that one person ingests in a single day is not really known. This value depends on the meal composition and way of preparation. The United States Food and Drug Administration (FDA) does not even consider sulfur as a nutrient [48]. This makes the task of quantifying the sulfur content of food even harder. Especially when most experts fail to account for all the sulfur-containing modifiers and food additives such as sulfur dioxide, sulfuric acid or carrageenan [48].

The primary dietary sources of sulfur are the sulfur-containing amino acids cysteine, methionine and taurine (**Figure 2B**) [49]. While the only source of methionine in mammals is the diet, cysteine can be produced from methionine via the transsulfuration pathway [49]. Taurine, on the other hand, can be synthesized in the cysteine/methionine oxidation pathway or be directly obtained from the diet [49]. For healthy humans, the daily requirement of sulfur amino acids (methionine plus cysteine) has been set as 14 mg/kg body weight [39]. Therefore, a person weighing 70 kg, independent of age or gender, requires the consumption of around 1.1 g per day.

Sulfur-containing amino acids are safer when supplied in a balanced stoichiometric ratio of methionine and cysteine. Di Buono *et al.* suggested that dietary cysteine can reduce the exogenous requirement for methionine in men [39]. This becomes exceedingly important when we consider that the largest concern associated with methionine intake is the production of homocysteine, an amino acid associated with several aspects of heart disease [50]. Some studies have examined the overall amount of the sulfur-containing amino acids (methionine and cysteine) in different types of diets [51]. The highest content (6.8 g per day) was reported in high-protein diets, which may be associated to an increased intake of heme, present in its highest concentrations in red meat [52]. Vegetarians and vegans, on the other hand, presented the lowest content of sulfur-containing amino acids: 3.0 g and 2.3 g per day, respectively [51]. A recently published study in the United States (U.S.) has shown that a typical American diet is already high in sulfur-containing amino acids given that a transition from a baseline diet to a “high sulfur” diet results in minor diet composition changes [53].

### 1.5.2. Endogenous

#### **a) Gut microbiota**

Typically, after digestion, diet-derived and endogenous proteins are efficiently absorbed in the small intestine [54]. However, a significant portion of luminal undigested or partially

digested proteins escapes digestion and enters the large intestine where it undergoes fermentation by intestinal bacteria [55, 56]. From this fermentation result amino acids, including cysteine, which are used for bacterial protein synthesis and/or for amino acid metabolism in order to synthesize bacterial metabolites [57, 58]. Among the several metabolites produced by gut microbiota is H<sub>2</sub>S [58]. Evidence suggests that the microbiota is a major regulator of the systemic bioavailability of H<sub>2</sub>S. Germ-free mice have 35% and 50-80% less free H<sub>2</sub>S and bound sulfane-sulfur in the plasma, respectively, than mice raised in a conventional animal facility [59]. In the colonic lumen, a significant number of bacterial species has been described to produce H<sub>2</sub>S, pyruvate and ammonia (NH<sub>3</sub>) from the fermentation of cysteine by cysteine desulfhydrase (**Figure 2C**). Among these species are *Escherichia coli*, *Salmonella enterica*, *Clostridia* and *Enterobacter* [57, 60–62].

H<sub>2</sub>S can also be produced via the reduction of inorganic sulfate by intestinal sulfate-reducing bacteria (SRB) or via microbial catabolism of sulfomucins (**Figure 2C**) [63]. Mucins are heavily glycosylated proteins responsible for the viscous properties of the colonic mucus barrier. These proteins can be either sulfated (sulfomucins) or sialylated (sialomucins). Although the majority of mucins found in the gut is sulfated, tissue sulfomucin content varies according to the intestinal portion we refer to: 86% in the rectum and 100% in the right colon [64]. A characteristically high sulfur diet (high in animal protein and fat, and low in fibers) leads to microbial nutrient deprivation and results in increased mucin sulfatase activity and mucin degradation, a pattern remarkably similar to that seen in ulcerative colitis (UC) [65–68]. In fact, evidence suggests that the combination of an increased mucin breakdown with an increased H<sub>2</sub>S production may lead to H<sub>2</sub>S concentrations that overwhelm the detoxification capacity of colonocytes and contribute to H<sub>2</sub>S toxicity [66, 69, 70]. However, it has been established that colonocytes are able to trigger adaptative responses to cope with the elevated levels of H<sub>2</sub>S [71].

SRB are microorganisms that obtain energy by coupling the oxidation of organic compounds or molecular hydrogen to the reduction of sulfate in a process known as sulfate respiration [72]. The concentration of SRB has been deeply correlated with the content of sulfomucins [73]. The dominant genera are *Desulfovibrio* (*D. piger*, *D. desulfuricans*), *Desulfobacter*, *Desulfobulbus* and *Desulfotomaculu* [53]. Nonetheless, recently, 13 new bacterial and archaeal phyla known to be capable of sulfate reduction have been described [74]. In both humans and rodents, the genus *Desulfovibrio* is regarded as the most abundant SRB and the primary producer of H<sub>2</sub>S [75, 76].

In both human and animal studies, a high protein diet results in fecal microbiota changes that increase H<sub>2</sub>S production [52]. Similarly, the consumption of processed foods expose

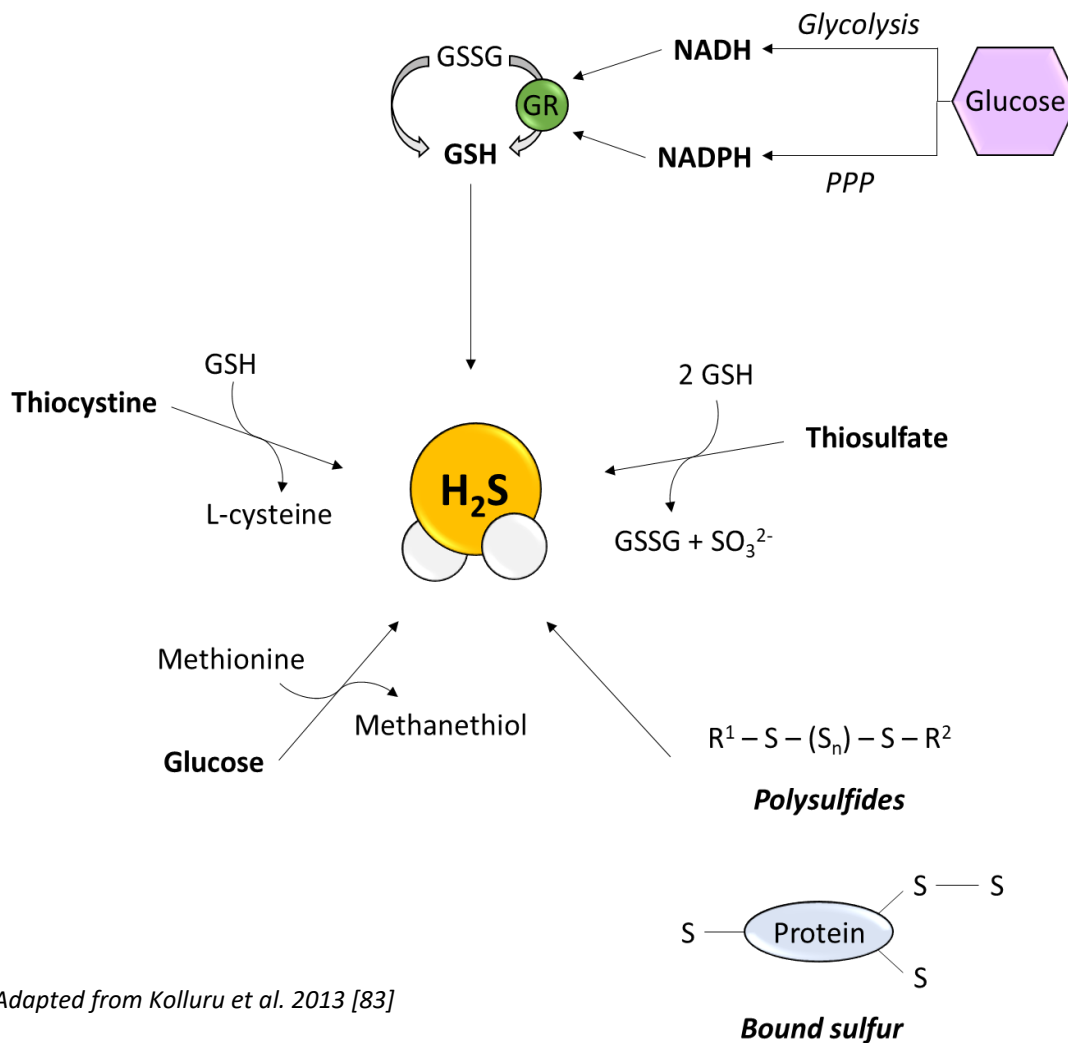
individuals to additives such as phosphates, nitrates, and emulsifiers, which have been shown to influence the composition of intestinal flora [77]. Mu *et al.* have found that rats fed a high-protein diet present a higher abundance of SRB and higher concentrations of colonic H<sub>2</sub>S [70]. Magee *et al.* have shown that individuals fed a high-meat diet for 10 days had 15 times more fecal sulfide than individuals fed a vegetarian diet for the same period of time [70]. This has been corroborated by David *et al.* who demonstrated that individuals on an animal-based diet presented elevated mRNA levels of sulfite reductases [78]. SRB have been associated to the development of intestinal bowel diseases (IBD) [79, 80]. However, they are typically not considered direct pathogens given that they are present in the gut of healthy individuals [79]. In fact, in 2017, Feng *et al.* compared fecal bacterial composition from one healthy donor and one diagnosed with irritable bowel syndrome [81]. Their results showed that the most abundant bacteria in the sick individual belonged to *Bilophila* and *Clostridium*, indicating that bacteria that utilize organic sulfur compounds rather than merely sulfate are relevant for human intestinal sulfur metabolism [81].

## **b) Tissue**

### Non-enzymatic production

In mammals, non-enzymatic H<sub>2</sub>S can be produced in the presence of reducing agents such as GSH, nicotinamide adenine dinucleotide (NADH) and nicotinamide adenine dinucleotide phosphate (NADPH) (**Figure 3**) [82, 83]. H<sub>2</sub>S can also be released from bound sulfur as well as organic or inorganic polysulfides (**Figure 3**) [83–85]. In human erythrocytes, for example, H<sub>2</sub>S is produced when elemental sulfur or inorganic polysulfides are supplied [86].

An additional non-enzymatical way to produce H<sub>2</sub>S is through thiosulfate (**Figure 3**) [83]. Koj *et al.* reported that glutathione disulfide (GSSG), H<sub>2</sub>S, and labelled sulfite were produced when rat liver mitochondria were incubated with oxygen, GSH, and [S<sup>35</sup>]thiosulfate [87]. Curiously, thiosulfate can also produce H<sub>2</sub>S in an enzymatic way. In 1966, Volini and Westley observed that, in bovine liver, the presence of the endogenous reductant, dihydrolipoic acid (DHLA), induced H<sub>2</sub>S production from thiosulfate by the enzyme rhodanase [88]. More recently, Mikami *et al.* described the same reaction in neural tissues [89]. Their findings suggested that this reaction is mediated by MPST, which combines 3-mercaptopyruvate (3-MP) with thioredoxin or DHLA in order to release H<sub>2</sub>S [89]. Literature has shown that this thiosulfate-derived mechanism of H<sub>2</sub>S production seems particularly important during hypoxic situations [90, 91].



Adapted from Kolluru et al. 2013 [83]

**Figure 3: Non-enzymatic production of  $H_2S$**

**NADH:** nicotinamide adenine dinucleotide; **NADPH:** nicotinamide adenine dinucleotide phosphate; **PPP:** pentose-phosphate pathway; **GR:** glutathione reductase; **GSH:** glutathione; **GSSG:** glutathione disulfide;  **$SO_3^{2-}$ :** sulfite



Yamagishi *et al.* have also demonstrated that glucose itself could react with methionine, homocysteine or cysteine to produce sulfur-containing gaseous compounds such as methanethiol and H<sub>2</sub>S (**Figure 3**) [92]. This non-enzymatic reaction appeared to be particularly active in patients with colon or lung cancer [92].

Other sources of spontaneous H<sub>2</sub>S production can include thiocystine and cysteine (**Figure 3**) [83]. The conversion of thiocystine into cysteine and the further reaction of cysteine with iron and vitamin B6 lead to H<sub>2</sub>S release [93, 94].

### Enzymatic production

Although non-enzymatic mechanisms for H<sub>2</sub>S synthesis have been identified it appears that the bulk of the H<sub>2</sub>S pool is enzymatically derived [82]. H<sub>2</sub>S is majorly synthesized as a by-product during the metabolism of the amino acids cysteine and homocysteine in the transsulfuration pathways. Nonetheless, methionine [95] and taurine [96] also contribute to increase the pool of total H<sub>2</sub>S.

“Forward transsulfuration” and “reverse transsulfuration” are two opposite processes involving the inter-conversion between the sulfur-containing amino acids cysteine and methionine (**Figure 4**). The “forward transsulfuration pathway” is used by bacteria, plants, and some fungi to produce methionine from cysteine, whereas “reverse transsulfuration” is used by vertebrates and some fungi to produce cysteine from methionine [97]. This reaction involves the catabolism of homocysteine, a molecule that when present in high concentrations is associated with cardiovascular diseases (CVD), strokes and defects of the neural tube [50]. Thus, this pathway not only allows the removal of toxic intermediates as it also contributes significantly to increase the cysteine pool, which is necessary for the biosynthesis of glutathione. In fact, studies have shown that, in mammalian liver, around 50% of the cysteine in the glutathione pool is derived from homocysteine [98].

Over decades, this process was extensively studied and systematically proven as a major H<sub>2</sub>S producer. The two enzymes that compose the transsulfuration process have been identified in the late 1960s: cystathionine β-synthase (CBS) is mainly expressed in the central nervous system whereas CSE is mainly expressed in the cardiovascular system. In liver and kidney, CSE and CBS are both expressed in high amounts. In addition, both proteins are vitamin B6-dependent cytoplasmic enzymes that present distinct capacities and use specific substrates [99].

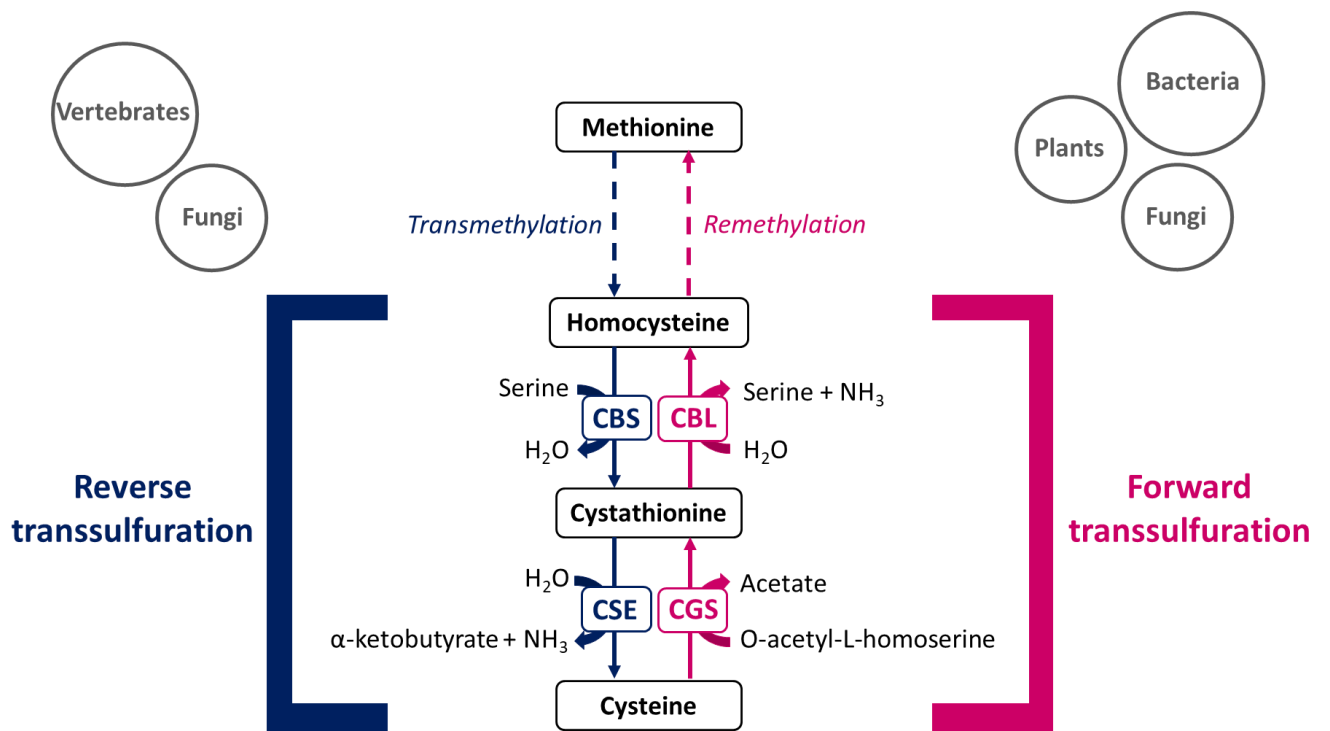


**Figure 4: Transsulfuration pathways**

**CBS:** cystathionine β-synthase; **CSE:** cystathionine γ-lyase; **CGS:** cystathionine γ-synthase; **CBL:** cystathionine β-lyase; **NH<sub>3</sub>:** ammonia

- Cystathionine  $\beta$ -synthase

CBS is the first enzyme in the reverse transsulfuration pathway. Isolated for the first time in 1969 by Braunstein *et al.*, this enzyme would receive different names in the years following its discovery [100]. In humans, the *CBS* gene is located on Chromosome 21, whereas in mice it is located on Chromosome 17. Due to its location, some studies have hypothesized that the development of Down's syndrome (DS) is somewhat related to this protein. Ichinohe *et al.* observed that DS patients have approximately three times higher CBS expression in their brains than normal individuals [101]. More recently, in 2019, Panagaki *et al.* showed that H<sub>2</sub>S overproduction generated by CBS inhibits mitochondrial Complex IV and suppresses oxidative phosphorylation in fibroblasts from DS patients [102].

### A) CBS structure

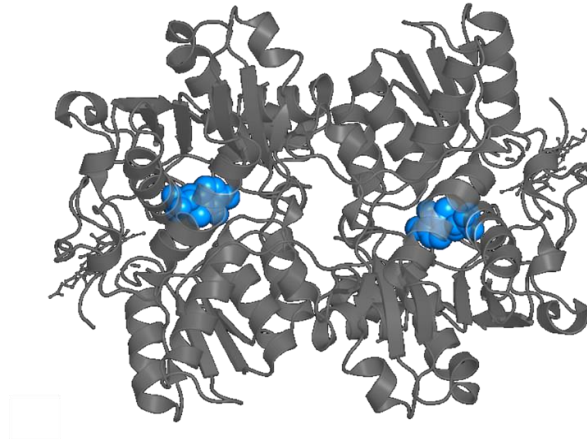
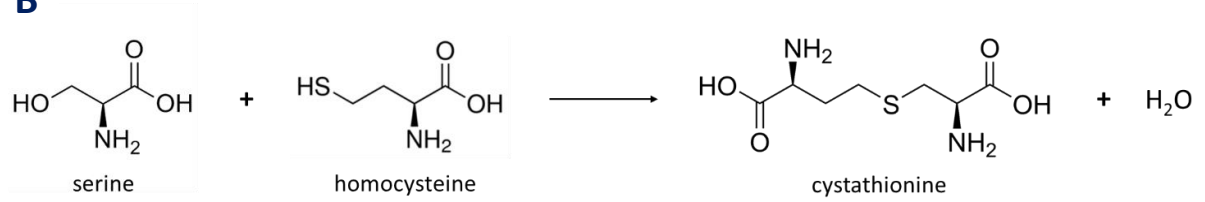
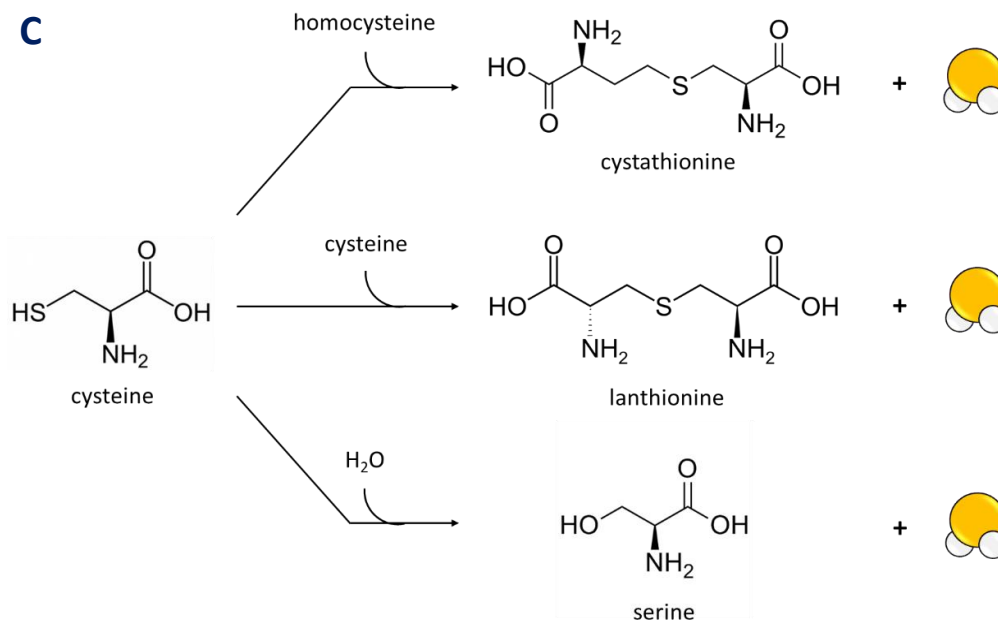
Human CBS is a 63-kDa cytosolic protein that consists of three architectural regions: the N-terminal domain binds the heme cofactor; the central catalytic core where catalysis occurs binds the pyridoxal-50-phosphate cofactor (PLP, the active form of vitamin B6); and the C-terminal domain is constituted by tandem repetitions of "CBS domains" (CBS1 and CBS2), which form binding clefts to house S-adenosylmethionine (SAM) (**Figure 5A**) [50].

The 70-amino acid long heme domain is unique for mammalian CBS and most studies suggest that it has no functional role in the catalytic activity of the enzyme. Evidence suggests that this domain rather serves as a redox sensor, given that its depletion renders CBS insensitive to oxidative stress [103]. However, it has also been demonstrated that, in its ferrous state, the heme domain is able to bind NO and CO, which subsequently prompts the inhibition of CBS activity [104]. On one hand, this inhibition demonstrates that the heme domain clearly interacts with the active site of the protein. On the other hand, it also suggests that the activity of CBS may be regulated not only by H<sub>2</sub>S but also by NO and CO.

The "CBS domains" of the C-terminus are able to bind SAM which, on one hand, stabilizes the homotetrameric state of the protein and on the other hand serves as an allosteric activator of CBS (increases enzyme activity approximately 2- to 5-fold) [23, 105–107].

### B) CBS reactions

The canonical reaction of CBS consists in the condensation of homocysteine and serine to yield cystathionine and H<sub>2</sub>O (**Figure 5B**). This reaction is the first and rate-limiting step of the

**A****B****C**

*Adapted from Yadav and Banerjee, 2012 [108]*

**Figure 5: Protein structure and reactions catalysed by CBS**

**A)** Schematic representation of the tertiary fold of a dimer of cystathionine  $\beta$ -synthase (CBS). In blue ball-and-stick representation is the active site pyridoxal phosphate (PLP). **B)** Canonical reaction. **C)** Reactions that release H<sub>2</sub>S

reverse transsulfuration process. Nonetheless, with broadly defined reaction specificity, CBS catalyses several alternative reactions that lead to the production of H<sub>2</sub>S [108].

In 2004, Chen *et al.* demonstrated that cysteine could react with homocysteine to produce cystathionine and H<sub>2</sub>S (**Figure 5C**) [109]. This reaction appeared to be stimulated by the presence of SAM. In addition, it was shown that, at physiologically relevant concentrations of serine, homocysteine, and cysteine, only 5% of the cystathionine formed came from cysteine [109]. This suggests that, from all the homocysteine metabolized by CBS, only a small portion reacts with cysteine and ends up releasing H<sub>2</sub>S as by-product. Nonetheless, when comparing all reactions, the condensation of homocysteine with cysteine accounts for nearly 96% of all CBS-mediated H<sub>2</sub>S-production [110].

Aside the two aforementioned reactions, CBS can also catalyse the condensation of two molecules of cysteine to yield lanthionine and H<sub>2</sub>S, and mediate the hydrolysis of cysteine to form serine (**Figure 5C**) [106].

### C) CBS mutations and KO models

Mutations in the *CBS* gene are the single most common cause of severe hereditary homocystinuria [111, 112]. This autosomal recessive disorder is characterized by an accumulation of the amino acid homocysteine in the serum and by its increased excretion in the urine. This illness is typically manifested as mental retardation, ocular lens dislocation, skeletal abnormalities, and vascular disease [113, 114]. Mutations in the *CBS* gene can alter either mRNA or enzyme stability, activity, binding of PLP and heme, or impair allosteric regulation [114]. CBS KO mice have 40x more the normal value of plasma homocysteine [115]. These animals suffer from severe growth retardation and the vast majority dies within 5 weeks after birth. Furthermore, histological examination of their liver shows hepatocyte enlargement and microvesicular steatosis [115]. On the other hand, heterozygous mutants for the *CBS* gene present 50% less hepatic CBS mRNA level and enzyme activity, accompanied by 2x more the normal plasma level of homocysteine [115].

#### • Cystathionine γ-lyase

CSE, also known as cystathionase (CTH), is the second PLP-dependent enzyme of the transsulfuration pathway. Located on Chromosome 1 in humans and Chromosome 3 in mice, the *CSE* gene is expressed in numerous organisms including mammals, amphibians, and plants.

Different CSE isoforms possess high sequence identity between phylogenetically distant organisms [116].

This cytosolic enzyme has been demonstrated to be abundantly expressed in the mammalian cardiovascular and respiratory systems [117]. In fact, in CSE knockout (KO) mice, endogenous levels of H<sub>2</sub>S are found 50% and 80% decreased in both serum and heart, respectively [118]. Moreover, these mice present elevated levels of the toxic amino acid homocysteine [118]. Additional evidence suggests that the most significant CSE-mediated H<sub>2</sub>S actions take place in the liver, kidney, heart, uterus, and pancreas [117–121].

### A) CSE structure

CSE is a 45 kDa PLP-dependent beta-replacing monomer that associates as a homotetramer in solution. X-ray crystallographic assays have shown PLP binding in only three of the four subunits [122].

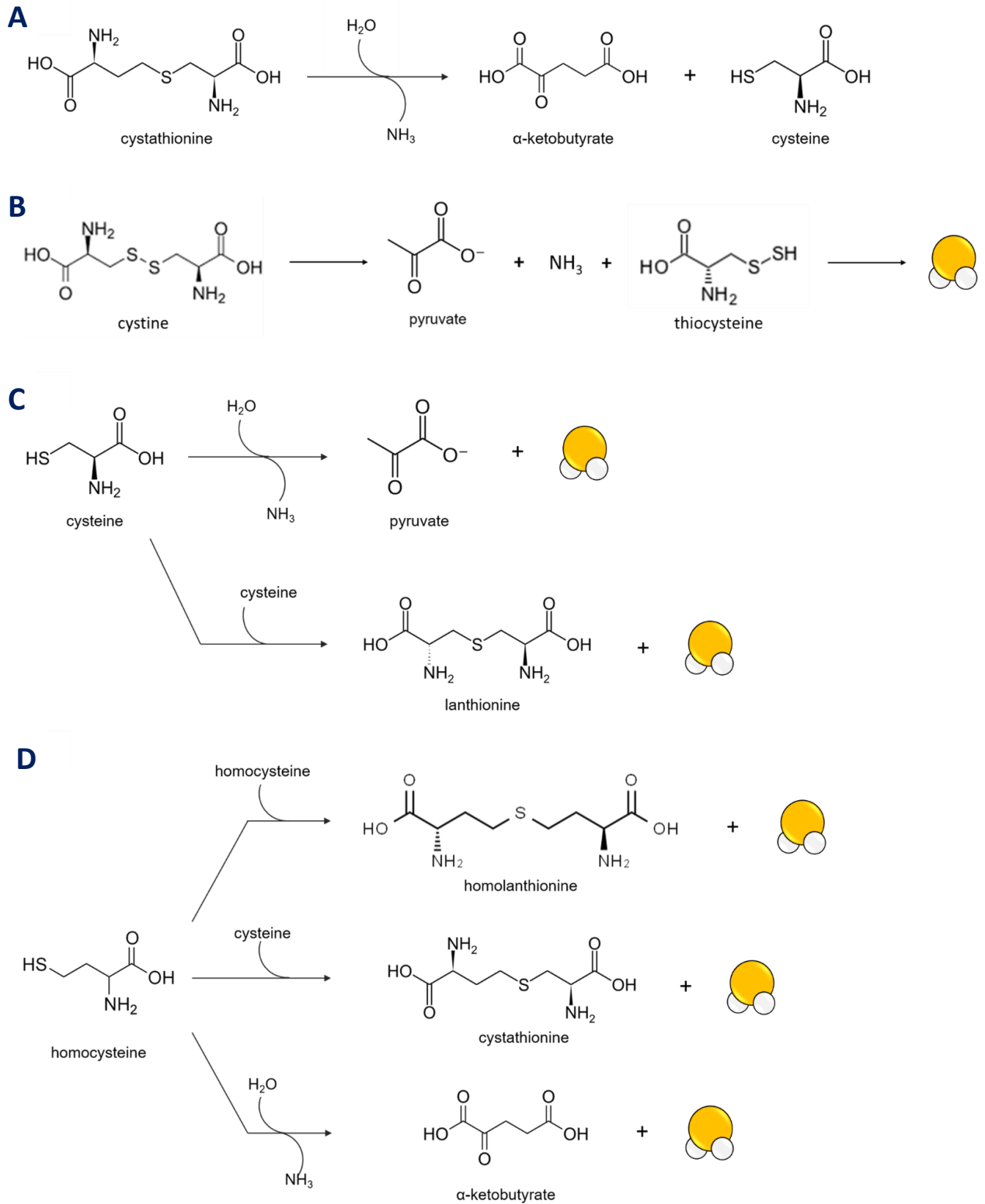
There are two separate isoforms of CSE, one of which is the result of a 132 base pair deletion [123]. While both isoforms are expressed, the longer form is the dominant form [123].

CSE responds to ER stress, with ER stressors inducing an increase in CSE expression levels (and subsequently H<sub>2</sub>S) and upregulating the activating transcription factor 4 (ATF4) [124]. Studies have suggested that CSE can be inactivated by phosphorylation [125] and activated by increased concentrations of Ca<sup>2+</sup>/calmodulin [117]. However, the mechanisms behind CSE regulation are still understudied. Researchers suggest that one possible site of regulation is the two CXXC motifs of the protein. A CXXC motif is characterized by two cysteine residues, intervened by two other random residues that together form an active site. For example, in the thioredoxin superfamily of enzymes, of which protein disulfide isomerase and thioredoxin are members, the CXXC motif is the active site [126]. The proximity of the two cysteine residues allows for the reduction or oxidation of the disulfide bonds, which may affect enzyme activity [123]. In CSE, these CXXC motifs may exert redox-sensitive allosteric regulation.

### B) CSE reactions

CSE has the ability to accommodate different substrates in the same binding pocket, such as cystathionine, homocysteine and cysteine, which leads to a competition between them.

The canonical reaction of CSE consists in the cleavage of a cystathionine molecule into cysteine,  $\alpha$ -ketobutyrate, and NH<sub>3</sub> (**Figure 6A**). However, there are several cysteine-, cysteine- and homocysteine-derived reactions catalysed by CSE that lead to the production of H<sub>2</sub>S [127]. The



Adapted from Chiku et al. 2009 [121]

**Figure 6: Reactions catalysed by CSE**

**A)** Canonical reaction of cystathionine  $\gamma$ -lyase (CSE). **B) C)** and **D)** Reactions that release  $\text{H}_2\text{S}$ .

first to notice these reactions were Yamanishi and Tuboi in 1980 [122]. According to their study, in rat liver, CSE would mediate the cleavage of cystine into pyruvate,  $\text{NH}_3$  and the intermediate thiocysteine. Thiocysteine would then decompose into  $\text{H}_2\text{S}$  in a non-enzymatic reaction with other thiols (**Figure 6B**) [122]. Aside this reaction, CSE also mediates the hydration of cysteine, which results in the production of pyruvate,  $\text{NH}_3$  and  $\text{H}_2\text{S}$ , and the condensation of two molecules of cysteine, which originates lanthionine and  $\text{H}_2\text{S}$  [127] (**Figure 6C**). In the presence of high concentrations of homocysteine, CSE appears to favour the condensation of two molecules of homocysteine to produce homolanthionine and  $\text{H}_2\text{S}$  (**Figure 6D**) [127, 128]. Additional studies have shown that CSE is also capable of mediating the hydration of homocysteine, which produces  $\alpha$ -ketobutyrate,  $\text{NH}_3$  and  $\text{H}_2\text{S}$ , as well as, catalysing the reaction between homocysteine and cysteine to form cystathionine and  $\text{H}_2\text{S}$  (**Figure 6D**).

When comparing all CSE-mediated reactions, the hydration of cysteine accounts for nearly 70% of all  $\text{H}_2\text{S}$ -produced, followed by the hydration of homocysteine, which accounts for approximately 29% [127].

### C) CSE mutations and KO models

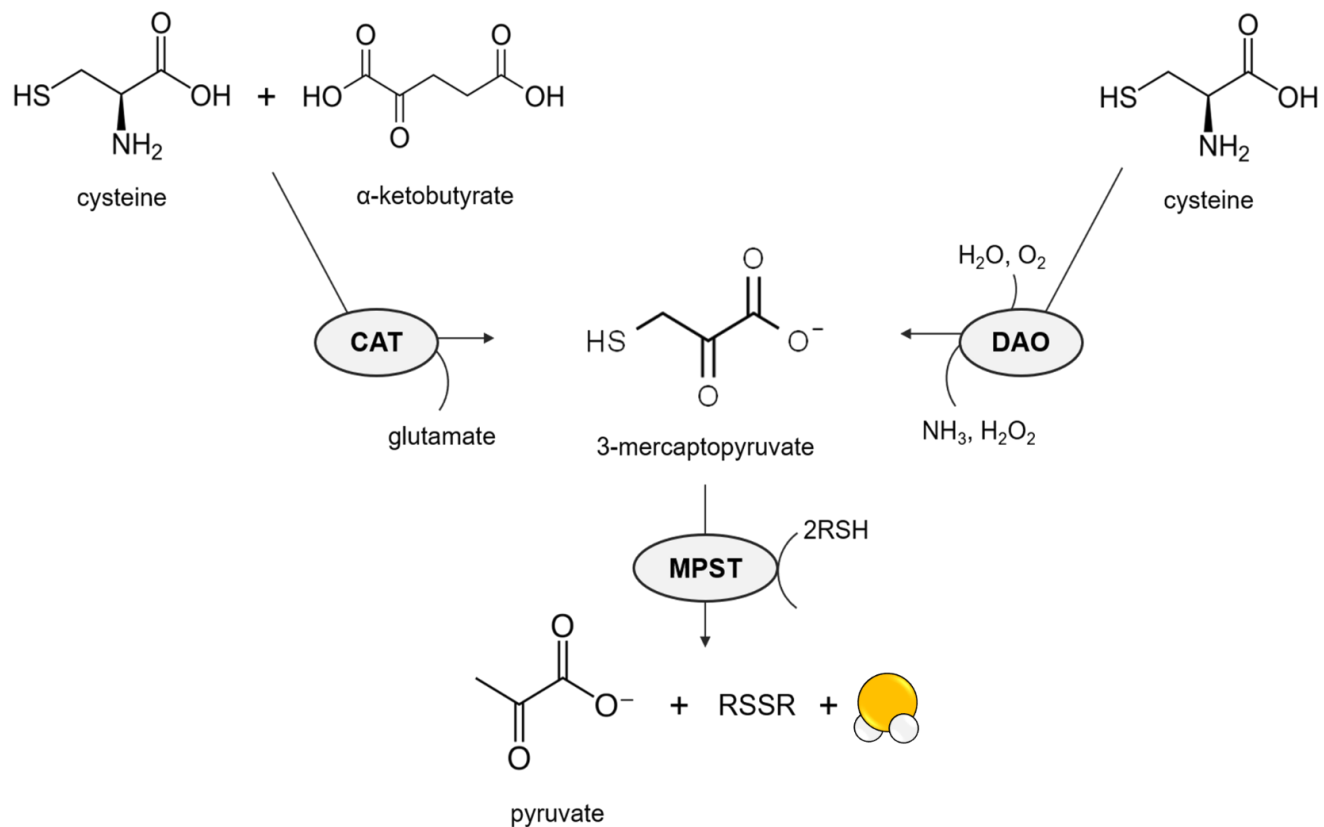
Mutations in the *CSE* gene cause cystathioninuria, an autosomal recessive inborn error characterized by an accumulation of cystathionine in the plasma and, subsequently, urine. Most affected individuals experience cystathioninuria as a mild disorder, displaying only the abnormal urinary excretion of cystathionine [128]. The same does not happen in rodents. Mice lacking CSE display pronounced hypertension, diminished endothelium-dependent vasorelaxation, skeletal muscle atrophy and vulnerability to oxidative injury [118, 129, 130]. However, since the activity of CSE in rat liver is five times as high as that in human liver, the role of this enzyme may be more important in rodents [131].

#### • 3-mercaptopyruvate sulfurtransferase (MPST)

Aside the two enzymes involved in the transsulfuration pathway, there is a third that mediates  $\text{H}_2\text{S}$ -producing reactions.

MPST is both a mitochondrial and cytosolic enzyme that belongs to the sulfurtransferase family. Located on Chromosome 22 in humans and Chromosome 15 in mice, MPST has 66% of homology with rhodanese, which is only located in mitochondria [23, 132–134]. Two splice variants of MPST, differing by 20 amino acids at the N terminus, give rise to the cytosolic MPST1





*Adapted from Yadav et al. 2013 [134]*

**Figure 7: Mitochondrial biosynthesis of H<sub>2</sub>S by the enzymes CAT/MPST or DAO/MPST**

**CAT:** cysteine aminotransferase; **DAO:** D-aminoacid oxidase; **MPST:** 3-mercaptopyruvate sulfurtransferase; **RSSR:** persulfide

and mitochondrial MPST2 isoforms [135]. Although the activity of MPST is found in both mitochondria and cytosol, its activity in the mitochondrion appears to be 3 times higher [134].

### **A) MPST structure**

Mercaptopyruvate sulfurtransferase is a 33-kDa protein that can function as a monomer or as a disulfide-linked homodimer [136]. This enzyme is well conserved among prokaryotes and eukaryotes, and has been implicated in important physiological roles related to sulfur metabolism. The enzyme comprises an N-terminal catalytically inactive domain and a C-terminal catalytically active domain. The catalytic cysteine, cysteine 248 (Cys<sup>248</sup>), is part of a conserved six amino acid motif that folds into a cradle-like loop and defines the active site pocket [136].

### **B) MPST reactions**

With the assistance of another PLP-dependent enzyme, the cysteine aminotransferase (CAT), MPST is capable of producing H<sub>2</sub>S [137]. CAT efficiently catalyses the transamination between cysteine and  $\alpha$ -ketoglutarate to produce glutamate and 3-mercaptopyruvate (3-MP), MPST substrate of interest [137]. 3-MP can also be produced directly from cysteine by the D-aminoacid oxidase (DAO), present in peroxisomes (**Figure 7**). MPST then transfers the sulfur from 3-MP to sulfite or other sulfur acceptors [137]. The direct outcome from the conjoined work of these two enzymes is the production of sulfane sulfur, not the free form of H<sub>2</sub>S (**Figure 7**). However, H<sub>2</sub>S can be formed upon the reduction of the atomic sulfur or released from persulfides and thiosulfate [138]. The former requires the presence of reductants such as glutathione or thioredoxin, and the latter, other specific sulfurtransferases [137].

### **C) MPST mutations and KO models**

This enzyme, which was first discovered in 1953 by Meister, Wood and Fiedler in rat liver, has been found expressed in both prokaryotes and eukaryotes [139, 140]. The specific activities of MPST vary from tissue to tissue, with the highest specific activity in the kidney followed by the liver. MPST activities in the heart, lung, cerebellum, thymus, cerebrum, and testis are less than half of that in the kidney [134].

One of the most important functions described for MPST is cyanide detoxification, since this enzyme transfers the sulfane sulfur from the 3-MP to the cyanide ion, producing nontoxic thiocyanate and pyruvate [138, 141]. Zinc is used as cofactor in this reaction.

Despite its broad expression and the fact that some abnormalities related to MPST deficiency have been already described [142], no life-threatening condition has ever been associated to this enzyme. In fact, partial deletion of MPST appears to improve hepatic steatosis in mice fed a high-fat diet (HFD) [142]. Furthermore, aside some anxiety-like behaviours, MPST KO animals show no pathological features compared to their wild-type (WT) counterparts when fed a normal diet [143]. In fact, MPST KO mice are born at the expected frequency and develop normally like their WT counterparts [144]. The only difference detected between WT and MPST KO mice was the enhanced passive systemic anaphylactic responses in the KO animals [144].

## **1.6. Catabolism of H<sub>2</sub>S**

Although many studies have highlighted the numerous biological reactions in which H<sub>2</sub>S plays a regulatory role, the truth is H<sub>2</sub>S remains a toxic molecule whose concentration must be under tight control. However, unlike the biosynthesis of H<sub>2</sub>S, the catabolism of this gaseous transmitter is not well studied, and several physiological experiments are still required.

Some studies have shown that the production of H<sub>2</sub>S is quick and in a continuous flux (several millimoles per day for a 70kg human being), which suggests that the detoxification mechanisms are very efficient [145]. In this manuscript, we will discuss three catabolic processes of H<sub>2</sub>S in mammals: expiration, methylation and oxidation.

### **1.6.1. Expiration**

Expiration is the process through which H<sub>2</sub>S escapes the body by the lungs. In 2010, a study has demonstrated that the basal level of exhaled H<sub>2</sub>S in healthy individuals is already higher than the ambient concentration of H<sub>2</sub>S [146]. The same study has described that the intravenous (IV) administration of Na<sub>2</sub>S would lead to a rapid elevation of exhaled H<sub>2</sub>S [146].

It is still unknown how much H<sub>2</sub>S is expelled through the lungs in a normal physiological situation. However, H<sub>2</sub>S exhalation is highly detectable in pathological situations such as septic shock and chronic obstructive pulmonary disease, conditions in which H<sub>2</sub>S is massively generated [147]. For this reason, it seems that expiration provides a route of disposal of H<sub>2</sub>S when its concentration is too high and might block mitochondrial H<sub>2</sub>S oxidation. However, given that the normal concentration of H<sub>2</sub>S in a mammalian body is extremely low, odds are that the loss of H<sub>2</sub>S through exhalation is very minimal. Nonetheless, due its strong link to inherent pathologies, H<sub>2</sub>S expiration is being more and more looked at as a possible diagnostic method [148].

### 1.6.2. Methylation

Methylation is another catabolic pathway of H<sub>2</sub>S that mainly takes place in the gut. As the name suggests, this process consists in the methylation of H<sub>2</sub>S into methanethiol, a colourless gas with a smell of rotten cabbage. Methanethiol can be further methylated by a thiol S-methyltransferase (TMT) into non-toxic dimethyl sulfide [149]. TMT is a microsomal enzyme with its highest activity in the colonic and cecal mucosa, although it has also been reported active in liver, lung, and kidney [149]. Although notably microsomal, TMT has been previously reported in the cytosol, conducting the S-methylation reaction of the pharmacologically active metabolite of Clopidogrel (an antiplatelet prodrug) [150]. A study conducted on 231 individuals from 47 randomly selected families has concluded that TMT activity in erythrocytes was dependent on inheritance (fivefold individual variation of enzyme activity) [151]. The authors of the study suggested that the variations found in erythrocyte TMT activity could reflect variations of the enzyme activity in other tissues and organs.

Given that the rate of H<sub>2</sub>S methylation appears to be many orders of magnitude less than that required to metabolize all H<sub>2</sub>S released in the colon, Levitt *et al.* have proposed an alternative method of intestinal H<sub>2</sub>S catabolism [152]. This process, called demethylation, consists in the transformation of methanethiol to H<sub>2</sub>S and subsequent oxidation of H<sub>2</sub>S to thiosulfate [152]. In fact, H<sub>2</sub>S oxidation has been shown to be 10 000 times faster than H<sub>2</sub>S methylation in colonic mucosa. When comparing colonic and non-colonic tissues (ileum, stomach, liver, muscle, erythrocytes and plasma), the oxidation of H<sub>2</sub>S into thiosulfate is at least eight times greater for cecal and right colonic mucosa than for the non-colonic tissues [153]. This implies that demethylation is a specialized detoxification system that allows intestinal tissues to rapidly metabolize H<sub>2</sub>S and methanethiol, preventing what could otherwise be injurious amounts of these two toxic compounds. In 1992, Aslam *et al.* described that a prolonged 4-hour perfusion of the rat colon with approximately 0.2 mM H<sub>2</sub>S produced increased mucosal apoptosis, goblet cell depletion, and superficial ulceration when compared with control animals [154, 155]. In 2011, Silva *et al.* described that several volatile sulphur-containing metabolites such as methanethiol were dramatically downregulated in the urine of cancer patients (leukaemia, colorectal and lymphoma) as a consequence of neoplastic cell presence [156]. However, a recent study has contradicted these findings by demonstrating that the fecal concentration of methanethiol in patients with colorectal cancer is much higher than that found in healthy subjects [157]. This contradiction may arise from the different type of samples used and from the cohort

heterogeneity. However, no differences were found concerning the fecal values of H<sub>2</sub>S between cancer patients and healthy individuals [157].

### 1.6.3. Mitochondrial oxidation

Sulfide-rich environments occur naturally in the sediments and grass marshes of the intertidal zone (seashore). Due to its highly toxic properties, microorganisms that dwell in these sulfidic habitats must have efficient ways to survive in such abiotic conditions. Thorough investigations soon showed that H<sub>2</sub>S was not only tolerated by these microorganisms, but rather exploited in an endosymbiotic way [152]. Looking closely to the lugworm *Arenicola marina*, it was possible to identify a new sulfide oxidation pathway, which was linked to the electron transport chain (ETC) at the level of ubiquinone via a sulfide quinone oxidoreductase (SQR) [158]. Additional evidence has demonstrated that, actually, SQR does not work alone in the detoxification of H<sub>2</sub>S [158, 159]. A mitochondrial pathway of three consecutive reactions has been identified in rat liver as well as in the body-wall tissue of *A. marina* [158, 159]. In these reactions cooperate with SQR three additional enzymes: persulfide dioxygenase or ethylmalonic encephalopathy protein 1 (ETHE1), thiosulfate sulfurtransferase (TST) and sulfite oxidase (SUOX). Together they form the sulfide oxidizing unit (SOU), whose work is the transformation of H<sub>2</sub>S into sulfite, thiosulfate and sulfate, respectively [159].

#### **a) Enzymes involved in H<sub>2</sub>S mitochondrial oxidation**

- Sulfide Quinone Oxidoreductase (SQR)

Located on Chromosome 15 in humans and Chromosome 2 in mice, SQR is a 50 kDa protein found in phylogenetically distant organisms, from prokaryotes to eukaryotes [159]. Although in animals and fungi the *SQR* gene can be traced back to a single acquisition from a eubacterial donor, the SQR protein is not a well-conserved protein (only approximately 20% sequence identity) [159].

#### **A) SQR structure**

SQR is a member of the flavin disulfide reductase (FDR) family, such as flavocytochrome c sulfide dehydrogenase (FCSD). SQR is characterized by having two redox centers, one of these being a flavin adenine dinucleotide (FAD). The other center, located close to the flavin, is a pair of cysteine residues separated by a chain of three sulfur atoms. SQR isolated from different eukaryotes and prokaryotes has showed that, while the structures are overall similar, significant

differences are perceived in the FAD binding mode and the configuration of active site residues [160]. Mechanistically, eukaryotic SQR is structurally more similar to the flavoprotein subunit of FCSD, a soluble bacterial H<sub>2</sub>S-oxidizing enzyme, than to the SQR of other prokaryotic species [161]. However, while FCSD uses cytochrome c as electron acceptor, SQR uses ubiquinone. Moreover, the reaction catalysed by SQR is more efficient. Example of this is the sulfur bacterium *Allochromatium vinosum*, which possesses both FCSD and SQR, but preferentially uses the latter for sulfide oxidation [162].

### **B) SQR mutations and KO models**

SQR KO models of *C. elegans* exposed to H<sub>2</sub>S present phosphorylation of eukaryotic translation initiation factor 2-alpha (IF2 $\alpha$ ) with subsequent inhibition of protein synthesis [163]. The organisms also present activation of endoplasmic reticulum (ER) and mitochondrial stress responses [163]. In humans, it has been recently reported the existence of two homozygous pathogenic variants of SQR, responsible for lack of protein and enzyme activity [164]. The first variant (c.637G > A) was associated with decreased cytochrome c oxidase (Complex IV) activity in liver and muscle, lactic acidosis, hypotonicity, brain lesions and multiorgan failure [164]. The patients presenting this mutation died before the age of 10 years. The second variant (c.446delT) was associated with lactic acidosis, ketosis, dicarboxylic aciduria, Complex IV inhibition, encephalopathy and basal ganglia lesions. The patient recovered after intravenous glucose administration. In all patients, the symptoms were triggered by infections or fasting, episodes associated with protein catabolism [164]. Furthermore, four single nucleotide polymorphisms (SNP) in the *SQR* gene were associated to extra susceptibility for osteoporosis in Chinese and Korean postmenopausal women [165, 166].

#### **• Ethylmalonic encephalopathy protein 1 (ETHE1)**

ETHE1 is a 27 kDa protein whose gene is located on Chromosome 19 in humans and on Chromosome 7 in mice. ETHE1 oxidizes persulfides in the mitochondrial matrix in an oxygen-dependent manner [167]. In mammals, ETHE1 is majorly expressed in the liver, intestines, nervous system, muscle, kidney and heart.

### **A) ETHE1 structure**

ETHE1 is a homodimer bound by a single iron atom and functions as a beta-lactamase-like iron-coordinating metalloprotein [168, 169]. The active site of human ETHE1 is very similar to an

ETHE1-like enzyme from *Arabidopsis thaliana* (60% sequence identity) [170]. The N-terminal sequence of 24 amino acids shows high similarity to mitochondrial targeting sequences.

### **B) ETHE1 mutations and KO models**

Mutations in the *ETHE1* gene were found to result in a devastating autosomal recessive disorder that affects the brain, gastrointestinal tract, and peripheral vessels, known as ethylmalonic encephalopathy (EE) [169, 171, 172]. ETHE1 deficiency affects the mitochondrial catabolism of fatty acids (FA) and branched-chain amino acids, resulting in high levels of ethylmalonic acid in the urine, high concentrations of C4 and C5 acylcarnitines in the blood, and low Complex IV activity in muscle and brain [169, 171].

#### • Thiosulfate sulfurtransferase (TST)

TST was initially described as a thiosulfate:cyanide sulfurtransferase [173]. The gene coding for this 33.4 kDa mitochondrial protein is located on Chromosome 22 in humans and on Chromosome 15 in mice. This ubiquitous enzyme is highly conserved across species and has been characterized in plants, bacteria, and fungi [174]. In mammals, TST is generally found with highest expression in the liver, with significant amounts in the kidney, adrenals, and thyroid glands [175].

### **A) TST structure**

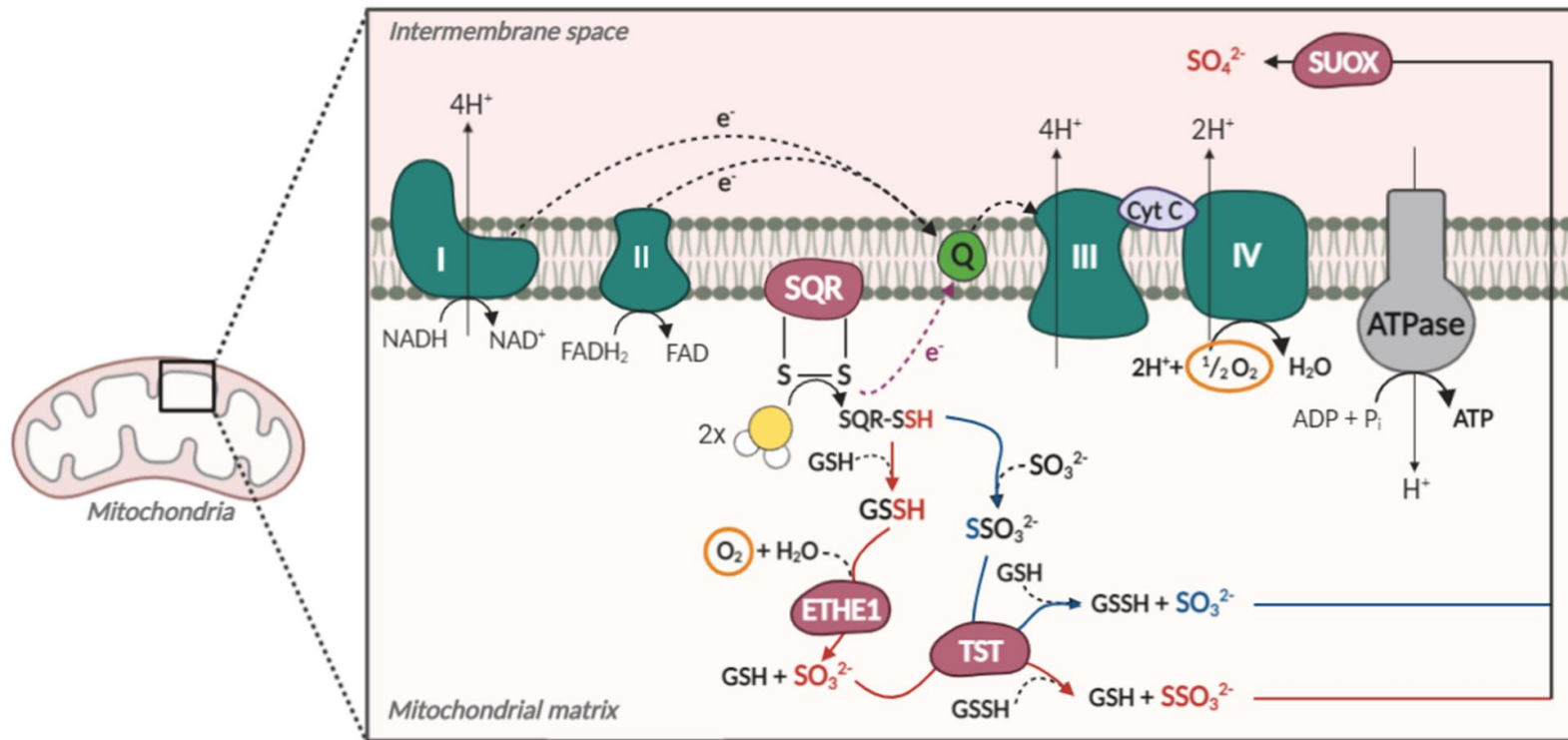
The crystal structure of TST consists of two domains (rhodanese domains) of similar size and nearly identical conformation, connected by a loop at the surface of the molecule [176]. The slightly smaller C-terminal domain hosts the active site, which is located near the interface between the N- and C-terminal domains. The catalytic cysteine (in humans Cys-248) is located in the active site cavity and is directly involved in the enzymatic reaction [176].

### **B) TST mutations and KO models**

TST mutations have been associated to patients suffering from ulcerative colitis and Chron's disease. These mutations compromise the activity of the enzyme and are linked to the accumulation of toxic sulfite [176, 177].

#### • Sulfite oxidase (SUOX)

SUOX is a 52 kDa protein present in the intermembrane mitochondrial space and whose gene is located on Chromosome 12 in humans and on Chromosome 10 in mice. *SUOX* has been



Adapted from Kabil and Banerjee, 2014 [122]

**Figure 8: Mitochondrial oxidation of H<sub>2</sub>S in a mammalian cell**

H<sub>2</sub>S is initially oxidized by **sulfide quinone oxidoreductase (SQR)**, generating an SQR-bound persulfide (SQR-SSH) and releasing electrons (e<sup>-</sup>) that are transferred to ubiquinone (Q) and carried down the electron transport chain (ETC). The SQR-SSH is transferred to a small molecule acceptor such as glutathione (GSH) (**red line**) or sulfite (SO<sub>3</sub><sup>2-</sup>) (**blue line**). If GSH acts as the acceptor, a molecule of glutathione persulfide (GSSH) is formed, which is then converted, with O<sub>2</sub> as co-substrate, by **persulfide dioxygenase (ETHE1)** to SO<sub>3</sub><sup>2-</sup> and GSH (**red line**). The SO<sub>3</sub><sup>2-</sup> formed can be converted, with GSSH as co-substrate, into thiosulfate (SSO<sub>3</sub><sup>2-</sup>) and GSH by **thiosulfate sulfurtransferase (TST)**. SSO<sub>3</sub><sup>2-</sup> is subsequently transformed into sulfate (SO<sub>4</sub><sup>2-</sup>) by **sulfite oxidase (SUOX)**. On the other hand, if SO<sub>3</sub><sup>2-</sup> is used as the SQR-SSH acceptor, SSO<sub>3</sub><sup>2-</sup> is formed (**blue line**). Since GSSH is necessary for ETHE1 to function, this SSO<sub>3</sub><sup>2-</sup> requires additional transformation into SO<sub>3</sub><sup>2-</sup> and GSSH by TST, using GSH as co-substrate (**blue line**). The resulting SO<sub>3</sub><sup>2-</sup> can be directly used by SUOX to produce SO<sub>4</sub><sup>2-</sup> (**blue line**).



found expressed in several human and rodent tissues, with liver, kidney, heart, placenta, brain, colon and small intestine presenting the most elevated expression [177].

### A) SUOX structure

SUOX uses molybdenum as cofactor to catalyse the oxidation of sulfite to sulfate [178]. Each subunit of this protein contains three domains. A small heme-containing N-terminal cytochrome b5 domain is connected to the rest of the protein via a flexible 10-residue-long loop region [178]. The central domain contains the active site of the enzyme. Finally, the C-terminal dimerization domain hosts a molybdopterin cofactor [178].

### B) SUOX mutations and KO models

SUOX deficiency is a life-threatening, autosomal recessive disease characterized by severe neurological impairment. Patients present neurological abnormalities, such as neonatal axial hypotonia and/or peripheral hypertonia, pharmacoresistant seizures or developmental delay and usually die at the age of 1 or 2 years [179, 180].

#### b) Steps of mitochondrial H<sub>2</sub>S oxidation

##### • Step 1

The H<sub>2</sub>S-oxidizing process starts with SQR (**Figure 8**). SQR is anchored to the inner mitochondrial membrane with its catalytic domain protruding into the matrix. This flavoprotein oxidizes H<sub>2</sub>S to form a transiently SQR-bound persulfide intermediate, which is then transferred to a small-molecule acceptor [159]. This oxidation yields two electrons that are transferred via FAD to ubiquinone and then to ubiquinol:cytochrome c oxidase (Complex III) of the ETC [159] [181]. Hence, SQR represents the third source of electrons for the ETC in addition to NADH dehydrogenase (Complex I) and succinate dehydrogenase (Complex II), which are involved in the oxidation of organic substrates.

The SQR-bound persulfide is then transferred to an acceptor such as GSH or sulfite (SO<sub>3</sub><sup>2-</sup>), generating GSSH (**Figure 8 – red line**) or thiosulfate (SSO<sub>3</sub><sup>2-</sup>) (**Figure 8 – blue line**), respectively. If thiosulfate is formed during this reaction, a TST is required to transfer the sulfane sulfur from SSO<sub>3</sub><sup>2-</sup> to GSH in order to produce GSSH to feed *ETHE1* [181]. However, recent studies using enzyme activity and nanodisc-incorporated enzymes have demonstrated that GSH is the predominant acceptor of the SQR-bound persulfide [182]. This premise is corroborated by the fact that the administration of cysteine to patients with mutations in the *ETHE1* gene improves H<sub>2</sub>S

Cell type	Cell line	Max stim.	JNaHS/initJO2
Colonic carcinoma	HT29	2.36	2.8
Monocytes	THP1	2.33	2.7
Myoblasts	p. c.	1.96	2.4
Colonic carcinoma	CaCo 2	1.74	1.4
Mammary carcinoma	ZR75-1	1.50	0.8
Myotubes	p. c.	1.50	1.2
Hepatoma	Hep G2	1.43	0.7
Mouse macrophages	p. c.	1.43	5.0
T cell	l. i. c.	1.38	1.7
Fibroblasts	NIH 3T3	1.31	0.6
Ovarian	Hela	1.28	0.5
Ovarian	CHO	1.20	0.7
Placenta	Jeg3	1.03	0.5
Neuroblastoma	SHS-Y5Y	1.03	0.2
Neuroblastoma	N2A	1.01	0.2

*Adapted from Lagoutte et al. 2010 [187]*

**Figure 9: Stimulation of cellular respiration by H<sub>2</sub>S in various cell types**

The different cell types are indicated with the maximal value of stimulation of oxygen consumption (Max stim.) and the relative sulfide exposure at which it occurs (JNaHS/initJO<sub>2</sub>). The name of established cell lines is indicated. Colonocytes (**yellow row**) present the highest capacity to oxidize H<sub>2</sub>S, while neural cells (**orange rows**) present the lowest.

**p. c.:** primary culture; **l. i. c.:** locally immortalized cell

clearance by increasing the levels of GSH, further implicating this molecule as the persulfide carrier [183].

- Step 2

ETHE1 is a dimeric enzyme located in the mitochondrial matrix that, using one molecule of  $O_2$  as cofactor, oxidizes GSSH to  $SO_3^{2-}$  and GSH [140].  $SO_3^{2-}$  can be readily oxidized by enzymes such as myeloperoxidase, prostaglandin H synthase and eosinophil peroxidase generating highly reactive products including the sulfite radical anion ( $SO_3^{\cdot-}$ ), the peroxymonosulfate ( $HSO_5$ ) and the sulfate radical anion ( $SO_4^{\cdot-}$ ) [184]. It is believed that cells limit the damaging potential of  $SO_3^{2-}$  by efficiently converting it to  $SSO_3^{2-}$  by TST, in a reaction in which GSSH acts as cofactor, or into sulfate ( $SO_4^{2-}$ ) by SUOX [140].

- Step 3

SUOX, a hemoprotein present in the intermitochondrial membrane space, oxidizes  $SSO_3^{2-}$  to  $SO_4^{2-}$  (**Figure 8 – red line**), although it can directly oxidize  $SO_3^{2-}$  into  $SO_4^{2-}$  (**Figure 8 – blue line**) [159, 181]. A study published in 1980 has demonstrated that, in rats,  $SO_4^{2-}$  is the major end-product of  $H_2S$  liver and kidney catabolism [185]. A recent study has corroborated these findings [182].

### **c) A double-faced molecule**

The mitochondrial  $H_2S$ -oxidation pathway couples the oxidation of  $H_2S$  to  $SSO_3^{2-}$  and  $SO_4^{2-}$  with the injection of electrons into ubiquinone. As  $O_2$  is required for this process, the efficiency of mitochondrial  $H_2S$  oxidation is expected to depend on  $O_2$  availability, being impaired under hypoxic conditions [186]. Based on the organization of the mitochondrial  $H_2S$  oxidation pathway presented in **Figure 8**, the oxidation of 2  $H_2S$  molecules is expected to require the consumption of 1.5  $O_2$  molecules (1 by ETHE1 and 0.5 by Complex IV) thus rendering the final  $O_2$  consumption per  $H_2S$  to be 0.75 [187, 188].

The real concentration of biologically active  $H_2S$  is determined by balancing  $H_2S$  production and the amount of  $O_2$  available for  $H_2S$  oxidation [189]. However, even the concept that eukaryotes need  $O_2$  to oxidize  $H_2S$  in a dose-depend manner is met with some judgement. For example, when mice were exposed to 80ppm (2.3 mM) of  $H_2S$  their  $O_2$  consumption dropped by 50% and so did their basal metabolic rate, putting them into a suspended animation-like state [9]. In this case, the cells did not use more  $O_2$  to oxidize increasing concentrations of  $H_2S$ .

Almost all cells present the capacity to oxidize H<sub>2</sub>S, with the exception of the central nervous system (**Figure 9**) [160]. In mammals, the main sites of sulfide oxidation are the liver and colon, and the enzyme activity is present in the mitochondria (**Figure 8**) [153, 185]. Previous studies showed that the liver capacity to oxidize H<sub>2</sub>S seems to be species-dependent, with human liver mitochondria showing the highest oxidation rates (followed by pig, rat and finally mouse) [190, 191]. In 2010, Lagoutte *et al.* demonstrated that mitochondrial affinity for H<sub>2</sub>S is very high, which allows its use as an energetic substrate at low micromolar concentrations (1–10 μM) [187]. However, if the supply of sulfide exceeds the oxidation rate, poisoning leads to a complete inhibition of Complex IV, which ultimately renders mitochondria inoperative [188, 192]. In fact, H<sub>2</sub>S inhibition of Complex IV is similar to that of cyanide in the aspect that they both block Complex IV in a non-competitive manner, decreasing the maximal activity without affecting the affinity for O<sub>2</sub> [193]. This makes H<sub>2</sub>S a very peculiar molecule from a bioenergetic point of view, with a double-faced effect on mitochondrial respiration: serving as an inorganic energetic substrate at low concentrations when the mitochondrial H<sub>2</sub>S oxidation pathway is fully operative or as an inhibitory molecule at higher concentrations when the activity of Complex IV becomes impaired [187, 181].

Mitochondria capability to oxidize H<sub>2</sub>S has led to the conventional belief that H<sub>2</sub>S is produced within the cytoplasm and consumed in mitochondria. However, there is evidence to suggest otherwise. MPST/CAT-mediated H<sub>2</sub>S production may occur inside mitochondria [194] and even CSE and CBS may possibly translocate from the cytosol to mitochondria [183]. Furthermore, evidence suggests that the physiological function of this pathway may go beyond the simple detoxification of H<sub>2</sub>S. **The impact of this mitochondrial H<sub>2</sub>S oxidation pathway on cell bioenergetics under specific physiological or pathological situations has to be further elucidated, as well as its ability to produce bioactive sulfur metabolites, such as SSO<sub>3</sub><sup>2-</sup>, whose physiological role has only recently begun to emerge** [195].

## 1.7. Biological effects of H<sub>2</sub>S

### 1.7.1. Vasorelaxation/Vasoconstriction

H<sub>2</sub>S is synthesized by CSE and CBS in various tissues involved in circulatory system homeostasis, including the heart, blood vessels, kidneys and the brain. Many studies conducted in both *in vitro* and *in vivo* models have demonstrated H<sub>2</sub>S as a modulator of the circulatory system, although results were sometimes contradictory (**Figure 10**).

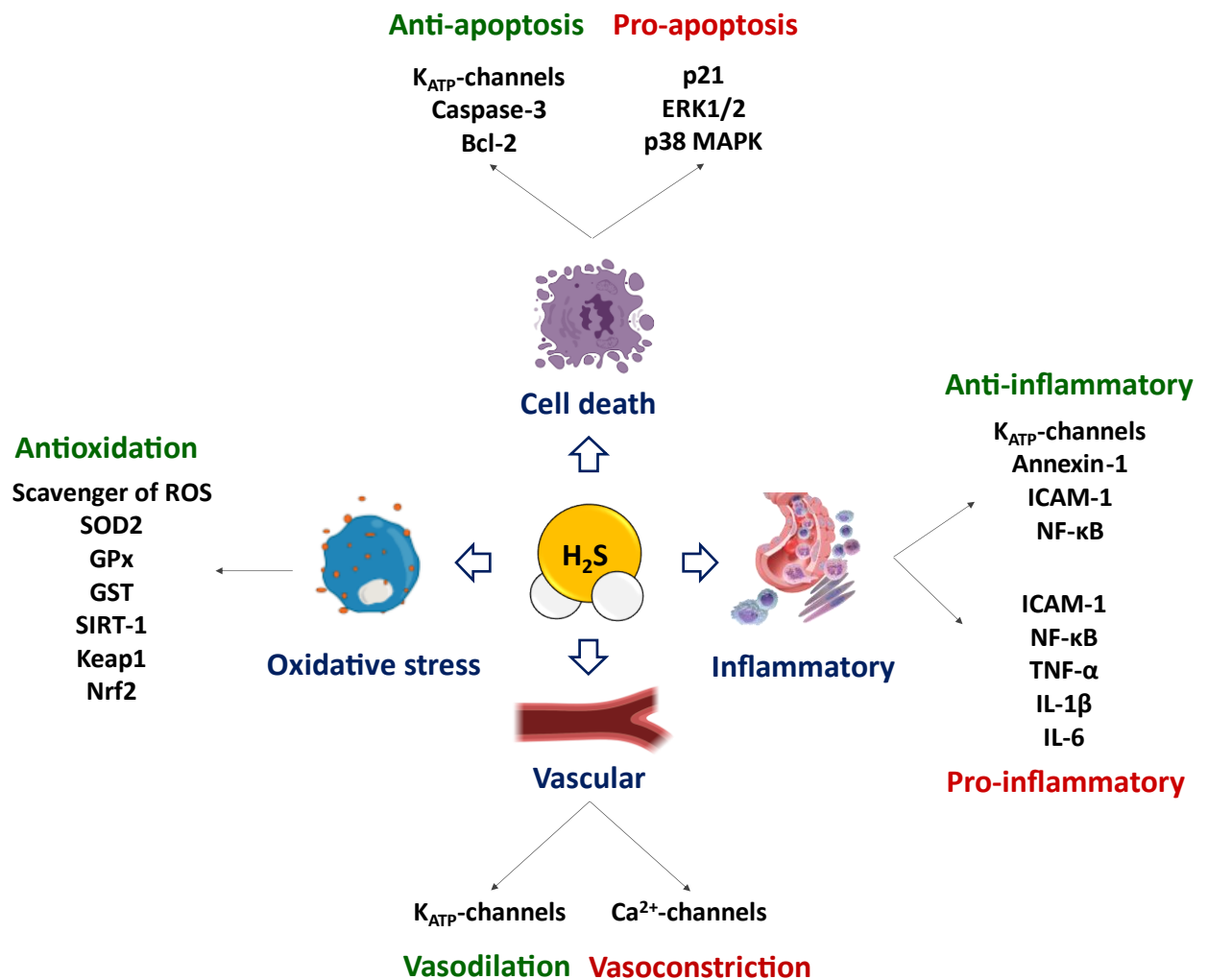


**Figure 10: Biological effects of H<sub>2</sub>S**

**K<sub>ATP</sub>-channel:** potassium ATP-sensitive channels; **Bcl-2:** B-cell lymphoma 2; **p21:** cyclin-dependant kinase inhibitor-1; **ERK1/2:** extracellular signal-regulated protein kinase 1/2; **p38 MAPK:** p38 mitogen-activated protein kinase; **ICAM-1:** intercellular adhesion molecule 1; **NF-κB:** nuclear factor kappa B; **TNFα:** tumour necrosis factor alpha; **IL-1β:** interleukin 1 beta; **IL-6:** interleukin 6; **Ca<sup>2+</sup>-channels:** calcium channels; **ROS:** reactive oxygen species; **SOD2:** superoxide dismutase 2; **GPx:** glutathione peroxidase; **GST:** glutathione S transferase; **SIRT-1:** sirtuin 1; **Keap1:** Kelch-like ECH-associated protein 1; **Nrf2:** nuclear factor erythroid-derived 2-like 2

Over the years, evidence has confirmed that endogenous H<sub>2</sub>S acts as a vasorelaxant, therefore serving as a key regulator of arterial blood pressure [18, 196, 197]. An early study using rat aortic cells has postulated that the mechanism through which H<sub>2</sub>S exerts its vasorelaxant-functions is the opening of ATP-sensitive potassium channels (K<sub>ATP</sub>) [18]. By doing so, H<sub>2</sub>S increases the flow of K<sup>+</sup> ions, which protect cells against excessive shrinkage, and lowers blood pressure by hyperpolarization [18, 198].

The vasorelaxation properties of H<sub>2</sub>S depend on its concentration, the status of the endothelium and the presence of NO. Evidence has shown that both exogenous and endogenous H<sub>2</sub>S are capable of limiting NO bioavailability by directly interacting with NO to produce nitroxyl (product of direct reaction of NO and H<sub>2</sub>S) [199–201]. Conversely, Predmore *et al.* observed that exogenous H<sub>2</sub>S increased the generation of NO by endogenous nitric oxide synthase (eNOS) through a protein kinase B- (Akt)-dependent manner, although the mechanism itself was not divulged [202]. Furthermore, Altaany *et al.* reported that H<sub>2</sub>S increased eNOS activity in mouse endothelial cell lysates through a novel post-translational modification (persulfidation) [203].

Some papers suggest that, aside K<sub>ATP</sub> channels, H<sub>2</sub>S exerts its functions of vasorelaxant/vasoconstrictor molecule through a Ca<sup>2+</sup>-dependent mechanism. In 2015, Zhong *et al.* demonstrated that a Ca<sup>2+</sup>-sensing receptor stimulated CSE-derived H<sub>2</sub>S production in rat vascular muscle cells [204]. A couple of years later, Wang *et al.* would corroborate these findings but, this time, in aorta endothelial cells from rats [205]. Given that H<sub>2</sub>S functions as an endothelial cell-derived relaxing factor, it is likely that H<sub>2</sub>S has a direct impact on vascular walls. Studies have shown that, in both mice and human models, the deprivation of endogenously produced H<sub>2</sub>S contributes to the development of hypertension, a key contributory factor in cardiovascular disease [118, 201]. Furthermore, in the vessel wall of spontaneously hypertensive rats, CSE levels are reduced, while CSE KO mice display elevated blood pressure and reduced endothelial-dependent responses [118, 206]. This suggests that H<sub>2</sub>S homeostasis may play an important role in the development of cardiovascular diseases. In fact, the administration of exogenous H<sub>2</sub>S has been reported to attenuate several cardiovascular perturbations, namely heart failure [207], ischemic myocardium [208], atherosclerosis [209], and hypertension [210].

However, other studies have suggested that H<sub>2</sub>S has vasoconstricting actions. Ping *et al.* found that H<sub>2</sub>S promoted vasocontraction of rat coronary artery by promoting Ca<sup>2+</sup> influx [211]. Similarly, Orlov *et al.* showed that H<sub>2</sub>S would trigger vasoconstriction in rat aortic rings through the activation of Ca<sup>2+</sup> influx via L-type channels, while Sun *et al.* showed that H<sub>2</sub>S would inhibit L-type Ca<sup>2+</sup>-channels in rat cardiomyocytes [212, 213]. Furthermore, in the brain, H<sub>2</sub>S facilitates the

induction of hippocampal long-term potentiation (LTP) [214]. For H<sub>2</sub>S this effect depends on the activation of N-methyl D-Aspartate (NMDA) receptors whereas for NO and CO this induction occurs independently of NMDA receptors [214].

### 1.7.2. Inflammation

Over the years, several papers have confirmed the involvement of H<sub>2</sub>S in inflammatory events, although results were sometimes contradictory (**Figure 10**).

#### **a) Anti-inflammatory**

One of the earliest events in an inflammatory reaction is the recruitment of leukocytes to the site of injury. According to Zanardo *et al.*, H<sub>2</sub>S acts as an anti-inflammatory agent by regulating the leukocyte-endothelial interface [215]. Inhibitors of CSE increased leukocyte-endothelial adhesion in rat mesenteric venules, while the use of H<sub>2</sub>S donors (NaHS and Na<sub>2</sub>S) suppressed the process [215]. According to the authors of this paper, the anti-inflammatory effects of H<sub>2</sub>S were exerted via activation of K<sub>ATP</sub> channels [215].

The mechanisms underlying the ability of H<sub>2</sub>S to inhibit leukocyte adherence to the vascular endothelium also involve the anti-inflammatory protein, annexin-1. Annexin-1 is contained within neutrophils, being released to restrain inflammation and restore homeostasis. In human neutrophils, NaHS triggers a striking translocation of annexin-1 from the cytosol to the cell surface, an event associated with inhibition of cell/endothelium interaction [216].

H<sub>2</sub>S has also been shown to suppress the expression of intracellular adhesion molecule-1 (ICAM-1) in response to high glucose concentrations in human umbilical vein endothelial cells [217]. This suppression resulted in a reduction of intracellular reactive oxygen species (ROS) levels and inhibition of the activity of nuclear factor-kappa B (NF-κB) – a pro-inflammatory transcription factor [217]. Additional evidence has demonstrated that H<sub>2</sub>S can directly downregulate NF-κB in a macrophage-like cell line, through the inhibition of its phosphorylation, nuclear translocation and DNA binding activity [218]. Recently, Sun *et al.* observed that H<sub>2</sub>S blocks the activation of the NF-κB signalling pathway, decreases the intracellular ROS production and downregulates the mRNA expression levels of several pro-inflammatory cytokines in a lipopolysaccharide- (LPS-) induced inflammation model [219].

## **b) Pro-inflammatory**

Contrarily to the evidence presented so far, some studies suggest that H<sub>2</sub>S can act as a pro-inflammatory mediator. Such is the case of Zhang *et al.* [220]. In their paper published in 2007, H<sub>2</sub>S upregulated the expression of adhesion molecules (ICAM-1, P-selectin, and E-selectin) in mouse lung and liver [220]. These results were later corroborated by the study of Tamizhselvi *et al.*, who have shown that H<sub>2</sub>S induces ICAM-1 expression and promotes neutrophil adhesion in an *in vitro* model of acute pancreatitis [221]. Zhi *et al.* have also demonstrated that human monocytes treated with NaHS presented activation of NF-κB phosphorylation and increased mRNA and protein levels of the pro-inflammatory cytokines tumour necrosis factor alpha (TNFα), IL-1β and IL-6 [222]. Recently, H<sub>2</sub>S has been associated with the development of human osteoarthritis [223] and rodent acute pancreatitis [224].

### 1.7.3. Apoptosis and cell proliferation

Apoptosis or programmed cell death is a highly regulated cellular suicide program that is critical for several biological processes such as normal development and maintenance of tissue homeostasis in multicellular organisms. In tumours, apoptosis allows cancerous cells to survive against oncogene activation, uncontrolled proliferation, and chemotherapy. Studies have shown that H<sub>2</sub>S is critical in the regulation of cell proliferation (**Figure 10**).

Pan *et al.* have demonstrated that inhibition of endogenous H<sub>2</sub>S/CSE pathway drastically decreased the proliferation of HepG2 and PLC/PRF/5 hepatoma cells, as it also increased ROS production, mitochondrial disruption, DNA damage and apoptosis [119]. Similarly, Zhen *et al.* observed that treatment with NaHS augmented cell viability in PLC/PRF/5 hepatoma cells by decreasing caspase-3 production [225]. Caspase-3 expression was also found decreased in C6 glioma cells after treatment with NaHS [226]. This and additional data indicate that H<sub>2</sub>S may serve as an anti-apoptotic molecule in the development of diseases that involve excessive cell growth and division. For example, overexpression of CBS in a human neuroblastoma cell line (SH-SY5Y) reduced cell death after 6-hydroxydopamine-induced apoptosis [227]. In 2020, Fouad *et al.* found that NaHS treatment in a rodent model of hepatotoxicity prevented apoptosis by downregulating the levels of the pro-apoptotic protein Bax and upregulating the levels of the anti-apoptotic protein Bcl-2 [228].

The preservation of mitochondrial integrity is key to the anti-apoptotic effect of H<sub>2</sub>S as mitochondria usually abet the apoptotic process. As previously mentioned, H<sub>2</sub>S has the capability to open K<sub>ATP</sub> channels in both plasma and mitochondrial membrane. Selectively blockade of



mitochondrial  $K_{ATP}$  channels with 5-hydroxydecanoate has been shown to reverse the protective effects of NaHS against rotenone-induced apoptosis of neuroblastoma cells [229]. In a similar way, blockade of mitochondrial  $K_{ATP}$  channels reversed the cardioprotective effects of NaHS against high glucose-induced cytotoxicity, apoptosis, oxidative stress and mitochondrial damage in H9c2 cardiac cells [230].

However, much like all other biological processes regulated by  $H_2S$ , the role of this gasotransmitter in apoptosis is also a matter of controversy. Yang *et al.* observed that smooth muscle cells isolated from CSE KO mice displayed higher proliferation rate and were more susceptible to apoptosis induced by exogenous  $H_2S$  [231]. According to the authors, these pro-apoptotic cellular effects of  $H_2S$  were mediated by an upregulation of cyclin-dependent kinase inhibitor 1 (p21) expression [231]. Another study has described that the overexpression of CSE in human aorta smooth muscle cells promotes apoptosis through increased extracellular signal-regulated protein kinase 1/2 (ERK1/2) activation, up-regulation of p21 and downregulation of cyclin D1 expression [232]. Yang *et al.* have also demonstrated that CSE overexpression or exogenously applied  $H_2S$  would decrease cell viability in INS-1E cells, an insulin-secreting beta cell line [233]. The pro-apoptosis effects of  $H_2S$  were linked to the activation of p38 mitogen-activated protein kinase (p38 MAPK) [233].

#### 1.7.4. Oxidative stress

Oxidative stress is characterized by an imbalance between free radicals (ROS) and antioxidants in your body. This imbalance can result in DNA damage, protein misfolding, organelle injury, and neuronal synaptic dysfunction. However, over the years, studies have shown that  $H_2S$  can reduce these detrimental impacts caused by oxidative stress (**Figure 10**).

The major ROS species produced in cells are superoxide ( $O_2^-$ ), hydrogen peroxide ( $H_2O_2$ ), and NO. In the ROS scavenging pathway, superoxide dismutase (SOD) transfers  $O_2^-$  to  $H_2O_2$ , which is converted to  $O_2$  and  $H_2O$  by catalase. Some papers have suggested that  $H_2S$  is a participant of this process by scavenging ROS. In 2004, Geng *et al.* reported that  $H_2S$  could reduce lipid peroxidation by scavenging  $H_2O_2$  and  $O_2^-$  following isoproterenol-induced myocardial ischemic injury [234]. Pei *et al.* have also observed that NaHS would protect cardiomyocytes from  $H_2O_2$ -induced apoptosis by upregulating SOD2-dependent ROS scavenging [235]. Similarly, H9c2 cardiomyocytes treated with NaHS presented decreased ROS production and enhanced expression of SOD, glutathione peroxidase (GPx) and glutathione-s-transferase (GST) after  $H_2O_2$ -induced oxidative stress [236]. These  $H_2S$  antioxidant effects were also associated to an

upregulation of sirtuin 1 (SIRT1) expression, a protein that promotes cell survival under oxidative stress [236].

Aside regulating the levels of  $O_2^-$  and  $H_2O_2$ ,  $H_2S$  acts as a direct scavenger of peroxynitrite ( $ONOO^-$ ), a cytotoxic species formed from rapid interaction of  $O_2^-$  and NO. Cell toxicity induced by  $ONOO^-$  can be significantly inhibited by NaHS treatment in the human neuroblastoma cell line, SH-SY5Y [237].

Additionally, it has been reported that  $H_2S$  can increase the levels of a major cellular antioxidant, GSH. Evidence has shown that  $H_2S$  enhances the transport of cysteine to increase GSH production rather than cystine transport in Neuro2a cells [238]. The efficiency of GSH production enhanced by  $H_2S$  was even 4-fold greater under oxidative stress [238]. In fact, the CSE/ $H_2S$  system appears to be crucial in maintaining cellular glutathione status. CSE-siRNA-transfected cells presented decreased GSH concentration and glutathione ratio (GSH/GSSG) [239]. However, incubation of these cells with exogenous  $H_2S$  increased the values of both GSH concentration and GSH/GSSG ratio [239]. Furthermore, the administration of exogenous  $H_2S$  preserved the cellular glutathione status under BSO (buthionine sulfoximine)-induced glutathione depletion [239]. These results were recently corroborated by Parsanathan and Jain [240]. In their study, the use of CSE siRNA to induce deficient endogenous  $H_2S$  production in  $C_2C_{12}$  myotubes caused an increase in  $H_2O_2$  and ROS levels, and downregulated GSH biosynthesis [240].

Dahl rats, a rodent model of hypertension and progressive kidney injury, submitted to a high-salt diet for 8 weeks presented increased blood pressure, impaired renal function and diminished  $H_2S$  content [241]. However, administration of the fast-release  $H_2S$  donor NaHS decreased blood pressure, increased antioxidant defences, and improved renal function. According to this study,  $H_2S$  activated nuclear factor erythroid 2-related factor 2 (Nfr2) by inducing Keap-1 persulfidation, leading in the end to the improvement of renal oxidative stress.

### 1.7.5. Protein modification

#### **a) The reaction**

First described in 2009, persulfidation is a novel post-translational modification mechanism that allows a simple gas molecule such as  $H_2S$  to interact with signalling proteins in our body [242]. In the literature, this modification is also referred to as “sulphydration”, which implies “hydration” and is inaccurate. Instead, the process involves “sulfuration”, ergo, the addition of a sulfur atom (S) [243]. The reaction itself consists in the conversion of the cysteine thiol (-SH) groups to persulfide (-SSH) groups (**Figure 11**).

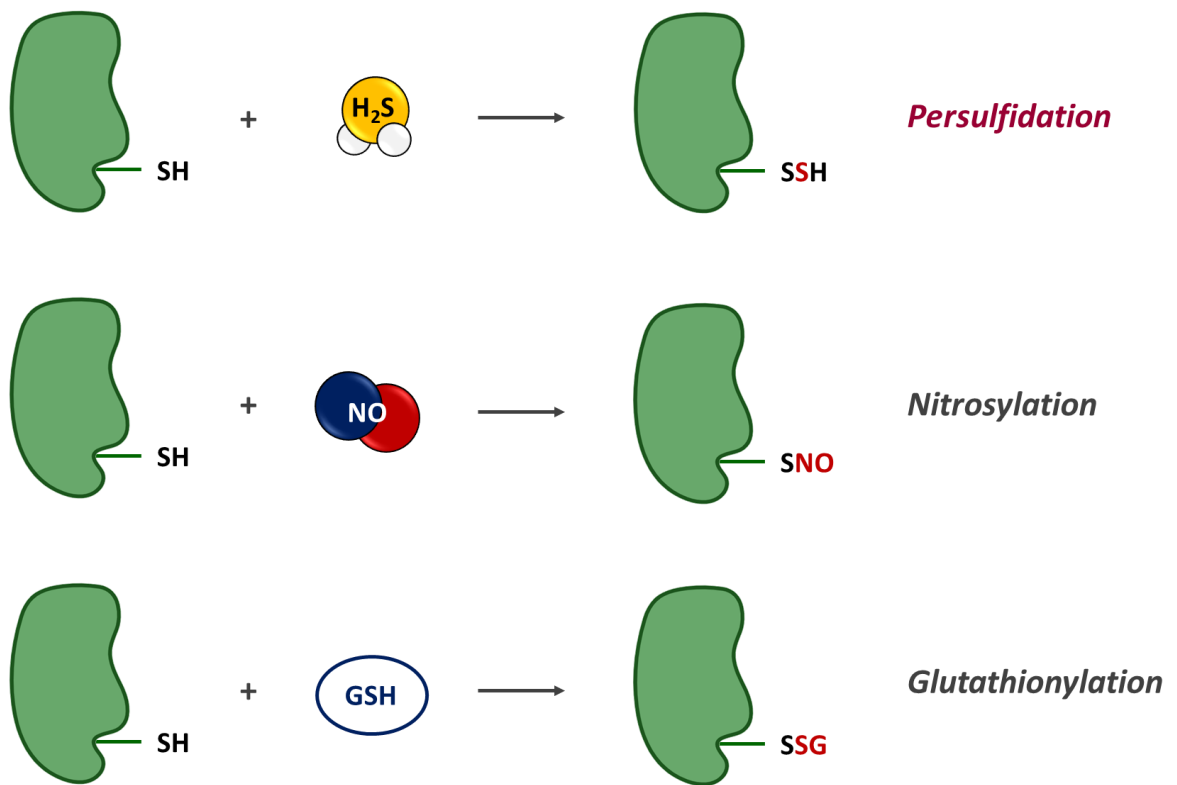
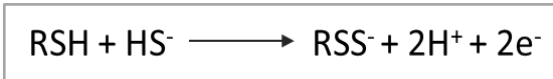


**Figure 11: Protein thiol modifications mediated by either the incorporation of H<sub>2</sub>S (persulfidation), NO (nitrosylation) or GSH (glutathionylation)**

**NO:** nitric oxide; **GSH:** glutathione

However, the original misconception of the persulfidation reaction was that H<sub>2</sub>S can react directly with the -SH groups in the proteins to form protein persulfide. This reaction is impossible due to the thermodynamic constraints. For this post-translation modification to occur, the cysteine residue must exist in an oxidized state, such as sulfenic acid or disulfide, which is subsequently attacked by the HS<sup>-</sup> anion to give a persulfide product [243]. The reaction between the HS<sup>-</sup> anion and the thiol residue to create the protein-bound persulfide is the following:



In oxidizing compartments, like the ER or the extracellular milieu, oxidized cysteines in proteins are relatively common. However, in the cytoplasmic compartment, which is reducing, oxidized cysteines in proteins have to be stabilized and set apart [242]. Since the imperative condition for persulfidation is the availability of free -SH groups, when this prerequisite cannot be met and the existence of a disulfide bond limits the access of H<sub>2</sub>S to the -SH groups, a two-step process takes place. First, H<sub>2</sub>S disrupts disulfide bonds within proteins by acting as a reducing agent. This would help expose the free -SH groups. Second, H<sub>2</sub>S persulfidates the cysteine residue [244].

Similar to other modifications in protein thiols such as S-nitrosylation and S-glutathionylation (**Figure 11**), H<sub>2</sub>S-mediated persulfidation has been found in several proteins and demonstrated to play a big role in H<sub>2</sub>S-mediated signalling processes. In fact, persulfidation and S-nitrosylation have striking similarities. Both involve the covalent modification of cysteines and both are reversible by reducing agents, such as dithiothreitol (DTT) [22].

However, some significant differences between the two processes have been identified. Whereas approximately 10–25% of endogenous glyceraldehyde 3-phosphate dehydrogenase (GAPDH), tubulin, and actin are persulfidated *in vivo*, only 1-2% of the same proteins are S-nitrosylated. Furthermore, unlike S-nitrosylation, persulfidation usually enhances the activity of the modified proteins. For example, it has been shown that GAPDH activity is significantly lower in CSE KO mice than in wild-type mice, and that exogenous H<sub>2</sub>S can increase GAPDH activity [22]. Compared to S-nitrosylation, persulfidation seems to be more stable and its detection by mass spectrometry appears to be relatively easy. Furthermore, persulfidation occurs without the need of physiological stimulation. This is demonstrated by the 25-30% reduction of liver GAPDH persulfidation in CSE KO animals while in KO of nitric oxide synthase (NOS) S-nitrosylation of GAPDH is not affected [242].

## **b) Importance of protein persulfidation**

The majority of proteins identified as targets for persulfidation is involved in metabolism and energy homeostasis, such as gluconeogenesis, FA oxidation and the TCA cycle [22]. In fact, a variety of key proteins of different cellular pathways are persulfidated by H<sub>2</sub>S in mammals, being known to regulate and affect the processes of cell survival/death, cell proliferation, mitochondrial bioenergetics, cellular metabolism, inflammation, ER stress, oxidative stress and even vasorelaxation [22].

Untereiner *et al.* have demonstrated that H<sub>2</sub>S upregulates the expression levels of peroxisome proliferator-activated receptor gamma coactivator 1-alpha (PGC-1α) and phosphoenolpyruvate carboxykinase (PEPCK) via glucocorticoid receptor; upregulates the expression levels of PGC-1α through the cAMP/PKA pathway and PGC-1α activity through persulfidation; and promotes persulfidation-dependent upregulation of both expression and activity of glucose-6-phosphatase (G6Pase) and fructose-1,6-biphosphatase (FBPase) [245].

Ju *et al.* found that *in vitro* stimulation with NaHS would augment pyruvate carboxylase (PC) activity in both HepG2 and mouse primary hepatocytes [246]. H<sub>2</sub>S also induced PC persulfidation at cysteine 265, reaction that was exacerbated by CSE overexpression and abrogated by CSE KO. This premise suggested that H<sub>2</sub>S enhances glucose production through persulfidation of PC. In addition, high-fat feeding of mice decreased both CSE expression and PC persulfidation in the liver, while glucose deprivation of HepG2 cells stimulated CSE expression [246].

Since it was first discovered, persulfidation has taken a considerable place under the spotlight as one of the most important and appealing mechanisms by which the H<sub>2</sub>S gasotransmitter acts upon a specific system. In fact, persulfidation appears to be common to a great deal of proteins, a considerable amount of which found to intervene in important metabolic pathways. In plants, the estimated percentage of persulfidated proteins varies from 5 – 25% of the entire proteome, depending on the method of detection and cellular model used [247]. However, we still require further elucidation on the specific sites targeted by this post-translational modification. Only then can we draw a wider picture and achieve a deeper comprehension on the protective effects of H<sub>2</sub>S.

### **1.8. Inhibitors of H<sub>2</sub>S biosynthesis**

In order to investigate the role of this new gasotransmitter, small-molecule inhibitors of the different H<sub>2</sub>S-producing enzymes have been commonly used to decrease H<sub>2</sub>S synthesis in

studies using isolated enzymes or cell culture models. These inhibitors can be small interfering RNA (siRNA) molecules, which are used to develop knock-down (KD) or KO models, or pharmacological agents [248–250]. However, given that genetic and siRNA approaches require additional expertise and access to specialized facilities, most researchers rely on pharmacological inhibitors.

Commonly used as CBS and/or CSE inhibitors with  $IC_{50}$  below 1mM are L-aminoethoxyvinylglycine (AVG, 1  $\mu$ M),  $\beta$ -cyano-L-alanine (BCA, 14  $\mu$ M), propargylglycine (PAG, 40  $\mu$ M) and aminooxyacetic acid (AOAA, 1.09  $\mu$ M) [251]. The first selective inhibitor of MPST (compound 3) has been very recently reported [252].

In 2013, Asimakopoulou *et al.* published a study in which they compared the efficiency of AVG, BCA, PAG and AOAA [251]. According to their results, AVG is a selective CSE inhibitor and the most powerful among all four inhibitors tested [251]. PAG, on the other hand, was described as the weakest inhibitor of all four. Also a CSE selective inhibitor, PAG could not inhibit recombinant CBS even when used at high millimolar concentrations (above 10 mM) [251]. In fact, the crystal structure of the covalent complex PAG-CSE is the only described so far [253]. The same study has shown that BCA is a more potent CSE inhibitor than PAG, although both substances exert their actions in a PLP-dependent manner. Interestingly, PAG is an irreversible inhibitor of CSE, while BCA is a reversible inhibitor [251]. AOAA, a typically CBS “selective” inhibitor, also exerted some effect on CSE [251]. Recently, Chao *et al.* found that the addition of a methyl ester group on AOAA enhances the cellular uptake of AOAA, and the new molecule (YD0171) presents higher potency and selectivity [254].

## **1.9. Donors of exogenous sulfide**

### **1.9.1. Fast-release donors**

#### **a) Sulfide salts**

Sulfide salts (NaHS and Na<sub>2</sub>S) are the most widely used H<sub>2</sub>S donors. Although commonly referred to as donors, sulfide salts are simply solid analogues of the gas, providing direct, instantaneous access to the biologically relevant forms of sulfide (HS<sup>-</sup> and H<sub>2</sub>S) [255].

Sulfide salts have been used to evaluate the therapeutic potential of exogenous H<sub>2</sub>S delivery in several pathological scenarios. For example, IV administration of 0.5 mg/kg Na<sub>2</sub>S has been shown to improve survival rate after cardiac arrest in mice [256] while the administration of 20 mg/kg Na<sub>2</sub>S has been shown to attenuate acute cerebral ischemia in rats [257]. Similarly, the

administration of 5.6 mg/kg NaHS has been shown to attenuate cerebral ischemia/reperfusion (I/R) injury in rats [258].

However, the use of sulfide salts triggers some concerns. Firstly, depending on the company and batch, commercially available reagents can have extremely poor quality. This is particularly true for NaHS, whose purity can go as low as 60%. Secondly, the liberation of H<sub>2</sub>S from sulfide salts does not match the slow and continuous release characteristic of endogenous H<sub>2</sub>S biosynthesis. In fact, the administration of a single bolus of NaHS or Na<sub>2</sub>S to *in vitro* or *in vivo* models may be detrimental, since H<sub>2</sub>S above a certain concentration level is extremely toxic [259]. Thirdly, since NaHS and Na<sub>2</sub>S hydrolyse immediately upon dissolution in water, once the solution is prepared volatilization of H<sub>2</sub>S occurs, lowering the overall concentration of sulfur species [45] [255]. To this issue can be added the air oxidation of HS<sup>-</sup> catalysed by trace metals in water, which further reduces the actual concentration of H<sub>2</sub>S in solution [45, 255].

#### **b) Thiosulfate (SSO<sub>3</sub><sup>2-</sup>)**

Until recently, thiosulfate (SSO<sub>3</sub><sup>2-</sup>) has been viewed as an inactive by-product of H<sub>2</sub>S catabolism. However, studies over the last 5 years have indicated that cells show the ability to reduce thiosulfate and regenerate H<sub>2</sub>S from it in a cell- and tissue-dependent fashion and, at least in part, via mechanisms that involve MPST and TST [87–89].

In experimental models, thiosulfate is administered under the form of sodium thiosulfate (STS, Na<sub>2</sub>S<sub>2</sub>O<sub>3</sub>). Unlike NaHS or Na<sub>2</sub>S, STS presents no apparent toxicity even when used at concentrations as high as 20 mM [260]. The therapeutic efficacy of STS has been seen in rodent models of LPS-induced lung injury [261], LPS-induced acute liver failure [262], angiotensin-induced hypertension [263] and hypertensive heart disease [210], cerebral ischemia [264], cardiac ischemia-reperfusion injury [265], vascular calcification [266] and renal dysfunction [260], at doses ranging from 10 to 2000 (mg/kg)/day. In humans, the short-term therapeutic use of STS has been proven safe for the treatment of calciphylaxis [267–269]. Furthermore, in clinical observational studies, plasma thiosulfate levels show positive correlations with improved clinical outcomes in renal transplantation [270, 271]. Ultimately, given that STS is a clinically safe drug that has been long used to treat cases of sodium nitroprusside/cyanide intoxication [272], the therapeutic application of STS in a variety of diseases that may benefit from H<sub>2</sub>S supplementation is considerable.

### 1.9.2. Slow-release donors

Driven by the limitations presented by sulfide salts or natural sulfide donors (ex: garlic), researchers have developed slow-release H<sub>2</sub>S donors that better mimic the gradual H<sub>2</sub>S production during enzymatic biosynthesis.

#### **a) GYY4137**

In 2008, Li *et al.* described the first slow-releasing H<sub>2</sub>S donor: morpholin-4-ium 4-methoxyphenyl(morpholino) phosphinodithioate (GYY4137) [273]. In aqueous solution at physiological pH and temperature, GYY4137 releases low quantities of H<sub>2</sub>S over a sustained period of time [273]. Intravenous or intraperitoneal injection (IP) of GYY4137 solutions (133 μmol/kg) in rats showed an increase in plasma sulfide levels after 30 min, which was sustained for 2 h [273]. Zheng *et al.* would later report that GYY4137 could maintain H<sub>2</sub>S levels in cell culture above baseline for over 7 days [274].

The release of H<sub>2</sub>S from GYY4137 occurs through a two-step hydrolytic degradation that appears to be pH and temperature dependent, with less H<sub>2</sub>S released at 4 °C and greater release at pH 3.0 [237, 239]. Due to its commercial availability and ease of handling, GYY4137 is the most widely studied H<sub>2</sub>S donor aside sulfide salts. Several papers have documented the pharmacological effects of GYY4137 as a vasorelaxant [237], an anti-inflammatory [275], an antithrombotic agent [276] and a tumour growth inhibitor [277] in both *in vitro* and *in vivo* models.

GYY4137 offers considerable advantages over the use of NaHS and Na<sub>2</sub>S. The slow rate of H<sub>2</sub>S generation from GYY4137 hydrolysis, rather than a single concentrated bolus of NaHS or Na<sub>2</sub>S, mirrors the enzymatic biosynthesis of H<sub>2</sub>S in mammalian systems [273, 278]. In a direct amperometric comparison of H<sub>2</sub>S release rates from GYY4137 and NaHS, GYY4137 released H<sub>2</sub>S with a peaking time of 10 min versus 10 seconds for NaHS in phosphate buffer pH 7.4 [273]. However, the peaking concentration for GYY4137 was 40-fold lower than for NaHS, even when the concentration of GYY4137 was increased 10x [273]. Researchers suggest that, although the final concentrations of GYY4137-generated H<sub>2</sub>S are lower, they are also likely more physiologically relevant than a single administration of concentrated sulfide salt. Another positive characteristic of GYY4137 is its high solubility in water, which allows concentrated stock solutions to be prepared and used immediately in *in vitro* or *in vivo* assays without the need for organic solvents (commonly required for other drugs).

GYY4137 enhanced mitochondrial function and glycolysis in the HCT116 human colorectal carcinoma cells [279]. H<sub>2</sub>S induced persulfidation of lactate dehydrogenase A (LDHA) at cysteine



163, stimulating its activity. This correlates with the higher lactate levels found in these cells. The isoform LDHB was also upregulated by H<sub>2</sub>S but at a somewhat lower extent. Furthermore, the incubation with GYY4137 significantly increased cell proliferation rate [279].

Although GYY4137 has proven to be a useful tool, some issues have been noticed regarding its use. For instance, GYY4137 is often prepared and sold as a dichloromethane complex, which is metabolized to CO, another gasotransmitter with biological effects similar to those of H<sub>2</sub>S [280]. Therefore, there is a general concern that part of the effects attributed to GYY4137-derived H<sub>2</sub>S may in fact come from CO. Furthermore, unlike NaHS or Na<sub>2</sub>S whose by-products can almost be neglected, synthetic donors such as GYY4137 are structurally complicated and may produce biologically active by-products after H<sub>2</sub>S release.

### **b) Other donors**

Recently, Feng *et al.* synthesized a series of compounds based on the structure of GYY4137 [281]. Among these compounds was 3-dihydro-2-phenyl-2-sulfanylenebenzo[d][1,3,2]oxazaphosphole (FW1256), which has shown a higher capacity to inhibit cancer development in MCF7 lines than GYY4137 (IC<sub>50</sub>: 5.7 μM for FW1256 versus 368 μM for GYY4137) [281]. FW1256 was later described as an anti-inflammatory agent for mice challenged with LPS [282].

## **1.10. Methods of H<sub>2</sub>S quantification**

As mentioned earlier in this chapter, in an aqueous solution, sulfide can be found as the gas H<sub>2</sub>S or one of its dissociated forms (HS<sup>-</sup> and S<sup>2-</sup>). Both HS<sup>-</sup> and H<sub>2</sub>S have a high propensity to oxidize, especially in the presence of oxygen (ex: water-based solutions) [28]. In addition, being a gas, H<sub>2</sub>S can rapidly diffuse across membranes and react with different biological matrixes (ex: proteins, heme, GSH...). Furthermore, H<sub>2</sub>S levels can differ according to the age, tissue and even measuring technique (**Figure 12**). Therefore, finding an accurate and 100% reliable method to quantify *in vivo* H<sub>2</sub>S reminds us of the quest to find the Holy Grail. Even so, in this manuscript, we describe general classes of analytical tools for H<sub>2</sub>S detection and quantification that are used today in analytical studies.

### **1.10.1. Lead acetate strips**

Lead acetate (Pb(C<sub>2</sub>H<sub>3</sub>O<sub>2</sub>)<sub>2</sub>) impregnated paper strips are widely used to qualitatively detect H<sub>2</sub>S in the atmosphere and in solution with high sensitivity [283]. Pb(C<sub>2</sub>H<sub>3</sub>O<sub>2</sub>)<sub>2</sub> reacts with

<b>Species</b>	<b>Sample</b>	<b>[H<sub>2</sub>S]</b>	<b>Method</b>
Rat	Plasma	300 μM	MB
Rat	Plasma	30-50 μM	Sensitive electrode
Mouse	Plasma	40 μM	Sensitive electrode
Mouse	Plasma	<100 nM	Polarographic sensor
Mouse	Plasma	100 pM	GC
Human	Plasma	25-80 μM	GC
Human	Plasma	1 μM	MB
Human	Plasma	38-70 μM	Sensitive electrode
Rat	Liver	26-144 μM	MBB/HPLC
Mouse	Liver	17 nM	GC
Mouse	Brain	2 μM	MB
Mouse	Brain	17 nM	GC
Rat	Kidney	40-200 μM	MBB/HPLC
Mouse	Kidney	6 μM	MB

**Figure 12: H<sub>2</sub>S quantification in different tissues and using different methods**

**MB:** methylene blue method; **MBB:** monobromobimane derivatization method; **HPLC:** high performance liquid chromatography; **GC:** gas chromatography

the H<sub>2</sub>S present to form lead sulfide (PbS) and acetic acid (2CH<sub>3</sub>COOH). PbS forms as a black precipitate that is proportional to the amount of H<sub>2</sub>S present in the sample. These strips are widely used for the qualitative detection of microbial H<sub>2</sub>S production by inserting a Pb(C<sub>2</sub>H<sub>3</sub>O<sub>2</sub>)<sub>2</sub>-soaked paper strip between the plug and inner wall of a culture tube, above the inoculated medium [284].

### 1.10.2. Methylene blue method

The methylene blue (MB) method published in 1949 is one of the earliest and most common methods used for H<sub>2</sub>S measurement [285]. In this method, H<sub>2</sub>S present in a given suspension is precipitated as zinc sulfide. The precipitate is redissolved, treated with an acid solution of p-aminodimethylaniline and allowed to react with a small amount of ferric chloride [285]. After some time, MB is formed. The optical density of this solution is then measured at 670nm and the results are calculated based on a previously prepared calibration curve of MB [285]. At the time, the minimum concentration of H<sub>2</sub>S that this method could detect was 3µg [285].

A couple of decades later, in 1969, the MB assay was perfected by using n,n-dimethyl-p-phenylenediamine sulfate, which ended up increasing the sensitivity of the method by 10% [286]. With this adaptation, the MB technique could detect H<sub>2</sub>S concentrations starting from 1µM [286] [287–290]. However, recent evidence has demonstrated that the detection limit of the MB method for H<sub>2</sub>S is only 2µM rather than the previously reported lower values [291]. Generally, the MB method is regarded as a low sensitive assay through which an overestimation of H<sub>2</sub>S may be achieved due to forceful sulfide-extraction under the highly acidic conditions. In 2020, Li *et al.* combined the MB assay with surface-enhanced Raman spectroscopy (a highly sensitive technique), which enhanced the detection limit of this method to the nanomolar range (concentrations above 3.7nM) [292]. Last but not least, the MB method has been adapted into a commercial assay kit to facilitate its use.

### 1.10.3. Monobromobimane derivatization

The Monobromobimane derivatization (MBB) method has been extensively used in biological samples to measure the concentration of H<sub>2</sub>S. This assay utilizes monobromobimane (mBB) to derivatize H<sub>2</sub>S under basic conditions (pH 9.5) [201, 206]. This reaction generates fluorescent sulfide dibimane (SdB) that is subsequently quantified by high performance liquid chromatography (HPLC) [31, 201, 206, 293].

The MBB method is very sensitive (detection limit of 2 nM) and allows the detection and quantification of all three sulfide biological forms: free hydrogen sulfide, acid-labile sulfide and

bound sulfane sulfur [291, 294, 295]. Recently, this method has proved itself useful in the detection and quantification of different poly- and persulfides, providing analytical information about these important reactive sulfur species [296]. However, it has been revealed that, for the same sample, the concentration of H<sub>2</sub>S measured under pH 9.5 seems to be higher than that under pH 8.0, possibly due to the release of H<sub>2</sub>S from some bound sulfide under basic conditions [294]. This means that, when comparing samples, the control of pH is absolutely imperative [294].

In 2017, the MBB method was improved by including <sup>36</sup>S-labeled sulfide-dibimane as an internal standard and by measuring the derivatized products by liquid chromatography with tandem mass spectrometry (LC-MS/MS) instead of HPLC [145]. These alterations conferred extra sensitivity and feasibility to the method and also made it suitable for large-scale analysis (300–400 samples per day). In fact, the updated MBB method allowed the quantification of H<sub>2</sub>S levels in a broad range of biological samples, such as blood, plasma, tissues (heart, liver and kidney) and cells across different species (yeast, mice, rat and human) [145].

#### 1.10.4. Gas chromatography

The gas chromatography (GC) method was first used in 1988 by Shigetoshi *et al.* [297]. This assay could successfully detect H<sub>2</sub>S levels in rat blood, being its lowest limit of detection 0.3 μM [297–299]. Recently, Furne *et al.* have improved this method by combining GC with a chemiluminescence sulfur detector [300]. This adaptation improved the sensitivity of the method to detect concentrations over 0.5 pmol [300]. Although sensitive and specific, the need for special equipment to process the samples make this method not widely used.

#### 1.10.5. Ion sensitive electrodes

Ion sensitive electrodes are easy to handle and relatively inexpensive [301, 302]. They are able to measure S<sup>2-</sup> ions in a given solution with near-perfect selectivity (detection limit of 100 nM) [117, 303–305]. The electronic voltage measured is further calculated as H<sub>2</sub>S concentration. This method does not require H<sub>2</sub>S derivatization, thus being suitable for real-time quantification [301, 302]. However, in order to apply this method, samples must undergo an alkaline pre-treatment to shift proton dissociation from H<sub>2</sub>S to S<sup>2-</sup> [302]. This means that the value of H<sub>2</sub>S obtained represents the total sulfide content instead of just the freely available H<sub>2</sub>S, which makes this value higher than what in reality is [214].

#### 1.10.6. Polarographic sensors

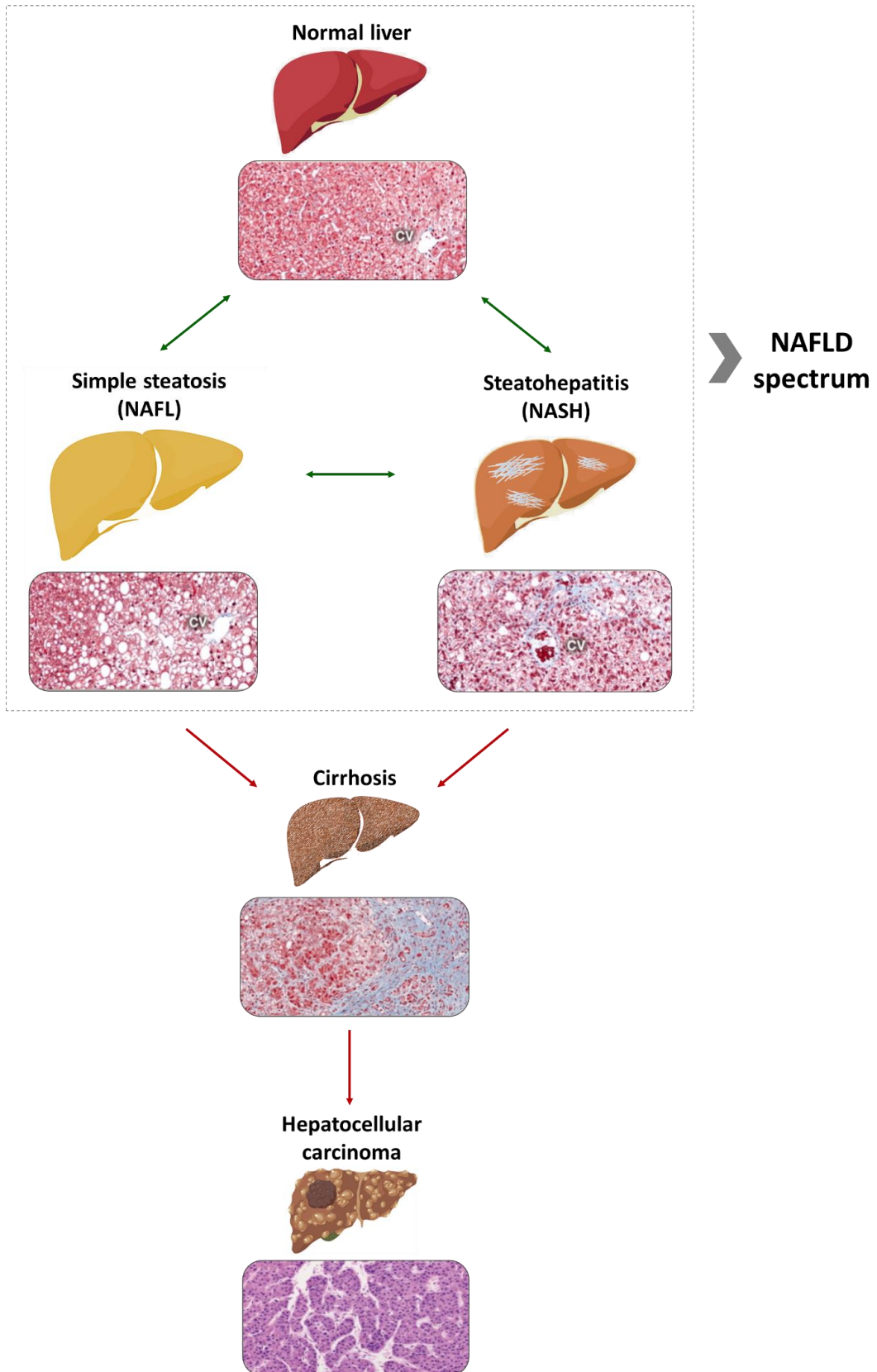
This amperometric method offers a reliable real-time quantification of H<sub>2</sub>S while using potassium ferricyanide (K<sub>3</sub>[Fe(CN)<sub>6</sub>]) as internal electrolyte and Na<sub>2</sub>S or NaHS as standard [302]. Besides the fact that samples do not suffer any alteration, polarographic sensors are incredibly stable and possess a detection limit within the nanomolar range (above 10nM) [302, 306].

This method has been used as a reliable tool for the measurement of H<sub>2</sub>S levels in various studies. Jeroschewski *et al.* were the first to try this technique, using a standard Clark-type oxygen electrode to measure H<sub>2</sub>S in aquatic environments [307]. However, in 2005, Doeller *et al.* modified the polarographic oxygen sensor to make real-time measurements of H<sub>2</sub>S [308]. One year later, the polarographic H<sub>2</sub>S sensor, as it would be known, was improved and used to measure rates of H<sub>2</sub>S production in biological samples, namely, rat liver, brain and heart [309]. Despite the advantages associated to H<sub>2</sub>S polarographic sensors, their main problem lies in the necessity of liquid electrolytes, which are prone to dryness, leakage and accumulation of impurities [302].

#### 1.10.7. Fluorometric probes

Fluorescent probes are highly sensitive and can be used for real-time measurements, even in specific tissues or cellular compartments [310]. The reactivity and specificity of these probes are based on a fluorescence-quenching group on a fluorophore that can be modified or removed selectively by H<sub>2</sub>S. The most common reaction-based detection involves azide reduction by H<sub>2</sub>S [311]. Up to now, several H<sub>2</sub>S-detecting probes have been reported, such as sulfidefluor-1 or -2 (SF1 or SF2), dansyl azide, sulfide-selective fluorescent probe-1 or -2 (SFP1 or SFP2, and 7-Azido-4-methylcoumarin [311–314].

Given that they provide access to live cell and tissue imaging experiments, fluorescent probes offer significantly higher resolution than other H<sub>2</sub>S quantification methods [310, 311]. However, even this assay has its problems. One of the first disadvantages of this method is the irreversible reaction between probe and H<sub>2</sub>S that leads to the quantification of accumulated probe activation rather than real-time H<sub>2</sub>S dynamics [310]. Driven by these limitations, Dulac *et al.* developed a new method of reversible quantification in biological fluids, detecting up to 200 nM of H<sub>2</sub>S at pH 7.4 using hemoglobin I from *Lucina pectinate* and a fluorophore [315]. Furthermore, the signal obtained from fluorescent probes can be tainted by tissue autofluorescence (when the emission/excitation wavelengths are similar) or by non-specific reactions with other biological thiols (GSH and cysteine) [311].



*Adapted from Cohen JC et al. 2011 [317] and Schlageter et al. 2014 [319]*

**Figure 13: Different stages of Non-Alcoholic Fatty Liver Disease (NAFLD)**

## 2. Non-Alcoholic Fatty Liver: a disease of the modern world

### 2.1. Description

Non-Alcoholic Fatty Liver Disease or more commonly known by its acronym “NAFLD” is an illness characterized by the excessive accumulation of fat in hepatocytes. The spectrum of NAFLD encompasses all liver lesions from simple steatosis (Non-Alcoholic Fatty Liver or NAFL) to a more complex pattern with active lesions of hepatocyte injury, apoptosis, cell death and inflammation (Non-Alcoholic Steatohepatitis or NASH) in the absence of alcohol intake (<20 or 30 g/day for men and <10 or 20 g for women) [316, 317] (**Figure 13**). NASH itself ranges from an initial stage of inflammation and liver cell damage to a latter one of fibrosis (scarring of the liver), which can further progress into cirrhosis and hepatocellular carcinoma (HCC) [317–319].

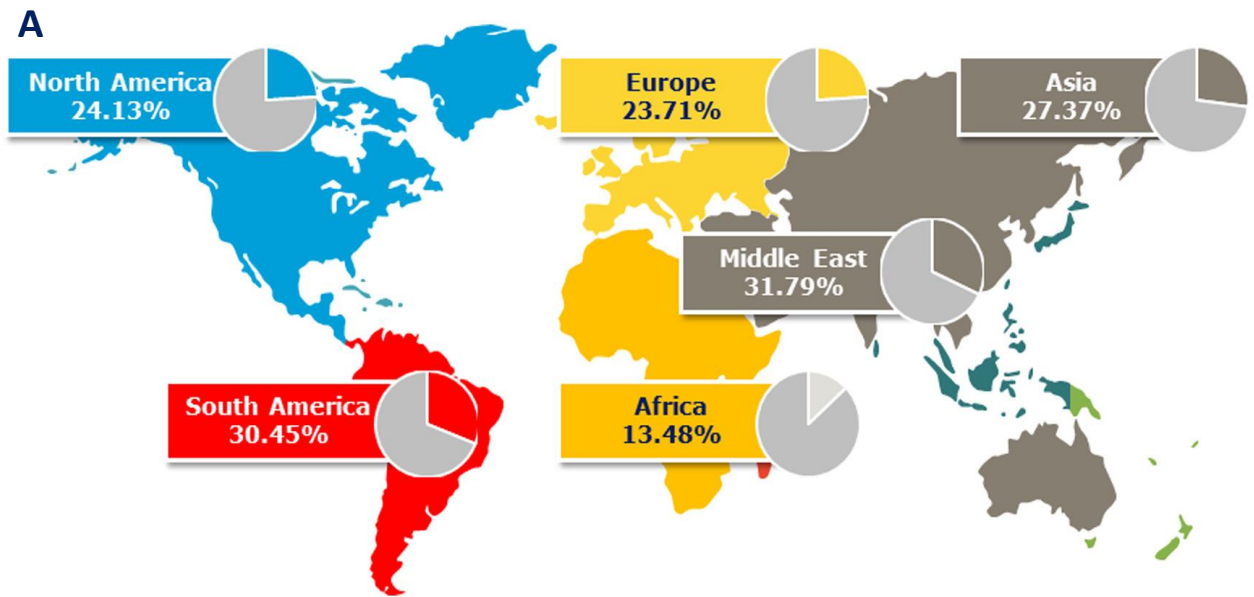
Ludwig *et al.* were among the first to describe the pathology in 1980. They examined biopsies taken from 20 patients evaluated at the Mayo Clinic over a 10-year period. These patients had histologic evidence suggestive of alcoholic hepatitis on liver biopsy (steatosis, lobular inflammation, ballooning and Mallory-Denk bodies) but no history of alcohol abuse. Mallory-Denk bodies are cytoplasmic hyaline inclusions composed by the protein p62, ubiquitin, and intermediate filament proteins keratins 8 and 18 that up to that moment were believed to be exclusive of Alcoholic Fatty Liver (AFL) [320].

The real definition of NAFLD still remains histological. NAFL is characterized by the presence of steatosis in at least 5% of hepatocytes in the absence of any significant inflammation or fibrosis, whereas NASH is characterized by steatosis, ballooning (hepatocyte dilation and enlargement) and inflammation, plus or minus fibrosis [321]. The illness is typically detected by biopsy or magnetic resonance imaging (MRI), and the final diagnosis is confirmed only after eliminating all other possible causes for the fatty liver, such as alcohol intake or drug medication.

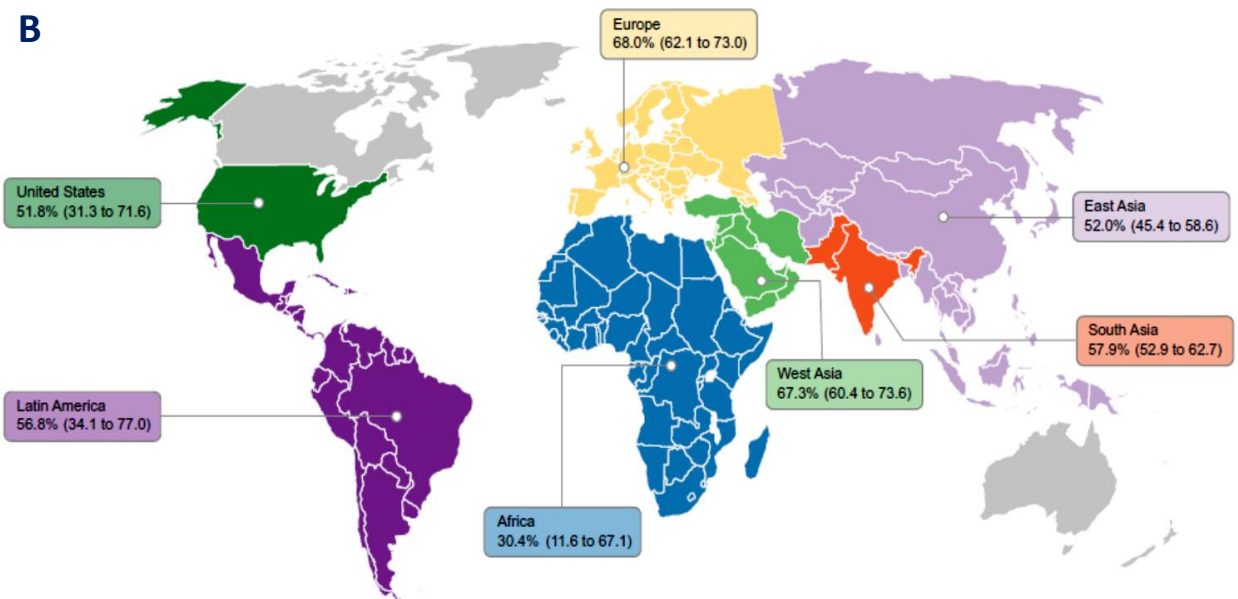
### 2.2. Epidemiology

NAFLD is considered the most prevalent liver disease in human history and the first chronic hepatic disease in the Western world. The scientific community estimates that this illness has a 25% worldwide prevalence, which means that two billion people are affected by it nowadays (**Figure 14A**) [322, 323].

Despite being a non-communicable disease (NCD) such as type 2 diabetes mellitus (T2DM), hypertension, CVD, and HCC, NAFLD continues to go unnoticed by the general population, policymakers and even the global health community. Although its numbers are already



Adapted from Younossi et al. 2018 [323]



Adapted from Younossi et al. 2019 [328]

**Figure 14: Worldwide prevalence of NAFLD in the general population (A) and among patients with T2DM (B)**

**T2DM:** type 2 diabetes mellitus



overwhelming, NAFLD is anticipated to become even more prevalent in the future, due to the increasing proportion of people of older age, obesity, low physical activity, unhealthy dietary habits, and T2DM [324].

NAFLD is often considered a self-inflicted disease, which implies that the person's behaviour is the main determinant for developing this illness. Due to socioeconomic reasons, in the Western countries, the major leading cause of NAFLD is overeating combined with poor physical exercise, which induces extra-hepatic fat accumulation [325]. Over the past few years, the scientific community has widely accepted NAFLD as the hepatic manifestation of the metabolic syndrome (MS) [322]. In fact, the prevalence of MS among NAFLD and NASH patients is 41% and 71%, respectively [322]. As part of the MS, NAFLD has become an established risk factor for the leading causes of death and disability in the twenty-first century, namely CVD, stroke, cancer, and T2DM. Nonetheless, despite the close association between NAFLD and MS, the two conditions do not always coexist in the same individual [51]. Recent studies suggest that pathogenetic processes beyond MS may also lead to NAFLD, such as genetic variants in the patatin-like phospholipase domain-containing protein 3 (*PNPLA3*) gene. In 2008, a genome-wide association study found that a missense mutation (I148M) in a *PNPLA3* allele was strongly associated with increased hepatic fat levels and hepatic inflammation [326]. The mutation was most common in Hispanics, the group most susceptible to NAFLD, and the hepatic fat content was more than two-fold higher in homozygotes than in noncarriers [326]. Recently, the I148M variant has been shown to not only influence hepatic fat accumulation, but also the susceptibility to more aggressive liver disease [327].

NAFLD is multi-factorial and the most notorious mechanisms for developing this disease are linked to changes in lipid and glucose homeostasis. The prevalence of NAFLD is 23% among the general population (**Figure 14A**), although this value increases to 51% in cases of obesity [322] and to 58-64% in T2DM obese people (**Figure 14B**) [243]. The prevalence of NASH is much lower (1.5-6.5%) but its incidence in T2DM and/or obese individuals is astonishing. There is an 82% correlation between NASH and obesity [322] and a 37% correlation between T2DM and NASH [328]. Of these, 17% are at risk of developing fibrosis [328].

NAFLD has a strong association with obesity and in fact the entire spectrum of obesity, ranging from overweight to obese and morbid obese, is associated with fatty liver. However, this is not always the case and patients who are not obese or morbid obese can also present NAFLD; this is known as "lean NAFLD" [329]. Although less common, individuals with lean NAFLD share an altered metabolic and cardiovascular profile as those who are obese, which in turn may lead to

collective risk for comorbidities, such as ischemic heart disease. In fact, people with lean NAFLD present higher rates of liver inflammation, ballooning, fibrosis and cirrhosis than overweight individuals [330]. The prognosis of lean individuals with NAFLD is still not well defined. However, a large, multi-centred, biopsy-proven cohort has shown that individuals with lean NAFLD were more commonly men, of non-Caucasian origin, and had a lower prevalence of T2DM, hypertension, hypertriglyceridemia, low cholesterol, central obesity and MS features as compared to non-lean NAFLD [331]. A recent study has shown that, when compared to obese NAFLD, lean NAFLD individuals have higher levels of bile acids and fibroblast growth factor 19 (FGF19) [332]. Bile acids and FGF19 increase energy expenditure, which can explain why lean individuals with fatty liver stay lean. In the same study, researchers found that, in lean NAFLD patients, the genetic variant rs58542926 of the transmembrane 6 superfamily member 2 (TM6SF2) had a higher prevalence than in obese individuals [332]. This variant was linked to impaired very low-density lipoprotein (VLDL) production.

Despite the strong association between obesity and abnormal metabolism, there are some obese subjects with normal metabolic profiles. These people are usually classified as metabolically healthy obese (MHO) and can account for up to 29% of the entire obese population [333]. Compared to metabolically abnormal obese people, MHO present lower visceral fat, higher insulin sensitivity, higher high-density lipoprotein (HDL) cholesterol level, and lower triglycerides (TG) level [333]. Some studies suggest that MHO individuals also present lower risk of cardiovascular disease or stroke when compared to metabolically abnormal obese people [334, 335]. However, when compared to metabolically healthy non-obese people, MHO individuals present 49% higher risk of coronary heart disease, 7% higher risk of cerebrovascular disease and 96% higher risk of heart failure [336].

Several studies have suggested that NAFLD has an age, gender, and ethnic bias. Increasing age is one of the most robust epidemiological factors for NAFLD, NASH and fibrosis. Although old age is not a risk factor for developing fatty liver, aged people have higher probability of mortality and disease progression to fibrosis and HCC [337].

The influence of gender on the development of NAFLD has been studied in the past few years and the conclusion is controversial. While some studies suggest that women are at a higher risk of developing the disease, others suggest that there is a male preponderance for it [338, 339]. In men, NAFLD prevalence increases from younger to middle age and starts to decline after the age of 50–60 years. As to women, the prevalence of NAFLD rises after the age of 50, peaking at 60–69 years and declining after the 7th decade of life [339]. Furthermore, men and post-

menopausal women appear to have a higher risk of developing fibrosis when compared to premenopausal women [339–341]. Some studies suggest that this difference is due to the protective effects of estrogen in fibrogenesis [339–341].

The role of ethnicity in the prevalence of NAFLD has been most evident in the studies from USA that involved multi-ethnic populations [342]. For example, when comparing individuals of European descent, Hispanic Americans and African Americans, Hispanic Americans have the highest prevalence of NAFLD while African Americans have the lowest [342]. The fact that African Americans seem to have a lower prevalence of NAFLD, despite having a higher prevalence of obesity, demonstrates the complexity of NAFLD, underlining the role of genetics and epigenetic factors (diet and lifestyle) in the development of this pathology.

## **2.3. Diagnosis**

### **2.3.1. Non- or minimally invasive methods**

#### **a) Biomarkers**

- **Hepatic transaminases**

In the majority of cases, symptoms associated to NAFLD are not felt until the person reaches a late stage in the development of the disease, which means that an early diagnosis is difficult to obtain.

If there is a suspicion of NAFLD, doctors will ask for a routine blood analysis to check the levels of aspartate aminotransferase (AST) and alanine aminotransferase (ALT). In a normal situation, these enzymes are predominantly contained within hepatocytes and to a lesser degree in muscle cells. When the liver is injured or damaged, hepatocytes spill these enzymes into the blood, increasing their concentration (1-4 times the upper limit of normal). Typically, ALT is a more specific marker of hepatic injury than AST and, according to recent evidence, ALT is often the first sign of NAFLD [343]. Individuals with NAFL and NASH present liver injury that is normally mirrored by elevated blood levels of these transaminases (normal levels of ALT range from 29 to 37 IU/l for males and 19 to 31 IU/l for females) [344, 345]. With the progression of hepatic steatosis to NASH and associated hepatic fibrosis, AST levels increase with a resultant rise in the AST:ALT ratio. Nonetheless, 50%-80% of NAFLD patients can have normal ALT and AST levels, and thus several biomarkers have been proposed to aid in the diagnosis [346, 347].

Gamma-glutamyltransferase (GGT) is another commonly assessed serum biomarker [348]. Studies have shown that GGT levels are increased in cases of NAFLD and it is possible to establish a positive correlation between GGT and insulin resistance (IR) [349, 350].

- MicroRNAs (miRNAs)

MicroRNAs (miRNAs) are short non-protein coding, single-strands RNAs of 19–22 nucleotides, that have a pivotal role in the regulation of gene expression [351]. miRNAs can target mRNAs through complementary base-pairing, thereby affecting protein synthesis at the post-transcriptional level. One miRNA can target multiple genes (multi-functionality), or multiple miRNAs can target a single gene (redundancy) [351]. There are thousands of miRNAs described in the literature. However, only a few have been linked to the diagnosis of NAFLD. Such is the case of miR34a, miR-122 and miR-21 [352, 353].

- **miR-34a** is the most characterized regulator of SIRT1 and a highly lipid responsive miRNA in the liver. miR-34a modulates oxidative stress and metabolism, and it has been demonstrated that it promotes cellular apoptosis and fibrosis through a miR-34a/SIRT1/p53 signalling pathway in rodents and humans [354, 355]. Serum levels of miR-34a and miR-122 were found to be significantly higher in NAFLD patients, being also positively correlated with VLDL and triglyceride levels [356]. Furthermore, evidence has shown that miR-34a expression increases from steatosis to less- and more-severe NASH [354].

- **miR-122** is the most abundant miRNA in human liver, representing more than 70% of the total liver miRNA pool [357]. Recent evidence has demonstrated that the inhibition of miR-122 alleviates lipid accumulation and inflammation in an *in vitro* model of NAFLD [358]. Several studies have confirmed that serum levels of miR-122 are significantly higher in NAFLD patients when compared to healthy subjects [356, 359]. Furthermore, much like miR-34a, the serum level of miR-122 is correlated with the severity of liver steatosis in NAFLD patients [360]. In fact, miR-122 is an important tumor suppressor and clinically its hepatic and circulating levels are a prognostic marker in patients with HCC [361, 362]. However, one study conducted on human liver organoids has shown the contrary, with the inhibition of miR-122 leading to liver inflammation, necrosis, and dysregulated insulin signalling [363].

- Since its identification, **miR-21** has called the attention of researchers in various fields, such as development, oncology, stem cell biology and aging. In individuals with fibrosing-NASH and HCC, miR-21 is highly up-regulated in both serum and liver [360, 364, 365]. Recently, a study has shown that the inhibition of miR-21 in a mouse model of NASH decreased liver injury,

inflammation and fibrosis by up-regulating peroxisome proliferator-activated receptor alpha (PPAR $\alpha$ ) [366]. Later, Rodrigues *et al.* corroborated these findings by demonstrating that miR-21 KO animals fed a fast food diet supplemented with obeticholic acid (OCA), a potent agonist of Farnesoid-X Activated Receptor (FXR), displayed minimal steatosis, inflammation and lipopoptosis through PPAR $\alpha$  up-regulation and FXR activation [367].

## **b) Imaging techniques**

### • Magnetic Resonance Imaging (MRI)

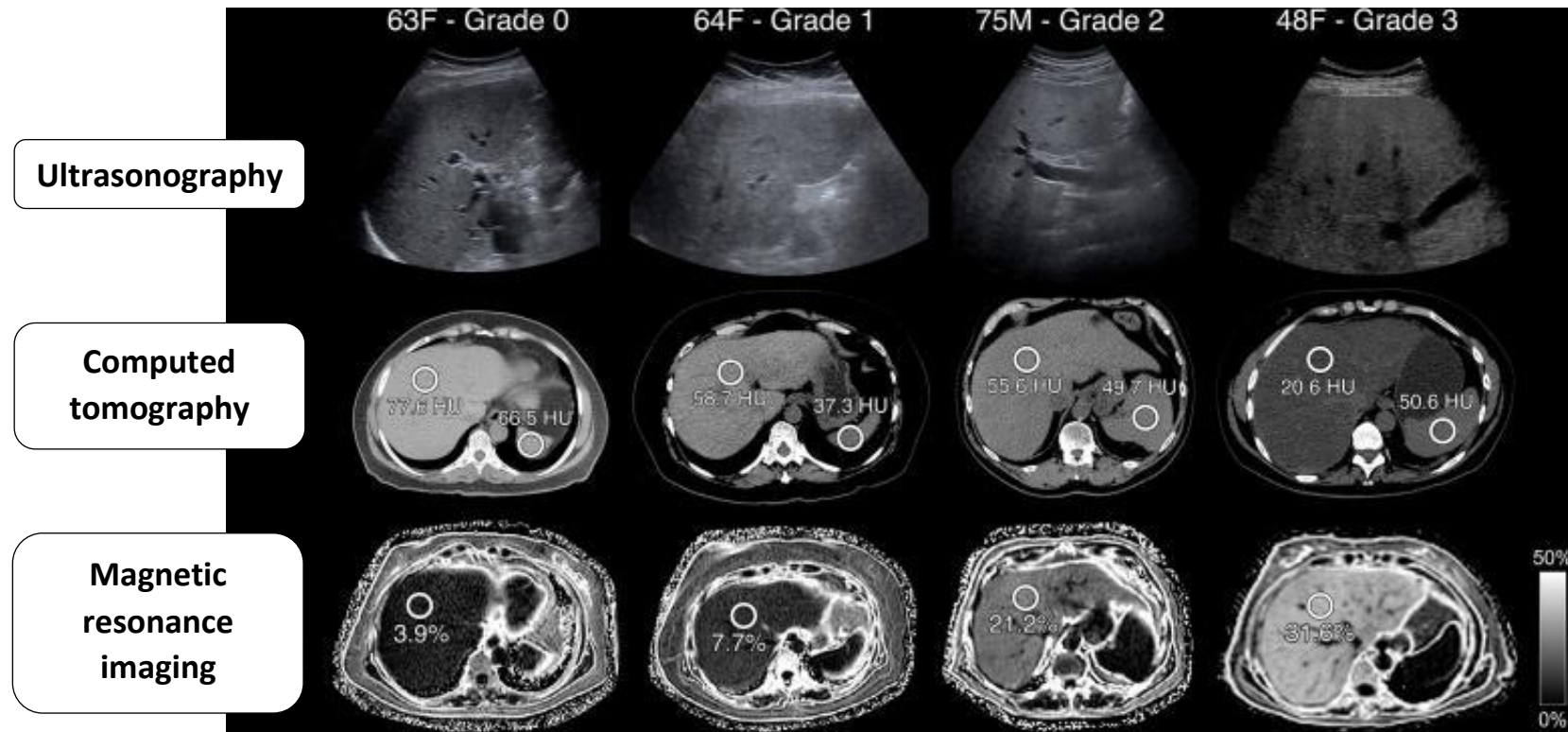
Magnetic resonance imaging (MRI) is one of the leading tools in the assessment of longitudinal changes in hepatic fat [368–370]. MRI measure the proton density fat fraction (PDFF), an objective and quantitative indicator of hepatic fat content across the entire liver, in an accurate and reproducible manner [368, 371]. In fact, MRI measures the signal intensity (brightness) of protons at different resonance frequencies (**Figure 15**).

One of the beneficial aspects of this technique is that it allows the screening and staging of NAFLD patients while avoiding ionizing radiation. Studies have shown that MRI not only shows high sensitivity and specificity (>80%) as it also accurately classifies grades and changes in hepatic steatosis [372, 373].

### • Transient elastography (TE)

Transient elastography (TE) is a commercial ultrasound-based modality that measures liver stiffness as a surrogate for hepatic fibrosis. TE uses vibrations of mild amplitude and low frequency to induce an elastic shear wave that propagates through the underlying tissue [374]. The propagation and velocity of the shear wave are directly related to tissue stiffness. However, some conflicting results have been observed while using TE for the diagnosis of obese NAFLD, given that subcutaneous fatty tissue attenuates elastic shear wave [375].

In order to fix this issue, TE diagnosis now uses the controlled attenuation parameter (CAP). This technique enables the simultaneous measurement of liver stiffness and steatosis. Several studies have already demonstrated that CAP significantly correlates with the percentage of steatosis and steatosis grade, representing a direct and easy-to-perform screening tool [376, 377].



Adapted from Zhang et al. 2018 [370]

**Figure 15: Steatosis detection using ultrasounds, computed tomography and magnetic resonance imaging**

The scans correspond to four different patients: three women (63F, 64F and 48F) and one man (75M). Steatosis grade increases from left to right in each row.

- Ultrasonography

Ultrasonography is a widely available method used for the detection of liver steatosis [370, 378]. When it encounters lipid droplets, the ultrasound beam causes more echo signals, which creates the appearance of a “bright” liver (**Figure 15**). In fact, liver brightness is directly associated to the severity of steatosis [378].

Ultrasonounds are widely used because they are safe and provide little patient discomfort. However, there are several clear disadvantages associated to this technique. Much like TE, large body weights attenuate the ultrasound beam, which leads to a poor estimation of liver steatosis [379]. In fact, the reported sensitivity of ultrasonounds for the detection of mild steatosis (fat content 5%-20%) is only 60-65% [378, 380]. This sensitivity increases to 80% when more than 20% of hepatocytes contain histologically visible fat droplets [381]. Additionally, this method is unable to differentiate mild fibrosis from steatosis, and, since it is operator- and reader-dependent, it presents low reproducibility [382].

- Computed tomography (CT)

Images obtained by computed tomography (CT) are generated by X-ray photons traversing tissues. The denser the tissue, the more attenuated the X-ray is and the brighter the corresponding image pixel [370, 383]. With increased steatosis, the liver tissue becomes hypoattenuating, which is translated by a darker image comparatively to the adjacent fat-free tissues (**Figure 15**).

CT allows a relatively fast acquisition and is easy to perform. This technique shows a sensitivity of 82% and a specificity of 100% in cases where the degree of steatosis is >30% [384, 385]. However, much like ultrasonounds, CT cannot accurately diagnose mild steatosis (fat content 5%-20%) [383]. In addition, CT obliges patients to be exposed to X-rays and results can vary when using different machines [383].

### 2.3.2. Invasive methods

Although serum biomarkers and imaging methods are useful in the detection of steatosis, almost all of them present some difficulty in differentiating between simple steatosis and steatohepatitis [386]. This differentiation can only be achieved through needle biopsy. Although an invasive method, the biopsy is up to now the only technique providing a diagnosis with high degree of certainty based on the detection of hepatic lesions, inflammation and fibrosis [387]. However, given that liver lesions may not be uniformly distributed, it becomes imperative to base the diagnosis on the comparison between at least two needle biopsies [387].

**A**

<b>0 ≤ NAS ≤ 2</b>	<b>No NASH</b>
<b>3 ≤ NAS ≤ 4</b>	<b>“borderline”</b>
<b>≥ 5 NAS</b>	<b>NASH</b>

**B**

STAGE	FEATURE
	<b>Steatosis</b>
<b>0</b>	<5%
<b>1</b>	5% to 33%
<b>2</b>	33% to 67%
<b>3</b>	>67%
	<b>Lobular inflammation</b>
<b>0</b>	No foci
<b>1</b>	<2 foci per 20x field
<b>2</b>	2-4 foci per 20x field
<b>3</b>	>4 foci per 20x field
	<b>Ballooning</b>
<b>0</b>	None
<b>1</b>	Few
<b>2</b>	Many
	<b>Fibrosis</b>
<b>0</b>	None
<b>1</b>	Perisinusoidal or periportal (3 substages characterized)
<b>2</b>	Perisinusoidal and periportal
<b>3</b>	Bridging fibrosis
<b>4</b>	Cirrhosis

*Adapted from Brunt et al. 1999 [388]*

**Table 3: Classification of patients according to the NAFLD Activity Score (NAS) (A) and the different criteria that compose the classification system (B)**



After retrieving the small tissue sample that constitutes the liver biopsy, the various stages of NAFLD are differentiated via well-established quantitative systems, such as the NAS score and the Bedossa algorithm.

#### **a) NAFLD Activity Score (NAS)**

According to Brunt *et al.* 1999, the grade and stage of NAFLD is not defined by one single characteristic but by the combination of multiple characteristics [388]. The system proposed by these researchers divided the grade of steatosis into mild, moderate, and severe categories, combined with 4 possible stages of fibrosis. Despite being universally accepted by the medical community, this system is not meant for grading cases not diagnosed as NASH [388].

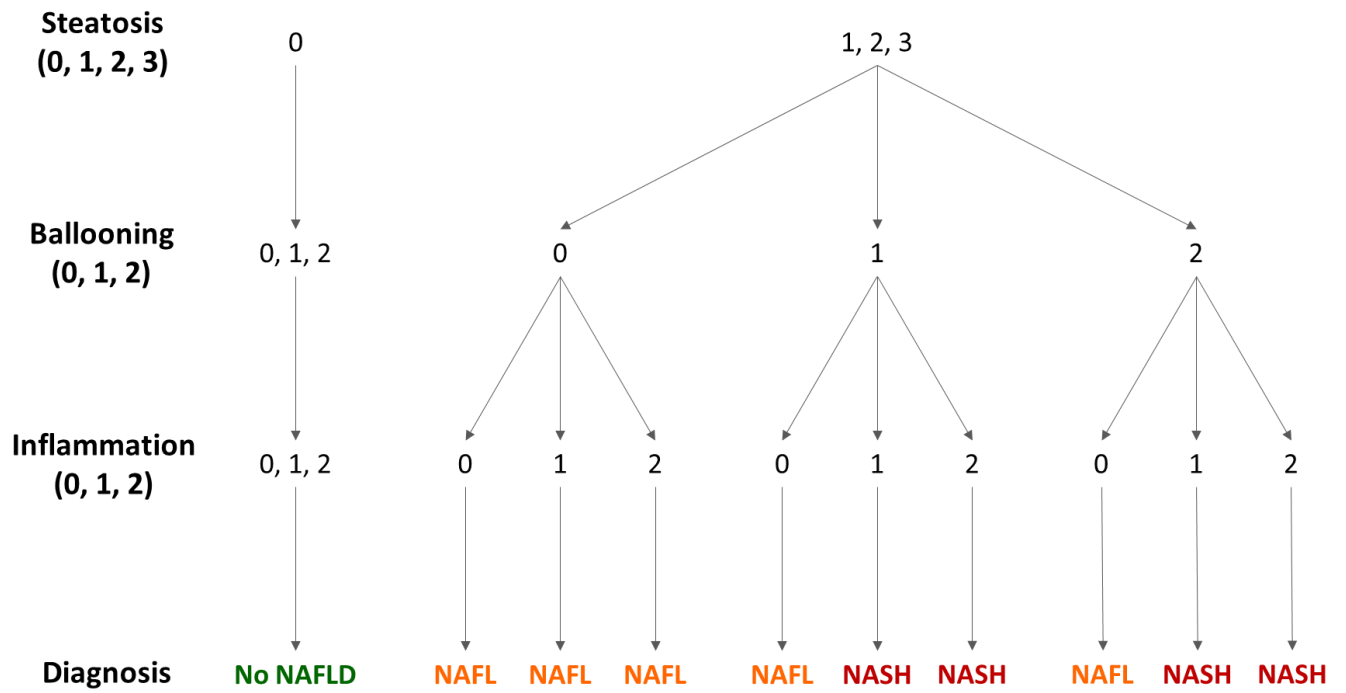
In 2002, the Pathology Committee of the NASH Clinical Research Network, sponsored by the National Institute of Diabetes and Digestive and Kidney Disease (NIDDKD), widened Brunt's score system to include all histological lesions caused by NAFLD, thus creating the NAFLD Activity Score (NAS) **(Table 3A)** [389]. This system allows patients to be differentiated into three categories.

The NAS score is defined as the sum of the scores for steatosis (0–3), lobular inflammation (0–3), and ballooning (0–2) **(Table 3B)** hence ranging from 0 to 8. If NAS has values between 0 and 2, the profile is determined “No NASH”; if the score is above or equal to 5 then patients are diagnosed with “NASH”; and when values range between 3 and 4 the situation is deemed “borderline” [389].

Fibrosis is not included in this semi-quantitative grade, since fibrosis is less reversible and thought to be the result of the disease activity rather than a potential driver lesion. Nonetheless, the fibrosis score (0, 1, 2, 3, 4) is evaluated before defining the diagnosis [389].

#### **b) Algorithm of Bedossa**

In 2012, Bedossa *et al.* developed an algorithm for the diagnosis of NAFLD using liver biopsies obtained during bariatric surgery [390]. The aim of their model was to build an algorithm along with a scoring system for histopathologic classification of liver lesions that could cover the entire spectrum of lesions in morbidly obese patients. The algorithm could segregate lesions into normal liver, NAFL, or NASH, and was built based on semi-quantitative evaluation of steatosis, hepatocellular ballooning, and lobular inflammation **(Figure 16)** [390].



*Adapted from Bedossa et al. 2012 [390]*

**Figure 16: Algorithm of Bedossa proposed for the diagnosis of NAFLD**

The algorithm of Bedossa starts with the classification of steatosis, which can range from 0 to 3. Following this is the classification of hepatocellular ballooning and inflammation, by this order, which can be classified on a scale of 0 to 2 [390].

According to this algorithm, in order to classify a patient as “NAFL”, the sample must present at least a level 1 steatosis and none of the two remaining criteria (ballooning and inflammation). On the other hand, in order to be classified as “NASH”, the sample must present a level 1 (minimum) in all three criteria [390].

## 2.4. Etiology of NAFLD

### 2.4.1. “Two-hits” hypothesis

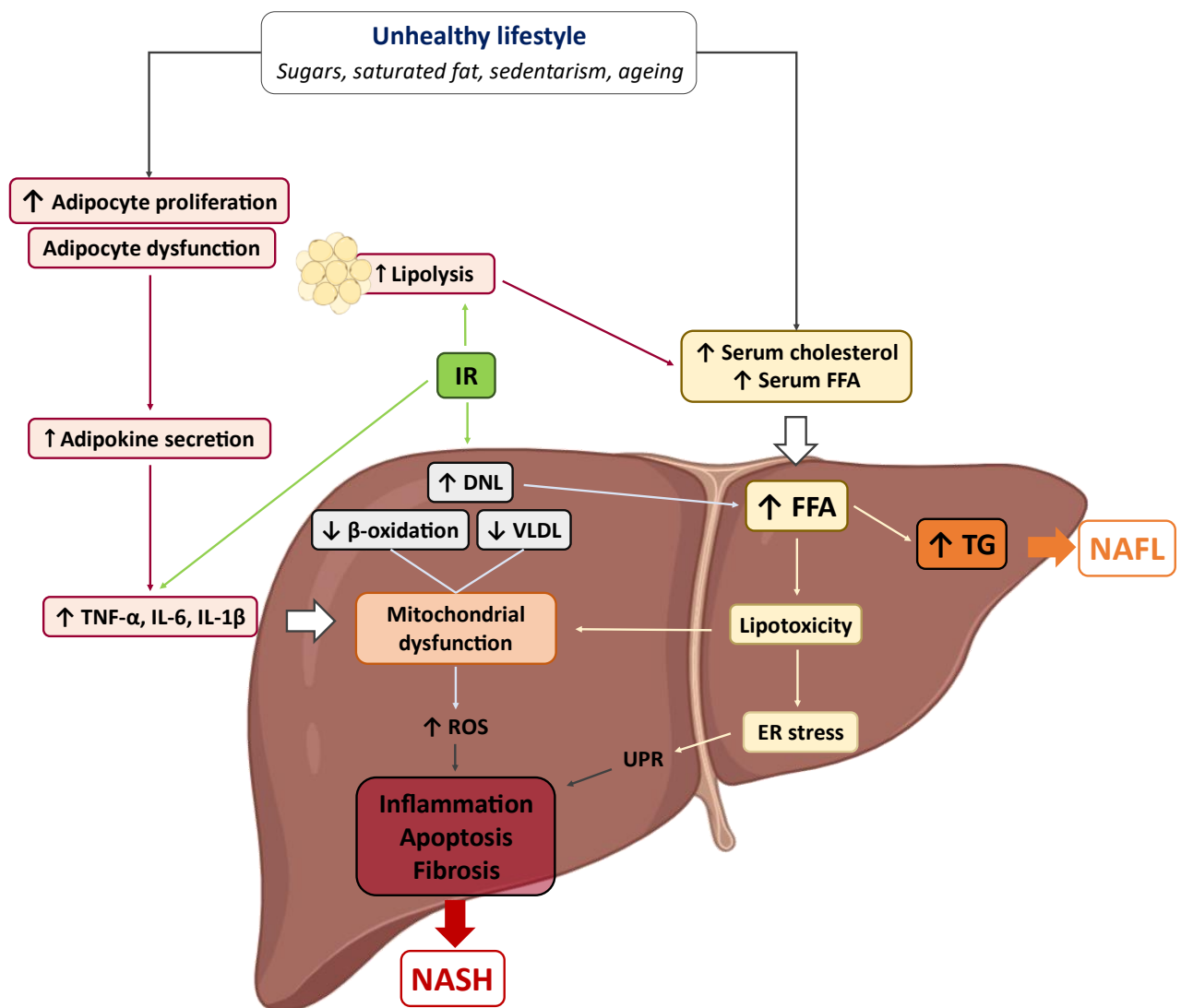
It was the idea of continuity from NAFL to NASH that led to the concept of the “two-hits” hypothesis in 1998 (**Figure 17**) [391]. According to this theory, NAFLD progresses from simple steatosis (NAFL) to steatosis accompanied by inflammation and ballooning (NASH), to fibrosis, cirrhosis and eventually HCC. This order of events indicates that the different features in the NAFLD spectrum have different degrees of severity, moving from less to more harmful. According to this theory, NAFLD begins with the hepatic accumulation of TG (“first hit”), which is due to an imbalance between their synthesis and their degradation [392]. This steatosis oversensitises the liver making it vulnerable to the effects of other stressors [391, 392]. Over time, all these elements contribute to cellular damage and oxidative stress-related fibrosis (“second hit”) [392].

#### a) **“First hit”: hepatic steatosis and insulin resistance**

- Increase in dietary fatty acids

Unhealthy lifestyle habits are translated into an imbalance between calory intake and energy expenditure, which results in TG accumulation in the liver (**Figure 17**). Dietary FA are taken up by the gut where they are assembled in small lipoprotein-rich structures (chylomicrons) that transport those lipids into the blood and lymph [393]. A great part of these chylomicron-contained lipids is absorbed by the adipose tissue and the rest is captured by the liver [393].

To this date, only one study has fully assessed the contribution of different FA sources to the total hepatic lipid content using FA stable-isotope tracers ([<sup>13</sup>C<sub>1</sub>] sodium acetate, [1,2,3,4-<sup>13</sup>C<sub>4</sub>] potassium palmitate, [<sup>2</sup>H<sub>31</sub>] glyceryl-tripalmitin and deuterated tripalmitate) [394]. In obese and insulin-resistant NAFLD individuals, 59% of hepatic lipids derive from an increased lipolysis of TG in the adipose tissue, 26% derive from hepatic *de novo* lipogenesis (DNL) and only 15% have its



Adapted from Petta et al. 2016 [392]

**Figure 17: Mechanisms behind Non-Alcoholic Fatty Liver Disease (NAFLD)**

Dietary and environmental factors lead to increased serum levels of free fatty acids (FFAs) and cholesterol. These enter the liver where they accumulate in high proportions. Fatty acid (FA) accumulation, which is strongly associated with insulin resistance (IR), leads to two different situations: synthesis and accumulation of triglycerides (TG), and accumulation of FAs, free cholesterol and other lipid metabolites, key-characteristics of non-alcoholic fatty liver (NAFL). IR is one of the key factors in the development of steatosis and results in both increased hepatic *de novo* lipogenesis (DNL) and impaired inhibition of adipose tissue lipolysis. Adipocyte hypertrophy leads to adipocyte dysfunction, in which the cells secrete abnormal amounts of pro-inflammatory cytokines and adipokines. The accumulated toxic metabolites and pro-inflammatory cytokines promote endoplasmic reticulum (ER) stress and mitochondria dysfunction, which leads to the activation of unfolded protein response (UPR) and increased production of reactive oxygen species (ROS), respectively. Collectively, the activation of these pathways eventually leads to hepatic inflammation, which is the key characteristic of non-alcoholic steatohepatitis (NASH).

**TNF $\alpha$** : tumour necrosis factor alpha; **IL-6**: interleukin 6; **IL-1 $\beta$** : interleukin 1 beta; **VLDL**: very low-density lipoprotein

origin in dietary fats and sugars [394]. In other studies, these ratios may differ according to the cohort, meal composition and size as well as to the time at which the samples are collected.

Evidence suggests that the FA nature plays a role in the development of NAFLD, as diets enriched in saturated FA lead to higher hepatic fat accumulation [395]. Moreover, some studies have shown that hypercaloric diets enriched in sugar and/or fat [396] increase hepatic TG content whereas caloric restriction [397] decreases it. In fact, since there is no effective therapy for NAFLD, caloric restriction has been progressively accepted as an effective non-pharmacological strategy to help the control of the progression of this illness. For example, obese individuals subjected to an 8-week long modified alternate-day calorie restriction present decreased levels of hepatic steatosis and fibrosis, body mass index, and plasma levels of ALT [398].

- Increase in adipose tissue lipolysis

In physiological conditions, the adipose tissue regulates energy homeostasis by serving as a safe storage unit for the excessive TG. However, when the incoming fat surpasses their maximum storage capacity, adipocytes undergo cellular hypertrophy and hyperplasia (**Figure 17**) [399]. Ultimately, this adipocyte remodelling leads to hypoxia and cellular death accompanied by a major secretion of inflammation-related cytokines. Some of these cytokines antagonize the action of insulin by phosphorylating the insulin receptor substrate-1 (IRS-1) and decreasing the expression of glucose transporter 4 (GLUT4), which, little by little, starts impairing the insulin signalling and leading to an insulin resistant phenotype [400]. Insulin is necessary to control the process of lipolysis and in cases of adipose IR lipolysis cannot be suppressed. This leads to substantial amounts of free fatty acids (FFA) being released into the bloodstream (**Figure 17**) [401].

Since the hepatic lipid uptake directly depends on the amount of FFA available in the plasma, adipose IR is ultimately responsible for a massive uptake and accumulation of lipids by the liver [399]. A recent study has shown that the administration of an inhibitor of adipose triglyceride lipase effectively reduces adipose tissue lipolysis, weight gain and IR in mice fed a HFD [402].

In mammals, two types of adipose tissue have been identified, the brown and the white, and they serve different purposes [399]. White adipose tissue stores energy in the form of TG whereas brown adipose tissue serves to dissipate the stored energy in the form of heat. In regard to white adipose tissue, we can further subdivide it into subcutaneous (SAT) and visceral (VAT). Other than their names, there are considerable anatomical differences in the distribution of both adipose tissues in the body [399].

SAT is responsible for the storage of nearly 80% of total body fat and, as an active participant of the endocrine system, it secretes adipokines that can sensitize the tissue for the actions of insulin, such as leptin and adiponectin [399, 403, 404]. SAT is located just under the skin in a gender-specific manner [399]. In men, SAT deposits in the back of the neck and shoulders whereas in women it deposits in the chest, hips, thighs, and buttocks [405]. This difference in adipose tissue composition between women and men is what creates the typical “pear” or “apple” shape, respectively [405]. Despite being considered the “safest” site for storing excess of fat, the truth is SAT continues to be the largest contributor of FFA in obese subjects [403].

VAT is the adipose tissue surrounding the internal intraperitoneal organs, which makes it mostly present in the intestinal mesentery and omentum [399]. Unlike SAT, VAT is anatomically linked to the liver via the portal vein. VAT is responsible for the secretion of pro-inflammatory adipokines that promote IR [406]. In cases of adipocyte hypertrophy where there is energy overload and massive scale apoptosis, immune cells, particularly macrophages, are summoned to the adipocytes in crisis where they release pro-inflammatory factors [401]. As a result, the overall production of pro-inflammatory adipokines and cytokines increases, leading to chronic inflammation and IR.

Several studies have pointed out that VAT plays a much more significant role in the progression of NAFLD than SAT, since VAT has typically larger macrophage-infiltration and macrophage-derived inflammation [407]. VAT is more sensitive to the lipolytic effects of catecholamines and less sensitive to the anti-lipolytic effects of insulin [408]. This grants this tissue a great capacity for FA mobilization and release to the portal circulation, but also makes it more prone to develop IR [408].

In IR adipose tissue, there is a massive delivery of FAs to the liver, which leads to excess hepatic TG synthesis and intracellular accumulation of toxic lipid products (**Figure 17**). This eventually impairs insulin signalling and activates inflammatory pathways. Although the connexion between adipose tissue IR and hepatic IR has been established, whether the degree of hepatic IR and steatohepatitis is proportional to the magnitude of adipose tissue IR is yet to be properly determined [408]. To date, only one study conducted in non-diabetic morbid obese NAFL patients has demonstrated that the levels of activated hepatic macrophages significantly correlated with adipose tissue IR and lipolysis [409].

Considering that both SAT and VAT have been said to play a role in the progression of NAFLD, the distribution of each tissue in the body might be more important than the tissue itself.

Lately, the visceral-to-subcutaneous fat ratio (VSR) has been considered a good predictor of NAFLD and fibrosis development [410, 411].

- Increase in hepatic lipogenesis

The liver plays an essential role when it comes to nutritional balance. At the same time, it can capture, stock, synthesize and export both glucose and lipids. After a meal, the liver uses the excess of glucose to refill its glycogen pool (glycogenesis) and to synthesize *de novo* long-chain fatty acids (LCFA), which are then esterified to store TG [412]. This process, known as DNL, is a complex and highly regulated metabolic pathway that can lead to adverse metabolic consequences when deregulated (**Figure 17**). The TG formed during the DNL are then transported as VLDL to the adipose tissue where they are stored [412].

Insulin plays an important role in the regulation of hepatic lipid accumulation. It favours glucose uptake by the liver, skeletal muscle and adipose tissue and promotes hepatic and muscle glycogenesis [413]. Furthermore, it redirects the surplus of glucose to the production of lipids by DNL and inhibits lipolysis in the adipose tissue. IR in the skeletal muscle participates to the hyperglycaemia and consequent hyperinsulinemia, favouring hepatic DNL. Moreover, IR in the adipose tissue impairs the suppression of lipolysis and increases FFA flux from the adipocytes to other tissues, such as the liver (**Figure 17**) [413]. A recent study has established that DNL contributes to 38% and 19% of hepatic TG content in obese patients with and without NAFLD, respectively [414].

Liver lipid homeostasis is under the regulation of several transcription factors, namely PPAR $\alpha$ , PPAR $\gamma$ , PPAR $\beta/\delta$ , sterol regulatory element-binding protein (SREBP)-1c, carbohydrate responsive element-binding protein (ChREBP), constitutive androstane receptor (CAR), liver X receptor (LXR), FXR, signal transducer and activator of transcription 5 (STAT5) and CCAAT/enhancer binding protein alpha (C/EBP $\alpha$ ) [415]. Over the years, different papers have shown the importance of these transcription factors in the development of NAFLD.

### **A) ChREBP and SREBP-1c**

In response to glucose and insulin, ChREBP and SREBP-1c are activated, inducing the expression of lipogenic genes, such as fatty acid synthase (FAS), acetyl-CoA carboxylase (ACC) and stearoyl-CoA desaturase-1 (SCD1) [416-418]. The expression of ChREBP has been found increased in the livers of NASH patients with a severe degree of steatosis [417]. Moreover, HFD-fed mice injected with a liver-specific ChREBP adenovirus display a higher degree of hepatic steatosis than

controls [417]. Conversely, ChREBP inhibition in liver of obese and insulin resistant *ob/ob* mice, through RNA interference (RNAi) or genetic ablation leads to reversal of hepatic steatosis [419] [420]. Studies have associated ChREBP to increased mitochondrial biogenesis, oxygen consumption rates, and ATP production [421]. Recently, Plant Homeodomain Finger 2 (Phf2), a new transcriptional co-activator of ChREBP has been linked to hepatic protection in a scenario of NAFLD [422]. Phf2 facilitates the incorporation of metabolic precursors into mono-unsaturated FFA, leading to the development of hepatosteatosis in the absence of inflammation and IR [422]. Furthermore, the specific co-recruitment of Phf2 and ChREBP to the promoter of nuclear factor erythroid 2 like 2 (Nrf2) reroutes glucose fluxes toward the pentose phosphate pathway and GSH biosynthesis, protecting the liver from oxidative stress and fibrogenesis in response to diet-induced obesity [422].

A transcription factor that acts in synergy with ChREBP is SREBP-1c. SREBP-1c has been found upregulated in the livers of mouse and human models of NAFLD, while SREBP1c KO mice display decreased expression of lipogenic enzymes (ACC, FAS and SCD1) [423]. Furthermore, a link between this transcription factor and the NAFLD-associated gene *PNPLA3* has been established [424, 425]. A recent study has reported that there is an interdependence between ChREBP (activated by glucose) and SREBP-1c (activated by insulin) for the full induction of glycolytic and lipogenic gene expression in mouse liver [426]. Viral re-establishment of the nuclear active form of SREBP-1c in the liver of ChREBP KO mice normalized lipogenic gene expression, while having no effect on glycolytic gene expression [426]. The mirror experiment, in which ChREBP expression was induced in the liver of SREBP-1c KO mice, rescued glycolytic gene expression but surprisingly not lipogenic gene expression, despite the well-known role of ChREBP in the control of DNL genes. Together, these results show that SREBP-1c and ChREBP are both required for coordinated induction of glycolytic and lipogenic mRNAs [426].

## **B) PPARs**

Hepatic lipid homeostasis is deeply controlled by PPARs, which coordinate transcriptional responses to altered metabolic conditions. When binding to FA, PPAR $\alpha$  becomes activated, promoting FA uptake and consumption through  $\beta$ -oxidation and ketogenesis [427]. Studies show that the hepatic expression of PPAR $\alpha$  is negatively correlated with the severity of NASH in human patients [428]. Furthermore, mice lacking hepatocyte PPAR $\alpha$  expression exhibit a more severe degree of steatosis, suggesting that this transcription factor plays a protective role during the development and progression of NAFLD [429]. Another member of the PPAR family is PPAR $\gamma$ ,



which is also activated upon FA binding and promotes lipogenesis and lipid accumulation [427]. The expression of isoform 2 of PPAR $\gamma$  (PPAR $\gamma$ 2) is upregulated in the liver and adipose tissue of obese individuals and HFD-fed mice [430]. Furthermore, total KO mice for PPAR $\gamma$  develop lipomatrophy, T2DM and hepatic steatosis [431]. Interestingly however, mice with hepatocyte-specific depletion of PPAR $\gamma$  are protected against HFD-induced steatosis and glucose intolerance [432]. PPAR $\beta/\delta$  is ubiquitously expressed and, much like PPAR $\alpha$  and PPAR $\gamma$ , is activated by FA [427]. In animal models of NASH, PPAR $\beta/\delta$  deficiency is associated to increased hepatotoxicity [433]. In fact, PPAR $\beta/\delta$  depletion leads to increased ER stress-related hepatic steatosis, which is accompanied by an increase in liver VLDL receptors [434]. A recent study has shown that PPAR $\beta/\delta$  reduces liver lipid content and stimulates FA  $\beta$ -oxidation by an autophagy-lysosomal pathway involving the 5' adenosine monophosphate-activated protein kinase/mammalian target of rapamycin (AMPK/mTOR) signalling [435].

### C) Nuclear receptors

The participation of nuclear receptors (NRs) in the regulation of several physiological and pathological processes has been highlighted throughout the years [436]. Evidence suggests that a dysregulation of NR may have a huge impact on the pathology of fatty liver, mainly due to the role NRs play in mediating hepatic detoxification of foreign chemicals (xenobiotics). CAR, LXR and FXR are examples of this NR family that have been linked to the pathogenesis of NAFLD [436].

- **CAR:** Animals fed a HFD for 12 weeks showed increased expression of the CAR target gene *CYP2B10* [437]. A recent study has corroborated this premise by showing that overweight, obese, and severely obese mice all present increased mRNA levels of *CAR* [438]. Activation of CAR using the TCPOBOP agonist appears to reduce obesity and improve T2DM by downregulating gluconeogenesis and improving insulin sensitivity [439]. However, in animal models of NASH, despite attenuating Fas (CD95/APO-1)-mediated liver injury and hepatic fibrosis [440], the activation of CAR worsened lipid peroxidation [441].

- **LXR:** this nuclear receptor regulates hepatic TG content by activating hepatic lipogenesis and TG transport to peripheral tissues. LXR KO mice present lower expression of lipogenic genes as well as PPAR $\alpha$  target genes involved in FA oxidation [442]. Evidence suggests that, in humans, the hepatic expression of LXR increases with the progression of NAFLD. Animals fed a HFD for 8, 12, 24 or 32 weeks showed increased levels of the LXR target genes *Abcg5* and *Abcg8* [437]. Furthermore, the expression of LXR $\alpha$  increases by 2- and 3-fold in the livers of NAFLD and NASH patients, respectively [443]. LXR target genes are involved in both cholesterol and FA metabolism,

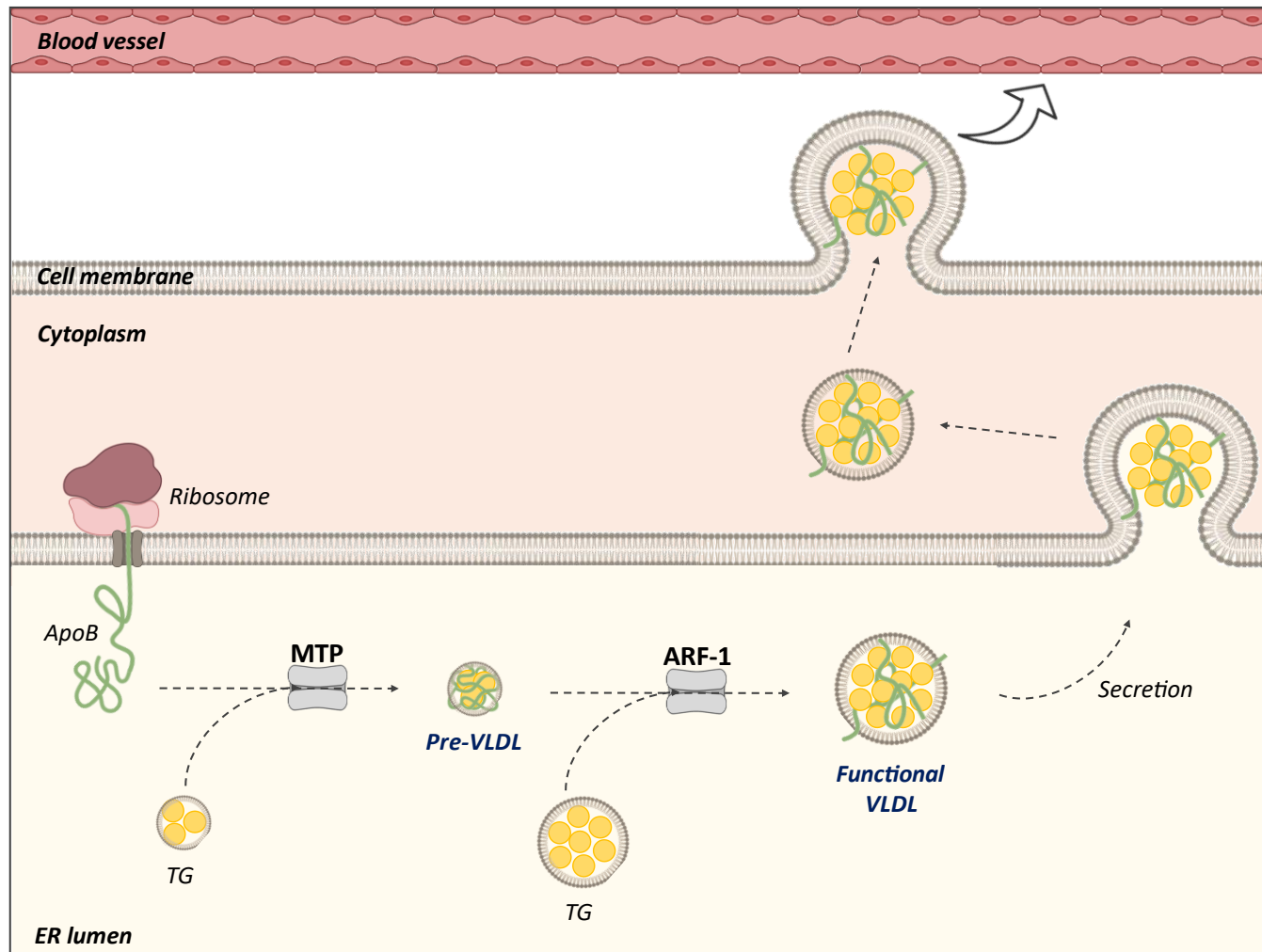


**Figure 18: Synthesis and secretion of VLDL**

ER: Endoplasmic reticulum; **ApoB**: Apolipoprotein B; **TG**: Triglycerides; **VLDL**: Very-low density lipoprotein; **MTP**: Microsomal transfer protein; **ARF-1**: ADP-ribosylation factor 1

such as SREBP-1c, FAS, ACC and the FA transporter cluster of differentiation 36 (CD36) [443]. LXR agonists increase steatosis but decrease inflammation, in part due to the IL-6 responsive gene product, *C/EBP-B*. Studies have shown that animal models of *C/EBPβ* depletion exhibit lower levels of steatosis in response to LXR agonists [444]. Recent evidence suggests that hepatic expression of the long noncoding RNA *Blnc1* (lipogenic factor) enhances the stimulatory effects of LXR agonists on DNL and is required for *in vivo* and *in vitro* LXR-mediated lipogenic activation [445].

- **FXR:** While LXR facilitates the storage of lipids, FXR decreases TG levels and improves glucose metabolism. FXR has a central role in the control of hepatic bile acids as well as lipid and glucose metabolism [446]. In obese rats, a deficiency in FXR promotes the expression of FAS, SREBP-1c and SCD1, resulting in hepatic steatosis, hyperglycaemia, hyperlipidaemia, and bile acid dysregulation [447]. Individuals with NASH present lower levels of FXR, and FXR-KO animals fed a methionine-choline deficient (MCD) diet present aggravated liver inflammation [448].

- Decrease in VLDL synthesis and export

The formation of hepatic VLDL is a two-step process that occurs in the lumen of the ER (**Figure 18**) [449]. In the first step, the microsomal transfer protein (MTP) mediates the partial lipidation of a recently formed apolipoprotein B (ApoB) by a small amount of TG in order to create a small and lipid-poor pre-VLDL. In the second step, ADP Ribosylation Factor-1 (ARF-1) mediates the fusion between primordial VLDL and TG-rich particles already present in the lumen in order to form a fully functional VLDL, which will be secreted and then transported to the adipose tissue where the TG are stored [449]. While only one molecule of ApoB is associated with each VLDL particle, the TG content in the VLDL can vary considerably [450].

Under normal circumstances, glucose from excess dietary carbohydrates undergoes glycolysis in liver and is eventually converted into FA to be esterified to TG for VLDL secretion (**Figure 19A**). VLDL synthesis is inhibited by insulin given that this hormone downregulates the expression of ApoB and MTP as well as the activity of ARF-1 [451]. However, NAFL individuals with hyperinsulinemia show impaired insulin suppression of VLDL secretion and concentration [452]. Moreover, obese individuals with NASH and hyperinsulinemia present decreased levels of *APOB* mRNA, as well as less production and secretion of VLDL [453]. In fact, genetic defects in *APOB* and *MTP* can impair VLDL secretion, therefore triggering hepatic steatosis that may further progress to NASH and fibrosis, even in the absence of obesity [454]. Recently, it has been reported that a deficiency of *PNPLA7* expression results in reduced VLDL secretion by increasing the degradation of ApoE (important for VLDL secretion and clearance) [455]. Interestingly though, studies suggest

that NAFLD may be much more associated to VLDL particle size rather than VLDL particle concentration, given that the former increases as the disease evolves from simple steatosis to NASH [456, 457]. Since particles with diameter above that of the sinusoidal endothelial pores cannot be secreted, the increase in particle size may present a problem and ultimately result in lipid retention and disease progression. Studies suggest that a prolonged exposure to FA, both *in vitro* and *in vivo*, leads to ER stress and post-translational degradation of ApoB [458, 459]. However, due to contradictory studies, the exact mechanisms behind the inadequate export of liver TG-VLDL in cases of hepatic steatosis are not completely understood. According to literature, obese people with NAFL have higher secretion of VLDL when compared to lean subjects, and moderate *in vitro* exposure to FA increases the levels of ApoB secretion [450, 458, 460].

- Changes in mitochondrial homeostasis

#### **A) Mitochondrial FA oxidation**

Mitochondrial FA oxidation or mitochondrial  $\beta$ -oxidation (mtFAO) is a process that allows the oxidation of FA of different lengths (**Figure 19B**), namely long-chain FA (LCFA) (13 to 21 carbons), medium-chain FA (MCFA) (6 to 12 carbons) and short-chain FA (SCFA) ( $\leq 5$  carbons) (**Figure 20**) [461]. Very long-chain FA (VLCFA) ( $\geq 22$  carbons) are preferentially oxidized in peroxisomes (**Figure 20**).

Regardless of their size, exogenous FA enter hepatocytes and must be activated into acyl-CoA before being metabolized. The activation of FA into molecules of acyl-CoA is catalysed by an acyl-CoA synthetase (ACS) specific to the length of the FA carbon chain (**Figure 21**) [462–464]. MCFA and SCFA enter mitochondria without secondary aid (due to their small size and high hydrosolubility) and are activated in the mitochondrial matrix by their respective ACS (medium-chain and short-chain ACS). By contrast, the situation for VLCFA and LCFA is not that simple, and they require a specific shuttle system to enter mitochondria (**Figure 21**) [464].

VLCFA and LCFA are activated into acyl-CoA in the cytosol by long-chain ACS that are located in the outer mitochondrial membrane (OMM), as well as peroxisomal and microsomal membranes. However, given that both the OMM and the inner mitochondrial membrane (IMM) are impermeable to acyl-CoA, the transport of these long-chain acyl-CoA to the mitochondrial matrix involves a special transport system: the carnitine palmitoyltransferase (CPT) shuttle (**Figure 21**) [461, 465]. This shuttle system involves three major entities: the carnitine palmitoyltransferase 1 (CPT1), the carnitine acylcarnitine translocase (CACT) and the carnitine palmitoyltransferase 2 (CPT2) [466]. The process begins with the transformation of the acyl-CoA molecules into

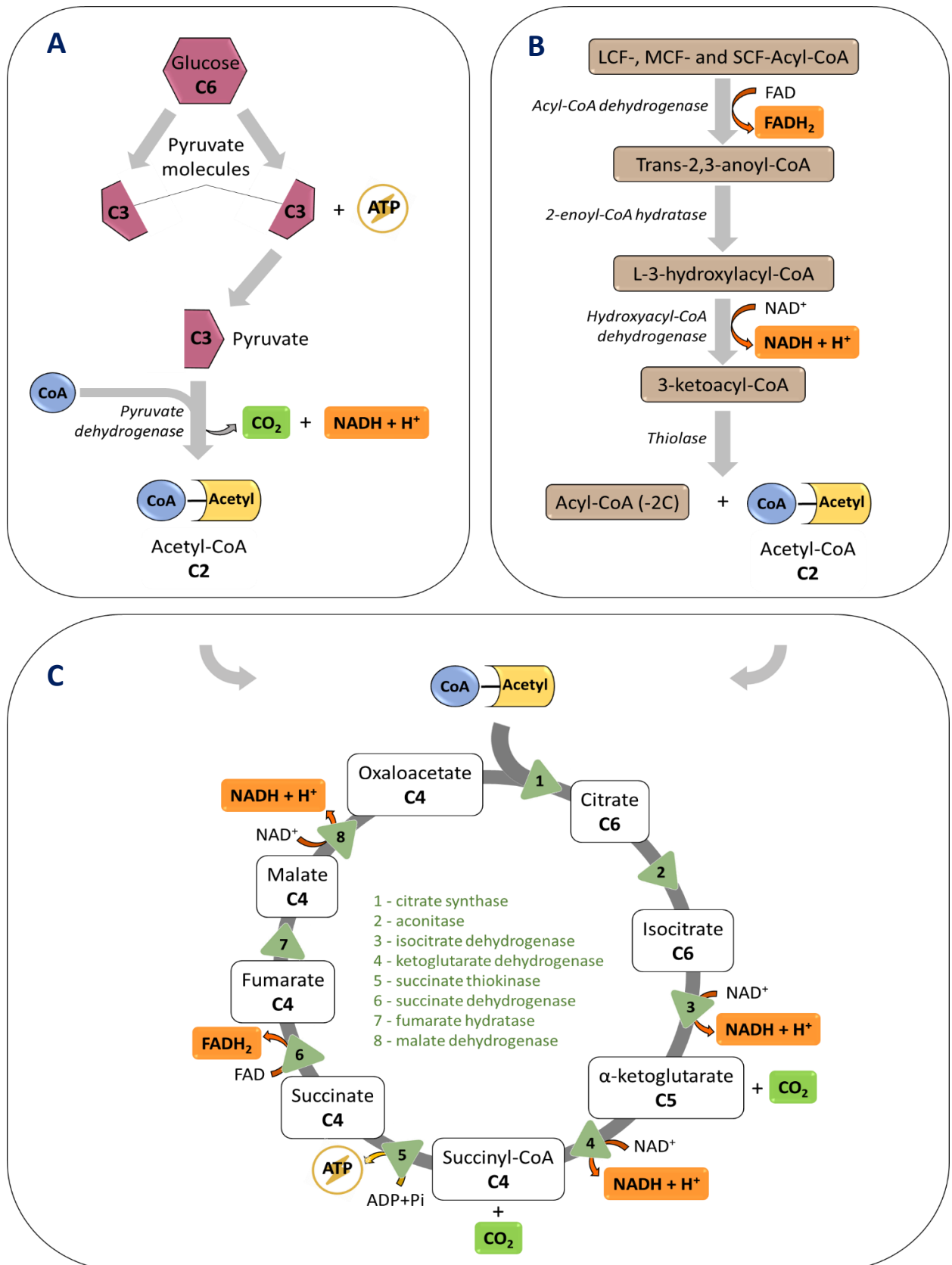
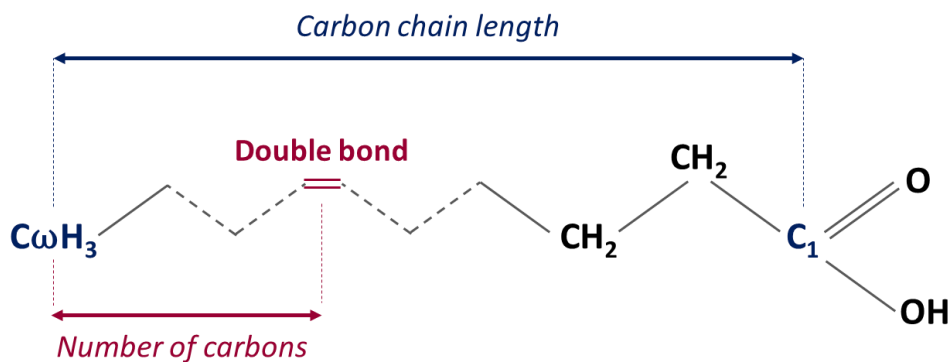


**Figure 19: Glycolysis (A), mitochondrial FA β-oxidation (B) and the Tricarboxylic Acid Cycle (C)**

The tricarboxylic acid (TCA) cycle comprises a series of chemical reactions used by all aerobic organisms to release energy through the oxidation of acetyl-CoA that mainly derives from carbohydrates (A) and fats (B).

LCF: long-chain fatty acyl-CoA; MCF: medium-chain fatty acyl-CoA; SCF: short-chain fatty acyl-CoA

- $\leq 5$  carbons: Short-chain fatty acid (SCFA)
- 6-12 carbons: Medium-chain fatty acid (MCFA)
- 13-21 carbons: Long-chain fatty acid (LCFA)
- $\geq 22$  carbons: Very-long chain fatty acid (VLCFA)



- $\omega 3$  family: 3 carbons separate the first or only double bond from  $C\omega$
- $\omega 6$  family: 6 carbons separate the first or only double bond from  $C\omega$
- $\omega 9$  family: 9 carbons separate the first or only double bond from  $C\omega$



***No double bond: saturated fatty acid***  
***One double bond: monounsaturated fatty acid***  
***Two or more double bonds: polyunsaturated fatty acid***

**Figure 20: Structure and designation of fatty acids**

acylcarnitines by CPT1, located in the OMM. Acylcarnitines are then translocated across the IMM into the mitochondrial matrix through the action of CACT. Finally, CPT2, located on the matrix face of IMM, transfers the acyl group from carnitine back to CoA, yielding acyl-CoA (**Figure 21**) [461, 465]. The importance of the CPT shuttle system in the hepatic oxidation of LCFA is accentuated by the phenotype of patients deficient in CPT1A (liver isoform of CPT1) [250, 467]. Human CPT1A deficits are manifested in hypoketotic hypoglycaemic episodes that begin in early childhood and are usually associated with fasting or illness, and display hepatic steatosis [250, 467]. The recurrent attacks leave dangerous neurological side-effects that most of the times lead to an untimely death.

Once inside the mitochondrial matrix, all acyl-CoA undergo the process of FA  $\beta$ -oxidation *per se*, which ultimately yields one acetyl-CoA molecule and an acyl-CoA shortened by two carbons [462–464]. This smaller acyl-CoA molecule is then further oxidized in other cycles of FA  $\beta$ -oxidation until its entirety is converted to molecules of acetyl-CoA [461]. Each FA  $\beta$ -oxidation cycle comprises 4 reactions (**Figure 19B**): 1) the conversion of acyl-CoA into trans-2,3-enoyl-CoA by acyl-CoA-dehydrogenase; 2) the conversion of trans-2,3-enoyl-CoA into L-3-hydroxyacyl-CoA by 2-enoyl-CoA hydratase; 3) the conversion of L-3-hydroxyacyl-CoA into 3-ketoacyl-CoA by hydroxyacyl-CoA dehydrogenase and, finally, 4) the conversion of 3-ketoacyl-CoA into acyl-CoA and acetyl-CoA by 3-oxoacyl-CoA thiolase [462–464]. The acetyl-CoA formed during this cycle is then condensed in order to form ketone bodies or directed towards the tricarboxylic acid (TCA) cycle, where it is completely oxidated into molecules of NADH, FADH<sub>2</sub> and CO<sub>2</sub> [462–464, 468].

### A) TCA cycle

The TCA cycle is the final step in the oxidation of sugars, lipids and proteins that allows the production of energy (ATP) and reducing equivalents (NADH, FADH<sub>2</sub>) [468]. This cycle occurs in the mitochondrial matrix and its enzymatic reactions may be schematically divided in 3 steps (**Figure 19C**) [468]:

- One molecule of acetyl-CoA (2C) and one molecule of oxaloacetate (4C) are combined through the actions of citrate synthase to form citrate (6C), which is subsequently transformed in isocitrate by aconitase;

- Then, isocitrate (6C) successively releases two of its carbons as CO<sub>2</sub> molecules in a pair of similar reactions that produce one molecule of NADH each time;

- The remaining 4C molecule (succinyl-CoA) undergoes a series of additional reactions; first generating an ATP molecule, then reducing the electron carrier FAD to FADH<sub>2</sub>, and finally

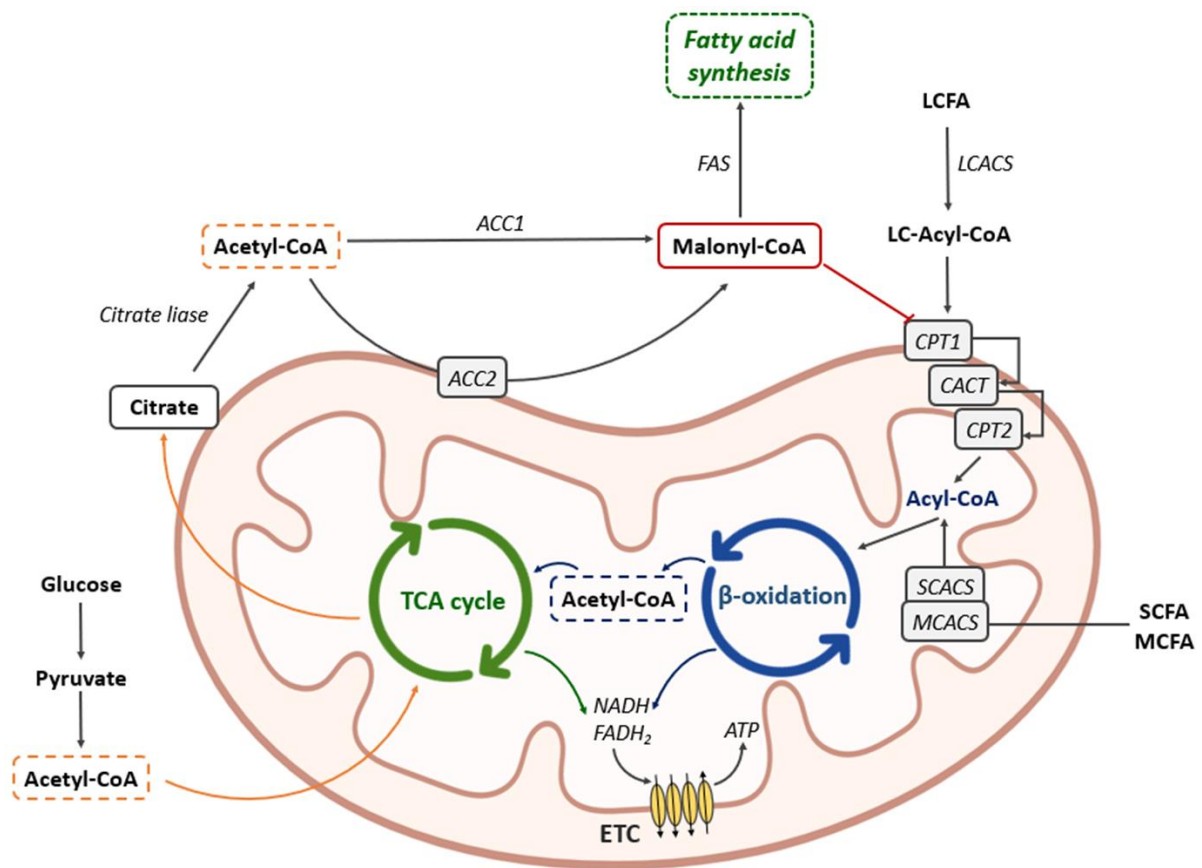


**Figure 21: Fatty acid metabolism**

In the cytosol, long-chain fatty acids (LCFA) are activated into LC-acyl-CoA via long-chain acyl-CoA synthetase (LCACS). The LC-acyl-CoA enter the mitochondrion via the carnitine palmitoyltransferase (CPT) shuttle, which comprises carnitine palmitoyltransferase 1 (CPT1), carnitine acylcarnitine translocase (CACT) and carnitine palmitoyltransferase 2 (CPT2). On the other hand, medium-chain fatty acids (MCFA) and short-chain fatty acids (SCFA) enter the mitochondrion without secondary aid and are directly activated in the mitochondrial matrix by medium-chain acyl-CoA synthetase (MCACS) and short-chain acyl-CoA synthetase (SCACS), respectively. Inside mitochondria, the acyl-CoA molecules are broken down in a series of enzymatic reactions known as  $\beta$ -oxidation. FADH<sub>2</sub> and NADH are released and used as co-factors in the electron transport chain (ETC). The ETC forms a proton gradient that drives the production of ATP by ATP synthase (ATPase). The acetyl-CoA formed during this cycle is then condensed and directed towards the tricarboxylic acid (TCA) cycle where it is completely oxidated into molecules of NADH, FADH<sub>2</sub> and CO<sub>2</sub>. Conversely, most of the acetyl-CoA that is used for fatty acid synthesis derives from carbohydrates via the glycolytic pathway. Pyruvate enters mitochondria and is converted to acetyl-CoA through the action of pyruvate dehydrogenase (PDH). This acetyl-CoA enters the TCA cycle, where it is oxidised for citrate production. Citrate is transported to the cytosol where it is reconverted to acetyl-CoA. Acetyl-CoA carboxylase 1 and 2 (ACC1 and ACC2) mediate the conversion of acetyl-CoA to malonyl-CoA. Malonyl-CoA is used as substrate by fatty acid synthase (FAS) for the production of fatty acids, while inhibiting CPT1 and impairing FA  $\beta$ -oxidation.



generating another NADH. These reactions allow the regeneration of oxaloacetate (the molecule that starts the cycle).

For each molecule of acetyl-CoA that enters the TCA cycle are produced 2 molecules of CO<sub>2</sub>, 3 molecules of NADH and H<sup>+</sup>, 1 molecule of FADH<sub>2</sub>, and 1 molecule of ATP [468] (**Figure 19C**). The reducing equivalents serve as electron carriers for Complex I (NADH) and Complex II (FADH<sub>2</sub>) of the ETC [468]. Located in the IMM, Complexes I, III and IV of the ETC pump H<sup>+</sup> across the membrane in order to generate the electrochemical H<sup>+</sup> gradient that drives mitochondrial ATP production by the ATP synthase (ATPase) (**Figure 8**) [468].

### A) Abnormal mtFAO

In cases of IR, lipolysis in the adipose tissue increases, thus augmenting the levels of circulating FA and FA uptake by the liver. Attempting to compensate the increasing hepatic TG deposition, liver mitochondria are able to boost the rate of mtFAO [461]. Although literature is slightly controversial about this matter, it is widely accepted that this raise of mtFAO is a metabolic adaptation observed in cases of NAFLD [461]. However, increased mtFAO leads to increased flow of reducing equivalents through the ETC, which leads to a higher release of mitochondrial ROS, mainly derived from Complexes I and III [469]. Eventually, mitochondria get overwhelmed with the increased liver fat load and end up getting impaired [461]. In fact, it is well documented that dysfunctions in mtFAO are directly associated to the development of hepatic steatosis [470–473] whereas increasing the expression or activity of hepatic enzymes involved in mtFAO reduces TG accumulation [474].

Dysfunctions in hepatic mtFAO can result from (1) the inhibition of CPT1A due to the overproduction of malonyl-CoA (**Figure 21**) resulting from enhanced DNL [475]; (2) the hepatic accumulation of toxic lipids such as ceramides and oxidized cardiolipin [476]; or (3) the increased mitochondrial oxidative stress that results from substrate overload [477]. Studies have shown that severe inhibition of mtFAO mainly induces microvesicular steatosis while moderate inhibition could lead to macrovesicular steatosis [478].

A study has shown that obese individuals in a late stage of NASH (presence of cirrhosis) display lower mRNA levels of *catalase*, *ACS* and *SOD1* [479]. On the contrary, Kohjima *et al.* have shown that NAFLD patients (both NAFL and NASH) have higher levels of catalase and SOD in order to neutralize the overproduced ROS, and that FAO by microsomes and peroxisomes is highly increased [480]. They have also reported that the mRNA levels of *CPT1A* in the NAFLD subjects were 50% decreased when compared to the controls [480]. In a similar way, animal models fed

for 4 weeks with MCD diet, in order to develop NASH, presented decreased liver CPT1A activity and, therefore, impaired mtFAO [481]. Following this line of thought, it has been reported that the liver overexpression of a malonyl-CoA-insensitive mutated form of CPT1A leads to a sustained rise of hepatic mtFAO and enhanced both glucose tolerance and insulin sensitivity in mice fed a high-fat/high-sucrose (HF/HS) diet [482]. Recently, it has been shown that the long-term expression of a constitutively active form of CPT1A in the liver of NAFLD animal models is responsible for the enhancement of mtFAO, glucose homeostasis and autophagy, as well as for the reduction of hepatic steatosis [475]. Indeed, impairment of mtFAO has been linked to a negative impact on hepatic gluconeogenesis. Given that acetyl-CoA is an allosteric activator of pyruvate carboxylase (PC), an enzyme that promotes gluconeogenesis and the TCA cycle, when the levels of acetyl-CoA are deeply reduced, the activity of PC is compromised [483]. Downregulation of PC can exacerbate the already existing hypoketoneemia-related ATP depletion, favouring organ damage [484].

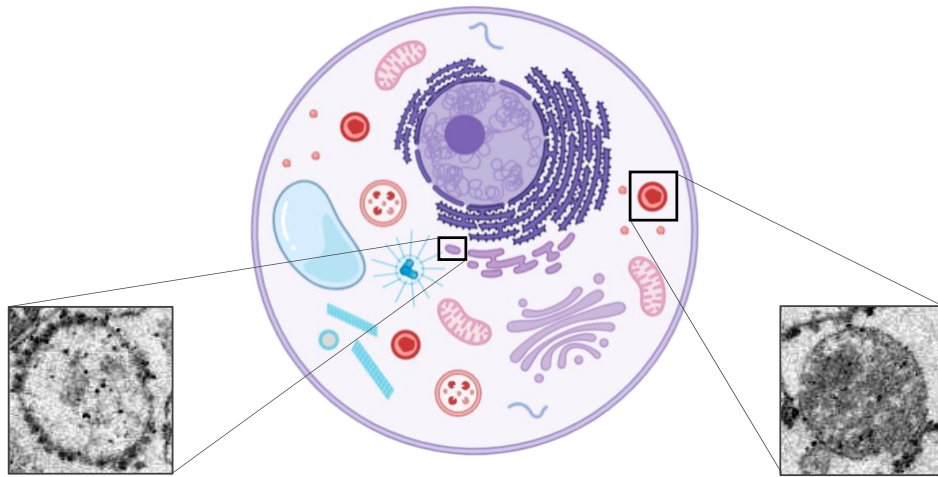
Despite the enormous amount of evidence pointing to dysfunctional mtFAO in cases of NAFLD, the variability found between the different studies is undeniable and could possibly result from differences in the dietary composition of the HF and control diets, treatment duration, genetic background of the animal models, and even the methods to assess mtFAO.

- Increased FAO in non-mitochondrial pathways

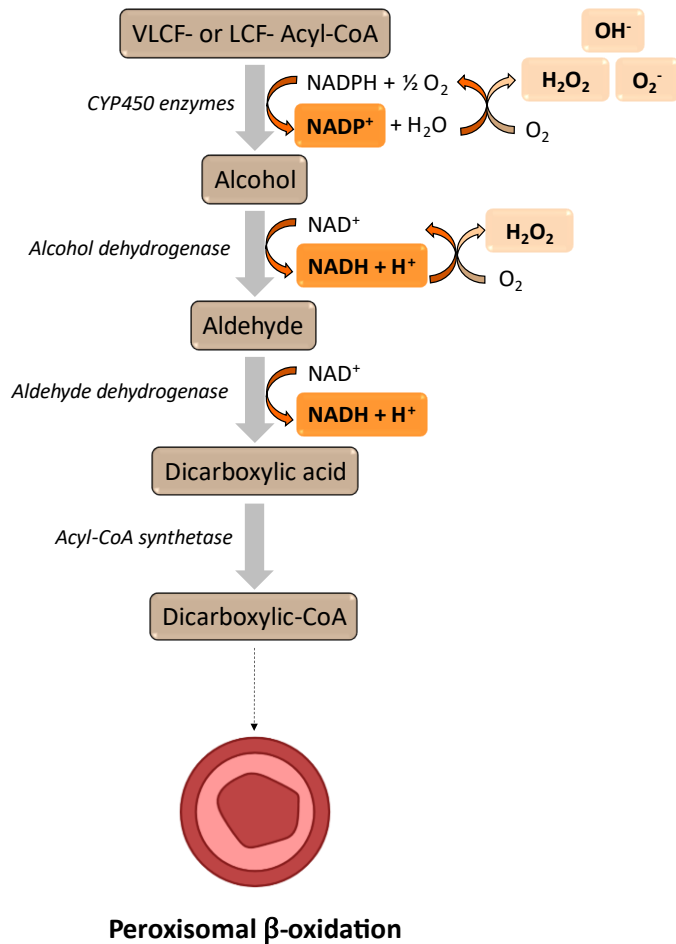
While the process of FAO primarily occurs in the mitochondria, lipid overload and/or compromised mitochondrial function forces a higher degree of FAO to take place in peroxisomes and microsomes.

### **A) Peroxisomal FA $\beta$ -oxidation**

As aforementioned, unlike SCFA, MCFA and LCFA, VLCFA are essentially oxidized in peroxisomes. This is due to the fact that mitochondria do not possess a very long-chain ACS [485]. The peroxisomal FA oxidation (pFAO) consists of a 4-step cycle in which participate 4 enzymes: acyl-CoA oxidase (AOX), enoyl-CoA hydratase, 3-hydroxyl-acyl-CoA dehydrogenase and  $\beta$ -ketothiolase [485, 486]. Much like mtFAO, pFAO yields one molecule of acetyl-CoA and an acyl-CoA shortened by two carbons in each cycle. Unlike mitochondria, peroxisomes do not have ETC, so the pFAO cycles are not coupled to oxidative phosphorylation, and hence no ATP production (**Figure 22**). Instead there is production of hydrogen peroxide ( $H_2O_2$ ), which is subsequently degraded in  $H_2O$  and  $O_2$  by catalase [485, 486]. Unlike mtFAO, in which the goal is to ultimately



### Microsomal $\omega$ -oxidation



### Peroxisomal $\beta$ oxidation

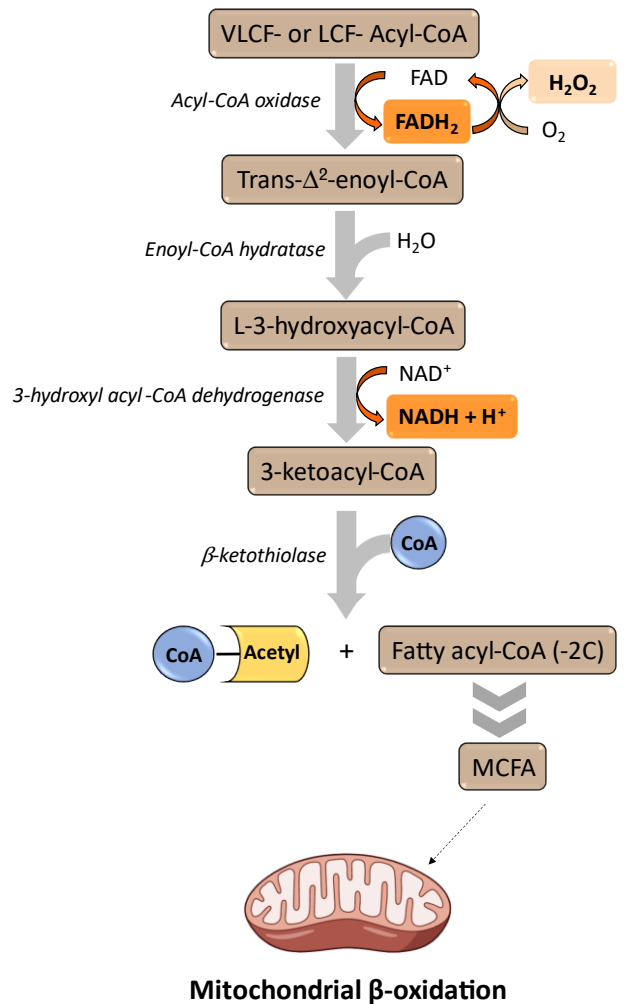


**Figure 22: Microsomal and peroxisomal fatty acid oxidation**

**VLCF:** very long-chain fatty acyl-CoA; **LCF:** long-chain fatty acyl-CoA

*The electronic micrographs used in this figure come from personal archive*

convert the entire acyl-CoA molecule into acetyl-CoA, in pFAO the VLCFA molecule is shortened until the acyl-CoA chain becomes MCFA. Then, the MCFA molecules leave peroxisomes and relocate towards mitochondria, where they are completely oxidized into acetyl-CoA molecules [485, 486].

### **B) Microsomal FA $\omega$ -oxidation**

Microsomal FA  $\omega$ -oxidation (mFAO) occurs in the ER and is controlled by members of the cytochrome P450 superfamily (such as CYP2E1). In physiological situations, mFAO is a minor pathway, but when the liver uptake of FA is too high or mtFAO is impaired, this pathway may be upregulated. During mFAO, LCFA are metabolized to dicarboxylic acids that serve as substrates for pFAO, process that leads to the production of  $O_2^-$  and  $H_2O_2$  (**Figure 22**) [487]. In fact, it has been shown that dicarboxylic acids can serve as biomarkers of lipid peroxidation in individuals with T2DM [487, 488]. Furthermore, the first step of mFAO, which is catalysed by the CYP450 superfamily, involves the transfer of active electrons from NADPH or NADH to  $O_2$ , generating large quantities of  $O_2^-$ ,  $H_2O_2$  and hydroxyethyl radicals [489, 490]. Throughout the years, several papers have reported increased hepatic expression or activity of CYP2E1 in obese patients with or without T2DM, individuals with NASH and animal models of obesity and fatty liver [491–494]. Moreover, recent studies suggest that the use of inhibitory substances of CYP2E1 may serve as therapeutic agents in the prevention or treatment of NAFLD [495, 496].

#### • Accumulation of toxic metabolites

When liver mitochondria, peroxisomes or microsomes cannot handle the massive release of FFA from dysfunctional and IR adipocytes, respiratory oxidation collapses, with subsequent impairment of lipid homeostasis, generation of lipid-derived toxic metabolites and overproduction of ROS. The most well-documented lipotoxic intermediates in the literature are ceramides, diacylglycerols (DAGs) and long-chain acyl-CoA (**Figure 23**). In fact, several studies show that hepatic lipotoxicity is not a consequence of excessive TG accumulation but rather accumulation of these lipid intermediaries, known to alter insulin signalling, to increase the production of pro-inflammatory cytokines and to participate in ER-stress.

Ceramides are a family of lipids that constitute the basis for sphingolipid and sphingomyelin biosynthesis. As bioactive lipids, ceramides have been implicated in a variety of physiological functions such as cellular differentiation, degeneration, and apoptosis. In mitochondria, ceramides suppress the ETC [497] and induce ROS production (**Figure 23**) [498]. A

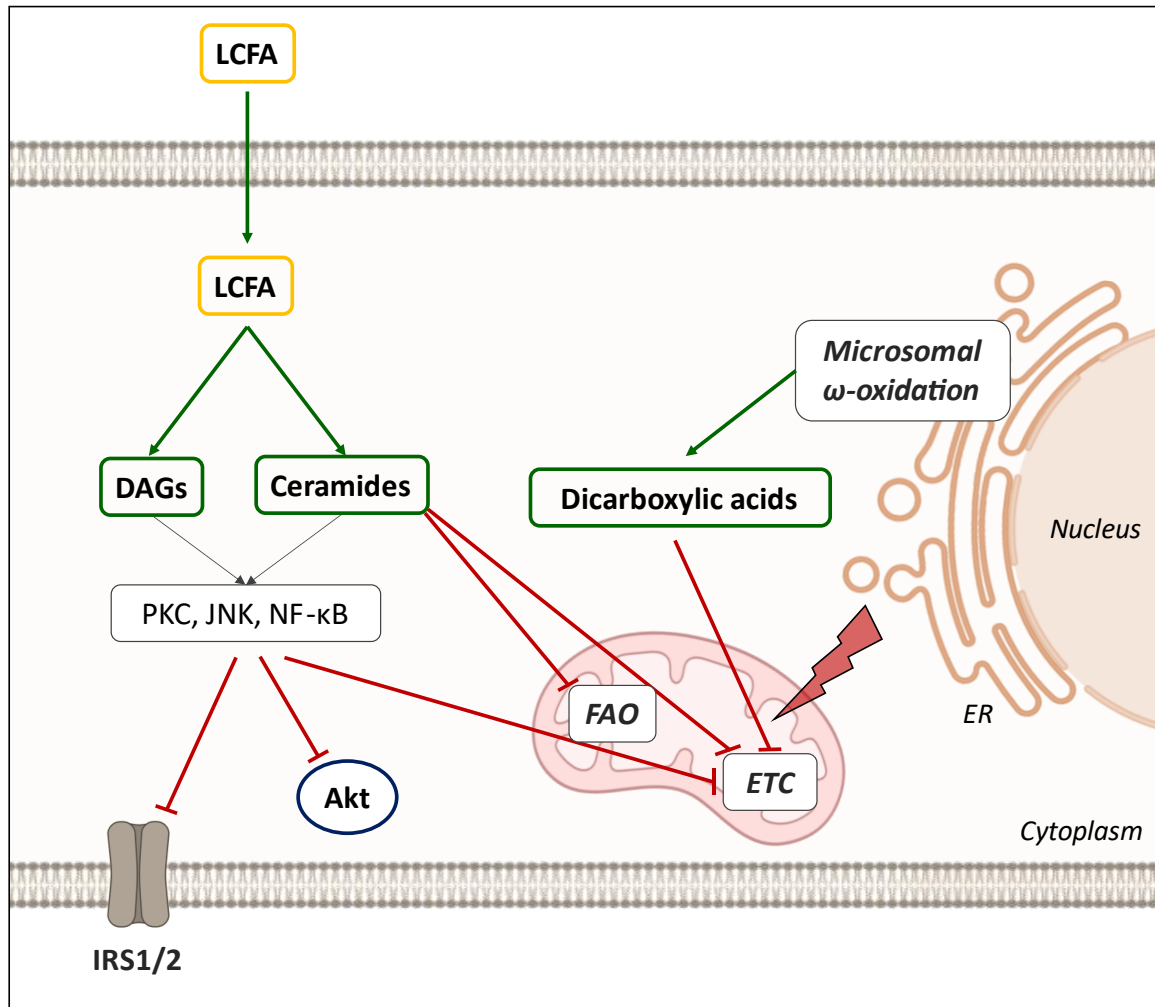


**Figure 23: Intracellular accumulation of toxic metabolites**

Up-regulation of peripheral adipose tissue lipolysis leads to an increased influx of free fatty acids (FFA) into the liver, especially long-chain fatty acids (LCFA). These LCFA can be converted into a number of different lipid species including triglycerides (TG) and diacylglycerols (DAGs), or undergo oxidation in mitochondria, microsomes, or peroxisomes. In cases of insulin resistance (IR), the rate of FFA flux exceeds the secretion of TG, or fat oxidation, resulting in a progressive increase in hepatic lipids, including TG and ceramides. Bioactive lipid species such as DAGs and ceramides have been mechanistically linked to the pathogenesis of IR through the blockade of insulin signalling and action. These metabolites have also been associated to the direct inhibition of mitochondrial electron transport chain (ETC). The accumulation of dicarboxylic acids from increased rates of microsomal fatty acid oxidation has also been linked to the impairment of ETC.

**ER:** endoplasmic reticulum; **PKC:** protein kinase C ; **JNK:** c-Jun N-terminal kinase; **NF-κB:** nuclear factor-kappa B; **IRS1/2:** insulin receptor substrate 1 or 2; **Akt:** protein kinase B; **FAO:** fatty acid oxidation

study published in 2019 has demonstrated that ceramide depletion, through dihydroceramide desaturase 1 (DES1), improved the activity of mitochondrial Complexes I, II and IV [497]. Additional evidence has shown that specific species within this class of lipids (ex: palmitoyl ceramide or C16:0 ceramide) are increased in the plasma, liver and adipose tissue of obese humans and mice [499–501]. These ceramides have been extensively associated to the inhibition of mtFAO and to the negative regulation of insulin signalling and energy expenditure (**Figure 23**) [499, 500]. In fact, studies have shown that ceramides induce skeletal muscle IR as a result of saturated fat activation of toll-like receptor 4 (TLR4) [502]. Ceramides have also been shown to induce IR in many tissues by inhibiting the Akt signalling pathway (**Figure 23**) [503]. In fact, a specific *in vivo* Knock-down (KD) model for hepatic ceramide synthase 6, responsible for C16:0 ceramide production, has shown an amelioration of IR, hyperglycaemia and obesity [501]. Similarly, the inhibition of ceramide synthase 1, responsible for the production of ceramide C18:0, has been shown to increase mtFAO in the skeletal muscle and to prevent TG accumulation in muscle and adipose tissue in NAFLD animal models [504]. Interestingly, however, this inhibition did not protect against diet-induced IR [504].

Similarly to ceramides, in biochemical signalling, DAGs function as both intermediates in lipid biosynthesis and signalling molecules. DAG is a physiological activator of protein kinase C (PKC). Increased concentrations of DAGs lead to activation of PKC in skeletal muscle and liver, which, in turn, decreases insulin-stimulated IRS-1/IRS-2 tyrosine phosphorylation, phosphatidylinositol-4,5-bisphosphate 3-kinase (PI3K) activation and downstream insulin signalling (**Figure 23**) [505]. A recent study using mouse embryonic fibroblasts has shown that the accumulation of DAGs upon palmitate treatment could deteriorate insulin signalling not only through PKC but also through the activation of JNK [506]. Furthermore, promoting mtFAO by knocking down ACC1 and ACC2 resulted in reduced DAG content, decreased PKC activation and protected from fat-induced hepatic IR [507]. Although a wide number of studies converge towards the conclusion that both DAGs and ceramides cause IR in metabolic organs, there are still some uncertainties on their mechanisms of action.

Dicarboxylic acids are another type of toxic metabolite that induces mitochondrial dysfunction (**Figure 23**). As previously discussed, when mtFAO can no longer cope with the excessive load of FFA, alternative pathways of FAO are activated, such as mFAO. The major products of mFAO are dicarboxylic acids. Studies have shown that, in rat liver, medium-chain dicarboxylic acids can inhibit Complexes I and II as well as coenzyme Q, thus impairing ATP production [508, 509].

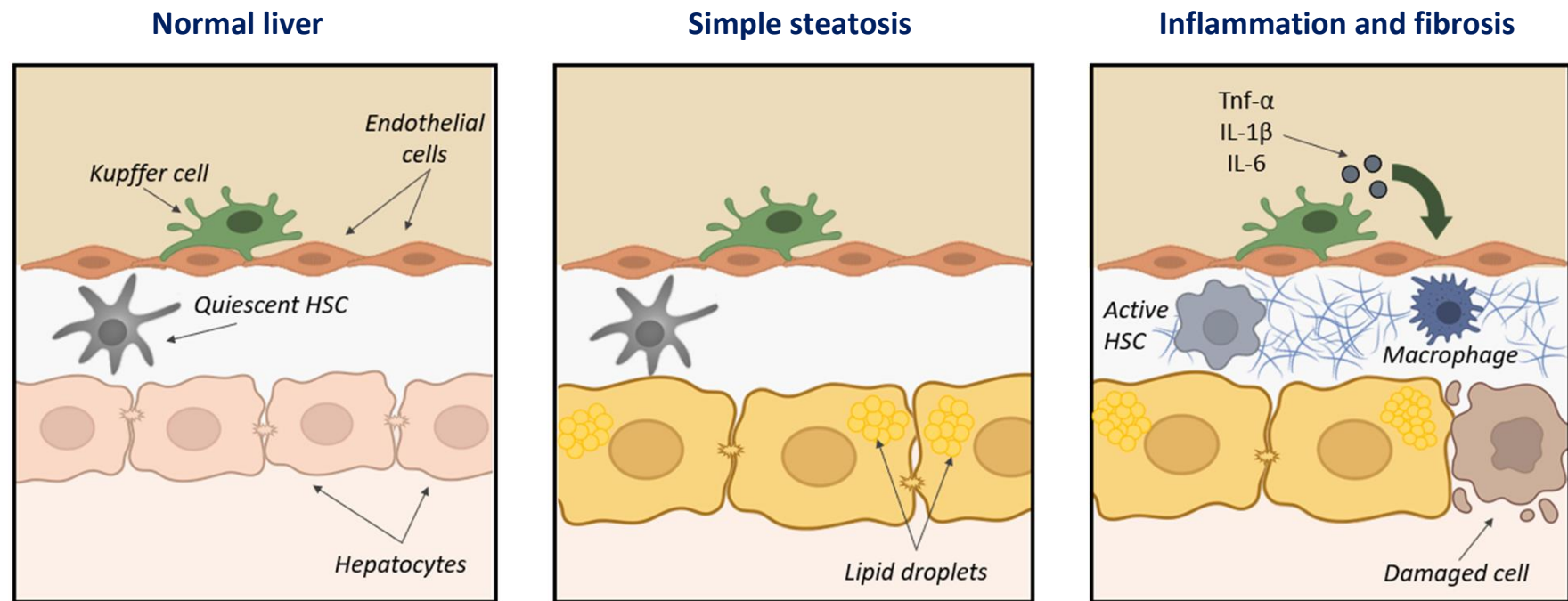


**Figure 24: Participation of inflammation in the development of Non-Alcoholic Fatty Liver Disease (NAFLD)**

During the development of NAFLD, the overload and altered composition of liver tissue lipids can modulate the biological activity of Kupffer cells, the resident liver macrophages, and hepatic stellate cells (HSC) [480]. HSC exist in the space between hepatocytes and endothelial cells. In a normal liver, HSC are described as being in a quiescent state. However, when the liver is damaged, HSC can change into an activated state. The activated HSC are characterized by proliferation and contractility, being responsible for the secretion of collagen that eventually leads to hepatic scarring. Additionally, activated Kupffer cells are a significant source of pro-inflammatory cytokines such as transforming growth factor  $\alpha$  (TNF $\alpha$ ), interleukin-1 $\beta$  (IL-1 $\beta$ ) and interleukin-6 (IL-6), that can serve as recruiters of other immune cells. The increase in inflammatory cells and mediators ends up inducing hepatocyte injury and liver scarring [480].

## b) “Second hit”: further insults

### • Inflammation

Chronic hepatic FA accumulation, excessive FAO and tissue insensitivity to insulin signalling make the liver extremely vulnerable to secondary insults such as inflammation. Several papers have demonstrated that hepatic inflammation is a major aggravating factor of liver steatosis [510]. At a cellular level, this task is carried out by activated hepatic stellate cells (HSC) and Kupffer cells (resident liver macrophages), as well as other pro-inflammatory cells that infiltrate the liver (**Figure 24**). HSCs account for 6% of the total number of liver cells and have been identified as the primary source of myofibroblasts in animal models of hepatotoxic liver injury [511]. Recently, it has been described that activated HSC isolated from mice subjected to western diet have almost 3000 overexpressed genes when compared to quiescent HSC. Among these are the transcriptional regulators ETS proto-oncogene-1 (ETS1) and Runt-related transcription factor-1 (RUNX1), which appear to act as drivers of NASH-associated HSC plasticity [512]. In fact, RUNX1 as well as its known targets chemokine (C-C motif) ligand-2 (CCL2), eNOS, phosphatidylinositol-4,5-bisphosphate 3-kinase catalytic subunit alpha (PI3KCA) and protein kinase C epsilon (PRKCE) have been found upregulated in patients with NASH [513]. Regarding Kupffer cells, they account for 15% of all liver cells, constituting the largest tissue specific population of macrophages in the body [514, 515]. These cells are rapid releasers of pro-inflammatory cytokines and chemokines such as TNF $\alpha$ , interleukin 1 $\beta$  (IL-1 $\beta$ ), IL-6, CCL2 and CCL5, which serve as recruiters of other immune cells (**Figure 24**) [510, 516]. A study has shown that the serum concentration of both TNF $\alpha$  and IL-6 are increased in obese people with or without T2DM [517]. Recently, it has been demonstrated that individuals with morbid obesity and advanced NASH present higher WAT mRNA levels of both *TNFA* and *IL-6* when compared to individuals with obesity and NAFL [518]. Interestingly though, this pattern was not found in the liver of the same patients [518]. Nonetheless, it had been already demonstrated by Crespo *et al.* that *TNFA* mRNA was overexpressed in the liver of NASH patients when compared to NAFL individuals [519]. Additionally, plasma levels of IL-1 $\beta$  and IL-6 were found augmented in NASH patients when compared to NAFL patients or healthy individuals [520].

A 2010 French study has quantified the expression of 222 genes involved in inflammatory and immune responses in biopsy-proven morbidly obese NAFLD patients [521]. Of those 222 genes, 47 were overexpressed when compared to samples recovered from lean individuals, and 58 were overexpressed in patients with already advanced NASH. Researchers concluded that the genetic differences found in the study may be present even before histological signs of inflammation or severe steatosis appear [521].



- Endoplasmic reticulum-associated stress

The ER is a very dynamic organelle involved in protein secretion and folding, calcium homeostasis and lipid biogenesis. Despite its remarkable capacity to adapt, under certain perturbing circumstances (ex: hyperlipidaemia, inflammation, viral infection, drugs), ER protein-folding is affected [522]. The consequence is a huge ER accumulation of misfolded proteins that triggers the Unfolded Protein Response (UPR), a conserved pathway aiming to restore ER homeostasis and resolve ER stress before it leads to cell death (**Figure 25**). UPR activation triggers a cascade of several coordinated responses such as 1) reduction of protein synthesis; 2) increased expression of chaperone proteins in order to promote protein folding and transport; and 3) increased degradation of misfolded proteins. If these mechanisms are not efficient enough for ER homeostasis recovering, the cell hits the self-destruct button through ER-induced apoptosis [522].

The UPR signal is transmitted by three ER transmembrane proteins: the Inositol-Requiring Enzyme 1 (IRE1), the PKR-like Endoplasmic-Reticulum Kinase (PERK) and the Activating Transcription Factor 6 (ATF6), all of which become activated once the chaperone protein BIP/GRP78 (Binding immunoglobulin protein/78 kDa glucose-regulated protein) dissociates from them [522]. If this adaptive response is insufficient due to chronic or acute ER stress, ER function cannot be preserved and a “terminal UPR” is triggered. The latter consists in the activation of the autophagy- and apoptosis-related proteins c-Jun Terminal Kinase (JNK) and CCAAT/enhancer-binding Homologous Protein (CHOP) [522].

Several studies have demonstrated a link between UPR activation and the progression of NAFLD. Human liver cell lines incubated with stearate (C18:0) present UPR activation before undergoing cellular apoptosis [523]. Curiously, cellular capacity to synthesize and stock TG is interrupted in the presence of stearate but remains unchanged in the presence of oleate (C18:1) [523]. Using HepG2 and primary human hepatocytes, researchers have found that CHOP is able to induce cell death and inflammatory responses after exposure to saturated FA by activating NF- $\kappa$ B through a pathway that involved expression of the Interleukin-1 receptor-associated kinase-like 2 (IRAK2) [524]. This activation leads to IL-8 and TNF $\alpha$  release from hepatocytes [524].

Recently, HFD-fed mice or patients with hepatic steatosis have been showed to present an inactivated form of IRE1 [525]. IRE1 plays a crucial role in preventing hepatic steatosis by functioning as a RNase to process a subset of miRNAs that are involved in hepatic lipid metabolism. The inactivation of IRE1 led to increased levels of miR-200 and miR-34, which decreased the expression of their targets, namely SIRT1 and PPAR $\alpha$ . This premise was corroborated by silencing IRE1, which exacerbated hepatic steatosis in mice [525]. In obese patients with NAFL or NASH, the

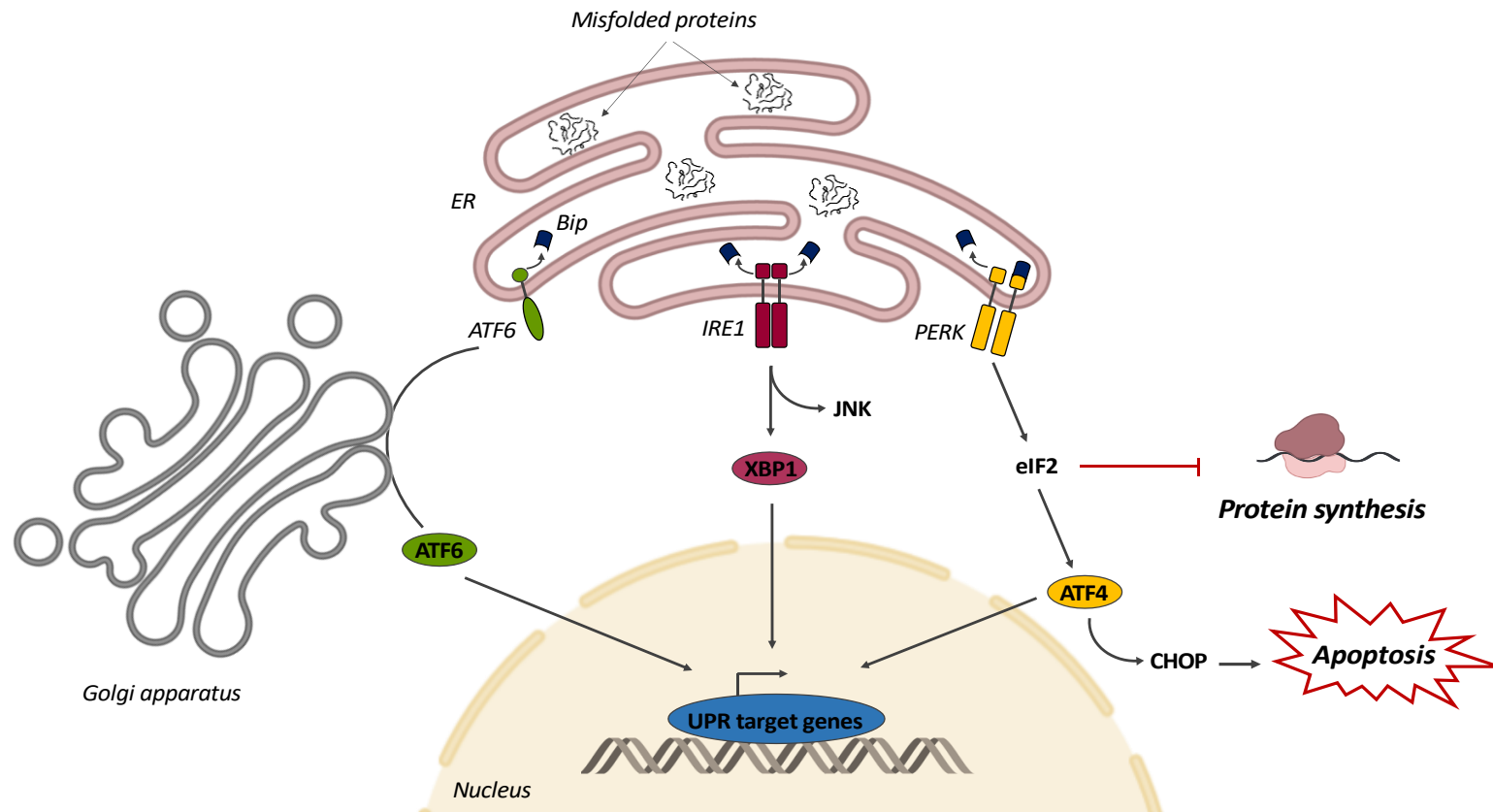


**Figure 25: Endoplasmic reticulum (ER)-associated stress and unfolding protein response (UPR)**

Under certain perturbing circumstances, ER protein-folding is affected. In order to restore ER homeostasis, the UPR pathway is triggered. The UPR signal is transmitted by three ER transmembrane proteins: the activating transcription factor 6 (ATF6), the inositol-requiring enzyme 1 (IRE1) and the PKR-like endoplasmic-reticulum kinase (PERK). These proteins become activated once the chaperone protein Bip dissociates from them. This activation induces a signalling cascade termed the UPR, which involves the downregulation of protein synthesis and the activation of transcription factors that regulate genes promoting ER homeostasis and cell survival. During prolonged or severe ER stress, genes that induce apoptosis are upregulated (JNK and CHOP).

**XBP1:** X-box binding protein 1; **ATF4:** activating transcription factor 4; **eIF2:** eukaryotic initiation factor 2; **CHOP:** CCAAT/enhancer-binding homologous protein; **JNK:** c-Jun N-terminal kinase

phosphorylation of the eukaryotic Initiation Factor-2  $\alpha$  (eIF2 $\alpha$ ), a target of PERK, is increased [526]. Interestingly though, in the same subjects, there was no change in the levels of other UPR intervenients such as CHOP or ATF4 [526]. However, more recently, Kaplon *et al.* have shown that obese individuals have higher expression of IRE1, PERK and ATF6 when compared to non-obese individuals [527].

X-Box binding protein-1 (XBP-1) is a main regulator of UPR, interacting with the PI3K insulin signalling pathway, with increased nuclear translocation induced by insulin. Chromatin immunoprecipitation (ChIP) analysis of both mouse primary hepatocytes and whole livers showed that XBP1 occupies the -743 to -523 site of the promoter of Tfeb (transcription factor EB), a master regulator of autophagy and lysosome biogenesis [528]. Interestingly, this occupancy was significantly reduced in livers from patients with steatosis. Furthermore, the overexpression of Tfeb in a liver KO mouse model for XBP1 fed HFD ameliorated glucose intolerance and hepatic steatosis [528].

#### • Oxidative stress

Oxidative stress is an important regulator of the transition between simple steatosis and steatohepatitis. It comprehends the production of ROS such as  $O_2^-$ , the hydroxyl radical ( $OH^\cdot$ ) and  $H_2O_2$ . In a cell, the main ROS producer is the mitochondrion through the simple operation of its respiratory chain. In fact, a given amount of oxygen is not completely reduced to  $H_2O$  and ends up forming  $O_2^-$  at the level of Complexes I and III. Apart from the mtFAO, ROS can also be produced during pFAO and mFAO (as mentioned in point 2.4.1.) (**Figure 22**). In normal physiological situations only a small part of ROS persists. The levels of ROS are controlled by natural antioxidant defences that cells possess. This system includes mitochondrial Manganese Superoxide Dismutase (MnSOD) and GSH. An imbalance between the level of pro-oxidative species ( $O_2^-$ ,  $H_2O_2$ ) and the amount of antioxidant defences (MnSOD, GSH) may increase the oxidative burden and lead to the damage of macromolecules, such as lipids, DNA, and proteins.

Increased ROS production participates in the progression of NAFL to NASH, and several mechanisms may explain why this production increases. Increased rates of mtFAO induce increased flow of reducing equivalents through the ETC, originating higher amounts of ROS. ROS can react with FA leading to lipid peroxidation and the formation of reactive aldehydes such as trans-4-hydroxy-2-nonenal (4-HNE) and malondialdehyde (MDA) [529]. In the literature there are several papers describing an increase in lipid peroxidation products, such as hydroperoxides and MDA, in the liver and serum of individuals with NAFL and NASH [530] [531] [532]. ROS have also

been shown to increase the expression of different cytokines such as TNF $\alpha$  and IL-8, which have been identified as playing a role in the progression of NAFLD [533]. Additionally, the overproduction of ROS has been linked to impaired liver insulin sensitivity through the activation of forkhead transcription factor 1 (Foxo1), which results in the upregulation of gluconeogenic and oxidative genes [534].

In addition to targeting macromolecules such as lipids and proteins, and due to its proximity to mitochondrial DNA (mtDNA), H<sub>2</sub>O<sub>2</sub> and O<sub>2</sub><sup>-</sup> can trigger several deleterious mutations, which can affect mitochondrial integrity and cellular homeostasis. In 2001, Sanyal *et al.* found that NASH patients presented ultrastructural mitochondrial disturbances, such as loss of mitochondrial cristae and paracrystalline inclusions, when compared to NAFL patients [535]. More recently, Sookoian *et al.* have demonstrated that, when compared to healthy subjects, NAFL patients have a higher mutational rate of liver mtDNA (1.28-fold), and that in NASH patients the mutational rate increases with the disease severity [536]. A great deal of the uncovered mtDNA mutations was found in genes of the ETC chain [536]. Interestingly, it has been shown that the activity of Complexes I, III, IV and V is decreased to 63%, 70%, 62% and 42%, respectively, in NASH patients when compared to healthy subjects [537]. In a similar way, animal models of NASH have shown a total of 21 dysregulated proteins, most of which are actively involved in mitochondrial oxidative phosphorylation, lipid metabolism and mtFAO [538]. Damages in mtDNA induce mitochondrial-specific endonucleases that target the defective mtDNA and cause its depletion. A study has reported that obese NAFL patients present lower liver mtDNA/nuclear DNA ratios when compared with control livers, thus suggesting a significant association between NAFLD and mtDNA depletion [539]. Carlos *et al.* corroborated this observation in a study including 90 NAFLD individuals (obese and insulin resistant NAFL and NASH) by showing that these patients had a significantly lower mtDNA copy number when compared to healthy subjects [540]. Similarly, HFD-fed mice presented decreased mtDNA copy number as well as lower activity of ETC Complexes I and III [538]. However, not all studies report the same evidence. In 2016, Kamfar *et al.* showed that mtDNA copy number in liver biopsy samples was 4.3- and 3.2-fold higher in patients with NAFL and NASH than in control subjects, respectively [541]. One possible reason for the contradictory results found between different NAFLD animal and human studies may be the discrepancies, for example, in sample size, participant ethnicity, animal genetic background, obesity degree, presence or absence of IR, T2DM and hyperlipidaemia.

### 2.4.2. “Multiple-hits” hypothesis

Evidence emphasizing the complexity of the various pathophysiological mechanisms, both hepatic and extrahepatic, behind the development and progression of NAFLD has made the “two-hits” hypothesis over-simplistic, and today the “multiple-hits” hypothesis is more widely accepted and provides a more accurate explanation of NAFLD pathogenesis [542].

This new hypothesis considers that the development of NAFLD derives from the interaction of genetic and environmental factors (diet and physical exercise) as well as changes in the crosstalk between different organs and tissues, including adipose tissue, pancreas, gut, and liver (**Figure 26**) [543]. It also categorizes NAFL and NASH as two separate diseases based on the fact that NAFL individuals seldomly develop inflammation and fibrosis, and that during the development of NASH, inflammation can precede steatosis [543]. Nonetheless, much like the “two-hits” theory, fat accumulation and IR still seem to represent the first triggers.

IR exacerbates fat accumulation in the liver by increasing hepatic DNL and impairing the inhibition of adipose tissue lipolysis [542]. At the same time, hepatic and adipose lipotoxicity caused by the high levels of FFA has its toll on mitochondrial production of ROS and on ER-associated stress. Oxidative stress, abnormal production of adipokines, activation of HSCs and intestinal dysbiosis are among the secondary multiple “hits” that follow the first impact. In fact, this model highlights the role of inflammatory cytokines (especially those originated from the adipose tissue and gut) in the origin of NASH and its possible progression into fibrosis and HCC (**Figure 26**) [542].

#### **a) Gut microbiota**

Since 1972, the general assumption was that inside the human gut there were 10 times more microorganisms than the total number of cells in the human body [544]. This claim was introduced to the world by the microbiologist Thomas Luckey, whose paper was based on a rough estimation of the number of human and microbial cells in the body. This theory, which has been questioned over the last few decades, has finally been debunked by a team of scientists who estimate the real microbial:human cells ratio to be 1.3:1 [545].

Human gut microbiota is constituted by bacteria, archaea, bacteriophages, yeast and fungi, altogether accounting for hundreds of different species. These microorganisms enclose 3.3 million genes, a number that is orders of magnitude bigger than the entire human genome [546]. Recent studies have gone further in postulating that the number of microbial genes surpasses the 20 millions [547].

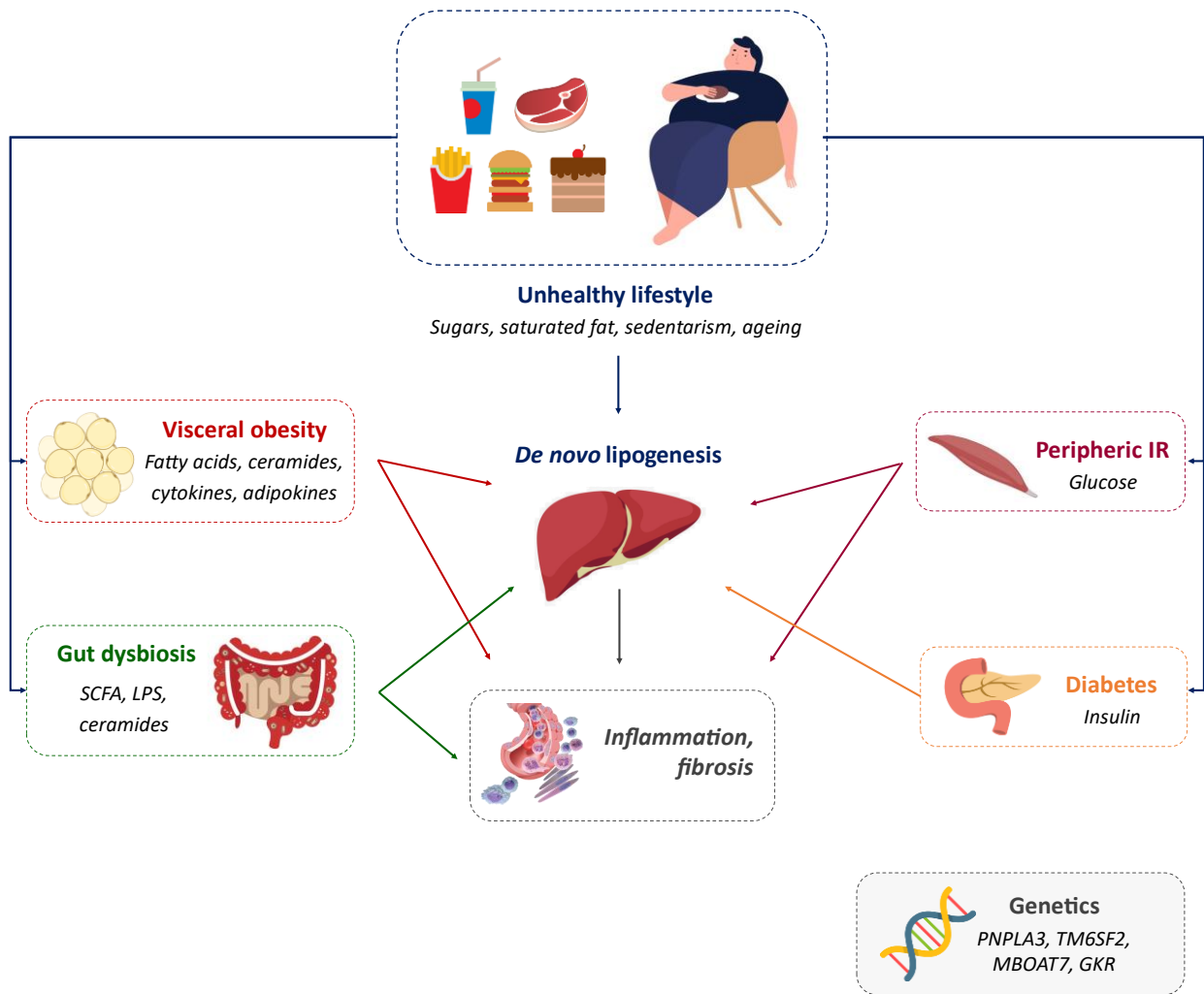


**Figure 26: “Multiple-hits” hypothesis**

Dietary habits and environmental factors can lead to the development of insulin resistance (IR), visceral obesity and changes in intestinal microbiota. IR is one of the key factors in the development of steatosis and results in both increased hepatic *de novo* lipogenesis (DNL) and impaired inhibition of adipose tissue lipolysis. These events are followed by an increased flux of fatty acids to the liver. IR also promotes adipose tissue dysfunction, which leads to abnormal production and secretion of adipokines and inflammatory cytokines. On the other hand, gut dysbiosis facilitates small bowel permeability, which allows the release of pro-inflammatory molecules into circulation. These molecules eventually reach the liver, where they promote hepatocyte inflammation and liver fibrosis. This process is amplified by the lipodystrophy phenotype manifested by the adipose tissue, which releases an uncontrolled quantity of fatty acids, ceramides, cytokines and adipokines. Last but not least, genetic predisposition for hepatic lipid accumulation, inflammation, and fibrosis also contributes to the pathogenesis of NAFLD.

**IR:** insulin resistance; **SCFA:** short-chain fatty acids; **LPS:** lipopolysaccharides; **PNPLA3:** patatin-like phospholipase domain-containing protein 3; **TM6SF2:** transmembrane-6 superfamily member 2; **MBOAT7:** membrane-bound O-acyltransferase domain-containing 7; **GKR:** glucokinase regulator

Of all gut microbial classes, none has been more investigated than bacteria. The human gut microbiota is mostly composed by two dominant bacterial populations: the Firmicutes and the Bacteroidetes [546]. Members of both groups produce SCFA from dietary compounds that escape digestion in the small intestine, thus supplying the host with an additional amount of energy. Normal colonic epithelia derive 60–70% of their energy supply from SCFA, particularly butyrate [548]. Although most SCFAs are utilized in the gut, some amount is transported to the bloodstream and reaches the liver via the portal vein. In the liver they can be channelled into the TCA cycle and become source of energy. In fact, propionate is largely taken up by the liver and is a good precursor for gluconeogenesis, DNL and protein synthesis [549]. Firmicutes and Bacteroidetes represent more than 90% of the total community (~27% Firmicutes and ~69% Bacteroidetes) [550]. The remaining percentage is accounted by other subdominant populations such as Proteobacteria and Actinobacteria [546, 550]. Over the past few decades, it has become clear that the intestinal microbiota is not an idle bystander but rather an interconnected and active player in physiology [551]. For example, when challenged with starvation, germ-free mice survive for a much shorter period of time than conventional mice, although weight loss was the same [552]. Additional studies have shown that gut microorganisms play an important role in host immunity through the secretion of bioactive metabolites, polysaccharide digestion, vitamin synthesis and lipid stocking [551].

The microbiota composition and function are shaped by a variety of host and environmental factors including diet, age, body weight, physical activity, geographical location, medication and intestinal/hepatic illnesses [553]. For instance, the microbiome of obese mice has an increased capacity to harvest energy from the diet and this trait appears to be transmissible upon microbiome colonization. Indeed, germ-free mice transplanted with the “obese microbiome” show significantly greater increase in total body fat than germ-free mice transplanted with a “lean microbiome” [554]. Moreover, if the equilibrium between bacteria and the host is compromised, such as in cases of bacterial overgrowth or changes in bacterial subpopulations, the intracellular junctions of the intestinal mucosa may become impaired and more permeable, which allows bacteria to translocate from the digestive tract into the blood [555, 556].

### **b) Gut-liver axis and intestinal dysbiosis in the development of NAFLD**

Over the years, it has been widely recognized that intestinal microorganisms are implicated in the development of NAFLD, through the gut-liver axis (GLA) (**Figure 27**) [557]. Due

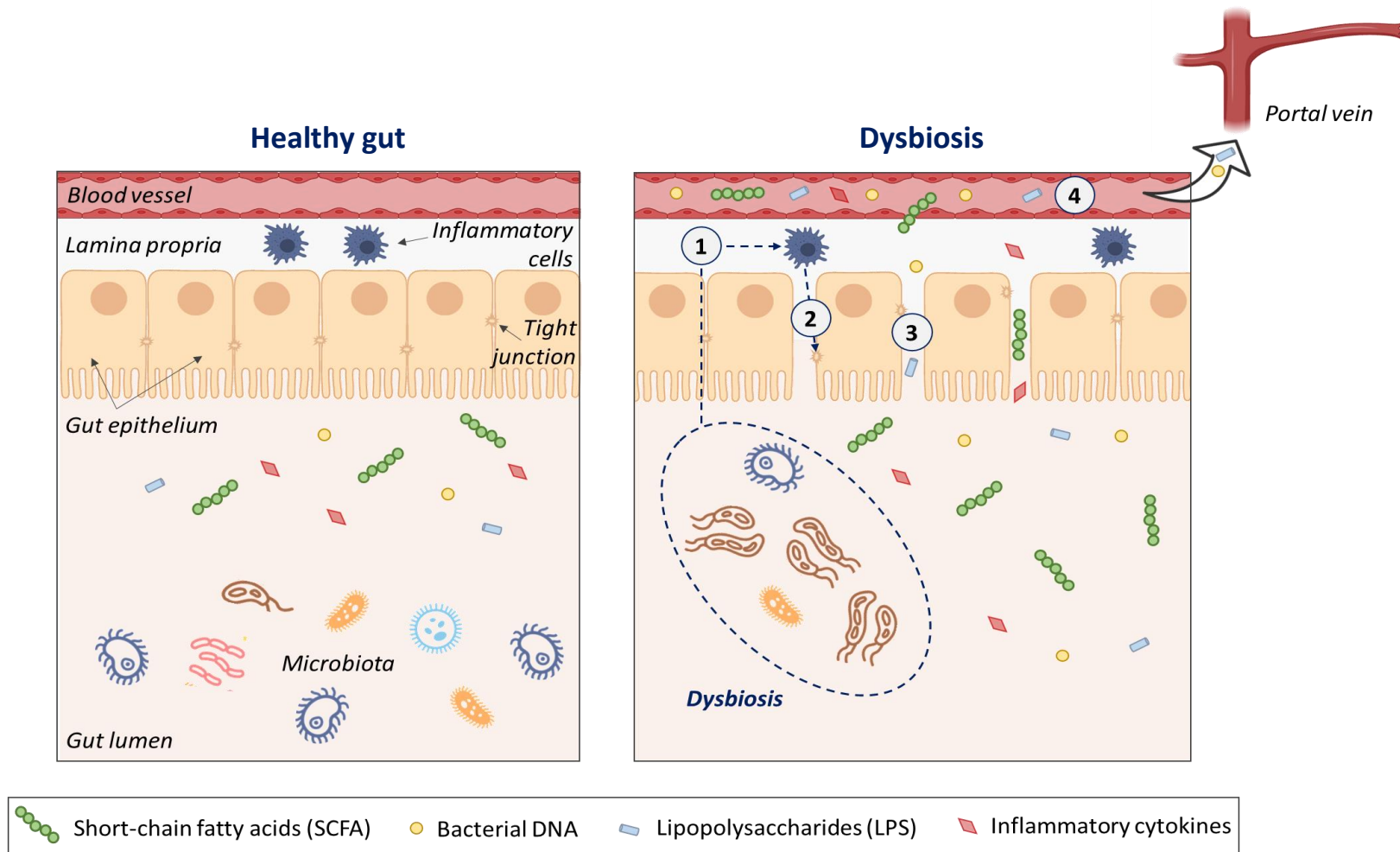


**Figure 27: Intestinal dysbiosis in the development of Non-Alcoholic Fatty Liver Disease (NAFLD)**

Intestinal bacterial overgrowth and dysbiosis cause activation of inflammatory cells residing on the lamina propria (1). Once activated, these cells secrete tumor necrosis factor alpha (TNF $\alpha$ ), which binds to its receptor on enterocytes and disrupts tight junctions (2). With a faulty gut barrier, microbial products can translocate from the intestinal lumen to the adjacent portal venous blood (3). Eventually, these microbial products reach the liver (4) where they activate hepatic stellate cells and Kupffer cells, and damage hepatocytes.



to the portal circulation, the liver is the first line of defense against the different products originated by gut microbiota, such as lipopolysaccharides (LPS), lipopeptides and even bacterial DNA [558]. In the liver, these pro-inflammatory toxins are met by a variety of resident immune cells (ex: Kupffer and HSCs) that become over-activated and trigger inflammatory responses [558]. This inflammatory feedback is conducted by the activation of TLR4, which recognizes the bacterial products and triggers a downstream inflammatory cascade [558]. In fact, studies suggest that the blockage of TLR4 is a potential therapy to alleviate hepatic inflammation and fibrosis [559, 560].

In a normal situation, bacterial products are tightly regulated and only a small portion of those enters the liver through the portal circulation. However, alterations in gut microbiota (dysbiosis) may lead to increased small bowel permeability, thus increasing the flow of bacterial endotoxins into the liver and damage the tissue via TLR signalling [496]. TLR in turn can activate a cascade of pro-inflammatory cytokines such IL-1 $\beta$ , IL-6, IL-12, IL-18 and TNF $\alpha$  [496]. When compared to healthy individuals, obese NAFLD patients have increased intestinal permeability and a higher prevalence of small intestine bacterial overgrowth [561]. This bacterial overgrowth may play a role in the progression of NAFL to NASH and fibrosis as suggested by some studies. Ley *et al.* demonstrated that genetically obese (*ob/ob*) mice show an increased proportion of the Firmicutes and a decrease in Bacteroidetes [562]. A further report indicated that the proportion of Bacteroidetes 16S rRNA sequences was diminished in feces from 12 obese human subjects [563]. In advanced NAFLD-related fibrosis, the ratio Firmicutes/Bacteroidetes is much higher [564], and in patients with NASH there is higher prevalence of Proteobacteria, Enterobacteria, Escherichia and Bacteroides (subpopulation of the Bacteroidetes) [565, 566]. Furthermore, NASH individuals display higher serum levels of LPS and a greater hepatic mRNA expression of *TNFA*, which supports the theory that bacterial endotoxemia is crucial in the worsening of NAFLD [567]. In one study, researchers tried to compare the human intestinal microbiota and the concentration of faecal SCFA in lean, overweight and obese subjects [568]. Their results showed that the total amount of SCFA, and specifically the concentration of propionate, was higher in the obese subject group than in the lean subject group. These authors also described that, in all groups, the two greatest bacterial populations were Firmicutes and Bacteroidetes. However, contrary to most studies, the ratio of Firmicutes to Bacteroidetes changed in favour of the Bacteroidetes in overweight and obese people [568]. Given that SCFA are directed towards the *de novo* synthesis of lipids and glucose, this study suggests that SCFA contribute to the development of obesity but that not all bacterial groups contribute in an equal manner to the development of obesity and its related co-morbidities [568]. In fact, Da Silva *et al.* have demonstrated that NAFL and NASH

patients have higher concentrations of fecal propionate and isobutyric acid than healthy controls [569]. In addition, these authors reported that NAFL and NASH patients have a higher Firmicutes/Bacteroidetes ratio and that this change is independent of BMI and IR status [569]. Recently, Yuan *et al.* reported that the high alcohol-producing *Klebsiella pneumoniae* (HiAlc Kpn) was detected in 61% of individuals with NAFLD (NAFL and NASH) in a Chinese cohort [570]. To further investigate this question, the authors fed specific-pathogen-free (SPF) mice with HiAlc Kpn and observed an induction of chronic hepatic steatosis [570].

Collectively, these studies suggest that some correlations can be made between bacterial composition and the different stages of NAFLD. However, due to the lack of reproducibility between human cohorts, there is still no precise explanation as to why dysbiosis occurs, and this affects the way researchers interpret data.

Aside NAFLD, dysbiosis has also been associated with several neurobehavioral and neurodegenerative disorders. In fact, the gut-brain axis (GBA) consists of a bidirectional communication system between the central (CNS), the enteric nervous systems (ENS) and peripheral intestinal functions that not only ensures the proper maintenance of gastrointestinal homeostasis as it also affects several cognitive functions [571, 572]. Due to this gut-brain connexion, microbial products can act as signalling molecules in the CNS and the ENS and modulate neurological functions. Labus *et al.* have demonstrated for the first time that the composition of gut microbiota is related to structural changes in the brain of humans suffering from irritable bowel syndrome (IBS), including sensory-related regions [573]. These results suggest that microbiota composition may alter the perception of pain in patients with IBS.

## **b) Genetic polymorphisms**

As we have seen so far, NAFLD is an overly complex disorder and the way it progresses depends on subtle genetic and environmental changes between individuals. In fact, over the years, genetics has been increasingly identified as an important player in the development of this pathology.

Among all analysed metabolism-related genes, polymorphisms in *PNPLA3* and *TM6SF2* are deemed to play the most significant role in the development of NAFLD. Human carriers of the E167K variant of the *TM6SF2* gene have lower circulating ApoB levels, increasing hepatocyte fat content and being at risk of developing NAFLD [574]. Membrane Bound O-Acyltransferase Domain Containing 7 (MBOAT7) catalyses acyl-chain remodelling of phosphatidylinositols (PIs). PIs are lipids, which regulate membrane dynamics and signal transduction pathways. Individuals carrying

the rs641738 C>T variant of this gene present a downregulation of MBOAT7 at both mRNA and protein levels and display an altered polyunsaturated PI metabolism [575]. A variation in the glucokinase regulator (GKR) gene locus has been also associated with NAFLD. GKR is a key regulator of DNL by controlling the flux of glucose into hepatocytes. Individuals carrying the rs1260326 variant of the gene display severe hepatic fat accumulation. This happens because fructose-6-phosphate (F6P) is unable to inhibit glucokinase (GK), and so glucose continues to be uptaken by hepatocytes [576].

Although the liver has several protective mechanisms to cope with a sudden increase in TG accumulation, in genetically predisposed individuals all these factors affect hepatic fat content and inflammatory environment, which lead the organ to a state of chronic inflammation, with possible worsening to hepatocellular death and development of fibrosis.

### 2.4.3. Controlling the disease

Due to its prevalence and association with other comorbidities, the implementation of specific treatments against NAFLD become of the utmost importance. Unfortunately, to date, there is no specific medication or therapy that can directly treat NAFLD, although several clinical trials are being conducted to revert this situation [577]. Currently, the only solution to this problem is managing the illness by adjusting the patient's lifestyle or, in more severe cases, by doing a surgical intervention.

#### **a) Diet and physical activity**

Sedentariness and high-calorie intake are crucial for the development and progression of NAFLD. Individuals with NAFLD have systematically been proven to do less physical exercise than age and sex-matched healthy controls [578] [579]. It is no surprise then that obesity runs high among NAFLD patients, thus making a balanced regime accompanied by regular physical activity the first mandatory adjustments towards disease amelioration [322, 328].

For some patients, these lifestyle adjustments are enough to mitigate IR and decrease the levels of hepatic transaminases (ALT and AST) [580–582]. Recent meta-analysis studies have shown that physical interventions lead not only to significant weight loss but also to an improvement of liver steatosis and stiffness as well as to a reduction in serum ALT, alkaline phosphatase and GGT [583, 584]. Evidence further suggests that when the decreased body weight is maintained, the levels of ALT continue to be within normal range [583]. Recently, a prospective study including 293 patients histologically diagnosed with NASH showed that 52 weeks of lifestyle

adjustment were enough to see a histological amelioration of the liver [585]. All patients who lost above 10% of their body weight presented lower NAS, whereas 90% presented a complete resolution of NASH and 45% presented a regression of fibrosis [585].

To date, there is no one perfect regime to fight NAFLD. However, several studies have suggested that diets known to improve insulin sensitivity are the best chance to ameliorate the individual's condition. Such is the case of the Mediterranean diet [586]. The foundation of this diet is vegetables, fruits, herbs, nuts, beans and whole grains. Red meat, processed foods and refined sugars are completely off menu [586]. One study subjected non-diabetic obese people with biopsy-proven NAFLD to a 6-week Mediterranean dietary intervention [587]. The results obtained showed that, even though there was no weight loss, diet intake was associated to a significant reduction in hepatic steatosis and to an improvement of insulin sensitivity [587]. In another study, 584 overweight/obese adult individuals with at least one CVD risk factor (ex: T2DM, arterial hypertension or dyslipidemia) were subjected to the Mediterranean diet [588]. Their results showed that patients with intermediate/high adherence to the diet had a progressive reduction of the degree of liver steatosis, IR and a more favourable glycometabolic profile [588]. Similarly, Gelli *et al.* accompanied 46 overweight/obese NAFLD individuals subjected to a Mediterranean diet for 6 months [589]. Their results showed that, at the end of the intervention, most patients had a lower degree of liver steatosis, as well as decreased levels of AST, ALT and GGT, lower body weight and higher insulin sensitivity [589].

Although these findings are intriguing, further validation is still required. Nonetheless, consistent changes in diet and physical activity remain the backbone of a meaningful management of NAFLD.

## **b) Pharmacological treatment**

Despite some ongoing trials [577], to date there is still no specific treatment for NAFLD. This means that all available pharmacological therapies aim to address coexisting conditions such as obesity, IR and dyslipidemia.

### **• Metformin**

Metformin was introduced to the world in the 1950s for the management of T2DM and obesity. Used as a first-line medication, metformin acts as an insulin sensitizing agent, lowering glycemia [590].

Given the association between NAFLD and T2DM, and after presenting striking results in the amelioration of hepatic steatosis and lipogenesis in rodents [591], metformin started to be commonly used in the treatment of NAFLD. In 2001, Marchesini *et al.* treated 20 overweight NASH patients with 500mg of metformin 3 times a day for 4 months [592]. This long-term treatment significantly reduced the concentrations of transaminases, decreased liver volume by 20% and significantly improved insulin sensitivity [592]. Subsequent studies have further confirmed the effect of metformin in reverting some of the pathological features associated with NAFLD [593, 594].

The mechanisms by which metformin exerts its actions are not, however, completely understood. As mentioned earlier in this chapter, the primary effect of metformin is the prominent decrease in hepatic glucose production. Several studies suggest that this effect is mainly due to an inhibition of Complex I of the ETC, which decreases ATP production [595]. This inhibition induces the activation of AMPK, an energetic sensor of the cell. Activated AMPK phosphorylates ACC, inhibiting DNL and promoting mtFAO instead, thus reducing hepatic lipid stores and enhancing hepatic insulin sensitivity [596]. However, in 2019 Wang *et al.* reported that, in fact, metformin increases the activity of ETC Complex I and mitochondrial density in the liver of HFD-fed mice [597]. For these authors, if metformin functions by inhibiting Complex I activity, that should further aggravate lipid accumulation and IR, contrary to the widespread clinical observations during metformin therapy in T2DM. According to these authors, the alleviated mitochondrial activity favours mtFAO, thus contributing to a decrease in hepatic lipid stores [597].

Although some studies suggest that metformin should be used in the treatment of T2DM and NAFL but not in cases of NASH, recent evidence has suggested that metformin can inhibit the formation of fibrosis through the activation of AMPK and the decreased expression of several fibrogenic genes [598]. Despite being extremely rare, some cases of metformin-related hepatotoxicity have been reported [599]. However, several meta-analysis studies have not been able to find an association between metformin and the exacerbation of liver injury.

- Thiazolidinediones

Thiazolidinediones (TZDs) (rosiglitazone and pioglitazone) are insulin sensitizing agents that exert their actions by binding to PPAR $\gamma$ . Among several mechanisms, PPAR $\gamma$  increases insulin sensitivity by enhancing lipid uptake and by stimulating adiponectin release from adipocytes [600].

Overweight NASH patients treated with rosiglitazone for nearly a year presented better insulin sensitivity, lower circulating levels of ALT and a lower degree of liver fibrosis [601]. In fact,

recent meta-analysis studies have consistently found that treatment for up to 24 months with TZDs was associated with improved advanced fibrosis and NASH resolution [600, 602]. Besides, several clinical trials have shown that TZDs treatment prevents subsequent events, such as an increase in oxidative stress, lipid peroxidation and pro-inflammatory cytokines that contribute to the development of NAFL to NASH [603, 604]. Animal models follow the same pattern found in the human studies. Rats given fructose-enriched diet (to develop metabolic syndrome) treated for 4 weeks with rosiglitazone presented decreased blood pressure, plasma TG levels, hepatic lipid content and MDA levels when compared to the control group [605]. Additionally, the same group of rats presented higher plasma levels of adiponectin [605].

Several adverse effects associated to the use of TZDs have been mentioned, edema being one of the most frequently observed. According to literature, TZDs-induced fluid retention results from the increase in tubular sodium and water reabsorption in the kidney [606]. Some studies have also made the connexion between TZDs and heart failure, which led physicians not to prescribe TZDs to patients with a high risk of heart disease [607]. Treatment with TZDs has also been associated to decreased bone density and increased risk of fractures [608, 609]. Furthermore, the cumulative evidence associating the intake of pioglitazone to the development of bladder cancer has led the French Agency for the Safety of Health Products and Germany's Federal Institute for Drugs and Medical Devices to withdraw this TZD from the market in 2011 [610, 611]. However, additional studies have reinstated that pioglitazone does not increase the risk of developing bladder cancer [612, 613].

#### • Vitamin E

As mentioned earlier in this manuscript, oxidative stress is highly implicated in the development of NAFLD [477]. Vitamin E has antioxidant properties and its use as a pharmacological approach in the treatment of NAFLD has gained some pertinence in the past few years [614].

Some studies have shown that NASH patients have low levels of vitamin E [615] and that administration of this vitamin reduces hepatic steatosis, inflammation and ballooning, as well as plasma levels of ALT, AST and 4-HNE in NAFLD individuals [616–619]. Whether the same improvements can still be achieved in the absence of coexisting lifestyle adjustments (ex: diet and physical exercise) is still a subject of great debate. Recently, mice fed a choline-deficient amino acid specific (CD/AA) diet and treated with nothing but vitamin E for 3 weeks presented decreased levels of oxidative stress and regression of the NAS score [620].

Evidence suggests that high doses of vitamin E are associated to a bigger risk of stroke and even death [621, 622]. However, most meta-analysis studies are criticized for not considering the consumption of other drugs, such as vitamin A, or other confounding factors, such as smoking. In this context, further monotherapy clinical trials and pharmacological evaluations are still needed to elucidate the underlying molecular mechanisms of prevention or therapy and possible adverse outcomes of vitamin E.

- Coenzyme Q10

Over the past few years, coenzyme Q10, also referred to as ubiquinone, has attracted much attention due to its envisaged health benefits [623]. Ubiquinone is present in all eukaryotic cells, and it is a crucial participant of the mitochondrial ETC.

Dietary intake of coenzyme Q10 is directly linked to enhanced levels of ubiquinol-10 within the human body, which is crucial for blocking lipid peroxidation by protecting against LDL oxidation in conditions of metabolic syndrome [624, 625]. Aside its impact on lipid peroxidation, several studies have demonstrated that ubiquinone ameliorates inflammation and improves adipokine secretion in conditions of metabolic syndrome [626–628]. For example, Farhangi *et al.* showed that obese NAFL patients supplemented for 4 weeks with coenzyme Q10 presented decreased BMI, lower serum AST level and decreased total antioxidant capacity [627]. Similarly, Farsi *et al.* reported that obese NAFL individuals supplemented with coenzyme Q10 for 12 weeks presented decreased serum levels of AST, ALT, GGT and TNF $\alpha$  [628]. Supplementation with coenzyme Q10 also increased the serum level of adiponectin [628]. Studies conducted in NAFLD animal models showed similar results to the clinical trials. For example, Chen *et al.* demonstrated that coenzyme Q10 supplementation to HFD-fed mice reduced weight gain and liver steatosis, while also decreasing serum levels of TG, total cholesterol and LDL-cholesterol [629]. In addition, the coenzyme Q10 supplementation downregulated the protein expression of SREBP-1c, ACC and FAS, while also upregulating the protein levels of PPAR $\alpha$  and CPT1 [629]. Similarly, Saleh *et al.* showed that a 2-week long supplementation with coenzyme Q10 to MCD-fed rats decreased the serum levels of ALT, AST and GGT while also decreasing the hepatic levels of NF- $\kappa$ B and IL-6 and the brain content of NO and NH<sub>3</sub> [630].

- Betaine

Betaine is an amino compound obtained from dietary sources (especially sea-food, spinach and beets) or synthesized endogenously from choline [631]. *In vivo*, betaine acts as a methyl donor for the conversion of homocysteine to methionine [631].

Oral betaine treatment has been evaluated in the treatment of NAFLD. Song *et al.* demonstrated that high sucrose diet (HSD)-fed mice treated with betaine presented increased protein levels of hepatic AMPK and decreased protein levels of SREBP-1c, ACC, and FAS [632]. Similarly, Wang *et al.* showed that betaine administration to HFD-fed mice decreased hepatic steatosis and IR while improving glucose tolerance and adipokine secretion [633]. Kathirvel *et al.* have also observed that betaine administration to HFD-fed mice reduced fasting glucose, plasma TG, liver steatosis and ameliorated IR [634].

The therapeutic effects of betaine on NAFLD have also been investigated and reported in clinical studies. Miglio *et al.* found that an 8-week long treatment with betaine in obese NASH patients ameliorated liver steatosis and decreased the hepatic levels of ALT, AST and GGT [635]. Similarly, Abdelmalek *et al.* showed that a one-year long betaine supplementation to obese NASH patients attenuated liver steatosis, necroinflammation and fibrosis [636]. A recent study has established a direct correlation between the serum levels of betaine and the severity of NAFLD, with obese NASH patients presenting significantly decreased serum levels of betaine when compared to obese individuals with NAFL [637].

- Statins

Statins are among the most widely prescribed lipid-lowering drugs to treat people at high risk of CVD. They inhibit 3-hydroxy-3-methyl-glutaryl-coenzyme A (HMG-CoA) reductase (catalysing the rate-limiting step in cholesterol production). It is well known that patients with NAFLD are among those people [318]. Several studies have reported that statins can significantly improve liver and cardiovascular outcome in patients with NAFLD. Kargiotis *et al.* have shown that, out of 20 obese NASH patients treated with rosuvastatin for one year, 19 showed complete resolution of hepatic inflammation as well as normalization of liver enzymes and blood glucose [638]. In another study, administration of atorvastatin to obese NASH patients for 33 weeks significantly reduced the levels of ALT, AST, GGT and TG [639]. It also decreased the extent of liver steatosis without changing the degree of fibrosis or inflammation [639]. Studies in mice present fairly similar results to those observed for humans. For example, a 6-week administration of a cocktail of statins (fluvastatin, pravastatin, simvastatin, atorvastatin, and rosuvastatin) to mice fed



MCD diet was able to prevent the development of diet-induced NASH [640]. The treatment with statins also induced *PPARA* gene expression and activated both mitochondrial and peroxisomal FAO [640].

Although there is general reluctance to prescribe statins to patients with suspected or conclusively proven chronic liver disease [641], serious liver injury as a direct causality of their use is rarely seen in clinical practice [642]. The guidelines emitted by the American Association for the Study of Liver Diseases (AASLD) specify that statins can be used to treat dyslipidaemia in adult patients suffering from any condition within the spectrum of NAFLD [321]. In fact, very recently, Vieira-Silva *et al.* observed that obesity-associated microbiota dysbiosis is negatively associated with statin treatment [643]. According to their results, the prevalence of *Bacteroides2* (Bact2), an intestinal microbiota that is associated with systemic inflammation, correlates with BMI, increasing from 3.90% in lean or overweight participants to 17.73% in obese participants [643]. Treatment with statins (48% of patients with simvastatin, 31% with atorvastatin and 21% with other statins) resulted in a decrease of Bact2 prevalence from 17.73% to 5.88% in the obese participants [643]. Nevertheless, evidence suggests that statins may impair mitochondrial morphology, membrane potential and oxidative phosphorylation. In fact, the use of statins has been linked to deficiencies in coenzyme Q10 [644], impairment of ETC Complexes [645] and even induction of mitochondrial apoptosis pathway [646]. Furthermore, several studies associate the use of statins to musculoskeletal pathologies, such as rhabdomyolysis, myalgia and/or mild hyperCKemia (elevated levels of creatine kinase) [647]. For this reason, the prolonged use of statins in NAFLD patients is a matter of concern for some physicians, given that these substances could aggravate an already compromised system.

- Bariatric surgery

Bariatric surgery is usually indicated to treat cases of morbid obesity when other medical treatments have failed to accomplish sustained weight loss [648]. The criteria for surgical intervention established in 1991 indicated that bariatric surgery was appropriate for all patients with BMI ( $\text{kg}/\text{m}^2$ ) > 40 (morbid obese) and for patients with BMI 35-40 with associated comorbid conditions (ex: T2DM, CVD, dyslipidemia) [649]. To this day, bariatric surgery remains one of the most successful methods of sustained weight loss for obese individuals. This type of surgical intervention aims to either restrict the volume of food that can be consumed or to induce nutritional malabsorption [648].

Although several studies have linked bariatric surgery to the amelioration/reversion of NAFLD, this type of intervention is recommended based on the presence and degree of obesity. In fact, a study using bariatric surgery as a primary treatment for NASH is not anticipated to be designed in the near future. Nonetheless, the available evidence suggests that NASH improves after bariatric surgery. From May 1994 to May 2013, 109 morbid obese patients with biopsy-proven NASH underwent bariatric surgery at the University Hospital of Lille [650]. One year after surgery, NASH had disappeared from 85% of the patients. These same individuals presented lower levels of ALT, GGT and higher insulin sensitivity. The mean NAS score was reduced from 5 (before the intervention) to 1 (one year after the surgery). Furthermore, hepatocellular ballooning was reduced in 69 individuals, lobular inflammation in 55 and fibrosis in 37 [650].

A retrospective study published in 2016 using 84 obese patients with ultrasound diagnosed NAFLD showed that 56% of them had complete disease resolution after being submitted to laparoscopic sleeve gastrectomy (LSG) [651]. In another study, Froylich *et al.* submitted 14 obese NASH patients to a Roux-en-Y gastric bypass (RYGB), an approach combining restriction and malabsorption. One and a half years after surgery, the average weight loss was 32% and the NAS score had significantly improved in all individuals [652]. More recently, 100 patients submitted to bariatric surgery (RYGB and LSG) presented significant improvements of BMI and total weight loss 1.5 years after the intervention [653]. Liver stiffness was also significantly improved, as were the levels of ALT, AST and GGT. Interestingly, between the two surgical approaches, RYGB appeared to be more effective than LSG [653]. In 2019, a meta-analysis study conducted on the impact of bariatric surgery on 32 different cohorts of NAFLD found that, after the intervention, the average weight loss was 25%. Furthermore, the resolution of steatosis, inflammation and fibrosis was observed in 66%, 50% and 40% of all cases, respectively [654]. Noteworthy is the development or worsening of NAFLD in some cases.

Although generally safe, mid- and long-term complications of bariatric surgery can occur, and these typically vary depending on the procedure. Among those well described are intestinal obstruction, malabsorption, marginal ulcer, ventral hernia, and gallstones [655].

### **3. H<sub>2</sub>S and liver pathophysiology: what lies beyond the stink**

#### **3.1. Context**

As a gasotransmitter, H<sub>2</sub>S is an important mediator in several biological systems. Noteworthy, the effects of H<sub>2</sub>S are invariably dependent on its concentration. For instance, at low

concentrations H<sub>2</sub>S is anti-inflammatory, while at high concentrations it is pro-inflammatory or toxic (**Figure 10**) [656].

Evidence suggests that the liver, a key organ to mammalian physiology with respect to energy substrate supply and body homeostasis, is likely exposed to high levels of H<sub>2</sub>S from both endogenous biosynthesis and exogenous sources. On one hand, all enzymes responsible for H<sub>2</sub>S production from amino acids (CSE, CBS and MPST) have been detected in the liver. On the other hand, H<sub>2</sub>S synthesis by the gastrointestinal microbiota may reach the liver through the portal circulation. Naturally, this premise makes us speculate about the importance of this molecule for the short- and long-term regulation of hepatic metabolism.

Although it is widely accepted that the liver is exceedingly well positioned to be exposed to elevated levels of H<sub>2</sub>S, nobody really knows how the liver copes with fluctuations in H<sub>2</sub>S concentrations. Several studies suggest that hepatic H<sub>2</sub>S is important for mitochondrial biogenesis and bioenergetics, insulin sensitivity, lipoprotein synthesis as well as glucose and lipid metabolism. Moreover, over the last few decades, alterations in H<sub>2</sub>S metabolism have been implicated in the development of several liver disorders, such as NAFL, NASH, fibrosis, cirrhosis and HCC.

## 3.2. H<sub>2</sub>S in liver functions

### 3.2.1. H<sub>2</sub>S and hepatic glucose metabolism

Glucose is a major energetic cell substrate whose blood levels vary according to food intake. Given that some tissues depend almost exclusively on this sugar, the organism has developed adaptive strategies to maintain glycemia fairly constant. As discussed earlier in this manuscript, the liver plays a crucial role in glucose homeostasis [657]. In the post-prandial state, the liver uses the surplus of glucose to restore glycogen pools and to synthesize LCFA, which are then esterified into TG and transported in VLDL to be stored in the adipose tissue (**Figure 28A**) [412, 657]. In a fasting state, the liver activates other pathways such as gluconeogenesis and glycogenolysis in order to generate and provide glucose for the tissues that solely depend on it (such as erythrocytes and the brain) [657]. The sophisticated homeostatic control of glucose metabolism in the liver is primarily directed by insulin and glucagon (**Figure 28B**). Hence, defects in the mechanisms by which these hormones exert their actions can disrupt glucose homeostasis and lead to metabolic disorders.

Several studies have demonstrated the role of H<sub>2</sub>S in glucose production (**Figure 29**) [658].

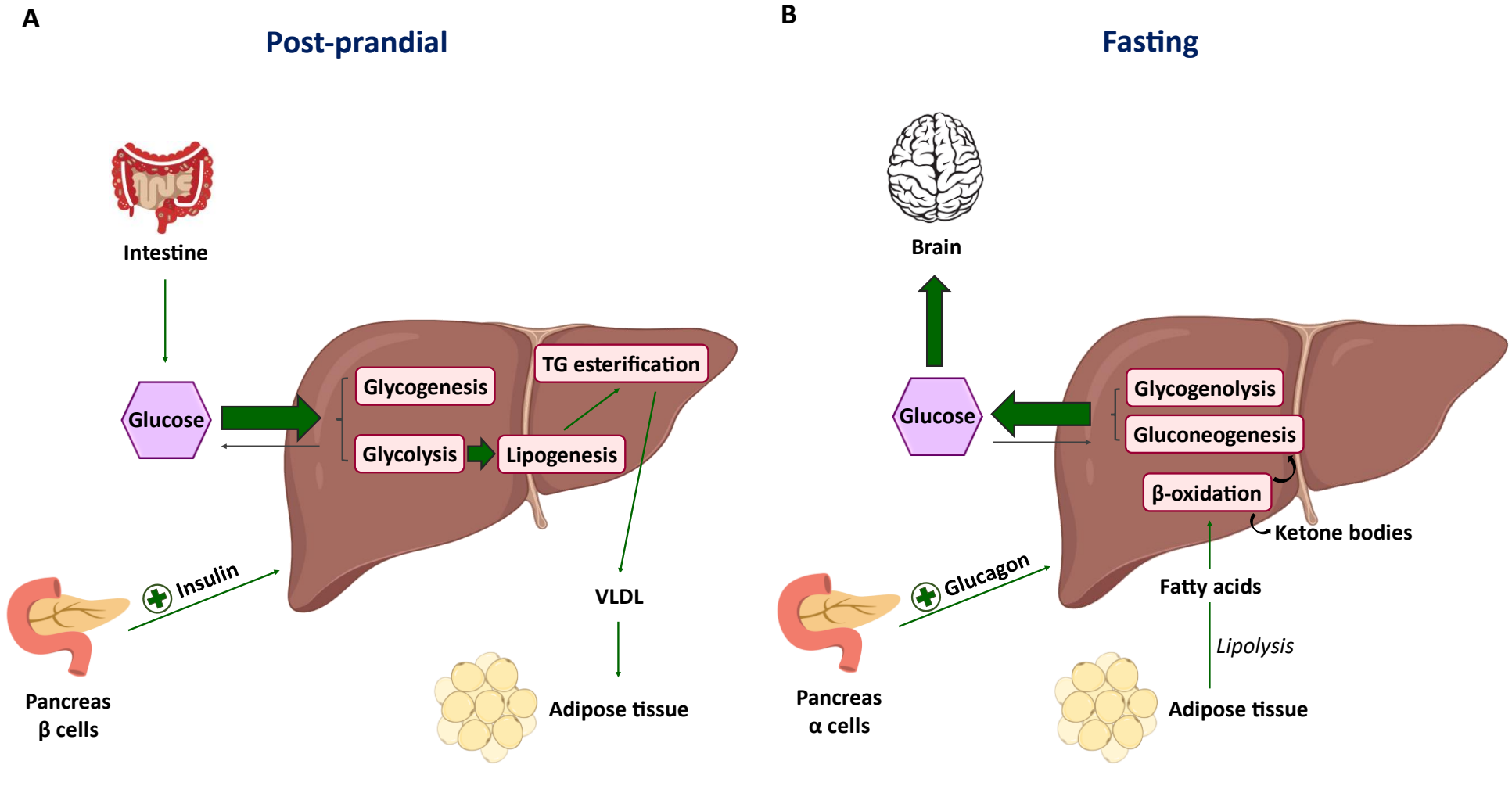


**Figure 28: Hepatic regulation of glucose and lipid metabolism in a post-prandial (A) and fasting (B) state**

VLDL: very-low density lipoprotein; TG: triglycerides

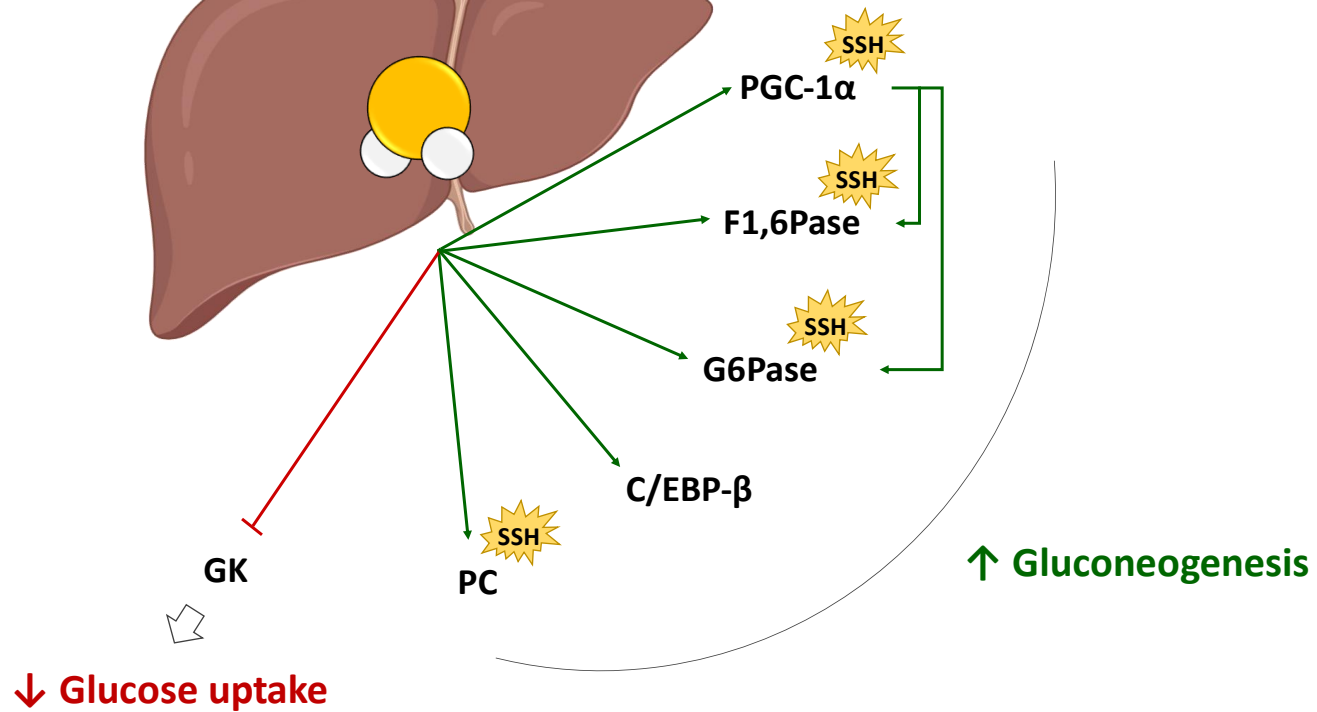


Figure 29: H<sub>2</sub>S regulation of liver glucose metabolism

**GK:** glucokinase; **PC:** pyruvate carboxylase; **C/EBP-β:** CCAAT/enhancer binding protein beta; **G6Pase:** glucose 6 phosphatase; **F1,6Pase:** fructose 1,6 biphosphatase; **PGC-1α:** peroxisome proliferator-activated receptor-gamma coactivator-1alpha; **SSH:** persulfidation

In the gut epithelium, H<sub>2</sub>S is produced in close proximity to the glucagon like peptide1 (GLP-1)–secreting cells. GLP-1 is a peptide hormone that plays pivotal roles in both glucose homeostasis and appetite regulation. In 2017, Pichette *et al.* reported that NaHS and GYY4137 can directly stimulate GLP-1 secretion in murine L-cells (GLUTag) and that this occurs through p38 mitogen-activated protein kinase (MAPK) without affecting cell viability [659]. They have further demonstrated that mice treated with chondroitin sulfate present elevated fecal levels of *Desulfovibrio piger* and increased colonic and fecal H<sub>2</sub>S concentration. Concomitantly, these mice also present enhanced GLP-1 and insulin secretion, improved oral glucose tolerance, and reduced food consumption [659].

Other studies have described a direct regulation of H<sub>2</sub>S on liver gluconeogenesis. Evidence has demonstrated that hepatocytes isolated from CSE KO mice show a reduced glycaemic response to chemical-induced activation of the cyclic adenosine monophosphate (cAMP)/protein kinase A (PKA) and glucocorticoid pathways compared with WT hepatocytes [245]. Furthermore, when comparing the *in vivo* glycaemic response to oral pyruvate administration, CSE KO mice show lower capacity to produce glucose than controls [245]. The *in vivo* administration of NaHS to CSE KO mice can normalize the rates of gluconeogenesis through the upregulation of both expression and activity of key gluconeogenic transcription factors such as PGC-1 $\alpha$  and C/EBP- $\beta$  (**Figure 29**) [245]. NaHS also upregulates the expression and the activities (by persulfidation) of G6Pase and fructose-1,6-bisphosphatase (F1,6Pase) [245]. Ju *et al.* corroborated these observations by showing that NaHS stimulates PC activity and gluconeogenesis in HepG2 cells and mouse primary hepatocytes [246]. They have further demonstrated that CSE overexpression stimulates PC persulfidation whereas CSE KO abates this reaction (**Figure 29**) [246]. Conversely, Zhang *et al.* demonstrated that insulin at the physiological range inhibits CSE expression while an insulin-resistant state elevates CSE expression [660]. In fact, Yusuf *et al.* showed that hepatic H<sub>2</sub>S and CSE mRNA levels in streptozotocin-induced diabetic rats were significantly higher than in non-diabetic controls [661]. Zhang *et al.* have further observed that adenovirus-mediated CSE overexpression increases endogenous H<sub>2</sub>S production and lowers glycogen content in HepG2 cells [660]. These findings were corroborated by the incubation of HepG2 cells with NaHS, given that the outcome was impaired glucose uptake and glycogen storage through a decrease in GK activity and increase in persulfidation of PC (**Figure 29**) [660].

### 3.2.2. H<sub>2</sub>S and hepatic lipid metabolism

Hepatic lipid metabolism is coordinated by a delicate combination of hormones, transcription factors, nuclear receptors and intracellular signalling pathways. As mentioned in Chapter 2 of this introduction, the excessive accumulation of lipids in the liver disrupts its functions and leads to the development of several hepatic disorders [662]. Jain *et al.* assessed fasting blood levels of H<sub>2</sub>S and lipids in healthy human subjects. Their results showed a significantly positive correlation between H<sub>2</sub>S, HDL-cholesterol and adiponectin as well as a negative correlation between H<sub>2</sub>S and LDL/HDL-cholesterol ratio [663].

Furthermore, according to the literature, both CBS and CSE are essential for liver lipid metabolism (**Figure 30**). Humans carrying a CBS variant and CBS KO mice exhibit the same traits of hyperhomocysteinemia, oxidative stress, liver steatosis and fibrosis [115, 664]. CBS KO mice present altered mRNA levels of proteins required for cholesterol and FA biosynthesis and uptake, namely upregulation of *LXR* and downregulation of *PPARA* (**Figure 30**) [665]. These animals have also been reported to have increased plasma levels of TG and non-esterified FA as well as lower hepatic activity of thiolase, a key enzyme for mtFAO [666]. Recent evidence has supported these findings by showing that CBS KO rabbits have higher plasma levels of TG, total cholesterol and LDL as well as an accumulation of hepatic microvesicular steatosis [667]. In 2017, Majtan *et al.* reinforced the importance of CBS in lipid metabolism and liver disorders. Subcutaneous administration of recombinant polyethyleneglycolylated human truncated CBS (PEG-CBS) 3 times a week prevented an otherwise fatal liver disease characterized by steatosis, death of hepatocytes, ER and mitochondrial abnormalities in CBS KO mice [668]. CBS KO mice have also shown a significant alteration of a broad range of hepatic phospholipids and phosphatidylcholines [669]. Some studies, however, describe an inverse correlation between CBS expression and the promotion of liver fat metabolism. In 2011, Gupta *et al.* showed that CBS *Tgl278T* deficient mice have significantly decreased body fat mass when compared to their heterozygous littermates [670]. This decrease in body fat mass was accompanied by a decrease in hepatic mRNA and protein levels of the critical lipid biosynthesizing enzyme SCD1 [670].

Unlike CBS-KO models, CSE-KO mice do not show hepatic steatosis or other pathological features in the liver when fed chow diet. In fact, a recent study has observed that these animals display significantly decreased plasma levels of TG when compared to control mice [129]. However, it has been demonstrated that the inhibition of hepatic CSE expression in a fetal hepatocyte line (L02) upregulates the SREBP-1c pathway, JNK phosphorylation and hepatic oxidative stress (**Figure 30**) [142].

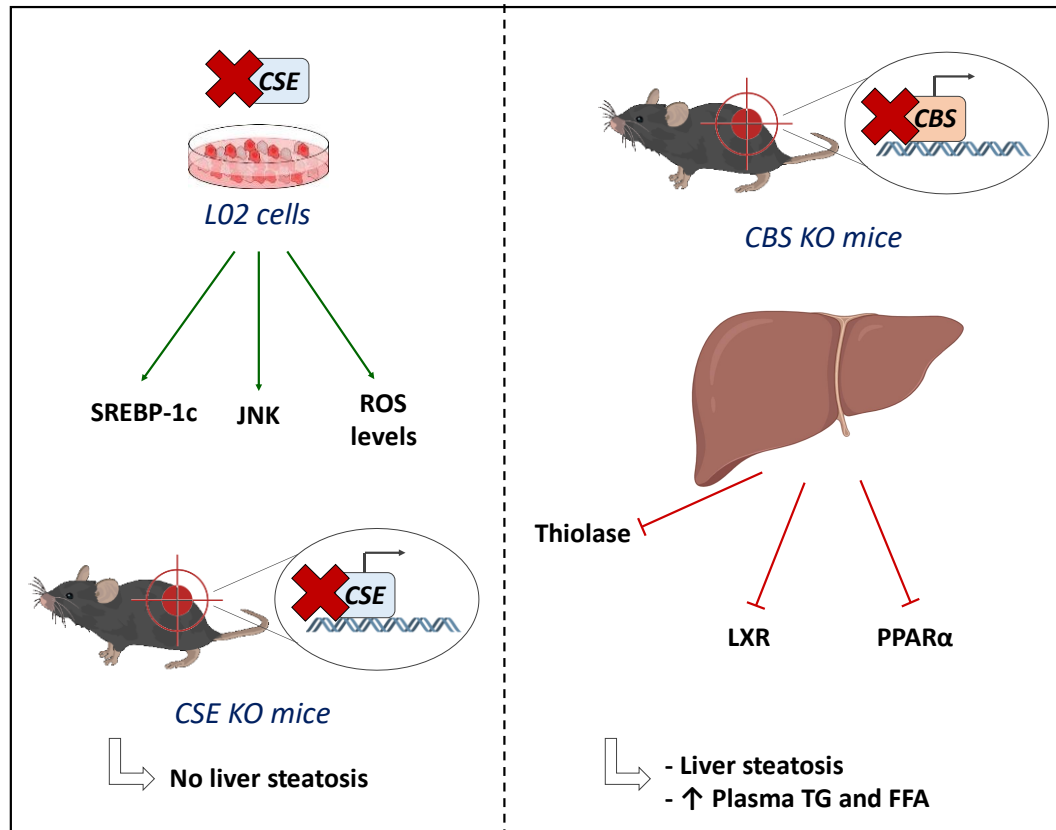


**Figure 30: H<sub>2</sub>S regulation of liver lipid metabolism**

The importance of H<sub>2</sub>S-producing enzymes to hepatic lipid metabolism has been investigated through *in vitro* and *in vivo* invalidation of CSE and CBS. Administration of H<sub>2</sub>S donors constitutes a different approach to investigate H<sub>2</sub>S effects on lipid metabolism.

**CSE:** cystathionine  $\gamma$ -lyase; **SREBP-1c:** sterol regulatory element-binding protein-1c; **JNK:** c-Jun N-terminal kinase; **ROS:** reactive oxygen species; **CBS:** cystathionine  $\beta$ -synthase; **LXR:** liver X receptor; **PPAR $\alpha$ :** peroxisome proliferator-activated receptor alpha; **TG:** triglycerides; **FFA:** free fatty acid



### 3.2.3. H<sub>2</sub>S and hepatic mitochondrial function

One major role of mitochondria is the production of the energy-rich molecule ATP through the metabolism of glucose, lipids and proteins. On a molecular level, H<sub>2</sub>S exhibits a dual role in mitochondrial respiration and ATP production. At high concentrations (typically 10-100 μM), H<sub>2</sub>S competitively binds to Complex IV, thereby inhibiting the binding of oxygen and, by extension, mitochondrial respiration. However, at low concentrations (1-10 μM), H<sub>2</sub>S can serve as an inorganic energetic substrate for mammalian mitochondria, providing electrons to the ETC and contributing to ATP production [187]. Similar results were observed with 3-MP, the substrate of MPST.

Indeed, low concentrations of 3-MP (10-100 nM) stimulate mitochondrial H<sub>2</sub>S production, enhance hepatic mitochondrial electron transport and promote cellular bioenergetics, whereas high concentrations of this substrate (>100 nM) inhibit cellular bioenergetics [194]. The same study has shown that low concentrations of NaHS (0.1-1 μM) prompt a significant increase in mitochondrial function while SQR silencing reduces basal bioenergetic parameters [194]. Additional studies have corroborated the duality of H<sub>2</sub>S in mitochondrial function. For example, Módis *et al.* showed that, at low concentrations (3-10 μM), NaHS appears to induce an elevation of cAMP and PKA levels when added to isolated rat liver mitochondria while also stimulating mitochondrial electron transport (**Figure 31**) [671]. On the other hand, Kai *et al.* have demonstrated that incubation with NaHS (>100 μM) and Na<sub>2</sub>S (>10 μM) decrease cellular O<sub>2</sub> consumption and lower protein accumulation of hypoxia-inducible factor 1 (HIF-1) in Hep3B and HeLa cell lines [672]. Furthermore, rats injected with relatively high concentrations of NaHS (3 or 5 mg/kg) and sacrificed 2h, 6h or 12h after injection displayed an inhibition of mitochondrial Complex IV activity, an increase in ROS production and an increase in the expression of mitochondrial apoptosis pathway-related proteins in a dose-dependent manner [673]. However, the concept of H<sub>2</sub>S duality (cytoprotective in low concentrations and detrimental in high concentrations) has been challenged by other studies. For example, Módis *et al.* have found that high concentrations of NaHS (50-300 μM) induced persulfidation of the α subunit of ATP synthase (ATP5A1) in HepG2 cells, rendering the ATP synthase enzyme more active (**Figure 31**) [674].

Aside serving as a mitochondrial energetic substrate, evidence has shown that H<sub>2</sub>S can modulate mitochondrial biogenesis and death. Untereiner *et al.* found that primary mouse hepatocytes isolated from CSE KO mice have less mtDNA and less mitochondria content [675]. *In vitro* treatment with NaHS abrogated the CSE KO effects on mitochondrial biogenesis. CSE KO hepatocytes also exhibited lower levels of mitochondrial transcription factors such as PGC-1α and

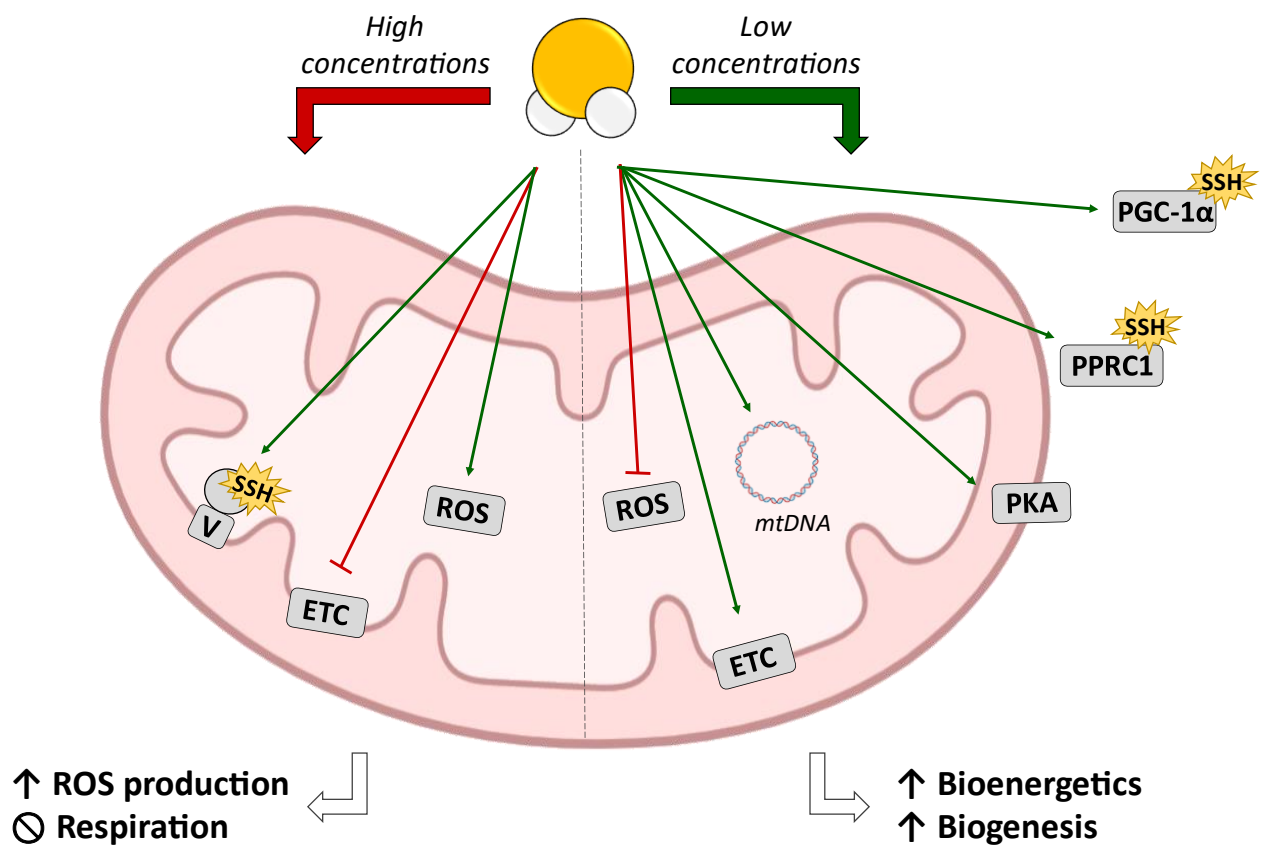


**Figure 31: Impacts of H<sub>2</sub>S on mitochondria**

Past reports of the actions of H<sub>2</sub>S focused solely on its toxic effects and the studies were conducted using extremely high doses of H<sub>2</sub>S donors. However, recent evidence has highlighted the beneficial role of H<sub>2</sub>S in cases where there is insufficiency of this signalling molecule.

**SSH:** persulfidation; **ETC:** electron transport chain; **ROS:** reactive oxygen species; **mtDNA:** mitochondrial DNA; **PKA:** phosphate kinase A; **PPRC1:** peroxisome proliferator-activated receptor gamma coactivator-related protein 1

peroxisome proliferator-activated receptor- $\gamma$  coactivator-related protein (PPRC1) (**Figure 31**) [675]. The administration of NaHS induced persulfidation of PPRC1. Furthermore, the knockdown of either PGC-1 $\alpha$  or PPRC1 significantly decreased NaHS-stimulated mitochondrial biogenesis, whereas knockdown of both genes completely abolished it [675]. In the rat hepatic cell line BRL, incubation with LPS increases CBS expression and H<sub>2</sub>S production [676]. The use of CBS siRNA decreases LPS-induced H<sub>2</sub>S production and increases mitochondrial membrane potential [676]. Conversely, in HepG2 cells, inhibition of the CSE/H<sub>2</sub>S pathway drastically decreased cellular proliferation while enhancing ROS production, mitochondrial disruption and increasing DNA damage [118].

Altogether, these results indicate that endogenous H<sub>2</sub>S plays a physiological role in the maintenance of mitochondrial bioenergetics. Considering that different concentrations of exogenous H<sub>2</sub>S can exert completely different effects, it is crucial to maintain a proper dose range of H<sub>2</sub>S in order to achieve optimal hepatic mitochondrial and cellular function.

#### 3.2.4. H<sub>2</sub>S and hepatic oxidative stress

Oxidative stress, which results from an imbalance between ROS production and ROS clearance, has been implicated in the development of several diseases (**Figure 32**) [677]. In the literature, it has been demonstrated that inhibition of mitochondrial Complex IV leads to the accumulation of NADH, which increases ROS production [678]. One study has reported that the short-term incubation of rat primary hepatocytes with 500  $\mu$ M NaHS could increase ROS formation through the inhibition of Complex IV and the depletion of GSH [679]. The use of genetically modified *in vivo* models has further investigated this connexion. When compared to their wild-type counterparts, CBS KO mice display higher hepatic levels of protein carbonylation and lipid peroxidation, common indicators of oxidative stress [664]. Similar results have been found in patients carrying a mutated variant of CBS [680].

Noteworthy, the interaction between ROS and H<sub>2</sub>S is bidirectional, and so, ROS can have a direct impact on H<sub>2</sub>S production. A study conducted on mitochondria isolated from murine hepatoma cells showed that H<sub>2</sub>O<sub>2</sub> treatment causes a concentration-dependent decrease in MPST activity and mitochondrial H<sub>2</sub>S production [681].

In animal models of liver injury, the administration of H<sub>2</sub>S donors demonstrates great potential as a new therapeutic strategy. Rats with carbon tetrachloride (CCl<sub>4</sub>)-induced hepatotoxicity and cirrhosis present reduced serum levels of H<sub>2</sub>S, hepatic H<sub>2</sub>S production and CSE expression [682]. However, when these animals are treated with NaHS, liver fibrosis and

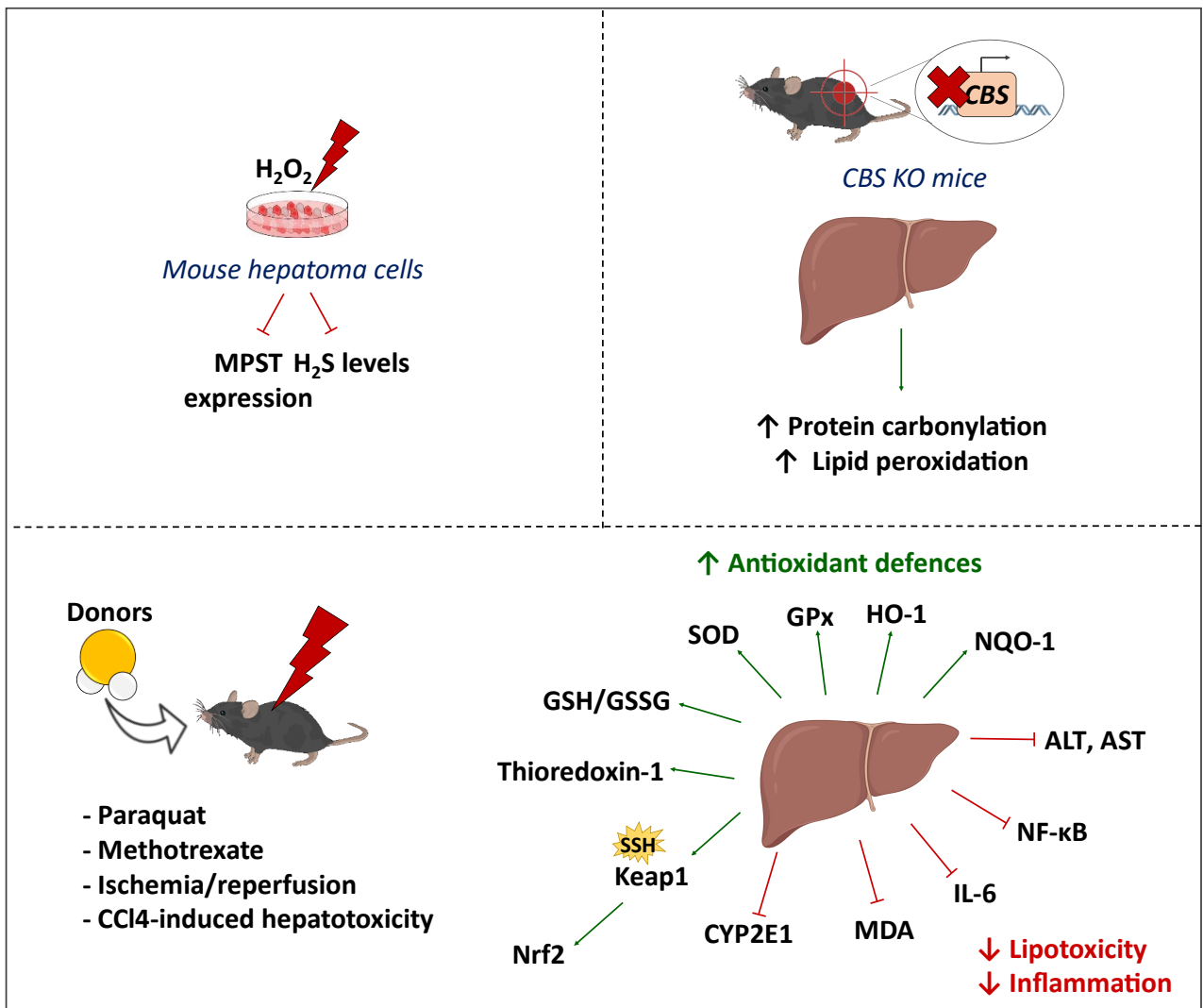


**Figure 32:  $H_2S$  as an antioxidant molecule**

Oxidative stress involves molecular or cellular damage caused by reactive oxygen species (ROS), due to a deficiency in antioxidant or in antioxidant enzyme systems. Excessive ROS can result in DNA damage, protein misfolding and organelle injury, playing an important role in the development of several diseases. Over the years, several papers have highlighted the importance of  $H_2S$  in the regulation of the oxidative/antioxidative balance in different *in vitro* and *in vivo* models.

**$H_2O_2$** : hydrogen peroxide; **MPST**: 3-mercaptopyruvate sulfurtransferase; **CBS**: cystathionine  $\beta$ -synthase; **GSH**: glutathione; **SOD**: superoxide dismutase; **MDA**: malondialdehyde; **CCl4**: carbon tetrachloride; **GPx**: glutathione peroxidase; **HO-1**: heme oxygenase-1; **NQO-1**: NAD(P)H dehydrogenase [quinone] 1; **ALT**: alanine aminotransferase; **AST**: aspartate aminotransferase; **IL-6**: interleukin 6; **SSH**: persulfidation; **Keap1**: Kelch-like ECH-associated protein 1; **Nrf2**: nuclear factor erythroid-derived 2-like 2; **CYP2E1**: Cytochrome P450 2E1

inflammation diminish, much due to a decrease in ALT, AST and MDA levels as well as to the inhibition of CYP2E1 activity [682]. A more recent study has corroborated this premise by demonstrating that, when treated with the slow-releasing H<sub>2</sub>S donor GYY4137, CCl<sub>4</sub>-treated mice present increased persulfidation of Keap1 and activated Nrf2 signalling pathway, which leads to decreased hepatic oxidative stress (**Figure 32**) [683]. Nrf2 is also involved in the production of H<sub>2</sub>S via the direct regulation of CBS, CSE and SQR expressions [684]. In another study using methotrexate to induce hepatotoxicity in rats, Na<sub>2</sub>S supplementation significantly reduced levels of ALT, MDA, IL-6 and NF-κB and increased hepatic total antioxidant capacity and endothelial levels of eNOS [228]. Administration of NaHS to rats suffering from paraquat-induced acute liver injury also attenuates the degree of liver injury and oxidative stress in a dose-dependent manner [685]. In this case, NaHS significantly decreased ROS and MDA levels while increasing the ratio of GSH/GSSG and the levels of antioxidant enzymes including SOD, GPx, Heme oxygenase-1 (HO-1), and NAD(P)H dehydrogenase [quinone] 1 (NQO-1) (**Figure 32**). In addition, NaHS also enhanced nuclear translocation of Nrf2 through the persulfidation of Keap1 [685].

Another study has demonstrated that preconditioning rats with NaHS prior to an I/R insult significantly increases serum H<sub>2</sub>S levels and decreases ALT and AST levels in the plasma [686]. The NaHS preconditioning also prevents hepatocytes from undergoing I/R-induced necrosis and drastically inhibits the mitochondrial permeability transition pore (MPTP) opening. The authors of this study concluded that mitochondrial-related cell death and apoptosis are prevented through the inhibition of MPTP opening and the activation of Akt-GSK-3β signalling pathway [686]. Likewise, Jha *et al.* showed that H<sub>2</sub>S administration to a mouse model of liver I/R increases the levels of GSH, attenuates the formation of lipid hydroperoxides and boosts the expression of thioredoxin-1 [687]. In fact, thioredoxin appears to regulate the MPST-catalysed reaction at physiologically relevant concentrations in the liver [135]. Interestingly, under normoxic conditions, the protein expression of CBS in liver mitochondria is found at a low level [688]. However, under hepatic ischemia/hypoxia events, CBS proteins accumulate in mitochondria, leading to increased H<sub>2</sub>S production. The augmentation in H<sub>2</sub>S levels prevents hypoxia-induced mitochondrial ROS production and mitochondrial Ca<sup>2+</sup>-mediated cytochrome c release [688].

Altogether, these results suggest that the concentration of H<sub>2</sub>S may be key to establish its role as pro-oxidant or antioxidant. Adjusting the dose of H<sub>2</sub>S appears to be essential to avoid any H<sub>2</sub>S-induced cytotoxicity in normal liver cells when it is used for the treatment of liver perturbances.

### 3.2.5. H<sub>2</sub>S in hepatic differentiation and liver cancer

#### **a) Hepatic differentiation**

Genetic and auto-immune disorders, viral infections and toxic injuries may cause severe hepatic lesions that can culminate in acute liver failure or chronic disease [689]. In several cases, liver transplantation is the primary, and sometimes only, method to treat these perturbations [690]. However, this medical approach is limited by a myriad of problems, such as high cost and immune rejection. In order to solve this issue, novel therapeutic strategies using stem-cells have emerged as possible alternative treatments [690].

In 2012, Ishkitiev *et al.* demonstrated that physiological concentrations of H<sub>2</sub>S could increase the capacity of human tooth-pulp stem cells (HTPC) to undergo hepatogenic differentiation [691]. Later on, the same set of researchers revealed that H<sub>2</sub>S increases hepatic differentiation of both HTPC and human bone marrow stem cells (hBMC) [692]. Recently, Yang *et al.* have demonstrated that H<sub>2</sub>S appears to maintain the function of dental pulp stem cells (DPSC) via the transient receptor potential action channel subfamily V member 1 (TRPV1) [693]. Once activated, TRPV1 facilitates the influx in Ca<sup>2+</sup>, which subsequently activates the β-catenin pathway. To further corroborate this premise, siRNA of CBS and CSE were used [693]. The results showed that blocking the expression of CBS and CSE has a huge impact on H<sub>2</sub>S levels, which is translated into a decrease of Ca<sup>2+</sup> levels and the deactivation of the β-catenin pathway, ultimately damaging the proliferation and differentiation of DPSC [693].

Interestingly, H<sub>2</sub>S had already been shown to regenerate insulin-producing pancreatic cells from HTPC cells [694]. The signalling pathways of PI3K-AKT and Wnt/Ca<sup>2+</sup> were found highly expressed after exposure to H<sub>2</sub>S. H<sub>2</sub>S also accelerated insulin synthesis and secretion from the regenerated pancreatic cells [694].

Stem cells may be used to generate functional hepatocytes, which may be transplanted into animal models suffering from different liver diseases. However, further investigations on the role of H<sub>2</sub>S in hepatic differentiation are still very much necessary.

#### **b) Hepatocarcinoma**

According to WHO, in 2018, HCC represented the fourth leading cause of cancer-related death around the world. Among the different etiologic factors for HCC are virus infections, NAFLD and alcoholic cirrhosis [695]. Given that most cases of HCC are diagnosed at a stage when the possibility of cure is already very slim, the majority of HCC-related deaths is due to tumour

recurrence [695]. Therefore, the development of more efficient curative strategies for HCC becomes of the utmost importance.

In recent years, a close relationship between H<sub>2</sub>S and HCC has been demonstrated. Some papers have reported that CSE and CBS are overexpressed in human hepatoma cells [118] [696]. The inhibition of the CSE/H<sub>2</sub>S pathway drastically decreases the proliferation of human hepatoma cells while concurrently enhancing ROS production, mitochondrial disruption, DNA damage and apoptosis [118]. Similarly, inhibiting the CBS/H<sub>2</sub>S pathway reduces the viability and growth rate of human hepatoma cells [696]. Another study has demonstrated that the expression of CSE, which was found positively correlated with the proliferation of human hepatoma cells, is regulated by the PI3K/Akt pathway via the transcription factor Sp1 [697]. Likewise, genetic depletion of CBS is capable of preventing the excessive proliferation of HCC cells through ferroptosis while the use of a CBS inhibitor substantially retards tumour growth in a xenograft mouse model of liver cancer [698]. Furthermore, treatment of PLC/PRF/5 hepatoma cells with NaHS for 24h increased the expression levels of CSE and CBS, activated NF- $\kappa$ B and decreased caspase-3 production [225]. As a result, cell viability of the hepatoma line increased and the number of apoptotic cells decreased [225]. Additional evidence has corroborated this premise by demonstrating that NaHS facilitates the proliferation and migration of PLC/PRF/5 hepatoma cells by activating the STAT3/cyclooxygenase-2 (COX-2) signalling pathway [699].

In 2018, Wang *et al.* established a link between drug resistance and high expression of CBS. According to their study, HepG2 cells with high CBS expression were less sensitive to the chemotherapeutic drugs doxorubicin (DOX) and sunitinib [700]. Additional evidence has further confirmed these results by showing that CBS depletion significantly elevated the sensitivity to both chemotherapeutic agents. According to the authors, CBS-induced drug resistance occurs through the activation of STAT3/Akt/Bcl-2 pathway and the inhibition of ROS production [700]. Pan *et al.* described similar findings using siRNA of CSE in HepG2 and PLC/PRF/5 hepatoma cell lines [701]. According to their study, the inhibition of CSE not only increased cellular radiosensitivity as it also suppressed the common radiation-enhanced invasive properties of HCC cells [701]. Similarly, Zhang *et al.* found that blocking the expression of CBS or CSE renders hepatoma cells sensitive to radiotherapy [702]. The knockdown of either enzyme significantly diminished the increased expressions of epithelial-mesenchymal transition (EMT)-related proteins induced by radiation through the p38MAPK pathway, leading to impaired invasion and metastasis of the residual HepG2 cells [702].

Contrarily to the data presented so far, other papers suggest that a lower expression of CBS promotes the proliferation of HCC. Using 120 samples from HCC patients, Kim *et al.* reported that a low expression of CBS significantly correlates with high tumour development and high levels of alpha-fetoprotein (a tumour marker) [703]. Additional evidence supporting the tumour-suppressive role of H<sub>2</sub>S has been demonstrated in 2017 when Wang *et al.* showed that treating HCC cell lines with NaHS induced autophagy and apoptosis through the activation of the PI3K/Akt/mTOR pathway [704]. Another study has shown that, in a subcutaneous HepG2 xenograft model, incubation with GYY4137 suppresses cell proliferation by inhibiting STAT3 activation [277]. Besides, gene expression of several downstream proteins of STAT3, including Bcl-2, cyclin D1, Mcl-1, vascular endothelial growth factor (VEGF) and HIF-1 $\alpha$ , was also decreased in the xenograft model [277]. Recently, Yang *et al.* have demonstrated the immunotherapeutic efficacy of H<sub>2</sub>S in murine hepatocellular carcinoma [705]. According to their study, NaHS inhibited the expression of immunosuppressive enzyme indoleamine 2, 3-dioxygenase 1 (IDO1) by blocking STAT3 and NF- $\kappa$ B pathways [705]. The use of CSE KO mice further corroborated this theory as H<sub>2</sub>S shortage increased IDO1 expression and activity, which ultimately favours an HCC immune escape [705].

Considering the evidence presented so far, it is possible to conclude that the role of H<sub>2</sub>S in cancer development and progression is rather controversial. One study has acknowledged this very same double-faced role of H<sub>2</sub>S. In 2017, Wu *et al.* found that low concentrations of NaHS (10-100  $\mu$ M) stimulated HCC proliferation whereas high concentrations of NaHS (600-1000  $\mu$ M) inhibited cell growth [706]. According to this study, the biphasic effects of NaHS are conducted through the epidermal growth factor receptor (EGFR)/extracellular regulated protein kinases (ERK)/matrix metalloproteinase 2 (MMP-2) and phosphatase and tensin homolog deleted on chromosome ten (PTEN)/Akt signalling pathways [706]. This study further suggests that low concentrations of H<sub>2</sub>S may favour pro-cancer activity, while high concentrations of H<sub>2</sub>S may inhibit the progression of HCC.

### **3.3. H<sub>2</sub>S in NAFLD and fibrosis**

As mentioned in Chapter 2 of this manuscript, among the critical contributors to the development of NAFLD are lipid metabolism alterations, oxidative stress, insulin resistance and inflammation. All of these pathological processes appear to be associated to dysregulations in hepatic H<sub>2</sub>S, which made researchers wonder what possible role could this gasotransmitter play in the onset and progression of NAFLD.



### 3.3.1. NAFLD

#### **a) Alterations in H<sub>2</sub>S metabolism in the development of NAFLD**

Some studies have reported that hepatic H<sub>2</sub>S levels or the activities of CBS and CSE are significantly lower in HFD-fed mice and rats when compared to the controls [707, 708]. These results have been corroborated by human studies, given that overweight individuals present lower plasma levels of H<sub>2</sub>S when compared to lean controls [709]. Similarly, in patients with T2DM, serum H<sub>2</sub>S levels are decreased when compared to healthy controls [710]. Furthermore, hepatic H<sub>2</sub>S biosynthesis is found impaired in a diet-induced rat model of NASH [711]. Nonetheless, some studies suggest that H<sub>2</sub>S biosynthesis is actually upregulated in NAFLD cases. HFD-fed mice present elevated mRNA and protein levels of CSE and CBS as well as higher levels of H<sub>2</sub>S in the liver [712]. Liver CBS and CSE were also found overactivated in T2DM obese diabetic rats [713]. The discrepancies found between these studies may arise from differences in the composition of the diets and/or the duration of feeding. However, they could also reflect spectrum-specific responses of these enzymes during the evolution of NAFLD.

In 2017, Takahashi *et al.* described that CSE KO mice fed HFD for 20 weeks exhibited impaired glucose-induced insulin secretion as well as reduced glucose tolerance [714]. A couple of years later, in 2019, the same group demonstrated that CSE KO mice were more prone to develop obesity and IR when fed HFD [715]. Their study showed that the CSE invalidation aggravated obesity-related IR by inhibiting hepatic Akt activity and repressing FoxO1 phosphorylation and degradation. This resulted in accumulation of nuclear FoxO1 and upregulation of PEPCK and G6Pase [715]. Additional evidence has demonstrated that CSE KO mice fed HFD present increased cholesterol levels in both plasma and liver. These results were associated to decreased mRNA expression of *LXR* and *LXR*-target gene *CYP7A1*, which halted cholesterol catabolism and led to its accumulation (**Figure 30**) [716]. According to this study, deficiencies in the CSE/H<sub>2</sub>S pathway result in high susceptibility to HFD-induced fatty liver. In fact, Ali *et al.* showed that HepG2 cells incubated with a mixture of FFA or high glucose presented lower levels of CSE expression and H<sub>2</sub>S production, as well as augmented intracellular levels of acetyl-CoA and lipids (**Figure 33**) [717]. Experiments using CSE KO mice fed high-fat/choline-deficient (HF/CD) diet have corroborated these results by showing an hepatic accumulation of acetyl-CoA and lipids [717]. Similarly, CSE KO mice fed HFD exhibit reduced plasmatic thiol levels, GSH, SOD activity and increased plasma MDA levels [129].

Species	Diet	Model	Treatment	Effect	Mechanisms	Reference
Mouse	HFD	NAFL	NaHS (56 µmol/kg/day)	Amelioration of HFD-induced NAFL	Activation of liver autophagy via the AMPK-mTOR pathway	[723]
Mouse	HFD	NAFL	NaHS (50 µmol/kg/day)	Amelioration of HFD-induced NAFL	Improvement of lipid metabolism And antioxidant potential	[722]
CSE KO Mouse	HF/CD	NAFL	Lack of CSE	Worsens HF/CD-induced NAFL	Upregulation of ACC, FAS, SREBP-1c, IL-6 and SMAα	[718]
Mouse	HFD	NAFL	NaHS (50 µmol/kg/day)	Amelioration of HFD-induced NAFL	Upregulation of UFA biosynthesis, mtFAO and lipid droplet degradation	[724]
Mouse	HFD	NAFL	Physical exercise for 24 days	Amelioration of HFD-induced NAFL	Physical exercise upregulated CBS, CSE and MPST expression, which decreased MDA levels as well as TNF-α and IL-6 expression	[725]
Mouse	HFD	NAFL	DADs (20, 50 and 100 mg/kg)	Amelioration of HFD-induced NAFL	Increased PPARα, inhibition of SCD1, SREBP-1c and ApoA-1	[726]
Mouse	MCD	NASH	DADs (20, 50 and 100 mg/kg)	Amelioration of MCD-induced NASH	Inhibition of lipid peroxidation through the downregulation of MDA, TNF-α, IL-6 and NF-κB	[726]
Rat	MCD	NASH	NaHS (28 µmol/kg/day)	Amelioration of MCD-induced NASH	Possibly through abating oxidative stress and suppressing inflammation	[711]
Mouse	MCD	NASH	SPRC (40 mg/kg/day)	Amelioration of MCD-induced NASH	Antioxidative effect through the PI3K/Akt/Nrf2/HO-1 signalling pathway	[721]

**Figure 33: Studies demonstrating the protective role of H<sub>2</sub>S in Non-Alcoholic Fatty Liver Disease (NAFLD)**

**HFD:** high-fat diet; **HF/CD:** high-fat/choline deficient diet; **MCD:** methionine-choline deficient diet; **NAFL:** non-alcoholic fatty liver; **NASH:** non-alcoholic steatohepatitis; **NaHS:** sodium hydrosulfide; **DADs:** diallyl disulfides; **SPRC:** s-propargyl-cysteine; **CBS:** cysteine β-synthase; **CSE:** cysteine γ-lyase; **MPST:** 3-mercaptopyruvate sulfurtransferase; **AMPK:** 5' AMP-activated protein kinase; **mTOR:** mechanistic target of rapamycin; **ACC:** acetyl-CoA carboxylase; **FAS:** fatty acid synthase; **SREBP-1c:** sterol regulatory element-binding protein-1c; **IL-6:** interleukin 6; **SMAα:** smooth muscle actin alpha; **UFA:** unsaturated fatty acids; **mtFAO:** mitochondrial fatty acid oxidation; **MDA:** malonaldehyde; **TNFα:** tumor necrosis factor alpha; **PPARα:** peroxisome proliferator-activated receptor alpha; **SCD1:** stearoyl-CoA desaturase-1; **ApoA-1:** apolipoprotein A1; **NF-κB:** nuclear factor-kappa B; **PI3K:** phosphoinositide 3-kinase; **Akt:** protein kinase B; **Nrf2:** nuclear factor erythroid-derived 2-like 2; **HO-1:** heme oxygenase 1

In 2019, Yang *et al.* have demonstrated that HFD-fed mice undergoing dietary methionine restriction for 22 weeks presented up-regulated hepatic protein expression and enzymatic activity of CSE as well as elevated H<sub>2</sub>S production [718]. These changes were associated to lower hepatic fat content, decreased lipid synthesis, increased mtFAO, glycolysis and TCA cycle metabolism, enhanced activity of GPx and reduced levels of oxidative damage products [718]. Another study has indicated that HFD-fed mice and NAFLD patients present an increased expression of hepatic MPST [142]. Both *in vivo* and *in vitro* inhibition of MPST significantly ameliorated intracellular fat accumulation. Interestingly though, H<sub>2</sub>S production was enhanced by the inhibition of MPST and inhibited by MPST overexpression. Additional experiments showed that MPST negatively regulates CSE expression, which promotes steatosis by the upregulation of SREBP-1c, JNK phosphorylation and hepatic oxidative stress [142]. This study highlights the complexity of H<sub>2</sub>S metabolism and the elaborate regulation to which all enzymes are subjected.

#### **b) H<sub>2</sub>S donors as a therapeutic agent in NAFLD**

Recently, a growing number of evidence has shown that H<sub>2</sub>S could be used as a drug for the treatment of NAFL/NASH. In 2014, Luo *et al.* described that an 8-week exposure to an MCD diet induced hepatic steatosis, inflammation and fibrosis in rats (**Figure 33**) [711]. Interestingly, these animals exhibited impaired hepatic H<sub>2</sub>S production. However, daily supplementation with NaHS prevented this MCD-diet-induced NASH phenotype by reducing Cyp2E1 expression, enhancing HO-1 expression and suppressing mitochondrial ROS formation [711]. Similarly, the treatment of MCD mice with S-propargyl-cysteine (SPRC), an H<sub>2</sub>S donor, for 4 weeks significantly reduced hepatic levels of ROS and MDA, and increased SOD activity [719]. In HepG2 cells, the CSE inhibitor DL-propargylglycine (PAG) completely abolished the antioxidant effects of SPRC through the downregulation of Akt phosphorylation, HO-1 and CSE expression, and by inhibiting Nrf2 translocation to the nucleus (**Figure 33**) [719]. On the other hand, incubation of HepG2 cells with NaHS increased the levels of CSE expression while simultaneously reducing the FFA-induced accumulation of acetyl-CoA and lipids [717]. According to the authors, the exogenous H<sub>2</sub>S blocked the transcription of DNL- (SREBP-1c), inflammation- (IL-6, TNF $\alpha$ ) and fibrosis- (SMA $\alpha$ ) related genes [717]. Additional studies have corroborated these results. Wang *et al.* demonstrated that pre-treating HepG2 cells with NaHS before exposing them to palmitic acid (PA) for 24h inhibits the expression of pro-inflammatory cytokines (TNF $\alpha$ , IL-6 and IL-1 $\beta$ ) and the activation of NF- $\kappa$ B [720]. In 2015, Wu *et al.* demonstrated that HFD-fed mice daily injected with NaHS for 4 weeks present a decrease in hepatic lipid content, lower expression levels of FAS, increased expression levels of

CPT1A, reduced levels of MDA and increased activity of both SOD and GPx (**Figure 33**) [721]. Additional studies have demonstrated that one of the mechanisms by which H<sub>2</sub>S may exert its NAFLD-protective role is through the activation of liver autophagy. Daily administration of NaHS to HFD-fed mice increased the expression of microtubule-associated protein 1A/1B-light chain 3 phosphatidylethanolamine conjugate (LC3II), a key protein required for autophagosome formation, and decreased p62 expression, one of the specific autophagy substrates (**Figure 33**) [722]. Furthermore, NaHS supplementation also increased AMPK phosphorylation, which subsequently reduced mTOR phosphorylation [722]. In 2020, Liu *et al.* showed that HFD-fed mice daily injected with NaHS for 4 weeks present lower liver weight, body weight and hepatic lipid content when compared to their respective HFD+NaCl controls [723]. Proteomics showed that 58 proteins whose expression had changed upon HFD-feeding were normalized after treatment with NaHS (**Figure 33**) [723]. The biological processes in which these proteins appear to be involved are fat digestion and absorption, FA metabolism, glutathione metabolism, drug metabolism-cytochrome P450 and steroid hormone biosynthesis [723].

Aside the direct H<sub>2</sub>S donors, other methods may be applied in order to modulate endogenous production of H<sub>2</sub>S. In 2017, Wang *et al.* have shown that HFD-fed mice subjected to moderate-intensity exercise for 24 weeks presented enhanced plasma and hepatic H<sub>2</sub>S levels as well as increased expression of CBS, CSE and MPST (**Figure 33**) [724]. These changes were accompanied by attenuated systemic insulin resistance and glucose intolerance, as well as mitigated hepatic steatosis and fibrosis [724]. In 2019, Zhang *et al.* demonstrated that administration of diallyl disulfides (DADs) (garlic derived organic polysulfide compounds that act as an H<sub>2</sub>S donor) to mice fed MCD diet or HFD for 4 or 20 weeks, respectively, ameliorated hepatic steatosis by downregulating mRNA levels of both *SREPB-1c* and apolipoprotein A1 (ApoA-1) and increasing mRNA levels of *FGF21* (**Figure 33**) [725]. In the HFD-fed group, DADs also prevented lipotoxicity through the increase in PPAR $\alpha$  expression and inhibition of SCD1 expression. As to the MCD-fed group, DADs markedly inhibited lipid peroxidation by decreasing MDA, TNF $\alpha$ , IL-6 levels, suppressing NF- $\kappa$ B activation and increasing SOD expression [725].

Collectively, these results demonstrate that H<sub>2</sub>S exerts a critical role in the development of NAFLD (**Figure 34**). The current studies mainly focus on the regulation of H<sub>2</sub>S levels by modulating the biosynthesis pathway or by the use of exogenous donors. **Whether H<sub>2</sub>S catalytic pathway, i.e. its mitochondrial oxidation, could also be important in the development and progression of NAFLD remains to be investigated.**

### 3.3.2. Fibrosis

Hepatic fibrosis is a scarring process caused by the excessive production of extracellular matrix (ECM) by activated HSCs that reflects the response of liver to injury [726]. Eventually, this process disrupts the architectural organization of hepatic functional units and blood flow. Fibrosis is the inevitable end of many chronic liver diseases, including NAFL, NASH and viral hepatitis [726]. However, if these hepatic injuries aggravate any further, hepatic fibrosis may progress to cirrhosis or even HCC.

It has been known that invalidation of CBS promotes fibrosis, oxidative stress, and steatosis in the mouse liver, suggesting a direct link between H<sub>2</sub>S and hepatic fibrosis [664]. In a similar way, gene knockout of CSE triggers an inflammatory response and exacerbates liver fibrosis by reducing H<sub>2</sub>S production [727]. Nonetheless, only recently have studies begun to show that H<sub>2</sub>S can be used to attenuate fibrogenesis both *in vivo* and *in vitro*.

Current evidence suggests that activated HSCs are the central players in fibrogenesis and that their inactivation may protect and treat liver fibrosis. In 2013, Fan *et al.* demonstrated that *in vitro* treatment with NaHS is able to suppress the proliferation of activated HSCs in a dose-dependent manner [728]. The H<sub>2</sub>S donor induced G1 phase cell cycle arrest and apoptosis at the same time that it reduced intracellular levels of ROS and Ca<sup>2+</sup>. In a similar way, the administration of NaHS to rats with CCl<sub>4</sub>-induced hepatic fibrosis attenuated the protein expression of collagen I [728]. These anti-fibrotic effects were mimicked in rats with CCl<sub>4</sub>-induced hepatic fibrosis [729]. S-allyl-cysteine (SAC), an endogenous H<sub>2</sub>S donor, has been shown to attenuate CCl<sub>4</sub>-induced liver Angiotensin II, a pro-fibrotic factor synthesized by activated HSCs, leads to the secretion of ECM components when bound to the angiotensin II type 1 receptor (AGTR1). In an *in vivo* model of liver fibrosis, treatment with NaHS resulted in a significant downregulation of AGTR1 expression whereas the use of PAG significantly increased the expression of this receptor [730]. Another study has shown that *in vitro* treatment of H<sub>2</sub>O<sub>2</sub>-induced HSCs with diallyl trisulfides (DATs) suppresses and reduces the expression of several fibrotic markers such as SMA, type I procollagen, fibronectin and TGF-β [731]. Exposure to DATs also elevated H<sub>2</sub>S levels and decreased intracellular ROS and lipid peroxides. This study has clearly demonstrated an H<sub>2</sub>S-associated mechanism underlying DATs-induced inhibition of fibrogenesis and alleviation of oxidative stress in HSCs [731]. Additional evidence has shown that the incubation of HSCs with DATs changes the expression profile of 21 proteins, most of which are involved in apoptotic pathways [731]. Another study has shown that NaHS exerts anti-proliferative effects on HSCs through a decrease in phospho-p38 and an increase in phospho-Akt expressions [729].

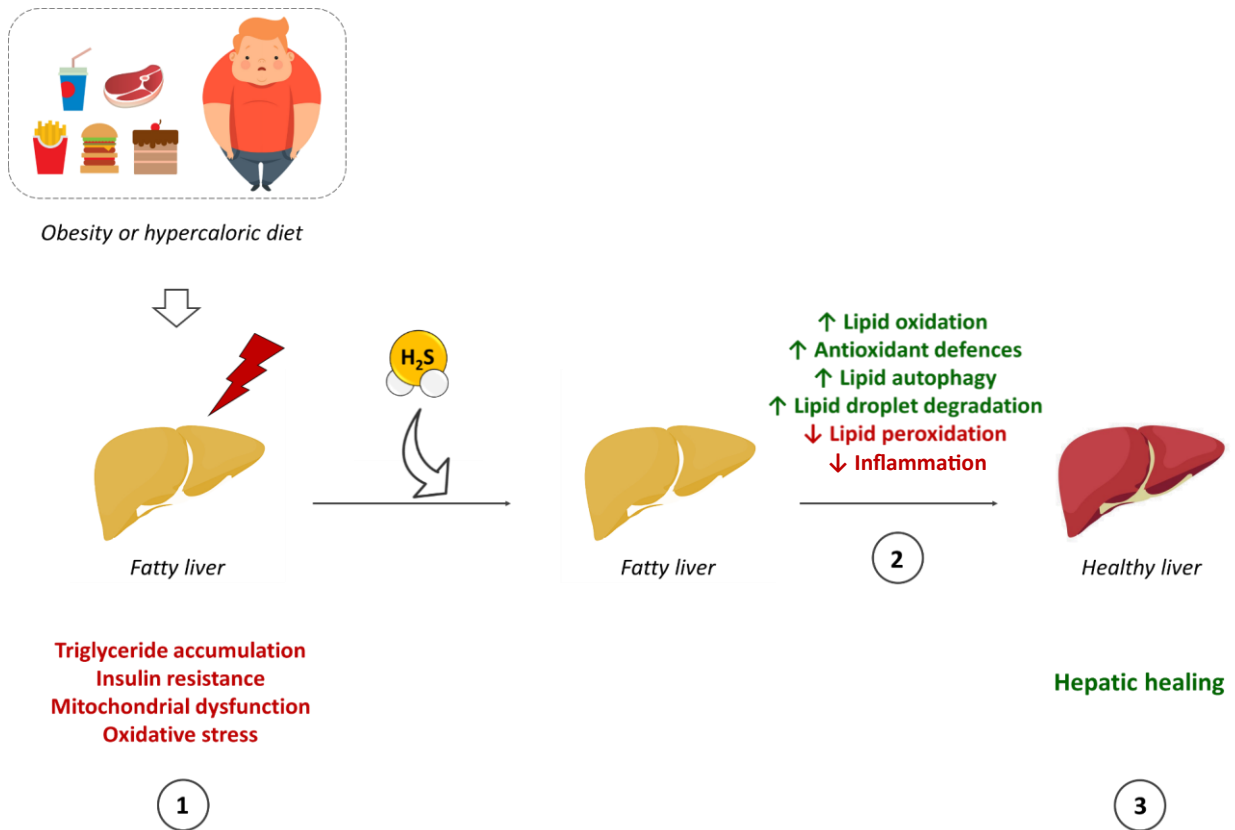


**Figure 34: H<sub>2</sub>S and Non-Alcoholic Fatty Liver Disease (NAFLD)**

Obesity, which is greatly impelled by poor dietary habits and sedentarism, is a well-characterized risk factor for the development of non-alcoholic fatty liver. This hepatic perturbation is associated not only with triglyceride accumulation, but also with insulin resistance, mitochondrial dysfunction and increased oxidative stress (1). Recent studies have suggested that hydrogen sulfide (H<sub>2</sub>S) can be used as a therapeutic agent in NAFLD. Administration of H<sub>2</sub>S to animal models of fatty liver is capable of increasing lipid oxidation and autophagy, increasing lipid droplet degradation, increasing the expression of antioxidant proteins, decreasing the amount of lipid peroxides and ameliorating inflammation (2). The regulation of these pathways by H<sub>2</sub>S appears to be a successful way to reverse or delay the development of fatty liver (3) fibrosis and plasma transaminase elevation in rats [732]. In the liver, SAC could also reduce the mRNA expression of inflammatory and fibrogenic cytokines/biomarkers, such as *IL-6*, *TNFA*, *TGFB*, *SMA*, *fibronectin* and *type I collagen*, as well as induce the mRNA expression of antioxidant enzymes, such as *SOD*, *catalase*, and *GPx* [732]. According to the authors, SAC-induced modulation of fibrogenic genes was accomplished by inhibiting the phosphorylation of SMAD3 and signal transducers and activators of transcription 3 (STAT3), which inhibited their binding ability to transcription promoters [732].

According to a recent paper, mRNA and protein expression of H<sub>2</sub>S synthesizing enzymes are low in HSCs when compared to hepatocytes and Kupffer cells [733]. In a very contradictory manner, this paper has also shown that H<sub>2</sub>S promotes HSCs activation [733]. In this study, incubation of rat HSCs with NaHS or GYY4137 increases HSC proliferation whereas CSE or CBS inhibitors reduce proliferation and the expression of fibrotic markers of HSCs [733]. Therefore, more experiments are required to determine the exact actions of H<sub>2</sub>S on HSCs activation and subsequent hepatic fibrosis.

### 3.4. Mitochondrial H<sub>2</sub>S oxidation in liver metabolism

While the studies discussed thus far largely concern the regulation of H<sub>2</sub>S levels through the modulation of its biosynthesis, mitochondrial H<sub>2</sub>S oxidation is another pathway that regulates the levels of this gasotransmitter and, therefore, its actions. Unfortunately, too few studies have been directly investigated the physiological relevance of this pathway in liver energy homeostasis.

- **Studies focusing SQR**

As mentioned earlier on Chapter 1, two homozygous pathogenic variants of SQR have been recently reported in humans [163]. These variants are responsible for lack of protein and enzyme activity, and are deeply associated with decreased hepatic Complex IV activity, lactic acidosis, ketosis, dicarboxylic aciduria and brain lesions. Interestingly, the symptoms are triggered by infections or fasting, episodes associated with protein catabolism [163].

Baiges *et al.* have reported that SQR mRNA levels are decreased by more than 50% in HFD-fed rats [734]. In a mouse model of kidney disease (Pdss2<sup>kd/kd</sup>), levels of SQR and its downstream enzymes were found decreased in association to increased H<sub>2</sub>S levels in the kidney [735]. These mice also showed low levels of thiosulfate in plasma and urine, and increased C4-C6 acylcarnitines in blood, due to inhibition of short-chain acyl-CoA dehydrogenase [735].

Butyrate is the preferred fuel source for normal colonocytes and is generated via microbial fermentation of undigested fiber remnants that reach the large intestine. Previous studies have demonstrated that butyrate and butyrate-based compounds revert IR and body fat accumulation in HFD-fed mice through the improvement of liver mitochondrial respiration, mtFAO and activation of the AMPK-ACC pathway [736]. H<sub>2</sub>S-mediated inhibition of colonocyte butyrate oxidation has been described in cases of ulcerative colitis [737]. Recently, the mechanism through which H<sub>2</sub>S conducts this inhibition has been further elucidated. Nanochips with human SQR have demonstrated that SQR includes CoA as an alternate sulfur acceptor, forming CoA persulfide (CoA-

SSH) in the process [738]. CoA-SSH associates with the cofactor FAD of butyryl-CoA dehydrogenase, a critical enzyme in butyrate metabolism, forming an inhibitory charge-transfer complex that ceases enzyme activity. A possible rationale for H<sub>2</sub>S modulation of butyryl-CoA dehydrogenase in colonocytes via SQR-derived CoA-SSH is prioritization of H<sub>2</sub>S oxidation under conditions of acute H<sub>2</sub>S exposure from gut microbial metabolism.

Up to now, not many studies have been reported regarding the modulation of SQR expression in mammals [739]. Using siRNA for SQR, Prieto-Lloret *et al.* demonstrated that the contraction of rat pulmonary arteries is largely caused by SQR-mediated sulfide metabolism, which, by donating electrons to ubiquinone, increases electron production by Complex III and thereby ROS production [739]. Another study has shown that SQR is required for H<sub>2</sub>S-mediated protection during nutrient/oxygen deprivation [740]. Hepa1-6 cells, with or without partial knockdown of SQR, were incubated with 5 μM NaHS and subjected to hypoxic conditions. The addition of exogenous H<sub>2</sub>S reduced LDH release during the ischemic phase and upon reperfusion. The later was upregulated in the cultures where SQR was partially depleted [740]. In addition, the increase in MTT activity during the reperfusion phase in the presence of NaHS was significantly reduced by SQR knockdown. Interestingly, SQR knockdown did not alter the effects of NaHS addition on nutrient/growth factor withdrawal in the absence of hypoxia [740]. It appears that the resistance to simulated I/R is linked to SQR capacity in donating electrons to the ETC via ubiquinone.

- **Studies focusing ETHE1**

Patients carrying a variant of ETHE1 and ETHE1 KO mice show abnormally high concentrations of H<sub>2</sub>S in the brain, liver, muscle, and colonic mucosa [171, 723]. These elevated levels of H<sub>2</sub>S lead to the inhibition of mitochondrial Complex IV activity and to the disruption of mitochondrial respiration [171, 723]. A proteomics study on fibroblast cells from patients with ETHE1 mutations revealed several downregulated proteins, including SQR, which can further explain the elevated H<sub>2</sub>S levels displayed by these patients [742]. Typically, patients carrying the variant allele are treated with metronidazole (antibiotic against H<sub>2</sub>S-producing bacteria) or with N-acetyl cysteine (a cell permeable precursor of GSH that accepts sulfur atoms from H<sub>2</sub>S and forms nontoxic compounds). Recently, it has been reported that liver transplant is also a therapeutic option for ethylmalonic encephalopathy [741].

A large proteomic study conducted on liver tissue from ETHE1 KO mice has demonstrated that the absence of ETHE1 is associated with the upregulation of three glycolytic enzymes: fructose



bisphosphate aldolase (FBA), pyruvate kinase (PK) and lactate dehydrogenase A (LDHA) [743]. These results present the idea that *ETHE1*-deficient cells favour glycolysis rather than mitochondrial respiration due to compromised Complex IV activity [743]. Moreover, the absence of *ETHE1* leads to the accumulation of short-chain acylcarnitines through the inhibition of short-chain acyl-CoA dehydrogenase activity, and to the accumulation of lactate [171, 723, 726]. Baiges *et al.* have reported that mRNA levels of *ETHE1* are decreased by more than 50% in HFD-fed rats [734]. Additional studies have demonstrated that *ETHE1* KO mice present decreased mRNA levels of the *E2* and *E3* subunits of the branched-chain  $\alpha$ -ketoacid dehydrogenase complex (BCKDH). BCKDH is the flux-generating step in the oxidation of branched-chain amino acids (valine, leucine and isoleucine), which occurs in the mitochondria, and has some steps overlapping with mtFAO [745].

- **Studies focusing TST**

In 2016, *TST* has been identified as a potential obesity-resistant gene. Morton *et al.* showed that *TST* mRNA levels were ~8-fold more expressed in the AT of lean mice when compared to obese animals [746]. In addition, mice injected with an adipocyte-specific *TST* adenovirus resisted to HFD-induced obesity and presented smaller fat cell size despite showing the same food intake as the controls [746]. This overexpression of *TST* in AT was associated with elevated hepatic *CPT1A* mRNA levels and increased mtFAO. *TST* expression was also found positively correlated with the mRNA levels of *GLUT4*, *IRS-1* and *PPARG* in AT. Similarly, higher *TST* mRNA levels were found in the AT of lean individuals when compared to obese individuals [746].

- **Studies focusing SUOX**

Up to now, no studies have been published regarding genetic manipulation of *SUOX*. However, studies have been conducted using a rat model of *SUOX* deficiency, which is achieved by using a diet low in molybdenum (cofactor of *SUOX*) with concurrent addition of tungsten (molybdenum competitor) to the drinking water. Daily administration of sodium metabisulfite to *SUOX* deficient rats for 6 weeks has increased plasma levels of lipid hydroperoxides and total oxidant status [747]. Interestingly, the same rat model has shown increased activity of erythrocyte glucose-6-phosphate dehydrogenase (G6PD), SOD and GPx [748]. In order to better understand the mechanisms through which hypertension influences hepatic function, a recent study has compared the whole liver proteome of hypertensive rats with their respective controls [749]. Among the differently expressed proteins was *SUOX*, which presented decreased expression in

the hypertensive group [749]. In humans, SUOX deficiency is an autosomal recessive disease characterized by severe neurological impairment. Patients present neurological abnormalities, pharmaco-resistant seizures or developmental delay and usually die at the age of 1 or 2 years [179, 180].

## Main issues for my PhD project

For many decades, H<sub>2</sub>S, the colourless gas with a strong odor of rotten eggs, has been recognized as a toxic molecule and an environmental pollutant. In the last two decades, the perception of H<sub>2</sub>S has changed from that of a noxious gas to a gasotransmitter with vast potential in pharmacotherapy. The ubiquitous distribution of H<sub>2</sub>S-producing enzymes, the remarkable diffusibility of H<sub>2</sub>S, and its high reactivity in different molecular pathways make this molecule unique among the regulators of cell survival and death. In fact, H<sub>2</sub>S appears to be an active participant in various biological pathways, especially in the liver. The unique position of this organ makes it likely to have high amounts of H<sub>2</sub>S coming from both exogenous (the gut) and endogenous (cysteine metabolism) sources.

Nonetheless, the effects of H<sub>2</sub>S can swiftly change from beneficial to detrimental when its concentrations surpass the physiological range, leading to the inhibition of Complex IV of the ETC. Although many studies have demonstrated the participation of H<sub>2</sub>S in different liver pathological scenarios, almost all lines of thought were focused on disruptions of the biosynthesis pathway and its consequences on tissue homeostasis. However, intracellular levels of H<sub>2</sub>S are not solely controlled by the enzymes that produce the gas, but also by the enzymes responsible for its degradation. The high efficiency of mitochondrial H<sub>2</sub>S oxidation catalysed by SQR serves as a protective shield against respiratory poisoning. Moreover, H<sub>2</sub>S oxidation leads to the formation of highly reactive persulfides, which could be important for protein persulfidation, a post-translational modification induced by H<sub>2</sub>S exposure.

**Given the evidence exposed herein, the objectives of my PhD were to investigate:**

- i) whether mouse liver mitochondrial H<sub>2</sub>S oxidation is regulated under different nutritional situations;**
- ii) whether liver mitochondrial H<sub>2</sub>S oxidation is regulated in mouse models of NAFLD and in obese humans;**
- iii) the pathophysiological effects of modulating H<sub>2</sub>S metabolism by *in vivo* H<sub>2</sub>S supplementation and liver SQR overexpression.**



## ***II. Methodology***

---

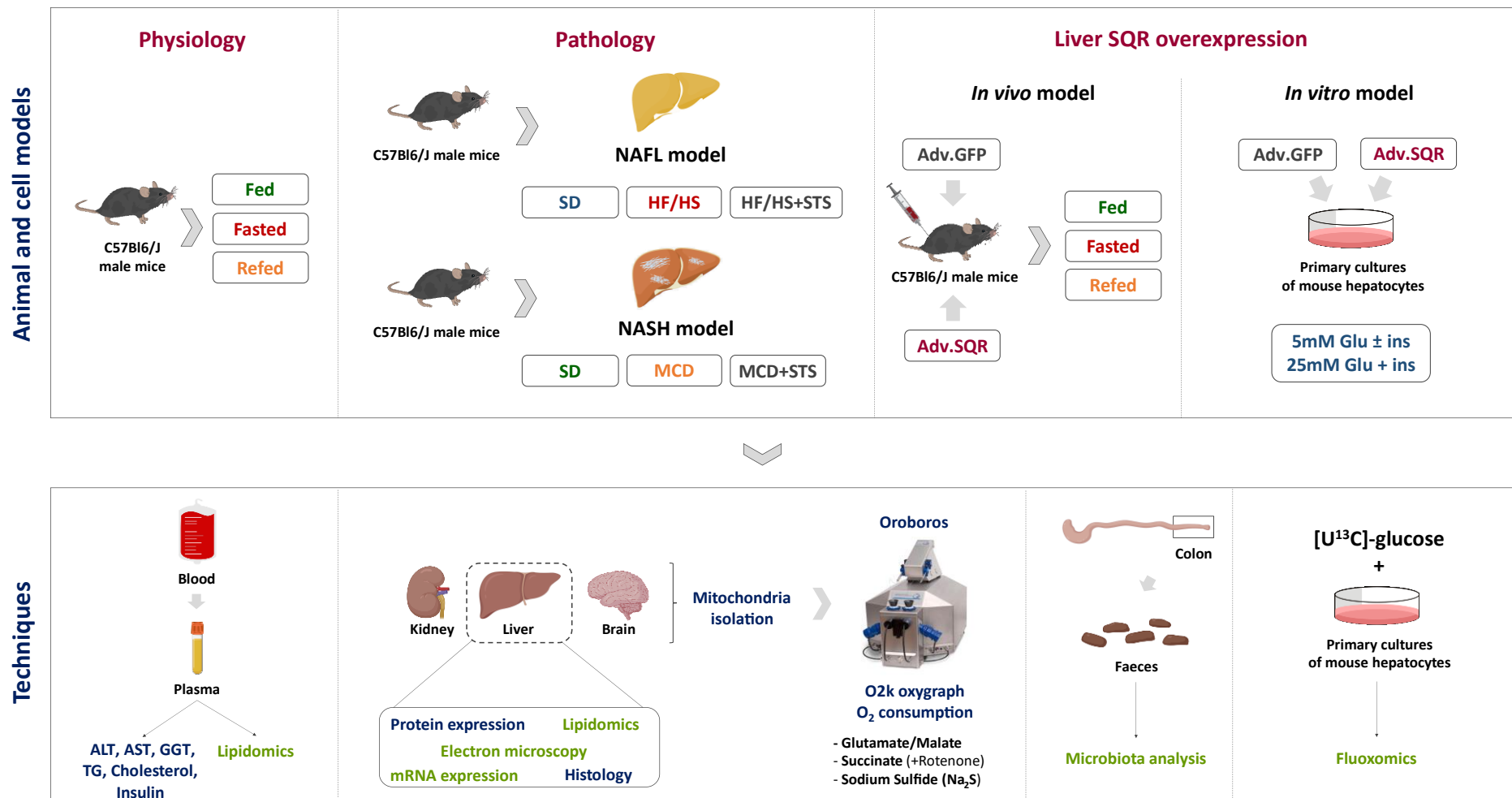


**Figure 35: Diagram of the different animal models and techniques used**

The techniques signalled in **green** were performed in collaboration with researchers from the home institute or other laboratories.

**SD:** standard diet; **HF/HS:** high fat/ high sucrose; **STS:** sodium thiosulfate; **MCD:** methionine-choline deficient diet; **Adv:** adenovirus; **GFP:** green fluorescent protein; **SQR:** sulfide quinone oxidoreductase; **Glu:** glucose; **Ins:** insulin; **ALT:** alanine aminotransferase; **AST:** aspartate aminotransferase; **GGT:** gamma-glutamyl transferase; **TG:** triglyceride

## II. Methodology

The different animal models and techniques used are indicated in **Figure 35**.

### 1. Animals

Adult male C57Bl6/J mice (Janvier Labs, Saint-Berthevin, France) were housed in colony cages under a 12h:12h light:dark cycle in a temperature- and humidity-controlled environment. Mice injected with adenovirus were kept in a conventional animal housing (Pitié Salpêtrière). All other animals were maintained in a Specific Pathogen Free (SPF) animal facility (Institut Cochin). Mice were settled to the housing conditions for at least 1 week before any study began, and had *ad libitum* access to water and food. All studies involving animals followed the European guidelines for the care and use of laboratory animals and were approved by the Paris Descartes University ethics committee (CEEA34). All *in vitro* (APAFIS #26042 N° 2019022717578208) and *in vivo* (APAFIS #15448 N° 2018012911055946) studies were approved by the French "Ministère de l'Education Nationale, de l'Enseignement Supérieur et de la Recherche".

### 2. Fasting/Refeeding experiments

Adult 8- to 16-week-old male C57Bl6/J mice were divided into three groups: one group of regularly fed mice (chow diet - SAFE A03, 61.3% carbohydrate, 13.5% fat, and 25.2% protein in terms of energy); one group of mice fasted for 24h prior to sacrifice; and one group of mice that, after being fasted for 24h, was refeed for 16h while receiving glucose (20% w/v) in the drinking water. Water was provided *ad libitum* to all groups. At the end of the experiment, the animals were euthanized by decapitation. Blood, liver, kidneys, heart, brain, adipose tissue and quadriceps were collected and frozen at -80°C until further use, with the exception of a liver piece that was immediately used for mitochondrial isolation.

### 3. NAFL and NASH animal models

In order to develop the NAFL model, 6-week-old adult male C57BL/6J mice were fed HF/HS diet (Research diets D12451, 35% carbohydrate, 45% fat, and 20% protein in terms of energy) while their controls received a specific control diet (SD) (Research diets D12450, 70% carbohydrate, 10% fat, and 20% protein in terms of energy). The animals were surveyed on a weekly-basis for body weight and food intake and sacrificed 10 or 20 weeks after diet intake. Before sacrifice, animals were subjected to glucose tolerance and insulin sensitivity tests.

To develop the NASH model, 27-week-old male C57BL/6J mice were fed MCD diet (Research diets A02082002BR) while their controls received a specific control diet (SD) (Research diets A02082003BY). Once again the animals were surveyed on a weekly-basis for body weight and food intake. All SD- and MCD-fed mice were sacrificed 4 weeks after the experiments began.

After sacrifice, blood, liver, kidneys, heart, brain, adipose tissue, quadriceps, colon (proximal and distal) and feces were collected. The livers were divided according to the experiments envisaged: mitochondria isolation, RNA and protein extraction, lipidomics and histological analysis (Platform of Histology, Cochin Institute). Plasma levels of ALT, AST, GGT, TG and cholesterol were measured at the Biochemical laboratory from Institut Claude Bernard - Bichat Hospital.

#### **4. *In vivo* supplementation of sodium thiosulfate (STS)**

Given that, in the literature, different studies use different sulfide donors and administration methods, we conducted a pilot study using MCD-fed mice and exposed them to two different sulfide donors for three weeks (Na<sub>2</sub>S and STS). The MCD-fed animals were divided into three groups: the first group was daily gavaged with 0.4 g STS/kg body weight; the second group received 3 mg STS/mL in the drinking water twice a week; and the third group was daily injected with 50 μmol Na<sub>2</sub>S/kg body weight. After 3 weeks of treatment, the animals were sacrificed, and liver histology was evaluated. Mice supplemented with STS showed less lipid accumulation than mice supplemented with Na<sub>2</sub>S. However, no differences were found between the two different supplementation methods of STS. Based on the obtained results, we decided to use STS as sulfide donor.

After 10 weeks of feeding, the HF/HS-fed mice were divided into HF/HS group and HF/HS + STS group. The mice from HF/HS group and HF/HS + STS group received an IP injection of either saline (0.9% w/v NaCl) or STS (0.4 g STS/kg body weight, dissolved in 0.9% w/v NaCl), respectively, twice a week. On the day of injection, the HF/HS + STS group received an additional STS supplementation in the drinking water (3 mg/mL). This course of treatment was pursued for 10 weeks. All animals were subjected to glucose tolerance and insulin sensitivity tests one week before being sacrificed.

In order to assess the effect of STS supplementation in an animal model of NASH, a subgroup of MCD-fed animals was supplemented with STS (using the same protocol as for the HF/HS-fed model) during all 4 weeks of MCD-feeding. At the end of the experiments, mice were sacrificed and tissue collection and use were performed as described in paragraph 1.3.



## **5. *In vivo* injection of adenovirus**

The pcDNA3 expression vector containing the human SQR (hSQR) coding sequence has been previously constructed by the team [187]. The resulting expression vector was sequenced to be certain of its exactitude. Afterwards, adenovirus coding green fluorescent protein (GFP) and hSQR were produced by the Laboratoire de thérapie génique (UMR 1089, Nantes, France). The adenovirus were delivered through penis injection ( $1 \times 10^9$  infectious particles (i.p.)/mouse) to adult C57Bl6/J mice and the animals were surveyed on a weekly-basis for body weight and food intake. Three weeks after the adenovirus injection, the animals were subjected to oral glucose tolerance test, insulin sensitivity test and pyruvate tolerance test. One week later, mice were sacrificed. Tissue collection and use were performed as described in paragraph 1.3.

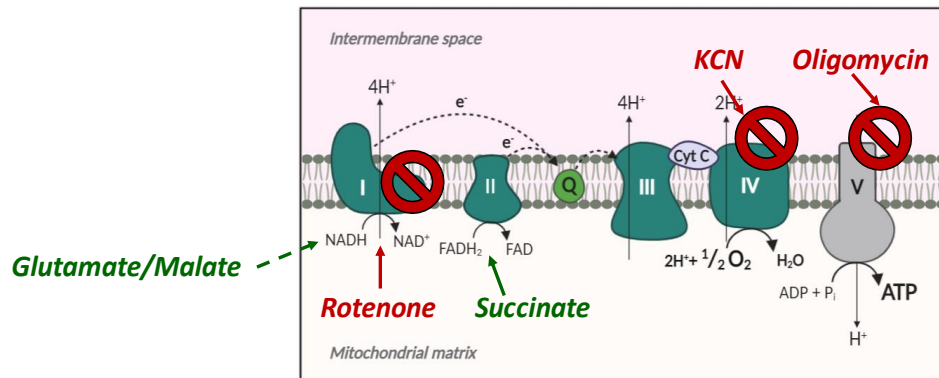
## **6. Physiological parameters**

To assess insulin sensitivity, mice were fasted for 5–6 h in the middle of the dark phase with *ad libitum* access to water. Actrapid HM human insulin (Novo Nordisk) was injected intraperitoneally (IP) at a dose of 0.75 U/kg body weight. To assess glucose tolerance, mice received a glucose solution by gavage (solvent: water; 1 g/kg body weight) after overnight fasting. To assess pyruvate tolerance, mice received an IP injection of sodium salt pyruvate (2 g/kg body weight) after an overnight fast. For all tests, tail blood glucose was monitored at 0, 15, 30, 60, 90 and 120 min using the Accu-Chek Aviva blood glucose monitor (Roche).

## **7. Isolation of mitochondria**

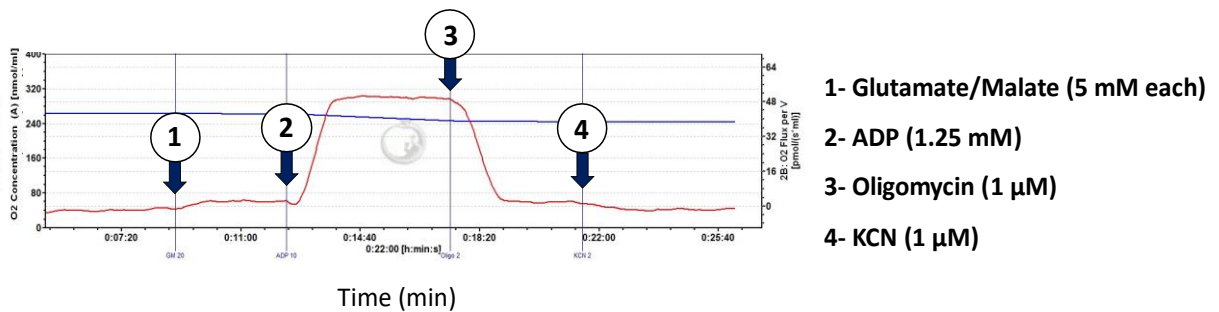
All steps were carried out at 4°C. Tissue mitochondria were isolated using differential centrifugation. Briefly, minced tissue samples were carefully homogenized (5 strokes at low speed rotation) at a ratio of 1 g of tissue/6 mL of isolation buffer (300 mM sucrose, 5 mM Tris-HCl, 1 mM EGTA, pH 7.4) containing 0.1% (w/v) fatty acid-free bovine serum albumin (BSA) using a glass Teflon homogenizer. After centrifugation at 600 g (10 min at 4°C), the supernatants containing mitochondria were further centrifuged at 8500 g (10 min at 4°C). The mitochondria pellets were resuspended in isolation buffer (without BSA) and protein concentration was determined by the Bicinchoninic Acid (BCA) assay using BSA as standard.

**A**



**B**

**Glutamate/Malate**



**C**

**Succinate + Rotenone**

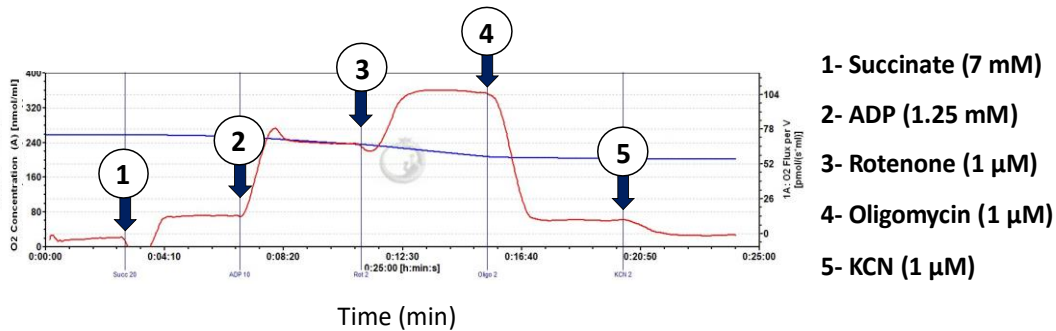


**Figure 36: O<sub>2</sub> consumption of isolated mitochondria was measured using an O2k oxygraph (Oroboros)**

**A)** Schematic representation of the different substrates and inhibitors used; **B)** Representative run of mitochondrial respiration using glutamate/malate; **C)** Representative run of mitochondrial respiration in the presence of succinate plus rotenone

O<sub>2</sub> concentration is represented by the blue line (left axis (nmol/mL) and O<sub>2</sub> consumption is represented by the red line (right axis (pmol/s.mL)).

**KCN:** potassium cyanide

## 8. Measurement of mitochondrial respiration and sulfide oxidation

Mitochondrial oxygen consumption was measured at 25°C using an Oroboros oxygraph-2k (Oroboros Instruments, Innsbruck, Austria). For mitochondrial respiration, mitochondria (~120 µg of proteins) were introduced into the respiratory chamber filled with 2 mL of respiration buffer (100 mM KCl, 40 mM sucrose, 10 mM TES, 5 mM MgCl<sub>2</sub>, 10 mM KPi, 1 mM EGTA, 0.4% (w/v) fatty acid-free BSA, pH 7.2). Measurements were conducted in the presence of either glutamate/malate (5 mM each) or succinate (7 mM) plus rotenone (1 µM) to assess Complex I- and Complex II-linked respiration rates, respectively. Mitochondrial respiration rate was determined successively in the presence of ADP (1.25 mM), oligomycin (1 µM), and lastly 1 mM potassium cyanide (KCN) to inhibit mitochondrial respiration and assess non-respiratory oxygen consumption (value to be subtracted to all values) (**Figure 36**). These measurements allowed the calculation of state 3 (substrates + ADP) and state 4 (oligomycin). State 3 - state 4 rate indicates oxygen consumption linked to ATP synthesis while state 3/state 4, defined as the respiratory control ratio (RCR), assesses the coupling between respiration and phosphorylation.

For H<sub>2</sub>S oxidation, a stock solution of 1 M Na<sub>2</sub>S was freshly prepared at the time of the experiment, diluted into water to a final concentration of 5 mM, and finally loaded into the high-pressure glass syringes of the injection Tip2k minipump (Oroboros Instruments). Sulfide oxidation measurements were performed using 2 mg of mitochondrial proteins per chamber. To be sure that the oxygen consumption observed upon sulfide addition to the chamber was specific to sulfide mitochondrial oxidation, previous assays were conducted comparing H<sub>2</sub>S-associated oxygen consumption in runs with or without mitochondria (**Figure 37A**). Furthermore, different tests were conducted to determine the best quantity of mitochondrial proteins to use and results showed that the lower the sample concentration is, the longer H<sub>2</sub>S oxidation takes (**Figure 37B and 37C**). The final assay for the measurement of H<sub>2</sub>S oxidation is depicted in **Figure 38**. Mitochondrial respiration was first settled to state 3 by addition of glutamate/malate (5 mM each) followed by ADP (1.25 mM). This allows the measurement of the reference state 3 rate to normalize mitochondrial H<sub>2</sub>S oxidation rate as percentage of state 3 rate. After addition of rotenone (1 µM), the chambers were reoxygenized, ADP (0.625 mM) was added and increasing concentrations (0.3125 µM - 25 µM) of Na<sub>2</sub>S were successively injected into the chamber. Finally, the run was ended by adding 1 mM KCN. Given that mitochondrial H<sub>2</sub>S oxidation follows Michaelis-Menten kinetics, we were able to calculate V<sub>max</sub> and K<sub>m</sub> for all experimental groups.

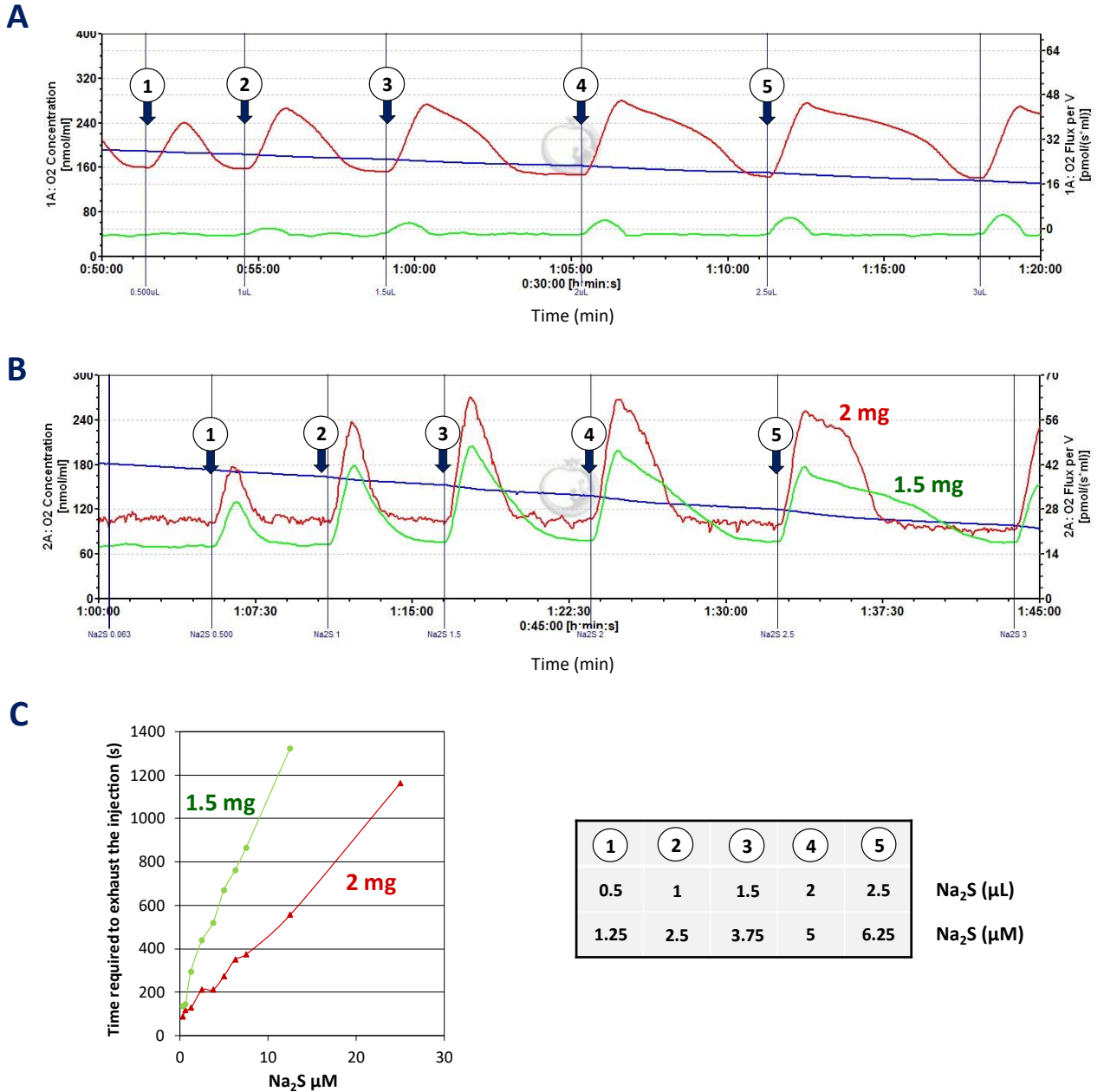


**Figure 37: Protocol to assess mitochondrial H<sub>2</sub>S oxidation**

Preliminary experiments were performed using isolated liver mitochondria. The mitochondria were successively exposed to glutamate/malate, ADP and rotenone before Na<sub>2</sub>S was injected in the chamber. **A)** In the absence of mitochondria (green line) there is a slight increase in O<sub>2</sub> consumption after Na<sub>2</sub>S injection. However, O<sub>2</sub> consumption is much higher when mitochondria are present (red line). **B)** The quantity of mitochondria present in the chamber also has an impact on the speed of the run. Compared to 2 mg of mitochondrial proteins (red line), the use of 1.5 mg (green line) delays the complete oxidation of each H<sub>2</sub>S injection. **C)** Time required to exhaust Na<sub>2</sub>S injection in the presence of 1.5 mg or 2 mg of mitochondria.

O<sub>2</sub> concentration is represented by the blue line (left axis (nmol/mL) and O<sub>2</sub> consumption is represented by the red line (right axis (pmol/s.mL)). The correspondence between Na<sub>2</sub>S volume and Na<sub>2</sub>S concentration is indicated. **Na<sub>2</sub>S:** sodium sulfide

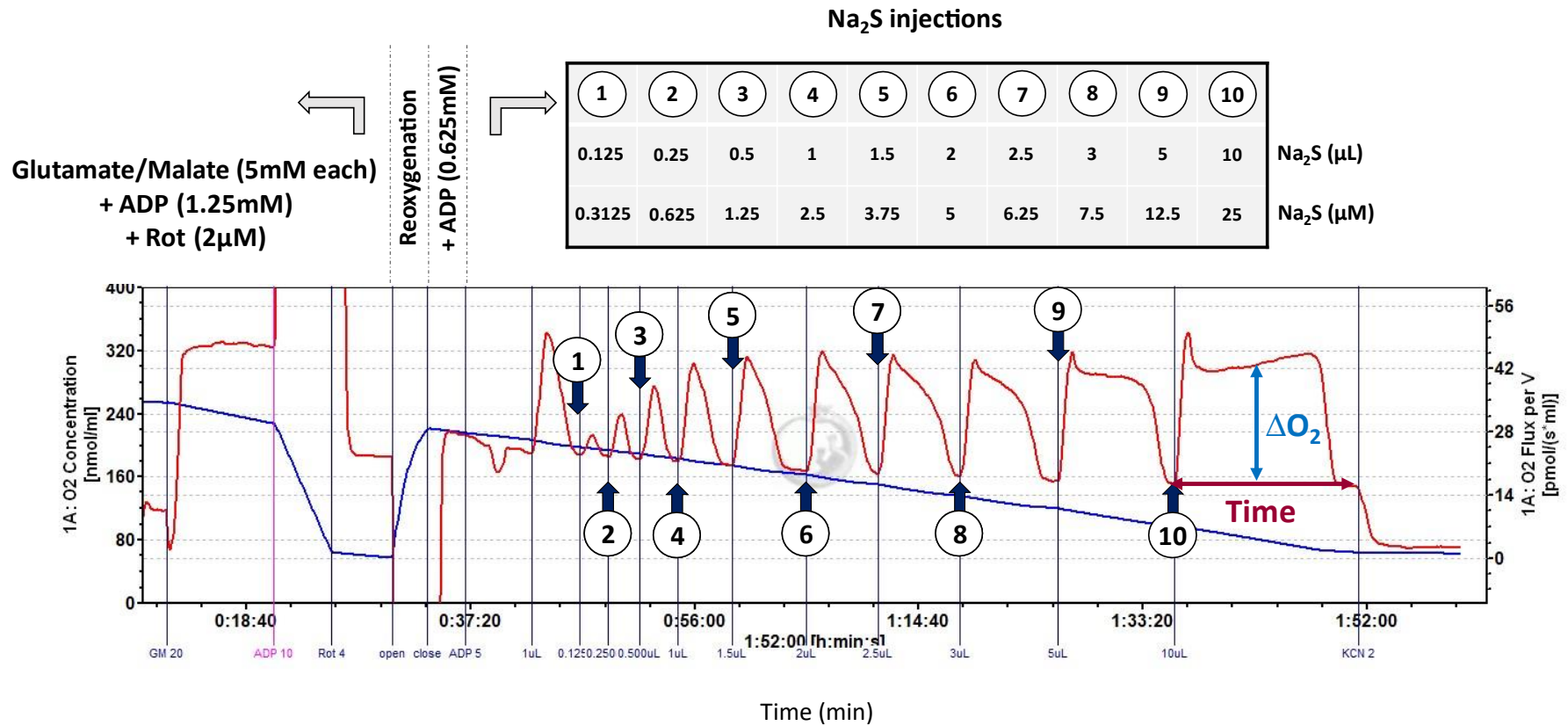


**Figure 38: Protocol to assess H<sub>2</sub>S oxidation capacity in isolated mitochondria**

Oxygen consumption ( $JO_2$ ) was measured using isolated mouse liver mitochondria (2mg of proteins) in the presence of sequential injections of Na<sub>2</sub>S. The quantification of  $JO_2$  associated to H<sub>2</sub>S oxidation started after injecting Na<sub>2</sub>S into the chamber. For each Na<sub>2</sub>S injection,  $JO_2$  increased with time, reached a transient maximal value, and then returned back to the previous basal  $JO_2$  once Na<sub>2</sub>S was totally oxidized. Sulfide oxidation rate was calculated as the difference in the  $JO_2$  rate after and before Na<sub>2</sub>S injection (represented in the graph by  $\Delta O_2$ ) and expressed per mg of protein. The correspondence between Na<sub>2</sub>S volume and Na<sub>2</sub>S concentration is indicated.

O<sub>2</sub> concentration is represented by the blue line (left axis (nmol/mL) and O<sub>2</sub> consumption is represented by the red line (right axis (pmol/s.mL)). **Rot**: rotenone; **Na<sub>2</sub>S**: sodium sulfide

## 9. Lipidomics analysis

To further performed fluoxomics using deuterated water ( $^2\text{H}_2\text{O}$ ,) animals were also injected with a solution of 38  $\mu\text{L/g}$  body weight of  $^2\text{H}_2\text{O}$  and 0.9% w/v NaCl 16h before being sacrificed. At the same time, these animals received a 5% v/v  $^2\text{H}_2\text{O}$  solution in their drinking water. TG and DAG species from liver tissue were extracted with a modified Folch method [750]. Briefly,  $\sim 25$  mg of liver tissues were homogenized with a tissue-lyser (2 cycles of 1 min at 25 Hz), and lipid species were extracted with 600  $\mu\text{l}$  of chloroform:methanol (3:1) and 100  $\mu\text{l}$  of  $\text{H}_2\text{O}$ , with the addition of internal standards. Lipid classes were separated with UHPLC (1290 Infinity, Agilent, Santa Clara, CA) equipped with ZORBAX Eclipse Plus C18 2.1  $\times$  100 mm 1.8  $\mu\text{m}$  column. Deuterium enrichment in the different lipid classes was measured with mass spectrometry (6540 QTOF, Agilent, Santa Clara, CA).

The analyses of *de novo* lipogenesis were done in collaboration with Dr. Amalia Gastaldelli and Sara Guerra from the Consiglio Nazionale delle Ricerche (Pisa, Italy).

## 10. Fecal microbiota analysis

After sacrifice, the feces were collected from the proximal and distal colon and kept at  $-80^\circ\text{C}$  until further use. The composition of mouse gut microbiota was determined according to the method described in Chassaing *et al.* 2015 [77]. Total RNAs were extracted from mouse feces using miRCUCY RNA Isolation- cell and plants kit (Exiqon) following the manufacturer's instructions with some modifications. Briefly, 100 mg of mouse feces were homogenized in 1 mL of sterile PBS, spun down at 300 g for 10 min. After centrifugation at 2000 g for 15 min, the supernatant was filtered through a 0.8  $\mu\text{m}$  filter (Millipore). Lysis buffer containing RNA Spike-In (UniSp2, UniSp4, and UniSp5) was added to fecal supernatant and followed by RNA isolation according to manufacturer's instruction (Exiqon). 16S rRNA gene amplification and sequencing were done using the Illumina MiSeq technology following the protocol of Earth Microbiome Project with their modifications to the MOBIO PowerSoil DNA Isolation Kit procedure for extracting DNA. The sequences were demultiplexed, qualitatively filtered using Quantitative Insights Into Microbial Ecology (QIIME, version 1.8.0) software package 39, and forward and reverse Illumina reads were joined using the fastq-join method.

The analyses of fecal microbiota composition were done in collaboration with Dr. Benoit Chassaing from Institut Cochin (Paris, France).

## 11. Primary cultures of mouse hepatocytes

Hepatocytes were isolated from the liver of mice (post-prandial state) by a modification of the collagenase method. Briefly, the liver was perfused with Hank's balanced salt solution (HBSS, KCl, 5.4 mM;  $\text{KH}_2\text{PO}_4$ , 0.45 mM; NaCl, 138 mM;  $\text{NaHCO}_3$ , 4.2 mM;  $\text{Na}_2\text{HPO}_4$ , 0.34 mM; glucose, 5.5 mM; HEPES, 1 M; EGTA, 50 mM;  $\text{CaCl}_2$ , 50 mM; pH 7.4) and washed at a rate of 5 mL/min using the portal vein. Afterwards, a solution of collagenase (4  $\mu\text{g}/\mu\text{L}$ ) was added. Cell viability was assessed by the trypan blue exclusion test, which was always higher than 60%. Hepatocytes were seeded in type I collagen pre-coated dishes (4  $\mu\text{g}/\mu\text{L}$  in 20 M acetic acid) at a density of  $1.5 \times 10^6$  cells/dish (in 60mm Petri dishes) in medium M199 (Invitrogen) supplemented with 2.5% v/v Nu serum, 10  $\mu\text{g}/\text{mL}$  of streptomycin, 100 units/mL of penicillin, 0.1% v/v ciprofloxacin, 1% v/v bovine serum albumin, 100 nM dexamethasone (Soludecadron, Merck Sharp), and 10 nM insulin (Actrapid, NovoNordisk). After cell attachment (3h), the medium was replaced by fresh M199 medium with different stimuli, namely 5 mM glucose  $\pm$  100 nM insulin, 25 mM insulin  $\pm$  100 nM insulin, 10  $\mu\text{M}$  forskolin, 10 nM glucagon, 100  $\mu\text{M}$  dibutyryl cyclic AMP (Bt2-cAMP), 300  $\mu\text{M}$  palmitic acid:oleic acid (1:2) or 600  $\mu\text{M}$  palmitic acid:oleic acid (1:2). The cells were kept in the new media for 24h after which they were collected for protein extraction.

For the *in vitro* experiments with adenovirus were also used mouse hepatocytes. These cells were isolated and cultured as previously described. After cell attachment (3h), the medium was replaced by fresh medium with 4 i.p./cell of adv.GFP or adv.SQR. After 24h, the medium was renewed by fresh M199 medium with different stimuli, namely 5 mM glucose  $\pm$  100 nM insulin or 25 mM insulin  $\pm$  100 nM insulin. After 24h, the medium was changed and 10% (v/v)  $^{13}\text{C}$ -glucose was added to each dish. The cells were kept in the new media for 24h after which they were collected for fluxomics.

## 12. Analysis of mRNA Expression by Real-time Quantitative PCR

Total RNA was extracted using Ribozol™ reagent (VWR International), according to the manufacturer's instructions. Total RNA was then quantified using a Qubit™ 2.0 fluorometer (Invitrogen). Total RNA was converted into cDNA using NZY Reverse Transcriptase (NZYTech, Lisbon, Portugal), according to the manufacturer's instructions. Quantitative real-time PCR (qRT-PCR) analyses were performed using the QuantStudio™ 7 Flex Real-Time PCR System (Applied Biosystems®). The expression levels of the genes of interest relative to the housekeeping gene hypoxanthine-guanine phosphoribosyl transferase (HPRT) were calculated using the relative standard curve method. Primer sequences are presented in **Table 4**.

	Gene		Sequence	Length (pb)
<b>Biosynthesis</b>	<b>CBS</b>	Sense	GATTTGATCCCCGAGTCC	118
		Antisense	TCATCGTAGTGTGCCAAAGG	
	<b>CSE</b>	Sense	ACAAGAGCCTGAGCAATGGA	106
		Antisense	GCTGTATTCAAACCCGAGGAC	
	<b>MPST</b>	Sense	CCGAGATGGCATCGAACCT	111
		Antisense	AACAGGCGTTTGATCTCCTC	
<b>Oxidation</b>	<b>SQR</b>	Sense	GAACCCAGTGAGAGGCACTT	111
		Antisense	CACTCCGGATGGAATCACAC	
	<b>ETHE1</b>	Sense	TGATTCCATCCGCTTTGGAC	91
		Antisense	CTGGTCGTTCAGGACAAAGG	
	<b>TST</b>	Sense	CAAAGAGTACCAGGAGCGAC	123
		Antisense	CCCACATAGTCCCAAAGTG	
	<b>SUOX</b>	Sense	CCCACACACCTATCGCTTAC	102
		Antisense	ACAGTGACCTCATGTTTGGG	

**Table 4: Primers used for Real-time Quantitative PCR**

The primers listed herein were designed using the Primer-BLAST software. These sequences were specifically designed to detect the mouse genes.

**CBS:** cystathionine  $\beta$ -synthase; **CSE:** cystathionine  $\gamma$ -lyase; **MPST:** 3-mercaptopyruvate sulfurtransferase; **SQR:** sulfide quinone oxidoreductase; **ETHE1:** ethylmalonic encephalopathy protein 1; **TST:** thiosulfate sulfurtransferase; **SUOX:** sulfite oxidase



This part of the project was conducted during a 3 month-long secondment at the laboratory of Professor Cecília Rodrigues (Faculty of Pharmacy – University of Lisbon, Lisbon, Portugal).

### **13. Western blots**

Proteins (20 µg/well) were subjected to SDS-PAGE separation in a 10% v/v or a Criterion TGX Stain-Free Pre Cast gradient 4-20% v/v polyacrylamide gel (Bio-Rad, California, USA), and transferred onto nitrocellulose membranes. REVERT™ 700 Total Protein Staining and protein immunodetection were performed using LI-COR Odyssey 9120 Imaging System for signal detection (LI-COR Biosciences, Lincoln, NE). After quantification of total protein staining, membranes were blocked in 5% (w/v) non-fat dry milk in Tris-buffered saline (TBS). The informations pertaining the primary antibodies used in this study are summarized in **Table 5**. For secondary antibodies, IRDye 680 goat anti-rabbit and IRDye 680 goat anti-mouse secondary antibodies (LI-COR Biosciences) were used in 5% (w/v) non-fat dry milk in TBS with 0.1% (v/v) Tween-20. Proteins were quantified using the Image studio software (Li-COR Biosciences). The fluorescence of each antibody was normalized by division with the total quantification of the REVERT signal.

### **14. Electron microscopy**

Electron microscopy was performed as described in Zischka *et al.* 2008 [751]. Briefly, 80 µg of isolated mitochondrial proteins were immediately pelleted, fixed in 2.5% (v/v) glutaraldehyde, postfixed with 1% (v/v) osmium tetroxide, dehydrated with ethanol, and embedded in Epon. Ultrathin sections were negative stained with uranyl acetate and lead citrate, and then analysed on a Zeiss EM 10 CR electron microscope. The electron micrographs were obtained as part of a collaboration with the laboratory of Dr. Hans Zischka from the Helmholtz Institute (Munich, Germany), where another 3 month-long secondment was completed.

### **15. Statistical analysis**

Results were expressed as means ± S.E.M. Statistical analyses were performed using GraphPad Prism (GraphPad Software, San Diego, CA, USA). Inter-group differences between two groups were assessed by Mann-Whitney test and were considered significant when  $p < 0.05$ .

Antibody	Concentration	Molecular weight (kDa)	Reference	Company
<i>SQR</i>	1:500	50	NBP1-84510	Novus Biologicals, Colorado, USA
<i>SUOX</i>	1:1000	60	NBP1-32423	Novus Biologicals
<i>ETHE1</i>	1:500	28	ab135589	Abcam, Cambridge, UK
<i>TST</i>	1:250	33	ab155320	Abcam
<i>CBS</i>	1:250	60	ab135626	Abcam
<i>CSE</i>	1:500	45	ab151769	Abcam
<i>MPST</i>	1:250	33	HPA001240	Atlas Antibodies, Bromma, Sweden
<i>MitoProfile Total OXPHOS</i>	1:250	CI: 20 CII: 30 CIII: 48 CIV: 40 CV: 55	ab110413	Abcam
<i>SOD1</i>	1:500	25	HPA001401	Atlas Antibodies
<i>SOD2</i>	1:500	25	HPA001814	Atlas Antibodies
<i>ATF4</i>	1:1000	49	11815	Cell Signalling Technology, Massachusetts, USA
<i>BiP</i>	1:1000	78	3183	Cell Signalling Technology
<i>Phospho-SAPK/JNK</i>	1:500	46, 54	4668	Cell Signalling Technology
<i>JNK</i>	1:500	46, 54	9258	Cell Signalling Technology
<i>CHOP</i>	1:1000	27	5554	Cell Signalling Technology
<i>Phospho-eIF2<math>\alpha</math></i>	1:1000	38	9721	Cell Signalling Technology
<i>eIF2</i>	1:1000	38	9722	Cell Signalling Technology
<i>pGSK3<math>\beta</math></i>	1:250	46	93365	Cell Signalling Technology
<i>GSK3<math>\beta</math></i>	1:250	46	9315	Cell Signalling Technology
<i>Phospho-IRE1</i>	1:500	110	ab124945	Abcam
<i>IRE<math>\alpha</math></i>	1:500	110	3294	Cell Signalling Technology
<i><math>\alpha</math>SMA</i>	1:500	40-45	ab7817	Abcam
<i>Phospho-Akt (Ser473)</i>	1:1000	60	4070	Cell Signalling Technology
<i>Akt</i>	1:1000	60	92725	Cell Signalling Technology
<i>FAS</i>	1:500	273	3180	Cell Signalling Technology
<i>ACC</i>	1:500	280	3662	Cell Signalling Technology
<i>AMPK</i>	1:500	62	2532	Cell Signalling Technology
<i>PEPCK1</i>	1:200	69	AP8093b	Abcepta, California, USA
<i>P70S6</i>	1:500	70, 85	9202	Cell Signalling Technology
<i>PC</i>	1:1000	130	-	Kind gift from Dr. Marc Foretz
<i>PRDX3</i>	1:10000	28	-	Kind gift from Prof. Bernard Knoops
<i>PPAR<math>\alpha</math></i>	1:1000	52	-	Kind gift from Dr. Chantal Dedouets

**Table 5: Primary antibodies used for Western blot**

## ***III. Results***

---



**Chapter 1:**  
**Mitochondrial H<sub>2</sub>S oxidation in**  
**liver physiology**



## **Problematic**

Although the enzymes responsible for H<sub>2</sub>S production and oxidation are expressed ubiquitously throughout the mammalian body, tissue-specific rates of H<sub>2</sub>S production and, especially, mitochondrial H<sub>2</sub>S oxidation are still up for debate. The balance between H<sub>2</sub>S production and clearance determines the tissue steady-state levels of H<sub>2</sub>S. More importantly, the regulation of either one of these processes, or both, represents a mechanism for modulating intracellular H<sub>2</sub>S levels. Some studies suggest that the rates of H<sub>2</sub>S production are directly correlated to the tissue levels of cysteine and homocysteine [146, 300, 752, 753]. However, since mammalian mitochondrial H<sub>2</sub>S oxidation is a fairly new process [159], tissue characterization of this pathway is still unknown. Almost all studies directed towards the investigation of this pathway were conducted in rodent and human cell lines or in isolated liver mitochondria from rat, human or pork [187]. Only one study has presented some preliminary data comparing mitochondrial H<sub>2</sub>S oxidation rates between the different tissues of the same animal (brain<liver<heart<kidney) [187]. Here, in order to have a larger picture on mammalian H<sub>2</sub>S metabolism, similar experiments were performed using mouse liver, kidney and brain to investigate mitochondrial H<sub>2</sub>S oxidation rates but also the protein expression level of enzymes involved in H<sub>2</sub>S oxidation and biosynthesis.

Secondly, considering the implications of H<sub>2</sub>S in the context of liver physiology, several studies have shown that H<sub>2</sub>S is involved in the regulation of many hepatic functions essential for its identity [658, 668, 679]. However, most of these studies, if not all, assess the importance of liver H<sub>2</sub>S metabolism through the modulation of its biosynthesis or by using H<sub>2</sub>S donors, completely bypassing the pathway of mitochondrial H<sub>2</sub>S oxidation. Since intracellular levels of H<sub>2</sub>S are determined by the rates of both production and oxidation, our working hypothesis is that changes in this pathway and/or in SQR activity may also influence the levels of H<sub>2</sub>S and, by extension, its effects on cell signalling networks. Therefore, in this study, we further assessed i) whether or not the nutritional status of the organism (fed state, fasting, refeeding) modulates the pathway of liver mitochondrial H<sub>2</sub>S oxidation, and ii) the physiological and metabolic consequences of overexpressing SQR in mouse liver.

## **Results**

Over the years, several studies have demonstrated that H<sub>2</sub>S plays a regulatory role in liver glucose metabolism with H<sub>2</sub>S promoting gluconeogenesis and inhibiting glucose utilisation. Our present results bring novel insights into liver H<sub>2</sub>S metabolism. First, they clearly demonstrated that

SQR is the key regulatory enzyme of liver mitochondrial H<sub>2</sub>S oxidation. Second, this pathway as well as SQR protein expression are negatively and positively regulated by fasting (characterized by increased gluconeogenesis) and refeeding (characterized by increased glucose utilisation), respectively. Third, in vivo liver overexpression of mitochondrial SQR, which increased hepatic H<sub>2</sub>S oxidation by 500%, increased glucose tolerance and liver insulin signalling, had no impact on pyruvate tolerance, and decreased liver fatty acid oxidation capacity. Fourth, in vitro studies using primary cultures of mouse hepatocytes and [U-13C]glucose revealed that SQR overexpression increases insulin-stimulated glucose utilisation at physiological glucose concentration.

## **Conclusions**

This study clearly demonstrated that SQR is the key regulatory enzyme of liver mitochondrial H<sub>2</sub>S oxidation. Changes in SQR protein expression also affect the protein expression of key enzymes involved in H<sub>2</sub>S biosynthesis, suggesting a coordinated regulation of these two pathways. Hepatic mitochondrial H<sub>2</sub>S oxidation is not only regulated by the nutritional status of the liver; it also directly impacts liver glucose homeostasis. This novel observation indicates that not only H<sub>2</sub>S biosynthesis but also mitochondrial H<sub>2</sub>S oxidation plays an important role in liver physiology. This represents a specific and previously ignored bioenergetic mechanism with consequences on glucose sensing and a potential target against the development of hepatic insulin resistance. In the future, further studies are required to better understand the underlying molecular mechanisms, and to reconsider whether the metabolic effects induced by modulating H<sub>2</sub>S biosynthesis could be due, at least partially, to changes in mitochondrial H<sub>2</sub>S oxidation.



## Original paper

ORIGINAL RESEARCH COMMUNICATIONS

### **Hepatic Hydrogen Sulfide Oxidation via Mitochondrial Sulfide Quinone Reductase Impacts Liver Glucose Metabolism**

Inês Mateus<sup>1</sup>, Sara Guerra<sup>2,3#</sup>, Véronique Lenoir<sup>1#</sup>, Fabrizia Carli<sup>2</sup>, Renaud Dentin<sup>1</sup>, Frédéric Bouillaud<sup>1</sup>, Amalia Gastaldelli<sup>2,3</sup> and Carina Prip-Buus<sup>1\*</sup>

<sup>1</sup> Université de Paris, Institut Cochin, INSERM, CNRS, 75014 Paris, France

<sup>2</sup> Cardiometabolic Risk Unit, Institute of Clinical Physiology, CNR, Pisa, Italy

<sup>3</sup> Institute of Life Sciences, Sant'Anna School of Advanced Studies, Pisa, Italy

# These authors contributed equally

\*Correspondence: Carina Prip-Buus, Institut Cochin, INSERM U1016, CNRS UMR 8104, Department of Endocrinology, Metabolism and Diabetes, 24 Rue du Faubourg Saint-Jacques, 75014, Paris, France ; Telephone number: +33153732704; Email: carina.prip-buus@inserm.fr.

**Running title:** Sulfide Oxidation Modulates Liver Metabolism

Number of words for abstract: 247

Work count: 4165 (except Legends, Methods and References)

Number of references: 53

Number of greyscale illustrations: 4

Number of coloured illustrations: 2

**Manuscript keywords:** Hydrogen sulfide; Mitochondria; Liver; Glucose metabolism; Homeostasis

## **Abstract**

**Aims:** To investigate the regulation of mouse liver mitochondrial hydrogen sulfide (H<sub>2</sub>S) oxidation under physiological conditions and its relevance in liver metabolism.

**Results:** We first showed that, by contrast to mouse brain mitochondria, mouse liver, and even more kidney, mitochondria efficiently oxidized H<sub>2</sub>S and expressed all enzymes involved in this pathway, including the mitochondrial sulfide quinone reductase (SQR). Interestingly, the nutritional status of the mouse tightly regulated liver mitochondrial H<sub>2</sub>S oxidation capacity and SQR protein expression, both being downregulated by a 24 h-fast while overnight refeeding after fasting totally abolished the fasting inhibitory effect. Moreover, adenovirus-mediated SQR overexpression in mouse liver clearly demonstrated that SQR is the key regulatory enzyme of hepatic mitochondrial H<sub>2</sub>S oxidation, allowing this pathway to no longer be under nutritional regulation. Liver SQR overexpressing mice had higher glucose tolerance, no change in pyruvate tolerance, lower insulinemia, decreased liver glycogen content and enhanced liver insulin signalling at the level of the Akt/GSK3 $\beta$  pathway. By using [<sup>14</sup>C]- and [<sup>13</sup>C]-labelled substrates, we further showed that liver SQR overexpression decreased liver fatty acid, but not glucose, oxidation fluxes, and increased in primary mouse hepatocyte cultures insulin-stimulated glucose metabolism at physiological glucose concentration.

**Innovation:** This study provides the first proof of concept that a direct modulation of liver mitochondrial H<sub>2</sub>S oxidation, through SQR overexpression, plays a pivotal role in regulating hepatic insulin signalling and glucose metabolism.

**Conclusion:** This study highlights that liver mitochondrial SQR-mediated H<sub>2</sub>S oxidation may represent a potential strategy to prevent and/or correct hepatic insulin resistance.

## Introduction

For a long time, hydrogen sulfide ( $H_2S$ ), a colourless and water-soluble gas with the characteristic smell of rotten eggs, was considered only as a toxin and an environmental pollutant inhibiting mitochondrial respiration at the level of cytochrome c oxidase [1].  $H_2S$  is now recognized as the third mammalian gasotransmitter besides nitric oxide (NO) and carbon monoxide (CO), playing an important role in inflammation, septic shock, ischemia reperfusion events, cardiovascular disease, and more recently liver pathophysiology [2, 3]. In contrast with NO and CO,  $H_2S$  at low concentrations (1-10  $\mu M$ ), lower than its toxic level, is an inorganic substrate for mammalian mitochondrial respiration through its oxidation by a mitochondrial Sulfide Quinone Reductase (SQR) [4, 5]. SQR is the first enzyme of the sulfide oxidizing unit (SOU), which also includes a dioxygenase (ETHE1) and a thiosulfate sulfurtransferase (TST). Together with sulfite oxidase (SUOX), they conduct the transformation of  $H_2S$  into sulfite, thiosulfate and sulfate, respectively [6]. In mammals, historically, the colon was the first main site considered for mitochondrial  $H_2S$  oxidation as this organ is particularly exposed to high  $H_2S$  levels arising from bacterial anaerobic sulfur metabolism [7, 8]. However, other tissues, such as the liver and the kidney, also exhibit the ability to oxidize  $H_2S$  [9, 10], the liver capacity being species-dependent with human liver mitochondria showing the highest oxidation rates [11, 12]. In fact, the presence of the SQR in many different cell types/organs of the mammalian organism suggests that the need to oxidize  $H_2S$  is not restricted to the gastrointestinal tract and that the spontaneous  $H_2S$  release by tissues has to be checked either to avoid toxic accumulation and/or to control  $H_2S$  signalling [4, 13].

Liver metabolism, which is finely regulated by hormones and nutrients, is central to energy homeostasis, and liver metabolic inflexibility is known to be associated with several metabolic diseases. The impact of  $H_2S$  on mitochondrial energy metabolism crucially depends on its bioavailability. Due to its location and function, the liver is exposed to different sources of  $H_2S$ .

First, H<sub>2</sub>S originated from the microbiota may escape the gut barrier and reach the liver through the portal vein [14, 15]. Indeed, compared to conventional mice, plasma free H<sub>2</sub>S level was decreased by 50-80% in germ-free mice, likely leading to reduced tissue bioavailability [16]. Second, H<sub>2</sub>S is a by-product generated by the transsulfuration pathway (metabolism of sulfur-containing amino acids) involving the cystathionine β-synthase (CBS), the cystathionine γ-lyase (CSE) and the 3-mercaptopyruvate sulfurtransferase (MPST) [17]. In the liver, H<sub>2</sub>S production is largely catalysed by CSE and, to a lesser degree, by CBS [18], and genetic deletion of CSE in mice markedly reduced liver H<sub>2</sub>S production [19, 20]. Over the past few decades, H<sub>2</sub>S emerged as a key regulator of many hepatic functions, including glucose and lipid metabolism [19, 21-23], mitochondrial function [23], oxidative stress [24], and cellular differentiation [25]. Importantly, a balanced and functionally intact CSE/H<sub>2</sub>S system has been reported to be important for adaptive liver energy metabolism. Indeed, exogenous H<sub>2</sub>S donors stimulated hepatic glucose production (gluconeogenesis) and down-regulated hepatic glucose uptake and glycogen storage [26]. Conversely, CSE knockout (CSE KO) mice had a reduced rate of gluconeogenesis, increased hepatic glucose consumption and a higher liver glycogen content [19]. All these studies exploring the physiological relevance of H<sub>2</sub>S in liver metabolism were focused on hepatic H<sub>2</sub>S biosynthesis pathway and/or used exogenous H<sub>2</sub>S donors. Whether hepatic mitochondrial H<sub>2</sub>S oxidation, in which SQR plays a crucial role [13], could also play an important role in liver metabolism remains totally unknown.

In this study, we first examined the capacity of mouse liver, kidney and brain mitochondria to oxidize H<sub>2</sub>S together with the protein expression levels of key enzymes involved in H<sub>2</sub>S mitochondrial oxidation and biosynthesis. We next investigated whether liver mitochondrial H<sub>2</sub>S oxidation is under nutritional regulation, and finally explored the physiological and metabolic consequences of overexpressing SQR in mouse liver and cultured mouse hepatocytes.

## Results

### *Mouse liver and kidney, but not brain, mitochondria efficiently oxidize H<sub>2</sub>S*

In the presence of low H<sub>2</sub>S concentrations, mitochondrial H<sub>2</sub>S oxidation occurs resulting in increased mitochondrial oxygen consumption, whereas high H<sub>2</sub>S concentrations inhibit mitochondrial respiration [1, 12]. Therefore, we used oxygraphy to study the capacity of mouse liver, kidney and brain mitochondria to oxidize increasing concentrations of an H<sub>2</sub>S salt (Na<sub>2</sub>S) (Fig. 1A). Results were plotted using the real values of oxygen consumption (Fig. 1B) or normalized as % of state 3 respiration rate (Fig. 1C) in order to consider possible variations in the respiration capacity of the mitochondria. Indeed, mouse liver, kidney and brain mitochondria showed differences in their respiratory mitochondrial capacity depending on the substrate used (Supplementary Fig. S1). Liver mitochondria had higher respiration rates (Supplementary Fig. S1A) and RCR (Supplementary Fig. S1C) in the presence of glutamate/malate while kidney mitochondria exhibited the highest preference for succinate (Supplementary Fig. S1B) and protein levels of OXPHOS Complexes (Supplementary Fig. S1D). Nevertheless, even when expressing mitochondrial H<sub>2</sub>S oxidation as % of state 3 respiration rate, liver and kidney mitochondria exhibited much higher H<sub>2</sub>S oxidative capacity (1.62-6.00% and 2.82-11.43% of state 3 respiration rate, respectively) than brain mitochondria (0.26-0.93% of state 3 respiration rate), kidney mitochondria showing the highest capacity (Fig. 1C). In agreement with previous studies [4], brain mitochondria displayed a very low capacity for H<sub>2</sub>S oxidation as this pathway became already saturated with 3.75 μM of Na<sub>2</sub>S, and oxygen consumption was inhibited in the presence of 7.5 μM of Na<sub>2</sub>S (Fig. 1B and Fig. 1C).

### *Liver, kidney and brain protein levels of enzymes involved in mitochondrial H<sub>2</sub>S oxidation and biosynthesis*

Mitochondrial H<sub>2</sub>S oxidation involves first the reaction catalysed by SQR, with the resulting persulfide undergoing a series of modification steps conducted by ETHE1, TST and SUOX (Fig. 2A). We thus assessed the protein expression level of these enzymes in mouse liver, kidney and brain

lysates. Compared to liver, kidney presented higher protein levels of SQR (+326%) and ETHE1 (+273%) but lower TST (-89%) and SUOX (-57%) protein levels (Fig. 2B and 2C). According to our previous observation showing higher kidney capacity for mitochondrial H<sub>2</sub>S oxidation rates (Fig. 1B and 1C), these results suggest that, among the SOU enzymes, SQR and ETHE1 may dictate the rate of this pathway. Interestingly, these two proteins could barely, if not, be detected by immunoblotting in the brain samples (Fig. 2B, Supplementary Fig. S3). Moreover, brain TST and SUOX protein levels represented only 8% and 4% of the corresponding liver protein level (Fig. 2B and 2C).

Conversely, H<sub>2</sub>S is a by-product of the desulfhydration of the amino acids cysteine and homocysteine conducted by CSE, CBS and MPST (Fig. 2A). Among the three tissues, immunoblotting experiments showed that the brain expressed the lowest protein levels of CBS and MPST, with no visible detection of the CSE protein. The MPST antibody has highlighted two bands of approximately the same size (33kDa) (Fig. 2B), which may correspond to the two splice variants of MPST that differ by 20 amino acids at the N terminus [28]. Kidney had lower protein levels of CBS (-47%), CSE (-28%) and MPST (-59%) when compared to liver (Fig. 2B and 2C), suggesting a higher liver capacity for H<sub>2</sub>S biosynthesis.

#### *Liver mitochondrial H<sub>2</sub>S oxidation is under nutritional regulation*

We next investigated whether mouse liver mitochondrial H<sub>2</sub>S oxidation could be subjected to nutritional regulation. Fig. 3A clearly showed that a 24 h-fasting period markedly decreased hepatic mitochondrial H<sub>2</sub>S oxidation capacity whereas overnight refeeding, after the fasting period, fully restored similar H<sub>2</sub>S oxidative rates than those measured in fed mouse liver mitochondria. Such nutritional regulation was not associated with parallel changes in liver mitochondrial respiratory capacity as fasting/refeeding had only a minor impact on mitochondrial respiratory rates, RCR and protein levels of OXPHOS Complexes (Supplementary Fig. S2A-S2D).

Interestingly, the nutritional regulation of mitochondrial H<sub>2</sub>S oxidation was associated with similar changes in liver SQR protein expression, with fasting decreasing by 50% SQR protein levels and refeeding abrogating the fasting inhibitory effect (Fig. 3B and 3C). In contrast to SQR, ETHE1 remained unaffected by the nutritional challenge whereas fasting significantly increased by 20% both TST and SUOX protein expression levels. Refeeding totally or partially counteracted the fasting effects on TST and SUOX protein levels (Fig. 3B and 3C). These results strongly suggest that SQR may be the key regulatory enzyme of liver mitochondrial H<sub>2</sub>S oxidation.

Liver H<sub>2</sub>S biosynthesis was also affected by the nutritional challenge. Indeed, a 24 h-fast respectively decreased by 32% and 34% the protein levels of CBS and MPST (Fig. 3B and 3C). Refeeding abrogated the fasting-induced inhibition only for CBS expression (Fig. 3B and 3C). Lastly, whereas CSE protein level remained unchanged by fasting, refeeding significantly decreased its protein expression by 24% when compared to fed mice (Fig. 3B and 3C).

#### *Liver SQR overexpression increases mitochondrial H<sub>2</sub>S oxidation capacity and abrogates the fasting/refeeding regulation*

As both liver mitochondrial H<sub>2</sub>S oxidation and SQR protein levels were similarly regulated by nutritional challenge, adenovirus-mediated SQR overexpression in mouse liver was performed to further investigate its physiological relevance. Four weeks after Adv-GFP and Adv-SQR injections in mice, immunoblot analysis showed specific overexpression of SQR in the mouse liver, but not in other tissues such as kidney, heart, brain, adipose tissue and skeletal muscle (Supplementary Fig. S3). Whatever the substrate used, liver SQR overexpression did not change the hepatic mitochondrial respiratory capacity of fed, fasted or refed mice, only RCR being slightly increased in the presence of succinate in the fed state (Supplementary Fig. S4). For Na<sub>2</sub>S concentrations above 3.75 μM, liver mitochondria isolated from fed Adv.SQR mice (54.6-245.9 pmol O<sub>2</sub>/s.mg) had a higher capacity to oxidize H<sub>2</sub>S than those isolated from the fed Adv.GFP mice

(47.0-68.7 pmol O<sub>2</sub>/s.mg) (Fig. 4A). Furthermore, the fasting/refeeding regulation of liver mitochondrial H<sub>2</sub>S oxidation was again observed in Adv-GFP mice but was totally abrogated following liver SQR overexpression (Fig. 4A). Importantly, by contrast to Adv.GFP liver mitochondria and whatever the nutritional condition considered, no saturation for mitochondrial H<sub>2</sub>S oxidation could be observed in Adv-SQR mice, even at 25 μM of Na<sub>2</sub>S. Moreover, the time necessary to consume this high Na<sub>2</sub>S concentration was twice as fast in Adv.SQR liver mitochondria compared to Adv.GFP liver mitochondria (217 ± 18 versus 432 ± 45 seconds, *p*<0.01). These results clearly show that hepatic SQR overexpression allowed liver mitochondria to cope with much higher H<sub>2</sub>S concentrations in a shorter period of time.

We next investigated whether liver SQR overexpression could impact the liver protein expression of H<sub>2</sub>S oxidation-related proteins ETHE1, SUOX and TST. In the fed Adv-SQR mice, liver ETHE1 (+17%) and SUOX (+15%), but not TST, protein levels were significantly increased when compared to fed Adv-GFP mice (Fig. 4B and 4C). In the fasting and refeeding conditions, only TST protein levels were significantly affected by SQR overexpression, with fasted and refed Adv.SQR mice having a respective 38% and 37% lower hepatic TST protein level when compared to fasted Adv.GFP mice (Fig. 4B and 4C).

Concerning the H<sub>2</sub>S production-related enzymes, liver SQR overexpression significantly decreased the protein levels of CBS (-13%), CSE (-21%) and MPST (-10%) in fed Adv-SQR mice compared to fed Adv-GFP mice (Fig. 4B and 4C). In the fasting and refeeding conditions, only liver CSE protein levels remained 29% lower in refed Adv-SQR mice compared to refed Adv-GFP mice (Fig. 4B and 4C). These results underline that, at least in fed mice, liver SQR overexpression not only increased hepatic mitochondrial H<sub>2</sub>S oxidation capacity but could also decrease liver H<sub>2</sub>S biosynthesis capacity.

*Liver SQR overexpression impacts mouse phenotype*



When fed standard chow for 4 weeks after adenovirus injections, Adv.GFP and Adv.SQR mice exhibited similar body weight, adiposity, muscle/body weight ratio, plasma triglycerides (TG), and postprandial glycemia (Table 1). However, compared to Adv-GFP mice, Adv.SQR mice displayed increased fasting glycemia, lower insulinemia in the postprandial state, and higher plasma total and HDL cholesterol (Table 1). Additionally, whereas liver histological analysis showed no discernible differences between both groups (Fig. 5A), fed Adv.SQR mice had higher liver/body weight ratio (+10%), lower hepatic levels of diacylglycerols (DAG) (-35%) and monoacylglycerols (MAG) (-39%) but similar hepatic TG levels, and decreased liver glycogen content (-28%) (Table 1). Interestingly, compared to Adv-GFP mice, Adv.SQR mice exhibited similar pyruvate tolerance but higher glucose tolerance and insulin sensitivity (Fig. 5B). To determine whether liver SQR overexpression could impact hepatic insulin signalling, we further examined the activation of Akt (phosphorylation at S473, p<sup>S473</sup>) and inactivation of GSK-3 $\beta$  (phosphorylation at S9, p<sup>S9</sup>) in the liver of fed, fasted and refed Adv-GFP and Adv-SQR mice (Fig. 5C and 5C). Compared to fed Adv-GFP mice, hepatic p<sup>S473</sup> Akt (+76%) and p<sup>S9</sup> GSK-3 $\beta$  (+22%) levels as well as the p<sup>S473</sup> Akt/total Akt ratio (+63%) were significantly increased in fed Adv-SQR mice (Fig. 5B and 5C). Moreover, the p<sup>S473</sup> Akt/total Akt ratio (+36%) was also increased in the fasted state whereas the p<sup>S9</sup> GSK-3 $\beta$ /total GSK-3 $\beta$  ratio increased both in fasted (+80%) and refed (+87%) Adv-SQR mice compared to Adv-GFP mice (Fig. 5B and 5C). These results indicate that liver SQR overexpression enhanced hepatic insulin signalling.

#### *Impact of liver SQR overexpression on hepatic metabolism*

To address this question, we first measured *ex-vivo* the rates of liver [U-<sup>14</sup>C]glucose and [1-<sup>14</sup>C]oleate oxidation into [<sup>14</sup>C]CO<sub>2</sub>. Whereas hepatic glucose oxidation remained unchanged by liver SQR overexpression (Fig. 6A), both oleate oxidation (Fig. 6B) and the protein level of carnitine palmitoyltransferase 1 (CPT1) (Fig. 6B), the key regulatory enzyme of mitochondrial long-chain

fatty acid oxidation, were significantly decreased (-16% and -25%, respectively). To further ascertain the role of SQR in liver glucose metabolism, we conducted a semi-quantitative estimate of [U-<sup>13</sup>C<sub>6</sub>]glucose-derived metabolites in primary cultures of mouse hepatocytes overexpressing either GFP or SQR (Fig. 6D). Whereas no significant changes in the metabolic [U-<sup>13</sup>C<sub>6</sub>]glucose routing could be observed in the presence of 5 mM glucose, Adv.SQR hepatocytes cultured in the presence of 5mM glucose + 100nM insulin showed significant increase in the levels of lactate m+3 (+44%), glutamine m+2 (+134%) and glutamate m+2 (+104%) as well a trend for increased alanine m+3 (p=0.571) and aspartate m+2 (p=0.573) (Fig. 6D). Interestingly, these metabolite levels reached values similar to those measured in Adv-GFP hepatocytes cultured in the presence of 25 mM glucose + 100nM insulin (Fig. 6D). These results indicate that liver SQR overexpression increased insulin-stimulated glycolysis and tricarboxylic acid cycle activity at physiological glucose concentrations.

## **Discussion**

Over the past decade, H<sub>2</sub>S emerges as a key regulator of liver glucose metabolism [21]. Balance between liver H<sub>2</sub>S biosynthesis and its mitochondrial oxidation controls the intrahepatic steady-state levels of H<sub>2</sub>S, and hence the signalling effects of this new gasotransmitter. While the hepatic H<sub>2</sub>S/CSE system was reported to be important for mouse liver glucose homeostasis, the relative contribution of liver mitochondrial SQR-mediated H<sub>2</sub>S oxidation has never been addressed. The present study provides the first proof of concept that this pathway also plays a pivotal role in the regulation of hepatic glucose metabolism.

First of all, our study reinforces previous reports [4, 18, 28] showing a high ability of mouse kidney and liver mitochondria to oxidize H<sub>2</sub>S, while brain mitochondria capacity remains extremely low. Importantly, we showed that these significant differences between tissues were associated to similar variations in the protein expression levels of the first two enzymes involved in H<sub>2</sub>S

oxidation, with liver and kidney expressing high SQR and ETHE1 protein levels while these proteins were barely immunodetected in the brain. Moreover, as previously shown [18, 28], liver and kidney expressed higher protein levels of H<sub>2</sub>S-producing enzymes (CSE, CBS and MPST) than brain, suggesting a high rate of H<sub>2</sub>S turn-over in these tissues that allows efficient regulation of H<sub>2</sub>S levels while preventing any toxic effect of H<sub>2</sub>S.

The liver is a highly flexible metabolic tissue characterized by its rapid adaptation to nutritional changes, essential for energy homeostasis. In the fed state, glucose oxidation, glycogen synthesis and lipogenesis are favoured whereas fatty acid oxidation and gluconeogenesis are induced during fasting [28]. Our study highlights novel insights into the crosstalk between H<sub>2</sub>S metabolism and liver physiology. First, we showed that both mouse liver mitochondrial H<sub>2</sub>S oxidation and SQR protein expression are regulated by the fed/fasting and fasting/refeeding transitions. Importantly, this nutritional regulation occurs without any change in the respiratory capacity of liver mitochondria. Second, SQR is the key regulatory enzyme of this pathway; its liver overexpression markedly increases mitochondrial H<sub>2</sub>S oxidation capacity, allowing liver mitochondria to cope with high H<sub>2</sub>S concentrations that otherwise would be detrimental. Third, increasing mitochondrial H<sub>2</sub>S oxidation capacity in mouse liver induces marked changes in liver glucose homeostasis, including improved glucose tolerance, enhanced hepatic insulin signalling and increased insulin-stimulated glucose utilisation at physiological glucose concentration.

As known for liver glucose and lipid metabolism [28], we herein show that liver mitochondrial H<sub>2</sub>S oxidation and SQR expression are also under nutritional regulation. Studies on the nutritional regulation of liver H<sub>2</sub>S metabolism remain up to now scarce and focused on H<sub>2</sub>S production [29]. Hepatic CSE protein expression was found downregulated by fasting [19] but also inhibited by insulin [26] whereas liver CSE and CBS were upregulated by caloric restriction [30]. Although further experiments will be needed to identify the nutritional and/or hormonal factors regulating SQR expression, we also cannot exclude H<sub>2</sub>S *per se* as such a regulatory factor. Indeed,

in mammals, studies performed in rat colonocytes [31] or cell lines [32] have shown that H<sub>2</sub>S exposure upregulated SQR expression. Such a regulation could be an ancestral mechanism conserved through evolution from bacteria to vertebrates [34–39], allowing adaptation to life in H<sub>2</sub>S-rich environments. Thus, conversely, the downregulated liver SQR expression in fasting could result from lower hepatic H<sub>2</sub>S levels [39], as supported by the decreased expression of two enzymes (CBS and MPST) involved in H<sub>2</sub>S production. The physiological relevance of this fasting-mediated regulation of mitochondrial H<sub>2</sub>S oxidation could be linked to the well-known stimulatory effect of H<sub>2</sub>S on hepatic gluconeogenesis. Indeed, H<sub>2</sub>S has been shown to increase by S-sulfhydration the activity of several gluconeogenic enzymes, namely pyruvate carboxylase, glucose 6-phosphatase and phosphoenolpyruvate carboxykinase [41, 42]. Therefore, in line with a lower liver H<sub>2</sub>S production in fasted mice, decreasing H<sub>2</sub>S oxidation could be a protective mechanism to preserve the hepatic level of H<sub>2</sub>S and its mediated stimulation of gluconeogenesis.

In the literature, the consequences of decreasing H<sub>2</sub>S levels in liver metabolism have been investigated through the use of CSE KO animal models. According to several studies, CSE KO mice present a lower rate of gluconeogenesis, a moderate increase in glucose tolerance and higher hepatic glycogen content and glucose uptake [19, 27, 41, 43]. Moreover, hepatocytes isolated from CSE KO mice showed higher glucose consumption, and HepG2 cells treated with NaHS presented diminished insulin signalling [26]. Although we did not measure liver H<sub>2</sub>S levels, our Adv.SQR mice displayed some physiological similarities to CSE KO mice, such as the higher glucose tolerance and enhanced hepatic insulin signalling. In addition to the increased phosphorylation level of liver Akt and GSK-3 $\beta$ , liver SQR overexpression also decreased the hepatic levels of DAGs, known to participate in the development of insulin resistance [43]. Interestingly however, our study reveals noticeable discrepancies between the phenotypes of Adv.SQR and CSE KO mice. Indeed, Adv.SQR mice presented higher liver weight, lower hepatic glycogen content and unchanged *in vivo* gluconeogenesis (as assessed by PTT) when compared to control mice. This

latter observation appears to be counterintuitive to the “pro-gluconeogenesis” role that has been associated to H<sub>2</sub>S. However, whereas SQR was overexpressed only in the liver, CSE KO mice exhibited a global invalidation of the CSE gene leading to other phenotypic traits. Indeed, the kidney also contributes to gluconeogenesis [44], and whether its gluconeogenic capacity might be affected in CSE KO mice remains unknown. Moreover, due to impaired inhibition of  $\beta$ -cell insulin secretion by endogenous pancreatic H<sub>2</sub>S [45], CSE KO mice present higher insulin secretion [20], which might impact liver glucose production independently of its intrinsic gluconeogenic capacity. Nevertheless, the lack of decreased glucose production in Adv.SQR mice is puzzling since these mice displayed enhanced hepatic insulin signalling under fasting conditions, suggesting a higher insulin sensitivity of the liver. Therefore, further experiments are needed to deeply investigate the gluconeogenic capacity of mouse hepatocytes overexpressing SQR. Considering the other phenotypic differences, several hypotheses can be considered. First, regarding the lower liver glycogen content in Adv.SQR mice, we could hypothesize that the glucose demand is so high in the liver that it limits the need to store it as glycogen. Second, the increased liver weight found in Adv.SQR mice could not be explained by higher glycogen storage or higher lipid accumulation. Liver hypertrophy is known to be correlated to portal blood flow and hypoxemia [23]. Furthermore, studies have shown that H<sub>2</sub>S participates in the regulation of liver blood flow and portal blood pressure [24]. Therefore, we cannot exclude that SQR-induced H<sub>2</sub>S oxidation might impact the vasoconstriction of the liver blood vessels and/or the portal vein. Another hypothesis for increased liver weight following SQR overexpression is hepatocyte proliferation. Interestingly, a recent study has demonstrated that enhanced liver insulin signalling was accompanied by a transient induction of S-phase entrance by quiescent hepatocytes, establishing a direct link between insulin sensitivity and mouse hepatocyte proliferation [26].

Due to its location, the liver is likely exposed to two different H<sub>2</sub>S sources: the endogenous generation rate (a property shared with other organs) and the possible H<sub>2</sub>S influx coming from the gut

microbiota delivered by the portal vein. The relative contribution of these distinct sources remains unknown. Nevertheless, liver SQR overexpression would impact both endogenous and exogenous H<sub>2</sub>S while CSE KO would address only the endogenous H<sub>2</sub>S rate, with at least direct consequences related to the transsulfuration pathway. Hence, the existence of phenotype discrepancies between Adv.SQR and CSE KO mice might also indicate specific SQR-mediated H<sub>2</sub>S signalling actions, independently of those mediated by the modulation of H<sub>2</sub>S biosynthesis. In other words, although H<sub>2</sub>S production and oxidation are both important to maintain the steady-state levels of H<sub>2</sub>S, the way by which these pathways control H<sub>2</sub>S actions in a cell may vary. Whereas H<sub>2</sub>S production is known to impact H<sub>2</sub>S ability to modify cysteine residues and regulate protein expression/activity [41, 46], mitochondrial H<sub>2</sub>S oxidation participates in mitochondrial bioenergetics by providing electrons to the respiratory chain while relying on oxygen consumption [12]. Therefore, we cannot exclude that an upregulation of this pathway may decrease oxygen tissue levels. This could impact oxygen sensing as well as the production of ROS and reactive sulfur species (such as persulfides and polysulfides), which have lately gained recognition as powerful cell signalling mediators [47]. Liver H<sub>2</sub>S metabolism may in fact have a greater degree of complexity. Indeed, we showed that liver SQR overexpression not only triggered a cascade of regulation on its downstream enzymes but also decreased the expression of H<sub>2</sub>S-producing enzymes. This intriguing finding reinforces previous studies suggesting the existence of a complex interplay and feedback mechanism(s) between H<sub>2</sub>S production and oxidation [31, 48].

While an increasing number of signalling roles and physiological effects are being attributed to H<sub>2</sub>S, our understanding of the mitochondrial H<sub>2</sub>S oxidation pathway and its consequences on liver energy homeostasis just started to emerge. This study clearly demonstrates the physiological relevance of liver SQR-mediated H<sub>2</sub>S oxidation in hepatic glucose metabolism and insulin signalling, strengthening the interest to further explore this pathway in metabolic diseases. This study also highlights that previous studies unravelling cell perturbations to

dysregulations in H<sub>2</sub>S production have ignored a major player of H<sub>2</sub>S-centered cell regulation. Therefore, assessment of mitochondrial H<sub>2</sub>S oxidation should be considered in the future when investigating H<sub>2</sub>S dysregulation in liver pathology.

## **Innovation**

Alterations in H<sub>2</sub>S levels have been associated to several metabolic pathologies, such as diabetes and NAFLD. However, most studies explore potential dysregulations in H<sub>2</sub>S biosynthesis and completely forsake H<sub>2</sub>S oxidation by mitochondrial SQR. The present study indicates that this pathway is nutritionally regulated and that increased SQR activity promotes liver glucose metabolism and insulin signalling, thus making this pathway a previously unrecognized target for overcoming hepatic insulin resistance. To our best knowledge, this is the first study to find a direct association between mitochondrial H<sub>2</sub>S oxidation and glucose metabolism.

## **Materials and Methods**

### *Animals and nutritional challenges*

Adult male C57Bl6/J mice (Janvier Labs, Saint-Berthevin, France) were housed in colony cages under a 12h:12h light:dark cycle in a temperature- and humidity-controlled environment. Adeno-injected mice were housed in a conventional animal housing (Pitié Salpêtrière, Paris, France). All other animals were maintained in a Specific Pathogen Free (SPF) animal facility (Institut Cochin, Paris, France). Mice were settled to the housing conditions for at least 1 week before the study began, and had *ad libitum* access to water and chow diet (SAFE A03, 61.3% carbohydrate, 13.5% fat, and 25.2% protein in term of energy) unless otherwise specified. For the fasting/refeeding experiments, mice were divided into three groups. The fed group had *ad libitum* access to food until the sacrifice. The fasted group was fed *ad libitum* and then fasted for 24 h prior to sacrifice. For the refeed group, mice fasted for 24 h were overnight refeed with the chow

diet and received additional 20% (w/v) glucose in the drinking water. At the end of the experiment, the animals were sacrificed. Blood, liver, kidneys, heart, brain, adipose tissue and quadriceps were collected and frozen at -80°C until further use, except for a part of the liver, kidney and brain that was immediately used for mitochondrial isolation. All studies involving animals followed the European guidelines for the care and use of laboratory animals and were approved by the Paris Descartes University ethics committee (CEEA34). *In vitro* (APAFIS #26042 N° 2019022717578208) and *in vivo* (APAFIS #15448 N° 2018012911055946) studies were approved by the French "Ministère de l'Education Nationale, de l'Enseignement Supérieur et de la Recherche".

#### *In vivo injection of adenovirus*

The pcDNA3 expression vector containing the human SQR (hSQR) coding sequence [4] was used for adenovirus production. Adenovirus coding green fluorescent protein (GFP) (Adv-GFP) and hSQR (Adv-SQR) were produced by the Laboratoire de thérapie génique (Nantes, France) and delivered through penis vein injection ( $1 \times 10^9$  infectious particles (i.p.)/mouse) to isoflurane anesthetized adult mice. Mice were surveyed on a weekly-basis for body weight and food intake. Three weeks after the adenovirus injection, mice were subjected to oral glucose tolerance test (OGTT), insulin sensitivity test (ITT) and pyruvate tolerance test (PTT). One week later, mice were sacrificed. Tissue collection and use were performed as previously described.

#### *Physiological parameters*

For ITT, mice were fasted for 5–6 h in the middle of the dark phase with *ad libitum* access to water. Actrapid HM human insulin (Novo Nordisk) was injected intraperitoneally (IP) at a dose of 0.75 U/kg body weight. For OGTT, mice received a glucose solution by gavage (solvent: water; 1 g/kg body weight) after overnight fasting. For PTT, mice received an IP injection of sodium salt pyruvate (2 g/kg body weight) after an overnight fast. For all tests, tail blood glucose was



monitored at 0, 15, 30, 60, 90 and 120 min using the Accu-Chek Aviva blood glucose monitor (Roche).

#### *Histology analysis and analytical procedures*

For histological studies, livers were fixed in 10% neutral buffered formalin and embedded in paraffin. Seven micrometre thick sections were cut and stained with haematoxylin–eosin. Plasma TG, cholesterol, alanine aminotransferase and aspartate aminotransferase concentrations were determined using an automated Monarch device (Laboratoire de Biochimie, Faculté de Médecine, Bichat, France). Serum insulin concentrations were determined using a rat insulin ELISA assay kit (Crystal Chem) using a mouse insulin standard. Liver TG, DAG, MAG and ceramides were quantified following extraction with a modified Folch method [49]. Briefly, ~ 25 mg of liver tissues were homogenized with a tissue-lyser (2 cycles of 1 min at 25 Hz), and lipid species were extracted with 600  $\mu$ L of chloroform:methanol (3:1) and 100  $\mu$ L of H<sub>2</sub>O, with the addition of internal standards (Avanti Polar Lipids, Merck KGaA, Darmstadt, Germany). Lipid classes were separated with UHPLC (1290 Infinity, Agilent, Santa Clara, CA) equipped with ZORBAX Eclipse Plus C18 2.1  $\times$  100 mm 1.8  $\mu$ m column (Agilent, Santa Clara, CA). Peak spectra were acquired with high resolution mass spectrometry (6540 QTOF, Agilent, Santa Clara, CA) equipped with an electrospray ion source (ESI), and concentrations of the different lipid classes were quantified with the Agilent MassHunter Profinder software (Agilent, Santa Clara, CA) with the use of internal standards.

#### *Isolation of mitochondria*

All steps were carried out at 4°C. Fresh liver, kidney and brain mitochondria were isolated using differential centrifugation. Briefly, minced tissue samples were carefully homogenized (5 strokes at low speed rotation) at a ratio of 1 g of tissue/6 mL of isolation buffer (300 mM sucrose, 5 mM Tris-HCl, 1 mM EGTA, pH 7.4) containing 0.1% (w/v) fatty acid-free bovine serum albumin

(BSA) using a glass Teflon homogenizer. After centrifugation at 600 g (10 min, 4°C), the supernatants containing mitochondria were further centrifuged at 8500 g (10 min, 4°C). The mitochondria pellets were resuspended in isolation buffer (without BSA) and protein concentration was determined by the Bicinchoninic Acid (BCA) assay using BSA as standard.

#### *Measurement of mitochondrial respiration and H<sub>2</sub>S oxidation*

Mitochondrial oxygen consumption was measured at 25°C using an Oroboros oxygraph-2k (Oroboros Instruments, Innsbruck, Austria). For mitochondrial respiration, mitochondria (~120 µg of proteins) were introduced into the respiratory chamber filled with 2 mL of respiration buffer (100 mM KCl, 40 mM sucrose, 10 mM TES, 5 mM MgCl<sub>2</sub>, 10 mM KPi, 1 mM EGTA, 0.4% (w/v) fatty acid-free BSA, pH 7.2). Measurements were conducted in the presence of either glutamate/malate (5 mM each) or succinate (7 mM) plus rotenone (1 µM) to assess Complex I- and Complex II-linked respiration rates, respectively. Mitochondrial respiration rate was determined successively in the presence of ADP (1.25 mM), oligomycin (1 µM), and lastly 1 mM potassium cyanide (KCN) to inhibit mitochondrial respiration and assess non-respiratory oxygen consumption (value to be subtracted to all values). These measurements allowed the calculation of state 3 (substrates + ADP) and state 4 (oligomycin). State 3 - state 4 rate indicates oxygen consumption linked to ATP synthesis while state 3/state 4, defined as the respiratory control ratio (RCR), assesses the coupling between respiration and phosphorylation.

For mitochondrial H<sub>2</sub>S oxidation, a stock solution of 1 M sodium sulfide (Na<sub>2</sub>S) was freshly prepared at the time of the experiment, diluted into water to a final concentration of 5 mM, and finally loaded into the high-pressure glass syringes of the injection Tip2k minipump (Oroboros Instruments). Na<sub>2</sub>S oxidation measurements were performed using 2 mg of mitochondrial proteins per chamber. Mitochondrial respiration was first settled to state 3 by addition of glutamate/malate (5 mM each) followed by ADP (1.25 mM). This allows the measurement of the

reference state 3 rate to normalize mitochondrial H<sub>2</sub>S oxidation rate as percentage of state 3 rate. After addition of rotenone (1 μM), the chambers were reoxygenized, ADP (0.625 mM) was added and increasing concentrations (0.3125 μM - 25 μM) of Na<sub>2</sub>S were successively injected into the chamber. Finally, the run was ended by adding 1 mM KCN. Mitochondrial Na<sub>2</sub>S oxidation was calculated by subtracting the values of O<sub>2</sub> consumption registered immediately before each injection and the maximum values registered for each injection peak. Subsequently all values were normalized by the concentration of protein inside the chambers. Na<sub>2</sub>S oxidation rate was expressed as pmol O<sub>2</sub>/s/mg of protein or % of state 3 respiration rate.

#### *Western blots*

Proteins (20 μg/well) were subjected to SDS-PAGE separation in an 10% or a Criterion TGX Stain-Free Pre Cast gradient 4-20% polyacrylamide gel (Bio-Rad, California, USA), and transferred onto nitrocellulose membrane. REVERT™ 700 Total Protein Staining and protein immunodetection were performed using LI-COR Odyssey 9120 Imaging System for signal detection (LI-COR Biosciences, Lincoln, NE). After quantification of total protein staining, membranes were blocked in 5% (w/v) non-fat dry milk in Tris-buffered saline (TBS). The antibodies used, diluted in TBS, were anti-SQR (1:500, NBP1-84510, Novus Biologicals, Colorado, USA), anti-SUOX (1:1000, NBP1-32423, Novus Biologicals), anti-ETHE1 (1:500, ab135589, Abcam, Cambridge, UK), anti-TST (1:250, ab155320, Abcam), anti-CBS (1:250, ab135626, Abcam), anti-CSE (1:500, ab151759, Abcam), anti-MPST (1:250, HPA001240, Atlas Antibodies, Bromma, Sweden), MitoProfile® Total OxPhOS Rodent WB Antibody Cocktail (1:250, ab110413, Abcam), anti-phospho Akt (Ser473) (1:1000, #4070, Cell Signaling Technology, Massachusetts, USA), anti-Akt (1:1000, #9272, Cell Signaling Technology), anti-phospho GSK3β (Ser9) (1:250, #9336, Cell Signaling Technology), anti-GSK3β (1:250, #9315, Cell Signaling Technology), and anti-CPT1A (1:1000,[50]). For secondary antibodies, IRDye 680 goat anti-rabbit and IRDye 680 goat anti-mouse secondary antibodies (LI-

COR Biosciences) were used in 5% (w/v) non-fat dry milk in TBS with 0.1% (v/v) Tween-20. Proteins were quantified using the Image studio software (Li-COR Biosciences). The fluorescence of each antibody-specific signal was normalized by division with the total quantification of the REVERT signal.

#### *[U-<sup>14</sup>C]glucose and [1-<sup>14</sup>C]oleate oxidation and [U-<sup>13</sup>C]glucose metabolism*

Liver [U-<sup>14</sup>C]glucose [51] and [1-<sup>14</sup>C]oleate [52] oxidation into [<sup>14</sup>C]CO<sub>2</sub> were measured *ex vivo* as described previously. [U-<sup>13</sup>C]glucose metabolism was measured *in vitro* in primary cultures of mouse hepatocytes. Mouse hepatocytes were isolated as described previously [53] and seeded in type I collagen pre-coated dishes at a density of 1.5x10<sup>6</sup> cells/dish (in 60mm Petri dishes) in M199 medium (Invitrogen) supplemented with 2.5% (v/v) Nu serum, 10 µg/mL of streptomycin, 100 units/mL of penicillin, 0.1% (v/v) ciprofloxacin, 1% (w/v) bovine serum albumin, 100 nM dexamethasone (Soludecadron, Merck Sharp), and 10 nM insulin (Actrapid, NovoNordisk). After cell attachment (3 h), the medium was replaced by fresh M199 medium with 4 i.p./cell of adv.GFP or adv.SQR. After 24 h, the medium was renewed by fresh M199 medium containing 5 mM ± 100 nM insulin or 25 mM glucose + 100 nM insulin (Novo Nordisk). After 24 h, the medium was changed and 10% (mol/mol) of [U-<sup>13</sup>C<sub>6</sub>]glucose (99%, Cambridge Isotope Laboratories, Inc., Tewksbury, MA) was added to each dish. Cells were collected 24 h after for fluxomic analyses. After homogenization with 600 µL cold methanol using Precellys 24 (Bertin Instrument, Montigny-le-Bretonneux, FRANCE), sample was kept in the freezer for 10 min and centrifuged for protein precipitation. The supernatant was transferred to a tube, chloroform (1200 µL) and water (400 µL) were added, and then the sample was centrifuged for phase separation. The upper phase was collected, filtered with 0.22 µm filters and dried under a gentle flux of N<sub>2</sub>. A 100 µL mix of acetonitrile: water (8:2) was added to the dry sample and transferred to a vial to be analysed by UHPLC-MS QTOF (1290 Infinity -6545 QTOF, Agilent, Santa Clara, CA) equipped with a UHand

InfinityLab Poroshell 120 HILIC-Z, 2.1mm x 150mm 2.7um, PEEK linked column (Agilent, Santa Clara, CA). Peaks of polar metabolites were extracted based on exact mass and <sup>13</sup>C enrichment was then quantified by Agilent MassHunter Profinder software (Agilent, Santa Clara, CA).

#### *Statistical analysis*

Results were expressed as means ± S.E.M. Statistical analyses were performed using GraphPad Prism (GraphPad Software, San Diego, CA, USA). Inter-group differences between two groups were assessed by Mann-Whitney test and were considered significant when  $p < 0.05$ .

#### **Acknowledgments**

We grateful thank all members of the Frédéric Bouillaud team (Institut Cochin) for helpful discussion and support of this project. We thank the staff of the Animal Facility and the HISTIM platform of the Institut Cochin and the staff at the Institute of Clinical Physiology for their help.

#### **Author contributions**

I.M., S.G., V.L., F.C., R.D., and C.P.-B. performed experiments; I.M., S.G., V.L., F.C., F.B., A.G., and C.P.-B. analysed data; I.M., A.G., and C.P.-B. interpreted results of experiments; I.M., and C.P.-B. prepared figures and drafted the manuscript; I.M., S.G., V.L., F.C., R.D., F.B., A.G., and C.P.-B. approved final version of manuscript; C.P.-B. conception and design of research; C.P.-B. edited and revised manuscript.

#### **Author disclosure statement**

The authors declare no conflict of interests, financial or otherwise, regarding the publication of this paper.

## Funding statements

This study was financially supported by the European Union's Horizon 2020 Research and Innovation programme under the Marie Skłodowska-Curie Grant Agreement No.722619 project "FOIE GRAS" (to C.P.-B. and A.G.) and by the Société Francophone du Diabète (SFD-Johnson & Johnson Diabetes Care Compagnie 2017 to C.P.-B.). I.M. and S.G. were recipient of an Early Stage Researcher grant under the FOIE GRAS project.

## References

- [1] Cooper C E and Brown G C. The inhibition of mitochondrial cytochrome oxidase by the gases carbon monoxide, nitric oxide, hydrogen cyanide and hydrogen sulfide: Chemical mechanism and physiological significance. *Journal of Bioenergetics and Biomembranes* 2008; 40(5): 533–539.
- [2] Wang R. Physiological implications of hydrogen sulfide: A whiff exploration that blossomed. *Physiol. Rev.* 2012; 92(2): 791–896.
- [3] Selzner M, Rüdiger H A, Sindram D, Madden J, and Clavien P A. Mechanisms of ischemic injury are different in the steatotic and normal rat liver. *Hepatology* 2000; 32(6): 1280–1288.
- [4] Lagoutte E, Mimoun S, Andriamihaja M, Chaumontet C, Blachier F, Bouillaud F. Oxidation of hydrogen sulfide remains a priority in mammalian cells and causes reverse electron transfer in colonocytes. *Biochim. Biophys. Acta - Bioenerg* 2010; 1797(8): 1500–1511.
- [5] Gubern M, Andriamihaja M, Nübel T, Blachier F, and Bouillaud F. Sulfide, the first inorganic substrate for human cells. *FASEB J.* 2007; 21(8): 1699–1706.
- [6] Theissen U, Hoffmeister M, Grieshaber M, and Martin W. Single eubacterial origin of

- eukaryotic sulfide:quinone oxidoreductase, a mitochondrial enzyme conserved from the early evolution of eukaryotes during anoxic and sulfidic times. *Mol. Biol. Evol.* 2003; 20(9): 1564–1574.
- [7] Gibson G R, Cummings J H, and Macfarlane G T. Growth and activities of sulphate-reducing bacteria in gut contents of healthy subjects and patients with ulcerative colitis. *FEMS Microbiol. Lett.* 1991; 86(2): 103–112.
- [8] Rey F E, Gonzalez M D, Cheng J, Wu M, Ahern P P, and Gordon J I. Metabolic niche of a prominent sulfate-reducing human gut bacterium. *Proc. Natl. Acad. Sci. U. S. A.* 2013; 110(33): 13582–13587.
- [9] Brito J A, Sousa F L, Stelter M, Bandejas T M, Vonrhein C, Teixeira M, Pereira M M and Archer M. Structural and functional insights into sulfide:quinone oxidoreductase. *Biochemistry* 2009; 48(24): 5613–5622.
- [10] Bartholomew T C, Powell G M, Dodgson K S, and Curtis C G. Oxidation of sodium sulphide by rat liver, lungs and kidney. *Biochem. Pharmacol.* 1980; 29(18): 2431–2437.
- [11] Helmy N, Prip-Buus C, Vons C, Lenoir V, Abou-Hamdan A, Guedouari-Bounihi H, Lombès A and Bouillaud F. Oxidation of hydrogen sulfide by human liver mitochondria. *Nitric Oxide* 2014; 41: 105–112.
- [12] Abou-Hamdan A, Guedouari-Bounihi H, Lenoir V, Andriamihaja M, Blachier F, and Bouillaud F. Oxidation of H<sub>2</sub>S in mammalian cells and mitochondria. *Methods in Enzymology* 2015; 554: 201–228.
- [13] Szabo C, Ransy C, Módis K, Andriamihaja M, Murghes B, Coletta C, Olah G, Yanagi K and Bouillaud F. Regulation of mitochondrial bioenergetic function by hydrogen sulfide. Part I. Biochemical and physiological mechanisms. *Br. J. Pharmacol.* 2014; 171(8): 2099–2122.

- [14] Blachier F, Mariotti F, Huneau J F, and Tomé D. Effects of amino acid-derived luminal metabolites on the colonic epithelium and physiopathological consequences. *Amino Acids* 2007; 33(4): 547–562.
- [15] Willis C L, Cummings J H, Neale G, and Gibson G R. In vitro effects of mucin fermentation on the growth of human colonic sulphate-reducing bacteria. *Anaerobe* 1996; 2: 117–122.
- [16] Shen X, Carlström M, Borniquel S, Jädert C, Kevil C G, and Lundberg J O. Microbial regulation of host hydrogen sulfide bioavailability and metabolism. *Free Radic. Biol. Med.* 2013; 60: 195–200.
- [17] Olson K R. H<sub>2</sub>S and polysulfide metabolism: Conventional and unconventional pathways. *Biochemical Pharmacology* 2018; 149: 77–90.
- [18] Kabil O, Vitvitsky V, Xie P, and Banerjee R. The quantitative significance of the transsulfuration enzymes for H<sub>2</sub>S production in murine tissues. *Antioxidants Redox Signal.* 2011; 15(2): 363–372.
- [19] Untereiner A A, Wang R, Ju Y, and Wu L. Decreased Gluconeogenesis in the Absence of Cystathionine Gamma-Lyase and the Underlying Mechanisms. *Antioxidants Redox Signal.* 2016; 24(3): 129–140.
- [20] Mani S, Li H, Yang G, Wu L, and Wang R. Deficiency of cystathionine gamma-lyase and hepatic cholesterol accumulation during mouse fatty liver development. *Sci. Bull.* 2015; 60(3): 336–347.
- [21] Untereiner A A and Wu L. Hydrogen Sulfide and Glucose Homeostasis: A Tale of Sweet and the Stink. *Antioxidants and Redox Signaling* 2018; 28(16): 1463–1482.
- [22] Majtan T, Hulková H, Parl I, Krijt J, Kozich V, Bublil E M and Kraus J P. Enzyme replacement prevents neonatal death, liver damage, and osteoporosis in murine



- homocystinuria. *FASEB J.* 2017; 31(12): 5495–5506.
- [23] Jain S K, Micinski D, Lieblong B J, and Stapleton T. Relationship between hydrogen sulfide levels and HDL-cholesterol, adiponectin, and potassium levels in the blood of healthy subjects. *Atherosclerosis* 2012; 225(1): 242–245.
- [24] Módis K, Ju YJ, Ahmad A, Untereiner A A, Altaany Z, Wu L, Szabo C and Wang R. S-Sulfhydration of ATP synthase by hydrogen sulfide stimulates mitochondrial bioenergetics. *Pharmacol. Res.* 2016; 113: 116–124.
- [25] Tan G, Pan S, Li J, Dong X, Kang K, Zhao M, Jiang X, Kanwar J R, Qiao H, Jiang H and Sun Z. Hydrogen sulfide attenuates carbon tetrachloride-induced hepatotoxicity, liver cirrhosis and portal hypertension in rats. *PLoS One* 2011; 6(10).
- [26] Ishkitiev N, Calenic B, Aoyama I, li H, Yaegaki K, and Imai T. Hydrogen sulfide increases hepatic differentiation in tooth-pulp stem cells. *J. Breath Res.* 2012; 6(1).
- [27] Zhang L, Yang G, Untereiner A, Ju Y, Wu L, and Wang R. Hydrogen sulfide impairs glucose utilization and increases gluconeogenesis in hepatocytes. *Endocrinology*, 2013; 154(1): 114–126.
- [28] Vitvitsky V, Kabil O, and Banerjee R. High turnover rates for hydrogen sulfide allow for rapid regulation of its tissue concentrations. *Antioxidants and Redox Signaling*. 2012; 17(1): 22–31.
- [29] Rui L. Energy metabolism in the liver. *Compr. Physiol.* 2014; 4(1): 177–197.
- [30] Hine C, Zhu Y, Hollenberg A N, and Mitchell J R. Dietary and Endocrine Regulation of Endogenous Hydrogen Sulfide Production: Implications for Longevity. *Antioxidants and Redox Signaling* 2018; 28(16): 1483–1502.
- [31] Hine C, Harputlugil E, Zhang Y, Ruckenstuhl C, Lee B C, Brace L, Longchamp A, Treviño-Villarreal J H, Mejia P, Ozaki C K, Wang R, Gladyshev V N, Madeo F, Mair W B and

- Mitchell J R. Endogenous hydrogen sulfide production is essential for dietary restriction benefits. *Cell* 2015; 160(1–2): 132–144.
- [32] Beaumont M, Andriamihaja M, Lan A, Khodorova N, Audebert M, Blouin JM, Grauso M, Lancha L, Benetti PH, Benamouzig R, Tomé D, Bouillaud F, Davila AM and Blachier F. Detrimental effects for colonocytes of an increased exposure to luminal hydrogen sulfide: The adaptive response. *Free Radic. Biol. Med.* 2016; 93: 155–164.
- [33] Wu D, Li J, Zhang Q, Tian W, Zhong P, Liu Z, Wang H, Wang H, Ji A and Li Y. Exogenous hydrogen sulfide regulates the growth of human thyroid carcinoma cells. *Oxid. Med. Cell. Longev.* 2019: 6927298-18.
- [34] Liu X, Zhang Z, Ma X, Li X, Zhou D, Gao B and Bai Y. Sulfide exposure results in enhanced *sqr* transcription through upregulating the expression and activation of HSF1 in echiuran worm *Urechis unicinctus*. *Aquat. Toxicol.* 2016; 170: 229–239.
- [35] Shimizu T, Shen J, Fang M, Zhang Y, Hori K, Trinidad J C, Bauer C E, Giedroc D P and Masuda S. Sulfide-responsive transcriptional repressor *SqrR* functions as a master regulator of sulfide-dependent photosynthesis. *Proc. Natl. Acad. Sci. U. S. A.* 2017; 114(9): 2355–2360.
- [36] Zhang T, Qin Z, Liu D, Wei M, Fu Z, Wang Q, Ma Y and Zhang Z. A novel transcription factor MRPS27 up-regulates the expression of *sqr*, a key gene of mitochondrial sulfide metabolism in echiuran worm *Urechis unicinctus*. *Comp. Biochem. Physiol. Part C Toxicol. Pharmacol.* 2021: 243: 108997.
- [37] Capdevila D A, Walsh B J C, Zhang Y, Dietrich C, Gonzalez-Gutierrez G, and Giedroc G P. Structural basis for persulfide-sensing specificity in a transcriptional regulator. *Nat. Chem. Biol.* 2021; 17(1): 65–70.
- [38] Ma YB, Zhang ZF, Shao MY, Kang KH, Shi XL, Dong YP and Li JL. Response of Sulfide:

- Quinone Oxidoreductase to Sulfide Exposure in the Echiuran Worm *Urechis unicinctus*. *Mar. Biotechnol.* 2012; 14(2): 245–251.
- [39] Kelley J L, Arias-Rodriguez L, Patacsil Martin D, Yee M C, Bustamante C D, and Tobler M. Mechanisms Underlying Adaptation to Life in Hydrogen Sulfide-Rich Environments. *Mol. Biol. Evol.* 2016; 33(6): 1419–1434.
- [40] Xiao A, Wang H, Lu X, Zhu J, Huang D, Xu T, Guo J, Liu C and Li J. H<sub>2</sub>S, a novel gasotransmitter, involves in gastric accommodation. *Sci. Rep.* 2015; 5: 16086.
- [41] Ju Y, Untereiner A A, Wu L, and Yang G. H<sub>2</sub>S-induced S-sulfhydration of pyruvate carboxylase contributes to gluconeogenesis in liver cells. *Biochim. Biophys. Acta - Gen. Subj.* 2015; 1850(11): 2293–2303.
- [42] Carter R N and Morton N M. Cysteine and hydrogen sulphide in the regulation of metabolism: Insights from genetics and pharmacology. *Journal of Pathology* 2016; 238(2): 321–332.
- [43] Yang G, Tang G, Zhang L, Wu L, and Wang R. The pathogenic role of cystathionine  $\gamma$ -lyase/hydrogen sulfide in streptozotocin-induced diabetes in mice. *Am. J. Pathol.* 2011; 179(2): 869–879.
- [44] Gerich J E, Woerle H J, Meyer C and Stumvoll M. Renal gluconeogenesis: Its importance in human glucose homeostasis. *Diabetes Care.* 2001; 24(2): 382-391.
- [45] Petersen M C, Madiraju A K, Gassaway B M, Marcel M, Nasiri A R, Butrico G, Marcucci M J, Zhang D, Abulizi A, Zhang XM, Phillbrick W, Hubbard S R, Jurczak M J, Samuel V T, Rinehart J and Shulman G I. Insulin receptor Thr1160 phosphorylation mediates lipid-induced hepatic insulin resistance. *J. Clin. Invest.* 2016; 126(11): 4361–4371.
- [46] Tang G, Zhang L, Yang G, Wu L, and Wang R. Hydrogen sulfide-induced inhibition of L-type Ca<sup>2+</sup> channels and insulin secretion in mouse pancreatic beta cells. *Diabetologia*

2013; 56(3): 533–541.

- [47] Zivanovic J, Kouroussis E, Kohl J B, Adhikari B, Bursac B, Schott-Roux S, Petrovic D, Miljkovic J L, Thomas-Lopez D, Jung Y, Miler M, Mitchell S, Milosevic V, Gomes J E, Benhar M, Gonzalez-Zorn B, Ivanovic-Burmazovic I, Torregrossa R, Mitchell J R, Whiteman M, Schwarz G, Snyder S H, Paul B D, Carroll K S and Filipovic M R. Selective Persulfide Detection Reveals Evolutionarily Conserved Antiaging Effects of S-Sulfhydration. *Cell Metab.* 2019; 30(6): 1152-1170.
- [48] Filipovic M R, Zivanovic J, Alvarez B, and Banerjee R. Chemical Biology of H<sub>2</sub>S Signaling through Persulfidation. *Chemical Reviews.* 2018; 118(3): 1253–1337.
- [49] Folch J, Lees M and Sloane Stanley G H. A simple method for the isolation and purification of total lipides from animal tissues. *J. Biol. Chem.* 1957; 226(1): 497–509.
- [50] Vavrova E, Lenoir V, Alves-Guerra MC, Denis R G, Castel J, Esnous C, Dyck J R B, Luquet S, Metzger D, Bouillaud F and Prip-Buus C. Muscle expression of a malonyl-CoA-insensitive carnitine palmitoyltransferase-1 protects mice against high-fat/high-sucrose diet-induced insulin resistance. *Am. J. Physiol. Endocrinol. Metab.* 2016; 311(3): E649–E660.
- [51] Bricambert J, Alves-Guerra MC, Esteves P, Prip-Buus C, Bertrand-Michel J, Guillou H, Chang C J, Vander Wal M N, Canonne-Hergaux F, Mathurin P, Raverdy V, Pattou F, Girard J, Postic C and Dentin R. The histone demethylase Phf2 acts as a molecular checkpoint to prevent NAFLD progression during obesity. *Nat. Commun.* 2018; 9(1): 1–18.
- [52] Monsénégo J, Mansouri A, Akkaoui M, Lenoir V, Esnous C, Fauveau V, Tavernier V, Girard J and Prip-Buus C. Enhancing liver mitochondrial fatty acid oxidation capacity in obese mice improves insulin sensitivity independently of hepatic steatosis. *J. Hepatol.*

2012; 56(3): 632–639.

- [53] Dentin R, Pégrier JP, Benhamed F, Foufelle F, Ferré P, Fauveau V, Magnuson M A, Girard J and Postic C. Hepatic Glucokinase Is Required for the Synergistic Action of ChREBP and SREBP-1c on Glycolytic and Lipogenic Gene Expression. *J. Biol. Chem.* 2004; 279(19): 20314–20326.

**Table 1: Metabolic variables in Adv.GFP and Adv.SQR mice**

	Fed			Fasted			Refed		
	Adv.GFP	Adv.SQR	<i>P value</i>	Adv.GFP	Adv.SQR	<i>P value</i>	Adv.GFP	Adv.SQR	<i>P value</i>
<b>Body weight (g)</b>	28.74 ± 0.58	28.70 ± 0.66	n.s.	24.90 ± 0.54	24.16 ± 0.28	n.s.	26.12 ± 0.65	26.19 ± 0.50	n.s.
<b>Liver (% body weight)</b>	5.06 ± 0.09	5.46 ± 0.08	**	4.19 ± 0.03	4.57 ± 0.13	*	6.48 ± 0.24	7.00 ± 0.17	n.s.
<b>Adipose tissue (% body weight)</b>	1.11 ± 0.07	1.01 ± 0.05	n.s.	0.99 ± 0.08	1.47 ± 0.25	n.s.	0.89 ± 0.10	0.97 ± 0.13	n.s.
<b>Quadriceps (% body weight)</b>	1.45 ± 0.03	1.41 ± 0.04	n.s.	1.24 ± 0.10	1.26 ± 0.06	n.s.	1.15 ± 0.07	1.15 ± 0.08	n.s.
<b>Glycemia at sacrifice (mM)</b>	7.89 ± 0.19	8.07 ± 0.20	n.s.	4.00 ± 0.15	4.84 ± 0.26	*	8.93 ± 0.33	8.56 ± 0.85	n.s.
<b>Fasting glycemia (mM)</b>	5.08 ± 0.14	5.58 ± 0.21	*	-	-		-	-	
<b>Insulinemia (µg insulin/L)</b>	0.449 ± 0.05	0.322 ± 0.04	*	0.12 ± 0.07	0.23 ± 0.11	n.s.	1.66 ± 0.28	3.50 ± 1.08	n.s.
<b>Plasma triglycerides (mM)</b>	1.24 ± 0.15	1.06 ± 0.08	n.s.	-	-		-	-	
<b>Total cholesterol (mM)</b>	2.40 ± 0.09	2.76 ± 0.09	*	-	-		-	-	
<b>HDL-cholesterol (mM)</b>	1.69 ± 0.09	2.02 ± 0.07	*	-	-		-	-	
<b>ALT (IU/L)</b>	65 ± 7.41	66.67 ± 4.63	n.s.	-	-		-	-	
<b>AST (IU/L)</b>	193 ± 25.46	210 ± 14.69	n.s.	-	-		-	-	
<b>Liver triglycerides (µg/g of liver)</b>	3011 ± 455.7	3312 ± 334.5	n.s.	-	-		-	-	
<b>Liver DAG (µg/g of liver)</b>	290.5 ± 44.64	189.0 ± 16.30	*	-	-		-	-	
<b>Liver MAG (µg/g of liver)</b>	78.82 ± 7.97	47.73 ± 6.30	*	-	-		-	-	
<b>Liver ceramides (µg/g of liver)</b>	68.47 ± 7.29	77.82 ± 4.82	n.s.	-	-		-	-	
<b>Glycogen (µmol/g of liver)</b>	233.8 ± 18.33	168.9 ± 11.95	**	14.94 ± 5.16	14.12 ± 3.81	n.s.	535.7 ± 28.34	477.2 ± 24.78	n.s.

*Plasma insulinemia, circulating TG, cholesterol, ALT and AST levels were measured after sacrifice.*

**ALT:** alanine aminotransferase; **AST:** aspartate aminotransferase; **DAG:** diacylglycerides; **MAG:** monoacylglycerides; **n.s.:** non-significant. Results are means ± S.E.M. \**p* < 0.05, \*\* *p* < 0.01.

## Figure Legends

### **FIG. 1. Mitochondrial H<sub>2</sub>S oxidation in isolated mouse liver, kidney and brain mitochondria. (A)**

Representative experimental runs of oxygen consumption due to H<sub>2</sub>S oxidation after injecting increasing concentrations of Na<sub>2</sub>S (0.313 μM-25 μM) into the chamber as indicated by the blue arrows on top of each graph. Oxygen concentration, represented by the blue line (left Y axis), and oxygen consumption, represented by the red line (right Y axis) are plotted against time (X axis). Every event (injection, addition, chamber opening/closing) is indicated by a vertical line. For each Na<sub>2</sub>S injection, oxygen consumption increased with time, reached a transient maximal value, and then returned back to the previous basal oxygen consumption rate once H<sub>2</sub>S was totally oxidized. H<sub>2</sub>S oxidation rate was calculated as the difference in the oxygen consumption rate after and before Na<sub>2</sub>S injection (represented in the graph by ΔO<sub>2</sub>). H<sub>2</sub>S oxidation rates were plotted as a function of Na<sub>2</sub>S concentration, and expressed as pmol O<sub>2</sub>/s/mg protein (**B**) or as percentage of state 3 respiration rate (**C**). Results are means ± S.E.M. (n=4 to 5 per tissue). \**p* <0.05 and \*\* *p* <0.01.

### **FIG. 2. Liver, kidney and brain protein expression of enzymes involved in H<sub>2</sub>S oxidation and biosynthesis. (A)**

Schematic representation of H<sub>2</sub>S oxidation and biosynthesis within a mammalian cell. H<sub>2</sub>S endogenous production occurs in the cytoplasm during the catabolism of cysteine and homocysteine by the transsulfuration pathway enzymes, cystathionine β-synthase (CBS) and cystathionine γ-lyase (CSE). The cysteine aminotransferase/3-mercaptopyruvate sulfurtransferase (CAT/MPST) pathway is common to both the cytoplasm and the mitochondrion. Endogenous and exogenous H<sub>2</sub>S is oxidized by sulfide quinone reductase (SQR) to generate persulfide. On a second step, the persulfide is oxidized by a dioxygenase (ETHE1) to generate sulfite that can either be oxidized by thiosulfate sulfurtransferase (TST) into thiosulfate or by sulfite oxidase (SUOX) into sulfate. Electrons released during the SQR reaction reduce ubiquinone, which transfers them to

the electron transport chain at the level of Complex III getting re-oxidized in the process. **(B)** Immunoblot analysis of the protein expression level of enzymes involved in H<sub>2</sub>S oxidation (SQR, ETHE1, TST, SUOX) and biosynthesis (CBS, CSE, MPST) using liver, kidney and brain lysates. **(C)** Immunoblot quantification was normalized by the total quantification of the REVERT signal. Results are means ± S.E.M. (n=5 per tissue) and expressed relative to liver. \$ *p*<0.05 and \$\$ *p*<0.01 versus liver; # *p*<0.05 and ## *p*<0.01 versus kidney.

**FIG. 3. Fasting and refeeding regulate liver mitochondrial H<sub>2</sub>S oxidation.** **(A)** Oxygen consumption rates due to H<sub>2</sub>S oxidation were measured in liver mitochondria isolated from fed, 24h-fasted and refed mice using increasing concentrations of Na<sub>2</sub>S (0.313 μM - 25 μM) as indicated in the legend of FIG. 2. H<sub>2</sub>S oxidation rates were plotted as a function of Na<sub>2</sub>S concentration, and expressed as pmol O<sub>2</sub>/s/mg protein or as percentage of state 3 respiration rate. **(B)** Immunoblot analysis of the protein expression level of enzymes involved in H<sub>2</sub>S oxidation (SQR, ETHE1, TST, SUOX) and biosynthesis (CBS, CSE, MPST) using liver lysates. **(C)** Immunoblot quantification was normalized by the total quantification of the REVERT signal. Results are means ± S.E.M. (n=7 per group) and expressed relative to the fed group. \$ *p*<0.05, \$\$ *p*<0.01 and \$\$\$ *p*<0.001 versus the fed group. # *p*<0.05 and ### *p*<0.001 versus the fasted group.

**FIG. 4. Liver SQR overexpression abrogates the nutritional regulation of hepatic mitochondrial H<sub>2</sub>S oxidation.** **(A)** Mice were injected with adenovirus (Adv) encoding either green fluorescent protein (Adv-GFP) or SQR (Adv-SQR). After 4 weeks, when indicated, mice were submitted to a fasting/refeeding challenge. Oxygen consumption rates due to H<sub>2</sub>S oxidation were measured in liver mitochondria isolated from fed, 24h-fasted and refed Adv-GFP and Adv-SQR mice using increasing concentrations of Na<sub>2</sub>S (0.313 μM - 25 μM) as indicated in the legend of FIG. 2. H<sub>2</sub>S oxidation rates were plotted as a function of Na<sub>2</sub>S concentration, and expressed as pmol O<sub>2</sub>/s/mg protein. **(B)** Immunoblot analysis of the protein expression level of enzymes involved in H<sub>2</sub>S



oxidation (SQR, ETHE1, TST, SUOX) and biosynthesis (CBS, CSE, MPST) using liver lysates. (C) Immunoblot quantification was normalized by the total quantification of the REVERT signal. Results are means  $\pm$  S.E.M. (n=5 to 22 per group) and expressed relative to the fed Adv.GFP or fasted Adv.GFP groups. \$  $p < 0.05$ , \$\$  $p < 0.01$  and \$\$\$  $p < 0.001$  versus the fed Adv.GFP or fasted Adv.GFP groups. #  $p < 0.05$  versus the refed Adv.GFP group.

**FIG. 5. Characterization of liver SQR overexpressing mice.** (A) Liver histological analysis by haematoxylin–eosin staining of Adv.GFP and Adv.SQR mice with an image magnification of 100X. (B) Oral glucose tolerance test (OGTT), insulin tolerance test (ITT) and pyruvate tolerance test (PTT) were performed in Adv.GFP and Adv.SQR mice. The respective area under the curve (AUC) is presented in each graph. (C) Immunoblot analysis of the protein expression level of phosphorylated ( $p^{S473}$ Akt and  $p^{S9}$ GSK-3 $\beta$ ) and total Akt and GSK-3 $\beta$  under the different nutritional conditions (D) Immunoblot quantification was normalized by the total quantification of the REVERT signal, and the  $p^{S473}$ Akt/Total Akt and  $p^{S9}$ GSK-3 $\beta$ /Total GSK-3 $\beta$  ratio are presented. Results are means  $\pm$  S.E.M. (n=5 to 18 per group) \* $p < 0.05$  and \*\*  $P < 0.01$ .

**FIG. 6. Hepatic SQR overexpression decreases oleate oxidation and increases insulin-stimulated glucose utilization.** Liver [ $U-^{14}C$ ]glucose (A) and [ $1-^{14}C$ ]oleate (B) oxidation into [ $^{14}C$ ]CO $_2$  were measured *ex-vivo* in Adv-GFP and Adv-SQR mice (n=5-6 per group). (C) Immunoblot quantification of the protein expression level of carnitine palmitoyltransferase 1A (CPT1A) (n=6 per group). (D) Primary cultures of mouse hepatocytes expressing either GFP or SQR were incubated for 24 h in the presence of 5 mM glucose  $\pm$  100 nM insulin or 25 mM glucose + 100 nM insulin, followed by a 24 h exposure to 10% (mol/mol) of [ $U-^{13}C_6$ ]glucose.  $^{13}C$ -enrichments of metabolites derived from [ $U-^{13}C_6$ ]glucose are shown. Results are means  $\pm$  S.E.M. (n=3 to 4 per group) \* $p < 0.05$ .

**Figure 1**

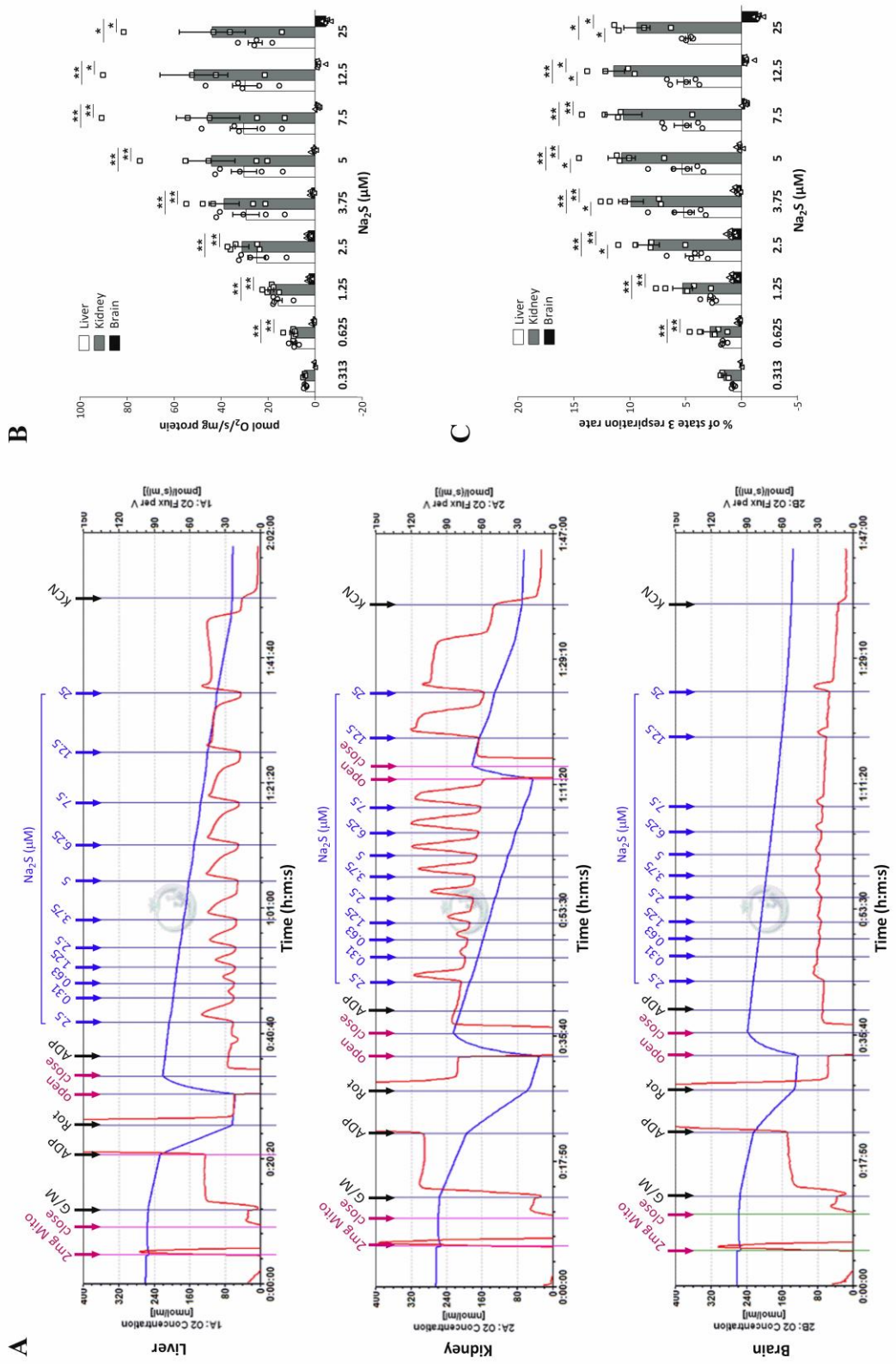
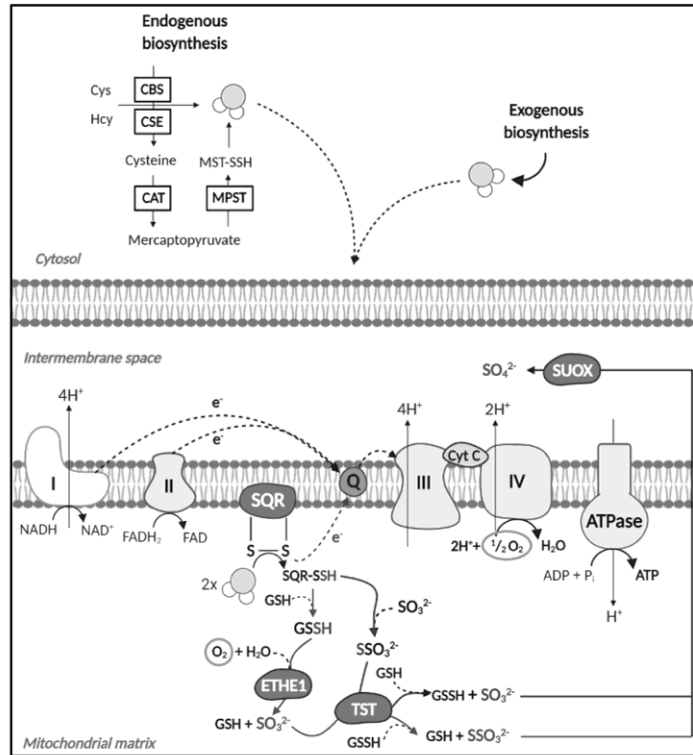
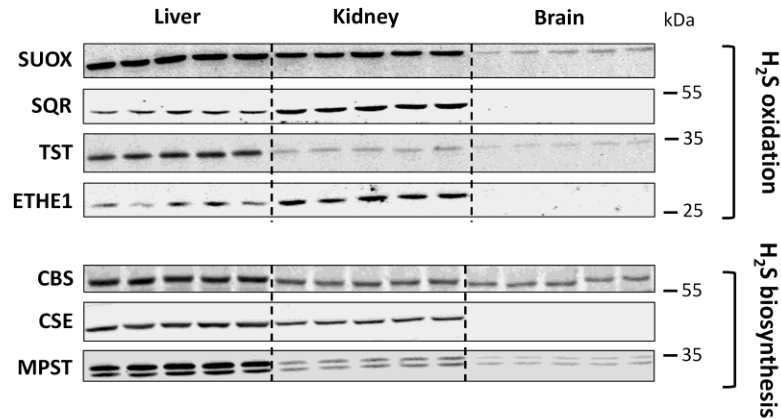


**Figure 2**

**A**



**B**



**C**

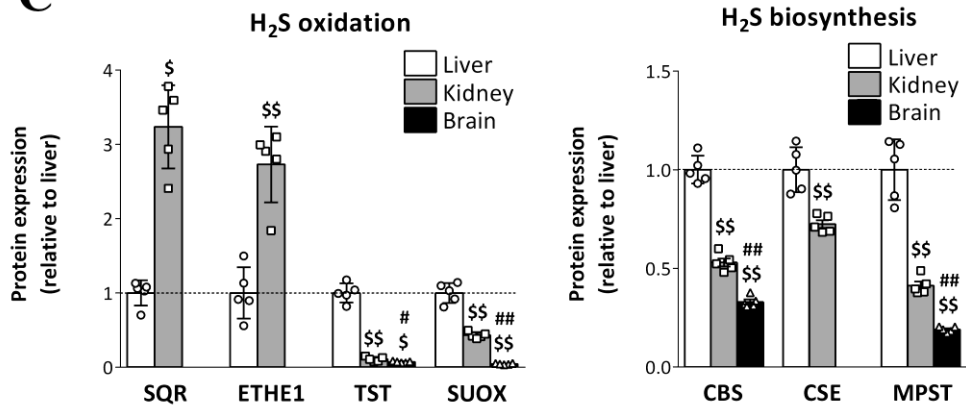
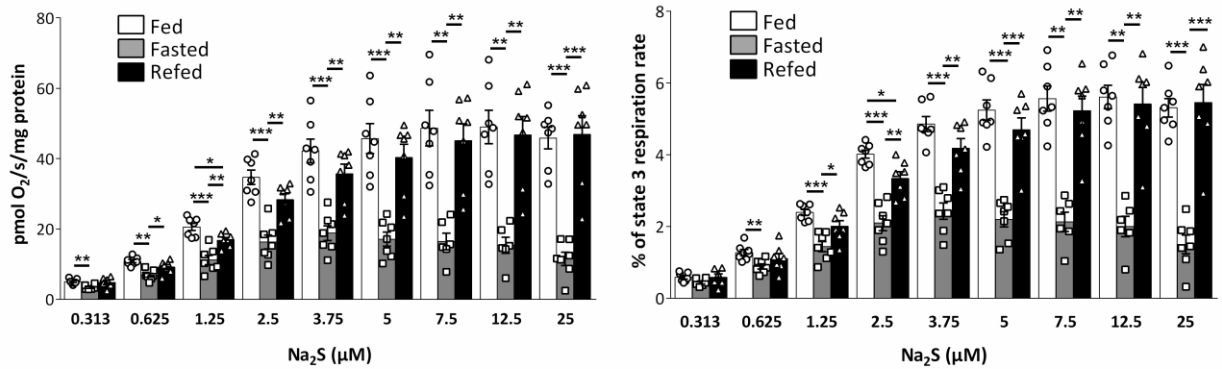
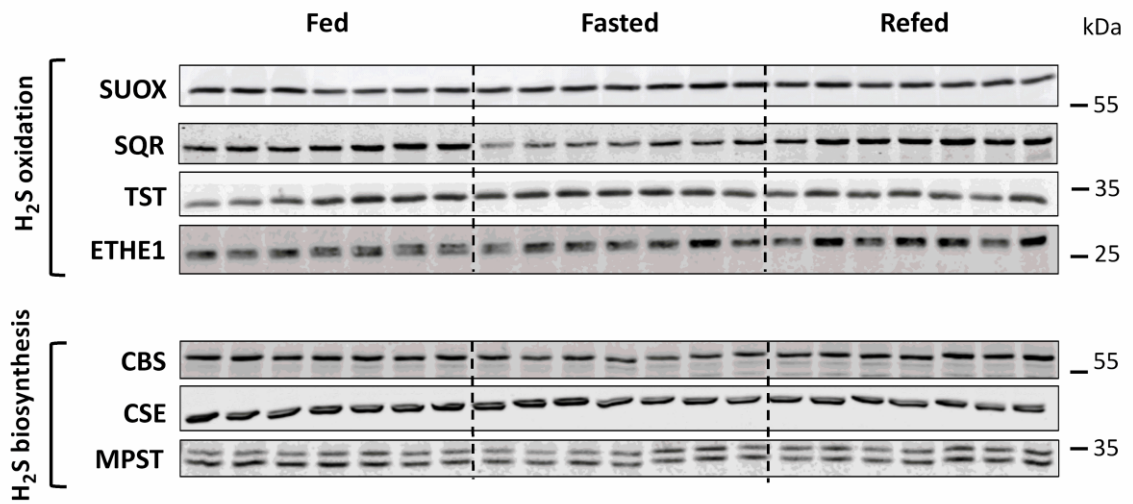


**Figure 3**

**A**



**B**



**C**

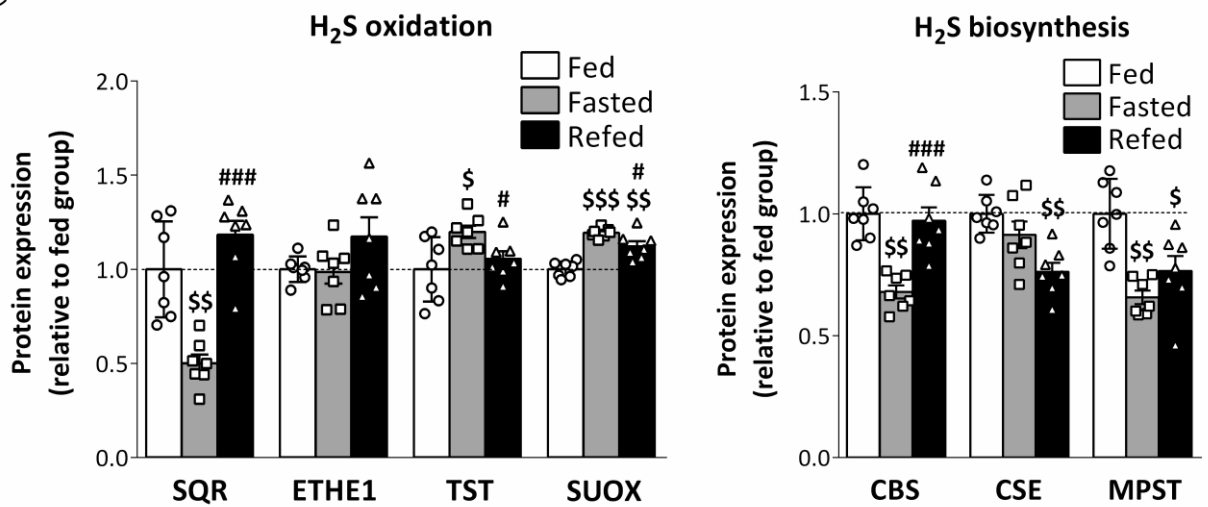


**Figure 4**

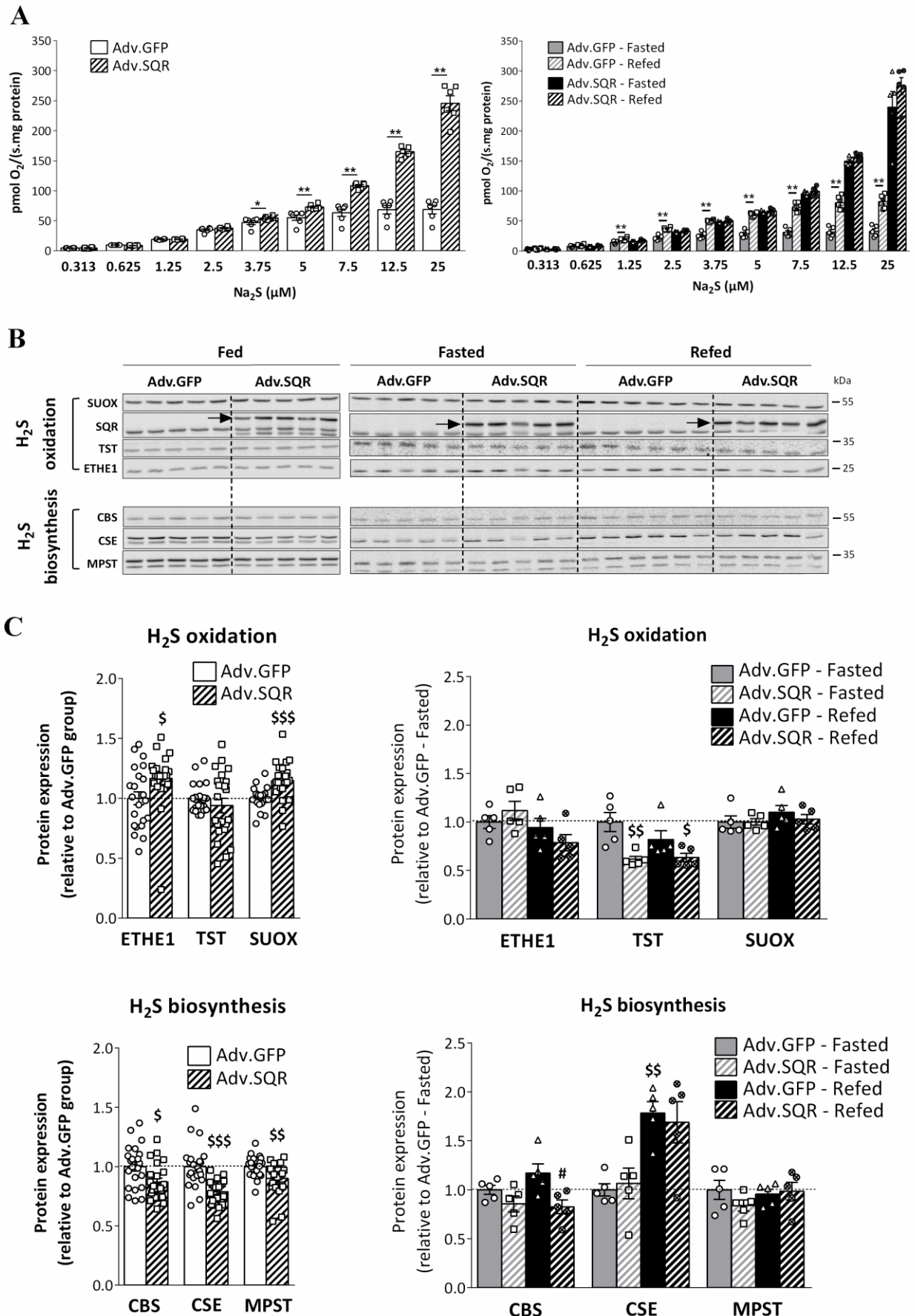
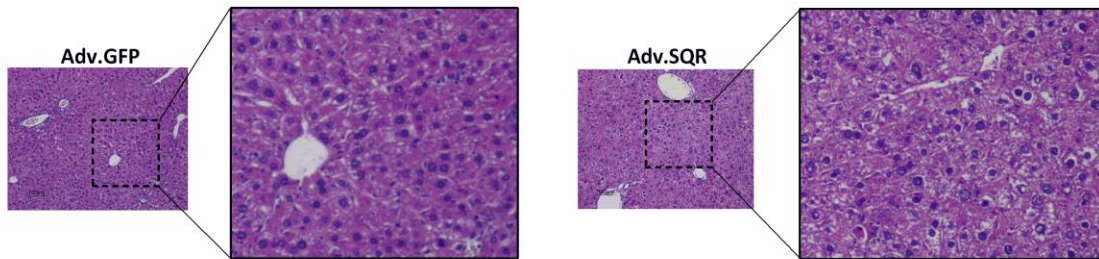
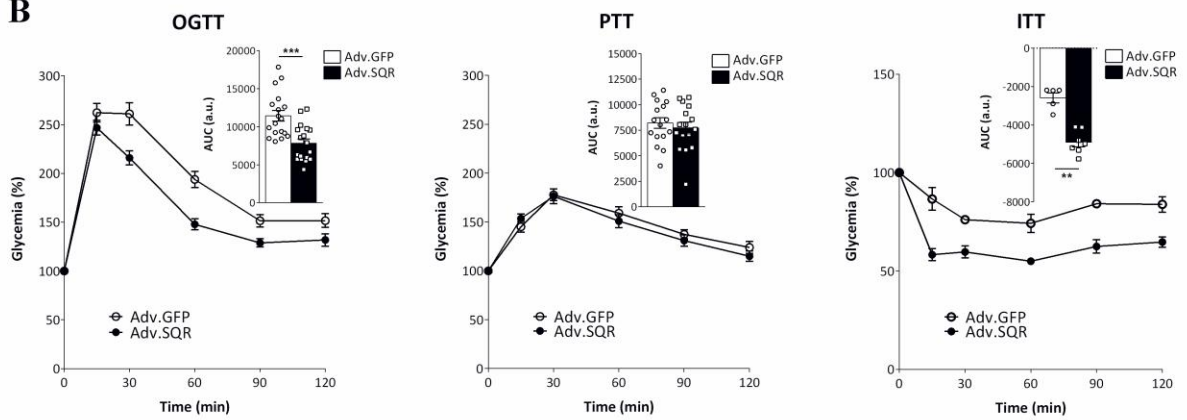


**Figure 5**

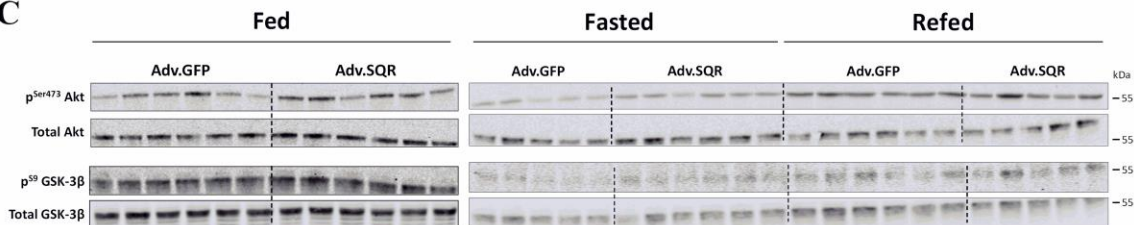
**A**



**B**



**C**



**D**

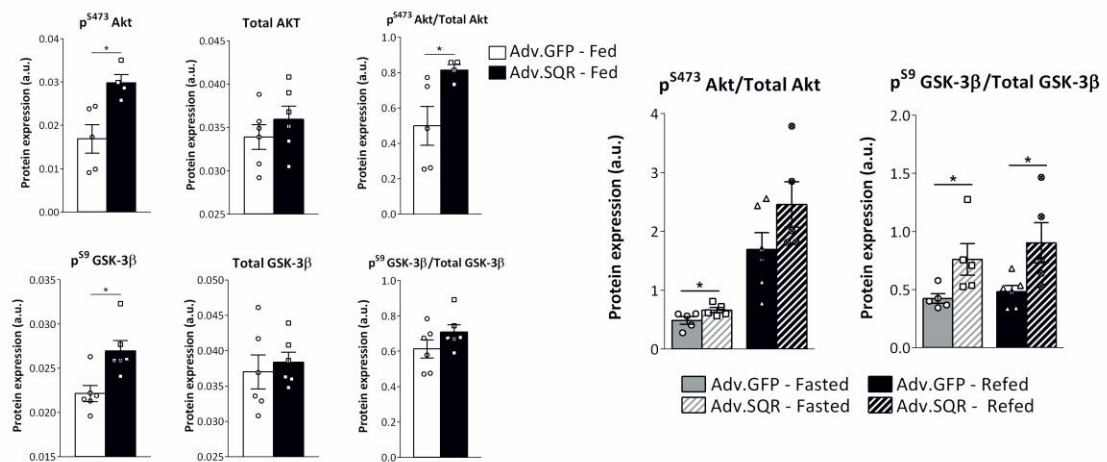
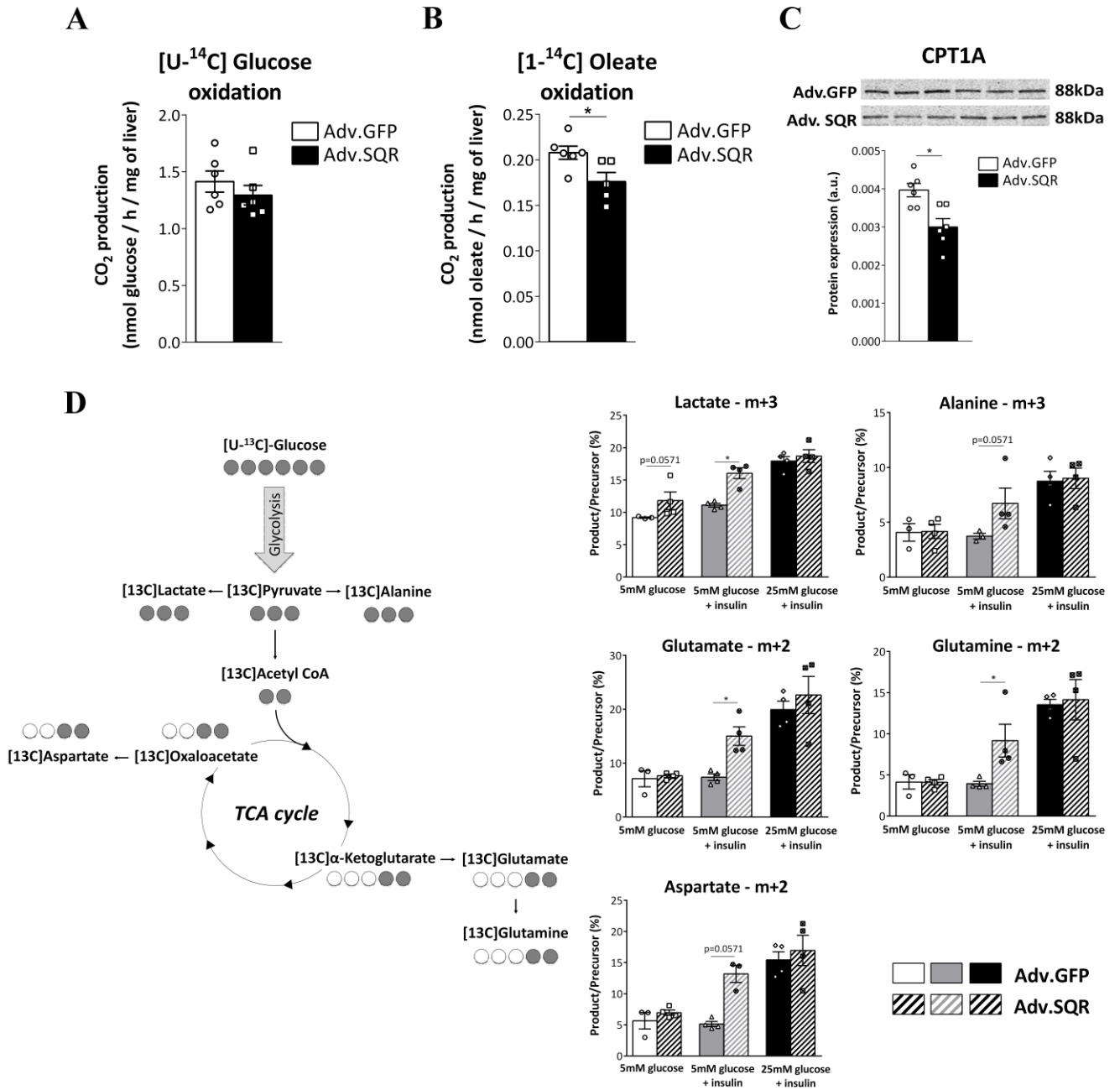


**Figure 6**



## Supplementary Figure Legends

**Supplementary FIG. 1.** Mitochondrial oxygen consumption rates were measured in liver, kidney and brain mitochondria isolated from fed mice (n=5 per tissue) using either glutamate/malate (**A**) or succinate plus rotenone (**B**) in the presence of ADP (state 3) or oligomycin (Oligo, state 4) to determine respiration linked to ATP synthesis (state 3-state 4) as well as (**C**) respiratory control ratio (RCR, state3/state 4). (**D**) Immunoblot analysis of the protein expression levels of OXPHOS Complexes (CI to CV) in mouse liver, kidney and brain mitochondria. Immunoblot quantification was normalized by the total quantification of the REVERT signal (n=4 to 5 per tissue). Results are means  $\pm$  S.E.M. \* $p < 0.05$ , \*\*  $p < 0.01$ .

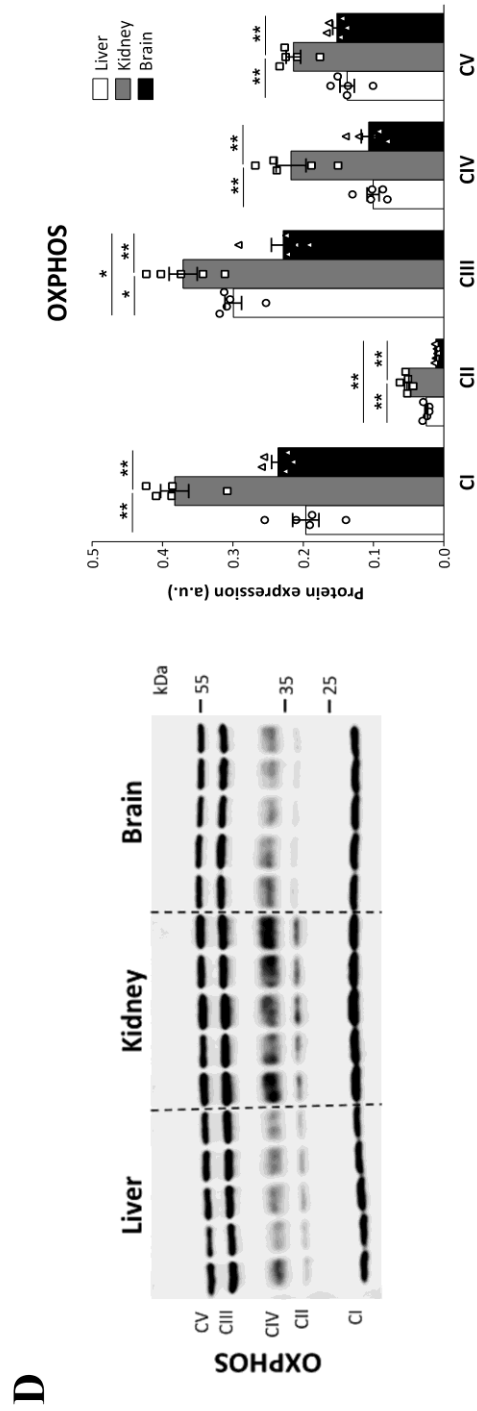
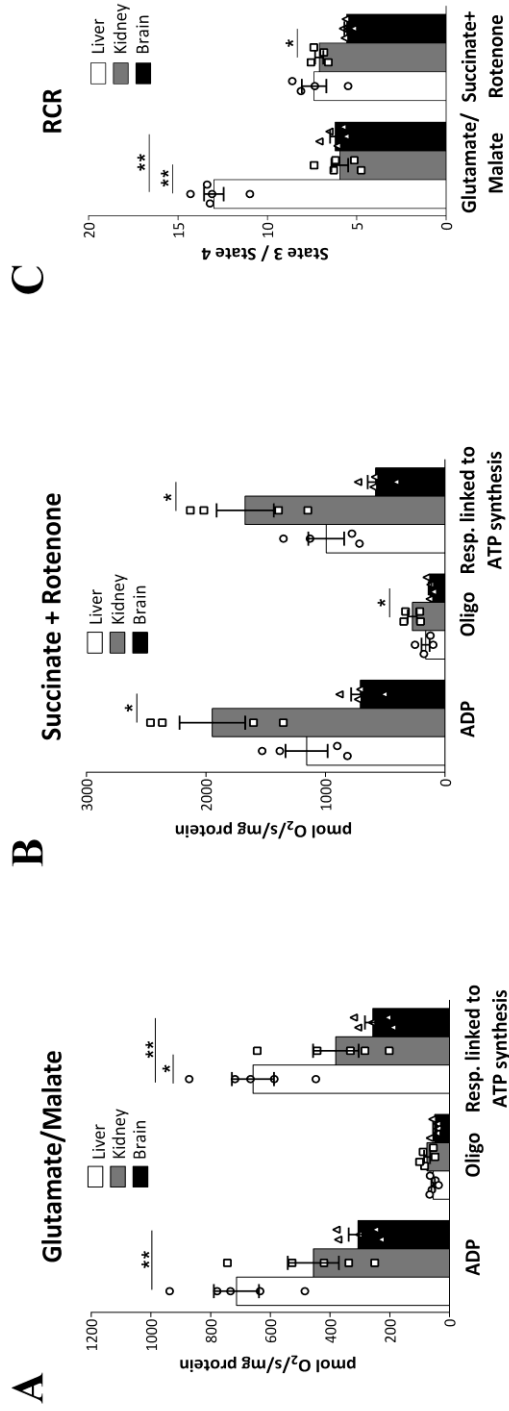
**Supplementary FIG. 2.** Mitochondrial respiratory capacity was measured in liver mitochondria isolated from fed, 24h-fasted and refed mice (n=7 per group) using either glutamate/malate (**A**) or succinate plus rotenone (**B**) in the presence of ADP (state 3) or oligomycin (Oligo, state 4) to determine respiration linked to ATP synthesis (state 3-state 4) as well as (**C**) respiratory control ratio (RCR, state3/state 4). (**D**) Immunoblot analysis of the protein expression levels of OXPHOS Complexes (CI to CV) in liver mitochondria isolated from fed, 24h-fasted and refed mice. Immunoblot quantification was normalized by the total quantification of the REVERT signal (n=7 per group). Results are means  $\pm$  S.E.M. \* $p < 0.05$ , \*\*  $p < 0.01$ , \*\*\*  $p < 0.001$ .

**Supplementary FIG. 3. Adenovirus-mediated specific liver overexpression of SQR protein in the mouse liver.** Adult mice were injected with adenovirus (Adv) encoding either green fluorescent protein (GFP) or human SQR (hSQR). Mice were sacrificed 4 weeks post-injection to analyse by immunoblotting SQR protein expression in the liver, the kidney, the heart, the brain, the adipose tissue and the skeletal muscle. The hSQR protein migrated more slowly in the SDS-PAGE gel, allowing it to be distinguished from the murine protein.

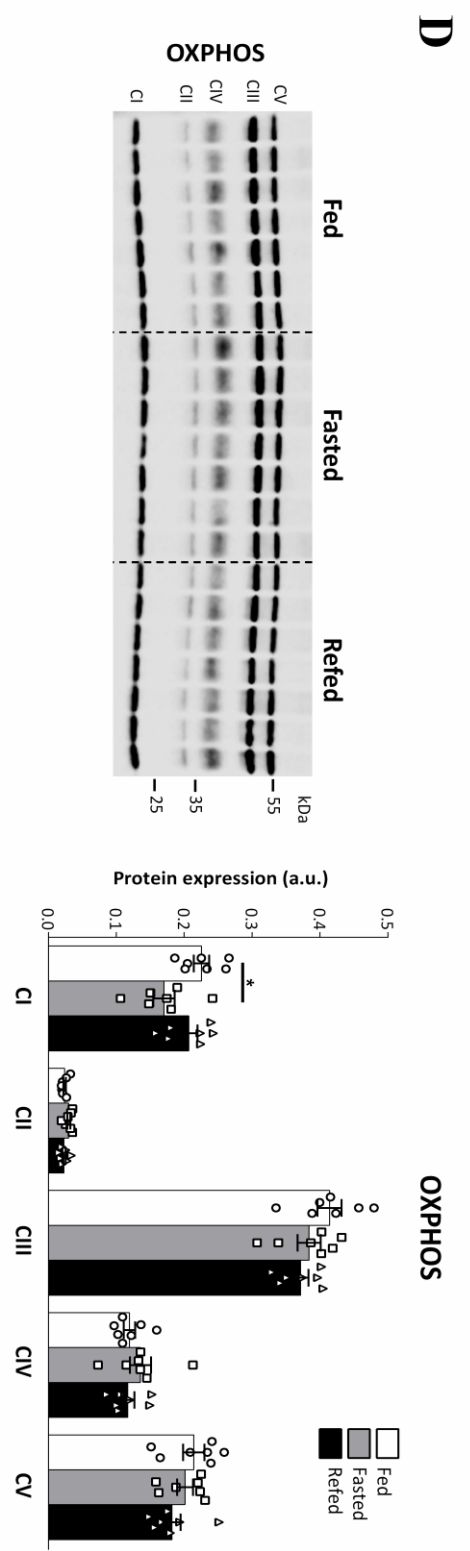
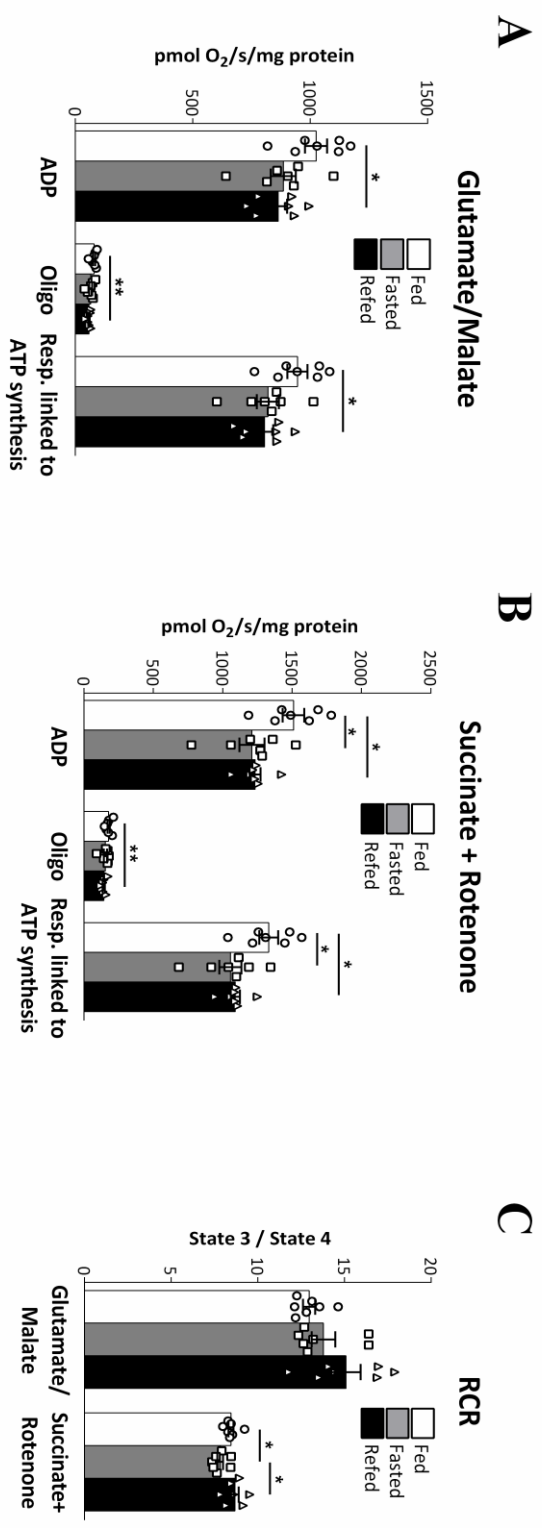


**Supplementary FIG. 4.** Mitochondrial respiratory capacity was measured in liver mitochondria isolated from fed (**A**), 24h-fasted (**B**) and refed (**C**) mice overexpressing GFP (Adv-GFP) or SQR (Adv-SQR) (n=6 per group) using either glutamate/malate or succinate plus rotenone in the presence of ADP (state 3) or oligomycin (Oligo, state 4) to determine respiration linked to ATP synthesis (state 3-state 4) as well as respiratory control ratio (RCR, state3/state 4). \*\*  $p < 0.01$ .

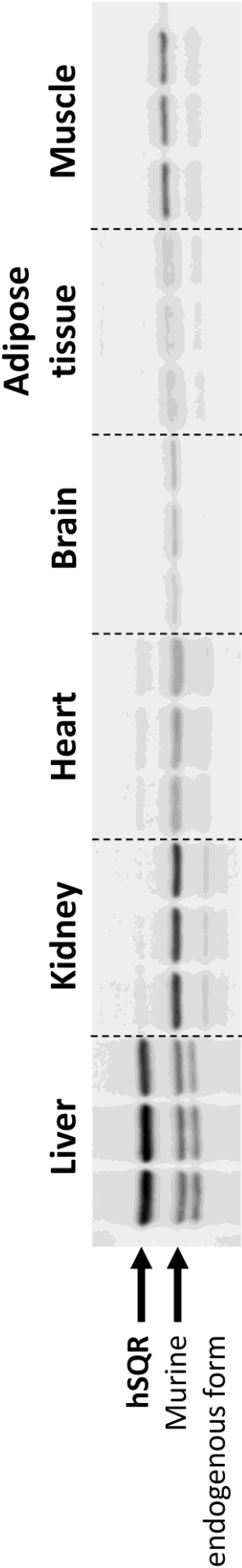
# Supplementary Figure 1



# Supplementary Figure 2



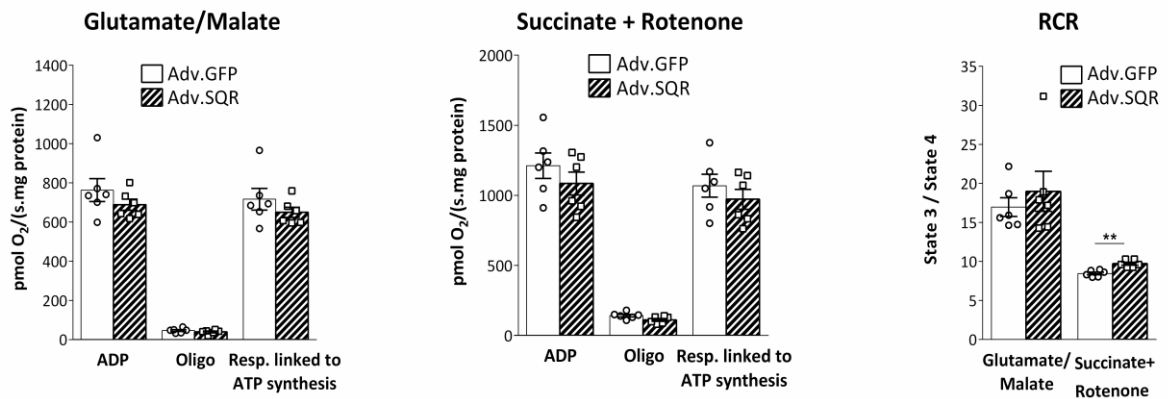
Supplementary Figure 3



# Supplementary Figure 4

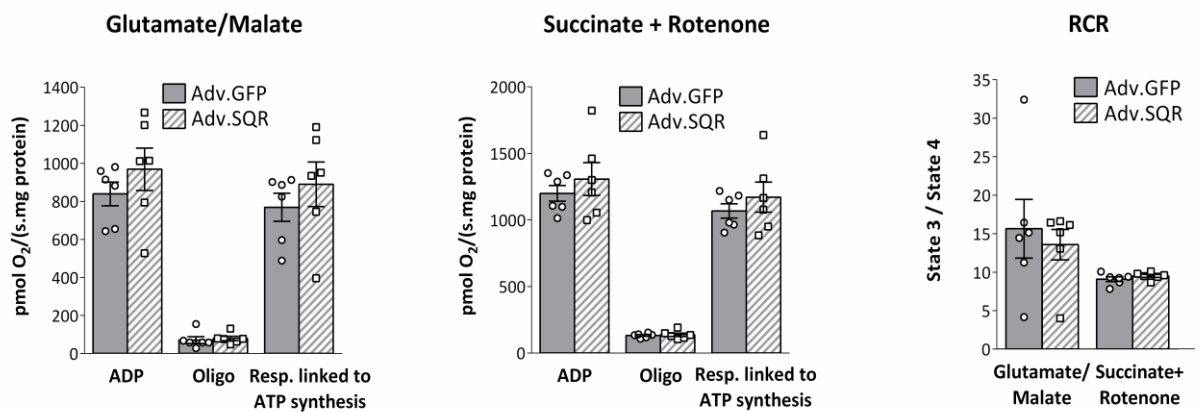
**A**

**Fed**



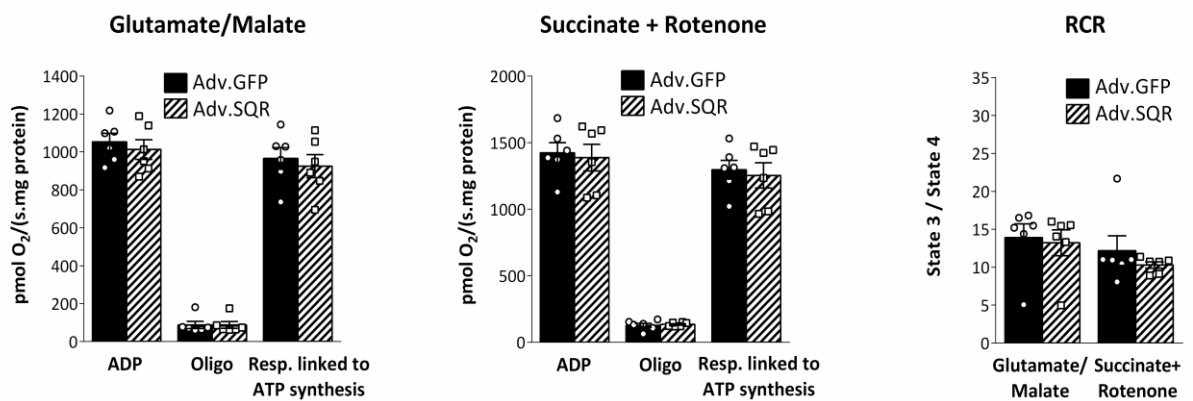
**B**

**Fasted**



**C**

**Refed**

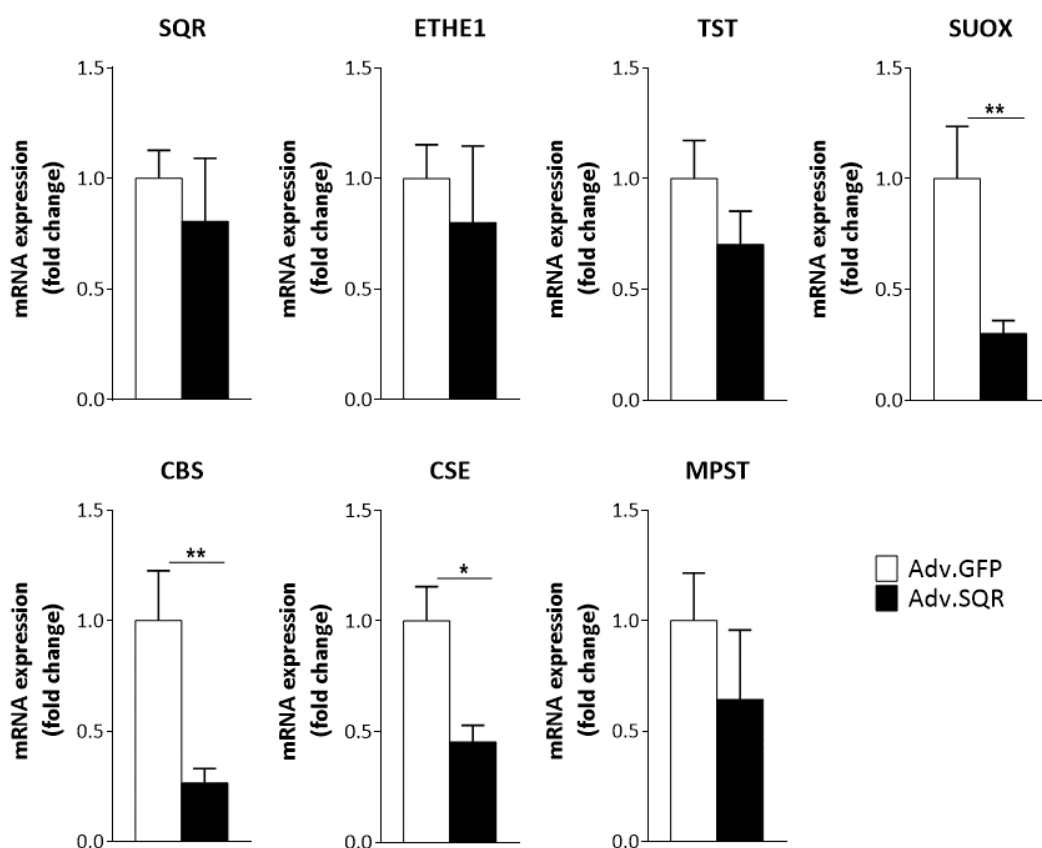




## Supplementary Results

The following mRNA analysis was obtained during my secondment in Lisbon with the help of Tawhidul Islam and Dr. André Santos, under the supervision of Dr. Rui Castro and Pr. Cecília Rodrigues. These data are complementary to the results presented and discussed in the previous paper.

### Genes involved in H<sub>2</sub>S oxidation and biosynthesis

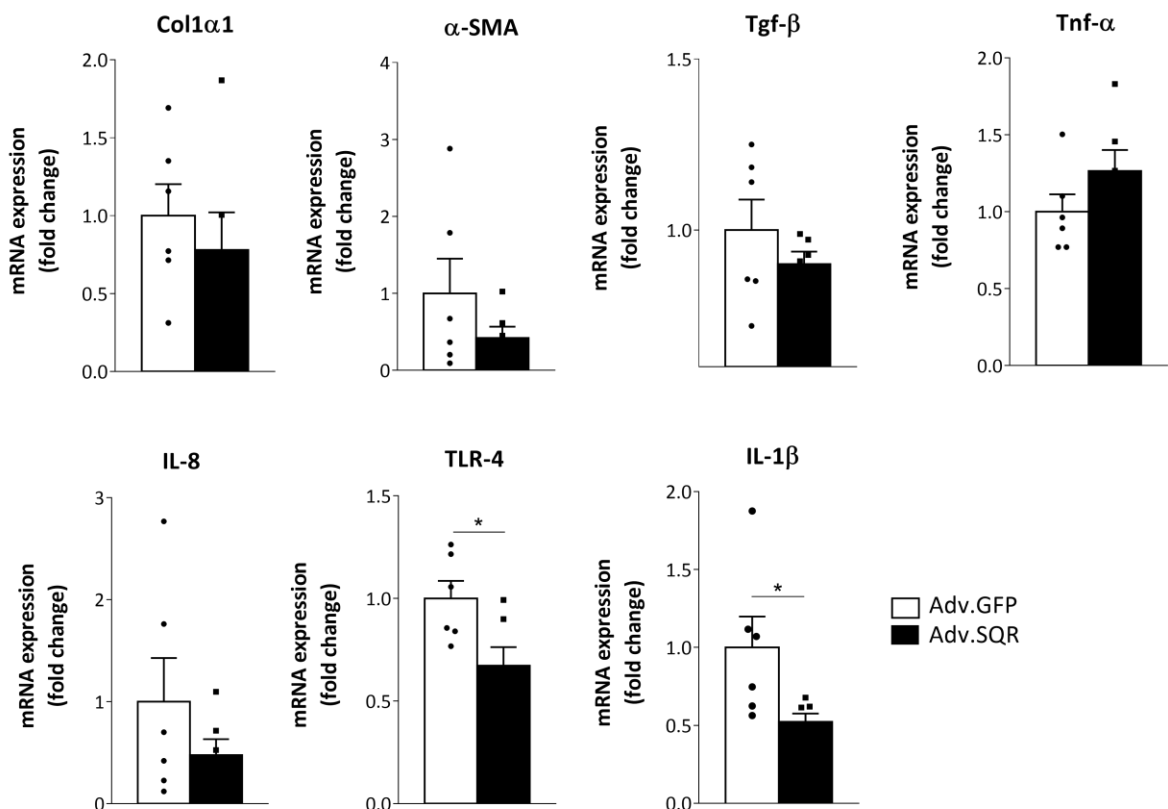


**SQR:** sulfide quinone oxidoreductase; **ETHE1:** dioxygenase; **TST:** thiosulfate sulfurtransferase; **SUOX:** sulfite oxidase; **CBS:** cystathionine  $\beta$ -synthase; **CSE:** cystathionine  $\gamma$ -lyase; **MPST:** 3-mercaptopyruvate sulfurtransferase. Results are represented as mean  $\pm$  SEM (n=6 per group). \* p<0.05, \*\* p<0.01 indicate significant differences (Mann Whitney U test).

By contrast to what observed at the protein level (see Article Figure 4B and 4C; increased hepatic protein levels of TST and SUOX), liver SQR overexpression induced a decrease in hepatic SUOX mRNA level whereas the mRNA levels of ETHE1 and TST remained unchanged. For H<sub>2</sub>S biosynthesis, CBS and CSE mRNA levels decreased following SQR overexpression, similarly to what observed for their protein levels (see Article Figure 4B and 4C). Only MPST mRNA level remained

unchanged. The absence of correlation between mRNA and protein levels could be due to several reasons, such as 1) complex, and not so well-defined, post-transcriptional regulation of these genes, 2) difference in their protein half-lives, and 3) unknown post-translational regulation. Additionally, as observed at the protein level (see Article Figure 4B), liver overexpression of the human SQR did not affect the transcriptional expression of the mouse SQR.

## Genes involved in inflammation and fibrosis



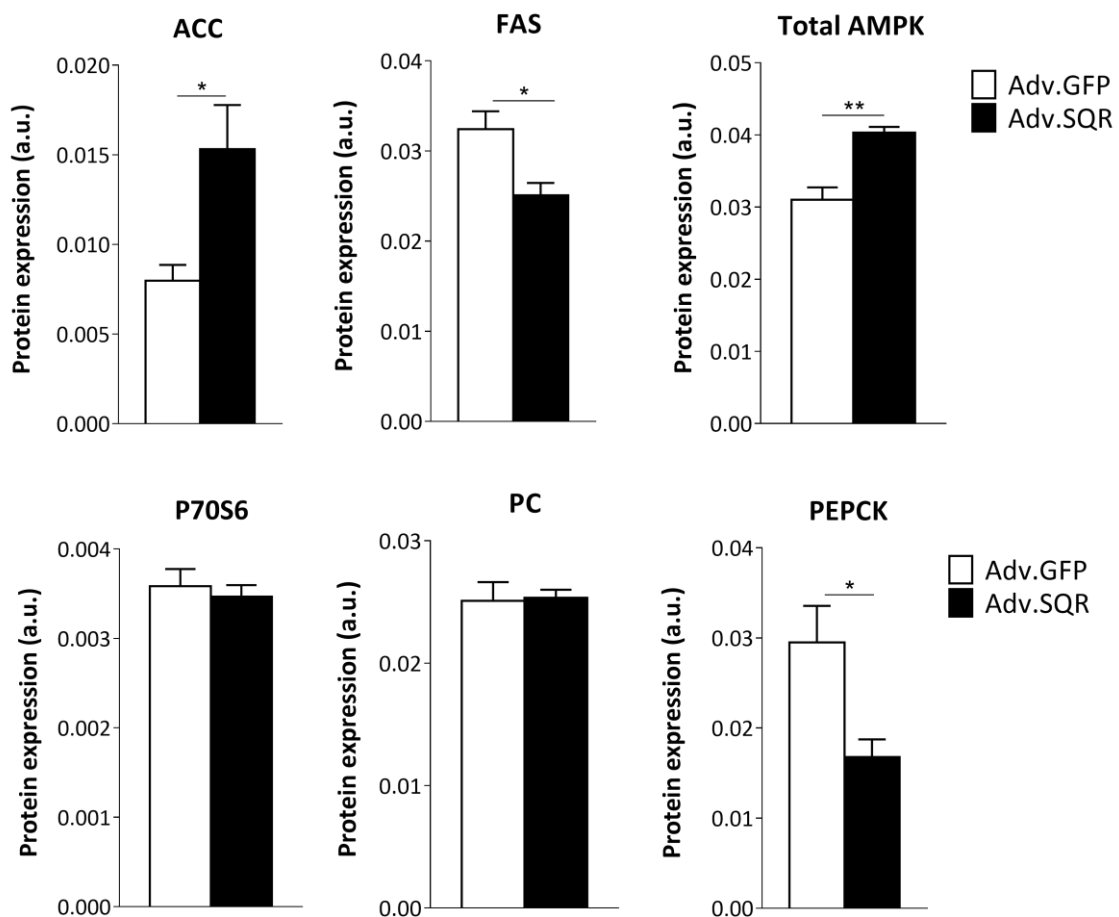
**Col1α1**: collagen type I alpha 1; **α-SMA**: alpha-smooth muscle actin; **Tgf-β**: Transforming growth factor beta; **TNFα**: tumor necrosis factor alpha; **IL-8**: interleukin 8; **TLR-4**: Toll-like receptor 4; **IL-1β**: interleukin 1 beta. Results are represented as mean ± SEM (n=6- per group). \* p<0.05,\*\* p<0.01 indicate significant differences (Mann Whitney U test)

The mRNA levels of key genes involved in inflammation (TGF-β, TNFα, IL-8, TLR-4 and IL-1β) and fibrosis (Col1α1 and α-SMA) were analysed. No significant change in fibrosis gene expression could be observed following liver SQR overexpression. Interestingly, Adv.SQR mice had lower hepatic mRNA level of two pro-inflammatory signalling mediators, TLR-4 and IL-1β. TLR-4 is activated upon the binding of the Gram-negative bacteria cell-wall component, LPS, generating inflammatory



cytokines, such as TNF $\alpha$  and IL-1 $\beta$ . Furthermore, TLR-4 activates pro-inflammatory kinases that impair insulin signal transduction [772]. Therefore, these results corroborate the beneficial effect of liver SQR overexpression on hepatic insulin signalling.

## Proteins involved in glucose metabolism and insulin signalling



**ACC:** acetyl-CoA carboxylase; **FAS:** fatty acid synthase; **AMPK:** 5' AMP-activated protein kinase; **P70S6:** ribosomal protein S6 kinase beta-1; **PC:** pyruvate carboxylase; **PEPCK:** phosphoenolpyruvate carboxykinase. Results are represented as mean  $\pm$  SEM (n=6 per group). \* p<0.05, \*\* p<0.01 indicate significant differences (Mann Whitney U test).

The protein expression levels of other genes involved in lipogenesis (ACC and FAS), glucose catabolism (PC), gluconeogenesis (PEPCK) and insulin signalling (P70S6) were analysed. Whereas P70S6 and PC protein levels remained unchanged, liver SQR overexpression increased ACC and AMPK protein levels and decreased FAS and PEPCK protein levels. These results could partially corroborate our finding that liver SQR overexpression decreases mitochondrial FA oxidation (increased ACC level). Surprisingly, although liver SQR overexpression did not impact pyruvate

tolerance test, it decreased hepatic PEPCK protein level, suggesting a decreased rate of gluconeogenesis.

**Chapter 2:**  
**Mitochondrial H<sub>2</sub>S oxidation in  
liver pathology**



## Problematic

The development of NAFLD is conditioned by alterations in lipid metabolism, oxidative stress, insulin signalling and inflammation [391, 392]. Several studies have shown that all of these pathological processes can be associated to dysregulations in hepatic H<sub>2</sub>S. Indeed, recent data from the literature suggest that hepatic H<sub>2</sub>S biosynthesis is impaired in NAFLD animal models and in obese individuals [707, 708, 710], and that administration of H<sub>2</sub>S donors (such as NaHS and Na<sub>2</sub>S) in these animals can prevent the further development of NASH by decreasing hepatic steatosis, oxidative stress and inflammation [711, 721, 723]. Although some preliminary reports allude to NAFLD animal models expressing less SQR [734], no study has ever been conducted to fully characterize the pathway of mitochondrial H<sub>2</sub>S oxidation in a mammalian model of NAFLD.

Therefore, in this study, we assessed i) whether or not liver mitochondrial H<sub>2</sub>S oxidation is regulated in mouse models of NAFLD and in obese humans, and ii) what are the pathophysiological effects of *in vivo* sodium thiosulfate (STS) supplementation on liver mitochondrial H<sub>2</sub>S oxidation and lipid metabolism. Furthermore, given that STS is an H<sub>2</sub>S donor majorly metabolized in the gut, we also assessed iii) whether or not STS supplementation led to changes in gut microbiota composition and how these changes could be associated to NAFLD profile.

Based on previous studies, our hypothesis was that STS supplementation would decrease liver steatosis in the HF/HS-fed mice and decrease inflammation and fibrosis in the MCD-fed mice. At the same time, we hoped these changes would be accompanied by shifts in liver mitochondrial H<sub>2</sub>S oxidation and microbiota composition.

## Results

### 1. Animal model of NAFL

In order to develop an animal model of NAFL, two diets were purchased from the company “Research Diets”: one diet of standard composition (SD) for the control group (D12451) and one diet enriched in fat and sucrose (HF/HS) (45% fat, 20% protein, 35% carbohydrates of which 17.4% corresponded to sucrose) for the model of NAFL (D12450J). The HF/HS diet has been used in rodents to increase blood glycemia, body weight, adiposity and IR [743-745]. Indeed, it is thought that this diet combination closely resembles the diet that has dramatically increased obesity levels in humans over the past few decades. Adult male C57Bl6/J mice were fed these two diets for 10 or 20 weeks. These animals were subjected to a weekly control of body weight and food intake.

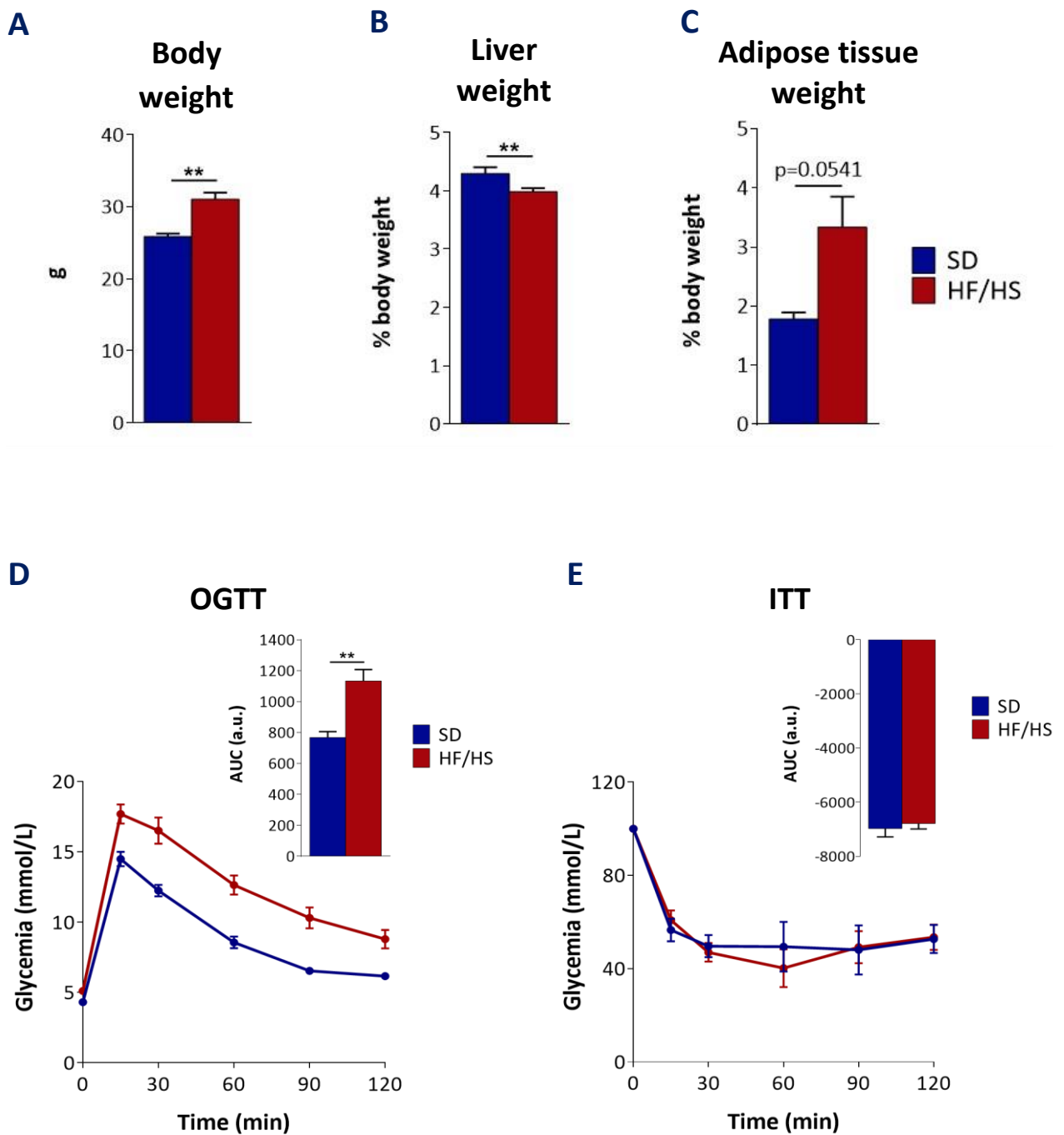


**Figure 39: Impact of 10 weeks of HF/HS feeding on mouse body weight (A), liver weight (B), adipose tissue weight (C), glucose tolerance (D) and insulin sensitivity (E)**

Results are represented as mean ± SEM (n=7-8 per group). \*\* p<0.01 indicates significant differences (Mann Whitney U test).

After the first 8 weeks of diet administration, oral glucose tolerance (OGTT) and insulin sensitivity tests (ITT) were performed. Ten weeks after the study began, a group of HF/HS- and SD-fed animals were sacrificed, while the remaining animals were set aside and fed for 10 more weeks (total of 20 weeks of diet challenge).

### 1.1. HF/HS-diet challenge for 10 weeks

#### **a) Body weight, glucose tolerance and insulin sensitivity**

Mice fed HF/HS diet for 10 weeks had a significantly increased body weight (+20%) (**Figure 39A**) and a lower liver/body weight ratio (**Figure 39B**). Adipose tissue weight increased by 87% without however reaching statistical significance (**Figure 39C**). As expected, HF/HS diet for 8 weeks induced glucose intolerance (**Figure 39D**) but no insulin resistance (**Figure 39D**).

#### **b) Liver mitochondrial H<sub>2</sub>S oxidation and respiration**

Liver mitochondria from mice fed HF/HS or SD diet for 10 weeks were analysed for their capacity to oxidize H<sub>2</sub>S by measuring O<sub>2</sub> consumption following successive injections into the Oroboros chamber of increasing concentrations of Na<sub>2</sub>S. Data were plotted using the real values (**Figure 40A**) or calculated as % of state 3 respiration rate by dividing each raw pmol O<sub>2</sub>/s.mg value by the state 3 value of each corresponding mouse (**Figure 40B**). Our results showed no significant differences in the mitochondrial capacity to oxidize H<sub>2</sub>S between SD- and HF/HS-fed mice. However, mitochondria isolated from the HF/HS-fed mice showed a slight tendency to oxidize less H<sub>2</sub>S than control mice (2.73-44.8 pmol O<sub>2</sub>/s.mg vs 3.02-57.5 pmol O<sub>2</sub>/s.mg). The values of the kinetic constants Km and Vmax were calculated by using the Michaelis-Menten equation. Despite observing a slight tendency, the Vmax and Km for H<sub>2</sub>S oxidation between SD- and HF/HS-fed mice were found unchanged (**Table 6**). The catalytic efficiency of the mitochondrial H<sub>2</sub>S oxidation reaction (Vmax/Km) was also found unchanged between SD- and HF/HS-fed mice (**Table 6**).

To evaluate the functionality of the mitochondrial preparations, we assessed mitochondrial respiratory capacity using classical carbon-based substrates: glutamate/malate for Complex I (**Figure 40C**) and succinate plus rotenone for Complex II (**Figure 40D**). Our results showed that mitochondria isolated from mice subjected to HF/HS diet feeding for 10 weeks displayed the same respiratory capacity as SD-fed mice whatever the substrate used. Moreover, RCR was also unchanged by the HF/HS diet.

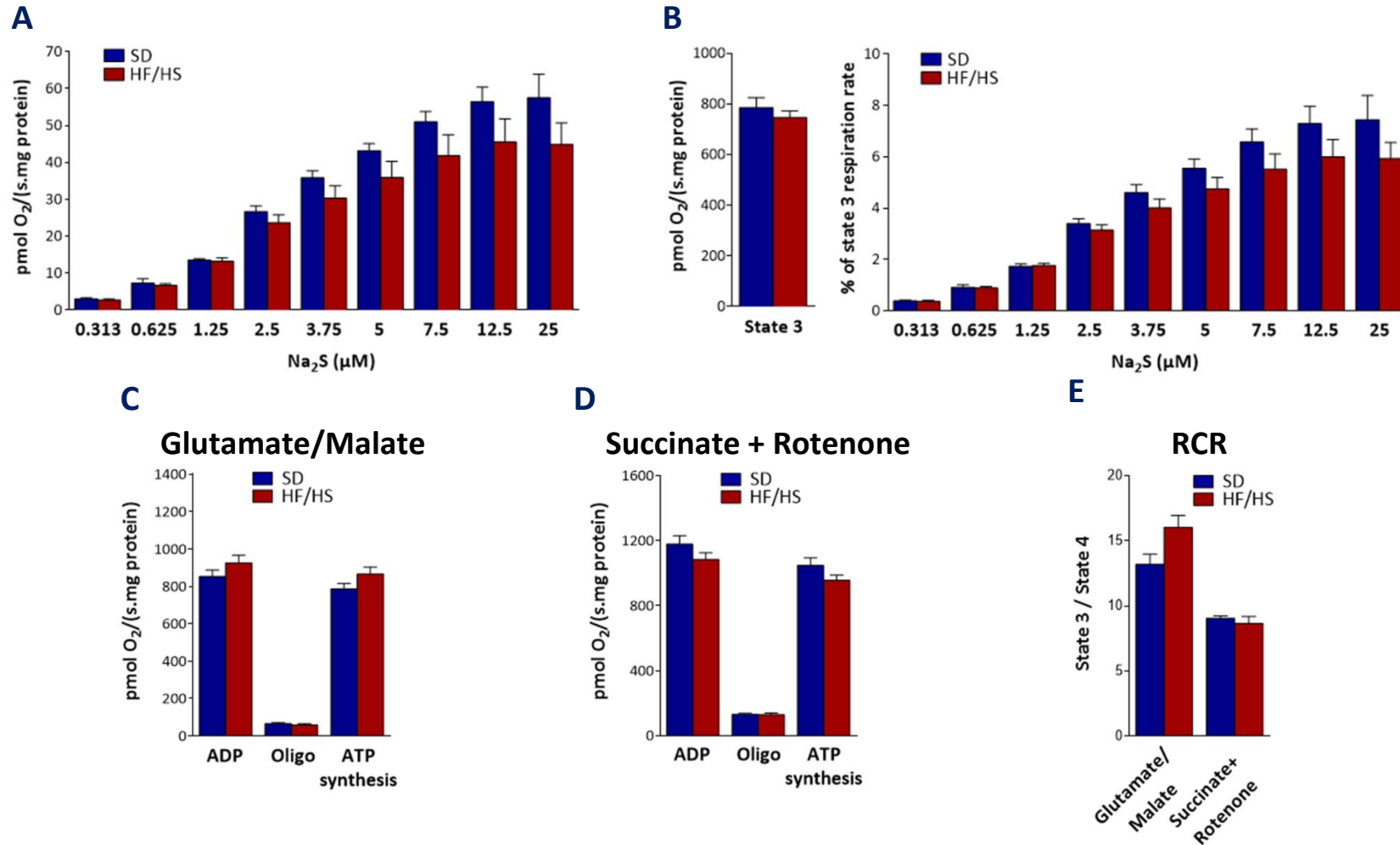


**Figure 40: Impact of 10 weeks of HF/HS-feeding on liver mitochondrial H<sub>2</sub>S oxidation and respiration**

**A)** Sulfide oxidation rates were plotted as a function of Na<sub>2</sub>S concentration and expressed as pmol O<sub>2</sub>/s/mg protein or **B)** as percentage of state 3 respiration rate. **C)** Mitochondrial oxygen consumption rate using either glutamate/malate or **D)** succinate plus rotenone in the presence of ADP (state 3) or oligomycin (Oligo, state 4) to determine respiration linked to ATP synthesis (state 3-state 4) as well as **E)** respiratory control ratio (RCR, state3/state 4). Results are represented as mean ± SEM (n=7-8 per group)



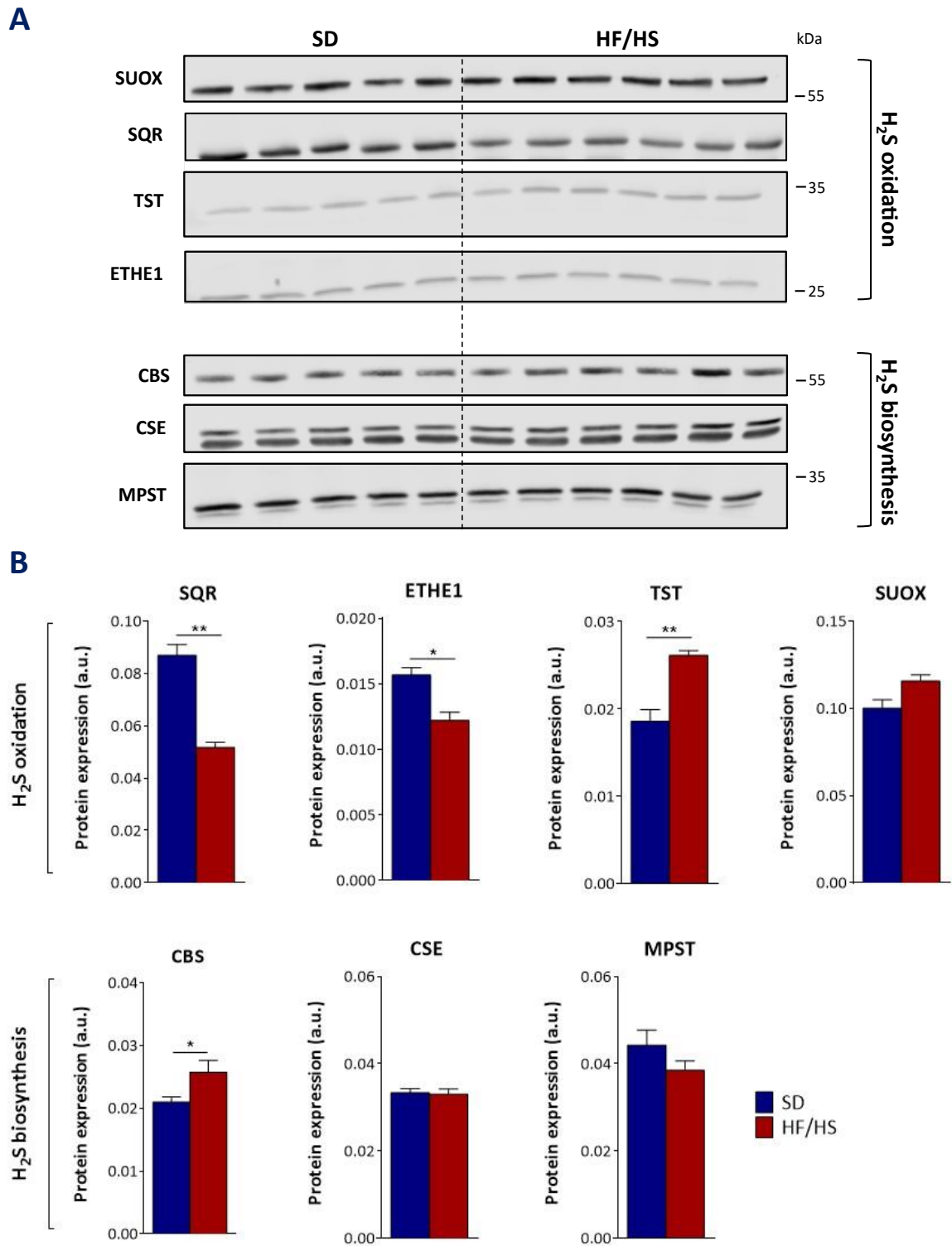


**Figure 41: Protein expression level of enzymes involved in H<sub>2</sub>S oxidation and biosynthesis**

**A)** Immunoblot analysis of the protein expression level of enzymes involved in H<sub>2</sub>S oxidation (SUOX, SQR, TST, ETHE1) and biosynthesis (CBS, CSE, MPST) using liver lysates from 10 weeks HF/HS- and SD-fed mice. **B)** Western blot quantification was normalized by the total quantification of the REVERT signal. Results are represented as mean  $\pm$  SEM (n=5-6 per group).

\* p<0.05, \*\* p<0.01 indicate significant differences (Mann Whitney U test).

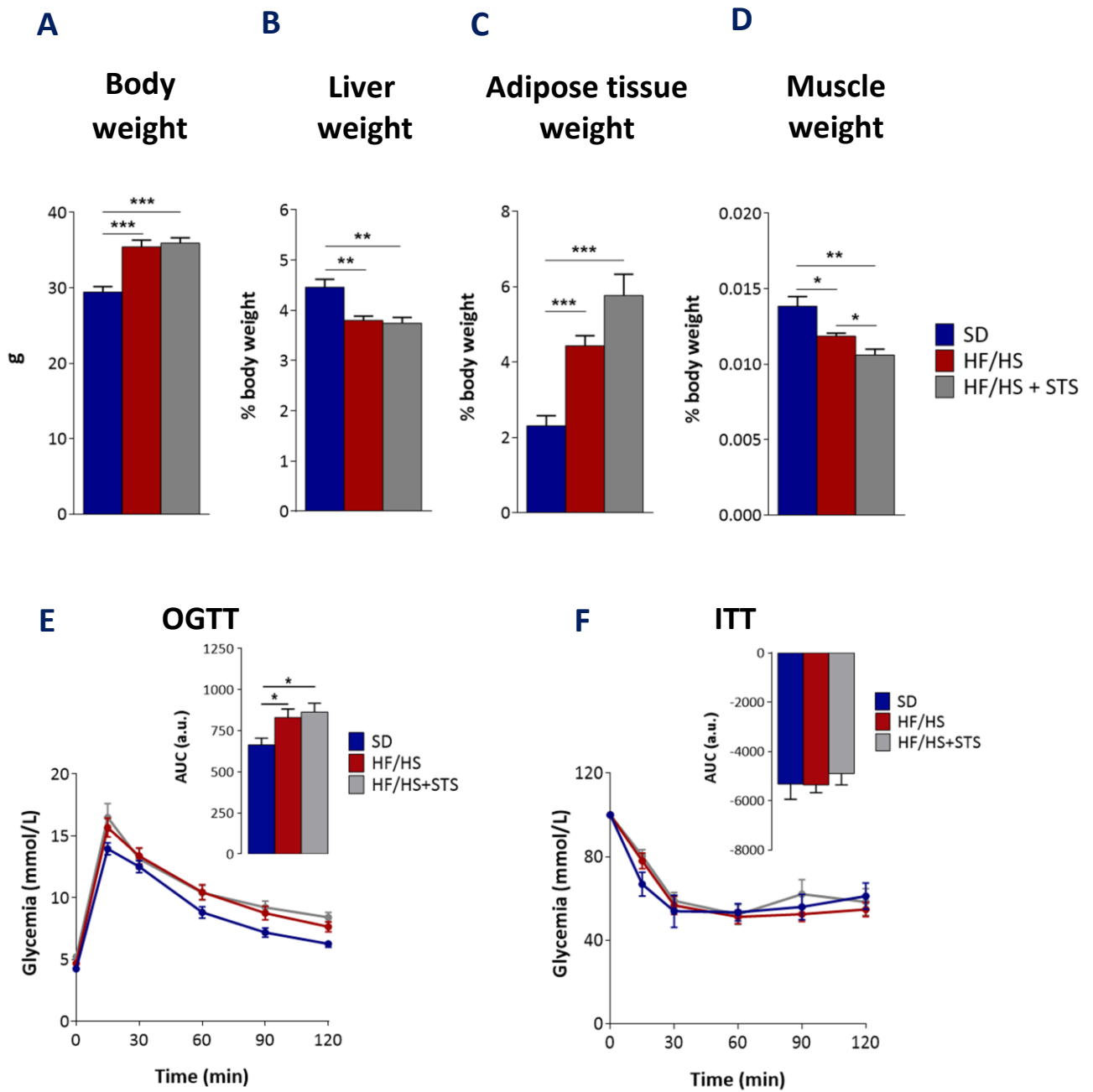


**Figure 42: Impact of 20 weeks of HF/HS feeding plus or minus STS supplementation on mouse body weight (A), liver weight (B), adipose tissue weight (C), muscle weight (D), glucose tolerance (E) and insulin sensitivity (F)**

Results are represented as mean  $\pm$  SEM (n=7-8 per group). \*\* p<0.01, \*\*\* p<0.001 indicate significant differences (Mann Whitney U test).

STS: sodium thiosulfate

### **c) Liver protein expression levels of key enzymes involved in mitochondrial H<sub>2</sub>S oxidation and biosynthesis**

Upon entering mitochondria, H<sub>2</sub>S is directly oxidized by SQR, with the resulting persulfide undergoing a series of modification steps conducted by ETHE1, TST and SUOX (**Figure 8**). Western blotting experiments using liver lysates showed that HF/HS-fed mice had lower protein expression levels of SQR (-40%) and ETHE1 (-22%) and higher TST protein expression level (+41%) when compared to the control mice (**Figure 41A and 41B**). Furthermore, given that H<sub>2</sub>S levels are controlled by both oxidation and biosynthesis, we also assessed the protein expression levels of CBS, CSE and MPST in the liver of HF/HS- and SD-fed mice. Our results showed that a 10 week period of HF/HS feeding significantly increased the hepatic protein expression level of CBS (+23%) whereas CSE and MPST protein expression levels remained unchanged (**Figure 41A and 41B**).

#### 1.2. HF/HS-diet challenge for 20 weeks minus or plus STS supplementation

After 10 weeks of diet intake, the HF/HS-fed animals were split into two groups: one began being supplemented with STS in addition to the HF/HS regime, while the second one received NaCl aside the HF/HS diet. The STS supplementation was done twice a week via IP (0.4 g STS/kg bw) and in the drinking water (3 mg STS/mL). This course of treatment continued for 10 weeks until the sacrifice of the mice. After 18 weeks of diet administration, OGTT and ITT were performed.

#### **a) Body weight, glucose tolerance and insulin sensitivity**

Compared to SD-fed mice, mice fed HF/HS diet for 20 weeks had a significant increase in body weight (+25%) (**Figure 42A**) and adiposity (+107%) (**Figure 42C**), lower liver/body weight ratio (**Figure 42B**) and muscle/body weight ratio (**Figure 42D**), and glucose intolerance (**Figure 42E**). Unexpectedly, after 18 weeks of diet intake, no insulin resistance could be observed in HF/HS-fed mice (**Figure 42F**). One explanation could be that, for the 10 week timepoint, we used the mice that presented the highest glucose intolerance, thus keeping the less- or non-responsive mice to be fed for a longer time with HF/HS diet. Another explanation for the lack of insulin resistance could be the existence of a questionable diet batch. Indeed, in a first series of HF/HS diet feeding for 20 weeks (in the same animal facility), HF/HS-fed mice displayed both glucose intolerance and insulin resistance (Results not shown). Unfortunately, a HF/HS-fed group + STS supplementation

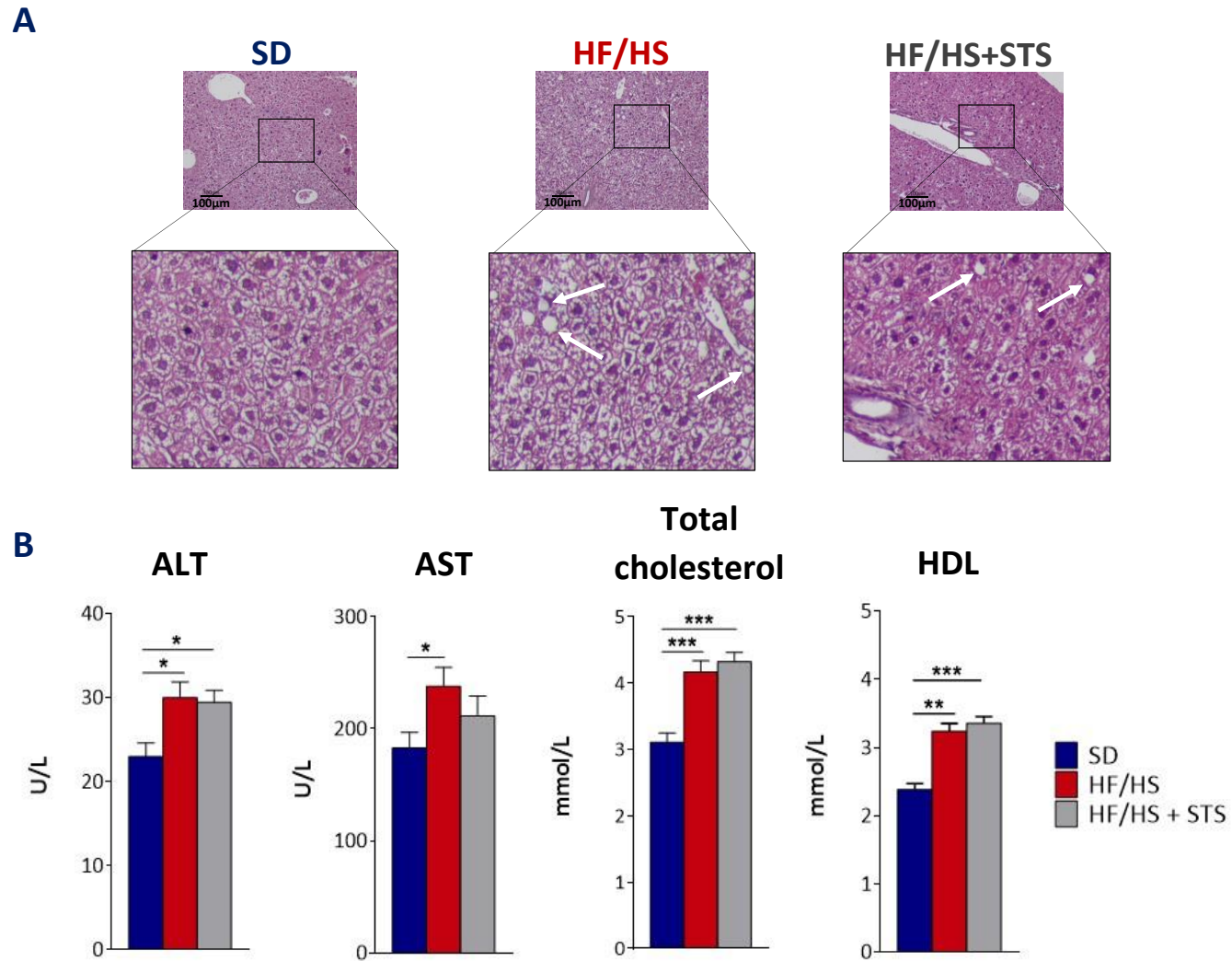


**Figure 43: Impact of 20 weeks of HF/HS feeding plus or minus STS supplementation on liver histology (A) and on different plasma parameters (B)**

Haematoxylin and eosin staining of liver sections (magnification x100). White arrows indicate lipid droplets Results are represented as mean  $\pm$  SEM (n=7-8 per group). \*  $p < 0.05$ , \*\*  $p < 0.01$ , \*\*\*  $p < 0.001$  indicate significant differences (Mann Whitney U test).. STS: sodium thiosulfate

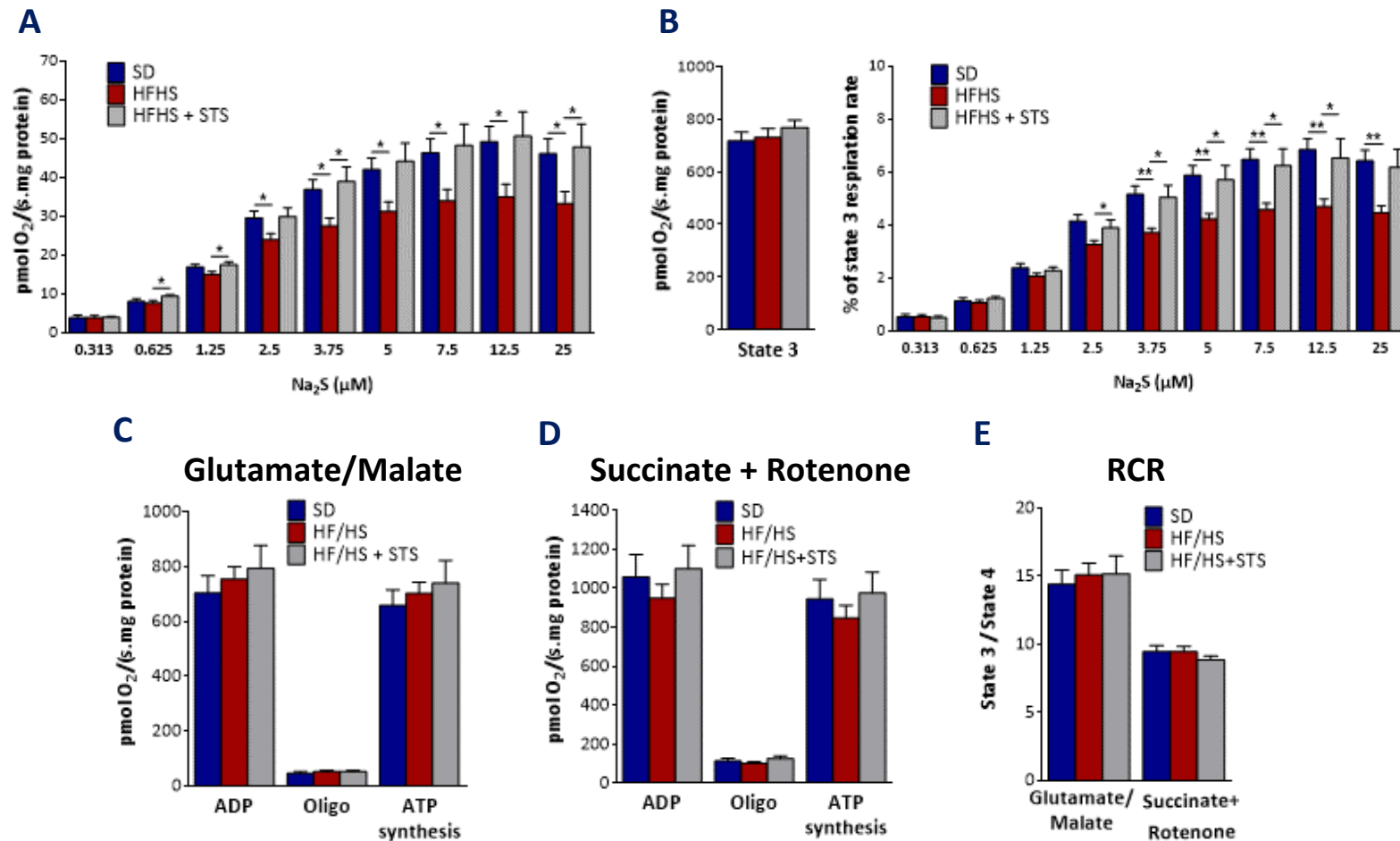


**Figure 44: Impact of 20 weeks of HF/HS-feeding plus or minus STS supplementation on liver mitochondrial H<sub>2</sub>S oxidation and respiration**

**A)** Sulfide oxidation rates were plotted as a function of Na<sub>2</sub>S concentration and expressed as pmol O<sub>2</sub>/s/mg protein or **B)** as percentage of state 3 respiration rate. **C)** Mitochondrial oxygen consumption rate using either glutamate/malate or **D)** succinate plus rotenone in the presence of ADP (state 3) or oligomycin (Oligo, state 4) to determine respiration linked to ATP synthesis (state 3-state 4) as well as **E)** respiratory control ratio (RCR, state3/state 4). Results are represented as mean ± SEM (n7-8 per group). \* p<0.05 and \*\* p<0.01 indicate significant differences (Mann Whitney U test). **STS:** sodium thiosulfate

**10 weeks**

	<b>Vmax</b>	<i>P value</i>	<b>Km</b>	<i>P value</i>	<b>Vmax/Km</b>	<i>P value</i>
<b>SD</b>	56.76 ± 4.90		2.32 ± 0.14		24.40 ± 1.36	
<b>HF/HS</b>	39.92 ± 4.03	n.s.	1.77 ± 0.20	n.s.	23.09 ± 1.22	n.s.

**20 weeks**

	<b>Vmax</b>	<i>P value</i>	<b>Km</b>	<i>P value</i>	<b>Vmax/Km</b>	<i>P value</i>
<b>SD</b>	56.76 ± 4.90		2.32 ± 0.14		24.40 ± 1.36	
<b>HF/HS</b>	39.92 ± 4.03	*p<0.05	1.77 ± 0.20	*p<0.05	23.09 ± 1.22	#p<0.05
<b>HF/HS+STS</b>	58.94 ± 7.78		2.21 ± 0.28		26.57 ± 0.86	

**Table 6: Determination of Vmax and Km values for mitochondrial H<sub>2</sub>S oxidation in SD-, HF/HS-fed mice and HF/HS+STS mice**

Results are represented as mean ± SEM (n=5-11 per group). \*HF/HS vs SD; # HF/HS+STS vs HF/HS

STS: sodium thiosulfate; n.s: not significant

was not included in this first series. In order to fully develop a NAFLD animal model, the study should have been continued for a few more months. This premise was further corroborated by histological staining of liver slices, which showed that HF/HS-fed mice presented very few lipid droplets (**Figure 43A**). Nevertheless, in this second series, the 20 weeks of HF/HS diet feeding already increased the plasma levels of ALT (+30%), AST (+30%), total cholesterol (+34%) and HDL cholesterol (+36%) (**Figure 43B**).

Next, we investigated the impact of STS supplementation during the last 10 weeks of HF/HS diet feeding. Our results showed that, when compared to HF/HS-fed animals, STS supplementation exerted no significant effect on body weight (**Figure 42A**), liver/body weight ratio (**Figure 42B**) or adiposity (**Figure 42C**). However, STS supplementation trend to decrease the muscle/body weight ratio, with HF/HS+STS mice showing a 10% decrease when compared to the HF/HS-fed mice (**Figure 42D**). Compared to HF/HS-fed mice, HF/HS+STS mice had similar glucose intolerance (**Figure 42E**) and insulin sensitivity (**Figure 42F**). When performing histological staining of liver sections, we observed no major differences between HF/HS+STS mice and HF/HS-fed mice (**Figure 43A**). Similarly, we could not detect alterations in different plasma parameters such as ALT, AST, total cholesterol or HDL-cholesterol between these two groups (**Figure 43B**). These results indicate that STS supplementation could not reverse the HF/HS-induced phenotypic changes.

### **b) Liver mitochondrial H<sub>2</sub>S oxidation and respiration**

Liver mitochondria from SD-, HF/HS- and HF/HS+STS-fed mice were tested for their capacity to oxidize H<sub>2</sub>S, as previously described for the 10 week-period of HF/HS diet feeding. Data were plotted using the real values (**Figure 44A**) or calculated as % of state 3 respiration rate by dividing each raw pmol O<sub>2</sub>/s.mg value by the state 3 value of each corresponding mouse (**Figure 44B**). For concentrations of Na<sub>2</sub>S between 3.75 μM and 25 μM, liver mitochondria from HF/HS-fed mice had a reduced capacity to oxidize H<sub>2</sub>S (3.82-4.44% of state 3 respiration) when compared to SD-fed mice (5.15-6.42% of state 3 respiration) (**Figure 44B**). Interestingly, this negative impact caused by a prolonged HF/HS diet feeding on mitochondrial H<sub>2</sub>S oxidation was abrogated by STS supplementation, with HF/HS+STS mice presenting values (5.04-6.17% of state 3 respiration) similar to those measured in SD-fed mice. We also calculated the values of the kinetic constants Km and Vmax using the Michaelis-Menten equation. HF/HS-fed animals presented lower Vmax and Km when compared to SD-fed animals (**Table 7**). STS supplementation increased the Vmax

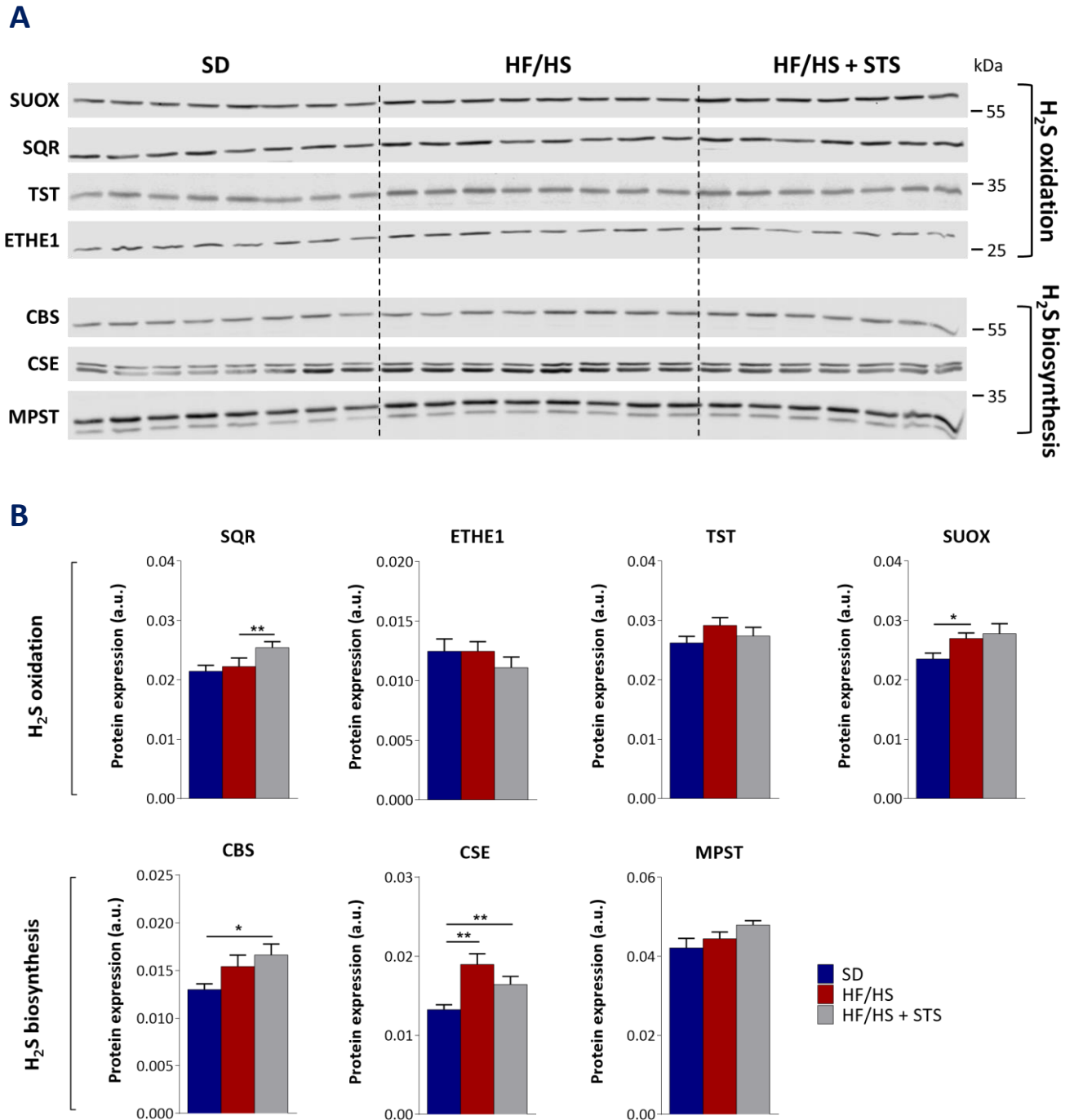


**Figure 45: Protein expression level of enzymes involved in H<sub>2</sub>S oxidation and biosynthesis**

**A)** Immunoblot analysis of the protein expression level of enzymes involved in H<sub>2</sub>S oxidation (SUOX, SQR, TST, ETHE1) and biosynthesis (CBS, CSE, MPST) using liver lysates from SD-, HF/HS-, HF/HS+STS-fed mice. **B)** Western blot quantification was normalized by the total quantification of the REVERT signal. Results are represented as mean  $\pm$  SEM (n=7-8 per group). \* p<0.05, \*\* p<0.01 indicate significant differences (Mann Whitney U test).

STS: sodium thiosulfate



and Km values without however reaching statistical significance (**Table 7**). Nevertheless, HF/HS+STS mice present higher catalytic efficiency ( $V_{max}/K_m$ ) than HF/HS-fed animals (**Table 7**).

The observed effects of HF/HS diet feeding and of STS supplementation on liver mitochondrial H<sub>2</sub>S oxidation could not be explained by changes in the functionality of isolated liver mitochondria. Indeed, liver mitochondria isolated from SD-, HF/HS- and HF/HS+STS mice displayed the same respiration rates in the presence of glutamate/malate (**Figure 44C**) and succinate plus rotenone (**Figure 44D**), and similar RCR values (**Figure 44E**).

### **c) Liver protein expression levels of key enzymes involved in mitochondrial H<sub>2</sub>S oxidation and biosynthesis**

By contrast to what observed after 10 weeks of HF/HS diet feeding, Western blotting experiments using liver lysates showed that HF/HS diet feeding for 20 weeks had only minor effects on the protein expression level of enzymes involved in H<sub>2</sub>S oxidation. Indeed, only the protein level of SUOX was significantly increased (+15%) (**Figure 45A and 45B**). Interestingly, HF/HS+STS mice presented a significant increase in the hepatic protein level of SQR (+14%) when compared to HF/HS-fed mice (**Figure 45A and 45B**). When assessing the protein expression of CBS, CSE and MPST in the liver of all three groups, we observed that HF/HS diet feeding for 20 weeks increased the hepatic protein level of CSE (+43%) while it had no effect on the protein expression level of MPST and CBS (only a tendency was noticed), the latter being however significantly increased by STS supplementation when compared to SD-fed mice (**Figure 45A and 45B**).

### **d) Plasma and liver lipids**

Using lipidomic techniques (collaboration with A. Gastaldelli and Sara Guerra, Pisa, Italy), we assessed the lipid content and lipid species composition of plasma (**Figure 46**) and liver (**Figure 47**). We observed that HF/HS diet feeding for 20 weeks increased the total circulating levels of TGs, ceramides, sphingomyelins and phosphatidylethanolamines (**Figure 46**). Interestingly, STS supplementation was able to revert this profile, with HF/HS+STS mice having circulating lipid levels similar to those measured in SD-fed mice (**Figure 46**). In the liver, we also observed a tendency for increased liver TGs content ( $p=0.0501$ ) in HF/HS-fed mice compared to SD-fed mice (**Figure 47**) although HF/HS diet had no significant impact on other liver lipid classes. Sadly, we were not able to quantify TGs by the lipidomics method in the liver of HF/HS+STS mice due to a technical problem.

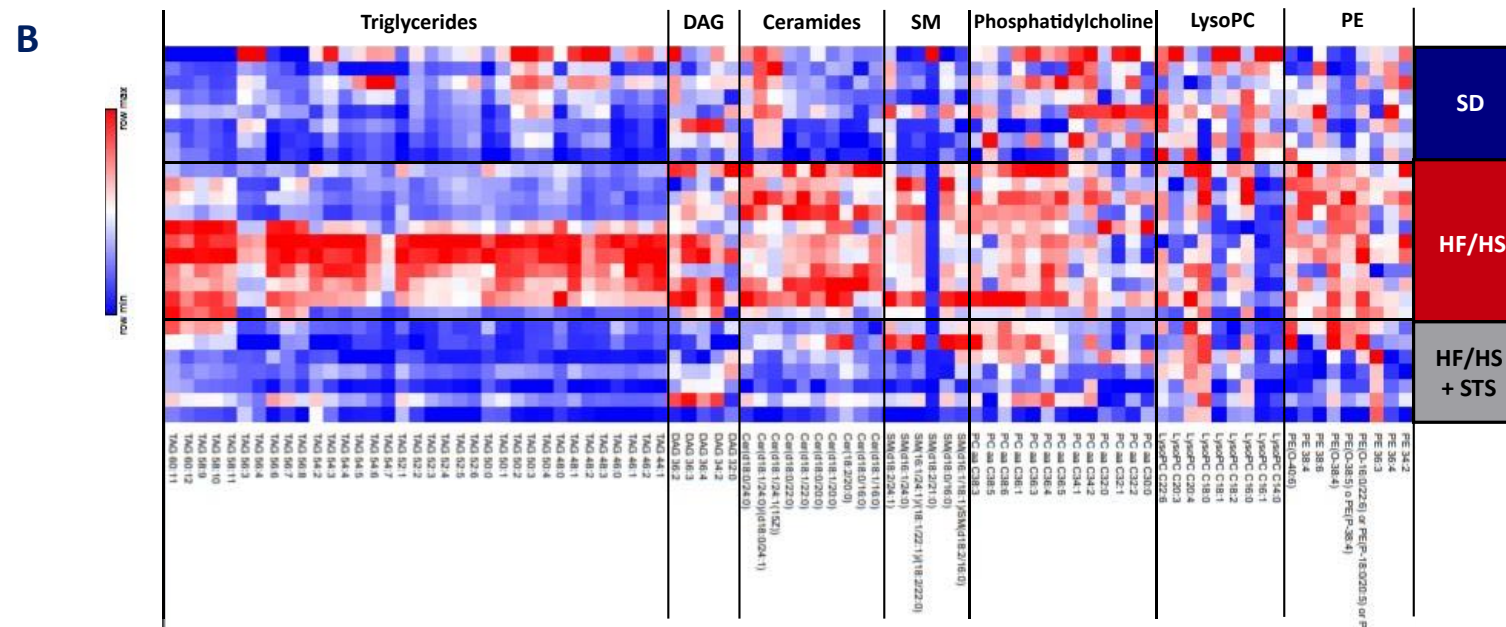
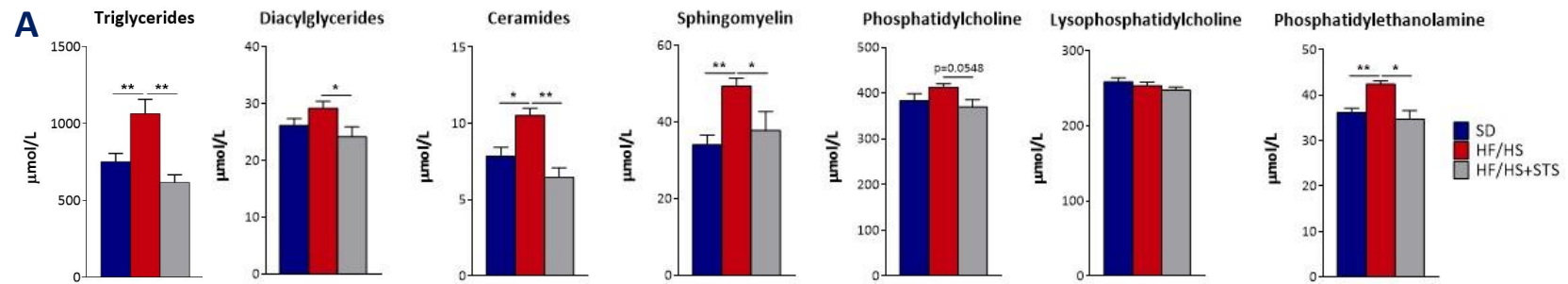
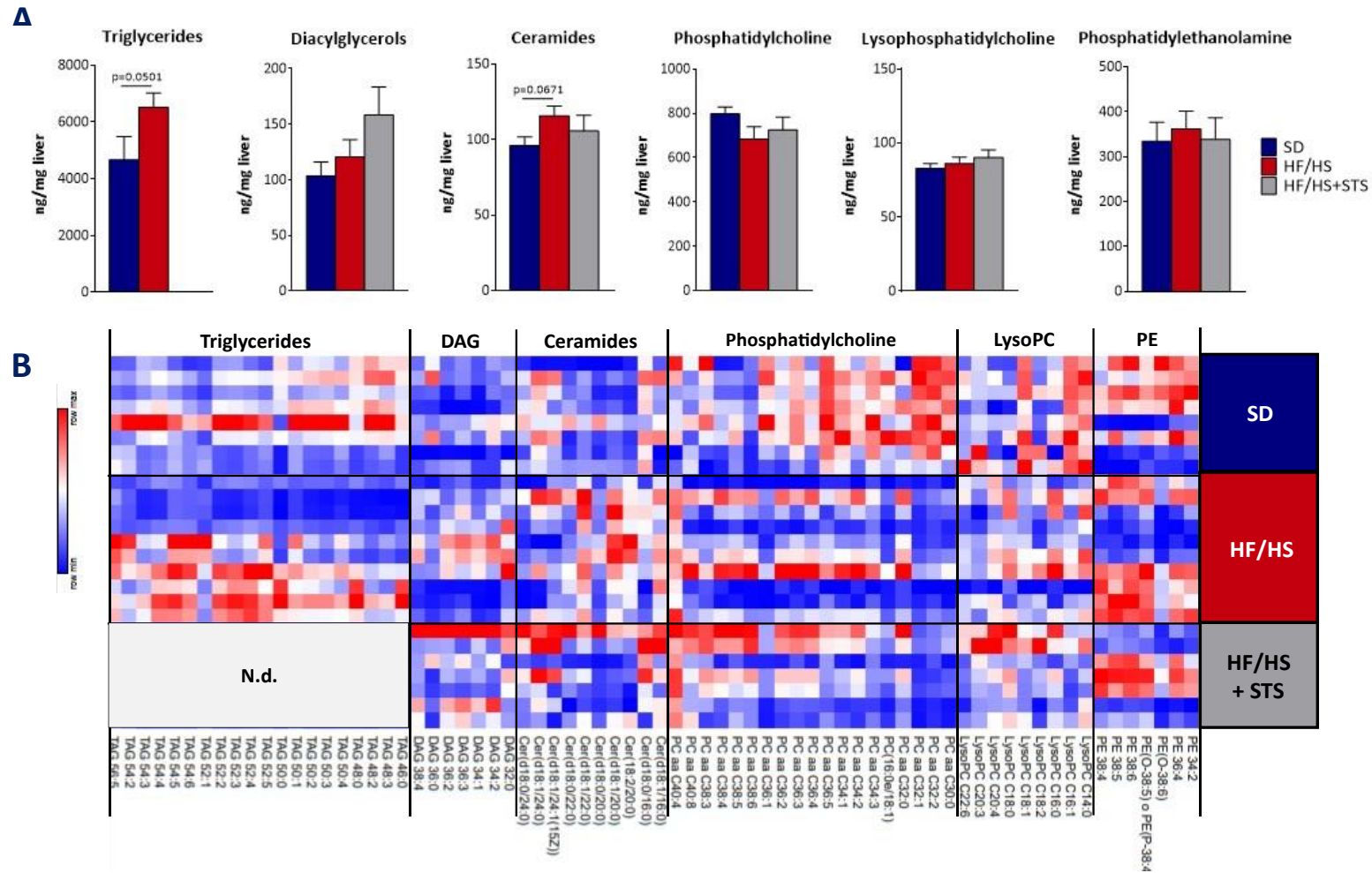


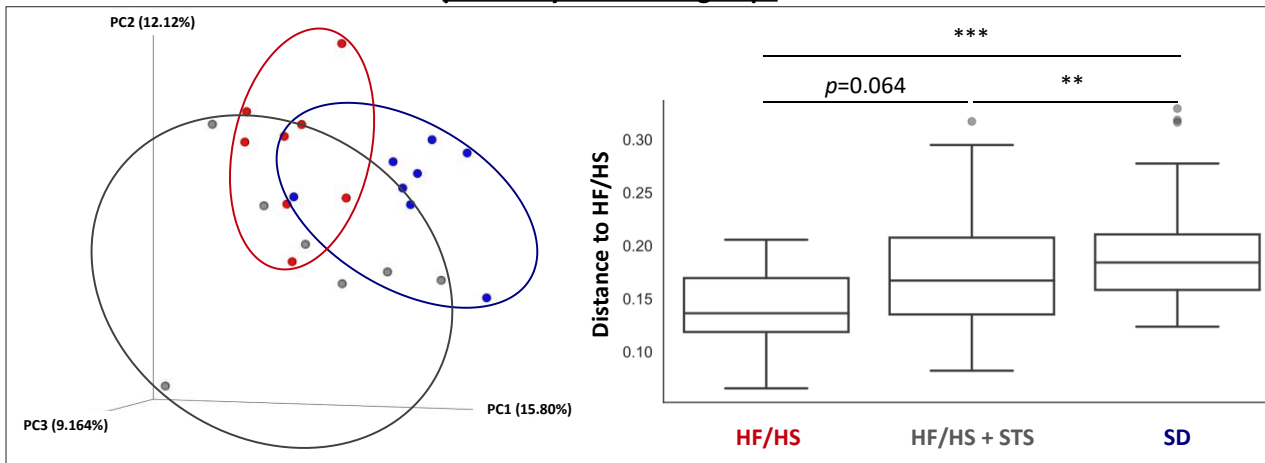
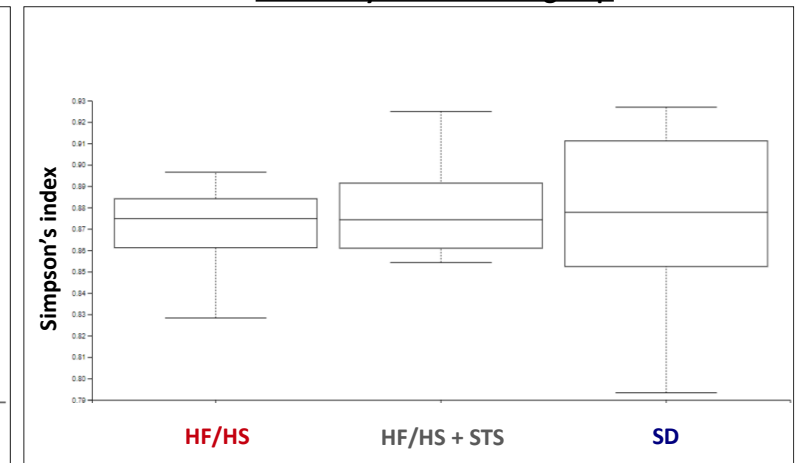
**Figure 46: Effect of HF/HS diet and STS supplementation on circulating lipids**

**A)** Lipidomic analysis of total plasma levels of triglycerides, diacylglycerides (DAG), ceramides, sphingomyelin (SM), phosphatidylcholine, lysophosphatidylcholine (LysoPC) and phosphatidylethanolamine (PE). **B)** Heat map showing the different lipid species present in the different lipid classes. Results are represented as mean  $\pm$  SEM (n=7-8 per group). \* p<0.05, \*\* p<0.01 indicate significant differences (Mann Whitney U test). **STS:** sodium thiosulfate

**B)**



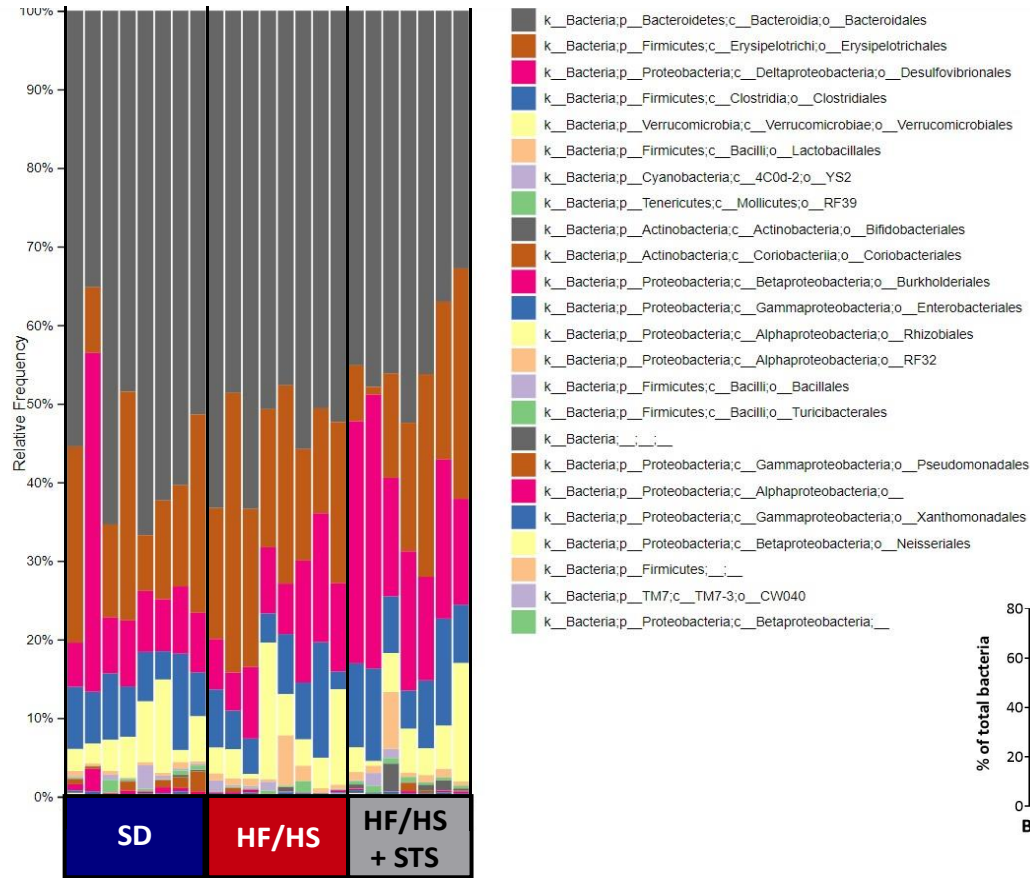
**A)** Lipidomic analysis of total liver levels of triglycerides, diacylglycerides (DAG), ceramides, phosphatidylcholine, lysophosphatidylcholine (LysoPC) and phosphatidylethanolamine (PE). **B)** Heat map showing the different lipid species present in the different lipid classes. Results are represented as mean  $\pm$  SEM (n=6-8 per group). \*  $p < 0.05$ , \*\*  $p < 0.01$  indicate significant differences (Mann Whitney U test). **N.d.**: not determined; **STS**: sodium thiosulfate

**A** **$\beta$  diversity – between groups****B** **$\alpha$  diversity – within each group****Figure 48: Effect of HF/HS diet and STS supplementation on gut microbiota diversity**

**A)** Principal component analysis (PCA) of the unweighted UniFrac distance matrix of fecal microbiota from SD-, HF/HS- and HF/HS+STS-fed mice. **B)** Microbiota richness and diversity in SD-, HF/HS- and HF/HS+STS-fed mice, based on the Simpson's Index. Categories were compared and statistical significance of clustering were determined via Permanova. Results are represented as mean  $\pm$  SEM (n=7-8 per group). \*\* p<0.01, \*\*\*p<0.001 indicate significant differences.

**STS:** sodium thiosulfate

**A**



**B**

	W
K_Bacteria;p__Bacteroidetes;c__Bacteroidia;o__Bacteroidales;f__Porphyromonadaceae	11
K_Bacteria;p__Actinobacteria;c__Actinobacteria;o__Bifidobacteriales;f__Bifidobacteriaceae	7
K_Bacteria;p__Firmicutes;c__Bacilli;o__Lactobacillales;f__Streptococcaceae	6
K_Bacteria;p__Bacteroidetes;c__Bacteroidia;o__Bacteroidales;f__Rikenellaceae	3
K_Bacteria;p__Actinobacteria;c__Coriobacterii;o__Coriobacteriales;f__Coriobacteriaceae	3
K_Bacteria;p__Bacteroidetes;c__Bacteroidia;o__Bacteroidales;f__	3
K_Bacteria;p__Proteobacteria;c__Deltaproteobacteria;o__Desulfuovibrionales;f__Desulfuovibrionaceae	2
K_Bacteria;p__Proteobacteria;c__Alphaproteobacteria;o__RF32;f__	2
K_Bacteria;p__Firmicutes;c__Erysipelotrichi;o__Erysipelotrichales;f__Erysipelotrichaceae	2
K_Bacteria;p__Bacteroidetes;c__Bacteroidia;o__Bacteroidales;f__	2
K_Bacteria;p__Bacteroidetes;c__Bacteroidia;o__Bacteroidales;f__S24-7	1
K_Bacteria;p__Proteobacteria;c__Gammaproteobacteria;o__Xanthomonadales;f__Xanthomonadaceae	1
K_Bacteria;p__Firmicutes;c__Clostridia;o__Clostridiales;f__Ruminococcaceae	1

**C**

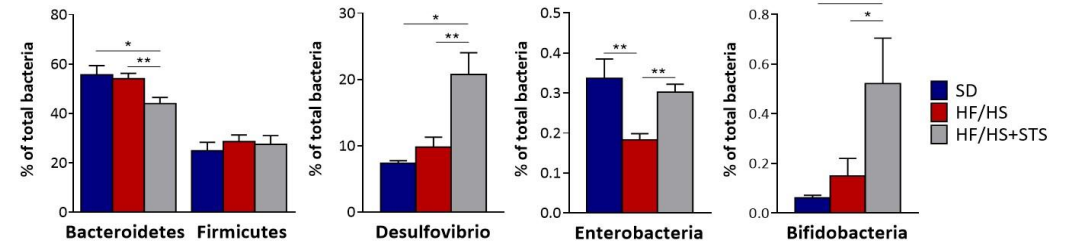


**Figure 49: Effect of HF/HS diet and STS supplementation on gut microbiota composition**

Bacterial-taxon–based analysis of feces at the phylum level. **B)** Differentially abundant microbial taxa identified by Analysis of Composition of Microbiomes (ANCOM). **C)** Fecal percentage of Bacteroidetes, Firmicutes, Desulfovibrio and Bifidobacteria in SD-, HF/HS- and HF/HS+STS-fed mice. Results are represented as mean ± SEM (n=7-8 per group). \* p<0.05 and \*\*p<0.01 indicate significant differences. **STS:** sodium thiosulfate

### 1.3. Impact of HF/HS diet and STS supplementation on gut microbiota

This part was performed with the helpful collaboration of Dr. Benoît Chassaing (Institut Cochin, Paris, France).

Through 16S RNA sequencing of fecal samples we were able to observe that HF/HS diet feeding for 20 weeks and STS supplementation had both an impact on gut microbiota (**Figure 48**). In accordance to the visual assessment of the PCA plots (**Figure 48A**), the UniFrac distances between SD- and HF/HS-fed mice or SD-fed and HF/HS+STS mice were significantly high (**Figure 48A**), which indicates that the microbial communities have changed between groups. We could further observe a tendency for microbial variation between HF/HS-fed and HF/HS+STS mice ( $p=0.064$ ) (**Figure 48A**). These altered compositions did not result from higher microbial richness within each mouse sample, as shown by the unchanging  $\alpha$ -diversity (**Figure 48B**). When looking at the taxonomy summary of all gut microbiota (at the class level), we could not perceive drastic changes caused by HF/HS diet feeding or STS supplementation (**Figure 49A**). However, when doing ANCOM statistical analysis, which indicates which organism(s) differentiate the groups, we observed some specific changes (**Figure 49B**). A closer analysis showed that, when compared to HF/HS-fed mice, HF/HS+STS mice presented a reduced percentage of Bacteroidetes (-19%) and increased percentages of Desulfovibrio (+250%) and Bifidobacteria (+66%) (**Figure 49C**). Interestingly, the percentage of Enterobacteria was decreased by 56% in HF/HS-fed mice when compared SD-fed mice, and this HF/HS-induced impact was abrogated by STS supplementation (**Figure 49C**).

## 2. Animal model of NASH

In order to develop an animal model of NASH, two diets were purchased from the company "Research Diets": a standard diet for the control group (A02082003BY, SD) and a methionine-choline deficient diet to induce NASH (A02082002BR, MCD). Although the MCD diet comprises high sucrose (40%) and fat (10%), it lacks methionine and choline, which are indispensable for VLDL synthesis [775]. As a result, animals fed with MCD diet rapidly develop steatohepatitis. Given that this diet has a drastic impact on mouse body weight, the experimental protocol was stopped after 4 weeks of MCD diet. All animals were subjected to thorough monitoring regarding weight loss and food intake. The MCD-fed animals were split into two groups: one began being supplemented with STS in addition to the MCD regime, while the second one received NaCl aside the MCD diet. The STS supplementation was done twice a week via IP (0.4 g STS/kg bw) and in the drinking water (3 mg STS/mL). This course of treatment lasted the entire period of diet intake.

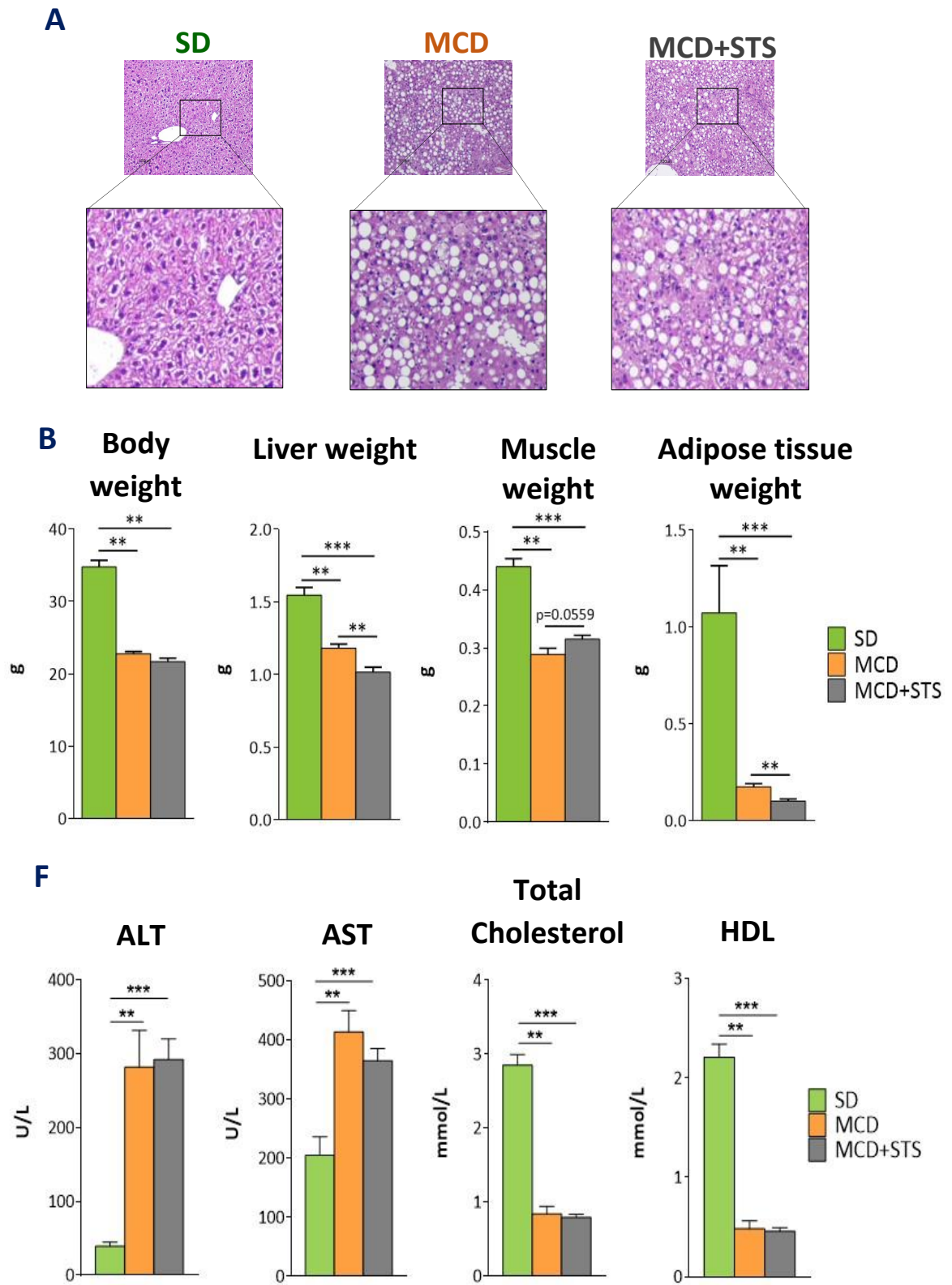


**Figure 50: Impact of MCD feeding and STS supplementation on liver histology (A), body weight (B), liver weight (C), adipose tissue weight (D), muscle weight (E) and on different plasma parameters (F)**

Haematoxylin and eosin staining of liver sections (magnification x100). Black arrows indicate lipid droplets and red circles indicate inflammation. Results are represented as mean  $\pm$  SEM (n=6-10 per group). \*p<0.05, \*\* p<0.01, \*\*\* p<0.001 indicate significant differences (Mann Whitney U test). **MCD**: methionine-choline deficient diet; **STS**: sodium thiosulfate

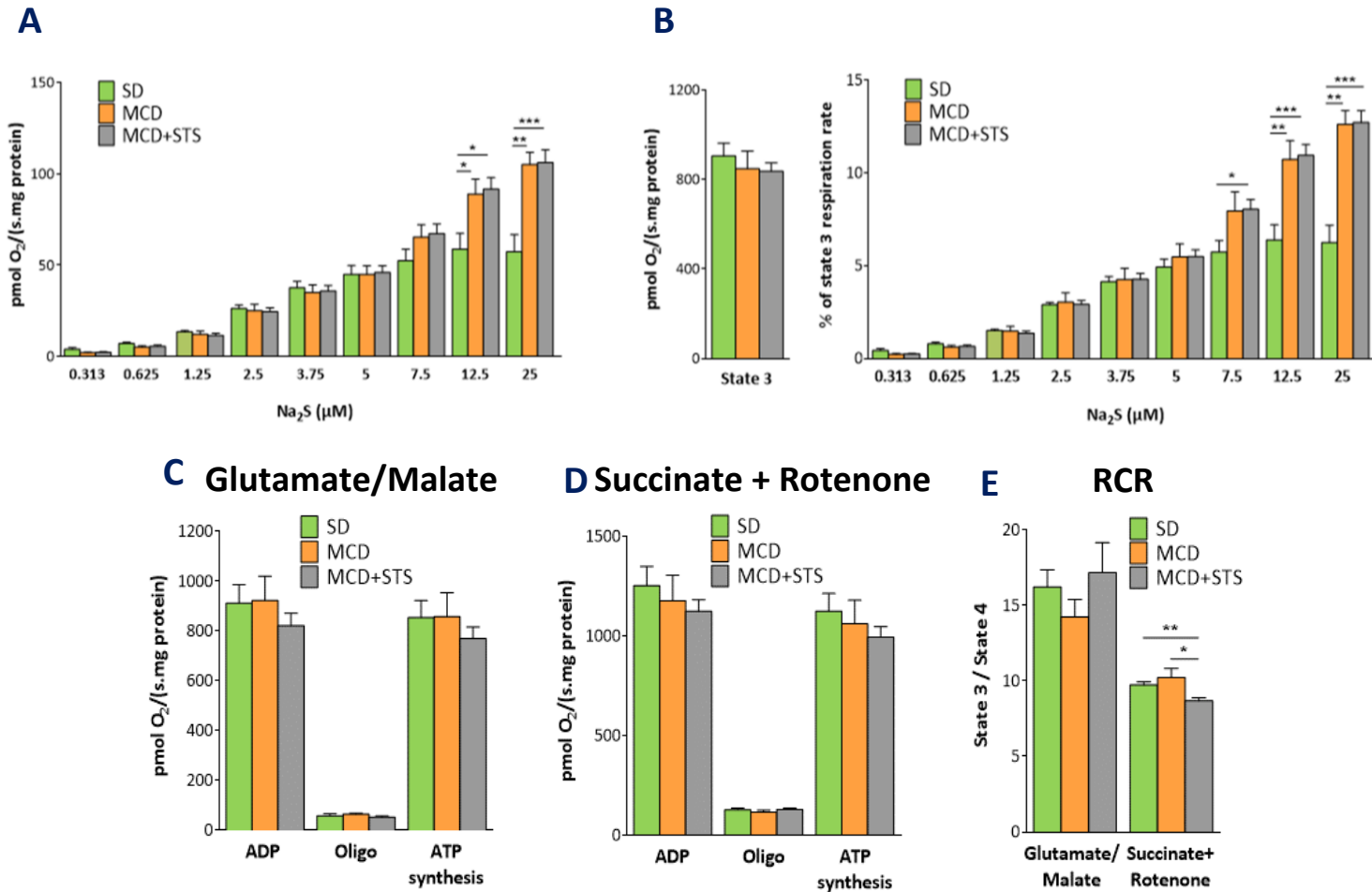


**Figure 51: Impact of MCD feeding and STS supplementation on liver mitochondrial H<sub>2</sub>S oxidation and respiration**

**A**) Sulfide oxidation rates were plotted as a function of Na<sub>2</sub>S concentration and expressed as pmol O<sub>2</sub>/s/mg protein or **B**) as percentage of state 3 respiration rate. **C**) Mitochondrial oxygen consumption rate using either glutamate/malate or **D**) succinate plus rotenone in the presence of ADP (state 3) or oligomycin (Oligo, state 4) to determine respiration linked to ATP synthesis (state 3-state 4) as well as **E**) respiratory control ratio (RCR, state3/state 4). Results are represented as mean ± SEM (n=6-10 per group). \* p<0.05, \*\* p<0.01, \*\*\*p<0.001 indicate significant differences (Mann Whitney U test). **MCD**: methionine-choline deficient diet; **STS**: sodium thiosulfate



	<b>Vmax</b>	<i>P value</i>	<b>Km</b>	<i>P value</i>	<b>Vmax/Km</b>	<i>P value</i>
<b>SD</b>	73.85 ± 12.29		3.66 ± 0.59		20.29 ± 0.73	
<b>MCD</b>	196.05 ± 34.02	**p<0.05; \$\$\$p<0.001	19.12 ± 6.89	**p<0.05; \$\$\$p<0.001	13.90 ± 2.36	*p<0.05; \$\$\$p<0.001
<b>MCD+STS</b>	180.76 ± 17.62		15.40 ± 3.11		14.02 ± 1.51	

**Table 7: Determination of Vmax and Km values for mitochondria H<sub>2</sub>S oxidation in SD-, MCD-fed mice and MCD+STS mice**

Results are represented as mean ± SEM (n=6-10 per group). \*MCD vs SD; \$ MCD+STS vs SD

**STS:** sodium thiosulfate

## 2.1. Impact of MCD diet and STS supplementation on mouse phenotype

Similarly to other studies using MCD diet to induce NASH [747, 748], liver histological analysis confirmed that MCD diet feeding for 4 weeks markedly induced liver steatosis and inflammation, which however could not be reversed or partially prevented by STS supplementation (**Figure 50A**). Liver steatosis in MCD-fed mice was accompanied by an increased liver/body weight ratio (+16%) compared to SD-fed mice, increase that however was not observed in the supplemented mice (**Figure 50C**). MCD-fed mice also displayed lower body weight (-35%) (**Figure 50B**) and a huge decrease in adipose tissue/body weight ratio (-75%) (**Figure 50D**). Despite having a similar body weight to that of MCD-fed mice, MCD+STS mice had significant lower liver/body weight ratio (**Figure 50C**) and adipose tissue/body weight ratio (**Figure 50B**) but higher muscle/body weight ratio (+14%) (**Figure 50E**). These observations indicated that STS supplementation further decreased liver and adipose tissue weight but exerted some protective effect on muscle mass.

MCD feeding also increased the plasma levels of ALT (+622%) and AST (+102%) (**Figure 50F**), while decreasing the plasma levels of total cholesterol (-71%) and HDL-cholesterol (-79%) (**Figure 50F**). STS supplementation exerted no significant effect on these plasma parameters (**Figure 50F**).

## 2.2. MCD diet increases liver mitochondrial H<sub>2</sub>S oxidation capacity

Liver mitochondria from SD-, MCD- and MCD+STS-fed mice were tested for their capacity to oxidize H<sub>2</sub>S. Data were plotted using the real values (**Figure 51A**) or calculated as % of state 3 respiration rate by dividing each raw pmol O<sub>2</sub>/s.mg value by the state 3 value of each corresponding mouse (**Figure 51B**). For concentrations of Na<sub>2</sub>S between 12.5 μM and 25 μM, liver mitochondria from MCD-fed mice presented a significant increase (+68% to +102 %) in their capacity to oxidize H<sub>2</sub>S (10.73-12.64% of state 3 respiration rate) when compared to SD-fed mice (6.40-6.25% of state 3 respiration rate) (**Figure 51B**). Interestingly, MCD and MCD+STS mice displayed the same capacity for H<sub>2</sub>S oxidation (**Figure 51B**), which made us hypothesize that perhaps in a condition of NASH H<sub>2</sub>S oxidation is already running at its maximum and cannot be increased any further. Thus, by contrast to SD-fed mice, no saturation could be reached in MCD and MCD+STS mice in the presence of H<sub>2</sub>S concentrations higher than 7.5 μM. This was associated with increased V<sub>max</sub> (MCD: +165%; MCD+STS: +144%) and higher K<sub>m</sub> (MCD: +421%; MCD+STS:

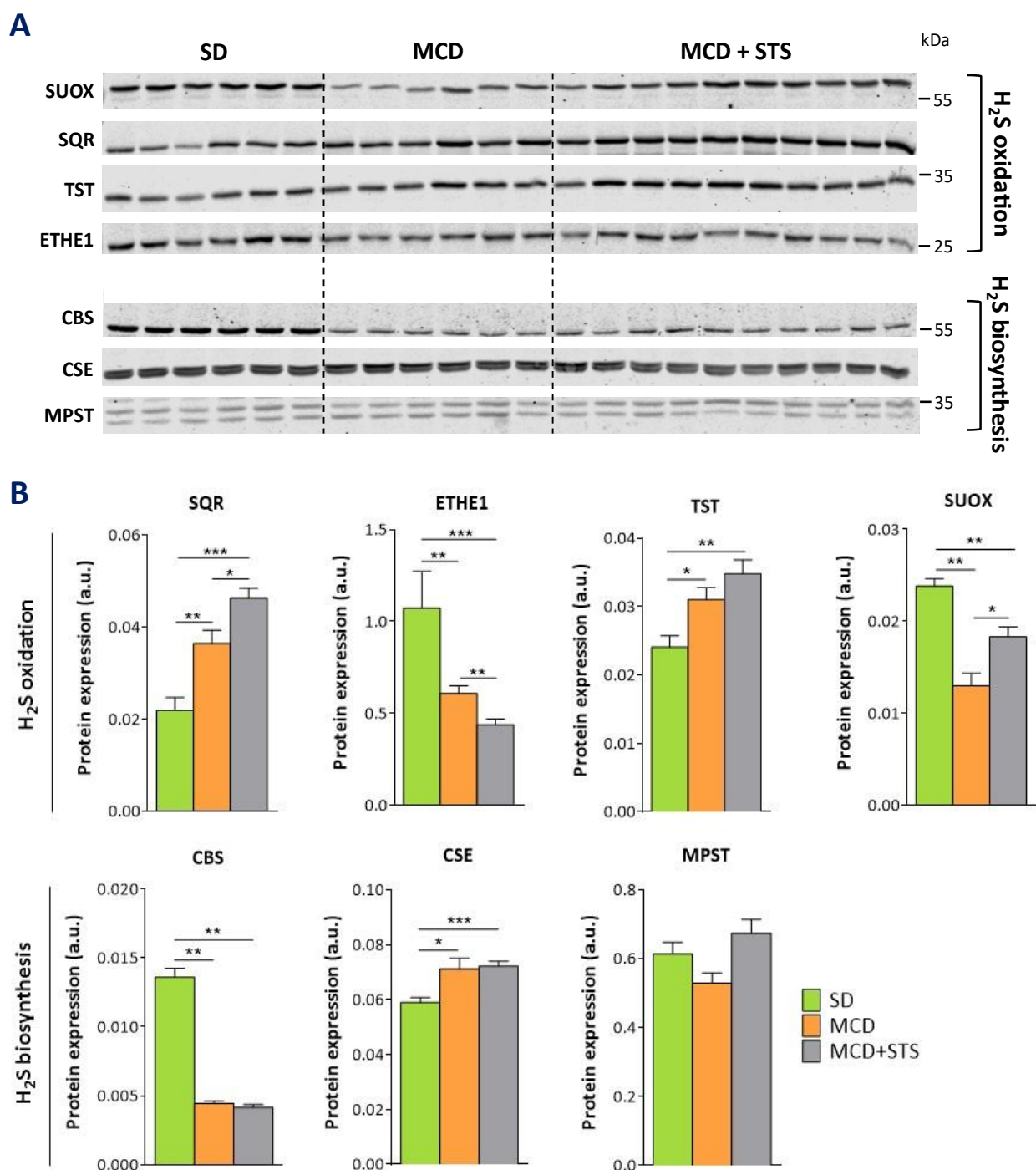
+320%) values for H<sub>2</sub>S oxidation but lower catalytic efficiency (V<sub>max</sub>/K<sub>m</sub>) (MCD: -32%; MCD+STS: -31%) (**Table 7**).

Once again, the observed effects of MCD diet feeding minus or plus STS supplementation on liver mitochondrial H<sub>2</sub>S oxidation could not be explained by changes in the functionality of isolated liver mitochondria. Indeed, liver mitochondria isolated from SD-, MCD- and MCD+STS mice displayed the same respiration rates in the presence of glutamate/malate (**Figure 51C**) and succinate plus rotenone (**Figure 51D**). RCR was found unchanged between the three groups when glutamate/malate was used as substrate (**Figure 51E**). However, mitochondria isolated from MCD+STS mice did display lower RCR than mitochondria from MCD- and SD-fed animals when succinate was used as substrate (SD: 9.74 ± 0.21; MCD: 10.24 ± 0.60; MCD+STS: 8.69 ± 0.20 (**Figure 51E**)). Nonetheless, the RCR value for the MCD+STS mice was deemed high enough to discard a possible mitochondrial uncoupling.

### 2.3. MCD diet and STS supplementation increase liver SQR protein expression

Western blotting experiments using liver lysates showed that MCD-fed mice exhibited higher liver protein expression of SQR (+66%) when compared to SD-fed mice (**Figure 52A** and **52B**). Interestingly, STS supplementation even further increased SQR protein expression (+27%) when compared to MCD-fed mice (**Figure 52A** and **52B**). Our results have also shown that MCD diet increases the expression of TST (+29%). Conversely, ETHE1 protein level was decreased in MCD-fed mice (-44%), with STS supplementation decreasing this level even further (-60%). Interestingly, we also observed that MCD feeding decreased SUOX expression (-46%), while STS supplementation slightly abrogated this effect (-23%).

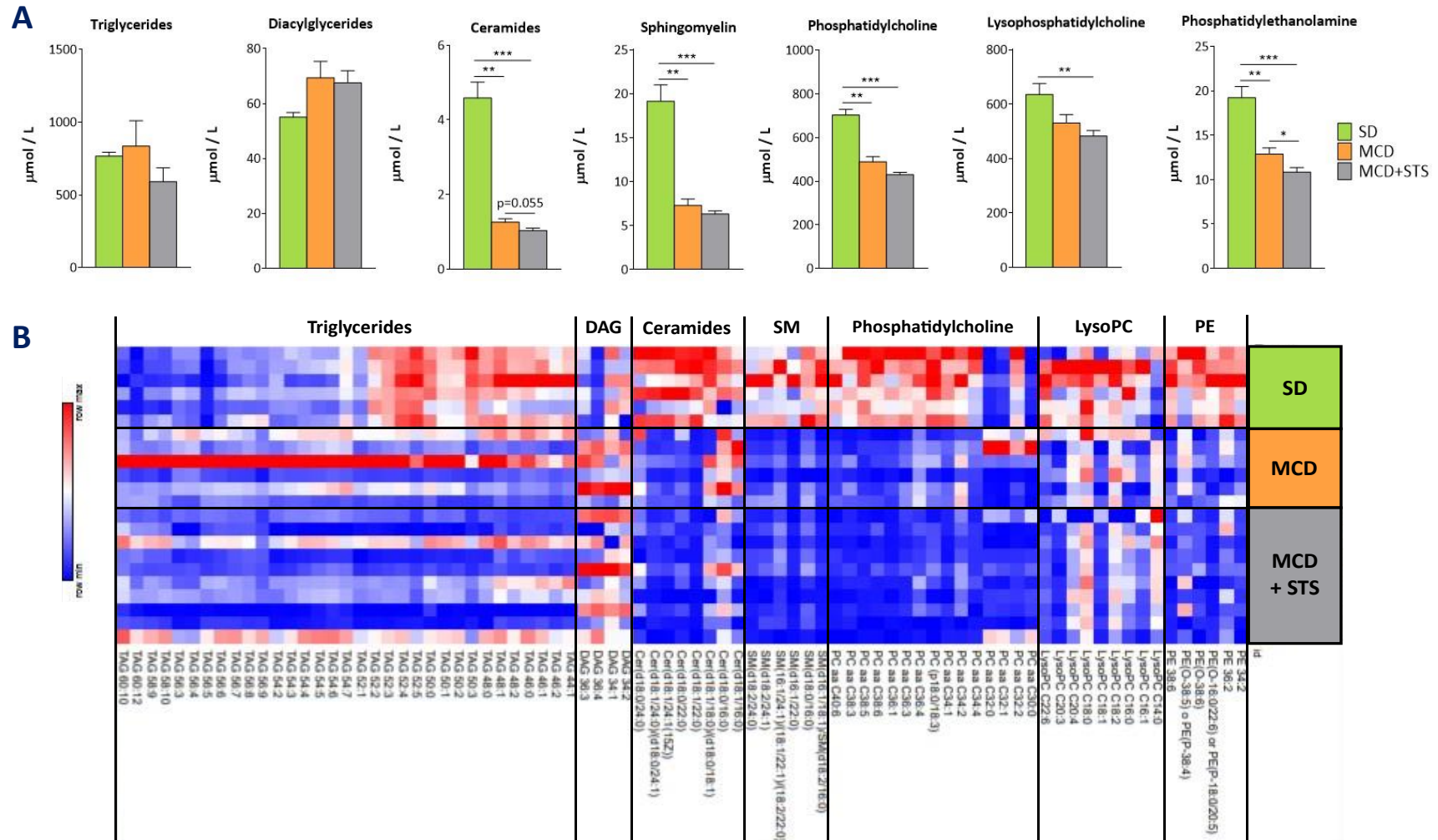
When assessing the protein expression of CBS, CSE and MPST in the liver of MCD and MCD+STS mice, we observed that MCD diet feeding markedly decreased the hepatic protein level of CBS (-68%) while it increased CSE protein level (+20%) (**Figure 52A** and **52B**). MPST protein level was not significantly altered by the MCD diet feeding, and STS supplementation did not change the protein expression levels of enzymes involved in H<sub>2</sub>S biosynthesis (**Figure 52A** and **Figure 52B**).



**Figure 52: Protein expression level of enzymes involved in H<sub>2</sub>S oxidation and biosynthesis**

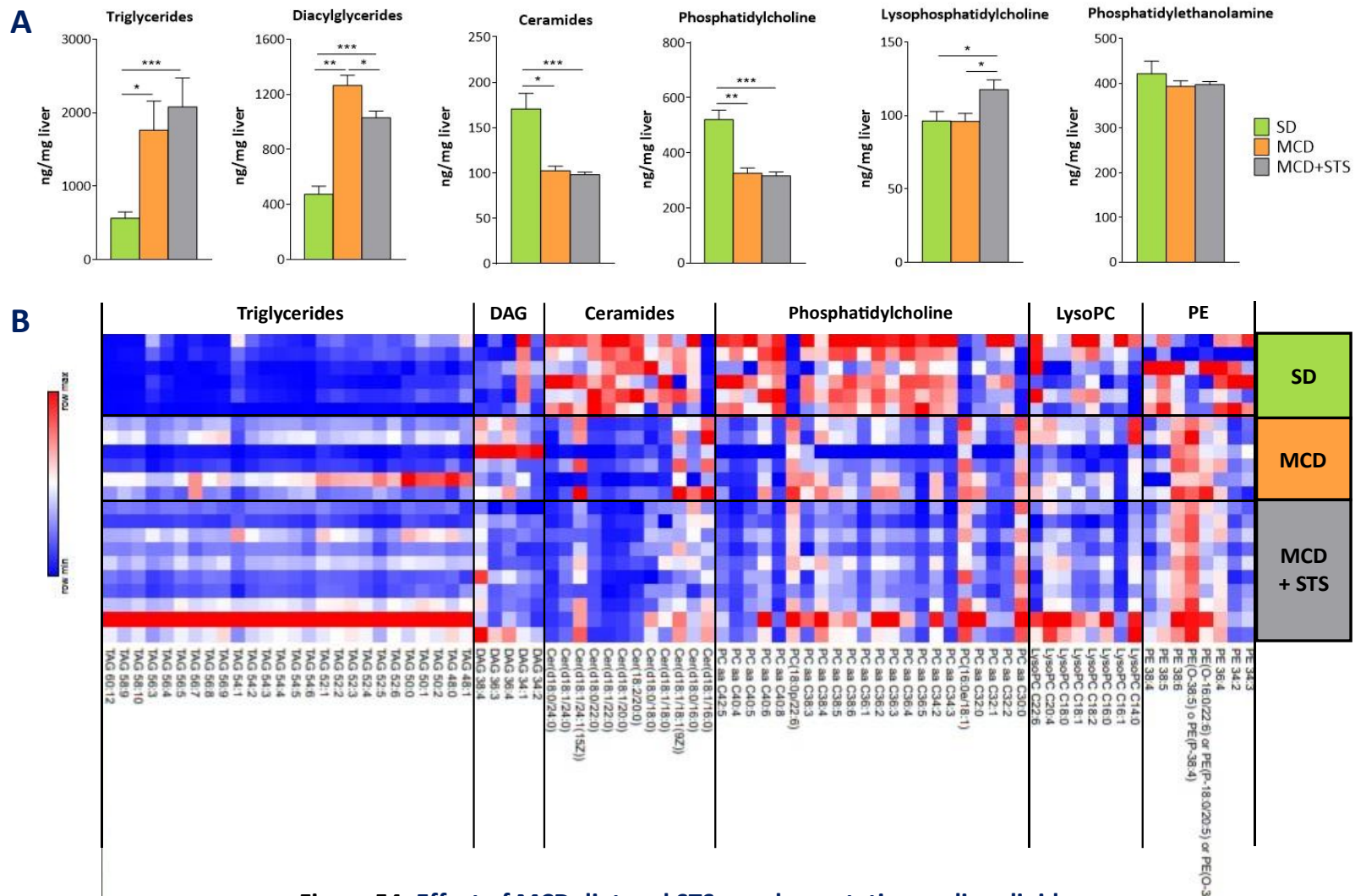
**A)** Immunoblot analysis of the protein expression level of enzymes involved in H<sub>2</sub>S oxidation (SUOX, SQR, TST, ETHE1) and biosynthesis (CBS, CSE, MPST) using liver lysates from SD-, MCD- and MCD+STS-fed mice. **B)** Western blot quantification was normalized by the total quantification of the REVERT signal. Results are represented as mean  $\pm$  SEM (n=6-10 per group). \* p<0.05, \*\* p<0.01, \*\*\* p<0.001 indicate significant differences (Mann Whitney U test).

**MCD:** methionine-choline deficient diet; **STS:** sodium thiosulfate



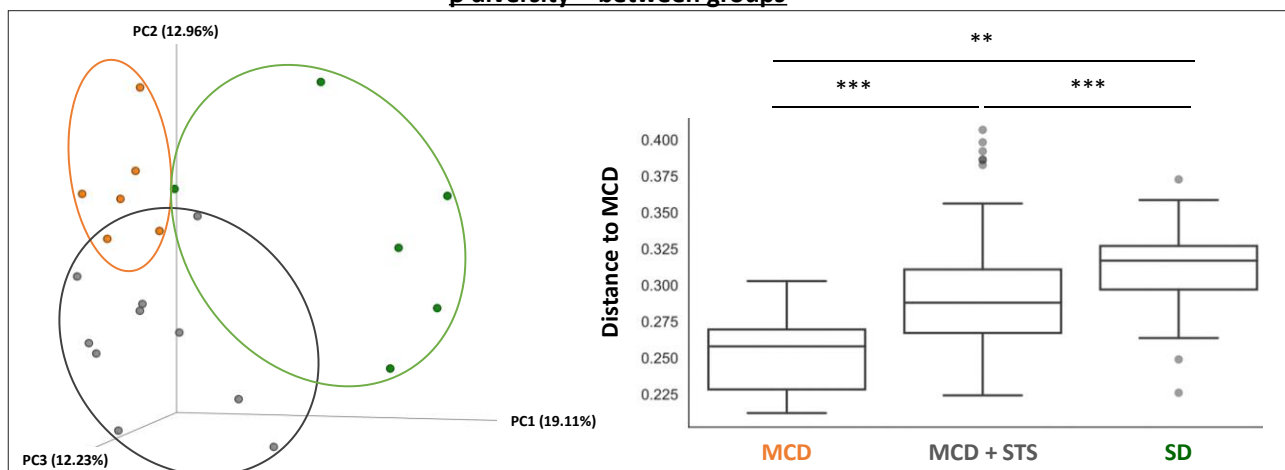
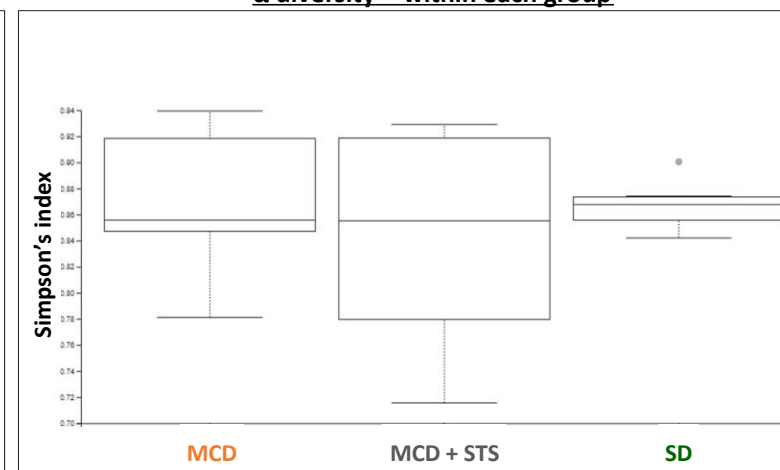
**Figure 53: Effect of MCD diet and STS supplementation on circulating lipids**

A) Lipidomic analysis of total plasma levels of triglycerides, diacylglycerides (DAG), ceramides, sphingomyelins (SM), phosphatidylcholine, lysophosphatidylcholine (LysoPC) and phosphatidylethanolamine (PE). B) Heat map showing the different lipid species present in the different lipid classes. Results are represented as mean ± SEM (n>6 per group). \* p<0.05, \*\* p<0.01, \*\*\* p<0.001 indicate significant differences (Mann Whitney U test). **MCD**: methionine-choline deficient diet; **STS**: sodium thiosulfate



**Figure 54: Effect of MCD diet and STS supplementation on liver lipids**

**A)** Lipidomic analysis of total liver levels of triglycerides, diacylglycerides (DAG), ceramides, phosphatidylcholine, lysophosphatidylcholine (LysoPC) and phosphatidylethanolamine (PE). **B)** Heat map showing the different lipid species present in the different lipid classes. Results are represented as mean  $\pm$  SEM (n=6-10 per group). \* p<0.05, \*\* p<0.01, \*\*\* p<0.001 indicate significant differences (Mann Whitney U test). **MCD:** methionine-choline deficient diet; **STS:** sodium thiosulfate

**A** **$\beta$  diversity – between groups****B** **$\alpha$  diversity – within each group****Figure 55: Effect of MCD diet and STS supplementation on gut microbiota diversity**

**A)** Principal component analysis (PCA) of the unweighted UniFrac distance matrix of fecal microbiota from SD-, MCD- and MCD+STS-fed mice. **B)** Microbiota richness and diversity in SD-, MCD- and MCD+STS-fed mice, based on the Simpson's Index. Categories were compared and statistical significance of clustering were determined via Permanova. Results are represented as mean  $\pm$  SEM (n=6-10 per group). \*\* p<0.01, \*\*\*p<0.001 indicate significant differences.

**MCD:** methionine-choline deficient diet; **STS:** sodium thiosulfate

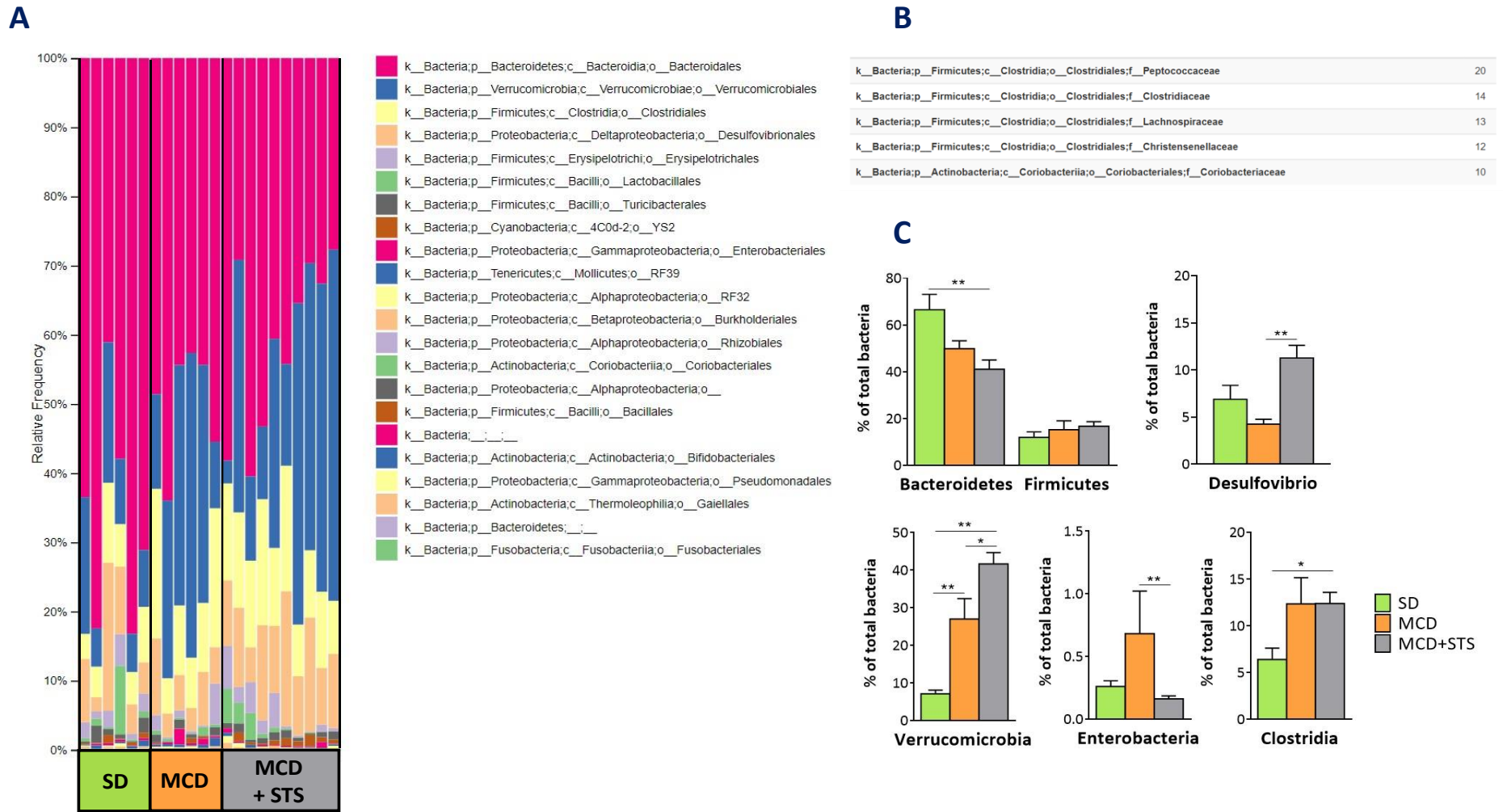


**Figure 56: Effect of MCD diet and STS supplementation on gut microbiota composition**

Bacterial-taxon-based analysis of feces at the phylum level. **B**) Differentially abundant microbial taxa identified by Analysis of Composition of Microbiomes (ANCOM). **C**) Fecal percentage of Bacteroidetes, Firmicutes, Desulfovibrio, Verrucomicrobia, Enterobacteria and Clostridia in SD-, MCD- and MCD+STS-fed mice. Results are represented as mean  $\pm$  SEM (n=6-10 per group). \* p<0.05, \*\*p<0.01 indicate significant differences. **MCD**: methionine-choline deficient diet; **STS**: sodium thiosulfate



## 2.4. Impact of MCD diet and STS supplementation on plasma and liver lipids

Using lipidomic techniques (collaboration with A. Gastaldelli and Sara Guerra, Pisa, Italy), we assessed the lipid content and lipid species composition of the plasma (**Figure 53**) and liver (**Figure 54**). We observed that MCD diet decreased the total circulating levels of ceramides, sphingomyelins, phosphatidylcholines and phosphatidylethanolamines (**Figure 53A and 53B**). Interestingly, STS supplementation even further decreased the levels of ceramides ( $p=0.055$ ) and phosphatidylethanolamines ( $p<0.05$ ) (**Figure 53A and 53B**). In the liver, as expected, MCD diet significantly increased the TG and diacylglycerol contents, while it decreased the levels of ceramides and phosphatidylcholines (**Figure 54A and 54B**). In agreement with liver histological analysis (**Figure 50A**), STS supplementation did not decrease the MCD diet-induced liver TG accumulation. However, STS supplementation partially reversed the MCD-induced increase in diacylglycerols, while it also increased the hepatic level of lysophosphatidylcholines (**Figure 54A and 54B**).

## 2.5. MCD diet and STS supplementation have an impact on gut microbiota

This part was performed with the helpful collaboration of Dr. Benoît Chassaing (Institut Cochin, Paris, France).

Through 16S RNA sequencing of fecal samples, we observed that MCD diet and STS supplementation both have an impact on gut microbiota (**Figure 55**). In accordance to the visual assessment of the PCA plots (**Figure 55A**), the UniFrac distances between SD and MCD, SD and MCD+STS or MCD and MCD+STS were significantly high (**Figure 55A**), which indicated that the microbial communities have changed between groups. These altered compositions did not result from higher microbial richness within each mouse sample, as shown by the unchanging  $\alpha$ -diversity (**Figure 55B**). When looking at the taxonomy summary of all gut microbiota (at the class level) we could not perceive drastic changes caused by MCD diet or STS supplementation (**Figure 56A**). However, when doing ANCOM statistical analysis, which indicates which organism(s) differentiate the groups, some changes were revealed (**Figure 56B**). A closer analysis showed that MCD+STS mice presented a decreased percentage of Bacteroidetes (-49%) when compared to SD-fed mice (**Figure 55C**). These STS supplemented mice also had increased levels of Desulfovibrio (+164%) when compared to MCD-fed mice, and higher levels of Clostridia (+93%) when compared to SD-fed mice (**Figure 55C**). When compared to SD-fed mice, MCD diet appeared to induce a

pronounced overgrowth of Verrucomicrobia (+277%), with STS supplementation increasing it even further (+481%) (**Figure 55C**). Interestingly, MCD diet promoted the development of Enterobacteria (+160%), while STS supplementation abrogated this overgrowth (**Figure 55C**).

### 3. Human obese patients

#### 3.1. Characteristics of the patients

A total of 18 female patients with morbid obesity (BMI>40) were studied in this project. In collaboration with physicians (C. Vons, N. Helmy, M. Zioli; Bondy), these patients (candidates for bariatric surgery) were previously included in a prospective study aimed to investigate the alterations in liver lipid metabolism in the context of obesity and NAFLD. Liver biopsies were collected during bariatric surgery and kept frozen at -80°C until investigation. In this study, the individuals were selected based on the absence of associated co-morbidities (T2DM, dyslipidemia, sleep apnea syndrome). Six of those obese individuals had normal liver histology (No NAFLD), 6 had simple steatosis (NAFL) and 6 had NASH. All these patients did not differ in age, fasting glycemia, BMI, blood cholesterol and GGT (**Table 8**). Obese NAFL and NASH patients had increased liver TG content, higher fasting insulinemia and HOMA-IR, an index of insulin resistance. When compared to the obese NAFL group, obese NASH patients had significant higher ALT levels (**Table 8**).

#### 3.2. NAFL patients present lower liver SQR protein expression

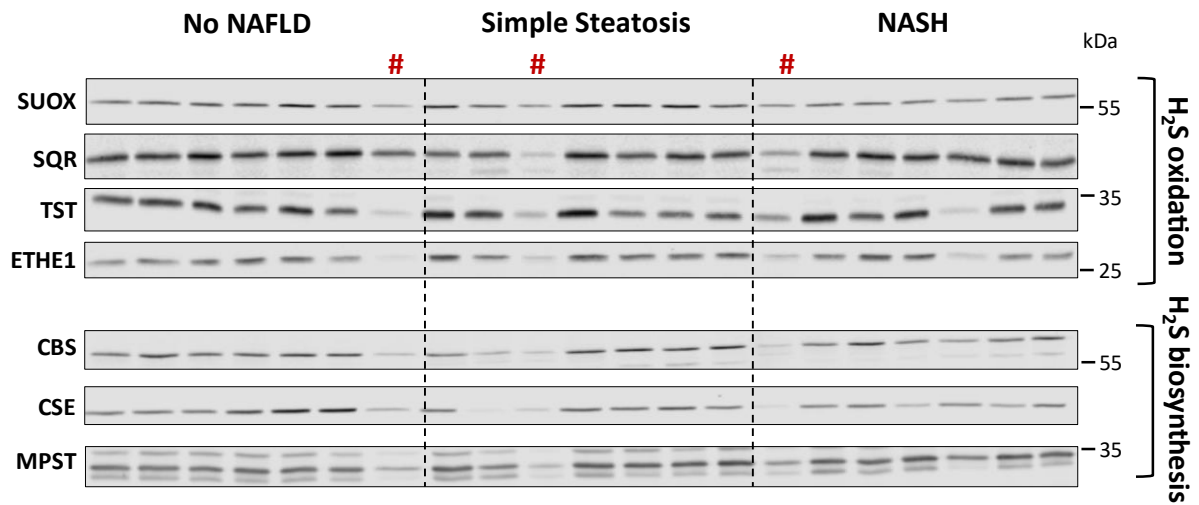
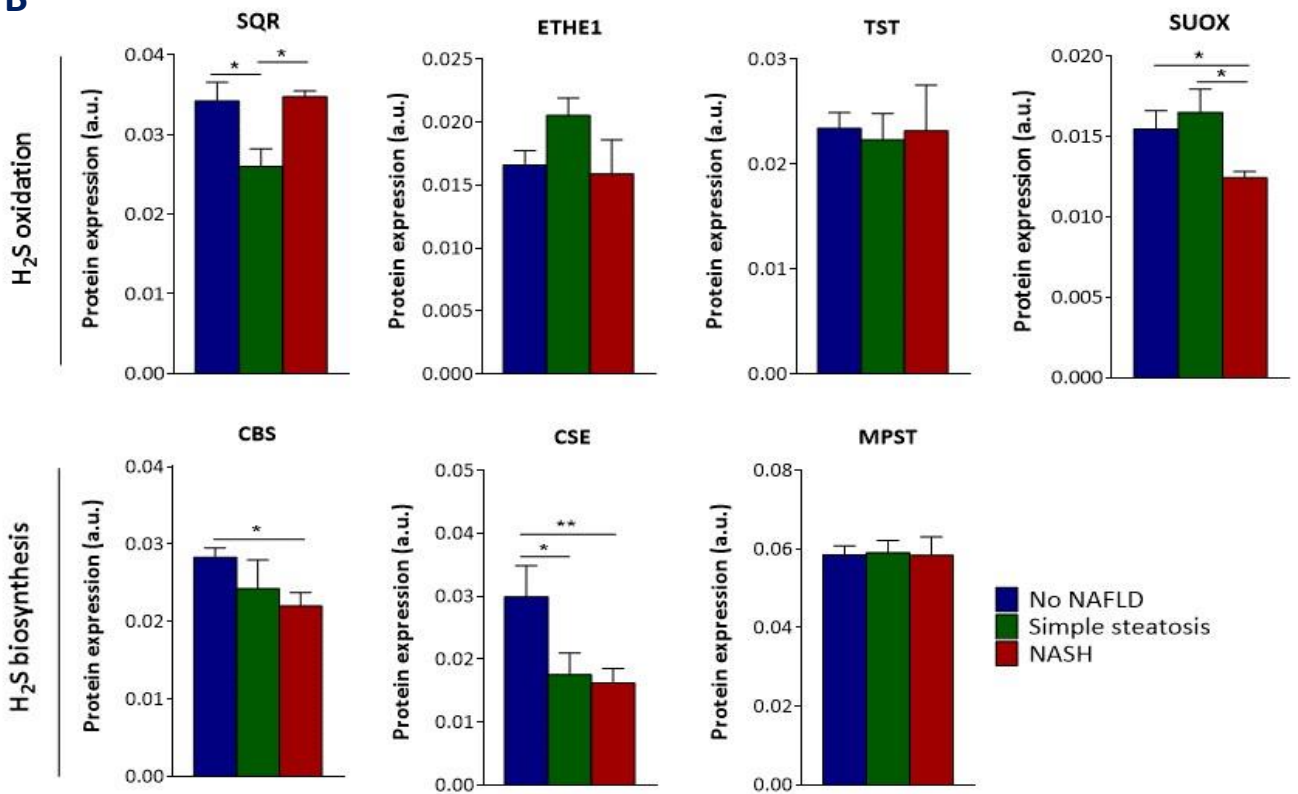
Western blotting experiments using liver lysates were performed to assess the protein expression level of enzymes involved in H<sub>2</sub>S oxidation and biosynthesis. Our results showed that NAFL patients presented a lower SQR protein level (-25%) when compared to the No NAFLD and NASH groups (**Figure 57A** and **57B**). Interestingly, NASH patients presented a 25% less protein expression of SUOX when compared to No NAFLD and NAFL individuals. When assessing the protein expression of CBS, CSE and MPST in the liver of these obese patients, we observed that NASH individuals presented decreased protein levels of both CBS and CSE (-23% and -46%, respectively), while NAFL patients only exhibited decreased CSE protein level (-42%). MPST protein expression was not changed in NAFL and NASH patients when compared to the No NAFLD group (**Figure 57A** and **57B**).

	No NAFLD	Simple steatosis	NASH	Statistics
	n=6	n=6	n=6	p value
Gender	Female	Female	Female	
Age (years)	35.00 ± 3.43	33.67 ± 3.80	37.00 ± 2.83	n.s.
BMI (kg/m <sup>2</sup> )	42.42 ± 0.93	45.08 ± 1.07	46.62 ± 1.25	n.s.
Fasting glycemia (mM)	4.83 ± 0.19	5.63 ± 0.66	5.53 ± 0.32	n.s.
Insulinemia (pmol/L)	36.13 ± 8.73	106.04 ± 25.47	171.55 ± 56.25	*p<0.05, ##p<0.01
HOMA-IR	1.17 ± 0.48	4.01 ± 1.13	6.33 ± 2.21	*p<0.05, ##p<0.01
Triglycerides (mg/g of liver)	5.60 ± 0.68	22.48 ± 10.06	24.99 ± 5.82	*p<0.05, ##p<0.01
Cholesterol (mM)	4.74 ± 0.38	5.18 ± 0.39	4.85 ± 0.35	n.s.
AST (IU/L)	23.00 ± 2.38	26.17 ± 5.42	32.83 ± 2.77	#p<0.05
ALT (IU/L)	19.17 ± 2.17	30.83 ± 12.03	43.83 ± 8.44	#p<0.05, \$p<0.05
γGT (IU/L)	20.50 ± 2.88	33.00 ± 9.64	29.83 ± 4.15	n.s.

**Table 8: Characteristics of the human obese patients**

Results are represented as mean ± SEM (n=6 per group). \*simple steatosis vs SD; # NASH vs SD; \$ NASH vs simple steatosis.

**n.s:** not significant; **NASH:** non-alcoholic steatohepatitis; **BMI:** body mass index; **HOMA-IR:** Homeostatic Model Assessment for Insulin Resistance; **AST:** aspartate aminotransferase; **ALT:** alanine aminotransferase; **GGT:** γ-glutamyltransferase.

**A****B**

**Figure 57: Protein expression level of enzymes involved in H<sub>2</sub>S oxidation and biosynthesis**

**A)** Immunoblot analysis of the protein expression level of enzymes involved in H<sub>2</sub>S oxidation (SUOX, SQR, TST, ETHE1) and biosynthesis (CBS, CSE, MPST) using liver lysates from healthy, NAFL and NASH individuals. **B)** Western blot quantification was normalized by the total quantification of the REVERT signal. Results are represented as mean ± SEM (n=6 per group). \* p<0.05 and \*\* p<0.01 indicate significant differences (Mann Whitney U test).

# represents samples that were disregarded for the quantification due to protein degradation

## Discussion

In this study, our objectives were to assess i) whether or not liver mitochondrial H<sub>2</sub>S oxidation is regulated in mouse models of NAFLD and in obese humans, and ii) what are the pathophysiological effects of *in vivo* sodium thiosulfate (STS) supplementation on liver mitochondrial H<sub>2</sub>S oxidation and lipid metabolism. Furthermore, given that STS is an H<sub>2</sub>S donor majorly metabolized in the gut, we also assessed iii) whether or not STS supplementation led to changes in gut microbiota composition and how these changes could be associated to NAFLD profile. The major findings of each experimental group from the investigated NAFLD mouse models and of liver biopsies from obese patients are summarized in **Table 9**.

### Diet-induced animal models of NAFL and NASH

The spectrum of NAFLD ranges from simple steatosis (NAFL) to steatohepatitis (NASH). The NAFL animal model used in this study was achieved by feeding C57Bl6/J mice with a 45% enriched in fat and sucrose (HF/HS) diet for 10 or 20 weeks. Our first observation was the rapid effect of HF/HS diet in increasing mouse body weight, adiposity and glucose intolerance. Indeed, previous studies had already reported significant changes after only 30 days of diet intake [778]. Additionally, we observed that 20 weeks of HF/HS diet resulted in dyslipidemia with increased plasma levels of TG, ceramides, sphingomyelins and phosphatidylethanolamines as well as in altered liver function as demonstrated by the increased plasma levels of ALT and AST. Liver lipidome of these mice only partly reflected the changes observed in the plasma, since HF/HS-fed mice showed a tendency to accumulate higher contents of TG and ceramides. These findings are supported by previous studies [779–781], although in our model liver steatosis developed very slowly. Unlike most reports, however, in this study, HF/HS diet had no impact on mitochondrial function and HF/HS-fed mice were unable to develop severe liver steatosis and insulin resistance (IR), even after 20 weeks of diet intake. One explanation could be that, for the 10 week timepoint, we used the mice that presented the highest glucose intolerance, thus keeping the less- or non-responsive mice to be fed for a longer time with HF/HS diet. Another explanation could be the existence of a questionable diet batch. Indeed, in a first series of HF/HS diet feeding for 20 weeks (in the same animal facility), HF/HS-fed mice displayed both glucose intolerance and IR (Results not shown). Another explanation could be the composition of the diet itself. A recent study by Pinyo *et al.* has shown that rats fed HFD or high-sucrose diet (HSD) alone more easily develop IR than rats fed HF/HS diet [782]. According to their study, the continuous ingestion of a diet

		NAFL animal model			NASH animal model		Obese patients	
		10 weeks	20 weeks		MCD versus SD	MCD+STS versus MCD	NAFL versus No NAFLD	NASH versus No NAFLD
		HS/HS versus SD	HS/HS versus SD	HF/HS+STS versus HF/HS				
<b>Energetic homeostasis</b>	Body weight	↑	↑	=	↓	=	=	=
	Fasting glycemia	↑	=	=	N.D.	N.D.	=	=
	Glucose tolerance	↓	↓	=	N.D.	N.D.	=	↓
	Insulin sensitivity	=	=	=	N.D.	N.D.	↓	↓
	Adiposity (% body weight)	↑	↑	=	↓	↓	N.D.	N.D.
	Muscle weight (% body weight)	N.D.	↓	↓	↓	↑	N.D.	N.D.
	ALT	N.D.	↑	=	↑	=	=	↑
	AST	N.D.	↑	=	↑	=	=	↑
<b>Lipid profile</b>	Liver TG	N.D.	↑	N.D.	↑	=	↑	↑
	Plasma TG	N.D.	↑	↓	=	=	=	↑
<b>Liver mitochondria</b>	Mitochondria respiration	=	=	=	=	=	N.D.	N.D.
	Mitochondrial H <sub>2</sub> S oxidation	=	↓	↑	↑ (≥12.5μM)	=	N.D.	N.D.
<b>Liver protein expression</b>	SQR protein expression	↓	=	↑	↑	↑	↓	=
	CSE protein expression	=	↑	=	↑	=	↓	↓
	CBS protein expression	↑	=	=	↓	=	=	↓
	MPST protein expression	=	=	=	=	=	=	=
<b>Microbiota</b>	<i>Bacteroidetes</i>	N.D.	=	↓	=	=	N.D.	N.D.
	<i>Firmicutes</i>	N.D.	=	=	=	=	N.D.	N.D.
	<i>Desulfovibrio</i>	N.D.	=	↑	=	↑	N.D.	N.D.
	<i>Enterobacteria</i>	N.D.	↓	↑	↑ (tendency)	↓	N.D.	N.D.

**Table 9: Summary of the main findings**

**NAFL:** non-alcoholic fatty liver; **NASH:** non-alcoholic steatohepatitis; **HF/HS:** high fat/high sugar diet; **SD:** standard diet; **STS:** sodium thiosulfate; **MCD:** methionine choline deficient diet; **N.D.:** not determined; **AST:** aspartate aminotransferase; **ALT:** alanine aminotransferase; **TG:** triglycerides; **SQR:** sulfide quinone reductase; **CSE:** cystathionine  $\gamma$  lyase; **CBS:** cystathionine  $\beta$  synthase; **MPST:** 3-mercaptopyruvate sulfurtransferase

combining high fat and high sugar increases the postprandial GLP-1 response to meal ingestion, which slows down the development of glucose intolerance and IR [782].

In this study, we also developed an *in vivo* model of NASH by feeding C57Bl6/J mice with MCD diet. Rodents consuming this regime develop steatohepatitis, necroinflammation, and fibrosis similar to human NASH [783]. However, unlike humans with NASH, rats or mice fed with MCD diet show significant weight loss and decreased serum TG and cholesterol levels [783]. Similar to what is described in the literature, in this study, mice fed MCD diet for four weeks presented a huge decrease in body, liver, muscle and adipose tissue weight, as well as decreased levels of total cholesterol and HDL-cholesterol. These MCD-fed mice also showed elevated levels of ALT and AST, clear indicators of liver injury. Furthermore, given that MCD diet impairs VLDL secretion, the liver of MCD-fed mice is unable to export TG, which, as demonstrated by our results, end up accumulating in the hepatic tissue. As presently reported for mice fed HF/HS diet, this MCD diet did not impact liver mitochondrial respiratory function.

#### **Regulation of mitochondrial H<sub>2</sub>S oxidation in animal models of NAFLD and in obese humans**

In this study, we showed for the first time that mitochondrial H<sub>2</sub>S oxidation is not only regulated during the development of NAFLD, as this regulation is different according to the stage of the illness. While 10 weeks of HF/HS diet only decreased liver SQR protein expression, 20 weeks of HF/HS diet downregulated hepatic mitochondrial H<sub>2</sub>S oxidation. This decrease, however, was not mimicked by lower SQR expression. Considering SQR as the key regulatory enzyme in mitochondrial H<sub>2</sub>S oxidation, the rate quantification of this pathway serves as an indirect measurement of SQR activity. One possible explanation to the impairment of mitochondrial H<sub>2</sub>S oxidation without changes in SQR protein expression could be the existence of post-translational modifications exerting a negative impact on SQR activity. However, this hypothesis remains to be deciphered. On the other hand, when using MCD diet, SQR protein expression was upregulated without a major increase in liver mitochondrial H<sub>2</sub>S oxidation. In fact, in MCD-fed mice, liver mitochondrial capacity to oxidize H<sub>2</sub>S is only increased when challenged with high concentrations of H<sub>2</sub>S, which suggests that these mitochondria possess higher tolerability to elevated incoming levels of H<sub>2</sub>S.

Although the animal models used in this study have their downsides (especially the HF/HS-induced NAFL model), these diet-induced changes in mitochondrial H<sub>2</sub>S oxidation capacity appear in accordance with what we observed in obese patients. Indeed, obese patients with simple

steatosis exhibited a decrease in liver SQR protein expression when compared to obese individuals with No NAFLD, suggesting a lower liver mitochondrial capacity to oxidize H<sub>2</sub>S. Conversely, obese NASH patients had higher liver SQR protein levels than obese NAFL patients, levels being similar to those measured in obese individuals with No NAFLD.

The implications of our findings remain open for interpretation, as it is difficult to decipher whether modulation of SQR protein expression in the liver is a causative mechanism or an adaptive response to the effects of HF/HS and MCD feeding. In the liver of HF/HS-fed mice, where SQR expression or activity are decreased, the transsulfuration pathway appears to suffer a boost, since CSE and CBS protein expressions are increased. It is possible that the activation of the transsulfuration pathway is an early adaptive response to hepatic oxidative stress in HF/HS-fed mice. Indeed, glutathione, the major endogenous direct antioxidant in the liver, lies downstream of this pathway, so increasing the transsulfuration rate would increase the levels of GSH. Moreover, since the first step of mitochondrial H<sub>2</sub>S oxidation involves the transfer of the SQR persulfide to GSH, decreasing the rates of this pathway would maintain higher concentration of free GSH to act as antioxidant. The increase in H<sub>2</sub>S production and decrease in H<sub>2</sub>S oxidation would lead to higher circulating levels of this gasotransmitter. Given that H<sub>2</sub>S itself acts as an antioxidant, increasing its levels could also serve as a protective mechanism against increased oxidative stress. Nonetheless, such beneficial associations should be interpreted with caution, as high levels of H<sub>2</sub>S also play a pathological role in inflammatory situations [220, 221]. In order to validate these assumptions, the levels of H<sub>2</sub>S and GSH should be measured.

On the other hand, in MCD-fed mice, where liver SQR protein expression was increased, the hepatic transsulfuration pathway is not so neatly regulated, with CBS levels decreasing and CSE levels increasing. One hypothesis to explain the elevated protein levels of SQR is the fact that mitochondria consume 5 times more oxygen when using H<sub>2</sub>S as substrate than when using NADH, for example. Since MCD diet is a highly detrimental regime when it comes to inducing inflammation and oxidative stress, the increase in mitochondrial H<sub>2</sub>S oxidation could serve as a mechanism to lower the levels of oxygen available for ROS production. Another hypothesis is that the increased CSE protein expression triggers a cascade of events, with H<sub>2</sub>S levels rising and promoting SQR gene transcription. Once again, in order to validate these hypothesis, the levels of liver H<sub>2</sub>S should be measured. As to the CBS levels, their decrease could demonstrate a coping mechanism in response to the lack of methionine in the MCD diet. In the transsulfuration pathway, CBS catalyses homocysteine to cystathionine. However, when methionine levels are low,



homocysteine can be redirected towards the production of methionine, which is converted to S-adenosyl-L-methionine (SAM), a valuable protector against fatty infiltration [784].

### **STS supplementation in animal models of NAFL and NASH**

Recent studies have proposed H<sub>2</sub>S as a therapeutic approach in the treatment of NAFLD, given that the use of H<sub>2</sub>S donors in animal models of NAFL or NASH decreases hepatic lipid accumulation, downregulates the inflammatory process and increases antioxidant defences [721, 723]. Our study demonstrated that the administration of STS to HF/HS-fed mice fails to reverse the diet-induced changes in hepatic steatosis, glucose intolerance and hypercholesterolemia. Similarly, the administration of STS to MCD-fed mice fails to reverse the diet-induced hepatic steatosis, fibrosis and inflammation. On the contrary, STS supplementation in MCD-fed mice further decreased liver and adipose tissue weight.

The discrepancy found between the lack of major physiological alterations induced by STS administration and already published data may come from the fact that most studies assessing the effect of H<sub>2</sub>S supplementation to animal models of NAFL and NASH use NaHS or Na<sub>2</sub>S as sulfide donors [721–723]. Indeed the use of STS in the context of liver metabolic reprogramming and cell signalling as an H<sub>2</sub>S donor is fairly recent. The therapeutic efficiency of STS has been seen in rodent models of lung injury, hypertension, cerebral ischemia and renal dysfunction [260-264]. Furthermore, unlike NaHS or Na<sub>2</sub>S, STS presents no apparent toxicity even when used at concentrations as high as 20 mM [260], thus making it a safe substance to use in humans. In fact, STS has been used for many years as an antidote against cases of cyanide poisoning [272] and more recently it has shown efficiency in treating human cases of calciphylaxis [268, 269].

In our study, STS supplementation in MCD-fed mice had no impact on mitochondrial H<sub>2</sub>S oxidation (already up-regulated by MCD diet), while its use in HF/HS-fed mice completely abrogated the HF/HS-induced negative impact on this pathway. Similarly, STS supplementation was unable to recover the plasma and liver lipid changes induced by MCD diet. However, when supplemented to HF/HS-fed mice, STS was able to normalize the diet-induced increase in circulating lipid levels. This decrease in plasma lipids may be due to higher tissue metabolization or to higher accumulation in the adipose tissue. This later premise is supported by the fact that HF/HS+STS mice presented slightly higher adiposity compared to HF/HS mice. Moreover, since most lipid species decreased by STS supplementation are considered “toxic” intermediaries in lipid metabolism, contributing to the development of IR [785–787], a downregulation of their

circulating levels could suggest a positive regulation of STS in insulin signalling and glucose metabolism. Further studies are required to thoroughly investigate this question.

### **STS supplementation impacts gut microbiota in animal models of NAFL and NASH**

NAFLD is a complex disease with many associated triggers, one of them being microbiota dysbiosis. The human gut microbiota is mostly composed by two dominant bacterial populations: the *Firmicutes* and the *Bacteroidetes* [546]. In normal situations, *Firmicutes* are in much lower abundance than *Bacteroidetes* [550]. However, in cases of NAFLD, the *Firmicutes/Bacteroidetes* ratio increases substantially [562-564]. Our study showed that STS supplementation in both HF/HS-fed and MCD-fed mice decreased the abundance of *Bacteroidetes* without increasing the population of *Firmicutes*. In HF/HS-fed mice, STS increased the abundance of *Desulfovibrio* and *Bifidobacteria*. *Desulfovibrio* is a gram-negative, obligate anaerobe that uses thiosulfate as substrate to produce H<sub>2</sub>S and sulfite. Some studies suggest that, due to their gram-negative nature, *Desulfovibrio* are associated to elevated levels of circulating LPS [788, 789]. However, HF/HS+STS mice showed a tendency to have lower hepatic mRNA levels of *TLR4* (with no statistical significance) (**Annex 1**). Given that STS supplementation increased the levels of *Bifidobacteria*, a well-known probiotic with anti-inflammatory properties, the potential *Desulfovibrio*-induced inflammation could be annulled. Our results further showed that HF/HS diet reduced the population of *Enterobacteria*, while STS supplementation stimulated it. Since most studies suggest that *Enterobacteria* promote obesity and IR, being found increased in animal models of NAFLD and in obese individuals [565, 790, 791], our contradictory findings call attention to the unideal animal model used. Indeed, when analysing the MCD model we could clearly see this increase in the abundance of *Enterobacteria*. Interestingly, STS supplementation decreased the levels of this bacterial subpopulation to levels similar to the controls. Apart from this, STS supplementation in the MCD model appears to favour gut dysbiosis and gut-derived inflammation, since it increased the levels of gram-negative bacteria such as *Clostridia* and *Verrucomicrobia*. In fact, MCD+STS mice showed increased mRNA levels of hepatic *IL-1B* and *TNFA* and decreased protein expression of SOD1 and PRDX3 (**Annex 2**). Altogether, these results contribute to the idea of STS favouring inflammation and oxidative stress in diet-induced NASH.

### **Conclusions**

In this study, we showed for the first time that liver mitochondrial H<sub>2</sub>S oxidation and/or its key regulatory enzyme (SQR) are altered in animal models and obese individuals with NAFL and

NASH. We also showed that, while STS supplementation does not appear to have a major impact on phenotypic diet-induced changes, it did alter mitochondrial H<sub>2</sub>S oxidation. Slight changes in this pathway may be substantial in the context of liver physiology and pathology, given that H<sub>2</sub>S levels are directly regulated by its oxidation rates. It is well-known in the literature that H<sub>2</sub>S acts as antioxidant in different pathological scenarios. The lower SQR protein expression found in animal models and humans with NAFL may be a protective mechanism to increase the circulating levels of H<sub>2</sub>S and GSH. On the other hand, the upregulation of SQR protein expression and activity in cases of NASH could represent an adaptation to the elevated production of H<sub>2</sub>S in the gut. Last but not least, the impact of H<sub>2</sub>S supplementation (especially orally) on gut microbiota in a context of NAFLD is something fairly new, with consequences on gut dysbiosis, intestinal permeability, hepatic inflammation and oxidative stress.



## **IV. General Discussion**



## General Discussion

Over the past few years, science has brought forward the regulatory role of H<sub>2</sub>S in liver pathophysiology. As a gasotransmitter, H<sub>2</sub>S controls a vast array of hepatic physiological functions, such as apoptosis, proliferation, inflammation, cellular metabolism, oxygen sensing, and protein modification. However, H<sub>2</sub>S is a tricky molecule and can quickly shift from cell signalling mediator to mitochondrial poison. This duality lies on the available tissue levels of H<sub>2</sub>S, which are governed by the rates of its biosynthesis and oxidation. The liver is one of the most metabolically active tissues in the body, even when it comes to H<sub>2</sub>S metabolism. Although many studies examine the role of H<sub>2</sub>S on a given system by assessing H<sub>2</sub>S production rates or through animal KO models of proteins involved in its biosynthesis, the truth is the pathway of mitochondrial H<sub>2</sub>S oxidation is seldomly checked. The present work carried out during my thesis provides new insights into the pathophysiological importance of liver mitochondrial H<sub>2</sub>S oxidation.

### Pathophysiological regulation of liver mitochondrial H<sub>2</sub>S oxidation

One major observation of my PhD work was that mitochondrial H<sub>2</sub>S oxidation is regulated in different physiological situations and during the development of NAFLD. While in a scenario of fasting mitochondrial H<sub>2</sub>S oxidation is downregulated, in refeeding after fasting this downregulation is annulled. On the other hand, in animal models of NAFL, mitochondrial H<sub>2</sub>S oxidation is downregulated, whereas in animal models of NASH it is upregulated. Interestingly, the protein levels of SQR were found deeply correlated with the rates of mitochondrial H<sub>2</sub>S oxidation. This suggests that SQR is the key regulatory enzyme in this pathway, as further confirmed by the *in vivo* liver SQR overexpression experiments.

Despite the clear nutritional regulation of mitochondrial H<sub>2</sub>S oxidation and SQR expression, to the full extent of our knowledge, no study has ever assessed the gene regulation of SQR by specific nutrients or hormones. In the future, *in vitro* studies must be conducted to evaluate whether or not glucose, specific fatty acids, specific amino acids, insulin or glucagon can for example directly regulate SQR expression/activity. One can assume that this regulation takes place since it has been shown that biochemical alterations, such as shifts in glucose or oxygen levels, directly regulate the expression or activity of the H<sub>2</sub>S-releasing enzymes [688, 792–794]. Nonetheless, several studies focused on the bacterial SQR have demonstrated that the transcription of this enzyme was induced by H<sub>2</sub>S [758–761]. Our results support these studies by

demonstrating that administration of STS to NAFL animal models not only increases liver SQR expression but also mitochondrial H<sub>2</sub>S oxidation. Therefore, further studies are required to determine whether or not such H<sub>2</sub>S-induced transcriptional regulation could also apply to the mammalian SQR. Apart from transcriptional regulation, a recent study has demonstrated that the treatment of HeLa cell lysates with STS induces the persulfidation of TST, increasing its activity [769]. However, this study failed to assess whether or not the same regulatory mechanism happened to the remaining enzymes involved in mitochondrial H<sub>2</sub>S oxidation [769].

Previous reports have demonstrated that animal models of NAFL and patients with fatty liver present lower levels of CoQ [795–797]. One possible explanation for the downregulated mitochondrial H<sub>2</sub>S oxidation pathway in our NAFL mouse model (despite no change in liver SQR protein levels) is a decrease in CoQ levels. SQR is the key enzyme in the mitochondrial H<sub>2</sub>S oxidation pathway and it absolutely requires CoQ as acceptor of electrons. Low levels of CoQ could affect the activity of SQR and its downstream reactions. In fact, a recent study has demonstrated that mice presenting severe CoQ deficiency (*Coq9*<sup>R239X</sup>) display a reduction in SQR levels and activity in the kidney [798]. Interestingly, in the same study was found that the reduction of SQR led to the upregulation of TST protein level and activity [798]. Our model of early-stage NAFL (10 weeks of HF/HS diet feeding) showed the exact same pattern, with SQR protein expression decreasing and the protein levels of TST protein expression increasing. One possible explanation for such regulation lies on the transsulfuration protein, CBS. The increased expression of this protein could lead to an elevation of H<sub>2</sub>S levels. As a consequence, the function of proteins that can be regulated by persulfidation would be affected, and the expression of enzymes potentially involved in the removal of persulfide groups, such as sulfurtransferases, might be induced. Aside modulating protein expression/activity, persulfidation is a protective mechanism against thiol oxidation (sulfenylation, sulfinylation, and sulfonylation) even with ROS levels within normal range [799].

Additionally, we cannot disregard the input of gut microbiota in regulating the expression of SQR by modulating the levels of H<sub>2</sub>S. Sulfate reducing bacteria (SRB) use thiosulfate and sulfate to produce H<sub>2</sub>S [800, 801]. Since it is a gas, H<sub>2</sub>S cannot be contained and some of it may escape the gut. Through the portal circulation, this H<sub>2</sub>S can easily reach the liver, where it is free to increase SQR protein expression and/or activity. Our study strongly supports this hypothesis by showing that *in vivo* administration of STS increases the abundance of SRB, such as *Desulfovibrio*, and that this increase is associated to increased SQR protein expression and mitochondrial H<sub>2</sub>S



oxidation in the liver. Such an observation could have direct implications on our daily life, since the Westernized dietary habits are filled with food additives and preservatives, some of which are sulfur-based [802]. In fact, a recent study has demonstrated that rats fed high-protein diet display increased intestinal luminal content of H<sub>2</sub>S, which coincided with increased expression of the *SQR* gene in colonocytes [71].

### **Importance of SQR-controlling H<sub>2</sub>S level in liver metabolism**

Due to its role as a gasotransmitter, studies showed that modulation of H<sub>2</sub>S levels impacts liver metabolism. Indeed, Zhang *et al.* showed that CSE KO animals (leading to lower liver H<sub>2</sub>S levels) present higher hepatic glycogen content and lower liver glucose production [660]. The same study showed that hepatocytes isolated from CSE KO mice showed higher glucose consumption and that HepG2 cells treated with NaHS presented remarkably diminished insulin signalling [660]. Tang *et al.* also showed that CSE KO mice present higher  $\beta$ -cell insulin secretion, which is abolished by the administration of NaHS [768]. Another study showed that CSE KO mice present a slight but significant increase in glucose tolerance [766]. Ju *et al.* further demonstrated that H<sub>2</sub>S is a direct stimulator of gluconeogenesis through the persulfidation of pyruvate carboxylase (PC), which leads to increased protein activity and glucose production [246]. These studies have been later corroborated by Untereiner *et al.* as CSE KO mice showed reduced rates of gluconeogenesis, which were reversed by administration of NaHS [245]. Moreover, incubation of isolated CSE KO hepatocytes with NaHS persulfidated PEPCK, FBPase, G6Pase and PGC-1 $\alpha$ , increasing their activity and contributing to higher glucose production [245].

Downregulation of CSE expression/activity and upregulation of SQR expression/activity are two completely different regulatory mechanisms of H<sub>2</sub>S metabolism. However, theoretically, both processes contribute to the same outcome: the decrease in intracellular H<sub>2</sub>S levels. By using *in vitro* and *in vivo* approaches, we showed that liver SQR overexpression has a positive effect on liver insulin signalling and glucose utilisation. Although we did not quantify H<sub>2</sub>S levels, the physiological alterations displayed by Adv.SQR mice suggest that the concentration of intracellular H<sub>2</sub>S decreased upon SQR overexpression, considering the phenotypic similarities to CSE KO mice and cells (higher glucose consumption and higher insulin signalling) [660]. In the future, the quantification of H<sub>2</sub>S levels in the liver of Adv.SQR mice will be important to corroborate this hypothesis. Nonetheless, our study demonstrated that modulation of either one of the pathways

involved in H<sub>2</sub>S metabolism (production or oxidation) has a direct impact on glucose metabolism and insulin signalling. This implies, for the first time, that changes in mitochondrial H<sub>2</sub>S oxidation may also have consequences on the development of IR and diabetes.

However, unlike CSE KO mice [660] or impact of exogenous H<sub>2</sub>S, our Adv.SQR mice exhibited no change in liver glucose production (as assessed by PTT) and had lower hepatic glycogen levels. In addition, we also noticed a higher liver/body weight ratio for the Adv.SQR mice. All these results appear to be counterintuitive when compared to the higher fasting glycemia, higher level of glucose-derived metabolites and increased liver insulin signalling observed in these mice. Several hypotheses could be put forward to explain these seemingly contradictory results. First, due to the observed increase in liver insulin signalling (even in the fasting state), liver glucose production could be less efficient. Thus, in the future, it would be interesting to conduct some *in vitro* experiments with mouse hepatocytes overexpressing SQR cultured in the presence of gluconeogenic precursors to confirm that SQR overexpression has no impact on glucose production. Second, regarding the lower liver glycogen content, we could hypothesize that glucose demand is so high in the liver that the need to consume this sugar supersedes the need to store it as glycogen. Third, the increased liver weight found in Adv.SQR mice could not be explained by higher glycogen storage or higher lipid accumulation. Liver hypertrophy is known to be correlated to portal blood flow and hypoxemia [803]. Furthermore, studies have shown that H<sub>2</sub>S participates in the regulation of liver blood flow and portal blood pressure [804, 805]. Therefore, we hypothesize that SQR-induced H<sub>2</sub>S oxidation might have vasoconstriction/vasodilation impact on the liver blood vessels and/or the portal vein. Another hypothesis for increased liver weight following SQR overexpression is hepatocyte proliferation. Interestingly, a recent study has demonstrated that enhanced insulin signalling upon growth factor receptor binding protein 14 (Grb14) inhibition was accompanied by a transient induction of S-phase entrance by quiescent hepatocytes, establishing a direct link between insulin sensitivity and mouse hepatocyte proliferation [806].

### **Specific SQR-mediated H<sub>2</sub>S signalling**

The observed differences in phenotype between CSE KO and Adv.SQR mice strongly suggest that SQR mediates some specific H<sub>2</sub>S signalling actions on mitochondrial/cell bioenergetics linked to glucose metabolism and cellular homeostasis that are independent from those mediated

by H<sub>2</sub>S biosynthesis modulation. According to our results, overexpressing SQR in mouse liver allowed the pathway of mitochondrial H<sub>2</sub>S oxidation to no longer be under nutritional regulation. This not only conclusively proves that SQR is the key regulatory enzyme in this pathway, as it also raises questions regarding the importance of SQR modulation in H<sub>2</sub>S signalling, protein persulfidation, redox balance and oxygen (O<sub>2</sub>) sensing. Indeed, since mitochondrial H<sub>2</sub>S oxidation relies on O<sub>2</sub> consumption, an upregulation of this pathway would significantly decrease O<sub>2</sub> tissue levels, which would impact O<sub>2</sub> sensing and ROS production. Although H<sub>2</sub>S production and oxidation are both important to maintain steady-state levels of H<sub>2</sub>S, the way by which these pathways control H<sub>2</sub>S actions in a cell may vary. The production of H<sub>2</sub>S has an impact on its ability to modify cysteine residues and regulate protein expression/activity, whereas the oxidation of H<sub>2</sub>S participates in mitochondrial respiration, controlling O<sub>2</sub> levels as well as the production of ROS and RSS. Indeed, RSS such as persulfides and polysulfides, have lately gained recognition as powerful cell signalling mediators [22].

### **Interplay between H<sub>2</sub>S production and oxidation**

There is a complex interplay and feedback mechanism(s) between the pathways of H<sub>2</sub>S production and oxidation, which regulates H<sub>2</sub>S signalling and the resultant phenotypic consequences. Indeed, we observed that when overexpressing SQR there was not only a cascade of regulation on its downstream enzymes, but also a modulation of CBS, CSE and MPST protein expression. Another example of this complexity is highlighted by the study of Shirozu *et al* [262]. In their study, hepatic levels of H<sub>2</sub>S in CSE KO mice were no different from those found in the control mice and liver SQR mRNA and protein levels were increased, which is unexpected in a model of H<sub>2</sub>S insufficiency [262]. This type of dual regulation has also been reported by Hine *et al.* in 2015 [740]. Their study has demonstrated that dietary restriction (DR) induces the production of H<sub>2</sub>S by the upregulation of CSE via mTOR activation. This increase in CSE expression presumes higher cysteine degradation into H<sub>2</sub>S while cysteine concentrations are low in the context of DR, which appears to be counterintuitive. However, the *in vivo* sources and substrates for CSE-derived H<sub>2</sub>S in cases of DR are not known, and free cysteine residues released upon autophagy could be a major fuel source for H<sub>2</sub>S production [740]. This study has further demonstrated that, *in vitro*, SQR is necessary for H<sub>2</sub>S-mediated cytoprotection during induced-IR. By donating electrons to the ETC, H<sub>2</sub>S serves as an alternate substrate when other sources of energy are scarce [740]. One interesting example of this H<sub>2</sub>S production/oxidation balance is the case of Nrf2. Several studies

have demonstrated that Keap1 is persulfidated by H<sub>2</sub>S, reaction that inactivates it and promotes Nrf2 signalling [685]. However, it has also been shown that Nrf2 itself controls the mRNA expression of SQR [807], which further corroborates the idea of a feedback loop between the pathways of H<sub>2</sub>S production and oxidation.

### **SQR response to cellular stress**

Recent studies have demonstrated a role of mitochondrial H<sub>2</sub>S oxidation in ER stress [163]. In *C. elegans* worms with partial ablation of SQR, exposure to even low concentrations of H<sub>2</sub>S leads to phosphorylation of eIF2 $\alpha$ , inhibition of protein synthesis and activation of UPR [163]. Thus, whereas in normal animals H<sub>2</sub>S is not known to induce either ER or mitochondrial stress, absence of SQR activity may lead to H<sub>2</sub>S-induced cellular stress [163]. It is possible that mitochondrial SQR uses H<sub>2</sub>S to generate a polysulfide, or sulfane sulfur, species that acts as a cell signal. In fact, mitochondria and ER are two organelles that share a close relationship through contact points known as mitochondria-ER associated membranes (MAMs). MAMs provide a platform to coordinate calcium transfer, inflammasome formation and the provision of membranes for autophagy. A very recent study has demonstrated that NO participates in maintaining MAMs integrity [808]. Given that previous studies have demonstrated that H<sub>2</sub>S can act through NO-dependent mechanisms [809], we can hypothesize that changes in SQR activity may modulate H<sub>2</sub>S-NO interaction and regulate pathways in which these two gasotransmitters are involved.

### **Concluding remarks**

While an increasing number of signalling roles and physiological effects are being attributed to H<sub>2</sub>S, our understanding of mitochondrial H<sub>2</sub>S oxidation pathway and its consequences in liver metabolic homeostasis is only now being investigated. Our study clearly demonstrates that SQR has an impact in liver glucose metabolism and insulin signalling. The differences found between CSE KO and Adv.SQR mice imply the existence of specific SQR-mediated cell signalling, which can either derive from the direct interaction with mitochondrial ETC or from the production of RSS with a highly reactive potential. My PhD work also highlights that all previous studies linking cell perturbations to dysregulations in H<sub>2</sub>S biosynthesis have ignored a major player of H<sub>2</sub>S-centered cell regulation, *i.e.* SQR-mediated H<sub>2</sub>S oxidation. From now on, it becomes imperative to include mitochondrial H<sub>2</sub>S oxidation in studies assessing the effects

of H<sub>2</sub>S dysregulation in pathological scenarios, since H<sub>2</sub>S oxidation and biosynthesis are now identified as two pathways actively interconnected. Moreover, the new finding that liver mitochondrial H<sub>2</sub>S oxidation can be modulated by changes in gut microbiota raises the question of whether or not this pathway could also be impacted by diet-induced intestinal changes. Due to the elevated rates of metabolic-related diseases, mitochondrial H<sub>2</sub>S oxidation must be looked at as a potential therapeutic target in the future.



## ***V. Annexes***

---





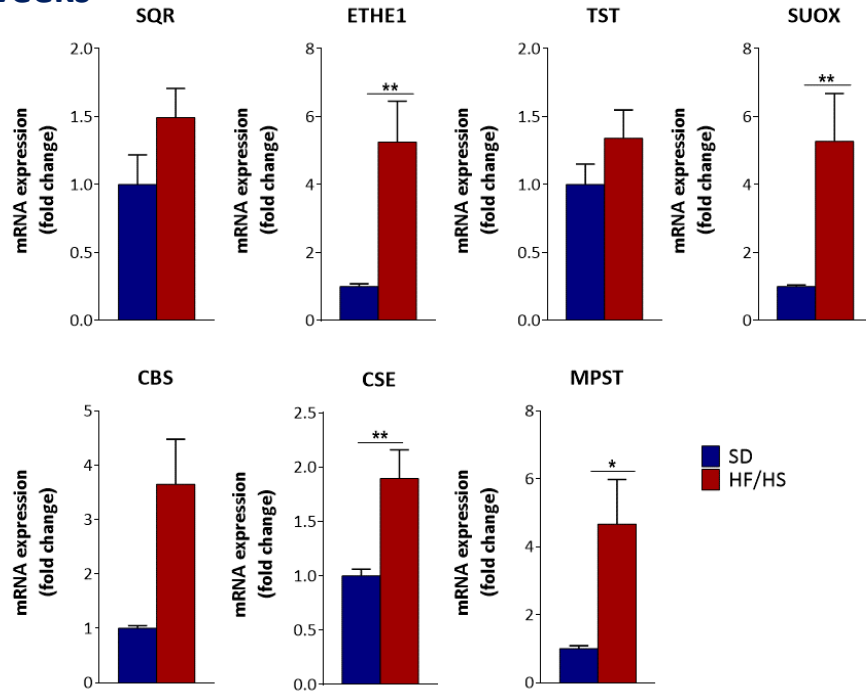
# **Annex 1: Complementary data on the HF/HS diet series**



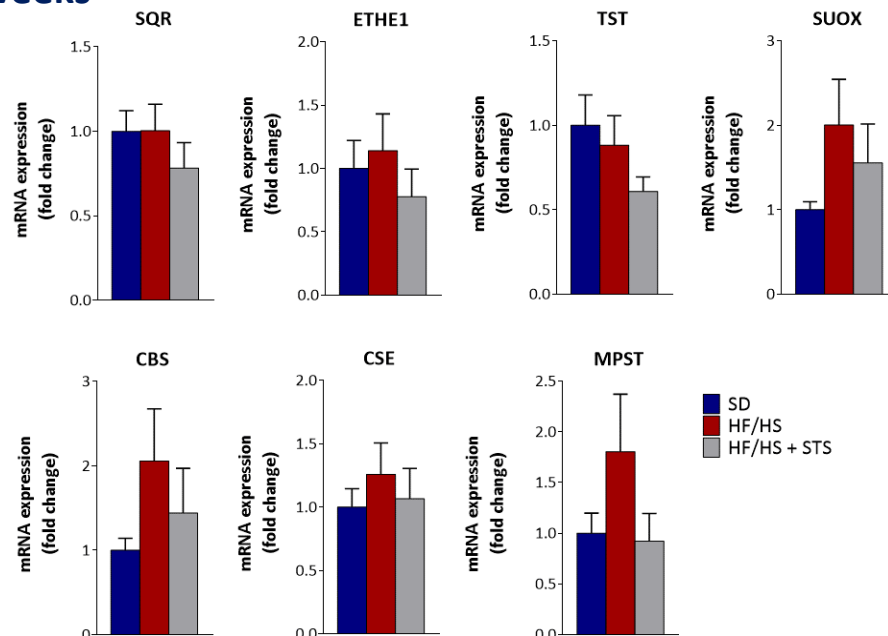
These results were obtained during my secondment in Lisbon with the help of Tawhidul Islam and under the supervision of Dr. Rui Castro and Pr. Cecília Rodrigues.

## Genes involved in H<sub>2</sub>S oxidation and biosynthesis

### 10 weeks



### 20 weeks



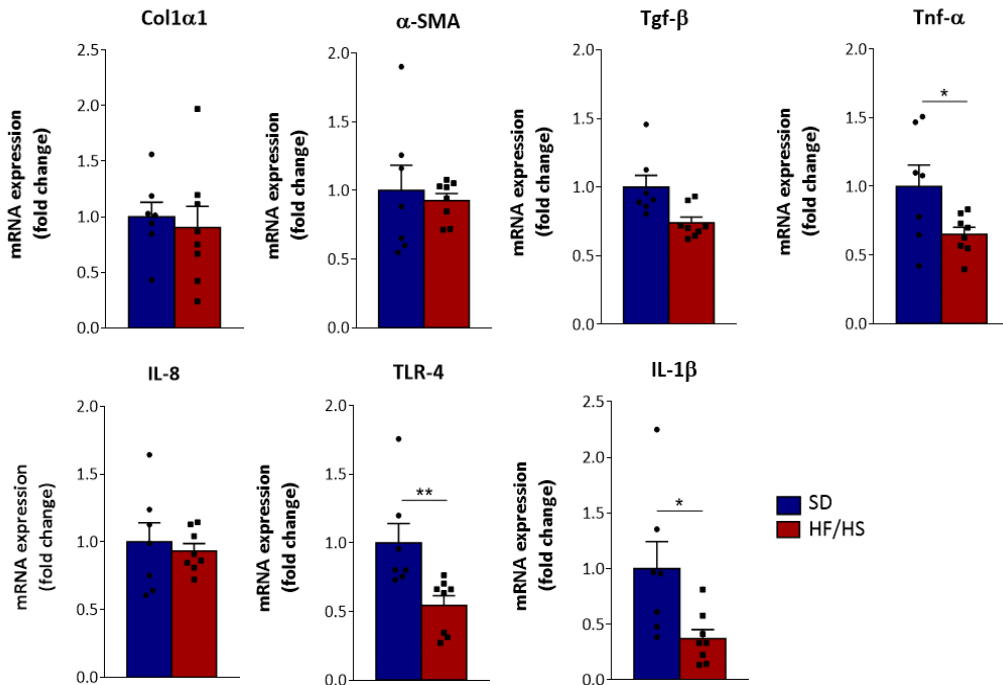
**SQR:** sulfide quinone oxidoreductase; **ETHE1:** dioxygenase; **TST:** thiosulfate sulfurtransferase; **SUOX:** sulfite oxidase; **CBS:** cystathionine  $\beta$ -synthase; **CSE:** cystathionine  $\gamma$ -lyase; **MPST:** 3-mercaptopyruvate sulfurtransferase. Results are represented as mean  $\pm$  SEM (n=6-11 per group). \* p<0.05, \*\* p<0.01 indicate significant differences (Mann Whitney U test).

After 10 weeks of HF/HS feeding, mice displayed significantly higher hepatic mRNA levels of ETHE1 and SUOX (H<sub>2</sub>S oxidation) and of CSE and MPST (H<sub>2</sub>S biosynthesis). After 20 weeks of HF/HS diet, these changes were no longer observed. Moreover, STS supplementation had no impact on the liver mRNA level of genes involved in H<sub>2</sub>S oxidation and H<sub>2</sub>S biosynthesis. These results are contradictory to what was previously observed at the protein level (see **Figures 41 and 45**), suggesting the existence of putative post-transcriptional regulation for these genes and/or differences in mRNA and protein half-lives.

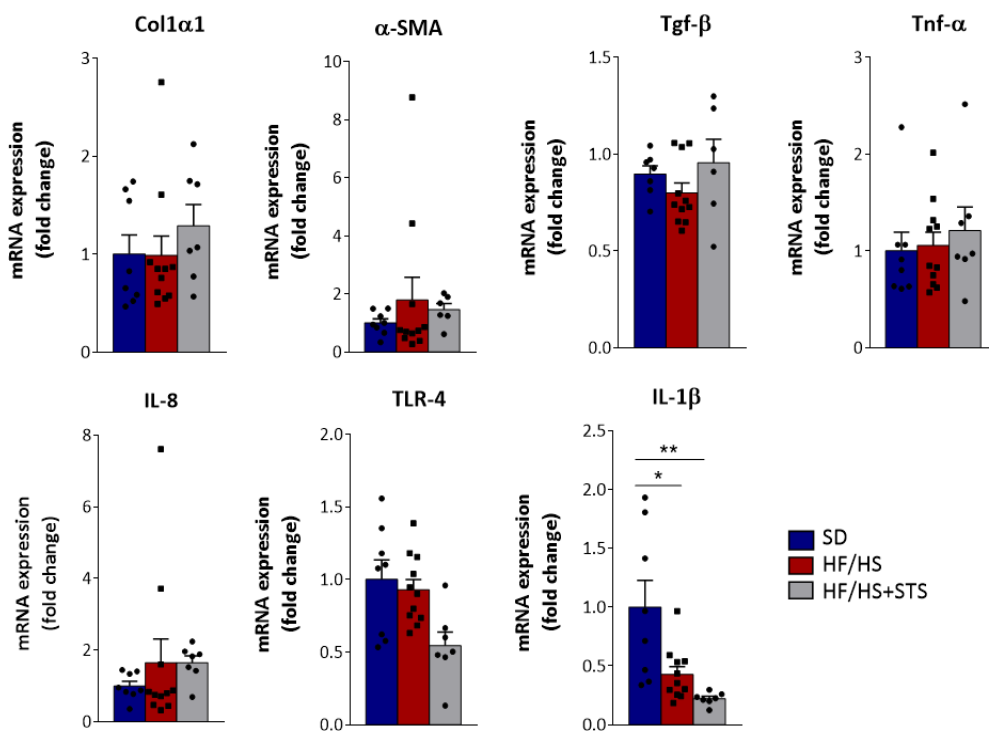
These results were obtained as part of a collaboration with Dr. André Santos and Pr Cecilia Rodrigues.

## Genes involved in inflammation and fibrosis

### 10 weeks



### 20 weeks



**Col1α1:** collagen type I alpha 1; **α-SMA:** alpha-smooth muscle actin; **Tgf-β:** Transforming growth factor beta; **TNFα:** tumor necrosis factor alpha; **IL-8:** interleukin 8; **TLR-4:** Toll-like receptor 4; **IL-1β:** interleukin 1 beta. Results are represented as mean ± SEM (n=6-11 per group). \* p<0.05, \*\* p<0.01 indicate significant differences (Mann Whitney U test).

The liver mRNA levels of key genes involved in inflammation (TGF- $\beta$ , TNF $\alpha$ , IL-8, TLR-4 and IL-1 $\beta$ ) and fibrosis (Col1 $\alpha$ 1 and  $\alpha$ -SMA) were analysed. Surprisingly, after 10 weeks of HF/HS diet, mice had lower hepatic mRNA level of three pro-inflammatory signalling mediators (TNF $\alpha$ , TLR-4 and IL-1 $\beta$ ) while mice fed this diet for 20 weeks only showed decreased hepatic mRNA levels of IL-1 $\beta$ . These findings are contradictory to other studies using NAFLD animal models and humans. This alludes back to the questionable diet batch used. On the other hand, STS supplementation appeared to have no effect on the expression of the different inflammation-related genes. Whether this is merely due to the inefficiency of STS as H<sub>2</sub>S donor or due to the lack of HF/HS diet-induced phenotype changes is not known.

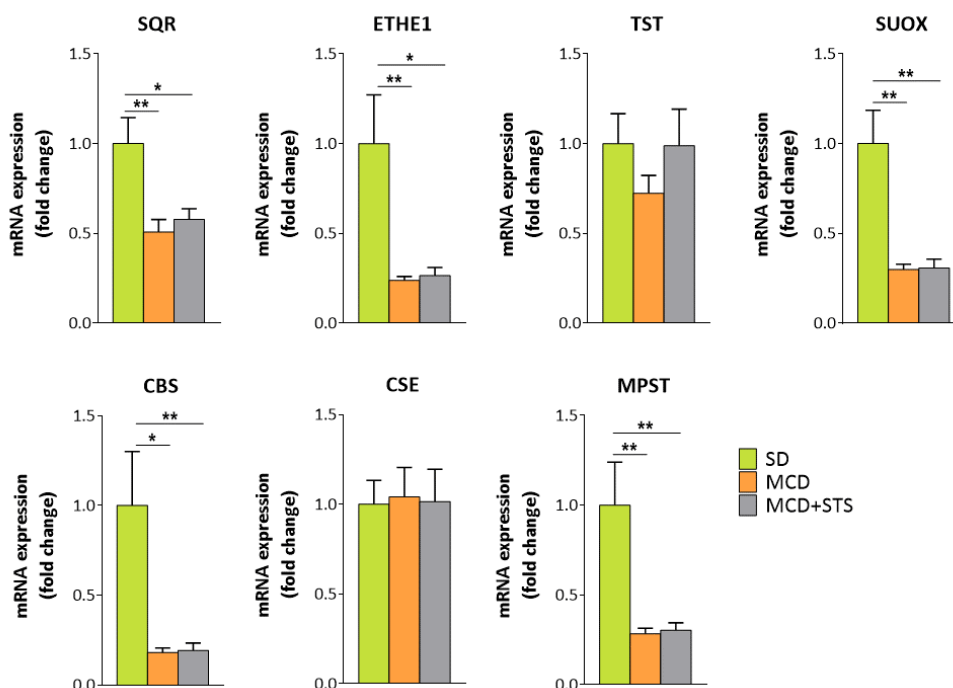
## **Annex 2: Complementary data on the MCD diet series**





These results were obtained during my secondment in Lisbon with the help of Tawhidul Islam and under the supervision of Dr. Rui Castro and Pr. Cecília Rodrigues.

## Genes involved in H<sub>2</sub>S oxidation and biosynthesis

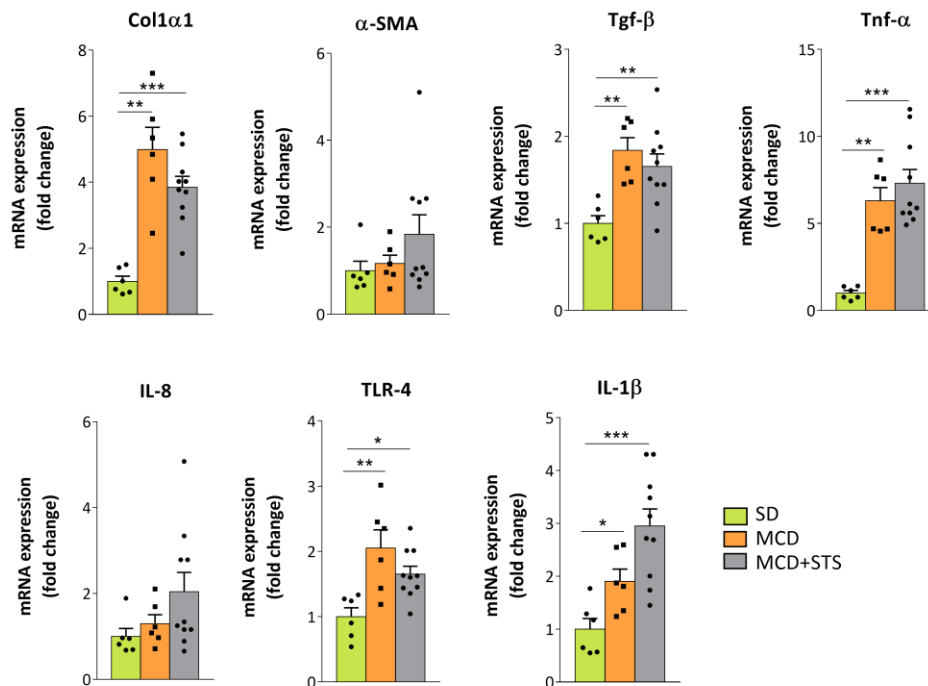


**SQR**: sulfide quinone oxidoreductase; **ETHE1**: dioxygenase; **TST**: thiosulfate sulfurtransferase; **SUOX**: sulfite oxidase; **CBS**: cystathionine  $\beta$ -synthase; **CSE**: cystathionine  $\gamma$ -lyase; **MPST**: 3-mercaptopyruvate sulfurtransferase. Results are represented as mean  $\pm$  SEM (n=6-11 per group). \* p<0.05, \*\* p<0.01 indicate significant differences (Mann Whitney U test).

After 4 weeks of MCD feeding, mice displayed significantly lower hepatic mRNA levels of SQR, ETHE1 and SUOX (H<sub>2</sub>S oxidation) and of CBS and MPST (H<sub>2</sub>S biosynthesis). Some of these results are contradictory to what was previously observed at the protein level (see **Figure 52**), suggesting the existence of putative post-transcriptional regulation for these genes and/or differences in mRNA and protein half-lives. In addition, STS supplementation did not revert the MCD diet-induced impact on the liver mRNA level of genes involved in H<sub>2</sub>S oxidation and H<sub>2</sub>S biosynthesis. Once again, these results were not entirely consistent with what was previously observed at the protein level (**Figure 52**).

These results were obtained as part of a collaboration with Dr. André Santos and Pr Cecilia Rodrigues.

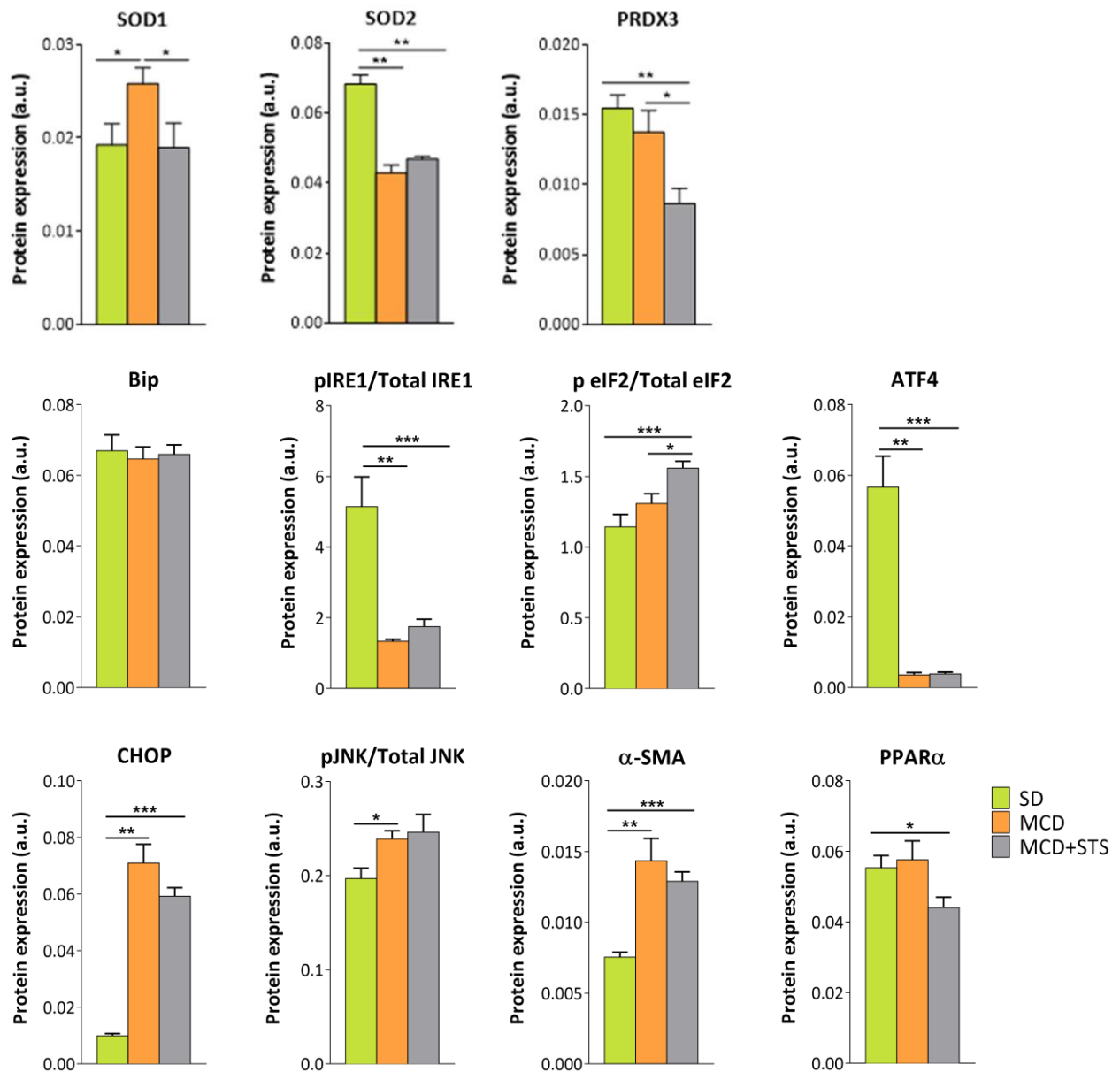
## Genes involved in inflammation and fibrosis



**Col1α1:** collagen type I alpha 1; **α-SMA:** alpha-smooth muscle actin; **Tgf-β:** Transforming growth factor beta; **Tnf-α:** tumor necrosis factor alpha; **IL-8:** interleukin 8; **TLR-4:** Toll-like receptor 4; **IL-1β:** interleukin 1 beta. Results are represented as mean ± SEM (n=6-11 per group). \* p<0.05, \*\* p<0.01 indicate significant differences (Mann Whitney U test).

The mRNA levels of key genes involved in inflammation (TGF-β, TNFα, IL-8, TLR-4 and IL-1β) and fibrosis (Col1α1 and α-SMA) were analysed. Mice fed MCD diet had increased hepatic mRNA levels of several pro-inflammatory (TGF-β, TNFα, TLR-4 and IL-1β) and fibrogenic (Col1α1) genes. These results are in accordance with what has already been published in the literature. Interestingly, however, STS supplementation proved itself to be ineffective in reverting the MCD diet-induced changes on the liver mRNA level of the aforementioned genes.

## Proteins involved in ER stress, inflammation and fibrosis



**SOD1**: superoxide dismutase 1; **SOD2**: superoxide dismutase2; **PRDX3**: peroxiredoxin 3; **Bip**: binding immunoglobulin protein; **IRE1**: inositol-requiring enzyme 1; **eIF2**: eukaryotic initiation factor 2; **ATF4**: activating transcription factor 4; **CHOP**: C/EBP homologous protein; **JNK**: c-Jun N-terminal kinases; **α-SMA**: alpha smooth muscle actin; **PPARα**: peroxisome proliferator-activated receptor alpha. Results are represented as mean ± SEM (n=6-10 per group). \* p<0.05, \*\* p<0.01, \*\*\*p<0.001 indicate significant differences (Mann Whitney U test).

The protein levels of major actors involved in antioxidant defense (SOD1, SOD2, PRDX3), endoplasmic reticulum (ER) stress (BIP, CHOP, IRE1, ATF4, eIF2), inflammation (JNK), fibrosis (α-SMA) and of PPARα were analysed.

Mice fed MCD diet presented higher liver protein expression of  $\alpha$ -SMA and increased pJNK/Total JNK ratio. Concerning ER stress, MCD diet increased hepatic CHOP protein level but decreased ATF4 protein level and pIRE1/Total IRE1 ratio whereas BIP and pelf2/Total eIF2 ratio remained unchanged. MCD diet also enhanced the liver protein level of SOD1 but decreased the protein level of SOD2. These results indicated that MCD diet impacted liver ER stress, inflammation, and antioxidant defences. STS supplementation proved itself to be ineffective in reverting the MCD diet-induced changes on SOD2, pIRE1/Total IRE1 ratio, ATF4, CHOP, pJNK/Total JNK ratio, and  $\alpha$ -SMA. However, STS supplementation did abrogate MCD-induced increase in SOD1 protein level. It also increased hepatic pelf2/total eIF2 ratio and decreased PRDX3 protein level compared to control and MCD mice, and decreased the PPAR $\alpha$  protein level when compared to control mice.

## ***VI. Bibliography***

---



- [1] R. Wang, "Toxic gas, lifesaver," *Scientific American*, vol. 302, no. 3, pp. 66–71, Mar. 2010.
- [2] G. Zhang *et al.*, "Redox chemistry changes in the Panthalassic Ocean linked to the end-Permian mass extinction and delayed Early Triassic biotic recovery," *Proceedings of the National Academy of Sciences of the United States of America*, vol. 114, no. 8, pp. 1806–1810, Feb. 2017.
- [3] L. R. Kump, A. Pavlov, and M. A. Arthur, "Massive release of hydrogen sulfide to the surface ocean and atmosphere during intervals of oceanic anoxia," *Geology*, vol. 33, no. 5, pp. 397–400, May 2005.
- [4] M. Tobler, C. N. Passow, R. Greenway, J. L. Kelley, and J. H. Shaw, "The Evolutionary Ecology of Animals Inhabiting Hydrogen Sulfide–Rich Environments," *Annual Review of Ecology, Evolution, and Systematics*, vol. 47, no. 1, pp. 239–262, Nov. 2016.
- [5] C. Szabo, "A timeline of hydrogen sulfide (H<sub>2</sub>S) research: From environmental toxin to biological mediator," *Biochemical Pharmacology*, vol. 149. Elsevier Inc., pp. 5–19, 01-Mar-2018.
- [6] S. L. M. Rubright, L. L. Pearce, and J. Peterson, "Environmental toxicology of hydrogen sulfide," *Nitric Oxide - Biology and Chemistry*, vol. 71. Academic Press Inc., pp. 1–13, 01-Dec-2017.
- [7] C. H. Foulkes, "*Gas!* : the story of the Special brigade. Andrews UK Limited, 2012.
- [8] S. Masood, "14 Die and Hundreds Sickened in Pakistan, and the Cause Is a Mystery," *The New York Times*, p. 4, 2020.
- [9] E. Blackstone, M. Morrison, and M. B. Roth, "H<sub>2</sub>S induces a suspended animation-like state in mice," *Science*, vol. 308, no. 5721, p. 518, Apr. 2005.
- [10] L. Wu and R. Wang, "Carbon monoxide: Endogenous production, physiological functions, and pharmacological applications," *Pharmacological Reviews*, vol. 57, no. 4. pp. 585–630, Dec-2005.
- [11] R. Wang, "Two's company, three's a crowd: can H<sub>2</sub>S be the third endogenous gaseous transmitter?," *The FASEB Journal*, vol. 16, no. 13, pp. 1792–1798, Nov. 2002.
- [12] R. F. Furchgott and J. V. Zawadzki, "The obligatory role of endothelial cells in the relaxation of arterial smooth muscle by acetylcholine," *Nature*, vol. 288, no. 5789, pp. 373–376, 1980.
- [13] A. Ahmad *et al.*, "Role of nitric oxide in the cardiovascular and renal systems," *International Journal of Molecular Sciences*, vol. 19, no. 9. MDPI AG, 03-Sep-2018.
- [14] A. Verma, D. J. Hirsch, C. E. Glatt, G. V. Ronnett, and S. H. Snyder, "Carbon monoxide: A putative neural messenger," *Science*, vol. 259, no. 5093, pp. 381–384, 1993.
- [15] S. W. Ryter and A. M. K. Choi, "Carbon monoxide: Present and future indications for a medical gas," *Korean Journal of Internal Medicine*, vol. 28, no. 2. Korean Association of Internal Medicine, pp. 123–140, Mar-2013.
- [16] H. H. Kim and S. Choi, "Therapeutic aspects of carbon monoxide in cardiovascular disease," *International Journal of Molecular Sciences*, vol. 19, no. 8. MDPI AG, 13-Aug-2018.
- [17] K. Abe and H. Kimura, "The possible role of hydrogen sulfide as an endogenous neuromodulator,"

- Journal of Neuroscience*, vol. 16, no. 3, pp. 1066–1071, Feb. 1996.
- [18] Z. Weimin, Z. Jing, L. Yanjie, and R. Wang, “The vasorelaxant effect of H<sub>2</sub>S as a novel endogenous gaseous KATP channel opener.,” *The EMBO Journal*, vol. 20, no. 21, pp. 6008–6016, 2001.
- [19] L. K. Wareham, H. M. Southam, and R. K. Poole, “Do nitric oxide, carbon monoxide and hydrogen sulfide really qualify as ‘gasotransmitters’ in bacteria?,” *Biochemical Society Transactions*, vol. 46, no. 5. Portland Press Ltd, pp. 1107–1118, 06-Sep-2018.
- [20] R. Hosoki, N. Matsuki, and H. Kimura, “The possible role of hydrogen sulfide as an endogenous smooth muscle relaxant in synergy with nitric oxide,” *Biochemical and Biophysical Research Communications*, vol. 237, no. 3, pp. 527–531, Aug. 1997.
- [21] H. F. Jin, J. B. Du, X. H. Li, Y. F. Wang, Y. F. Liang, and C. S. Tang, “Interaction between hydrogen sulfide/cystathionine  $\gamma$ -lyase and carbon monoxide/heme oxygenase pathways in aortic smooth muscle cells,” *Acta Pharmacologica Sinica*, vol. 27, no. 12, pp. 1561–1566, Dec. 2006.
- [22] M. R. Filipovic, J. Zivanovic, B. Alvarez, and R. Banerjee, “Chemical Biology of H<sub>2</sub>S Signaling through Persulfidation,” *Chemical Reviews*, vol. 118, no. 3. American Chemical Society, pp. 1253–1337, 14-Feb-2018.
- [23] R. Wang, “Physiological implications of hydrogen sulfide: A whiff exploration that blossomed,” *Physiological Reviews*, vol. 92, no. 2, pp. 791–896, Apr. 2012.
- [24] J. C. Mathai *et al.*, “No facilitator required for membrane transport of hydrogen sulfide,” *Proceedings of the National Academy of Sciences of the United States of America*, vol. 106, no. 39, pp. 16633–16638, Sep. 2009.
- [25] M. A. A. Schoonen and H. L. Barnes, “An approximation of the second dissociation constant for H<sub>2</sub>S,” *Geochimica et Cosmochimica Acta*, vol. 52, no. 3, pp. 649–654, Mar. 1988.
- [26] M. N. Hughes, M. N. Centelles, and K. P. Moore, “Making and working with hydrogen sulfide. The chemistry and generation of hydrogen sulfide in vitro and its measurement in vivo: A review,” *Free Radical Biology and Medicine*, vol. 47, no. 10. pp. 1346–1353, 15-Nov-2009.
- [27] R. Karunya *et al.*, “Rapid measurement of hydrogen sulphide in human blood plasma using a microfluidic method,” *Scientific Reports*, vol. 9, no. 1, pp. 1–11, Dec. 2019.
- [28] M. L. Jennings, “Transport of H<sub>2</sub>S and HS<sup>-</sup> across the human red blood cell membrane: Rapid H<sub>2</sub>S diffusion and AE1-mediated Cl<sup>-</sup>/HS<sup>-</sup> exchange,” *American Journal of Physiology - Cell Physiology*, vol. 305, no. 9, Nov. 2013.
- [29] L. Geng *et al.*, “A simple and reliable method reducing sulfate to sulfide for multiple sulfur isotope analysis,” *Rapid Communications in Mass Spectrometry*, vol. 32, no. 4, pp. 333–341, Feb. 2018.
- [30] T. V. Mishanina, M. Libiad, and R. Banerjee, “Biogenesis of reactive sulfur species for signaling by hydrogen sulfide oxidation pathways,” *Nature Chemical Biology*, vol. 11, no. 7. Nature Publishing



Group, pp. 457–464, 20-Jul-2015.

- [31] Y. Ogasawara, S. Isoda, and S. Tanabe, "Tissue and Subcellular Distribution of Bound and Acid-Labile Sulfur, and the Enzymic Capacity for Sulfide Production in the Rat.," *Biological & Pharmaceutical Bulletin*, vol. 17, no. 12, pp. 1535–1542, Dec. 1994.
- [32] H. Zhong *et al.*, "Hydrogen Sulfide and Endoplasmic Reticulum Stress: A Potential Therapeutic Target for Central Nervous System Degeneration Diseases," *Frontiers in Pharmacology*, vol. 11, p. 702, May 2020.
- [33] M. Ishigami, K. Hiraki, K. Umemura, Y. Ogasawara, K. Ishii, and H. Kimura, "A source of hydrogen sulfide and a mechanism of its release in the brain," *Antioxidants and Redox Signaling*, vol. 11, no. 2, pp. 205–214, Feb. 2009.
- [34] A. M. Porcelli, A. Ghelli, C. Zanna, P. Pinton, R. Rizzuto, and M. Rugolo, "pH difference across the outer mitochondrial membrane measured with a green fluorescent protein mutant," *Biochemical and Biophysical Research Communications*, vol. 326, no. 4, pp. 799–804, Jan. 2005.
- [35] J. I. Toohey, "Sulfur signaling: Is the agent sulfide or sulfane?," *Analytical Biochemistry*, vol. 413, no. 1. Academic Press, pp. 1–7, 01-Jun-2011.
- [36] S. L. Budaev, A. A. Batoeva, and B. A. Tsybikova, "Degradation of thiocyanate in aqueous solution by persulfate activated ferric ion," *Minerals Engineering*, vol. 81, pp. 88–95, Aug. 2015.
- [37] J. I. Toohey, "Sulphane sulphur in biological systems: A possible regulatory role," *Biochemical Journal*, vol. 264, no. 3. Portland Press Ltd, pp. 625–632, 1989.
- [38] N. Shibuya *et al.*, "3-Mercaptopyruvate sulfurtransferase produces hydrogen sulfide and bound sulfane sulfur in the brain," *Antioxidants and Redox Signaling*, vol. 11, no. 4, pp. 703–714, Apr. 2009.
- [39] M. Di Buono, L. J. Wykes, R. O. Ball, and P. B. Pencharz, "Dietary cysteine reduces the methionine requirement in men," *American Journal of Clinical Nutrition*, vol. 74, no. 6, pp. 761–766, 2001.
- [40] K. A. Black and P. C. Dos Santos, "Shared-intermediates in the biosynthesis of thio-cofactors: Mechanism and functions of cysteine desulfurases and sulfur acceptors," *Biochimica et Biophysica Acta - Molecular Cell Research*, vol. 1853, no. 6. Elsevier, pp. 1470–1480, 01-Jun-2015.
- [41] M. Čavuzić and Y. Liu, "Biosynthesis of sulfur-containing tRNA modifications: A comparison of bacterial, archaeal, and eukaryotic pathways," *Biomolecules*, vol. 7, no. 1. MDPI AG, 11-Mar-2017.
- [42] A. Finazzi Agrò, I. Mavelli, C. Cannella, and G. Federici, "Activation of porcine heart mitochondrial malate dehydrogenase by zero valence sulfur and rhodanese," *Biochemical and Biophysical Research Communications*, vol. 68, no. 2, pp. 553–560, Jan. 1976.
- [43] F. B. Hill, "Atmospheric sulfur and its links to the biota.," *Brookhaven symposia in biology*, no. 30, pp. 159–181, Aug. 1973.
- [44] T. L. Guidotti, "Hydrogen sulfide intoxication," in *Handbook of Clinical Neurology*, vol. 131, Elsevier B.V.,

2015, pp. 111–133.

- [45] E. Blackstone and M. B. Roth, “Suspended animation-like state protects mice from lethal hypoxia,” *Shock*, vol. 27, no. 4, pp. 370–372, Apr. 2007.
- [46] Z. H. Han, Y. Jiang, Y. Y. Duan, X. Y. Wang, Y. Huang, and T. Z. Fang, “Protective effects of hydrogen sulfide inhalation on oxidative stress in rats with cotton smoke inhalation-induced lung injury,” *Experimental and Therapeutic Medicine*, vol. 10, no. 1, pp. 164–168, 2015.
- [47] S. Faller, S. W. Ryter, A. M. K. Choi, T. Loop, R. Schmidt, and A. Hoetzel, “Inhaled hydrogen sulfide protects against ventilator-induced lung injury,” *Anesthesiology*, vol. 113, no. 1, pp. 104–115, Jul. 2010.
- [48] “Food Additive Status List | FDA.” [Online]. Available: <https://www.fda.gov/food/food-additives-petitions/food-additive-status-list>. [Accessed: 09-Dec-2020].
- [49] J. T. Brosnan and M. E. Brosnan, “The sulfur-containing amino acids: An overview,” in *Journal of Nutrition*, 2006, vol. 136, no. 6.
- [50] K. Zuhra, F. Augsburger, T. Majtan, and C. Szabo, “Cystathionine- $\beta$ -synthase: Molecular Regulation and Pharmacological Inhibition,” *Biomolecules*, vol. 10, no. 5, p. 697, Apr. 2020.
- [51] M. E. Nimni, B. Han, and F. Cordoba, “Are we getting enough sulfur in our diet?,” *Nutrition and Metabolism*, vol. 4. BioMed Central, p. 24, 2007.
- [52] N. Ijssennagger *et al.*, “Gut microbiota facilitates dietary heme-induced epithelial hyperproliferation by opening the mucus barrier in colon,” *Proceedings of the National Academy of Sciences of the United States of America*, vol. 112, no. 32, pp. 10038–10043, Aug. 2015.
- [53] A. Dostal Webster *et al.*, “Influence of short-term changes in dietary sulfur on the relative abundances of intestinal sulfate-reducing bacteria,” *Gut Microbes*, vol. 10, no. 4, pp. 447–457, Jul. 2019.
- [54] Y. He *et al.*, “Protein hydrolysates’ absorption characteristics in the dynamic small intestine in vivo,” *Molecules*, vol. 23, no. 7, 2018.
- [55] C. Gaudichon *et al.*, “Ileal losses of nitrogen and amino acids in humans and their importance to the assessment of amino acid requirements,” *Gastroenterology*, vol. 123, no. 1, pp. 50–59, 2002.
- [56] A. Amaretti *et al.*, “Profiling of Protein Degraders in Cultures of Human Gut Microbiota,” *Frontiers in Microbiology*, vol. 10, Nov. 2019.
- [57] N. Awano, M. Wada, H. Mori, S. Nakamori, and H. Takagi, “Identification and functional analysis of *Escherichia coli* cysteine desulfhydrases,” *Applied and Environmental Microbiology*, vol. 71, no. 7, pp. 4149–4152, Jul. 2005.
- [58] F. Blachier, F. Mariotti, J. F. Huneau, and D. Tomé, “Effects of amino acid-derived luminal metabolites on the colonic epithelium and physiopathological consequences,” *Amino Acids*, vol. 33, no. 4. Amino Acids, pp. 547–562, Nov-2007.
- [59] X. Shen, M. Carlström, S. Borniquel, C. Jädert, C. G. Kevil, and J. O. Lundberg, “Microbial regulation of

- host hydrogen sulfide bioavailability and metabolism," *Free Radical Biology and Medicine*, vol. 60, pp. 195–200, Jul. 2013.
- [60] T. Oguri, B. Schneider, and L. Reitzer, "Cysteine catabolism and cysteine desulfhydrase (CdsH/STM0458) in salmonella enterica serovar typhimurium," *Journal of Bacteriology*, vol. 194, no. 16, pp. 4366–4376, Aug. 2012.
- [61] H. Gu *et al.*, "Novel cysteine desulfidase CdsB involved in releasing cysteine repression of toxin synthesis in *Clostridium difficile*," *Frontiers in Cellular and Infection Microbiology*, vol. 7, no. JAN, p. 531, Jan. 2018.
- [62] F. Blachier, M. Beaumont, and E. Kim, "Cysteine-derived hydrogen sulfide and gut health: a matter of endogenous or bacterial origin," *Current opinion in clinical nutrition and metabolic care*, vol. 22, no. 1. NLM (Medline), pp. 68–75, 01-Jan-2019.
- [63] C. L. Willis, J. H. Cummings, G. Neale, and G. R. Gibson, "In vitro effects of mucin fermentation on the growth of human colonic sulphate-reducing bacteria," *Anaerobe*, vol. 2, pp. 117–122, 1996.
- [64] G. Lennon *et al.*, "Correlations between colonic crypt mucin chemotype, inflammatory grade and *Desulfovibrio* species in ulcerative colitis," *Colorectal Disease*, vol. 16, no. 5, 2014.
- [65] F. E. Rey, M. D. Gonzalez, J. Cheng, M. Wu, P. P. Ahern, and J. I. Gordon, "Metabolic niche of a prominent sulfate-reducing human gut bacterium," *Proceedings of the National Academy of Sciences of the United States of America*, vol. 110, no. 33, pp. 13582–13587, Aug. 2013.
- [66] M. S. Desai *et al.*, "A Dietary Fiber-Deprived Gut Microbiota Degrades the Colonic Mucus Barrier and Enhances Pathogen Susceptibility," *Cell*, vol. 167, no. 5, pp. 1339–1353.e21, Nov. 2016.
- [67] H. H. Tsai, A. D. Dwarakanath, C. A. Hart, J. D. Milton, and J. M. Rhodes, "Increased faecal mucin sulphatase activity in ulcerative colitis: A potential target for treatment," *Gut*, vol. 36, no. 4, pp. 570–576, 1995.
- [68] F. Carbonero, A. C. Benefiel, A. H. Alizadeh-Ghamsari, and H. R. Gaskins, "Microbial pathways in colonic sulfur metabolism and links with health and disease," *Frontiers in Physiology*, vol. 3 NOV, 2012.
- [69] E. A. Magee, C. J. Richardson, R. Hughes, and J. H. Cummings, "Contribution of dietary protein to sulfide production in the large intestine: an in vitro and a controlled feeding study in humans," *The American Journal of Clinical Nutrition*, vol. 72, no. 6, pp. 1488–1494, Dec. 2000.
- [70] C. Mu, Y. Yang, Z. Luo, L. Guan, and W. Zhu, "The colonic microbiome and epithelial transcriptome are altered in rats fed a high-protein diet compared with a normal-protein diet," *Journal of Nutrition*, vol. 146, no. 3, pp. 474–483, 2016.
- [71] M. Beaumont *et al.*, "Detrimental effects for colonocytes of an increased exposure to luminal hydrogen sulfide: The adaptive response," *Free Radical Biology and Medicine*, vol. 93, pp. 155–164, Apr. 2016.
- [72] H. D. PECK, "Enzymatic basis for assimilatory and dissimilatory sulfate reduction.," *Journal of*

- bacteriology*, vol. 82, no. 6, pp. 933–939, Dec. 1961.
- [73] J. A. Croix, F. Carbonero, G. M. Nava, M. Russell, E. Greenberg, and H. R. Gaskins, “On the relationship between sialomucin and sulfomucin expression and hydrogenotrophic microbes in the human colonic mucosa,” *PLoS ONE*, vol. 6, no. 9, Sep. 2011.
- [74] K. Anantharaman *et al.*, “Expanded diversity of microbial groups that shape the dissimilatory sulfur cycle,” *ISME Journal*, vol. 12, no. 7, pp. 1715–1728, Jun. 2018.
- [75] J. Kováč, M. Vítězová, and I. Kushkevych, “Metabolic activity of sulfate-reducing bacteria from rodents with colitis,” *Open Medicine*, vol. 13, no. 1, pp. 344–349, 2018.
- [76] G. R. Gibson, J. H. Cummings, and G. T. Macfarlane, “Growth and activities of sulphate-reducing bacteria in gut contents of healthy subjects and patients with ulcerative colitis,” *FEMS Microbiology Letters*, vol. 86, no. 2, pp. 103–112, Dec. 1991.
- [77] B. Chassaing *et al.*, “Dietary emulsifiers impact the mouse gut microbiota promoting colitis and metabolic syndrome,” *Nature*, vol. 519, no. 7541, pp. 92–96, Mar. 2015.
- [78] L. A. David *et al.*, “Diet rapidly and reproducibly alters the human gut microbiome,” *Nature*, vol. 505, no. 7484, pp. 559–563, 2014.
- [79] J. Loubinoux, J.-P. Bronowicki, I. A. C. Pereira, J.-L. Mougénel, and A. E. Faou, “Sulfate-reducing bacteria in human feces and their association with inflammatory bowel diseases,” *FEMS Microbiology Ecology*, vol. 40, no. 2, pp. 107–112, May 2002.
- [80] I. Kushkevych *et al.*, “The Sulfate-Reducing Microbial Communities and Meta-Analysis of Their Occurrence during Diseases of Small–Large Intestine Axis,” *Journal of Clinical Medicine*, vol. 8, no. 10, p. 1656, Oct. 2019.
- [81] Y. Feng, A. J. M. Stams, W. M. de Vos, and I. Sánchez-Andrea, “Enrichment of sulfidogenic bacteria from the human intestinal tract,” *FEMS Microbiology Letters*, vol. 364, no. 4. Oxford University Press, pp. 1–7, 01-Feb-2017.
- [82] D. G. Searcy and S. H. Lee, “Sulfur reduction by human erythrocytes,” *Journal of Experimental Zoology*, vol. 282, no. 3, pp. 310–322, Oct. 1998.
- [83] G. K. Kolluru, X. Shen, S. C. Bir, and C. G. Kevil, “Hydrogen sulfide chemical biology: Pathophysiological roles and detection,” *Nitric Oxide - Biology and Chemistry*, vol. 35. NIH Public Access, pp. 5–20, 2013.
- [84] A. I. Bhuiyan, V. T. Papajani, M. Paci, and S. Melino, “Glutathione–Garlic sulfur conjugates: Slow hydrogen sulfide releasing agents for therapeutic applications,” *Molecules*, vol. 20, no. 1, pp. 1731–1750, Jan. 2015.
- [85] R. Tocmo, Y. Wu, D. Liang, V. Fogliano, and D. Huang, “Boiling enriches the linear polysulfides and the hydrogen sulfide-releasing activity of garlic,” *Food Chemistry*, vol. 221, pp. 1867–1873, Apr. 2017.
- [86] G. A. Benavides *et al.*, “Hydrogen sulfide mediates the vasoactivity of garlic,” *Proceedings of the*

- National Academy of Sciences of the United States of America*, vol. 104, no. 46, pp. 17977–17982, Nov. 2007.
- [87] A. Koj, J. Frendo, and Z. Janik, “[35S]thiosulphate oxidation by rat liver mitochondria in the presence of glutathione.,” *The Biochemical journal*, vol. 103, no. 3, pp. 791–795, 1967.
- [88] M. Volini and J. Westley, “The Mechanism of the Rhodanese-catalyzed Thiosulfate Reaction KINETIC ANALYSIS\*,” 1966.
- [89] Y. Mikami, N. Shibuya, Y. Kimura, N. Nagahara, Y. Ogasawara, and H. Kimura, “Thioredoxin and dihydrolipoic acid are required for 3-mercaptopyruvate sulfurtransferase to produce hydrogen sulfide,” *Biochemical Journal*, vol. 439, no. 3, pp. 479–485, Nov. 2011.
- [90] A. Leskova, S. Pardue, J. D. Glawe, C. G. Kevil, and X. Shen, “Role of thiosulfate in hydrogen sulfide-dependent redox signaling in endothelial cells,” *American Journal of Physiology - Heart and Circulatory Physiology*, vol. 313, no. 2, pp. H256–H264, 2017.
- [91] K. R. Olson *et al.*, “Thiosulfate: A readily accessible source of hydrogen sulfide in oxygen sensing,” *American Journal of Physiology - Regulatory Integrative and Comparative Physiology*, vol. 305, no. 6, pp. R592–R603, Sep. 2013.
- [92] K. Yamagishi *et al.*, “Generation of gaseous sulfur-containing compounds in tumour tissue and suppression of gas diffusion as an antitumour treatment,” *Gut*, vol. 61, no. 4, pp. 554–561, Apr. 2012.
- [93] J. Yang *et al.*, “Non-enzymatic hydrogen sulfide production from cysteine in blood is catalyzed by iron and vitamin B6,” *Communications Biology*, vol. 2, no. 1, Dec. 2019.
- [94] E. Marutani and F. Ichinose, “Emerging pharmacological tools to control hydrogen sulfide signaling in critical illness,” *Intensive Care Medicine Experimental*, vol. 8, no. 1, pp. 1–14, Dec. 2020.
- [95] C. Hine and J. R. Mitchell, “Calorie restriction and methionine restriction in control of endogenous hydrogen sulfide production by the transsulfuration pathway,” *Experimental Gerontology*, vol. 68, pp. 26–32, Aug. 2015.
- [96] S. C. Peck, K. Denger, A. Burrichter, S. M. Irwin, E. P. Balskus, and D. Schleheck, “A glycol radical enzyme enables hydrogen sulfide production by the human intestinal bacterium *Bifidobacterium wadsworthia*,” *Proceedings of the National Academy of Sciences of the United States of America*, vol. 116, no. 8, pp. 3171–3176, Feb. 2019.
- [97] B. Francis Binklisy and V. nu VIGNISAUD, “THE FORMATION OF CYSTEINE FROM HOMOCYSTEINE: AND SERINE BY LIVER TISSUE OF RATS\*,” *Journal of Biological Chemistry*, vol. 144, pp. 507–511, 1942.
- [98] E. Mosharov, M. R. Cranford, and R. Banerjee, “The quantitatively important relationship between homocysteine metabolism and glutathione synthesis by the transsulfuration pathway and its regulation by redox changes,” *Biochemistry*, vol. 39, no. 42, pp. 13005–13011, Oct. 2000.
- [99] K. R. Olson, “H<sub>2</sub>S and polysulfide metabolism: Conventional and unconventional pathways,”

*Biochemical Pharmacology*, vol. 149. Elsevier Inc., pp. 77–90, 01-Mar-2018.

- [100] A. E. Braunstein, E. V. Goryachenkova, and N. D. Lac, "Reactions catalysed by serine sulfhydryase from chicken liver," *BBA - Enzymology*, vol. 171, no. 2, pp. 366–368, Feb. 1969.
- [101] A. Ichinohe, T. Kanaumi, S. Takashima, Y. Enokido, Y. Nagai, and H. Kimura, "Cystathionine  $\beta$ -synthase is enriched in the brains of Down's patients," *Biochemical and Biophysical Research Communications*, vol. 338, no. 3, pp. 1547–1550, Dec. 2005.
- [102] T. Panagaki, E. B. Randi, F. Augsburg, and C. Szabo, "Overproduction of H<sub>2</sub>S, generated by CBS, inhibits mitochondrial Complex IV and suppresses oxidative phosphorylation in down syndrome," *Proceedings of the National Academy of Sciences of the United States of America*, vol. 116, no. 38, pp. 18769–18771, Sep. 2019.
- [103] M. Yamanishi, O. Kabil, S. Sen, and R. Banerjee, "Structural insights into pathogenic mutations in heme-dependent cystathionine- $\beta$ -synthase," *Journal of Inorganic Biochemistry*, vol. 100, no. 12. Elsevier, pp. 1988–1995, 01-Dec-2006.
- [104] S. Taoka and R. Banerjee, "Characterization of NO binding to human cystathionine  $\beta$ -synthase: Possible implications of the effects of CO and NO binding to the human enzyme," *Journal of Inorganic Biochemistry*, vol. 87, no. 4, pp. 245–251, Dec. 2001.
- [105] J. D. Finkelstein, W. E. Kyle, J. J. Martin, and A. M. Pick, "Activation of cystathionine synthase by adenosylmethionine and adenosylethionine," *Biochemical and Biophysical Research Communications*, vol. 66, no. 1, pp. 81–87, Sep. 1975.
- [106] J. Ereno-Orbea, T. Majtan, I. Oyenarte, J. P. Kraus, and L. A. Martinez-Cruz, "Structural insight into the molecular mechanism of allosteric activation of human cystathionine  $\beta$ -synthase by S-adenosylmethionine," *Proceedings of the National Academy of Sciences of the United States of America*, vol. 111, no. 37, pp. E3845–E3852, Sep. 2014.
- [107] T. Majtan, A. L. Pey, and J. P. Kraus, "Kinetic stability of cystathionine beta-synthase can be modulated by structural analogs of S-adenosylmethionine: Potential approach to pharmacological chaperone therapy for homocystinuria," *Biochimie*, vol. 126, pp. 6–13, Jul. 2016.
- [108] P. K. Yadav and R. Banerjee, "Detection of reaction intermediates during human cystathionine  $\beta$ -synthase-monitored turnover and H<sub>2</sub>S production," *Journal of Biological Chemistry*, vol. 287, no. 52, pp. 43464–43471, Dec. 2012.
- [109] X. Chen, K. H. Jhee, and W. D. Kruger, "Production of the neuromodulator H<sub>2</sub>S by cystathionine  $\beta$ -synthase via the condensation of cysteine and homocysteine," *Journal of Biological Chemistry*, vol. 279, no. 50, pp. 52082–52086, Dec. 2004.
- [110] S. Singh, D. Padovani, R. A. Leslie, T. Chiku, and R. Banerjee, "Relative contributions of cystathionine  $\beta$ -synthase and  $\gamma$ -cystathionase to H<sub>2</sub>S biogenesis via alternative trans-sulfuration reactions," *Journal of Biological Chemistry*, vol. 284, no. 33, pp. 22457–22466, Aug. 2009.

- [111] B. Renga, "Hydrogen sulfide generation in mammals: The molecular biology of cystathionine- $\beta$ -synthase (CBS) and cystathionine- $\gamma$ -lyase (CSE)," *Inflammation and Allergy - Drug Targets*, vol. 10, no. 2. Bentham Science Publishers B.V., pp. 85–91, 2011.
- [112] A. Mazaheri, N. Mostofizadeh, and M. Hashemipour, "Homocystinuria with Stroke and Positive Familial History," *Advanced Biomedical Research*, vol. 6, no. 1, p. 132, 2017.
- [113] S. Fatima, A. Hafeez, A. Ijaz, N. Asif, A. Awan, and A. Sajid, "Classical homocystinuria in a juvenile patient," *Journal of the College of Physicians and Surgeons Pakistan*, vol. 28, no. 6, pp. 488–489, Jun. 2018.
- [114] E. M. Bublil and T. Majtan, "Classical homocystinuria: From cystathionine beta-synthase deficiency to novel enzyme therapies," *Biochimie*, vol. 173. Elsevier B.V., pp. 48–56, 01-Jun-2020.
- [115] M. Watanabe *et al.*, "Mice deficient in cystathionine  $\beta$ -synthase: Animal models for mild and severe homocyst(e)inemia," *Proceedings of the National Academy of Sciences of the United States of America*, vol. 92, no. 5, pp. 1585–1589, Feb. 1995.
- [116] I. Ishii *et al.*, "Murine cystathionine  $\gamma$ -lyase: Complete cDNA and genomic sequences, promoter activity, tissue distribution and developmental expression," *Biochemical Journal*, vol. 381, no. 1, pp. 113–123, Jul. 2004.
- [117] G. Yang *et al.*, "H<sub>2</sub>S as a physiologic vasorelaxant: Hypertension in mice with deletion of cystathionine  $\gamma$ -lyase," *Science*, vol. 322, no. 5901, pp. 587–590, Oct. 2008.
- [118] Y. Pan, S. Ye, D. Yuan, J. Zhang, Y. Bai, and C. Shao, "Hydrogen sulfide (H<sub>2</sub>S)/cystathionine  $\gamma$ -lyase (CSE) pathway contributes to the proliferation of hepatoma cells," *Mutation Research - Fundamental and Molecular Mechanisms of Mutagenesis*, vol. 763–764, pp. 10–18, 2014.
- [119] S. Huang, H. Li, and J. Ge, "A cardioprotective insight of the cystathionine  $\gamma$ -lyase/hydrogen sulfide pathway," *IJC Heart and Vasculature*, vol. 7, pp. 51–57, Jun. 2015.
- [120] S. J. Han *et al.*, "Hydrogen sulfide-producing cystathionine  $\gamma$ -lyase is critical in the progression of kidney fibrosis," *Free Radical Biology and Medicine*, vol. 112, pp. 423–432, Nov. 2017.
- [121] T. Chiku, D. Padovani, W. Zhu, S. Singh, V. Vitvitsky, and R. Banerjee, "H<sub>2</sub>S biogenesis by human cystathionine  $\gamma$ -lyase leads to the novel sulfur metabolites lanthionine and homolanthionine and is responsive to the grade of hyperhomocysteinemia," *Journal of Biological Chemistry*, vol. 284, no. 17, pp. 11601–11612, Apr. 2009.
- [122] O. Kabil and R. Banerjee, "Enzymology of H<sub>2</sub>S biogenesis, decay and signaling," *Antioxidants and Redox Signaling*, vol. 20, no. 5. Antioxid Redox Signal, pp. 770–782, 10-Feb-2014.
- [123] A. L. Levonen, R. Lapatto, M. Saksela, and K. O. Raivio, "Human cystathionine  $\gamma$ -lyase: Developmental and in vitro expression of two isoforms," *Biochemical Journal*, vol. 347, no. 1, pp. 291–295, Apr. 2000.
- [124] J. G. Dickhout *et al.*, "Integrated stress response modulates cellular redox state via induction of

- cystathionine  $\gamma$ -lyase: Cross-talk between integrated stress response and thiol metabolism," *Journal of Biological Chemistry*, vol. 287, no. 10, pp. 7603–7614, Mar. 2012.
- [125] G. Yuan *et al.*, "Protein kinase G-regulated production of H<sub>2</sub>S governs oxygen sensing," *Science Signaling*, vol. 8, no. 373, Apr. 2015.
- [126] D. E. Fomenko and V. N. Gladyshev, "Identity and functions of CxxC-derived motifs," *Biochemistry*, vol. 42, no. 38, pp. 11214–11225, Sep. 2003.
- [127] T. Yamanishi and S. Tuboi, "The mechanism of the L-cystine cleavage reaction catalyzed by rat liver  $\gamma$ -cystathionase," *Journal of Biochemistry*, vol. 89, no. 6, pp. 1913–1921, Apr. 1981.
- [128] J. E. Vargas, S. H. Mudd, S. E. Waisbren, and H. L. Levy, "Maternal  $\gamma$ -cystathionase deficiency: Absence of both teratogenic effects and pregnancy complications," *American Journal of Obstetrics and Gynecology*, vol. 181, no. 3, pp. 753–755, 1999.
- [129] S. Mani *et al.*, "Decreased endogenous production of hydrogen sulfide accelerates atherosclerosis," *Circulation*, vol. 127, no. 25, pp. 2523–2534, Jun. 2013.
- [130] A. M. Rao, M. R. Drake, and M. H. Stipanuk, "Role of the transsulfuration pathway and of  $\gamma$ -cystathionase activity in the formation of cysteine and sulfate from methionine in rat hepatocytes," *Journal of Nutrition*, vol. 120, no. 8, pp. 837–845, 1990.
- [131] N. Nagahara, T. Okazaki, and T. Nishino, "Cytosolic mercaptopyruvate sulfurtransferase is evolutionarily related to mitochondrial rhodanese: Striking similarity in active site amino acid sequence and the increase in the mercaptopyruvate sulfurtransferase activity of rhodanese by site-directed mutagenesis," *Journal of Biological Chemistry*, vol. 270, no. 27, pp. 16230–16235, Jul. 1995.
- [132] N. Nagahara and T. Nishino, "Role of amino acid residues in the active site of rat liver mercaptopyruvate sulfurtransferase: cDNA cloning, overexpression, and site-directed mutagenesis," *Journal of Biological Chemistry*, vol. 271, no. 44, pp. 27395–27401, 1996.
- [133] N. Nagahara, T. Ito, H. Kitamura, and T. Nishino, "Tissue and subcellular distribution of mercaptopyruvate sulfurtransferase in the rat: Confocal laser fluorescence and immunoelectron microscopic studies combined with biochemical analysis," *Histochemistry and Cell Biology*, vol. 110, no. 3, pp. 243–250, 1998.
- [134] P. K. Yadav, K. Yamada, T. Chiku, M. Koutmos, and R. Banerjee, "Structure and kinetic analysis of H<sub>2</sub>S production by human mercaptopyruvate sulfurtransferase," *Journal of Biological Chemistry*, vol. 288, no. 27, pp. 20002–20013, Jul. 2013.
- [135] P. K. Yadav, V. Vitvitsky, S. Carballal, J. Seravalli, and R. Banerjee, "Thioredoxin regulates human mercaptopyruvate sulfurtransferase at physiologically-relevant concentrations," *Journal of Biological Chemistry*, vol. 295, no. 19, pp. 6299–6310, May 2020.
- [136] D. Bordo and P. Bork, "The rhodanese/Cdc25 phosphatase superfamily. Sequence-structure-function relations," *EMBO Reports*, vol. 3, no. 8. European Molecular Biology Organization, pp. 741–746, 2002.



- [137] N. Nagahara, "Multiple role of 3-mercaptopyruvate sulfurtransferase: antioxidative function, H<sub>2</sub>S and polysulfide production and possible SO<sub>x</sub> production," *British Journal of Pharmacology*, vol. 175, no. 4, pp. 577–589, Feb. 2018.
- [138] A. Meister, "Conversion of the  $\alpha$ -keto analog of cysteine to pyruvate and sulfur," *Federation Proceeding*, vol. 12, no. 245, 1953.
- [139] J. L. Wood and H. Fiedler, "Beta-Mercapto-pyruvate, a substrate for rhodanese," *The Journal of biological chemistry*, vol. 205, no. 1, pp. 231–234, 1953.
- [140] N. Nagahara, Q. Li, and N. Sawada, "Do antidotes for acute cyanide poisoning act on mercaptopyruvate sulfurtransferase to facilitate detoxification?," *Current drug targets. Immune, endocrine and metabolic disorders*, vol. 3, no. 3. Curr Drug Targets Immune Endocr Metabol Disord, pp. 198–204, 2003.
- [141] B. Sörbo, "3-Mercaptopyruvate, 3-Mercaptolactate and Mercaptoacetate," *Methods in Enzymology*, vol. 143, no. C, pp. 178–182, Jan. 1987.
- [142] M. Li *et al.*, "Fatty acids promote fatty liver disease via the dysregulation of 3-mercaptopyruvate sulfurtransferase/hydrogen sulfide pathway," *Gut*, vol. 67, no. 12, Sep. 2017.
- [143] N. Akahoshi *et al.*, "Increased urinary 3-mercaptolactate excretion and enhanced passive systemic anaphylaxis in mice lacking mercaptopyruvate sulfurtransferase, a model of mercaptolactate-cysteine disulfiduria," *International Journal of Molecular Sciences*, vol. 21, no. 3, Feb. 2020.
- [144] K. R. Olson, E. R. DeLeon, and F. Liu, "Controversies and conundrums in hydrogen sulfide biology," *Nitric Oxide - Biology and Chemistry*, vol. 41. Academic Press Inc., pp. 11–26, 15-Sep-2014.
- [145] B. Tan *et al.*, "New method for quantification of gasotransmitter hydrogen sulfide in biological matrices by LC-MS/MS," *Scientific Reports*, vol. 7, Apr. 2017.
- [146] V. Vitvitsky, O. Kabil, and R. Banerjee, "High turnover rates for hydrogen sulfide allow for rapid regulation of its tissue concentrations," *Antioxidants and Redox Signaling*, vol. 17, no. 1. Mary Ann Liebert, Inc., pp. 22–31, 01-Jul-2012.
- [147] C. F. Toombs *et al.*, "Detection of exhaled hydrogen sulphide gas in healthy human volunteers during intravenous administration of sodium sulphide," *British Journal of Clinical Pharmacology*, vol. 69, no. 6, pp. 626–636, Jun. 2010.
- [148] J. Zhang, X. Wang, Y. Chen, and W. Yao, "Exhaled hydrogen sulfide predicts airway inflammation phenotype in COPD," *Respiratory Care*, vol. 60, no. 2, pp. 251–258, 2015.
- [149] J. H. Cha, D. H. Kim, S. J. Choi, W. T. Koo, and I. D. Kim, "Sub-Parts-per-Million Hydrogen Sulfide Colorimetric Sensor: Lead Acetate Anchored Nanofibers toward Halitosis Diagnosis," *Analytical Chemistry*, vol. 90, no. 15, pp. 8769–8775, Aug. 2018.
- [150] R. A. Weisiger, L. M. Pinkus, and W. B. Jakoby, "Thiol S-methyltransferase: suggested role in detoxication of intestinal hydrogen sulfide," *Biochemical Pharmacology*, vol. 29, no. 20, pp. 2885–2887,

Oct. 1980.

- [151] C. Liu *et al.*, "Human liver cytochrome P450 enzymes and microsomal thiol methyltransferase are involved in the stereoselective formation and methylation of the pharmacologically active metabolite of clopidogrel," *Drug Metabolism and Disposition*, vol. 43, no. 10, pp. 1632–1641, Oct. 2015.
- [152] R. A. Keith, J. Van Loon, L. F. Wussow, and R. M. Weinshilboum, "Thiol methylation pharmacogenetics: Heritability of human erythrocyte thiol methyltransferase activity," *Clinical Pharmacology and Therapeutics*, vol. 34, no. 4, pp. 521–528, Oct. 1983.
- [153] M. D. Levitt, J. Furne, J. Springfield, F. Suarez, and E. DeMaster, "Detoxification of hydrogen sulfide and methanethiol in the cecal mucosa," *Journal of Clinical Investigation*, vol. 104, no. 8, pp. 1107–1114, 1999.
- [154] J. Furne, J. Springfield, T. Koenig, E. DeMaster, and M. D. Levitt, "Oxidation of hydrogen sulfide and methanethiol to thiosulfate by rat tissues: A specialized function of the colonic mucosa," *Biochemical Pharmacology*, vol. 62, no. 2, pp. 255–259, Jul. 2001.
- [155] M. Aslam, J. J. Batten, T. H. J. Florin, R. L. Sidebotham, and J. H. Baron, "Hydrogen sulphide induced damage to the colonic mucosal barrier in the rat," *Gut*, vol. 33, no. 69. 1992.
- [156] C. L. Silva, M. Passos, and J. S. Cmara, "Investigation of urinary volatile organic metabolites as potential cancer biomarkers by solid-phase microextraction in combination with gas chromatography-mass spectrometry," *British Journal of Cancer*, vol. 105, no. 12, pp. 1894–1904, Dec. 2011.
- [157] A. Ishibe *et al.*, "Detection of gas components as a novel diagnostic method for colorectal cancer," *Annals of Gastroenterological Surgery*, vol. 2, no. 2, pp. 147–153, Mar. 2018.
- [158] S. Völkel and M. K. Grieshaber, "SULPHIDE OXIDATION AND OXIDATIVE PHOSPHORYLATION IN THE MITOCHONDRIA OF THE LUGWORM ARENICOLA MARINA," *The Journal of Experimental Biology*, vol. 200, pp. 83–92, 1997.
- [159] U. Theissen, M. Hoffmeister, M. Grieshaber, and W. Martin, "Single eubacterial origin of eukaryotic sulfide:quinone oxidoreductase, a mitochondrial enzyme conserved from the early evolution of eukaryotes during anoxic and sulfidic times," *Molecular Biology and Evolution*, vol. 20, no. 9, pp. 1564–1574, Sep. 2003.
- [160] J. A. Brito *et al.*, "Structural and functional insights into sulfide:quinone oxidoreductase," *Biochemistry*, vol. 48, no. 24, pp. 5613–5622, Jun. 2009.
- [161] M. Marcia, U. Ermler, G. Peng, and H. Michel, "A new structure-based classification of sulfide: Quinone oxidoreductases," *Proteins: Structure, Function and Bioinformatics*, vol. 78, no. 5. Proteins, pp. 1073–1083, 2010.
- [162] M. Reinartz, J. Tschäpe, T. Brüser, H. G. Trüper, and C. Dahl, "Sulfide oxidation in the phototrophic sulfur bacterium *Chromatium vinosum*," *Archives of Microbiology*, vol. 170, no. 1, pp. 59–68, 1998.

- [163] J. W. Horsman and D. L. Miller, "Mitochondrial sulfide quinone oxidoreductase prevents activation of the unfolded protein response in hydrogen sulfide," *Journal of Biological Chemistry*, vol. 291, no. 10, pp. 5320–5325, Mar. 2016.
- [164] M. W. Friederich *et al.*, "Pathogenic variants in SQOR encoding sulfide:quinone oxidoreductase are a potentially treatable cause of Leigh disease," *Journal of Inherited Metabolic Disease*, vol. 43, no. 5, pp. 1024–1036, Sep. 2020.
- [165] H.-S. Jin *et al.*, "Association of the I264T Variant in the Sulfide Quinone Reductase-Like (SQRDL) Gene with Osteoporosis in Korean Postmenopausal Women," *PLOS ONE*, vol. 10, no. 8, p. e0135285, Aug. 2015.
- [166] X. Cai, X. Yi, Y. Zhang, D. Zhang, L. Zhi, and H. Liu, "Genetic susceptibility of postmenopausal osteoporosis on sulfide quinone reductase-like gene," *Osteoporosis International*, vol. 29, no. 9, pp. 2041–2047, Sep. 2018.
- [167] T. M. Hildebrandt and M. K. Grieshaber, "Three enzymatic activities catalyze the oxidation of sulfide to thiosulfate in mammalian and invertebrate mitochondria," *FEBS Journal*, vol. 275, no. 13, pp. 3352–3361, Jul. 2008.
- [168] I. Pettinati, J. Brem, M. A. McDonough, and C. J. Schofield, "Crystal structure of human persulfide dioxygenase: Structural basis of ethylmalonic encephalopathy," *Human Molecular Genetics*, vol. 24, no. 9, pp. 2458–2469, May 2015.
- [169] V. Tiranti *et al.*, "Ethylmalonic Encephalopathy Is Caused by Mutations in ETHE1, a Gene Encoding a Mitochondrial Matrix Protein," *American Journal of Human Genetics*, vol. 74, no. 2, pp. 239–252, 2004.
- [170] J. G. McCoy, C. A. Bingman, E. Bitto, M. M. Holdorf, C. A. Makaroff, and G. N. Phillips, "Structure of an ETHE1-like protein from *Arabidopsis thaliana*," *Acta Crystallographica Section D: Biological Crystallography*, vol. 62, no. 9, pp. 964–970, Sep. 2006.
- [171] V. Tiranti *et al.*, "Loss of ETHE1, a mitochondrial dioxygenase, causes fatal sulfide toxicity in ethylmalonic encephalopathy," *Nature Medicine*, vol. 15, no. 2, pp. 200–205, 2009.
- [172] A. Reza TAVASOLI, P. Rostami, M. Reza ASHRAFI, and P. Karimzadeh, "Neurological and Vascular Manifestations of Ethylmalonic Encephalopathy," Shahid Beheshti University of Medical Sciences, 2017.
- [173] J. Westley, "Thiosulfate: Cyanide Sulfurtransferase (Rhodanese)," *Methods in Enzymology*, vol. 77, no. C, pp. 285–291, Jan. 1981.
- [174] J. WESTLEY, H. ADLER, L. WESTLEY, and C. NISHIDA, "The sulfurtransferases," *Fundamental and Applied Toxicology*, vol. 3, no. 5, pp. 377–382, Sep. 1983.
- [175] R. Cipollone, P. Ascenzi, and P. Visca, "Common themes and variations in the rhodanese superfamily," *IUBMB Life*, vol. 59, no. 2, pp. 51–59, 2007.
- [176] M. Libiad, A. Sriraman, and R. Banerjee, "Polymorphic variants of human rhodanese exhibit differences

- in thermal stability and sulfur transfer kinetics," *Journal of Biological Chemistry*, vol. 290, no. 39, pp. 23579–23588, Sep. 2015.
- [177] W. H. Woo, H. Yang, K. P. Wong, and B. Halliwell, "Sulphite oxidase gene expression in human brain and in other human and rat tissues," *Biochemical and Biophysical Research Communications*, vol. 305, no. 3, pp. 619–623, Jun. 2003.
- [178] C. Kisker *et al.*, "Molecular basis of sulfite oxidase deficiency from the structure of sulfite oxidase," *Cell*, vol. 91, no. 7, pp. 973–983, Dec. 1997.
- [179] S. H. Mudd, F. Irreverre, and L. Laster, "Sulfite oxidase deficiency in man: Demonstration of the enzymatic defect," *Science*, vol. 156, no. 3782, pp. 1599–1602, 1967.
- [180] M. Boyer, M. Sowa, R. Wang, and J. Abdenur, "Isolated Sulfite Oxidase Deficiency: Response to Dietary Treatment in a Patient with Severe Neonatal Presentation," *Journal of Inborn Errors of Metabolism and Screening*, vol. 7, 2019.
- [181] A. Giuffrè and J. B. Vicente, "Hydrogen sulfide biochemistry and interplay with other gaseous mediators in mammalian physiology," *Oxidative Medicine and Cellular Longevity*, vol. 2018. Hindawi Limited, 2018.
- [182] M. Libiad, P. K. Yadav, V. Vitvitsky, M. Martinov, and R. Banerjee, "Organization of the human mitochondrial hydrogen sulfide oxidation pathway," *Journal of Biological Chemistry*, vol. 289, no. 45, pp. 30901–30910, Nov. 2014.
- [183] E. M. Bos, H. van Goor, J. A. Joles, M. Whiteman, and H. G. D. Leuvenink, "Hydrogen sulfide: physiological properties and therapeutic potential in ischaemia," *British Journal of Pharmacology*, vol. 172, no. 6, pp. 1479–1493, Mar. 2015.
- [184] A. Kumar *et al.*, "Sulfite-induced protein radical formation in LPS aerosol-challenged mice: Implications for sulfite sensitivity in human lung disease," *Redox Biology*, vol. 15, pp. 327–334, May 2018.
- [185] T. C. Bartholomew, G. M. Powell., K. S. Dodgson, and C. G. Curtis, "Oxidation of sodium sulphide by rat liver, lungs and kidney," *Biochemical Pharmacology*, vol. 29, no. 18, pp. 2431–2437, Sep. 1980.
- [186] F. Malagrìno *et al.*, "Hydrogen sulfide oxidation: Adaptive changes in mitochondria of SW480 colorectal cancer cells upon exposure to hypoxia," *Oxidative Medicine and Cellular Longevity*, vol. 2019, 2019.
- [187] E. Lagoutte, S. Mimoun, M. Andriamihaja, C. Chaumontet, F. Blachier, and F. Bouillaud, "Oxidation of hydrogen sulfide remains a priority in mammalian cells and causes reverse electron transfer in colonocytes," *Biochimica et Biophysica Acta - Bioenergetics*, vol. 1797, no. 8, pp. 1500–1511, Aug. 2010.
- [188] M. Gubern, M. Andriamihaja, T. Nübel, F. Blachier, and F. Bouillaud, "Sulfide, the first inorganic substrate for human cells," *The FASEB Journal*, vol. 21, no. 8, pp. 1699–1706, Jun. 2007.
- [189] K. R. Olson, "Hydrogen sulfide as an oxygen sensor," *Antioxidants and Redox Signaling*, vol. 22, no. 5. Mary Ann Liebert Inc., pp. 377–397, 10-Feb-2015.

- [190] N. Helmy *et al.*, "Oxidation of hydrogen sulfide by human liver mitochondria," *Nitric Oxide*, vol. 41, pp. 105–112, Sep. 2014.
- [191] A. Abou-Hamdan, H. Guedouari-Bounihi, V. Lenoir, M. Andriamihaja, F. Blachier, and F. Bouillaud, "Oxidation of H<sub>2</sub>S in mammalian cells and mitochondria," in *Methods in Enzymology*, vol. 554, Academic Press Inc., 2015, pp. 201–228.
- [192] X. Leschelle *et al.*, "Adaptative metabolic response of human colonic epithelial cells to the adverse effects of the luminal compound sulfide," *Biochimica et Biophysica Acta - General Subjects*, vol. 1725, no. 2, pp. 201–212, Sep. 2005.
- [193] C. E. Cooper and G. C. Brown, "The inhibition of mitochondrial cytochrome oxidase by the gases carbon monoxide, nitric oxide, hydrogen cyanide and hydrogen sulfide: Chemical mechanism and physiological significance," *Journal of Bioenergetics and Biomembranes*, vol. 40, no. 5. Springer, pp. 533–539, 07-Oct-2008.
- [194] K. Módis, C. Coletta, K. Erdélyi, A. Papapetropoulos, and C. Szabo, "Intramitochondrial hydrogen sulfide production by 3-mercaptopyruvate sulfurtransferase maintains mitochondrial electron flow and supports cellular bioenergetics," *The FASEB Journal*, vol. 27, no. 2, pp. 601–611, Feb. 2013.
- [195] K. Isoherranen, L. Bouchard, and N. Kluger, "Benefits of intralesional injections of sodium thiosulfate in the treatment of calciphylaxis," *International Wound Journal*, vol. 14, no. 6, pp. 955–959, Dec. 2017.
- [196] L. Tomasova *et al.*, "Intracolonic hydrogen sulfide lowers blood pressure in rats," *Nitric Oxide - Biology and Chemistry*, vol. 60, pp. 50–58, Nov. 2016.
- [197] I. A. Sziártó *et al.*, "Cystathionine  $\gamma$ -lyase-produced hydrogen sulfide controls endothelial bioavailability and blood pressure," *Hypertension*, vol. 71, no. 6, pp. 1210–1217, 2018.
- [198] G. Tang, L. Wu, W. Liang, and R. Wang, "Direct stimulation of KATP channels by exogenous and endogenous hydrogen sulfide in vascular smooth muscle cells," *Molecular Pharmacology*, vol. 68, no. 6, pp. 1757–1764, Dec. 2005.
- [199] Q. C. Yong, L. F. Hu, S. Wang, D. Huang, and J. S. Bian, "Hydrogen sulfide interacts with nitric oxide in the heart: Possible involvement of nitroxyl," *Cardiovascular Research*, vol. 88, no. 3, pp. 482–491, Dec. 2010.
- [200] M. Eberhardt *et al.*, "H<sub>2</sub>S and NO cooperatively regulate vascular tone by activating a neuroendocrine HNO-TRPA1-CGRP signalling pathway," *Nature Communications*, vol. 5, Jul. 2014.
- [201] J. L. Greaney, J. L. Kutz, S. W. Shank, S. Jandu, L. Santhanam, and L. M. Alexander, "Impaired Hydrogen Sulfide-Mediated Vasodilation Contributes to Microvascular Endothelial Dysfunction in Hypertensive Adults," *Hypertension*, vol. 69, no. 5, pp. 902–909, May 2017.
- [202] B. L. Predmore, D. Julian, and A. J. Cardounel, "Hydrogen Sulfide Increases Nitric Oxide Production from Endothelial Cells by an Akt-Dependent Mechanism," *Frontiers in Physiology*, vol. 2, p. 104, Dec. 2011.

- [203] Z. Altaany, Y. J. Ju, G. Yang, and R. Wang, "The coordination of S-sulfhydration, S-nitrosylation, and phosphorylation of endothelial nitric oxide synthase by hydrogen sulfide," *Science Signaling*, vol. 7, no. 342, pp. ra87–ra87, Sep. 2014.
- [204] X. Zhong *et al.*, "Calcium Sensing Receptor Regulating Smooth Muscle Cells Proliferation Through Initiating Cystathionine-Gamma-Lyase/Hydrogen Sulfide Pathway in Diabetic Rat," *Cellular Physiology and Biochemistry*, vol. 35, no. 4, pp. 1582–1598, Apr. 2015.
- [205] Y. Wang *et al.*, "Calcium sensing receptor initiating cystathionine-gamma-lyase/hydrogen sulfide pathway to inhibit platelet activation in hyperhomocysteinemia rat," *Experimental Cell Research*, vol. 358, no. 2, pp. 171–181, Sep. 2017.
- [206] H. Yan, J. Du, and C. Tang, "The possible role of hydrogen sulfide on the pathogenesis of spontaneous hypertension in rats," *Biochemical and Biophysical Research Communications*, vol. 313, no. 1, pp. 22–27, Jan. 2004.
- [207] M. Abdelmonem, N. N. Shahin, L. A. Rashed, H. A. A. Amin, A. A. Shamaa, and A. A. Shaheen, "Hydrogen sulfide enhances the effectiveness of mesenchymal stem cell therapy in rats with heart failure: In vitro preconditioning versus in vivo co-delivery," *Biomedicine and Pharmacotherapy*, vol. 112, Apr. 2019.
- [208] Y. D. Bai *et al.*, "Hydrogen Sulfide Alleviates Acute Myocardial Ischemia Injury by Modulating Autophagy and Inflammation Response under Oxidative Stress," *Oxidative Medicine and Cellular Longevity*, vol. 2018, 2018.
- [209] S. H. Cheung and J. Y. W. Lau, "Hydrogen sulfide mediates athero-protection against oxidative stress via S-sulfhydration," *PLoS ONE*, vol. 13, no. 3, Mar. 2018.
- [210] P. M. Snijder *et al.*, "Exogenous administration of thiosulfate, a donor of hydrogen sulfide, attenuates angiotensin II-induced hypertensive heart disease in rats," *British Journal of Pharmacology*, vol. 172, no. 6, pp. 1494–1504, 2015.
- [211] N.-N. Ping, S. Li, Y.-N. Mi, L. Cao, and Y.-X. Cao, "Hydrogen sulphide induces vasoconstriction of rat coronary artery via activation of Ca<sup>2+</sup> influx," *Acta Physiologica*, vol. 214, no. 1, pp. 88–96, May 2015.
- [212] S. N. Orlov, S. V. Gusakova, L. V. Smaglii, S. V. Koltsova, and S. V. Sidorenko, "Vasoconstriction triggered by hydrogen sulfide: Evidence for Na<sup>+</sup>,K<sup>+</sup>,2Cl<sup>-</sup>-cotransport and L-type Ca<sup>2+</sup> channel-mediated pathway.," *Biochemistry and biophysics reports*, vol. 12, pp. 220–227, Dec. 2017.
- [213] Y.-G. Sun, Y.-X. Cao, W.-W. Wang, S.-F. Ma, T. Yao, and Y.-C. Zhu, "Hydrogen sulphide is an inhibitor of L-type calcium channels and mechanical contraction in rat cardiomyocytes," *Cardiovascular Research*, vol. 79, no. 4, pp. 632–641, Sep. 2008.
- [214] M. Zhuo, S. A. Small, E. R. Kandel, and R. D. Hawkins, "Nitric oxide and carbon monoxide produce activity-dependent long-term synaptic enhancement in hippocampus," *Science*, vol. 260, no. 5116, pp. 1946–1950, 1993.
- [215] R. C. O. Zanardo *et al.*, "Hydrogen sulfide is an endogenous modulator of leukocyte-mediated

- inflammation," *The FASEB Journal*, vol. 20, no. 12, pp. 2118–2120, Oct. 2006.
- [216] V. Brancaleone, E. Mitidieri, R. J. Flower, G. Cirino, and M. Perretti, "Annexin a1 mediates hydrogen sulfide properties in the control of inflammation," *Journal of Pharmacology and Experimental Therapeutics*, vol. 351, no. 1, pp. 96–104, Oct. 2014.
- [217] Q. Guan *et al.*, "Hydrogen sulfide suppresses high glucose-induced expression of intercellular adhesion molecule-1 in endothelial cells," *Journal of Cardiovascular Pharmacology*, vol. 62, no. 3, pp. 278–284, Sep. 2013.
- [218] J. Du *et al.*, "Hydrogen Sulfide Suppresses Oxidized Low-density Lipoprotein (Ox-LDL)-stimulated Monocyte Chemoattractant Protein 1 generation from Macrophages via the Nuclear Factor  $\kappa$ B (NF- $\kappa$ B) Pathway," *Journal of Biological Chemistry*, vol. 289, no. 14, pp. 9741–9753, Apr. 2014.
- [219] L. Sun *et al.*, "Exogenous hydrogen sulfide prevents lipopolysaccharide-induced inflammation by blocking the TLR4/NF- $\kappa$ B pathway in MAC-T cells," *Gene*, vol. 710, pp. 114–121, Aug. 2019.
- [220] H. Zhang, L. Zhi, S. M. Moochhala, P. K. Moore, and M. Bhatia, "Endogenous hydrogen sulfide regulates leukocyte trafficking in cecal ligation and puncture-induced sepsis," *Journal of Leukocyte Biology*, vol. 82, no. 4, pp. 894–905, Oct. 2007.
- [221] R. Tamizhselvi, Y. H. Koh, J. Sun, H. Zhang, and M. Bhatia, "Hydrogen sulfide induces ICAM-1 expression and neutrophil adhesion to caerulein-treated pancreatic acinar cells through NF- $\kappa$ B and Src-family kinases pathway," *Experimental Cell Research*, vol. 316, no. 9, pp. 1625–1636, 2010.
- [222] L. Zhi, A. D. Ang, H. Zhang, P. K. Moore, and M. Bhatia, "Hydrogen sulfide induces the synthesis of proinflammatory cytokines in human monocyte cell line U937 via the ERK-NF- $\kappa$ B pathway," *Journal of Leukocyte Biology*, vol. 81, no. 5, pp. 1322–1332, May 2007.
- [223] N. Muniraj, L. K. Stamp, A. Badiei, A. Hegde, V. Cameron, and M. Bhatia, "Hydrogen sulfide acts as a pro-inflammatory mediator in rheumatic disease," *International Journal of Rheumatic Diseases*, vol. 20, no. 2, pp. 182–189, Feb. 2017.
- [224] Y. Liu, R. Liao, Z. Qiang, and C. Zhang, "Pro-inflammatory cytokine-driven PI3K/Akt/Sp1 signalling and H<sub>2</sub>S production facilitates the pathogenesis of severe acute pancreatitis," *Bioscience Reports*, vol. 37, no. 2, Apr. 2017.
- [225] Y. Zhen *et al.*, "Exogenous hydrogen sulfide exerts proliferation/anti-apoptosis/angiogenesis/migration effects via amplifying the activation of NF- $\kappa$ B pathway in PLC/PRF/5 hepatoma cells," *International Journal of Oncology*, vol. 46, no. 5, pp. 2194–2204, May 2015.
- [226] Y. Zhen *et al.*, "Exogenous hydrogen sulfide promotes C6 glioma cell growth through activation of the p38 MAPK/ERK1/2-COX-2 pathways," *Oncology Reports*, vol. 34, no. 5, pp. 2413–2422, Nov. 2015.
- [227] L. Xie, C. X. Tiong, and J. S. Bian, "Hydrogen sulfide protects SH-SY5Y cells against 6-hydroxydopamine-induced endoplasmic reticulum stress," *American Journal of Physiology - Cell Physiology*, vol. 303, no. 1, Jul. 2012.

- [228] A. A. Fouad, H. M. Hafez, and A. A. H. Hamouda, "Hydrogen sulfide modulates IL-6/STAT3 pathway and inhibits oxidative stress, inflammation, and apoptosis in rat model of methotrexate hepatotoxicity," *Human and Experimental Toxicology*, vol. 39, no. 1, pp. 77–85, Jan. 2020.
- [229] L. F. Hu, M. Lu, Z. Y. Wu, P. T. H. Wong, and J. S. Bian, "Hydrogen sulfide inhibits rotenone-induced apoptosis via preservation of mitochondrial function," *Molecular Pharmacology*, vol. 75, no. 1, pp. 27–34, Jan. 2009.
- [230] W. Liang *et al.*, "ATP-sensitive K<sup>+</sup> channels contribute to the protective effects of exogenous hydrogen sulfide against high glucose-induced injury in H9c2 cardiac cells," *International Journal of Molecular Medicine*, vol. 37, no. 3, pp. 763–772, Mar. 2016.
- [231] G. Yang, L. Wu, S. Bryan, N. Khaper, S. Mani, and R. Wang, "Cystathionine gamma-lyase deficiency and overproliferation of smooth muscle cells," *Cardiovascular Research*, vol. 86, no. 3, pp. 487–495, Jun. 2010.
- [232] G. Yang, L. Wu, and R. Wang, "Pro-apoptotic effect of endogenous H<sub>2</sub>S on human aorta smooth muscle cells," *The FASEB Journal*, vol. 20, no. 3, pp. 553–555, Mar. 2006.
- [233] G. Yang, W. Yang, L. Wu, and R. Wang, "H<sub>2</sub>S, endoplasmic reticulum stress, and apoptosis of insulin-secreting beta cells," *Journal of Biological Chemistry*, vol. 282, no. 22, pp. 16567–16576, Jun. 2007.
- [234] B. Geng *et al.*, "Endogenous hydrogen sulfide regulation of myocardial injury induced by isoproterenol," *Biochemical and Biophysical Research Communications*, vol. 318, no. 3, pp. 756–763, Jun. 2004.
- [235] J. Pei *et al.*, "Hydrogen Sulfide Promotes Cardiomyocyte Proliferation and Heart Regeneration via ROS Scavenging," *Oxidative Medicine and Cellular Longevity*, vol. 2020, 2020.
- [236] D. Wu, Q. Hu, X. Liu, L. Pan, Q. Xiong, and Y. Z. Zhu, "Hydrogen sulfide protects against apoptosis under oxidative stress through SIRT1 pathway in H9c2 cardiomyocytes," *Nitric Oxide - Biology and Chemistry*, vol. 46, pp. 204–212, Apr. 2015.
- [237] M. Whiteman *et al.*, "The novel neuromodulator hydrogen sulfide: An endogenous peroxynitrite 'scavenger'?" *Journal of Neurochemistry*, vol. 90, no. 3, pp. 765–768, Aug. 2004.
- [238] Y. Kimura, Y. I. Goto, and H. Kimura, "Hydrogen sulfide increases glutathione production and suppresses oxidative stress in mitochondria," *Antioxidants and Redox Signaling*, vol. 12, no. 1, pp. 1–13, Jan. 2010.
- [239] Z. W. Lee, Y. L. Low, S. Huang, T. Wang, and L. W. Deng, "The cystathionine  $\gamma$ -lyase/hydrogen sulfide system maintains cellular glutathione status," *Biochemical Journal*, vol. 460, no. 3, pp. 425–435, Jun. 2014.
- [240] R. Parsanathan and S. K. Jain, "Hydrogen sulfide increases glutathione biosynthesis, and glucose uptake and utilisation in C2C12 mouse myotubes," *Free Radical Research*, vol. 52, no. 2, pp. 288–303, Feb. 2018.



- [241] P. Huang *et al.*, "Hydrogen sulfide inhibits high-salt diet-induced renal oxidative stress and kidney injury in Dahl rats," *Oxidative Medicine and Cellular Longevity*, vol. 2016, 2016.
- [242] A. K. Mustafa *et al.*, "H<sub>2</sub>S signals through protein S-Sulfhydration," *Science Signaling*, vol. 2, no. 96, Nov. 2009.
- [243] W. H. Koppenol and P. L. Bounds, "Signaling by sulfur-containing molecules. Quantitative aspects," *Archives of Biochemistry and Biophysics*, vol. 617, pp. 3–8, Mar. 2017.
- [244] B. Jiang, G. Tang, K. Cao, L. Wu, and R. Wang, "Molecular mechanism for H<sub>2</sub>S-induced activation of K ATP channels," *Antioxidants and Redox Signaling*, vol. 12, no. 10, pp. 1167–1178, May 2010.
- [245] A. A. Untereiner, R. Wang, Y. Ju, and L. Wu, "Decreased Gluconeogenesis in the Absence of Cystathionine Gamma-Lyase and the Underlying Mechanisms," *Antioxidants and Redox Signaling*, vol. 24, no. 3, pp. 129–140, Jan. 2016.
- [246] Y. Ju, A. Untereiner, L. Wu, and G. Yang, "H<sub>2</sub>S-induced S-sulfhydration of pyruvate carboxylase contributes to gluconeogenesis in liver cells," *Biochimica et Biophysica Acta - General Subjects*, vol. 1850, no. 11, pp. 2293–2303, Nov. 2015.
- [247] A. Aroca, J. M. Benito, C. Gotor, and L. C. Romero, "Persulfidation proteome reveals the regulation of protein function by hydrogen sulfide in diverse biological processes in Arabidopsis," *Journal of Experimental Botany*, vol. 68, no. 17, pp. 4915–4927, Aug. 2017.
- [248] B. Fox *et al.*, "Inducible hydrogen sulfide synthesis in chondrocytes and mesenchymal progenitor cells: Is H<sub>2</sub>S a novel cytoprotective mediator in the inflamed joint?," *Journal of Cellular and Molecular Medicine*, vol. 16, no. 4, pp. 896–910, 2012.
- [249] C. Szabo *et al.*, "Tumor-derived hydrogen sulfide, produced by cystathionine- $\beta$ -synthase, stimulates bioenergetics, cell proliferation, and angiogenesis in colon cancer," *Proceedings of the National Academy of Sciences of the United States of America*, vol. 110, no. 30, pp. 12474–12479, Jul. 2013.
- [250] P. Phowthongkum, K. Suphapeetiporn, and V. Shotelersuk, "Carnitine palmitoyl transferase 1A deficiency in an adult with recurrent severe steato hepatitis aggravated by high pathologic or physiologic demands: A roller-coaster for internists," *Clinical and Molecular Hepatology*, vol. 25, no. 4. Korean Association for the Study of the Liver, pp. 412–416, 01-Dec-2019.
- [251] A. Asimakopoulou *et al.*, "Selectivity of commonly used pharmacological inhibitors for cystathionine  $\beta$  synthase (CBS) and cystathionine  $\gamma$  lyase (CSE)," *British Journal of Pharmacology*, vol. 169, no. 4, pp. 922–932, Jun. 2013.
- [252] K. Hanaoka *et al.*, "Discovery and mechanistic characterization of selective inhibitors of H<sub>2</sub>S-producing Enzyme: 3-Mercaptopyruvate," *Scientific Reports*, vol. 7, no. 1, pp. 1–12, Jan. 2017.
- [253] Q. Sun *et al.*, "Structural basis for the inhibition mechanism of human cystathionine  $\gamma$ -lyase, an enzyme responsible for the production of H<sub>2</sub>S," *Journal of Biological Chemistry*, vol. 284, no. 5, pp. 3076–3085, Jan. 2009.

- [254] C. Chao *et al.*, "Cystathionine- $\beta$ -synthase inhibition for colon cancer: Enhancement of the efficacy of aminooxyacetic acid via the prodrug approach," *Molecular Medicine*, vol. 22, pp. 361–379, 2016.
- [255] C. R. Powell, K. M. Dillon, and J. B. Matson, "A review of hydrogen sulfide (H<sub>2</sub>S) donors: Chemistry and potential therapeutic applications," *Biochemical Pharmacology*, vol. 149. Elsevier Inc., pp. 110–123, 01-Mar-2018.
- [256] S. Minamishima *et al.*, "Hydrogen sulfide improves survival after cardiac arrest and cardiopulmonary resuscitation via a nitric oxide synthase 3-dependent mechanism in mice," *Circulation*, vol. 120, no. 10, pp. 888–896, 2009.
- [257] H. Q. Shi *et al.*, "Sodium Sulfide, a Hydrogen Sulfide-Releasing Molecule, Attenuates Acute Cerebral Ischemia in Rats," *CNS Neuroscience and Therapeutics*, vol. 22, no. 7, pp. 625–632, Jul. 2016.
- [258] W. W. Jiang, B. S. Huang, Y. Han, L. H. Deng, and L. X. Wu, "Sodium hydrosulfide attenuates cerebral ischemia/reperfusion injury by suppressing overactivated autophagy in rats," *FEBS Open Bio*, vol. 7, no. 11, pp. 1686–1695, Nov. 2017.
- [259] C. Szabo *et al.*, "Regulation of mitochondrial bioenergetic function by hydrogen sulfide. Part I. Biochemical and physiological mechanisms," *British Journal of Pharmacology*, vol. 171, no. 8, pp. 2099–2122, Apr. 2014.
- [260] R. K. Bijarnia, M. Bachtler, P. G. Chandak, H. Van Goor, and A. Pasch, "Sodium thiosulfate ameliorates oxidative stress and preserves renal function in hyperoxaluric rats," *PLoS ONE*, vol. 10, no. 4, Apr. 2015.
- [261] M. Sakaguchi *et al.*, "Sodium thiosulfate attenuates acute lung injury in Mice," *Anesthesiology*, vol. 121, no. 6, pp. 1248–1257, Dec. 2014.
- [262] K. Shirozu, K. Tokuda, E. Marutani, D. Lefer, R. Wang, and F. Ichinose, "Cystathionine  $\gamma$ -Lyase deficiency protects mice from Galactosamine/lipopolysaccharide-induced acute liver failure," *Antioxidants and Redox Signaling*, vol. 20, no. 2, pp. 204–216, Jan. 2014.
- [263] P. M. Snijder *et al.*, "Sodium thiosulfate attenuates angiotensin II-induced hypertension, proteinuria and renal damage," *Nitric Oxide - Biology and Chemistry*, vol. 42, pp. 87–98, Nov. 2014.
- [264] E. Marutani *et al.*, "Thiosulfate mediates cytoprotective effects of hydrogen sulfide against neuronal ischemia," *Journal of the American Heart Association*, vol. 4, no. 11, Nov. 2015.
- [265] S. Ravindran, S. Jahir Hussain, S. R. Boovarahan, and G. A. Kurian, "Sodium thiosulfate post-conditioning protects rat hearts against ischemia reperfusion injury via reduction of apoptosis and oxidative stress," *Chemico-Biological Interactions*, vol. 274, pp. 24–34, Aug. 2017.
- [266] N. Subhash, R. Sriram, and G. A. Kurian, "Sodium thiosulfate protects brain in rat model of adenine induced vascular calcification," *Neurochemistry International*, vol. 90, pp. 193–203, Nov. 2015.
- [267] M. Brucculeri, J. Cheigh, G. Bauer, and D. Serur, "Long-term intravenous sodium thiosulfate in the treatment of a patient with calciphylaxis," *Seminars in Dialysis*, vol. 18, no. 5, pp. 431–434, Sep. 2005.

- [268] R. P. Singh, H. Derendorf, and E. A. Ross, "Simulation-based sodium thiosulfate dosing strategies for the treatment of Calciphylaxis," *Clinical Journal of the American Society of Nephrology*, vol. 6, no. 5, pp. 1155–1159, May 2011.
- [269] B. Zuhaili and K. Al-Talib, "Successful treatment of single infected calciphylaxis lesion with intralesional injection of sodium thiosulfate at high concentration," *Wounds*, vol. 31, no. 8, pp. E54–E57, Jan. 2019.
- [270] E. Van Den Berg *et al.*, "Urinary sulfur metabolites associate with a favorable cardiovascular risk profile and survival benefit in renal transplant recipients," *Journal of the American Society of Nephrology*, vol. 25, no. 6, pp. 1303–1312, Jun. 2014.
- [271] A. R. S. Frenay *et al.*, "Serum free sulfhydryl status is associated with patient and graft survival in renal transplant recipients," *Free Radical Biology and Medicine*, vol. 99, pp. 345–351, Oct. 2016.
- [272] V. A. Hall and J. M. Guest, "Sodium nitroprusside-induced cyanide intoxication and prevention with sodium thiosulfate prophylaxis," *American journal of critical care : an official publication, American Association of Critical-Care Nurses*, vol. 1, no. 2. American Association of Critical-Care Nurses, pp. 19–25, 01-Sep-1992.
- [273] L. Li *et al.*, "Characterization of a novel, water-soluble hydrogen sulfide-releasing molecule (GY4137): New insights into the biology of hydrogen sulfide," *Circulation*, vol. 117, no. 18, pp. 2351–2360, May 2008.
- [274] Z. W. Lee *et al.*, "The slow-releasing Hydrogen Sulfide donor, GY4137, exhibits novel anti-cancer effects in vitro and in vivo," *PLoS ONE*, vol. 6, no. 6, 2011.
- [275] L. Li, M. Salto-Tellez, C. H. Tan, M. Whiteman, and P. K. Moore, "GY4137, a novel hydrogen sulfide-releasing molecule, protects against endotoxic shock in the rat," *Free Radical Biology and Medicine*, vol. 47, no. 1, pp. 103–113, Jul. 2009.
- [276] E. Grambow *et al.*, "The effects of hydrogen sulfide on platelet–leukocyte aggregation and microvascular thrombolysis," *Platelets*, vol. 28, no. 5, pp. 509–517, Jul. 2017.
- [277] S. Lu, Y. Gao, X. Huang, and X. Wang, "GY4137, a hydrogen sulfide (H<sub>2</sub>S) donor, shows potent anti-hepatocellular carcinoma activity through blocking the STAT3 pathway," *International Journal of Oncology*, vol. 44, no. 4, pp. 1259–1267, Apr. 2014.
- [278] Z. Chen, J. Tang, P. Wang, J. Zhu, and Y. Liu, "GY4137 Attenuates Sodium Deoxycholate-Induced Intestinal Barrier Injury Both in Vitro and in Vivo," *BioMed Research International*, vol. 2019, 2019.
- [279] A. A. Untereiner, G. Oláh, K. Módis, M. R. Hellmich, and C. Szabo, "H<sub>2</sub>S-induced S-sulfhydration of lactate dehydrogenase a (LDHA) stimulates cellular bioenergetics in HCT116 colon cancer cells," *Biochemical Pharmacology*, vol. 136, pp. 86–98, Jul. 2017.
- [280] B. E. Alexander *et al.*, "Investigating the generation of hydrogen sulfide from the phosphoramidodithioate slow-release donor GY4137," *MedChemComm*, vol. 6, no. 9, pp. 1649–1655, Jul. 2015.

- [281] W. Feng *et al.*, "Discovery of New H<sub>2</sub>S Releasing Phosphordithioates and 2,3-Dihydro-2-phenyl-2-sulfanylenebenzo[d][1,3,2]oxazaphospholes with Improved Antiproliferative Activity," *Journal of Medicinal Chemistry*, vol. 58, no. 16, pp. 6456–6480, Aug. 2015.
- [282] C. W. Huang, W. Feng, M. T. Peh, K. Peh, B. W. Dymock, and P. K. Moore, "A novel slow-releasing hydrogen sulfide donor, FW1256, exerts anti-inflammatory effects in mouse macrophages and in vivo," *Pharmacological Research*, vol. 113, pp. 533–546, Nov. 2016.
- [283] D. F. S. Natusch, J. R. Sewell, and R. L. Tanner, "Determination of Hydrogen Sulfide in Air—An Assessment of Impregnated Paper Tape Methods," *Analytical Chemistry*, vol. 46, no. 3, pp. 410–415, Mar. 1974.
- [284] S. Korshunov and J. Imlay, "Quantification of Hydrogen Sulfide and Cysteine Excreted by Bacterial Cells," *BIO-PROTOCOL*, vol. 8, no. 10, 2018.
- [285] J. K. Fogo and M. Popowsky, "Spectrophotometric Determination of Hydrogen Sulfide," *Analytical Chemistry*, vol. 21, no. 6, pp. 732–734, Jun. 1949.
- [286] J. D. CLINE, "SPECTROPHOTOMETRIC DETERMINATION OF HYDROGEN SULFIDE IN NATURAL WATERS," *Limnology and Oceanography*, vol. 14, no. 3, pp. 454–458, May-1969.
- [287] Z. Chunyu, D. Junbao, B. Dingfang, Y. Hui, T. Xiuying, and T. Chaoshu, "The regulatory effect of hydrogen sulfide on hypoxic pulmonary hypertension in rats," *Biochemical and Biophysical Research Communications*, vol. 302, p. 810, 2003.
- [288] H. L. Wei, C. Y. Zhang, H. F. Jin, C. S. Tang, and J. B. Du, "Hydrogen sulfide regulates lung tissue-oxidized glutathione and total antioxidant capacity in hypoxic pulmonary hypertensive rats," *Acta Pharmacologica Sinica*, vol. 29, no. 6, pp. 670–676, Jun. 2008.
- [289] R. R. Gaddam, S. Chambers, D. Murdoch, G. Shaw, and M. Bhatia, "Circulating levels of hydrogen sulfide and substance P in patients with sepsis," *Journal of Infection*, vol. 75, no. 4, pp. 293–300, Oct. 2017.
- [290] B. Wiliński, J. Wiliński, E. Somogyi, J. Piotrowska, and W. Opoka, "Vitamin D3 (cholecalciferol) boosts hydrogen sulfide tissue concentrations in heart and other mouse organs," *Folia Biologica (Czech Republic)*, vol. 60, no. 3–4, pp. 243–247, 2012.
- [291] X. Shen, E. A. Peter, S. Bir, R. Wang, and C. G. Kevil, "Analytical measurement of discrete hydrogen sulfide pools in biological specimens," *Free Radical Biology and Medicine*, vol. 52, no. 11–12. Elsevier Inc., pp. 2276–2283, 2012.
- [292] P. Li, D. Yuan, and K. Lin, "Determination of nanomolar dissolved sulfides in water by coupling the classical methylene blue method with surface-enhanced Raman scattering detection," *Spectrochimica Acta - Part A: Molecular and Biomolecular Spectroscopy*, 2020.
- [293] T. W. Mitchell, J. C. Savage, and D. H. Gould, "High-performance liquid chromatography detection of sulfide in tissues from sulfide-treated mice," *Journal of Applied Toxicology*, vol. 13, no. 6, pp. 389–394, 1993.

- [294] X. Shen, C. B. Pattillo, S. Pardue, S. C. Bir, R. Wang, and C. G. Kevil, "Measurement of plasma hydrogen sulfide in vivo and in vitro," *Free Radical Biology and Medicine*, vol. 50, no. 9. Elsevier Inc., pp. 1021–1031, 01-May-2011.
- [295] E. A. Wintner *et al.*, "A monobromobimane-based assay to measure the pharmacokinetic profile of reactive sulphide species in blood," *British Journal of Pharmacology*, vol. 160, no. 4, pp. 941–957, 2010.
- [296] T. Ida *et al.*, "Reactive cysteine persulfides and S-polythiolation regulate oxidative stress and redox signaling," *Proceedings of the National Academy of Sciences of the United States of America*, vol. 111, no. 21, pp. 7606–7611, May 2014.
- [297] K. Shigetoshi, T. Nagata, K. Kimura, and K. Kudo, "Extractive Alkylation and Gas Chromatographic Analysis of Sulfide," *Journal of Forensic Sciences*, vol. 33, no. 1, p. 12453J, Jan. 1988.
- [298] C. J. Richardson, E. A. M. Magee, and J. H. Cummings, "A new method for the determination of sulphide in gastrointestinal contents and whole blood by microdistillation and ion chromatography," *Clinica Chimica Acta*, vol. 293, no. 1–2, pp. 115–125, 2000.
- [299] R. Hyšpler *et al.*, "A simple, optimized method for the determination of sulphide in whole blood by GC-MS as a marker of bowel fermentation processes," in *Journal of Chromatography B: Analytical Technologies in the Biomedical and Life Sciences*, 2002, vol. 770, no. 1–2, pp. 255–259.
- [300] J. Furne, A. Saeed, and M. D. Levitt, "Whole tissue hydrogen sulfide concentrations are orders of magnitude lower than presently accepted values," *American Journal of Physiology - Regulatory Integrative and Comparative Physiology*, vol. 295, no. 5, Nov. 2008.
- [301] J. A. Velázquez-Moyado and A. Navarrete, "The detection and quantification, in vivo and in real time, of hydrogen sulfide in ethanol-induced lesions in rat stomachs using an ion sensitive electrode," *Journal of Pharmacological and Toxicological Methods*, vol. 89, pp. 54–58, Jan. 2018.
- [302] T. Xu *et al.*, "Electrochemical hydrogen sulfide biosensors," *Analyst*, vol. 141, no. 4. Royal Society of Chemistry, pp. 1185–1195, 21-Feb-2016.
- [303] L. Chang *et al.*, "Hydrogen sulfide inhibits myocardial injury induced by homocysteine in rats," *Amino Acids*, vol. 34, no. 4, pp. 573–585, 2008.
- [304] Y. H. Chen *et al.*, "Endogenous hydrogen sulfide in patients with COPD," *Chest*, vol. 128, no. 5, pp. 3205–3211, 2005.
- [305] Y. H. Chen, W. Z. Yao, Y. L. Ding, B. Geng, M. Lu, and C. S. Tang, "Effect of theophylline on endogenous hydrogen sulfide production in patients with COPD," *Pulmonary Pharmacology and Therapeutics*, vol. 21, no. 1, pp. 40–46, 2008.
- [306] N. L. Whitfield, E. L. Kreimier, F. C. Verdial, N. Skovgaard, and K. R. Olson, "Reappraisal of H<sub>2</sub>S/sulfide concentration in vertebrate blood and its potential significance in ischemic preconditioning and vascular signaling," *American Journal of Physiology - Regulatory Integrative and Comparative Physiology*, vol. 294, no. 6, Jun. 2008.

- [307] P. Jeroschewski, C. Steuckart, and M. Kuhl, "An amperometric microsensor for the determination of H<sub>2</sub>S in aquatic environments," *Analytical Chemistry*, vol. 68, no. 24, pp. 4351–4357, 1996.
- [308] D. W. Kraus and J. E. Doeller, "Sulfide consumption by mussel gill mitochondria is not strictly tied to oxygen reduction: Measurements using a novel polarographic sulfide sensor," *Journal of Experimental Biology*, vol. 207, no. 21, pp. 3667–3679, Oct. 2004.
- [309] J. E. Doeller *et al.*, "Polarographic measurement of hydrogen sulfide production and consumption by mammalian tissues," *Analytical Biochemistry*, vol. 341, no. 1, pp. 40–51, Jun. 2005.
- [310] Y. Takano, H. Echizen, and K. Hanaoka, "Fluorescent Probes and Selective Inhibitors for Biological Studies of Hydrogen Sulfide-and Polysulfide-Mediated Signaling," *Antioxidants and Redox Signaling*, vol. 27, no. 10. Mary Ann Liebert Inc., pp. 669–683, 01-Oct-2017.
- [311] A. R. Lippert, E. J. New, and C. J. Chang, "Reaction-based fluorescent probes for selective imaging of hydrogen sulfide in living cells," *Journal of the American Chemical Society*, vol. 133, no. 26, pp. 10078–10080, Jul. 2011.
- [312] K. Wang, H. Peng, N. Ni, C. Dai, and B. Wang, "2,6-dansyl azide as a fluorescent probe for hydrogen sulfide," *Journal of Fluorescence*, vol. 24, no. 1, pp. 1–5, Jan. 2014.
- [313] Y. Qian *et al.*, "Selective fluorescent probes for live-cell monitoring of sulphide," *Nature Communications*, vol. 2, no. 1, pp. 1–7, Oct. 2011.
- [314] Q. L. Xie, W. Liu, X. J. Liu, F. Ouyang, Y. Q. Kuang, and J. H. Jiang, "An azidocoumarin-based fluorescent probe for imaging lysosomal hydrogen sulfide in living cells," *Analytical Methods*, vol. 9, no. 19, pp. 2859–2864, May 2017.
- [315] M. Dulac, A. Melet, and E. Galardon, "Reversible Detection and Quantification of Hydrogen Sulfide by Fluorescence Using the Hemoglobin i from *Lucina pectinata*," *ACS Sensors*, vol. 3, no. 10, pp. 2138–2144, Oct. 2018.
- [316] G. Marchesini *et al.*, "EASL-EASD-EASO Clinical Practice Guidelines for the management of non-alcoholic fatty liver disease," *Journal of Hepatology*, vol. 64, no. 6, pp. 1388–1402, Jun. 2016.
- [317] J. C. Cohen, J. D. Horton, and H. H. Hobbs, "Human fatty liver disease: Old questions and new insights," *Science*, vol. 332, no. 6037. Science, pp. 1519–1523, 24-Jun-2011.
- [318] D. Kim, A. Touros, and W. R. Kim, "Nonalcoholic Fatty Liver Disease and Metabolic Syndrome," *Clinics in Liver Disease*, vol. 22, no. 1. W.B. Saunders, pp. 133–140, 01-Feb-2018.
- [319] M. Schlageter, L. M. Terracciano, S. D'Angelo, and P. Sorrentino, "Histopathology of hepatocellular carcinoma," *World Journal of Gastroenterology*, vol. 20, no. 43. WJG Press, pp. 15955–15964, 21-Nov-2014.
- [320] J. Ludwig, T. R. Viggiano, D. B. McGill, and B. J. Oh, "Nonalcoholic steatohepatitis: Mayo Clinic experiences with a hitherto unnamed disease," *Mayo Clin Proc*, vol. 55, no. 7, pp. 434–438, 1980.

- [321] N. Chalasani *et al.*, “The diagnosis and management of non-alcoholic fatty liver disease: Practice Guideline by the American Association for the Study of Liver Diseases, American College of Gastroenterology, and the American Gastroenterological Association,” *Hepatology*, vol. 55, no. 6, pp. 2005–2023, Jun. 2012.
- [322] Z. M. Younossi, A. B. Koenig, D. Abdelatif, Y. Fazel, L. Henry, and M. Wymer, “Global epidemiology of nonalcoholic fatty liver disease—Meta-analytic assessment of prevalence, incidence, and outcomes,” *Hepatology*, vol. 64, no. 1, pp. 73–84, Jul. 2016.
- [323] Z. Younossi *et al.*, “Global Perspectives on Nonalcoholic Fatty Liver Disease and Nonalcoholic Steatohepatitis,” *Hepatology*, vol. 69, no. 6. John Wiley and Sons Inc., pp. 2672–2682, 01-Jun-2018.
- [324] J. V. Lazarus *et al.*, “NAFLD — sounding the alarm on a silent epidemic,” *Nature Reviews Gastroenterology and Hepatology*, vol. 17, no. 7. Nature Research, pp. 377–379, 01-Jul-2020.
- [325] K. P. H. Sharp, M. Schultz, and K. J. Coppell, “Is non-alcoholic fatty liver disease a reflection of what we eat or simply how much we eat?,” *JGH Open*, vol. 2, no. 2, pp. 59–74, Apr. 2018.
- [326] S. Romeo *et al.*, “Genetic variation in PNPLA3 confers susceptibility to nonalcoholic fatty liver disease,” *Nature Genetics*, vol. 40, no. 12, pp. 1461–1465, Dec. 2008.
- [327] F. V. Bruschi *et al.*, “The PNPLA3 I148M variant modulates the fibrogenic phenotype of human hepatic stellate cells,” *Hepatology*, vol. 65, no. 6, pp. 1875–1890, Jun. 2017.
- [328] Z. M. Younossi *et al.*, “The global epidemiology of NAFLD and NASH in patients with type 2 diabetes: A systematic review and meta-analysis,” *Journal of Hepatology*, vol. 71, no. 4, pp. 793–801, Oct. 2019.
- [329] C. Ding, Z. Chan, and F. Magkos, “Lean, but not healthy: The ‘metabolically obese, normal-weight’ phenotype,” *Current Opinion in Clinical Nutrition and Metabolic Care*, vol. 19, no. 6. Lippincott Williams and Wilkins, pp. 408–417, 01-Nov-2016.
- [330] L. Denkmayr *et al.*, “Lean Patients with Non-Alcoholic Fatty Liver Disease Have a Severe Histological Phenotype Similar to Obese Patients,” *Journal of Clinical Medicine*, vol. 7, no. 12, p. 562, Dec. 2018.
- [331] A. C. Dela Cruz *et al.*, “Characteristics and long-term prognosis of lean patients with nonalcoholic fatty liver disease,” Elsevier BV, May 2014.
- [332] F. Chen *et al.*, “Lean NAFLD: A Distinct Entity Shaped by Differential Metabolic Adaptation,” *Hepatology*, vol. 71, no. 4, pp. 1213–1227, Apr. 2020.
- [333] B. Wang *et al.*, “Prevalence of Metabolically Healthy Obese and Metabolically Obese but Normal Weight in Adults Worldwide: A Meta-Analysis,” *Hormone and Metabolic Research*, vol. 47, no. 11, pp. 839–845, Sep. 2015.
- [334] K. K. Aung, C. Lorenzo, M. A. Hinojosa, and S. M. Haffner, “Risk of developing diabetes and cardiovascular disease in metabolically unhealthy normal-weight and metabolically healthy obese individuals,” *Journal of Clinical Endocrinology and Metabolism*, vol. 99, no. 2, pp. 462–468, Feb. 2014.

- [335] M. Gao *et al.*, "Metabolically healthy obesity, transition to unhealthy metabolic status, and vascular disease in Chinese adults: A cohort study," *PLoS Medicine*, vol. 17, no. 10, Oct. 2020.
- [336] R. Caleyachetty *et al.*, "Metabolically Healthy Obese and Incident Cardiovascular Disease Events Among 3.5 Million Men and Women," *Journal of the American College of Cardiology*, vol. 70, no. 12, pp. 1429–1437, Sep. 2017.
- [337] C. D. Williams *et al.*, "Prevalence of nonalcoholic fatty liver disease and nonalcoholic steatohepatitis among a largely middle-aged population utilizing ultrasound and liver biopsy: A prospective study," *Gastroenterology*, vol. 140, no. 1, pp. 124–131, 2011.
- [338] A. Lonardo *et al.*, "Sex Differences in Nonalcoholic Fatty Liver Disease: State of the Art and Identification of Research Gaps," *Hepatology*, vol. 70, no. 4. John Wiley and Sons Inc., pp. 1457–1469, 01-Oct-2019.
- [339] J. D. Yang *et al.*, "Gender and menopause impact severity of fibrosis among patients with nonalcoholic steatohepatitis," *Hepatology*, vol. 59, no. 4, pp. 1406–1414, 2014.
- [340] J. S. Klair *et al.*, "A longer duration of estrogen deficiency increases fibrosis risk among postmenopausal women with nonalcoholic fatty liver disease," *Hepatology*, vol. 64, no. 1, pp. 85–91, Jul. 2016.
- [341] S. I. Kojima, N. Watanabe, M. Numata, T. Ogawa, and S. Matsuzaki, "Increase in the prevalence of fatty liver in Japan over the past 12 years: Analysis of clinical background," *Journal of Gastroenterology*, vol. 38, no. 10, pp. 954–961, Oct. 2003.
- [342] N. E. Rich *et al.*, "Racial and Ethnic Disparities in Nonalcoholic Fatty Liver Disease Prevalence, Severity, and Outcomes in the United States: A Systematic Review and Meta-analysis," *Clinical Gastroenterology and Hepatology*, vol. 16, no. 2, pp. 198-210.e2, Feb. 2018.
- [343] D. S. B, "A Study to Correlate AST/ALT Ratio and GGT Levels in Patients with NonAlcoholic Fatty liver Disease," *journal of Medical Science And clinical Research*, vol. 7, no. 4, Apr. 2019.
- [344] J. K. Lee *et al.*, "Estimation of the healthy upper limits for serum alanine aminotransferase in Asian populations with normal liver histology," *Hepatology*, vol. 51, no. 5, pp. 1577–1583, May 2010.
- [345] D. Q. Huang *et al.*, "ALT Levels for Asians With Metabolic Diseases: A Meta-analysis of 86 Studies With Individual Patient Data Validation," *Hepatology Communications*, vol. 4, no. 11, pp. 1624–1636, Nov. 2020.
- [346] B. JD *et al.*, "Prevalence of hepatic steatosis in an urban population in the United States: impact of ethnicity," *Hepatology (Baltimore, Md)*, vol. 40, no. 6, 2004.
- [347] M. Nouredin and R. Loomba, "Nonalcoholic fatty liver disease: Indications for liver biopsy and noninvasive biomarkers," *Clinical Liver Disease*, vol. 1, no. 4, pp. 104–107, Sep. 2012.
- [348] J. Wang *et al.*, "Diagnostic value of alcoholic liver disease (ALD)/ nonalcoholic fatty liver disease (NAFLD) index combined with  $\gamma$ -glutamyl transferase in differentiating ALD and NAFLD," *Korean Journal*



of *Internal Medicine*, vol. 31, no. 3, pp. 479–487, May 2016.

- [349] S. Petta *et al.*, “Serum  $\gamma$ -glutamyl Transferase Levels, Insulin Resistance and Liver Fibrosis in Patients with Chronic Liver Diseases,” *PLoS ONE*, vol. 7, no. 12, Dec. 2012.
- [350] G. Marchesini *et al.*, “Aminotransferase and gamma-glutamyltranspeptidase levels in obesity are associated with insulin resistance and the metabolic syndrome,” *Journal of Endocrinological Investigation*, vol. 28, no. 4, pp. 333–339, 2005.
- [351] J. O’Brien, H. Hayder, Y. Zayed, and C. Peng, “Overview of microRNA biogenesis, mechanisms of actions, and circulation,” *Frontiers in Endocrinology*, vol. 9, no. AUG. Frontiers Media S.A., p. 402, 03-Aug-2018.
- [352] J. Liu *et al.*, “A circulating microRNA signature as noninvasive diagnostic and prognostic biomarkers for nonalcoholic steatohepatitis,” *BMC Genomics*, vol. 19, no. 1, Mar. 2018.
- [353] S. S. Pillai *et al.*, “Predicting nonalcoholic fatty liver disease through a panel of plasma biomarkers and micrnas in female West Virginia population,” *International Journal of Molecular Sciences*, vol. 21, no. 18, pp. 1–20, Sep. 2020.
- [354] R. E. Castro *et al.*, “MiR-34a/SIRT1/p53 is suppressed by ursodeoxycholic acid in the rat liver and activated by disease severity in human non-alcoholic fatty liver disease,” *Journal of Hepatology*, vol. 58, no. 1, pp. 119–125, Jan. 2013.
- [355] X. Li, W. Zhang, K. Xu, and J. Lu, “miR-34a promotes liver fibrosis in patients with chronic hepatitis via mediating Sirt1/p53 signaling pathway,” *Pathology Research and Practice*, vol. 216, no. 5, May 2020.
- [356] N. C. Salvoza, D. C. Klinzing, J. Gopez-Cervantes, and M. O. Baclig, “Association of circulating serum MIR-34a and MIR-122 with dyslipidemia among patients with non-alcoholic fatty liver disease,” *PLoS ONE*, vol. 11, no. 4, Apr. 2016.
- [357] J. Chang *et al.*, “miR-122, a mammalian liver-specific microRNA, is processed from hcr mRNA and may downregulate the high affinity cationic amino acid transporter CAT-1,” *RNA biology*, vol. 1, no. 2, pp. 106–113, Jul. 2004.
- [358] Y. Hu, G. Du, G. Li, X. Peng, Z. Zhang, and Y. Zhai, “The miR-122 inhibition alleviates lipid accumulation and inflammation in NAFLD cell model,” *Archives of Physiology and Biochemistry*, pp. 1–5, Jul. 2019.
- [359] K. Jampoka, P. Muangpaisarn, K. Khongnomnan, S. Treeprasertsuk, P. Tangkijvanich, and S. Payungporn, “Serum miR-29a and miR-122 as Potential Biomarkers for Non-Alcoholic Fatty Liver Disease (NAFLD),” *MicroRNA*, vol. 7, no. 3, pp. 215–222, May 2018.
- [360] H. Yamada *et al.*, “Associations between circulating microRNAs (miR-21, miR-34a, miR-122 and miR-451) and non-alcoholic fatty liver,” *Clinica Chimica Acta*, vol. 424, pp. 99–103, Sep. 2013.
- [361] C. Coulouarn, V. M. Factor, J. B. Andersen, M. E. Durkin, and S. S. Thorgeirsson, “Loss of miR-122 expression in liver cancer correlates with suppression of the hepatic phenotype and gain of metastatic properties,” *Oncogene*, vol. 28, no. 40, pp. 3526–3536, Oct. 2009.

- [362] J. Xu *et al.*, "Circulating MicroRNAs, miR-21, miR-122, and miR-223, in patients with hepatocellular carcinoma or chronic hepatitis," *Molecular Carcinogenesis*, vol. 50, no. 2, pp. 136–142, Feb. 2011.
- [363] H. Sendi *et al.*, "miR-122 inhibition in a human liver organoid model leads to liver inflammation, necrosis, steatofibrosis and dysregulated insulin signaling," *PLoS ONE*, vol. 13, no. 7, Jul. 2018.
- [364] J. Zhao *et al.*, "MiR-21 simultaneously regulates ERK1 signaling in HSC activation and hepatocyte EMT in hepatic fibrosis," *PLoS ONE*, vol. 9, no. 10, Oct. 2014.
- [365] P. P. Becker *et al.*, "Performance of serum microRNAs-122,-192 and-21 as biomarkers in patients with non-Alcoholic steatohepatitis," *PLoS ONE*, vol. 10, no. 11, Nov. 2015.
- [366] L. X *et al.*, "Liver microRNA-21 is overexpressed in non-alcoholic steatohepatitis and contributes to the disease in experimental models by inhibiting PPAR $\alpha$  expression," *Gut*, vol. 65, no. 11, 2016.
- [367] P. M. Rodrigues *et al.*, "MiR-21 ablation and obeticholic acid ameliorate nonalcoholic steatohepatitis in mice," *Cell Death and Disease*, vol. 8, no. 4, Apr. 2017.
- [368] M. S. Middleton *et al.*, "Agreement Between Magnetic Resonance Imaging Proton Density Fat Fraction Measurements and Pathologist-Assigned Steatosis Grades of Liver Biopsies From Adults With Nonalcoholic Steatohepatitis," *Gastroenterology*, vol. 153, no. 3, pp. 753–761, Sep. 2017.
- [369] T. H. Kim *et al.*, "Accuracy of proton magnetic resonance for diagnosing non-alcoholic steatohepatitis: a meta-analysis," *Scientific Reports*, vol. 9, no. 1, pp. 1–8, Dec. 2019.
- [370] Y. Zhang *et al.*, "Liver fat imaging-a clinical overview of ultrasound, CT, and M R imaging," *British Journal of Radiology*, vol. 91, no. 1089. British Institute of Radiology, 2018.
- [371] A. Tang *et al.*, "Nonalcoholic fatty liver disease: MR imaging of liver proton density fat fraction to assess hepatic steatosis," *Radiology*, vol. 267, no. 2, pp. 422–431, May 2013.
- [372] X. M. Wang, X. J. Zhang, and L. Ma, "Diagnostic performance of magnetic resonance technology in detecting steatosis or fibrosis in patients with nonalcoholic fatty liver disease A meta-analysis," *Medicine (United States)*, vol. 97, no. 21, 2018.
- [373] R. Loomba *et al.*, "Multicenter Validation of Association Between Decline in MRI-PDFF and Histologic Response in NASH," *Hepatology*, vol. 72, no. 4, pp. 1219–1229, Oct. 2020.
- [374] E. B. Tapper and R. Loomba, "Noninvasive imaging biomarker assessment of liver fibrosis by elastography in NAFLD," *Nature Reviews Gastroenterology and Hepatology*, vol. 15, no. 5. Nature Publishing Group, pp. 274–282, 01-May-2018.
- [375] S. Petta, V. Di Marco, C. Cammà, G. Butera, D. Cabibi, and A. Craxì, "Reliability of liver stiffness measurement in non-alcoholic fatty liver disease: The effects of body mass index," *Alimentary Pharmacology and Therapeutics*, vol. 33, no. 12, pp. 1350–1360, Jun. 2011.
- [376] V. de Lédinghen *et al.*, "Controlled attenuation parameter for the diagnosis of steatosis in non-alcoholic fatty liver disease," *Journal of Gastroenterology and Hepatology (Australia)*, vol. 31, no. 4, pp. 848–855,

Apr. 2016.

- [377] T. Karlas *et al.*, "Individual patient data meta-analysis of controlled attenuation parameter (CAP) technology for assessing steatosis," *Journal of Hepatology*, vol. 66, no. 5, pp. 1022–1030, May 2017.
- [378] J. R. Van Werven *et al.*, "Assessment of hepatic steatosis in patients undergoing liver resection: Comparison of US, CT, T1-weighted dual-echo MR imaging, and point-resolved 1H MR spectroscopy," *Radiology*, vol. 256, no. 1, pp. 159–168, Jul. 2010.
- [379] G. Xiao, S. Zhu, X. Xiao, L. Yan, J. Yang, and G. Wu, "Comparison of laboratory tests, ultrasound, or magnetic resonance elastography to detect fibrosis in patients with nonalcoholic fatty liver disease: A meta-analysis," *Hepatology*, vol. 66, no. 5, pp. 1486–1501, Nov. 2017.
- [380] S. Dasarathy, J. Dasarathy, A. Khiyami, R. Joseph, R. Lopez, and A. J. McCullough, "Validity of real time ultrasound in the diagnosis of hepatic steatosis: A prospective study," *Journal of Hepatology*, vol. 51, no. 6, pp. 1061–1067, Dec. 2009.
- [381] A. Shannon *et al.*, "Ultrasonographic quantitative estimation of hepatic steatosis in children With NAFLD," *Journal of Pediatric Gastroenterology and Nutrition*, vol. 53, no. 2, pp. 190–195, Aug. 2011.
- [382] R. G. Barr *et al.*, "Elastography assessment of liver fibrosis: Society of radiologists in ultrasound consensus conference statement," *Radiology*, vol. 276, no. 3, pp. 845–861, Sep. 2015.
- [383] N. F. Schwenzer, F. Springer, C. Schraml, N. Stefan, J. Machann, and F. Schick, "Non-invasive assessment and quantification of liver steatosis by ultrasound, computed tomography and magnetic resonance," *Journal of Hepatology*, vol. 51, no. 3, pp. 433–445, Sep. 2009.
- [384] S. H. Park *et al.*, "Macrovesicular hepatic steatosis in living liver donors: Use of CT for quantitative and qualitative assessment," *Radiology*, vol. 239, no. 1. Radiology, pp. 105–112, Apr-2006.
- [385] K. M. Haberal, H. Turnaoglu, and A. N. H. Reyhan, "Is unenhanced computed tomography reliable in the assessment of macrovesicular steatosis in living liver donors?," *Experimental and Clinical Transplantation*, vol. 17, no. 6, pp. 749–752, Dec. 2019.
- [386] Q. Li, M. Dhyani, J. R. Grajo, C. Sirlin, and A. E. Samir, "Current status of imaging in nonalcoholic fatty liver disease," *World Journal of Hepatology*, vol. 10, no. 8, pp. 530–542, Aug. 2018.
- [387] P. Bedossa, "Diagnosis of non-alcoholic fatty liver disease/non-alcoholic steatohepatitis: Why liver biopsy is essential," *Liver International*, vol. 38, pp. 64–66, Feb. 2018.
- [388] E. M. Brunt, C. G. Janney, A. M. Di Bisceglie, B. A. Neuschwander-Tetri, and B. R. Bacon, "Nonalcoholic steatohepatitis: a proposal for grading and staging the histological lesions," *The American Journal of Gastroenterology*, vol. 94, no. 9, pp. 2467–2474, Sep. 1999.
- [389] D. E. Kleiner *et al.*, "Design and validation of a histological scoring system for nonalcoholic fatty liver disease," *Hepatology*, vol. 41, no. 6, pp. 1313–1321, Jun. 2005.
- [390] P. Bedossa *et al.*, "Histopathological algorithm and scoring system for evaluation of liver lesions in

- morbidly obese patients," *Hepatology*, vol. 56, no. 5, pp. 1751–1759, Nov. 2012.
- [391] C. P. Day and O. F. W. James, "Steatohepatitis: A tale of two 'Hits'?", *Gastroenterology*, vol. 114, no. 4 I. W.B. Saunders, pp. 842–845, 1998.
- [392] S. Petta *et al.*, "Pathophysiology of non alcoholic fatty liver disease," *International Journal of Molecular Sciences*, vol. 17, no. 12. MDPI AG, 11-Dec-2016.
- [393] S. Dash, C. Xiao, C. Morgantini, and G. F. Lewis, "New Insights into the Regulation of Chylomicron Production," *Annual Review of Nutrition*, vol. 35, no. 1. Annual Reviews Inc., pp. 265–294, 17-Jul-2015.
- [394] K. L. Donnelly, C. I. Smith, S. J. Schwarzenberg, J. Jessurun, M. D. Boldt, and E. J. Parks, "Sources of fatty acids stored in liver and secreted via lipoproteins in patients with nonalcoholic fatty liver disease," *Journal of Clinical Investigation*, vol. 115, no. 5, pp. 1343–1351, May 2005.
- [395] P. K. Luukkonen *et al.*, "Saturated fat is more metabolically harmful for the human liver than unsaturated fat or simple sugars," in *Diabetes Care*, 2018, vol. 41, no. 8, pp. 1732–1739.
- [396] V. Lecoultre *et al.*, "Effects of fructose and glucose overfeeding on hepatic insulin sensitivity and intrahepatic lipids in healthy humans," *Obesity*, vol. 21, no. 4, pp. 782–785, Apr. 2013.
- [397] C. C. L. Wang, R. L. Adochio, J. W. Leitner, I. M. Abeyta, B. Draznin, and M. A. Cornier, "Acute effects of different diet compositions on skeletal muscle insulin signalling in obese individuals during caloric restriction," *Metabolism: Clinical and Experimental*, vol. 62, no. 4, pp. 595–603, Apr. 2013.
- [398] M. I. Johari *et al.*, "A Randomised Controlled Trial on the Effectiveness and Adherence of Modified Alternate-day Calorie Restriction in Improving Activity of Non-Alcoholic Fatty Liver Disease," *Scientific Reports*, vol. 9, no. 1, pp. 1–9, Dec. 2019.
- [399] A. Gómez-Hernández, N. Beneit, S. Díaz-Castroverde, and Ó. Escribano, "Differential Role of Adipose Tissues in Obesity and Related Metabolic and Vascular Complications," *International Journal of Endocrinology*, vol. 2016. Hindawi Limited, 2016.
- [400] E. Carvalho, P. Jansson, I. Nagaev, A. Wentzel, and U. Smith, "Insulin resistance with low cellular IRS-1 expression is also associated with low GLUT4 expression and impaired insulin-stimulated glucose transport 1," *The FASEB Journal*, vol. 15, no. 6, pp. 1101–1103, Apr. 2001.
- [401] K. Janochova, M. Haluzik, and M. Buzga, "Visceral fat and insulin resistance – what we know?," *Biomedical Papers*, vol. 163, no. 1, pp. 19–27, 2019.
- [402] M. Schweiger *et al.*, "Pharmacological inhibition of adipose triglyceride lipase corrects high-fat diet-induced insulin resistance and hepatosteatosis in mice," *Nature Communications*, vol. 8, no. 1, pp. 1–15, Mar. 2017.
- [403] P. Mårin *et al.*, "The morphology and metabolism of intraabdominal adipose tissue in men," *Metabolism*, vol. 41, no. 11, pp. 1242–1248, 1992.
- [404] K. V. Pivtorak, N. A. Shevchuk, N. A. Pivtorak, and I. V. Fedzhaga, "Correction of adipocyte secretion

- disorders in patients with non-alcoholic fatty liver disease with overweight and obesity," *Wiadomosci lekarskie (Warsaw, Poland : 1960)*, vol. 72, no. 8, pp. 1477–1480, Aug. 2019.
- [405] E. Chang, M. Varghese, and K. Singer, "Gender and Sex Differences in Adipose Tissue," *Current Diabetes Reports*, vol. 18, no. 9. Current Medicine Group LLC 1, p. 69, 01-Sep-2018.
- [406] Y. Miyazaki and R. A. DeFronzo, "Visceral fat dominant distribution in male type 2 diabetic patients is closely related to hepatic insulin resistance, irrespective of body type," *Cardiovascular Diabetology*, vol. 8, Aug. 2009.
- [407] C. Y. Han *et al.*, "Adipocyte-Derived Versican and Macrophage-Derived Biglycan Control Adipose Tissue Inflammation in Obesity," *Cell Reports*, vol. 31, no. 13, p. 107818, Jun. 2020.
- [408] M. Gaggini, C. Saponaro, and A. Gastaldelli, "Not all fats are created equal: Adipose vs. ectopic fat, implication in cardiometabolic diseases," *Hormone Molecular Biology and Clinical Investigation*, vol. 22, no. 1, pp. 7–18, Apr. 2015.
- [409] C. Rosso *et al.*, "Crosstalk between adipose tissue insulin resistance and liver macrophages in non-alcoholic fatty liver disease," *Journal of Hepatology*, vol. 71, no. 5, pp. 1012–1021, Nov. 2019.
- [410] D. Kim *et al.*, "Body Fat Distribution and Risk of Incident and Regressed Nonalcoholic Fatty Liver Disease," *Clinical Gastroenterology and Hepatology*, vol. 14, no. 1, pp. 132-138.e4, Jan. 2016.
- [411] C. H. Jung, E. J. Rhee, H. Kwon, Y. Chang, S. Ryu, and W. Y. Lee, "Visceral-to-subcutaneous abdominal fat ratio is associated with nonalcoholic fatty liver disease and liver fibrosis," *Endocrinology and Metabolism*, vol. 35, no. 1, pp. 165–176, Mar. 2020.
- [412] A. Lonardo, F. Nascimbeni, M. Maurantonio, A. Marrazzo, L. Rinaldi, and L. E. Adinolfi, "Nonalcoholic fatty liver disease: Evolving paradigms," *World Journal of Gastroenterology*, vol. 23, no. 36. Baishideng Publishing Group Co., Limited, pp. 6571–6592, 28-Sep-2017.
- [413] C. Rosso *et al.*, "Peripheral insulin resistance predicts liver damage in nondiabetic subjects with nonalcoholic fatty liver disease," *Hepatology*, vol. 63, no. 1, pp. 107–116, Jan. 2016.
- [414] G. I. Smith *et al.*, "Insulin resistance drives hepatic de novo lipogenesis in nonalcoholic fatty liver disease," *Journal of Clinical Investigation*, vol. 130, no. 3, pp. 1453–1460, Mar. 2020.
- [415] S. Steensels, J. Qiao, and B. A. Ersoy, "Transcriptional regulation in non-alcoholic fatty liver disease," *Metabolites*, vol. 10, no. 7. MDPI AG, pp. 1–34, 01-Jul-2020.
- [416] C. Postic and J. Girard, "The role of the lipogenic pathway in the development of hepatic steatosis," *Diabetes and Metabolism*, vol. 34, no. 6 PART 2, pp. 643–648, 2008.
- [417] F. Benhamed *et al.*, "The lipogenic transcription factor ChREBP dissociates hepatic steatosis from insulin resistance in mice and humans," *Journal of Clinical Investigation*, vol. 122, no. 6, pp. 2176–2194, Jun. 2012.
- [418] W. Swiatek, K. M. Parnell, G. A. Nickols, B. F. Scharschmidt, and J. Rutter, "Validation of PAS Kinase, a

- Regulator of Hepatic Fatty Acid and Triglyceride Synthesis, as a Therapeutic Target for Nonalcoholic Steatohepatitis," *Hepatology Communications*, vol. 4, no. 5, pp. 696–707, May 2020.
- [419] R. Dentin *et al.*, "Liver-specific inhibition of ChREBP improves hepatic steatosis and insulin resistance in ob/ob mice," *Diabetes*, vol. 55, no. 8, pp. 2159–2170, Aug. 2006.
- [420] K. Iizuka, B. Miller, and K. Uyeda, "Deficiency of carbohydrate-activated transcription factor ChREBP prevents obesity and improves plasma glucose control in leptin-deficient (ob/ob) mice," *American Journal of Physiology - Endocrinology and Metabolism*, vol. 291, no. 2, 2006.
- [421] A. Kumar *et al.*, "Activation of Nrf2 is required for normal and ChREBP-augmented glucose-stimulated B-cell proliferation," *Diabetes*, vol. 67, no. 8, pp. 1561–1575, Aug. 2018.
- [422] J. Bricambert *et al.*, "The histone demethylase Phf2 acts as a molecular checkpoint to prevent NAFLD progression during obesity," *Nature Communications*, vol. 9, no. 1, pp. 1–18, Dec. 2018.
- [423] G. Liang, J. Yang, J. D. Horton, R. E. Hammer, J. L. Goldstein, and M. S. Brown, "Diminished hepatic response to fasting/refeeding and liver X receptor agonists in mice with selective deficiency of sterol regulatory element-binding protein-1c," *Journal of Biological Chemistry*, vol. 277, no. 11, pp. 9520–9528, Mar. 2002.
- [424] M. Kohjima *et al.*, "SREBP-1c, regulated by the insulin and AMPK signaling pathways, plays a role in nonalcoholic fatty liver disease," *International Journal of Molecular Medicine*, vol. 21, no. 4, pp. 507–511, Apr. 2008.
- [425] L. Chen *et al.*, "The additive effects of the TM6SF2 E167K and PNPLA3 I148M polymorphisms on lipid metabolism," *Oncotarget*, vol. 8, no. 43, pp. 74209–74216, 2017.
- [426] A. G. Linden *et al.*, "Interplay between ChREBP and SREBP-1c coordinates postprandial glycolysis and lipogenesis in livers of mice," *Journal of Lipid Research*, vol. 59, no. 3, pp. 475–487, 2018.
- [427] A. Fougerat, A. Montagner, N. Loiseau, H. Guillou, and W. Wahli, "Peroxisome Proliferator-Activated Receptors and Their Novel Ligands as Candidates for the Treatment of Non-Alcoholic Fatty Liver Disease," *Cells*, vol. 9, no. 7. NLM (Medline), 08-Jul-2020.
- [428] S. Francque *et al.*, "PPAR $\alpha$  gene expression correlates with severity and histological treatment response in patients with non-alcoholic steatohepatitis," *Journal of Hepatology*, vol. 63, no. 1, pp. 164–173, Jul. 2015.
- [429] M. Régnier *et al.*, "Hepatocyte-specific deletion of Ppar $\alpha$  promotes NAFLD in the context of obesity," *Scientific Reports*, vol. 10, no. 1, pp. 1–15, Dec. 2020.
- [430] M. Inoue *et al.*, "Increased expression of PPAR $\gamma$  in high fat diet-induced liver steatosis in mice," *Biochemical and Biophysical Research Communications*, vol. 336, no. 1, pp. 215–222, Oct. 2005.
- [431] F. Gilardi *et al.*, "Systemic PPAR $\gamma$  deletion in mice provokes lipoatrophy, organomegaly, severe type 2 diabetes and metabolic inflexibility," *Metabolism: Clinical and Experimental*, vol. 95, pp. 8–20, Jun.

2019.

- [432] E. Morán-Salvador *et al.*, "Role for PPAR $\gamma$  in obesity-induced hepatic steatosis as determined by hepatocyte- and macrophage-specific conditional knockouts," *The FASEB Journal*, vol. 25, no. 8, pp. 2538–2550, Aug. 2011.
- [433] W. Shan *et al.*, "Peroxisome proliferator-activated receptor- $\beta/\delta$  protects against chemically induced liver toxicity in mice," *Hepatology*, vol. 47, no. 1, pp. 225–235, Jan. 2008.
- [434] M. Zarei *et al.*, "Hepatic regulation of VLDL receptor by PPAR $\beta/\delta$  and FGF21 modulates non-alcoholic fatty liver disease," *Molecular Metabolism*, vol. 8, pp. 117–131, Feb. 2018.
- [435] L. Tong *et al.*, "PPAR $\delta$  attenuates hepatic steatosis through autophagy-mediated fatty acid oxidation," *Cell Death and Disease*, vol. 10, no. 3, Mar. 2019.
- [436] M. C. Cave *et al.*, "Nuclear receptors and nonalcoholic fatty liver disease," *Biochimica et Biophysica Acta - Gene Regulatory Mechanisms*, vol. 1859, no. 9, pp. 1083–1099, Sep. 2016.
- [437] X. Li, Z. Wang, and J. E. Klaunig, "Modulation of xenobiotic nuclear receptors in high-fat diet induced non-alcoholic fatty liver disease," *Toxicology*, vol. 410, pp. 199–213, Dec. 2018.
- [438] P. Wang *et al.*, "Impact of obese levels on the hepatic expression of nuclear receptors and drug-metabolizing enzymes in adult and offspring mice," *Acta Pharmaceutica Sinica B*, vol. 10, no. 1, pp. 171–185, Jan. 2020.
- [439] B. Dong *et al.*, "Activation of nuclear receptor CAR ameliorates diabetes and fatty liver disease," *Proceedings of the National Academy of Sciences of the United States of America*, vol. 106, no. 44, pp. 18831–18836, Nov. 2009.
- [440] E. S. Baskin-Bey *et al.*, "Constitutive androstane receptor (CAR) ligand, TCPOBOP, attenuates Fas-induced murine liver injury by altering Bcl-2 proteins," *Hepatology*, vol. 44, no. 1, pp. 252–262, Jul. 2006.
- [441] Y. Yamazaki *et al.*, "The role of the nuclear receptor constitutive androstane receptor in the pathogenesis of non-alcoholic steatohepatitis," *Gut*, vol. 56, no. 4, pp. 565–574, Apr. 2007.
- [442] S. Ducheix *et al.*, "A systems biology approach to the hepatic role of the oxysterol receptor LXR in the regulation of lipogenesis highlights a cross-talk with PPAR $\alpha$ ," *Biochimie*, vol. 95, no. 3, pp. 556–567, Mar. 2013.
- [443] S. B. Ahn, K. Jang, D. W. Jun, B. H. Lee, and K. J. Shin, "Expression of Liver X Receptor Correlates with Intrahepatic Inflammation and Fibrosis in Patients with Nonalcoholic Fatty Liver Disease," *Digestive Diseases and Sciences*, vol. 59, no. 12, pp. 2975–2982, Nov. 2014.
- [444] S. M. Rahman, M. Choudhury, R. C. Janssen, K. C. Baquero, M. Miyazaki, and J. E. Friedman, "CCAAT/enhancer binding protein  $\beta$  deletion increases mitochondrial function and protects mice from LXR-induced hepatic steatosis," *Biochemical and Biophysical Research Communications*, vol. 430, no. 1,

pp. 336–339, Jan. 2013.

- [445] X. Y. Zhao *et al.*, “Long noncoding RNA licensing of obesity-linked hepatic lipogenesis and NAFLD pathogenesis,” *Nature Communications*, vol. 9, no. 1, pp. 1–14, Dec. 2018.
- [446] Y. Xi and H. Li, “Role of farnesoid X receptor in hepatic steatosis in nonalcoholic fatty liver disease,” *Biomedicine and Pharmacotherapy*, vol. 121. Elsevier Masson SAS, p. 109609, 01-Jan-2020.
- [447] J. Prawitt *et al.*, “Farnesoid X receptor deficiency improves glucose homeostasis in mouse models of obesity,” *Diabetes*, vol. 60, no. 7, pp. 1861–1871, Jul. 2011.
- [448] C. D. Fuchs, T. Claudel, H. Scharnagl, T. Stojakovic, and M. Trauner, “FXR controls CHOP expression in steatohepatitis,” *FEBS Letters*, vol. 591, no. 20, pp. 3360–3368, Oct. 2017.
- [449] F. Perla, M. Prelati, M. Lavorato, D. Visicchio, and C. Anania, “The Role of Lipid and Lipoprotein Metabolism in Non-Alcoholic Fatty Liver Disease,” *Children*, vol. 4, no. 6, p. 46, Jun. 2017.
- [450] E. Fabbrini, B. S. Mohammed, F. Magkos, K. M. Korenblat, B. W. Patterson, and S. Klein, “Alterations in Adipose Tissue and Hepatic Lipid Kinetics in Obese Men and Women With Nonalcoholic Fatty Liver Disease,” *Gastroenterology*, vol. 134, no. 2, pp. 424–431, 2008.
- [451] B. Vergès, “Pathophysiology of diabetic dyslipidaemia: where are we?,” *Diabetologia*, vol. 58, no. 5. Springer Verlag, pp. 886–899, 01-May-2015.
- [452] M. K. Poulsen, B. Nellemann, H. Stødkilde-Jørgensen, S. B. Pedersen, H. Grønbaek, and S. Nielsen, “Impaired insulin suppression of VLDL-triglyceride kinetics in nonalcoholic fatty liver disease,” *Journal of Clinical Endocrinology and Metabolism*, vol. 101, no. 4, pp. 1637–1646, Apr. 2016.
- [453] M. Charlton, R. Sreekumar, D. Rasmussen, K. Lindor, and K. Sreekumaran Nair, “Apolipoprotein Synthesis in Nonalcoholic Steatohepatitis,” 2002.
- [454] M. Di Filippo *et al.*, “Homozygous MTP and APOB mutations may lead to hepatic steatosis and fibrosis despite metabolic differences in congenital hypocholesterolemia,” *Journal of Hepatology*, vol. 61, no. 4, pp. 891–902, Oct. 2014.
- [455] X. Wang *et al.*, “The patatin-like phospholipase domain containing protein 7 facilitates VLDL secretion by modulating ApoE stability,” *Hepatology*, p. hep.31161, Feb. 2020.
- [456] Z. G. Jiang *et al.*, “Steatohepatitis and liver fibrosis are predicted by the characteristics of very low density lipoprotein in nonalcoholic fatty liver disease,” *Liver International*, vol. 36, no. 8, pp. 1213–1220, Aug. 2016.
- [457] M. Martínez-Uña *et al.*, “S-Adenosylmethionine increases circulating very-low density lipoprotein clearance in non-alcoholic fatty liver disease,” *Journal of Hepatology*, vol. 62, no. 3, pp. 673–681, Mar. 2015.
- [458] T. Ota, C. Gayet, and H. N. Ginsberg, “Inhibition of apolipoprotein B100 secretion by lipid-induced hepatic endoplasmic reticulum stress in rodents,” *Journal of Clinical Investigation*, vol. 118, no. 1, pp.



316–332, Jan. 2008.

- [459] D. M. Conlon *et al.*, “Inhibition of apolipoprotein B synthesis stimulates endoplasmic reticulum autophagy that prevents steatosis,” *Journal of Clinical Investigation*, vol. 126, no. 10, pp. 3852–3867, Oct. 2016.
- [460] B. Mittendorfer, M. Yoshino, B. W. Patterson, and S. Klein, “VLDL triglyceride kinetics in lean, overweight, and obese men and women,” *Journal of Clinical Endocrinology and Metabolism*, vol. 101, no. 11, pp. 4151–4160, Nov. 2016.
- [461] B. Fromenty, “Inhibition of mitochondrial fatty acid oxidation in drug-induced hepatic steatosis,” *Liver Research*, vol. 3, no. 3–4. KeAi Communications Co., pp. 157–169, 01-Dec-2019.
- [462] F. Lynen, “Participation of Coenzyme a in the Oxidation of Fat,” *Nature*, vol. 174, no. 4438, pp. 962–965, 1954.
- [463] S. Ochoa, “Enzymes of fatty acid metabolism: a commentary on ‘Enzymes of fatty acid metabolism’ by F. Lynen and S. Ochoa *Biochim. Biophys. Acta* 12 (1953) 299-314,” *BBA - Biochimica et Biophysica Acta*, vol. 1000, no. C, pp. 279–296, Jan. 1989.
- [464] S. Eaton, K. Bartlett, and M. Pourfarzam, “Mammalian mitochondrial  $\beta$ -oxidation,” 1996.
- [465] J. D. McGarry and N. F. Brown, “The mitochondrial carnitine palmitoyltransferase system. From concept to molecular analysis,” *European Journal of Biochemistry*, vol. 244, no. 1. Blackwell Publishing Ltd, pp. 1–14, 1997.
- [466] J. P. Bonnefont, F. Djouadi, C. Prip-Buus, S. Gobin, A. Munnich, and J. Bastin, “Carnitine palmitoyltransferases 1 and 2: Biochemical, molecular and medical aspects,” *Molecular Aspects of Medicine*, vol. 25, no. 5–6, pp. 495–520, 2004.
- [467] N. F. Brown *et al.*, “Molecular characterization of L-CPT I deficiency in six patients: Insights into function of the native enzyme,” *Journal of Lipid Research*, vol. 42, no. 7, pp. 1134–1142, 2001.
- [468] H. A. Krebs, “The tricarboxylic acid cycle,” *The Harvey lectures*, vol. 44, pp. 165–169, 1948.
- [469] Q. Chen, E. J. Vazquez, S. Moghaddas, C. L. Hoppel, and E. J. Lesnefsky, “Production of Reactive Oxygen Species by Mitochondria: central role of complex III.,” *Journal of Biological Chemistry*, vol. 278, no. 38, pp. 36027–36031, Sep. 2003.
- [470] R. S. Rector *et al.*, “Mitochondrial dysfunction precedes insulin resistance and hepatic steatosis and contributes to the natural history of non-alcoholic fatty liver disease in an obese rodent model,” *Journal of Hepatology*, vol. 52, no. 5, pp. 727–736, May 2010.
- [471] J. Lee *et al.*, “Loss of Hepatic Mitochondrial Long-Chain Fatty Acid Oxidation Confers Resistance to Diet-Induced Obesity and Glucose Intolerance,” *Cell Reports*, vol. 20, no. 3, pp. 655–667, Jul. 2017.
- [472] L. Diao, C. Auger, H. Konoeda, A. R. Sadri, S. Amini-Nik, and M. G. Jeschke, “Hepatic steatosis associated with decreased  $\beta$ -oxidation and mitochondrial function contributes to cell damage in obese mice after

- thermal injury article," *Cell Death and Disease*, vol. 9, no. 5, pp. 1–11, May 2018.
- [473] L. Barbier-Torres *et al.*, "Silencing hepatic MCJ attenuates non-alcoholic fatty liver disease (NAFLD) by increasing mitochondrial fatty acid oxidation," *Nature Communications*, vol. 11, no. 1, pp. 1–15, Dec. 2020.
- [474] M. Stefanovic-Racic, G. Perdomo, B. S. Mantell, I. J. Sipula, N. F. Brown, and R. M. O'Doherty, "A moderate increase in carnitine palmitoyltransferase 1a activity is sufficient to substantially reduce hepatic triglyceride levels," *American Journal of Physiology - Endocrinology and Metabolism*, vol. 294, no. 5, May 2008.
- [475] M. Weber *et al.*, "Liver CPT1A gene therapy reduces diet-induced hepatic steatosis in mice and highlights potential lipid biomarkers for human NAFLD," *The FASEB Journal*, vol. 34, no. 9, pp. 11816–11837, Sep. 2020.
- [476] M. Jiang, C. Li, Q. Liu, A. Wang, and M. Lei, "Inhibiting ceramide synthesis attenuates hepatic steatosis and fibrosis in rats with non-alcoholic fatty liver disease," *Frontiers in Endocrinology*, vol. 10, no. SEP, p. 665, Sep. 2019.
- [477] H. B. Eccleston *et al.*, "Chronic exposure to a high-fat diet induces hepatic steatosis, impairs nitric oxide bioavailability, and modifies the mitochondrial proteome in mice," *Antioxidants and Redox Signaling*, vol. 15, no. 2, pp. 447–459, Jul. 2011.
- [478] J. Massart, K. Begriche, N. Buron, M. Porceddu, A. Borgne-Sanchez, and B. Fromenty, "Drug-Induced Inhibition of Mitochondrial Fatty Acid Oxidation and Steatosis," *Current Pathobiology Reports*, vol. 1, no. 3, pp. 147–157, Sep. 2013.
- [479] R. Sreekumar, B. Rosado, D. Rasmussen, and M. Charlton, "Hepatic gene expression in histologically progressive nonalcoholic steatohepatitis," *Hepatology*, vol. 38, no. 1, pp. 244–251, Jul. 2003.
- [480] M. Kohjima *et al.*, "Re-evaluation of fatty acid metabolism-related gene expression in nonalcoholic fatty liver disease," *International Journal of Molecular Medicine*, vol. 20, no. 3, pp. 351–358, 2007.
- [481] G. Serviddio *et al.*, "Oxidation of hepatic carnitine palmitoyl transferase-I (CPT-I) impairs fatty acid beta-oxidation in rats fed a methionine-choline deficient diet," *PLoS ONE*, vol. 6, no. 9, p. 24084, Sep. 2011.
- [482] J. Monsénégo *et al.*, "Enhancing liver mitochondrial fatty acid oxidation capacity in obese mice improves insulin sensitivity independently of hepatic steatosis," *Journal of Hepatology*, vol. 56, no. 3, pp. 632–639, Mar. 2012.
- [483] A. Adina-Zada, T. N. Zeczycki, and P. V. Attwood, "Regulation of the structure and activity of pyruvate carboxylase by acetyl CoA," *Archives of Biochemistry and Biophysics*, vol. 519, no. 2. Arch Biochem Biophys, pp. 118–130, 15-Mar-2012.
- [484] A. A. David Cappel, aw Deja, J. A. Duarte, P. Mishra, J. D. Browning, and S. C. Burgess Correspondence, "Pyruvate-Carboxylase-Mediated Anaplerosis Promotes Antioxidant Capacity by Sustaining TCA Cycle and Redox Metabolism in Liver," *Cell Metabolism*, vol. 29, pp. 1291-1305.e8, 2019.

- [485] P. S. Brady, R. R. Ramsay, and L. J. Brady, "Regulation of the long-chain carnitine acyltransferases," *The FASEB Journal*, vol. 7, no. 11, pp. 1039–1044, Aug. 1993.
- [486] M. Fransen, C. Lismont, and P. Walton, "The peroxisome-mitochondria connection: How and why?," *International Journal of Molecular Sciences*, vol. 18, no. 6. MDPI AG, 01-Jun-2017.
- [487] J. Vamecq, J. P. Draye, and J. Brison, "Rat liver metabolism of dicarboxylic acids," *American Journal of Physiology - Gastrointestinal and Liver Physiology*, vol. 256, no. 4, 1989.
- [488] M. Inouye, T. Mio, and K. Sumino, "Dicarboxylic acids as markers of fatty acid peroxidation in diabetes," *Atherosclerosis*, vol. 148, no. 1, pp. 197–202, Jan. 2000.
- [489] A. I. Cederbaum, "Cytochrome P450 2E1-dependent oxidant stress and upregulation of anti-oxidant defense in liver cells," in *Journal of Gastroenterology and Hepatology (Australia)*, 2006, vol. 21, no. SUPPL. 3, pp. S22–S25.
- [490] A. Mahli *et al.*, "Identification of cytochrome CYP2E1 as critical mediator of synergistic effects of alcohol and cellular lipid accumulation in hepatocytes in vitro," *Oncotarget*, vol. 6, no. 39, pp. 41464–41478, 2015.
- [491] H. Chtioui, D. Semela, M. Ledermann, A. Zimmermann, and J. F. Dufour, "Expression and activity of the cytochrome P450 2E1 in patients with nonalcoholic steatosis and steatohepatitis," *Liver International*, vol. 27, no. 6, pp. 764–771, Aug. 2007.
- [492] R. Zhu *et al.*, "Systematic transcriptome analysis reveals elevated expression of alcohol-metabolizing genes in NAFLD livers," *Journal of Pathology*, vol. 238, no. 4, pp. 531–542, Mar. 2016.
- [493] Y. Liu, F. Cheng, Y. X. Luo, P. Hu, H. Ren, and M. L. Peng, "[The role of cytochrome P450 in nonalcoholic fatty liver induced by high-fat diet: a gene expression profile analysis].," *Zhonghua gan zang bing za zhi = Zhonghua ganzangbing zazhi = Chinese journal of hepatology*, vol. 25, no. 4, pp. 285–290, Apr. 2017.
- [494] J. Xu *et al.*, "The role of human cytochrome P450 2E1 in liver inflammation and fibrosis," *Hepatology Communications*, vol. 1, no. 10, pp. 1043–1057, Dec. 2017.
- [495] T. Jian *et al.*, "Hepatoprotective effect of loquat leaf flavonoids in PM2.5-induced non-alcoholic fatty liver disease via regulation of IRs-1/Akt and CYP2E1/JNK pathways," *International Journal of Molecular Sciences*, vol. 19, no. 10, Oct. 2018.
- [496] T. Gopal *et al.*, "Nanoformulated SOD1 ameliorates the combined NASH and alcohol-associated liver disease partly via regulating CYP2E1 expression in adipose tissue and liver," *American Journal of Physiology - Gastrointestinal and Liver Physiology*, vol. 318, no. 3, pp. G428–G438, 2020.
- [497] B. Chaurasia *et al.*, "Targeting a ceramide double bond improves insulin resistance and hepatic steatosis," *Science*, vol. 365, no. 6451, pp. 386–392, Jul. 2019.
- [498] S. Schüll *et al.*, "Cytochrome c oxidase deficiency accelerates mitochondrial apoptosis by activating ceramide synthase 6," *Cell death & disease*, vol. 6, no. 3, p. e1691, Mar. 2015.

- [499] S. M. Turpin *et al.*, "Obesity-induced CerS6-dependent C16:0 ceramide production promotes weight gain and glucose intolerance," *Cell Metabolism*, vol. 20, no. 4, pp. 678–686, Oct. 2014.
- [500] S. Raichur *et al.*, "CerS2 haploinsufficiency inhibits  $\beta$ -oxidation and confers susceptibility to diet-induced steatohepatitis and insulin resistance," *Cell Metabolism*, vol. 20, no. 4, pp. 687–695, Oct. 2014.
- [501] S. Raichur *et al.*, "The role of C16:0 ceramide in the development of obesity and type 2 diabetes: CerS6 inhibition as a novel therapeutic approach," *Molecular Metabolism*, vol. 21, pp. 36–50, Mar. 2019.
- [502] W. L. Holland *et al.*, "Lipid-induced insulin resistance mediated by the proinflammatory receptor TLR4 requires saturated fatty acid-induced ceramide biosynthesis in mice," *Journal of Clinical Investigation*, vol. 121, no. 5, pp. 1858–1870, May 2011.
- [503] J. A. Chavez, M. M. Siddique, S. T. Wang, J. Ching, J. A. Shayman, and S. A. Summers, "Ceramide and glucosylceramides are independent antagonists of insulin signaling," *Journal of Biological Chemistry*, vol. 289, no. 2, pp. 723–734, Jan. 2014.
- [504] N. Turner *et al.*, "A selective inhibitor of ceramide synthase 1 reveals a novel role in fat metabolism," *Nature Communications*, vol. 9, no. 1, Dec. 2018.
- [505] M. C. Petersen *et al.*, "Insulin receptor Thr1160 phosphorylation mediates lipid-induced hepatic insulin resistance," *Journal of Clinical Investigation*, vol. 126, no. 11, pp. 4361–4371, Nov. 2016.
- [506] Y. J. Kim, P. Greimel, and Y. Hirabayashi, "GPCR5B-Mediated Sphingomyelin Synthase 2 Phosphorylation Plays a Critical Role in Insulin Resistance," *iScience*, vol. 8, pp. 250–266, Oct. 2018.
- [507] D. B. Savage *et al.*, "Reversal of diet-induced hepatic steatosis and hepatic insulin resistance by antisense oligonucleotide inhibitors of acetyl-CoA carboxylases 1 and 2," *Journal of Clinical Investigation*, vol. 116, no. 3, pp. 817–824, Mar. 2006.
- [508] S. Passi, M. Picardo, M. Nazzaro-Porro, A. Breathnach, A. M. Confaloni, and G. Serlupi-Crescenzi, "Antimitochondrial effect of saturated medium chain length (C8-C13) dicarboxylic acids," *Biochemical Pharmacology*, vol. 33, no. 1, pp. 103–108, Jan. 1984.
- [509] J. H. Tonsgard and G. S. Getz, "Effect of Reye's syndrome serum on isolated chinchilla liver mitochondria," *Journal of Clinical Investigation*, vol. 76, no. 2, pp. 816–825, 1985.
- [510] J.-Y. Cha, D.-H. Kim, and K.-H. Chun, "The role of hepatic macrophages in nonalcoholic fatty liver disease and nonalcoholic steatohepatitis," *Laboratory Animal Research*, vol. 34, no. 4, p. 133, 2018.
- [511] I. Mederacke *et al.*, "Fate tracing reveals hepatic stellate cells as dominant contributors to liver fibrosis independent of its aetiology," *Nature Communications*, vol. 4, no. 1, pp. 1–11, Nov. 2013.
- [512] A. B. Marcher *et al.*, "Transcriptional regulation of Hepatic Stellate Cell activation in NASH," *Scientific Reports*, vol. 9, no. 1, Dec. 2019.
- [513] S. Kaur *et al.*, "Increased Expression of RUNX1 in Liver Correlates with NASH Activity Score in Patients with Non-Alcoholic Steatohepatitis (NASH)," *Cells*, vol. 8, no. 10, Oct. 2019.

- [514] L. Bouwens, M. Baekeland, R. de Zanger, and E. Wisse, "Quantitation, tissue distribution and proliferation kinetics of kupffer cells in normal rat liver," *Hepatology*, vol. 6, no. 4, pp. 718–722, 1986.
- [515] Z. Kmiec, "Cooperation of liver cells in health and disease.," *Advances in anatomy, embryology, and cell biology*, vol. 161. 2001.
- [516] O. Krenkel and F. Tacke, "Liver macrophages in tissue homeostasis and disease," *Nature Reviews Immunology*, vol. 17, no. 5. Nature Publishing Group, pp. 306–321, 01-May-2017.
- [517] K. Popko *et al.*, "Proinflammatory cytokines IL-6 and TNF- $\alpha$  and the development of inflammation in obese subjects," *European Journal of Medical Research*, vol. 15, no. 2, pp. 120–122, Nov. 2010.
- [518] A. S. B. Jorge *et al.*, "Body mass index and the visceral adipose tissue expression of IL-6 and TNF-alpha are associated with the morphological severity of non-alcoholic fatty liver disease in individuals with class III obesity," *Obesity Research and Clinical Practice*, vol. 12, no. 1, pp. 1–8, Jan. 2018.
- [519] J. Crespo *et al.*, "Gene expression of tumor necrosis factor  $\alpha$  and TNF-receptors, p55 and p75, in nonalcoholic steatohepatitis patients," *Hepatology*, vol. 34, no. 6, pp. 1158–1163, 2001.
- [520] A. Hadinia, A. H. Doustimotlagh, H. R. Goodarzi, A. Arya, and M. Jafarina, "Circulating levels of pro-inflammatory cytokines in patients with nonalcoholic fatty liver disease and non-alcoholic steatohepatitis," *Iranian Journal of Immunology*, vol. 16, no. 4, pp. 327–333, Sep. 2019.
- [521] A. Bertola *et al.*, "Hepatic Expression Patterns of Inflammatory and Immune Response Genes Associated with Obesity and NASH in Morbidly Obese Patients," *PLoS ONE*, vol. 5, no. 10, p. e13577, Oct. 2010.
- [522] A. S. Henkel, "Unfolded Protein Response Sensors in Hepatic Lipid Metabolism and Nonalcoholic Fatty Liver Disease," *Seminars in Liver Disease*, vol. 38, no. 4, pp. 320–332, Nov. 2018.
- [523] M. D. Mantzaris, E. V. Tsianos, and D. Galaris, "Interruption of triacylglycerol synthesis in the endoplasmic reticulum is the initiating event for saturated fatty acid-induced lipotoxicity in liver cells," *FEBS Journal*, vol. 278, no. 3, pp. 519–530, Feb. 2011.
- [524] J. A. Willy, S. K. Young, J. L. Stevens, H. C. Masuoka, and R. C. Wek, "CHOP links endoplasmic reticulum stress to NF- $\kappa$ B activation in the pathogenesis of nonalcoholic steatohepatitis," *Molecular Biology of the Cell*, vol. 26, no. 12, pp. 2190–2204, Jun. 2015.
- [525] J. M. Wang *et al.*, "IRE1 prevents hepatic steatosis by processing and promoting the degradation of select microRNAs," *Science Signaling*, vol. 11, no. 530, May 2018.
- [526] P. Puri *et al.*, "Activation and Dysregulation of the Unfolded Protein Response in Nonalcoholic Fatty Liver Disease," *Gastroenterology*, vol. 134, no. 2, pp. 568–576, 2008.
- [527] R. E. Kaplon, E. Chung, L. Reese, K. Cox-York, D. R. Seals, and C. L. Gentile, "Activation of the unfolded protein response in vascular endothelial cells of Nondiabetic obese adults," *Journal of Clinical Endocrinology and Metabolism*, vol. 98, no. 9, p. E1505, Sep. 2013.

- [528] Z. Zhang *et al.*, "The unfolded protein response regulates hepatic autophagy by sXBP1-mediated activation of TFEB," *Autophagy*, pp. 1–15, 2020.
- [529] S. Sutti *et al.*, "Adaptive immune responses triggered by oxidative stress contribute to hepatic inflammation in NASH," *Hepatology*, vol. 59, no. 3, pp. 886–897, Mar. 2014.
- [530] C. P. M. S. Oliveira *et al.*, "Lipid peroxidation in bariatric candidates with nonalcoholic fatty liver disease (NAFLD) - Preliminary findings," *Obesity Surgery*, vol. 15, no. 4, pp. 502–505, Apr. 2005.
- [531] S. Zelber-Sagi *et al.*, "Serum malondialdehyde is associated with non-alcoholic fatty liver and related liver damage differentially in men and women," *Antioxidants*, vol. 9, no. 7, pp. 1–15, Jul. 2020.
- [532] C. T. Shearn, L. M. Saba, J. R. Roede, D. J. Orlicky, A. H. Shearn, and D. R. Petersen, "Differential carbonylation of proteins in end-stage human fatty and nonfatty NASH," *Free Radical Biology and Medicine*, vol. 113, pp. 280–290, Dec. 2017.
- [533] I. H. Bahcecioglu *et al.*, "Levels of serum hyaluronic acid, TNF- $\alpha$  and IL-8 in patients with nonalcoholic steatohepatitis," *Hepato-Gastroenterology*, vol. 52, no. 65, pp. 1549–1553, Sep. 2005.
- [534] L. Gu *et al.*, "Spexin alleviates insulin resistance and inhibits hepatic gluconeogenesis via the foxo1/pgc-1 $\alpha$  pathway in high-fat-diet-induced rats and insulin resistant cells," *International Journal of Biological Sciences*, vol. 15, no. 13, pp. 2815–2829, 2019.
- [535] S. AJ *et al.*, "Nonalcoholic steatohepatitis: association of insulin resistance and mitochondrial abnormalities," *Gastroenterology*, vol. 120, no. 5, 2001.
- [536] S. Sookoian *et al.*, "Mitochondrial genome architecture in non-alcoholic fatty liver disease," *Journal of Pathology*, vol. 240, no. 4, pp. 437–449, Dec. 2016.
- [537] M. Pérez-Carreras *et al.*, "Defective hepatic mitochondrial respiratory chain in patients with nonalcoholic steatohepatitis," *Hepatology*, vol. 38, no. 4, pp. 999–1007, Oct. 2003.
- [538] Y. You *et al.*, "Protein profiling and functional analysis of liver mitochondria from rats with nonalcoholic steatohepatitis," *Molecular Medicine Reports*, vol. 16, no. 3, pp. 2379–2388, Sep. 2017.
- [539] S. Sookoian *et al.*, "Epigenetic regulation of insulin resistance in nonalcoholic fatty liver disease: Impact of liver methylation of the peroxisome proliferator-activated receptor  $\gamma$  coactivator 1 $\alpha$  promoter," *Hepatology*, vol. 52, no. 6, pp. 1992–2000, Dec. 2010.
- [540] C. J. Pirola *et al.*, "Epigenetic modifications in the biology of nonalcoholic fatty liver disease: The role of DNA hydroxymethylation and TET proteins," *Medicine (United States)*, vol. 94, no. 36, Sep. 2015.
- [541] S. Kamfar *et al.*, "Liver mitochondrial DNA copy number and deletion levels may contribute to nonalcoholic fatty liver disease susceptibility," *Hepatitis Monthly*, vol. 16, no. 12, p. 40774, Dec. 2016.
- [542] Y. L. Fang, H. Chen, C. L. Wang, and L. Liang, "Pathogenesis of non-alcoholic fatty liver disease in children and adolescence: From 'two hit theory' to 'multiple hit model,'" *World Journal of Gastroenterology*, vol. 24, no. 27. Baishideng Publishing Group Co., Limited, pp. 2974–2983, 21-Jul-

2018.

- [543] H. Tilg and A. R. Moschen, "Evolution of inflammation in nonalcoholic fatty liver disease: The multiple parallel hits hypothesis," *Hepatology*, vol. 52, no. 5, pp. 1836–1846, Nov. 2010.
- [544] T. D. Luckey, "Introduction to intestinal microecology.," *The American journal of clinical nutrition*, vol. 25, no. 12, pp. 1292–1294, 1972.
- [545] R. Sender, S. Fuchs, and R. Milo, "Revised estimates for the number of human and bacteria cells in the body," *bioRxiv*, p. 036103, Jan. 2016.
- [546] J. Qin *et al.*, "A human gut microbial gene catalogue established by metagenomic sequencing," *Nature*, vol. 464, no. 7285, pp. 59–65, 2010.
- [547] B. T. Tierney *et al.*, "The Landscape of Genetic Content in the Gut and Oral Human Microbiome," *Cell Host and Microbe*, vol. 26, no. 2, pp. 283–295.e8, Aug. 2019.
- [548] W. Scheppach, "Effects of short chain fatty acids on gut morphology and function," *Gut*, vol. 35, no. 1 SUPPL., 1994.
- [549] T. M. S. Wolever, P. Spadafora, and H. Eshuis, "Interaction between colonic acetate and propionate in humans," *American Journal of Clinical Nutrition*, vol. 53, no. 3, pp. 681–687, 1991.
- [550] Z. Chen *et al.*, "Diversity of macaque microbiota compared to the human counterparts OPEN."
- [551] C. Gérard and H. Vidal, "Impact of gut microbiota on host glycemic control," *Frontiers in Endocrinology*, vol. 10, no. JAN. Frontiers Media S.A., p. 29, 2019.
- [552] B. Tennant, O. J. Malm, R. E. Horowitz, and S. M. Levenson, "Response of germfree, conventional, conventionalized and E. coli monocontaminated mice to starvation.," *The Journal of nutrition*, vol. 94, no. 2, pp. 151–160, 1968.
- [553] N. Hasan and H. Yang, "Factors affecting the composition of the gut microbiota, and its modulation," *PeerJ*, vol. 2019, no. 8. PeerJ Inc., 2019.
- [554] P. J. Turnbaugh, R. E. Ley, M. A. Mahowald, V. Magrini, E. R. Mardis, and J. I. Gordon, "An obesity-associated gut microbiome with increased capacity for energy harvest," *Nature*, vol. 444, no. 7122, pp. 1027–1031, Dec. 2006.
- [555] L. A. Ding, J. S. Li, Y. S. Li, N. T. Zhu, F. N. Liu, and L. Tan, "Intestinal barrier damage caused by trauma and lipopolysaccharide," *World Journal of Gastroenterology*, vol. 10, no. 16, pp. 2373–2378, Aug. 2004.
- [556] G. B. Saffouri *et al.*, "Small intestinal microbial dysbiosis underlies symptoms associated with functional gastrointestinal disorders," *Nature Communications*, vol. 10, no. 1, Dec. 2019.
- [557] K. Brandl and B. Schnabl, "Intestinal microbiota and nonalcoholic steatohepatitis," *Current Opinion in Gastroenterology*, vol. 33, no. 3. Lippincott Williams and Wilkins, pp. 128–133, 01-May-2017.
- [558] R. K. Ernst and C. E. Chandler, "Bacterial lipids: Powerful modifiers of the innate immune response," *F1000Research*, vol. 6. Faculty of 1000 Ltd, p. 1334, 2017.

- [559] L. S. Hou *et al.*, "Rutin mitigates hepatic fibrogenesis and inflammation through targeting TLR4 and P2X7 receptor signaling pathway in vitro and in vivo," *Journal of Functional Foods*, vol. 64, p. 103700, Jan. 2020.
- [560] C. Engelmann *et al.*, "Toll-like receptor 4 is a therapeutic target for prevention and treatment of liver failure," *Journal of Hepatology*, vol. 73, no. 1, pp. 102–112, Jul. 2020.
- [561] L. Miele *et al.*, "Increased intestinal permeability and tight junction alterations in nonalcoholic fatty liver disease," *Hepatology*, vol. 49, no. 6, pp. 1877–1887, Jun. 2009.
- [562] R. E. Ley, F. Bäckhed, P. Turnbaugh, C. A. Lozupone, R. D. Knight, and J. I. Gordon, "Obesity alters gut microbial ecology," *Proceedings of the National Academy of Sciences of the United States of America*, vol. 102, no. 31, pp. 11070–11075, Aug. 2005.
- [563] R. E. Ley, P. J. Turnbaugh, S. Klein, and J. I. Gordon, "Microbial ecology: Human gut microbes associated with obesity," *Nature*, vol. 444, no. 7122, pp. 1022–1023, Dec. 2006.
- [564] R. Loomba *et al.*, "Gut Microbiome-Based Metagenomic Signature for Non-invasive Detection of Advanced Fibrosis in Human Nonalcoholic Fatty Liver Disease," *Cell Metabolism*, vol. 25, no. 5, pp. 1054-1062.e5, May 2017.
- [565] L. Zhu *et al.*, "Characterization of gut microbiomes in nonalcoholic steatohepatitis (NASH) patients: A connection between endogenous alcohol and NASH," *Hepatology*, vol. 57, no. 2, pp. 601–609, Feb. 2013.
- [566] J. Boursier *et al.*, "The severity of nonalcoholic fatty liver disease is associated with gut dysbiosis and shift in the metabolic function of the gut microbiota," *Hepatology*, vol. 63, no. 3, pp. 764–775, Mar. 2016.
- [567] A. Guerra Ruiz *et al.*, "Lipopolysaccharide-binding protein plasma levels and liver TNF-alpha gene expression in obese patients: Evidence for the potential role of endotoxin in the pathogenesis of non-alcoholic steatohepatitis," *Obesity Surgery*, vol. 17, no. 10, pp. 1374–1380, Oct. 2007.
- [568] A. Schwartz *et al.*, "Microbiota and SCFA in lean and overweight healthy subjects," *Obesity*, vol. 18, no. 1, pp. 190–195, Jan. 2010.
- [569] H. E. Da Silva *et al.*, "Nonalcoholic fatty liver disease is associated with dysbiosis independent of body mass index and insulin resistance," *Scientific Reports*, vol. 8, no. 1, Dec. 2018.
- [570] J. Yuan *et al.*, "Fatty Liver Disease Caused by High-Alcohol-Producing *Klebsiella pneumoniae*," *Cell Metabolism*, vol. 30, no. 4, pp. 675-688.e7, Oct. 2019.
- [571] J. B. Furness, "The enteric nervous system and neurogastroenterology," *Nature Reviews Gastroenterology and Hepatology*, vol. 9, no. 5. Nature Publishing Group, pp. 286–294, 06-May-2012.
- [572] J. H. Ding *et al.*, "Role of gut microbiota via the gut-liver-brain axis in digestive diseases," *World Journal of Gastroenterology*, vol. 26, no. 40, pp. 6141–6162, Oct. 2020.



- [573] J. S. Labus *et al.*, "Differences in gut microbial composition correlate with regional brain volumes in irritable bowel syndrome," *Microbiome*, vol. 5, no. 1, pp. 1–17, May 2017.
- [574] S. Prill *et al.*, "The TM6SF2 E167K genetic variant induces lipid biosynthesis and reduces apolipoprotein B secretion in human hepatic 3D spheroids," *Scientific Reports*, vol. 9, no. 1, p. 11585, Dec. 2019.
- [575] P. K. Luukkonen *et al.*, "The MBOAT7 variant rs641738 alters hepatic phosphatidylinositols and increases severity of non-alcoholic fatty liver disease in humans," *Journal of Hepatology*, vol. 65, no. 6. Elsevier B.V., pp. 1263–1265, 01-Dec-2016.
- [576] L. Valenti, A. Alisi, and V. Nobili, "Unraveling the genetics of fatty liver in obese children: Additive effect of P446L GCKR and I148M PNPLA3 polymorphisms," *Hepatology*, vol. 55, no. 3, pp. 661–663, Mar. 2012.
- [577] S. L. Friedman, B. A. Neuschwander-Tetri, M. Rinella, and A. J. Sanyal, "Mechanisms of NAFLD development and therapeutic strategies," *Nature Medicine*, vol. 24, no. 7. Nature Publishing Group, pp. 908–922, 01-Jul-2018.
- [578] S. Zelber-Sagi *et al.*, "Role of leisure-time physical activity in nonalcoholic fatty liver disease: A population-based study," *Hepatology*, vol. 48, no. 6, pp. 1791–1798, 2008.
- [579] Y. F. Li *et al.*, "Dose-response association between physical activity and non-alcoholic fatty liver disease: A case-control study in a Chinese population," *BMJ Open*, vol. 9, no. 3, Mar. 2019.
- [580] I. J. Hickman *et al.*, "Modest weight loss and physical activity in overweight patients with chronic liver disease results in sustained improvements in alanine aminotransferase, fasting insulin, and quality of life," *Gut*, vol. 53, no. 3, pp. 413–419, Mar. 2004.
- [581] S. R. Bird and J. A. Hawley, "Update on the effects of physical activity on insulin sensitivity in humans," *BMJ Open Sport and Exercise Medicine*, vol. 2, no. 1. BMJ Publishing Group, p. 143, 01-Mar-2017.
- [582] C. N. Katsagoni, M. Georgoulis, G. V. Papatheodoridis, D. B. Panagiotakos, and M. D. Kontogianni, "Effects of lifestyle interventions on clinical characteristics of patients with non-alcoholic fatty liver disease: A meta-analysis," *Metabolism: Clinical and Experimental*, vol. 68, pp. 119–132, Mar. 2017.
- [583] A. Suzuki *et al.*, "Effect of changes on body weight and lifestyle in nonalcoholic fatty liver disease," *Journal of Hepatology*, vol. 43, no. 6, pp. 1060–1066, Dec. 2005.
- [584] D. A. Koutoukidis *et al.*, "Association of Weight Loss Interventions with Changes in Biomarkers of Nonalcoholic Fatty Liver Disease: A Systematic Review and Meta-analysis," *JAMA Internal Medicine*, vol. 179, no. 9, pp. 1262–1271, Sep. 2019.
- [585] E. Vilar-Gomez *et al.*, "Weight loss through lifestyle modification significantly reduces features of nonalcoholic steatohepatitis," *Gastroenterology*, vol. 149, no. 2, pp. 367-378.e5, Aug. 2015.
- [586] C. Anania, F. Massimo Perla, F. Olivero, L. Pacifico, and C. Chiesa, "Mediterranean diet and nonalcoholic fatty liver disease," *World Journal of Gastroenterology*, vol. 24, no. 19. Baishideng Publishing Group Co.,

Limited, pp. 2083–2094, 21-May-2018.

- [587] M. C. Ryan *et al.*, “The Mediterranean diet improves hepatic steatosis and insulin sensitivity in individuals with non-alcoholic fatty liver disease,” *Journal of Hepatology*, vol. 59, no. 1, pp. 138–143, Jul. 2013.
- [588] F. Baratta *et al.*, “Adherence to Mediterranean Diet and Non-Alcoholic Fatty Liver Disease: Effect on Insulin Resistance,” *American Journal of Gastroenterology*, vol. 112, no. 12, pp. 1832–1839, Dec. 2017.
- [589] C. Gelli, M. Tarocchi, L. Abenavoli, L. Di Renzo, A. Galli, and A. De Lorenzo, “Effect of a counseling-supported treatment with the Mediterranean diet and physical activity on the severity of the non-alcoholic fatty liver disease,” *World Journal of Gastroenterology*, vol. 23, no. 17, pp. 3150–3162, May 2017.
- [590] M. Stumvoll, N. Nurjhan, G. Perriello, G. Dailey, and J. E. Gerich, “Metabolic Effects of Metformin in Non-Insulin-Dependent Diabetes Mellitus,” *New England Journal of Medicine*, vol. 333, no. 9, pp. 550–554, Aug. 1995.
- [591] H. Z. Lin, S. Q. Yang, C. Chuckaree, F. Kuhajda, G. Ronnet, and A. M. Diehl, “Metformin reverses fatty liver disease in obese, leptin-deficient mice,” *Nature Medicine*, vol. 6, no. 9, pp. 998–1003, Sep. 2000.
- [592] G. Marchesini, M. Brizi, G. Bianchi, S. Tomassetti, M. Zoli, and N. Melchionda, “Metformin in non-alcoholic steatohepatitis,” *Lancet*, vol. 358, no. 9285, pp. 893–894, Sep. 2001.
- [593] W. Feng *et al.*, “Randomized trial comparing the effects of gliclazide, liraglutide, and metformin on diabetes with non-alcoholic fatty liver disease,” *Journal of Diabetes*, vol. 9, no. 8, pp. 800–809, Aug. 2017.
- [594] W. Feng *et al.*, “Effects of liraglutide, metformin and gliclazide on body composition in patients with both type 2 diabetes and non-alcoholic fatty liver disease: A randomized trial,” *Journal of Diabetes Investigation*, vol. 10, no. 2, pp. 399–407, Mar. 2019.
- [595] M. R. Owen, E. Doran, and A. P. Halestrap, “Evidence that metformin exerts its anti-diabetic effects through inhibition of complex 1 of the mitochondrial respiratory chain,” *Biochemical Journal*, vol. 348, no. 3, pp. 607–614, Jun. 2000.
- [596] R. J. Ford *et al.*, “Metformin and salicylate synergistically activate liver AMPK, inhibit lipogenesis and improve insulin sensitivity,” *Biochemical Journal*, vol. 468, no. 1, pp. 125–132, May 2015.
- [597] Y. Wang *et al.*, “Metformin Improves Mitochondrial Respiratory Activity through Activation of AMPK,” *Cell Reports*, vol. 29, no. 6, pp. 1511–1523.e5, Nov. 2019.
- [598] T. Luo *et al.*, “AMPK activation by metformin suppresses abnormal extracellular matrix remodeling in adipose tissue and ameliorates insulin resistance in obesity,” *Diabetes*, vol. 65, no. 8, pp. 2295–2310, Aug. 2016.
- [599] C. J. Cone, A. M. Bachyrycz, and G. H. Murata, “Hepatotoxicity associated with metformin therapy in

- treatment of type 2 diabetes mellitus with nonalcoholic fatty liver disease," *Annals of Pharmacotherapy*, vol. 44, no. 10, pp. 1655–1659, Oct. 2010.
- [600] L. He, X. Liu, L. Wang, and Z. Yang, "Thiazolidinediones for nonalcoholic steatohepatitis: A meta-analysis of randomized clinical trials," *Medicine (United States)*, vol. 95, no. 42, 2016.
- [601] B. A. Neuschwander-Tetri, E. M. Brunt, K. R. Wehmeier, D. Oliver, and B. R. Bacon, "Improved nonalcoholic steatohepatitis after 48 weeks of treatment with the PPAR- $\gamma$  ligand rosiglitazone," *Hepatology*, vol. 38, no. 4, pp. 1008–1017, Oct. 2003.
- [602] G. Musso, M. Cassader, E. Paschetta, and R. Gambino, "Thiazolidinediones and advanced liver fibrosis in nonalcoholic steatohepatitis: A meta-analysis," *JAMA Internal Medicine*, vol. 177, no. 5, pp. 633–640, May 2017.
- [603] H. M. Al-Muzafar and K. A. Amin, "Thiazolidinedione induces a therapeutic effect on hepatosteatosis by regulating stearyl-CoA desaturase-1, lipase activity, leptin and resistin," *Experimental and Therapeutic Medicine*, vol. 16, no. 4, pp. 2938–2948, Oct. 2018.
- [604] J. Li and X. Shen, "Effect of rosiglitazone on inflammatory cytokines and oxidative stress after intensive insulin therapy in patients with newly diagnosed type 2 diabetes," *Diabetology and Metabolic Syndrome*, vol. 11, no. 1, p. 35, May 2019.
- [605] Z. Ackerman *et al.*, "Hepatic effects of rosiglitazone in rats with the metabolic syndrome," *Basic and Clinical Pharmacology and Toxicology*, vol. 107, no. 2, pp. 663–668, 2010.
- [606] J. Bętkowski, J. Rachańczyk, and M. Włodarczyk, "Thiazolidinedione-induced fluid retention: Recent insights into the molecular mechanisms," *PPAR Research*, vol. 2013, 2013.
- [607] P. M. Seferović *et al.*, "Type 2 diabetes mellitus and heart failure: a position statement from the Heart Failure Association of the European Society of Cardiology," *European Journal of Heart Failure*, vol. 20, no. 5, pp. 853–872, May 2018.
- [608] D. Bilik *et al.*, "Thiazolidinediones and fractures: Evidence from translating research into action for diabetes," *Journal of Clinical Endocrinology and Metabolism*, vol. 95, no. 10, pp. 4560–4565, 2010.
- [609] E. O. Billington, A. Grey, and M. J. Bolland, "The effect of thiazolidinediones on bone mineral density and bone turnover: systematic review and meta-analysis," *Diabetologia*, vol. 58, no. 10, pp. 2238–2246, Oct. 2015.
- [610] A. Neumann, A. Weill, P. Ricordeau, J. P. Fagot, F. Alla, and H. Allemand, "Pioglitazone and risk of bladder cancer among diabetic patients in France: A population-based cohort study," *Diabetologia*, vol. 55, no. 7, pp. 1953–1962, Jul. 2012.
- [611] H. E. Lebovitz, "Thiazolidinediones: the Forgotten Diabetes Medications," *Current Diabetes Reports*, vol. 19, no. 12. Springer, pp. 1–13, 01-Dec-2019.
- [612] M. B. Davidson, "Pioglitazone (Actos) and bladder cancer: Legal system triumphs over the evidence,"

- Journal of Diabetes and its Complications*, vol. 30, no. 6. Elsevier Inc., pp. 981–985, 01-Aug-2016.
- [613] E. Filipova, K. Uzunova, K. Kalinov, and T. Vekov, "Pioglitazone and the Risk of Bladder Cancer: A Meta-Analysis," *Diabetes Therapy*, vol. 8, no. 4, pp. 705–726, Aug. 2017.
- [614] H. El Hadi, R. Vettor, and M. Rossato, "Vitamin E as a treatment for nonalcoholic fatty liver disease: Reality or myth?," *Antioxidants*, vol. 7, no. 1. MDPI AG, 01-Mar-2018.
- [615] A. Erhardt, W. Stahl, H. Sies, F. Lirussi, A. Donner, and D. Häussinger, "Plasma levels of vitamin E and carotenoids are decreased in patients with nonalcoholic steatohepatitis (NASH)," *European Journal of Medical Research*, vol. 16, no. 2, pp. 76–78, Feb. 2011.
- [616] S. A. Harrison, S. Torgerson, P. Hayashi, J. Ward, and S. Schenker, "Vitamin E and Vitamin C Treatment Improves Fibrosis in Patients with Nonalcoholic Steatohepatitis," *American Journal of Gastroenterology*, vol. 98, no. 11, pp. 2485–2490, 2003.
- [617] F. Yakaryilmaz *et al.*, "Effects of vitamin e treatment on peroxisome proliferator-activated receptor- $\alpha$  expression and insulin resistance in patients with non-alcoholic steatohepatitis: Results of a pilot study," *Internal Medicine Journal*, vol. 37, no. 4, pp. 229–235, Apr. 2007.
- [618] H. F. Ji, Y. Sun, and L. Shen, "Effect of vitamin E supplementation on aminotransferase levels in patients with NAFLD, NASH, and CHC: Results from a meta-analysis," *Nutrition*, vol. 30, no. 9, pp. 986–991, 2014.
- [619] M. C. Podszun, J. Y. Chung, K. Ylaya, D. E. Kleiner, S. M. Hewitt, and Y. Rotman, "4-HNE Immunohistochemistry and Image Analysis for Detection of Lipid Peroxidation in Human Liver Samples Using Vitamin E Treatment in NAFLD as a Proof of Concept," *Journal of Histochemistry and Cytochemistry*, vol. 68, no. 9, pp. 635–643, Sep. 2020.
- [620] G. Karimian, M. Kirschbaum, Z. J. Veldhuis, F. Bomfati, R. J. Porte, and T. Lisman, "Vitamin E attenuates the progression of non-alcoholic fatty liver disease caused by partial hepatectomy in mice," *PLoS ONE*, vol. 10, no. 11, Nov. 2015.
- [621] E. R. Miller, R. Pastor-Barriuso, D. Dalal, R. A. Riemersma, L. J. Appel, and E. Guallar, "Meta-analysis: High-dosage vitamin E supplementation may increase all-cause mortality," *Annals of Internal Medicine*, vol. 142, no. 1. American College of Physicians, 04-Jan-2005.
- [622] M. Schürks, R. J. Glynn, P. M. Rist, C. Tzourio, and T. Kurth, "Effects of vitamin E on stroke subtypes: Meta-analysis of randomised controlled trials," *BMJ (Online)*, vol. 341, no. 7781, p. 1033, Nov. 2010.
- [623] D. Mantle and I. P. Hargreaves, "Coenzyme Q10 supplementation in non-alcoholic fatty liver disease: An overview," *Gastrointestinal Nursing*, vol. 18, no. 2. MA Healthcare Ltd, pp. 22–27, 02-Mar-2020.
- [624] P. Orlando *et al.*, "Aspalathin-rich green rooibos extract lowers LDL-cholesterol and oxidative status in high-fat diet-induced diabetic vervet monkeys," *Molecules*, vol. 24, no. 9, p. 1713, 2019.
- [625] G. P. Littarru and L. Tiano, "Bioenergetic and antioxidant properties of coenzyme Q10: Recent developments," in *Molecular Biotechnology*, 2007, vol. 37, no. 1, pp. 31–37.

- [626] N. B. Nesami, H. Mozaffari-Khosravi, A. Najarzadeh, and E. Salehifar, "The effect of coenzyme Q10 supplementation on pro-inflammatory factors and adiponectin in mildly hypertensive patients: A randomized, double-blind, placebo-controlled trial," *International Journal for Vitamin and Nutrition Research*, vol. 85, no. 3–4, pp. 156–164, 2015.
- [627] M. A. Farhangi, B. Alipour, E. Jafarvand, and M. Khoshbaten, "Oral Coenzyme Q10 Supplementation in Patients with Nonalcoholic Fatty Liver Disease: Effects on Serum Vaspin, Chemerin, Pentraxin 3, Insulin Resistance and Oxidative Stress," *Archives of Medical Research*, vol. 45, no. 7, pp. 589–595, Oct. 2014.
- [628] F. Farsi, M. Mohammadshahi, P. Alavinejad, A. Rezazadeh, M. Zarei, and K. A. Engali, "Functions of Coenzyme Q10 Supplementation on Liver Enzymes, Markers of Systemic Inflammation, and Adipokines in Patients Affected by Nonalcoholic Fatty Liver Disease: A Double-Blind, Placebo-Controlled, Randomized Clinical Trial," *Journal of the American College of Nutrition*, vol. 35, no. 4, pp. 346–353, May 2016.
- [629] K. Chen *et al.*, "Coenzyme Q10 attenuates high-fat diet-induced non-alcoholic fatty liver disease through activation of the AMPK pathway," *Food and Function*, vol. 10, no. 2, pp. 814–823, Feb. 2019.
- [630] D. O. Saleh, R. F. Ahmed, and M. M. Amin, "Modulatory role of co-enzyme Q10 on methionine and choline deficient diet-induced non-alcoholic steatohepatitis (NASH) in albino rats," *Applied Physiology, Nutrition and Metabolism*, vol. 42, no. 3, pp. 243–249, 2017.
- [631] S. A. S. Craig, "Betaine in human nutrition," *American Journal of Clinical Nutrition*, vol. 80, no. 3. American Society for Nutrition, pp. 539–549, 2004.
- [632] Z. Song *et al.*, "Involvement of AMP-activated protein kinase in beneficial effects of betaine on high-sucrose diet-induced hepatic steatosis," *American Journal of Physiology - Gastrointestinal and Liver Physiology*, vol. 293, no. 4, p. G894, Oct. 2007.
- [633] Z. Wang, T. Yao, M. Pini, Z. Zhou, G. Fantuzzi, and Z. Song, "Betaine improved adipose tissue function in mice fed a high-fat diet: A mechanism for hepatoprotective effect of betaine in nonalcoholic fatty liver disease," *American Journal of Physiology - Gastrointestinal and Liver Physiology*, vol. 298, no. 5, p. G634, May 2010.
- [634] E. Kathirvel *et al.*, "Betaine improves nonalcoholic fatty liver and associated hepatic insulin resistance: A potential mechanism for hepatoprotection by betaine," *American Journal of Physiology - Gastrointestinal and Liver Physiology*, vol. 299, no. 5, p. G1068, Nov. 2010.
- [635] F. Miglio, L. C. Rovati, A. Santoro, and I. Setnikar, "Efficacy and safety of oral betaine glucuronate in non-alcoholic steatohepatitis: A double-blind, randomized, parallel-group, placebo-controlled prospective clinical study," *Arzneimittel-Forschung/Drug Research*, vol. 50, no. 8, pp. 722–727, 2000.
- [636] M. F. Abdelmalek, P. Angulo, R. A. Jorgensen, P. B. Sylvestre, and K. D. Lindor, "Betaine, a promising new agent for patients with nonalcoholic steatohepatitis: results of a pilot study," *The American Journal of Gastroenterology*, vol. 96, no. 9, pp. 2711–2717, Sep. 2001.

- [637] S. Sookoian *et al.*, "Nonalcoholic steatohepatitis is associated with a state of betaine-insufficiency," *Liver International*, vol. 37, no. 4, pp. 611–619, Apr. 2017.
- [638] K. Kargiotis *et al.*, "Resolution of non-alcoholic steatohepatitis by rosuvastatin monotherapy in patients with metabolic syndrome," *World Journal of Gastroenterology*, vol. 21, no. 25, pp. 7860–7868, Jul. 2015.
- [639] R. Cioboată *et al.*, "Pharmacological management of non-alcoholic fatty liver disease: Atorvastatin versus pentoxifylline," *Experimental and Therapeutic Medicine*, vol. 13, no. 5, pp. 2375–2381, May 2017.
- [640] H. S. Park *et al.*, "Statins increase mitochondrial and peroxisomal fatty acid oxidation in the liver and prevent non-alcoholic steatohepatitis in mice," *Diabetes and Metabolism Journal*, vol. 40, no. 5, pp. 376–385, 2016.
- [641] P. Blais, M. Lin, J. R. Kramer, H. B. El-Serag, and F. Kanwal, "Statins Are Underutilized in Patients with Nonalcoholic Fatty Liver Disease and Dyslipidemia," *Digestive Diseases and Sciences*, vol. 61, no. 6, pp. 1714–1720, Jun. 2016.
- [642] E. Björnsson, E. I. Jacobsen, and E. Kalaitzakis, "Hepatotoxicity associated with statins: Reports of idiosyncratic liver injury post-marketing," *Journal of Hepatology*, vol. 56, no. 2, pp. 374–380, Feb. 2012.
- [643] S. Vieira-Silva *et al.*, "Statin therapy is associated with lower prevalence of gut microbiota dysbiosis," *Nature*, vol. 581, no. 7808, pp. 310–315, May 2020.
- [644] S. Tavintharan, C. N. Ong, K. Jeyaseelan, M. Sivakumar, S. C. Lim, and C. F. Sum, "Reduced mitochondrial coenzyme Q10 levels in HepG2 cells treated with high-dose simvastatin: A possible role in statin-induced hepatotoxicity?," *Toxicology and Applied Pharmacology*, vol. 223, no. 2, pp. 173–179, Sep. 2007.
- [645] S. Pierno *et al.*, "Statins and fenofibrate affect skeletal muscle chloride conductance in rats by differently impairing ClC-1 channel regulation and expression," *British Journal of Pharmacology*, vol. 156, no. 8, pp. 1206–1215, Apr. 2009.
- [646] T. Hattori *et al.*, "Statin-induced Ca(2+) release was increased in B lymphocytes in patients who showed elevated serum creatine kinase during statin treatment.," *Journal of atherosclerosis and thrombosis*, vol. 16, no. 6, pp. 870–877, 2009.
- [647] A. Selva-O'Callaghan *et al.*, "Statin-induced myalgia and myositis: an update on pathogenesis and clinical recommendations," *Expert Review of Clinical Immunology*, vol. 14, no. 3. Taylor and Francis Ltd, pp. 215–224, 04-Mar-2018.
- [648] B. M. Wolfe, E. Kvach, and R. H. Eckel, "Treatment of obesity," *Circulation Research*, vol. 118, no. 11. Lippincott Williams and Wilkins, pp. 1844–1855, 27-May-2016.
- [649] "Gastrointestinal surgery for severe obesity: National Institutes of Health Consensus Development Conference Statement," in *Consensus statement*, 1991, vol. 9, no. 1, pp. 1–20.

- [650] G. Lassailly *et al.*, "Bariatric surgery reduces features of nonalcoholic steatohepatitis in morbidly obese patients," *Gastroenterology*, vol. 149, no. 2, pp. 379–388, Aug. 2015.
- [651] A. Algooneh, S. Almazeedi, S. Al-Sabah, M. Ahmed, and F. Othman, "Non-alcoholic fatty liver disease resolution following sleeve gastrectomy," *Surgical Endoscopy*, vol. 30, no. 5, pp. 1983–1987, May 2016.
- [652] D. Froylich, R. Corcelles, C. Daigle, M. Boules, S. Brethauer, and P. Schauer, "Effect of Roux-en-Y gastric bypass and sleeve gastrectomy on nonalcoholic fatty liver disease: A comparative study," in *Surgery for Obesity and Related Diseases*, 2016, vol. 12, no. 1, pp. 127–131.
- [653] F. Nickel *et al.*, "Bariatric Surgery as an Efficient Treatment for Non-Alcoholic Fatty Liver Disease in a Prospective Study with 1-Year Follow-up: BariScan Study," *Obesity Surgery*, vol. 28, no. 5, pp. 1342–1350, May 2018.
- [654] Y. Lee *et al.*, "Complete Resolution of Nonalcoholic Fatty Liver Disease After Bariatric Surgery: A Systematic Review and Meta-analysis," *Clinical Gastroenterology and Hepatology*, vol. 17, no. 6, pp. 1040-1060.e11, May 2019.
- [655] I. T. Ma and J. A. Madura, "Gastrointestinal complications after bariatric surgery," *Gastroenterology and Hepatology*, vol. 11, no. 8, pp. 526–535, Aug. 2015.
- [656] M. Bhatia, "H<sub>2</sub>S and Inflammation: An Overview," in *Chemistry, Biochemistry and Pharmacology of Hydrogen Sulfide*, P. K. Moore and M. Whiteman, Eds. Springer, 2015, pp. 165–180.
- [657] L. Rui, "Energy metabolism in the liver," *Comprehensive Physiology*, vol. 4, no. 1, pp. 177–197, 2014.
- [658] A. Untereiner and L. Wu, "Hydrogen Sulfide and Glucose Homeostasis: A Tale of Sweet and the Stink," *Antioxidants and Redox Signaling*, vol. 28, no. 16. Mary Ann Liebert Inc., pp. 1463–1482, 01-Jun-2018.
- [659] J. Pichette, N. Fynn-Sackey, and J. Gagnon, "Hydrogen sulfide and sulfate prebiotic stimulates the secretion of GLP-1 and improves glycemia in male mice," *Endocrinology*, vol. 158, no. 10, pp. 3416–3425, Oct. 2017.
- [660] L. Zhang, G. Yang, A. Untereiner, Y. Ju, L. Wu, and R. Wang, "Hydrogen sulfide impairs glucose utilization and increases gluconeogenesis in hepatocytes," *Endocrinology*, vol. 154, no. 1, pp. 114–126, Jan. 2013.
- [661] M. Yusuf, B. T. K. Huat, A. Hsu, M. Whiteman, M. Bhatia, and P. K. Moore, "Streptozotocin-induced diabetes in the rat is associated with enhanced tissue hydrogen sulfide biosynthesis," *Biochemical and Biophysical Research Communications*, vol. 333, no. 4, pp. 1146–1152, Aug. 2005.
- [662] J. D. Schumacher and G. L. Guo, "Mechanistic review of drug-induced steatohepatitis," *Toxicology and Applied Pharmacology*, vol. 289, no. 1, pp. 40–47, Nov. 2015.
- [663] S. K. Jain, D. Micinski, B. J. Lieblong, and T. Stapleton, "Relationship between hydrogen sulfide levels and HDL-cholesterol, adiponectin, and potassium levels in the blood of healthy subjects," *Atherosclerosis*, vol. 225, no. 1, pp. 242–245, Nov. 2012.

- [664] K. Robert *et al.*, "Cystathionine  $\beta$  synthase deficiency promotes oxidative stress, fibrosis, and steatosis in mice liver," *Gastroenterology*, vol. 128, no. 5, pp. 1405–1415, 2005.
- [665] J. Hamelet, K. Demuth, J. L. Paul, J. M. Delabar, and N. Janel, "Hyperhomocysteinemia due to cystathionine beta synthase deficiency induces dysregulation of genes involved in hepatic lipid homeostasis in mice," *Journal of Hepatology*, vol. 46, no. 1, pp. 151–159, Jan. 2007.
- [666] K. Namekata, Y. Enokido, I. Ishii, Y. Nagai, T. Harada, and H. Kimura, "Abnormal lipid metabolism in cystathionine  $\beta$ -synthase-deficient mice, an animal model for hyperhomocysteinemia," *Journal of Biological Chemistry*, vol. 279, no. 51, pp. 52961–52969, Dec. 2004.
- [667] T. Zhang *et al.*, "Hyperhomocysteinemia and dyslipidemia in point mutation G307S of cystathionine  $\beta$ -synthase-deficient rabbit generated using CRISPR/Cas9," *Lipids in Health and Disease*, vol. 19, no. 1, Dec. 2020.
- [668] T. Majtan *et al.*, "Enzyme replacement prevents neonatal death, liver damage, and osteoporosis in murine homocystinuria," *FASEB Journal*, vol. 31, no. 12, pp. 5495–5506, 2017.
- [669] R. L. Jacobs *et al.*, "Cystathionine beta-synthase deficiency alters hepatic phospholipid and choline metabolism: Post-translational repression of phosphatidylethanolamine N-methyltransferase is a consequence rather than a cause of liver injury in homocystinuria," *Molecular Genetics and Metabolism*, vol. 120, no. 4, pp. 325–336, Apr. 2017.
- [670] S. Gupta and W. D. Kruger, "Cystathionine Beta-Synthase Deficiency Causes Fat Loss in Mice," *PLoS ONE*, vol. 6, no. 11, p. e27598, Nov. 2011.
- [671] K. Módis, P. Panopoulos, C. Coletta, A. Papapetropoulos, and C. Szabo, "Hydrogen sulfide-mediated stimulation of mitochondrial electron transport involves inhibition of the mitochondrial phosphodiesterase 2A, elevation of cAMP and activation of protein kinase A," *Biochemical Pharmacology*, vol. 86, no. 9, pp. 1311–1319, 2013.
- [672] S. Kai *et al.*, "Hydrogen sulfide inhibits hypoxia-but not anoxia-induced hypoxia-inducible factor 1 activation in a von Hippel-Lindau-and mitochondria-dependent manner," *Antioxidants and Redox Signaling*, vol. 16, no. 3, pp. 203–216, Feb. 2012.
- [673] X. Feng, H. Zhang, M. Shi, Y. Chen, T. Yang, and H. Fan, "Toxic effects of hydrogen sulfide donor NaHS induced liver apoptosis is regulated by complex IV subunits and reactive oxygen species generation in rats," *Environmental Toxicology*, vol. 35, no. 3, pp. 322–332, Mar. 2020.
- [674] K. Módis *et al.*, "S- Sulfhydration of ATP synthase by hydrogen sulfide stimulates mitochondrial bioenergetics," *Pharmacological Research*, vol. 113, no. Pt A, pp. 116–124, Nov. 2016.
- [675] A. A. Untereiner, M. Fu, K. Módis, R. Wang, Y. J. Ju, and L. Wu, "Stimulatory effect of CSE-generated H<sub>2</sub>S on hepatic mitochondrial biogenesis and the underlying mechanisms," *Nitric Oxide - Biology and Chemistry*, vol. 58, pp. 67–76, Aug. 2016.
- [676] J. Yan, F. Teng, W. Chen, Y. Ji, and Z. Gu, "Cystathionine  $\beta$ -synthase-derived hydrogen sulfide regulates



- lipopolysaccharide-induced apoptosis of the BRL rat hepatic cell line in vitro," *Experimental and Therapeutic Medicine*, vol. 4, no. 5, pp. 832–838, Nov. 2012.
- [677] I. Liguori *et al.*, "Oxidative stress, aging, and diseases," *Clinical Interventions in Aging*, vol. 13. Dove Medical Press Ltd., pp. 757–772, 01-Jan-2018.
- [678] X. Li, P. Fang, J. Mai, E. T. Choi, H. Wang, and X. F. Yang, "Targeting mitochondrial reactive oxygen species as novel therapy for inflammatory diseases and cancers," *Journal of Hematology and Oncology*, vol. 6, no. 1. BioMed Central Ltd., pp. 1–19, 25-Feb-2013.
- [679] D. H. Truong, M. A. Eghbal, W. Hindmarsh, S. H. Roth, and P. J. O'Brien, "Molecular mechanisms of hydrogen sulfide toxicity," in *Drug Metabolism Reviews*, 2006, vol. 38, no. 4, pp. 733–744.
- [680] C. S. Vanzin *et al.*, "Lipid, Oxidative and Inflammatory Profile and Alterations in the Enzymes Paraoxonase and Butyrylcholinesterase in Plasma of Patients with Homocystinuria Due CBS Deficiency: The Vitamin B12 and Folic Acid Importance," *Cellular and Molecular Neurobiology*, vol. 35, no. 6, pp. 899–911, Aug. 2015.
- [681] K. Módis, A. Asimakopoulou, C. Coletta, A. Papapetropoulos, and C. Szabo, "Oxidative stress suppresses the cellular bioenergetic effect of the 3-mercaptopyruvate sulfurtransferase/hydrogen sulfide pathway," *Biochemical and Biophysical Research Communications*, vol. 433, no. 4, pp. 401–407, Apr. 2013.
- [682] G. Tan *et al.*, "Hydrogen sulfide attenuates carbon tetrachloride-induced hepatotoxicity, liver cirrhosis and portal hypertension in rats," *PLoS ONE*, vol. 6, no. 10, 2011.
- [683] S. Zhao *et al.*, "Hydrogen sulfide alleviates liver injury via S-sulhydrated-Keap1/Nrf2/LRP1 pathway," *Hepatology*, Mar. 2020.
- [684] J. M. Hourihan, J. G. Kenna, and J. D. Hayes, "The gasotransmitter hydrogen sulfide induces Nrf2-target genes by inactivating the Keap1 ubiquitin ligase substrate adaptor through formation of a disulfide bond between Cys-226 and Cys-613," *Antioxidants and Redox Signaling*, vol. 19, no. 5, pp. 465–481, Aug. 2013.
- [685] Z. Liu, X. Wang, L. Li, G. Wei, and M. Zhao, "Hydrogen Sulfide Protects against Paraquat-Induced Acute Liver Injury in Rats by Regulating Oxidative Stress, Mitochondrial Function, and Inflammation," *Oxidative Medicine and Cellular Longevity*, vol. 2020, 2020.
- [686] N. Shinya and M. Yamaguchi, "Stimulatory effect of calcium administration on regucalcin mRNA expression is attenuated in the kidney cortex of rats ingested with saline," *Molecular and Cellular Biochemistry*, vol. 178, no. 1–2, pp. 275–281, 1998.
- [687] S. Jha, J. W. Calvert, M. R. Duranski, A. Ramachandran, and D. J. Lefer, "Hydrogen sulfide attenuates hepatic ischemia-reperfusion injury: Role of antioxidant and antiapoptotic signaling," *American Journal of Physiology - Heart and Circulatory Physiology*, vol. 295, no. 2, Aug. 2008.
- [688] H. Teng, B. Wu, K. Zhao, G. Yang, L. Wu, and R. Wang, "Oxygen-sensitive mitochondrial accumulation of

- cystathionine  $\beta$ -synthase mediated by Lon protease," *Proceedings of the National Academy of Sciences of the United States of America*, vol. 110, no. 31, pp. 12679–12684, Jul. 2013.
- [689] C. Hu and L. Li, "In Vitro and in Vivo Hepatic Differentiation of Adult Somatic Stem Cells and Extraembryonic Stem Cells for Treating End Stage Liver Diseases," *Stem Cells International*, vol. 2015. Hindawi Publishing Corporation, 2015.
- [690] S. Zhang, Y. Yang, L. Fan, F. Zhang, and L. Li, "The clinical application of mesenchymal stem cells in liver disease: the current situation and potential future," *Annals of Translational Medicine*, vol. 8, no. 8, pp. 565–565, Apr. 2020.
- [691] N. Ishkitiev, B. Calenic, I. Aoyama, H. li, K. Yaegaki, and T. Imai, "Hydrogen sulfide increases hepatic differentiation in tooth-pulp stem cells," *Journal of Breath Research*, vol. 6, no. 1, Mar. 2012.
- [692] M. Okada *et al.*, "Hydrogen sulphide increases hepatic differentiation of human tooth pulp stem cells compared with human bone marrow stem cells," *International Endodontic Journal*, vol. 47, no. 12, pp. 1142–1150, Dec. 2014.
- [693] R. Yang *et al.*, "Hydrogen sulfide maintains dental pulp stem cell function via TRPV1-mediated calcium influx," *Cell Death Discovery*, vol. 4, no. 1, Dec. 2018.
- [694] M. Okada, T. Imai, K. Yaegaki, N. Ishkitiev, and T. Tanaka, "Regeneration of insulin-producing pancreatic cells using a volatile bioactive compound and human teeth," *Journal of Breath Research*, vol. 8, no. 4, Dec. 2014.
- [695] L.-Y. Mak *et al.*, "Global Epidemiology, Prevention, and Management of Hepatocellular Carcinoma," *American Society of Clinical Oncology Educational Book*, no. 38, pp. 262–279, May 2018.
- [696] H. Jia, J. Ye, J. You, X. Shi, W. Kang, and T. Wang, "Role of the cystathionine  $\beta$ -synthase/H<sub>2</sub>S system in liver cancer cells and the inhibitory effect of quinolone-indolone conjugate QIC2 on the system," *Oncology Reports*, vol. 37, no. 5, pp. 3001–3009, May 2017.
- [697] P. Yin *et al.*, "Sp1 is involved in regulation of cystathionine  $\gamma$ -lyase gene expression and biological function by PI3K/Akt pathway in human hepatocellular carcinoma cell lines," *Cellular Signalling*, vol. 24, no. 6, pp. 1229–1240, Jun. 2012.
- [698] L. Wang *et al.*, "A pharmacological probe identifies cystathionine  $\beta$ -synthase as a new negative regulator for ferroptosis," *Cell Death and Disease*, vol. 9, no. 10, Oct. 2018.
- [699] Y. Zhen *et al.*, "Exogenous hydrogen sulfide promotes hepatocellular carcinoma cell growth by activating the STAT3-COX-2 signaling pathway," *Oncology Letters*, vol. 15, no. 5, pp. 6562–6570, May 2018.
- [700] L. Wang, H. Hannawi, Y. Liu, X. Zhang, X. Shi, and T. Wang, "Cystathionine  $\beta$ -synthase Induces Multidrug Resistance and Metastasis in Hepatocellular Carcinoma," *Current Molecular Medicine*, vol. 18, no. 7, pp. 496–506, Dec. 2018.

- [701] Y. Pan, C. Zhou, D. Yuan, J. Zhang, and C. Shao, "Radiation Exposure Promotes Hepatocarcinoma Cell Invasion through Epithelial Mesenchymal Transition Mediated by H<sub>2</sub>S/CSE Pathway," *Radiation Research*, vol. 185, no. 1, pp. 96–105, Jan. 2016.
- [702] H. Zhang *et al.*, "Blocking Endogenous H<sub>2</sub>S Signaling Attenuated Radiation-Induced Long-Term Metastasis of Residual HepG2 Cells through Inhibition of EMT," *Radiation Research*, vol. 190, no. 4, pp. 374–384, Oct. 2018.
- [703] J. Kim *et al.*, "Expression of cystathionine  $\beta$ -synthase is downregulated in hepatocellular carcinoma and associated with poor prognosis," *Oncology Reports*, vol. 21, no. 6, pp. 1449–1454, 2009.
- [704] S. S. Wang *et al.*, "Hydrogen sulfide promotes autophagy of hepatocellular carcinoma cells through the PI3K/Akt/mTOR signaling pathway," *Cell Death and Disease*, vol. 8, no. 3, 2017.
- [705] D. Yang *et al.*, "H<sub>2</sub>S suppresses indoleamine 2, 3-dioxygenase 1 and exhibits immunotherapeutic efficacy in murine hepatocellular carcinoma," *Journal of Experimental and Clinical Cancer Research*, vol. 38, no. 1, Feb. 2019.
- [706] D. Wu *et al.*, "Hydrogen sulfide acts as a double-edged sword in human hepatocellular carcinoma cells through EGFR/ERK/MMP-2 and PTEN/AKT signaling pathways," *Scientific Reports*, vol. 7, no. 1, Dec. 2017.
- [707] M. T. Peh, A. B. Anwar, D. S. W. Ng, M. S. B. M. Atan, S. D. Kumar, and P. K. Moore, "Effect of feeding a high fat diet on hydrogen sulfide (H<sub>2</sub>S) metabolism in the mouse," *Nitric Oxide*, vol. 41, pp. 138–145, Sep. 2014.
- [708] E. Bravo *et al.*, "High fat diet-induced non alcoholic fatty liver disease in rats is associated with hyperhomocysteinemia caused by down regulation of the transsulphuration pathway," *Lipids in Health and Disease*, vol. 10, 2011.
- [709] M. Whiteman *et al.*, "Adiposity is a major determinant of plasma levels of the novel vasodilator hydrogen sulphide," *Diabetologia*, vol. 53, no. 8, pp. 1722–1726, Aug. 2010.
- [710] S. K. Jain *et al.*, "In African American Type 2 diabetic patients, is vitamin d deficiency associated with lower blood levels of hydrogen sulfide and cyclic adenosine monophosphate, and elevated oxidative stress?," *Antioxidants and Redox Signaling*, vol. 18, no. 10. Antioxid Redox Signal, pp. 1154–1158, 01-Apr-2013.
- [711] Z.-L. Luo *et al.*, "Effects of treatment with hydrogen sulfide on methionine-choline deficient diet-induced non-alcoholic steatohepatitis in rats," *Journal of Gastroenterology and Hepatology*, vol. 29, no. 1, pp. 215–222, Jan. 2014.
- [712] S.-Y. Hwang, L. K. Sarna, Y. L. Siow, and K. O, "High-fat diet stimulates hepatic cystathionine  $\beta$ -synthase and cystathionine  $\gamma$ -lyase expression," *Canadian Journal of Physiology and Pharmacology*, vol. 91, no. 11, pp. 913–919, Nov. 2013.
- [713] E. P. Wijekoon, B. Hall, S. Ratnam, M. E. Brosnan, S. H. Zeisel, and J. T. Brosnan, "Homocysteine

- metabolism in ZDF (Type 2) diabetic rats," *Diabetes*, vol. 54, no. 11, pp. 3245–3251, Nov. 2005.
- [714] N. Takahashi *et al.*, "Reactive sulfur species regulate tRNA methylation and contribute to insulin secretion," *Nucleic Acids Research*, vol. 45, no. 1, pp. 435–445, 2017.
- [715] W. Guo *et al.*, "Cystathionine  $\gamma$ -lyase deficiency aggravates obesity-related insulin resistance via FoxO1-dependent hepatic gluconeogenesis," *FASEB Journal*, vol. 33, no. 3, pp. 4212–4224, Mar. 2019.
- [716] S. Mani, H. Li, G. Yang, L. Wu, and R. Wang, "Deficiency of cystathionine gamma-lyase and hepatic cholesterol accumulation during mouse fatty liver development," *Science Bulletin*, vol. 60, no. 3, pp. 336–347, Feb. 2015.
- [717] A. Ali *et al.*, "Cystathionine gamma-lyase/H2S system suppresses hepatic acetyl-CoA accumulation and nonalcoholic fatty liver disease in mice," *Life Sciences*, vol. 252, Jul. 2020.
- [718] Y. Yang *et al.*, "Dietary methionine restriction reduces hepatic steatosis and oxidative stress in high-fat-fed mice by promoting H<sub>2</sub>S production," *Food and Function*, vol. 10, no. 1, pp. 61–77, Jan. 2019.
- [719] W. Li *et al.*, "S-Propargyl-cysteine Exerts a Novel Protective Effect on Methionine and Choline Deficient Diet-Induced Fatty Liver via Akt/Nrf2/HO-1 Pathway," *Oxidative Medicine and Cellular Longevity*, vol. 2016, 2016.
- [720] Y. Di Wang, J. Y. Li, Y. Qin, Q. Liu, Z. Z. Liao, and X. H. Xiao, "Exogenous Hydrogen Sulfide Alleviates-Induced Intracellular Inflammation in HepG2 Cells," *Experimental and Clinical Endocrinology and Diabetes*, vol. 128, no. 3, pp. 137–143, Mar. 2020.
- [721] D. Wu *et al.*, "Exogenous hydrogen sulfide mitigates the fatty liver in obese mice through improving lipid metabolism and antioxidant potential," *Medical Gas Research*, vol. 5, no. 1, p. 1, Jan. 2015.
- [722] L. Sun *et al.*, "Hydrogen sulfide reduces serum triglyceride by activating liver autophagy via the AMPK-mTOR pathway," *American Journal of Physiology-Endocrinology and Metabolism*, vol. 309, no. 11, pp. E925–E935, Dec. 2015.
- [723] Z. Liu *et al.*, "Metabolomic-proteomic combination analysis reveals the targets and molecular pathways associated with hydrogen sulfide alleviating NAFLD," *Life Sciences*, 2020.
- [724] B. Wang, J. Zeng, and Q. Gu, "Exercise restores bioavailability of hydrogen sulfide and promotes autophagy influx in livers of mice fed with high-fat diet," *Canadian Journal of Physiology and Pharmacology*, vol. 95, no. 6, pp. 667–674, 2017.
- [725] N. Zhang *et al.*, "Diallyl disulfide attenuates non-alcoholic steatohepatitis by suppressing key regulators of lipid metabolism, lipid peroxidation and inflammation in mice," *Molecular Medicine Reports*, vol. 20, no. 2, pp. 1363–1372, 2019.
- [726] M. Pinzani and J. Maclas-Barragan, "Update on the pathophysiology of liver fibrosis," *Expert Review of Gastroenterology and Hepatology*, vol. 4, no. 4. Taylor & Francis, pp. 459–472, Aug-2010.
- [727] L. Ci *et al.*, "Cystathionine  $\gamma$ -Lyase Deficiency Exacerbates CCl<sub>4</sub>-Induced Acute Hepatitis and Fibrosis in

- the Mouse Liver," *Antioxidants & Redox Signaling*, vol. 27, no. 3, pp. 133–149, Jul. 2017.
- [728] H. N. Fan *et al.*, "Protective effects of hydrogen sulfide on oxidative stress and fibrosis in hepatic stellate cells," *Molecular Medicine Reports*, vol. 7, no. 1, pp. 247–253, Jan. 2013.
- [729] H. N. Fan *et al.*, "Decreased expression of p38 MAPK mediates protective effects of hydrogen sulfide on hepatic fibrosis," *European Review for Medical and Pharmacological Sciences*, vol. 17, pp. 644–652, 2013.
- [730] H. N. Fan, N. W. Chen, W. L. Shen, X. Y. Zhao, and J. Zhang, "Endogenous hydrogen sulfide is associated with angiotensin II type 1 receptor in a rat model of carbon tetrachloride-induced hepatic fibrosis," *Molecular Medicine Reports*, vol. 12, no. 3, pp. 3351–3358, Sep. 2015.
- [731] F. Zhang *et al.*, "Diallyl trisulfide suppresses oxidative stress-induced activation of hepatic stellate cells through production of hydrogen sulfide," *Oxidative Medicine and Cellular Longevity*, vol. 2017, 2017.
- [732] Z. Gong *et al.*, "S-allyl-cysteine attenuates carbon tetrachloride-induced liver fibrosis in rats by targeting STAT3/SMAD3 pathway," *American Journal of Translational Research*, vol. 10, no. 5, pp. 1337–1346, May 2018.
- [733] T. Damba, M. Zhang, M. Buist-Homan, H. van Goor, K. N. Faber, and H. Moshage, "Hydrogen sulfide stimulates activation of hepatic stellate cells through increased cellular bio-energetics," *Nitric Oxide - Biology and Chemistry*, vol. 92, pp. 26–33, Nov. 2019.
- [734] I. Baiges, J. Palmfeldt, C. Bladé, N. Gregersen, and L. Arola, "Lipogenesis is decreased by grape seed proanthocyanidins according to liver proteomics of rats fed a high fat diet," *Molecular and Cellular Proteomics*, vol. 9, no. 7, pp. 1499–1513, 2010.
- [735] C. M. Quinzii, M. Luna-Sanchez, M. Ziosi, A. Hidalgo-Gutierrez, G. Kleiner, and L. C. Lopez, "The role of sulfide oxidation impairment in the pathogenesis of primary CoQ deficiency," *Frontiers in Physiology*, vol. 8, no. JUL. Frontiers Media S.A., 25-Jul-2017.
- [736] M. P. Mollica *et al.*, "Butyrate regulates liver mitochondrial function, efficiency, and dynamics in insulin-resistant obese mice," *Diabetes*, vol. 66, no. 5, pp. 1405–1418, May 2017.
- [737] W. Babidge, S. Millard, and W. Roediger, "Sulfides impair short chain fatty acid  $\beta$ -oxidation at acyl-CoA dehydrogenase level in colonocytes: Implications for ulcerative colitis," *Molecular and Cellular Biochemistry*, vol. 181, no. 1–2, pp. 117–124, 1998.
- [738] A. P. Landry *et al.*, "A Catalytic Trisulfide in Human Sulfide Quinone Oxidoreductase Catalyzes Coenzyme A Persulfide Synthesis and Inhibits Butyrate Oxidation," *Cell Chemical Biology*, vol. 26, no. 11, pp. 1515-1525.e4, Nov. 2019.
- [739] J. Prieto-Lloret *et al.*, "Role of reactive oxygen species and sulfide-quinone oxidoreductase in hydrogen sulfide-induced contraction of rat pulmonary arteries," *American Journal of Physiology - Lung Cellular and Molecular Physiology*, vol. 314, no. 4, pp. L670–L685, Apr. 2018.

- [740] C. Hine *et al.*, "Endogenous hydrogen sulfide production is essential for dietary restriction benefits," *Cell*, vol. 160, no. 1–2, pp. 132–144, Jan. 2015.
- [741] A. Tam *et al.*, "Improved clinical outcome following liver transplant in patients with ethylmalonic encephalopathy," *American Journal of Medical Genetics, Part A*, vol. 179, no. 6, pp. 1015–1019, Jun. 2019.
- [742] J. Palmfeldt *et al.*, "Proteomics reveals that redox regulation is disrupted in patients with ethylmalonic encephalopathy," *Journal of Proteome Research*, vol. 10, no. 5, pp. 2389–2396, May 2011.
- [743] N. Sahebkhari *et al.*, "Quantitative proteomics suggests metabolic reprogramming during ETHE1 deficiency," *Proteomics*, vol. 16, no. 7, pp. 1166–1176, Apr. 2016.
- [744] M. Boyer *et al.*, "Response to medical and a novel dietary treatment in newborn screen identified patients with ethylmalonic encephalopathy," *Molecular Genetics and Metabolism*, vol. 124, no. 1, pp. 57–63, May 2018.
- [745] T. M. Hildebrandt, I. Di Meo, M. Zeviani, C. Viscomi, and H. P. Braun, "Proteome adaptations in Ethe1-deficient mice indicate a role in lipid catabolism and cytoskeleton organization via post-translational protein modifications," *Bioscience Reports*, vol. 33, no. 4, pp. 575–584, 2013.
- [746] N. M. Morton *et al.*, "Genetic identification of thiosulfate sulfurtransferase as an adipocyte-expressed antidiabetic target in mice selected for leanness," *Nature Medicine*, vol. 22, no. 7, pp. 771–779, Jul. 2016.
- [747] E. N. Herken, E. Kocamaz, O. Erel, H. Celik, and V. Kucukatay, "Effect of sulfite treatment on total antioxidant capacity, total oxidant status, lipid hydroperoxide, and total free sulfhydryl groups contents in normal and sulfite oxidase-deficient rat plasma," *Cell Biology and Toxicology*, vol. 25, no. 4, pp. 355–362, Aug. 2009.
- [748] O. H. Ozturk, S. Oktar, M. Aydin, and V. Kucukatay, "Effect of sulfite on antioxidant enzymes and lipid peroxidation in normal and sulfite oxidase-deficient rat erythrocytes," *Journal of Physiology and Biochemistry*, vol. 66, no. 3, pp. 205–212, Sep. 2010.
- [749] D. S. Svoboda and M. D. Kawaja, "Changes in hepatic protein expression in spontaneously hypertensive rats suggest early stages of non-alcoholic fatty liver disease," *Journal of Proteomics*, vol. 75, no. 6, pp. 1752–1763, Mar. 2012.
- [750] J. FOLCH, M. LEES, and G. H. SLOANE STANLEY, "A simple method for the isolation and purification of total lipides from animal tissues.," *The Journal of biological chemistry*, vol. 226, no. 1, pp. 497–509, May 1957.
- [751] H. Zischka *et al.*, "Electrophoretic analysis of the mitochondrial outer membrane rupture induced by permeability transition," *Analytical Chemistry*, vol. 80, no. 13, pp. 5051–5058, Jul. 2008.
- [752] D. R. Linden *et al.*, "Production of the gaseous signal molecule hydrogen sulfide in mouse tissues," *Journal of Neurochemistry*, vol. 106, no. 4, pp. 1577–1585, Aug. 2008.

- [753] M. D. Levitt, M. S. Abdel-Rehim, and J. Furne, "Free and acid-labile hydrogen sulfide concentrations in mouse tissues: Anomalously high free hydrogen sulfide in aortic tissue," *Antioxidants and Redox Signaling*, vol. 15, no. 2, pp. 373–378, Jul. 2011.
- [754] M. Selzner, H. A. Rüdiger, D. Sindram, J. Madden, and P. A. Clavien, "Mechanisms of ischemic injury are different in the steatotic and normal rat liver," *Hepatology*, vol. 32, no. 6, pp. 1280–1288, 2000.
- [755] O. Kabil, V. Vitvitsky, P. Xie, and R. Banerjee, "The quantitative significance of the transsulfuration enzymes for H<sub>2</sub>S production in murine tissues," *Antioxidants and Redox Signaling*, vol. 15, no. 2, pp. 363–372, Jul. 2011.
- [756] C. Hine, Y. Zhu, A. N. Hollenberg, and J. R. Mitchell, "Dietary and Endocrine Regulation of Endogenous Hydrogen Sulfide Production: Implications for Longevity," *Antioxidants and Redox Signaling*, vol. 28, no. 16. Mary Ann Liebert Inc., pp. 1483–1502, 01-Jun-2018.
- [757] D. Wu *et al.*, "Exogenous hydrogen sulfide regulates the growth of human thyroid carcinoma cells," *Oxidative Medicine and Cellular Longevity*, vol. 2019, 2019.
- [758] X. Liu *et al.*, "Sulfide exposure results in enhanced *sqr* transcription through upregulating the expression and activation of HSF1 in echiuran worm *Urechis unicinctus*," *Aquatic Toxicology*, vol. 170, pp. 229–239, Jan. 2016.
- [759] T. Shimizu *et al.*, "Sulfide-responsive transcriptional repressor SqrR functions as a master regulator of sulfide-dependent photosynthesis," *Proceedings of the National Academy of Sciences of the United States of America*, vol. 114, no. 9, pp. 2355–2360, Feb. 2017.
- [760] T. Zhang *et al.*, "A novel transcription factor MRPS27 up-regulates the expression of *sqr*, a key gene of mitochondrial sulfide metabolism in echiuran worm *Urechis unicinctus*," *Comparative Biochemistry and Physiology Part C: Toxicology & Pharmacology*, vol. 243, p. 108997, Feb. 2021.
- [761] D. A. Capdevila, B. J. C. Walsh, Y. Zhang, C. Dietrich, G. Gonzalez-Gutierrez, and D. P. Giedroc, "Structural basis for persulfide-sensing specificity in a transcriptional regulator," *Nature Chemical Biology*, vol. 17, no. 1, pp. 65–70, Jan. 2021.
- [762] Y. Bin Ma *et al.*, "Response of Sulfide: Quinone Oxidoreductase to Sulfide Exposure in the Echiuran Worm *Urechis unicinctus*," *Marine Biotechnology*, vol. 14, no. 2, pp. 245–251, Apr. 2012.
- [763] J. L. Kelley, L. Arias-Rodriguez, D. Patacsil Martin, M. C. Yee, C. D. Bustamante, and M. Tobler, "Mechanisms Underlying Adaptation to Life in Hydrogen Sulfide-Rich Environments," *Molecular Biology and Evolution*, vol. 33, no. 6, pp. 1419–1434, Jun. 2016.
- [764] A. Xiao *et al.*, "H<sub>2</sub>S, a novel gasotransmitter, involves in gastric accommodation," *Scientific Reports*, vol. 5, Nov. 2015.
- [765] R. N. Carter and N. M. Morton, "Cysteine and hydrogen sulphide in the regulation of metabolism: Insights from genetics and pharmacology," *Journal of Pathology*, vol. 238, no. 2. John Wiley and Sons Ltd, pp. 321–332, 01-Jan-2016.

- [766] G. Yang, G. Tang, L. Zhang, L. Wu, and R. Wang, "The pathogenic role of cystathionine  $\gamma$ -lyase/hydrogen sulfide in streptozotocin-induced diabetes in mice," *American Journal of Pathology*, vol. 179, no. 2, pp. 869–879, Aug. 2011.
- [767] J. E. Gerich, H. J. Woerle, C. Meyer, and M. Stumvoll, "Renal gluconeogenesis: Its importance in human glucose homeostasis," *Diabetes Care*, vol. 24, no. 2. American Diabetes Association Inc., pp. 382–391, 2001.
- [768] G. Tang, L. Zhang, G. Yang, L. Wu, and R. Wang, "Hydrogen sulfide-induced inhibition of L-type Ca<sup>2+</sup> channels and insulin secretion in mouse pancreatic beta cells," *Diabetologia*, vol. 56, no. 3, pp. 533–541, Mar. 2013.
- [769] J. Zivanovic *et al.*, "Selective Persulfide Detection Reveals Evolutionarily Conserved Antiaging Effects of S-Sulfhydration," *Cell Metabolism*, vol. 30, no. 6, pp. 1152–1170.e13, Dec. 2019.
- [770] E. Vavrova *et al.*, "Muscle expression of a malonyl-CoA-insensitive carnitine palmitoyltransferase-1 protects mice against high-fat/high-sucrose diet-induced insulin resistance," *American journal of physiology Endocrinology and metabolism*, vol. 311, no. 3, pp. E649–E660, Sep. 2016.
- [771] R. Dentin *et al.*, "Hepatic Glucokinase Is Required for the Synergistic Action of ChREBP and SREBP-1c on Glycolytic and Lipogenic Gene Expression," *Journal of Biological Chemistry*, vol. 279, no. 19, pp. 20314–20326, May 2004.
- [772] L. Jia *et al.*, "Hepatocyte toll-like receptor 4 regulates obesity-induced inflammation and insulin resistance," *Nature Communications*, vol. 5, May 2014.
- [773] C. Fernandes-Santos, R. E. Carneiro, L. de Souza Mendonca, M. B. Aguila, and C. A. Mandarim-de-Lacerda, "Pan-PPAR agonist beneficial effects in overweight mice fed a high-fat high-sucrose diet," *Nutrition*, vol. 25, no. 7–8, pp. 818–827, Jul. 2009.
- [774] S. Moreno-Fernández, M. Garcés-Rimón, G. Vera, J. Astier, J. F. Landrier, and M. Miguel, "High fat/high glucose diet induces metabolic syndrome in an experimental rat model," *Nutrients*, vol. 10, no. 10, Oct. 2018.
- [775] Q. M. Anstee and R. D. Goldin, "Mouse models in non-alcoholic fatty liver disease and steatohepatitis research," *International Journal of Experimental Pathology*, vol. 87, no. 1. Int J Exp Pathol, pp. 1–16, Feb-2006.
- [776] S. J. Lee, J. H. Kang, W. Iqbal, and O. S. Kwon, "Proteomic analysis of mice fed methionine and choline deficient diet reveals marker proteins associated with steatohepatitis," *PLoS ONE*, vol. 10, no. 4, Apr. 2015.
- [777] M. Kong, X. Chen, H. Xu, Wenping, M. Fang, and Y. Xu, "Hepatocyte-specific deletion of Brg1 alleviates methionine-and-choline-deficient diet (MCD) induced non-alcoholic steatohepatitis in mice," *Biochemical and Biophysical Research Communications*, vol. 503, no. 1, pp. 344–351, Sep. 2018.
- [778] S. Nakajima, T. Hira, and H. Hara, "Postprandial glucagon-like peptide-1 secretion is increased during



- the progression of glucose intolerance and obesity in high-fat/high-sucrose diet-fed rats," *British Journal of Nutrition*, vol. 113, no. 9, pp. 1477–1488, May 2015.
- [779] K. Eisinger *et al.*, "Lipidomic analysis of the liver from high-fat diet induced obese mice identifies changes in multiple lipid classes," *Experimental and Molecular Pathology*, vol. 97, no. 1, pp. 37–43, Aug. 2014.
- [780] M. R. Chun *et al.*, "Differential effects of high-carbohydrate and high-fat diet composition on muscle insulin resistance in rats," *Journal of Korean Medical Science*, vol. 25, no. 7, pp. 1053–1059, Jul. 2010.
- [781] Z. H. Yang, H. Miyahara, J. Takeo, and M. Katayama, "Diet high in fat and sucrose induces rapid onset of obesity-related metabolic syndrome partly through rapid response of genes involved in lipogenesis, insulin signalling and inflammation in mice," *Diabetology and Metabolic Syndrome*, vol. 4, no. 1, 2012.
- [782] J. Pinyo, T. Hira, and H. Hara, "Continuous feeding of a combined high-fat and high-sucrose diet, rather than an individual high-fat or high-sucrose diet, rapidly enhances the glucagon-like peptide-1 secretory response to meal ingestion in diet-induced obese rats," *Nutrition*, vol. 62, pp. 122–130, Jun. 2019.
- [783] M. E. Rinella, M. S. Elias, R. R. Smolak, T. Fu, J. Borensztajn, and R. M. Green, "Mechanisms of hepatic steatosis in mice fed a lipogenic methionine choline-deficient diet," in *Journal of Lipid Research*, 2008, vol. 49, no. 5, pp. 1068–1076.
- [784] A. J. Barak, H. C. Beckenhauer, M. Junnila, and D. J. Tuma, "Dietary Betaine Promotes Generation of Hepatic S-Adenosylmethionine and Protects the Liver from Ethanol-Induced Fatty Infiltration," *Alcoholism: Clinical and Experimental Research*, vol. 17, no. 3, pp. 552–555, 1993.
- [785] C. Zhang, E. L. Klett, and R. A. Coleman, "Lipid signals and insulin resistance," *Clinical Lipidology*, vol. 8, no. 6. NIH Public Access, pp. 659–667, Dec-2013.
- [786] N. Taltavull *et al.*, "Protective effects of fish oil on pre-diabetes: A lipidomic analysis of liver ceramides in rats," *Food and Function*, vol. 7, no. 9, pp. 3981–3988, Sep. 2016.
- [787] P. Zabielski, H. R. Hady, M. Chacinska, K. Roszczyc, J. Gorski, and A. U. Blachnio-Zabielska, "The effect of high fat diet and metformin treatment on liver lipids accumulation and their impact on insulin action," *Scientific Reports*, vol. 8, no. 1, p. 7249, Dec. 2018.
- [788] G. Xie *et al.*, "Distinctly altered gut microbiota in the progression of liver disease," *Oncotarget*, vol. 7, no. 15, pp. 19355–19366, Apr. 2016.
- [789] M. Qiu *et al.*, "Modulation of intestinal microbiota by glycyrrhizic acid prevents high-fat diet-enhanced pre-metastatic niche formation and metastasis," *Mucosal Immunology*, vol. 12, no. 4, pp. 945–957, Jul. 2019.
- [790] F. Shen, R. D. Zheng, X. Q. Sun, W. J. Ding, X. Y. Wang, and J. G. Fan, "Gut microbiota dysbiosis in patients with non-alcoholic fatty liver disease," *Hepatobiliary and Pancreatic Diseases International*, vol. 16, no. 4, pp. 375–381, Aug. 2017.

- [791] N. Fei *et al.*, “Endotoxin producers overgrowing in human gut microbiota as the causative agents for nonalcoholic fatty liver disease,” *mBio*, vol. 11, no. 1, Jan. 2020.
- [792] R. Wang *et al.*, “Endogenous CSE/hydrogen sulfide system regulates the effects of glucocorticoids and insulin on muscle protein synthesis,” *Oxidative Medicine and Cellular Longevity*, vol. 2019, 2019.
- [793] H. P. Harding *et al.*, “An integrated stress response regulates amino acid metabolism and resistance to oxidative stress,” *Molecular Cell*, vol. 11, no. 3, pp. 619–633, Mar. 2003.
- [794] C. Hine *et al.*, “Hypothalamic-Pituitary Axis Regulates Hydrogen Sulfide Production,” *Cell Metabolism*, vol. 25, no. 6, pp. 1320–1333.e5, Jun. 2017.
- [795] E. Bravo *et al.*, “Coenzyme Q metabolism is disturbed in high fat diet-induced non alcoholic fatty liver disease in rats,” *International Journal of Molecular Sciences*, vol. 13, no. 2, pp. 1644–1657, Feb. 2012.
- [796] Z. Yesilova *et al.*, “Systemic markers of lipid peroxidation and antioxidants in patients with nonalcoholic fatty liver disease,” *American Journal of Gastroenterology*, vol. 100, no. 4, pp. 850–855, Apr. 2005.
- [797] K. M. Botham, M. Napolitano, and E. Bravo, “The emerging role of disturbed CoQ metabolism in nonalcoholic fatty liver disease development and progression,” *Nutrients*, vol. 7, no. 12. MDPI AG, pp. 9834–9846, 01-Dec-2015.
- [798] M. Luna-Sánchez *et al.*, “CoQ deficiency causes disruption of mitochondrial sulfide oxidation, a new pathomechanism associated with this syndrome,” *EMBO Molecular Medicine*, vol. 9, no. 1, pp. 78–95, Jan. 2017.
- [799] R. Millikin *et al.*, “The chemical biology of protein hydropersulfides: Studies of a possible protective function of biological hydropersulfide generation,” *Free Radical Biology and Medicine*, vol. 97, pp. 136–147, Aug. 2016.
- [800] H. L. A. Tarr, “The enzymic formation of hydrogen sulphide by certain heterotrophic bacteria,” *Biochemical Journal*, vol. 27, no. 6, pp. 1869–1874, Jan. 1933.
- [801] B. B. Jørgensen, “The sulfur cycle of freshwater sediments: Role of thiosulfate,” *Limnology and Oceanography*, vol. 35, no. 6, pp. 1329–1342, Sep. 1990.
- [802] *Safety evaluation of certain food additives Prepared by the Sixty-ninth meeting of the Joint FAO/WHO Expert Committee on Food Additives (JECFA) WHO FOOD ADDITIVES SERIES: 60 IPCS-International Programme on Chemical Safety.* 2009.
- [803] B. Le Roy, A. Dupré, A. Gallon, P. Chabrot, J. Gagnière, and E. Buc, “Liver hypertrophy: Underlying mechanisms and promoting procedures before major hepatectomy,” *Journal of Visceral Surgery*, vol. 155, no. 5. Elsevier Masson SAS, pp. 393–401, 01-Oct-2018.
- [804] P. I. Yanchuk and L. A. Slobodanyk, “THE ROLE OF HYDROGEN SULFIDE IN REGULATION OF CIRCULATION BLOOD LIVER,” *Fiziolohichnyi zhurnal (Kiev, Ukraine : 1994)*, vol. 61, no. 3, pp. 28–34, 2015.

- [805] T. Huc, H. Jurkowska, M. Wróbel, K. Jaworska, M. Onyszkiewicz, and M. Ufnal, "Colonic hydrogen sulfide produces portal hypertension and systemic hypotension in rats," *Experimental Biology and Medicine*, vol. 243, no. 1, pp. 96–106, Jan. 2018.
- [806] L. Morzyglod *et al.*, "Growth factor receptor binding protein 14 inhibition triggers insulin-induced mouse hepatocyte proliferation and is associated with hepatocellular carcinoma," *Hepatology*, vol. 65, no. 4, pp. 1352–1368, Apr. 2017.
- [807] J. M. Hourihan, J. G. Kenna, and J. D. Hayes, "The gasotransmitter hydrogen sulfide induces Nrf2-target genes by inactivating the Keap1 ubiquitin ligase substrate adaptor through formation of a disulfide bond between Cys-226 and Cys-613," *Antioxidants and Redox Signaling*, vol. 19, no. 5, pp. 465–481, Aug. 2013.
- [808] A. Bassot *et al.*, "Regulation of Mitochondria-Associated Membranes (MAMs) by NO/sGC/PKG Participates in the Control of Hepatic Insulin Response," *Cells*, vol. 8, no. 11, Oct. 2019.
- [809] C. L. Bianco and J. M. Fukuto, "Examining the reaction of NO and H<sub>2</sub>S and the possible cross-talk between the two signaling pathways," *Proceedings of the National Academy of Sciences of the United States of America*, vol. 112, no. 34, National Academy of Sciences, pp. 10573–10574, 25-Aug-2015.